Design and Application of Probes to Understand Peroxisomal Localisation of BODIPYs

BOYE ZHU

Design and Application of Probes to Understand Peroxisomal Localisation of BODIPYs

朱博也 (Boye Zhu)

Supervised by Prof. Patrick G. Steel

A thesis submitted in partial fulfilment of the requirement for the degree of Doctor of Philosophy in Science

Department of Chemistry

Durham University

United Kingdom

July 2022

ABSTRACT

BODIPYs (4,4-difluoro-4-bora-3a,4a-diaza-s-indacene) constitute an important class of fluorophores. The excellent qualities of BODIPY comprise relatively high fluorescence quantum yields and molar absorption coefficients, narrow emission bandwidths, high elevated stability towards chemicals and light, and the extra feature of excitation/emission wavelengths in the visible region.

Previous work in our group generated a small set of BODIPY fluorophores, including one, nitro-BODIPY, 1,3,5,7-tetramethyl-8-(4-nitrophenyl)-BODIPY, that is intrinsically non-fluorescent but upon incubation of cells with this compound, fluorescence is observed at the target site. The target site in plant cells was identified as peroxisomes, as verified by co-localization with an SKL-FP construct (peroxisome-specific carboxyl-terminal targeting sequence fluorescent proteins). It is key to future applications to be able to understand how this is occurring at a molecular level.

These objectives are challenged by a lack of knowledge of this protein target and the physicochemical profile of nitro-BODIPY. This leads to the specific aims of this project which are: 1. To develop a 'toolbox' of analogues that enable multicolour visualisation. 2. To confirm the nature of the binding process between nitro-BODIPY and the target protein and to determine its reversibility. 3. To identify the target protein of nitro-BODIPY in plant peroxisomes.

Therefore, a family of red-shifted nitro-BODIPY probes were synthesised. Most of them showed selectivity towards plant peroxisomes and their emission wavelength could reach to a maximum of around 700 nm. Water-soluble probes were prepared and proved to exhibit selective labelling towards plant peroxisomes as well. In addition, a group of dual-fluorophore probes (nitro-BODIPY probes with a second fluorophore including Rhodamine B, Cy5, dansyl and NBD) were developed to determine whether nitro-BODIPY only localizes at peroxisome or somewhere else. Although several dual-fluorophore probes showed selective labelling of the peroxisome, the reporter function of the second fluorophore in all probes was challenged by various degrees of FRET. Finally, a photoaffinity labelling probe (nitro-BODIPY core attatched with a benzophenone photoaffinity group) was prepared to determine the target proteins of nitro-BODIPY in plant peroxisomes. Several potential protein targets of nitro-BODIPY in plant peroxisomes were detected by this photoaffinity labelling probe via SDS-PAGE technique.

ABBREVIATIONS

BODIPY: 4,4-difluoro-4-bora-3a,4a-diaza-s-indacene

BTEA·ICl_2: benzyltrimethylammonium dichloroiodate

Cy5: Sulfo-Cyanine5

CYS: Cysteine

Dansyl: 5-(dimethylAmino)Naphthalene-1-Sulfonyl chloride

DDQ: 2,3-Dichloro-5,6-dicyano-1,4-benzoquinone

DIBAL-H: diisobutylaluminium hydride

DIPEA: N,N-diisopropylethylamine

DMAP: 4-dimethylaminopyridine

DMF: N,N-dimethylformamide

DMSO: dimethyl sulfoxide

EDC: 1-ethyl-3-(3-dimethylaminopropyl)carbodiimide

FRET: Förster resonance energy transfer

GFP: green fluorescent protein

GFP-SKL fusion protein: peroxisome-specific carboxyl-terminal targeting sequence fluorescent proteins

GSH: Glutathione

HBTU: hexafluorophosphate benzotriazole tetramethyl uronium

HCY: Homocysteine

HEPES: 4-(2-hydroxyethyl)-1-piperazineethanesulfonic acid

HOBt: hydroxybenzotriazole

HOMO: highest occupied molecular orbital

ICT: intramolecular charge transfer

IUPAC: international union of pure and applied chemistry

LCMS: liquid chromatography-mass spectrometry

LDS: lithiumdodecyl sulphate

LUMO: lowest unoccupied molecular orbital

MPO: myeloperoxidase

NBD: nitrobenzoxadiazole

NBS: N-Bromosuccinimide

NCS: N-Chlorosuccinimide

NHS: N-hydroxysuccinimide

NIR: near infrared

Nitro-BODIPY: 1,3,5,7-tetramethyl-8-(4-nitrophenyl)-BODIPY

NMR: nuclear magnetic resonance

PAL: photoaffinity labelling

PEG: poly(ethylene glycol)

PET: photoinduced electron transfer

PRG: photoaffinity groups

PTS1/2: peroxisomal targeting signal type 1/2

RNS: reactive nitrogen species

Rodamine B: 9-(2-carboxyphenyl)-6-(diethylamino)-N,N-diethyl-3H-xanthen-3-iminium chloride

ROS: reactive oxygen species

SDS: sodium lauryl sulfate

SDS-PAGE: sodium dodecyl sulfate–polyacrylamide gel electrophoresis

SKL: C-terminal tripeptide, Ser-Lys-Leu

SO_3-Pyr: sulfur trioxide pyridine complex

TBAI: tetra-n-butylammonium iodide

TD-DFT: time-dependent density-functional theory

TFA: trifluoroacetic acid

TLC: thin layer chromatograph

Tris: 2-amino-2-(hydroxymethyl)propane-1,3-diol

Triton X-100: 2-[4-(2,4,4-trimethylpentan-2-yl)phenoxy]ethanol

TsCl: 4-toluenesulfonyl chloride

VLCFA: very long chain fatty acids

λ_{abs}: ultraviolet maximum absorption wavelength

λ_{em}: fluorescence emission wavelength

φ_f: fluorescence quantum yield

DECLARATION

The scientific work described in this thesis was carried out in the Department of Chemistry, Durham University, United Kingdom between October 2018 and March 2021. This work has not been previously submitted for a degree at this or any other institution.

STATEMENT OF COPYRIGHT

ACKNOWLEDGEMENTS

During my journey in search of my PhD, I have received the support from many individuals. Therefore, it is my pleasure to take the time and express my gratitude. First and foremost, I would like to thank my supervisor Prof Patrick Steel for his guidance, patient and encouragement to the completion of my project and thesis. I would also like to express gratitude to my secondary supervisor Prof Andrew Beeby who friendly provided me a laboratory space during the tough Covid period. I would also like to warmly thank Prof Andrei Smertenko (Washington State University) for his advices, support and cooperation for my research project. Significantly, I would also like to thank China Scholarship Council (CSC) and Durham University for funding my research which without, I would be unable to achieve a doctorate.

In the PGS group, I have met many individuals past and present who made working in CG001 a pleasure. I would like to individually thank Dr Exequiel Porta, Dr Jaime Isern, Dr Niranjan Thota, Dr Michaela Buerdsell, Dr Vanessa Lyne, Dr Jonathon Reuven, Victor Agostino, Dr Angelo Machado, Dr Katherine Norman and Sam Yates. You all have provided great scientific feedback as well as continued support, encouragement.

Finally, I would like to thank my friends and family back in China for their unconditional love, support and encouragement during the past four years. I would also like to thank my friends in Durham, Dr Qiuhan He, Dr Yi Guo, Dr Difu Shi and Lai Zhang who brought a lot of joy to me during the past four years.

Table of Contents

1 INTRODUCTION

1.1 BODIPYs

BODIPY is the technical common name of 4,4-difluoro-4-bora-3a,4a-diaza-*s*-indacene ($C_9H_7BN_2F_2$)[1], a molecule which consists of a boron difluoride group BF_2 joined to a dipyrromethene group $C_9H_7N_2$. The common name is an abbreviation for 'boron-dipyrromethene'. It is a red crystalline solid. BODIPYs constitute an important class of fluorophores discovered in 1968 by Treibs and Kreuzer[2]. The excellent qualities of BODIPY comprise relatively high fluorescence quantum yields and molar absorption coefficients, narrow emission bandwidths with high peak intensities, high stability towards chemicals and light, and the extra feature of excitation/emission wavelengths in the visible region.

1.1.1 Structures and properties of simple BODIPYs

The IUPAC numbering system for BODIPY dyes is different to that used for dipyrromethenes[3], and this can lead to confusion. However, the terms α, β and meso positions are used in just the same way for both systems.

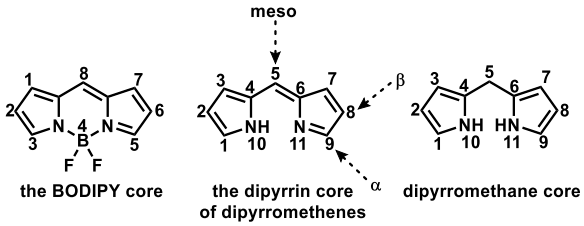

Figure 1 numbering system for BODIPYs.

There are still synthetic limitations for even some simple BODIPY systems. The unsubstituted parent system BODIPY core (BODIPY **1**) was one among them because the dipyrromethene precursor is unstable and decomposes above -30 to -40 °C[4]. Due to the difficulty in its synthesis, the core BODIPY **1** has not been reported for decades. In 2013, Alison found a effective way to synthesis BODIPY **1** from dipyrromethene precursor under low temperature with p-chloranil as a dehydrogenating agent[5], whilst the symmetrical, dimethyl-substituted compound **2** has also been prepared[6-7]. The symmetrically substituted systems **3** and **4** have apparently not been reported, reflecting synthetic limitations for even some simple BODIPY systems.

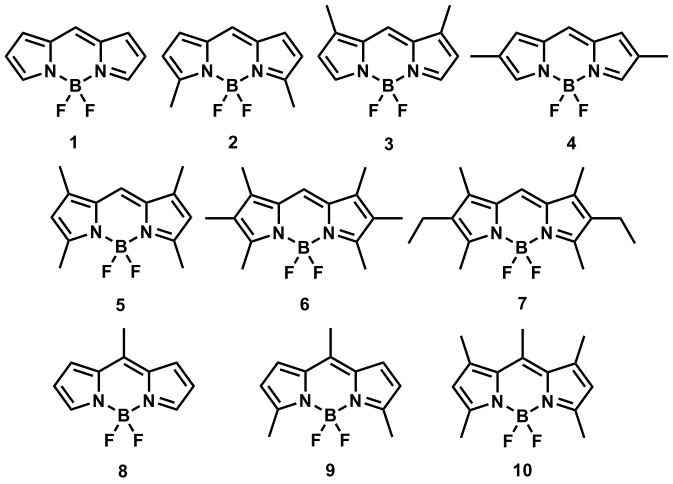

Figure 2 simple symmetrical BODIPYs 1-10.

In contrast, the symmetrically substituted, tetra-, hexa-, and hepta-alkylated systems **5**[8], **6** and **7**[9] have been synthesised from substituted 2-formyl pyrrole (Scheme 1). Zhang reported an efficient method to synthesis a series of symmetrical BODIPYs which includes BODIPY **1**, **2**, **5**, **7**, **8**, **9** and **10** (Scheme 2)[10]. This method requires one pyrrole and one acyl chloride (R_4 could be alkyl or aryl) to afford the substituted dipyrromethene, which is then treated with DDQ as a dehydrogenating agent.

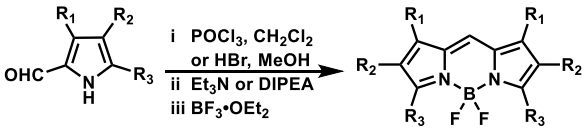

Scheme 1 synthesis of simple symmetrical BODIPYs 5, 6, 7.

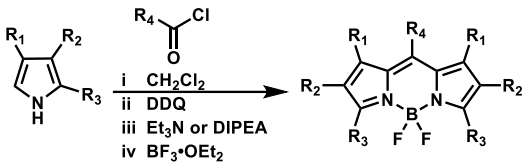

Scheme 2 synthesis of simple symmetrical BODIPYs 1, 2, 5, 7, 8, 9, 10.

Because of the synthetic difficulties, only a few examples of simple unsymmetric BODIPYs have been reported. The unsymmetrically substituted BODIPYs **11**[11] and **12**[12] have been prepared in a similar way to BODIPYs **5-7** (scheme 3). Using a pyrrole with a formyl group or a formyl chloride group, unsymmetrical BODIPYs with one, two, and three methyl groups (BODIPY **11**, **13**, **14** and **15**) were synthesised easily and efficiently[10] (Scheme 4). A self-condensation can occur so these pyrroles must be used in excess in the reaction.

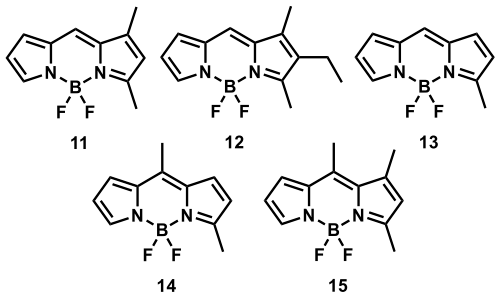

Figure 3 unsymmetrical BODIPYs 11-15.

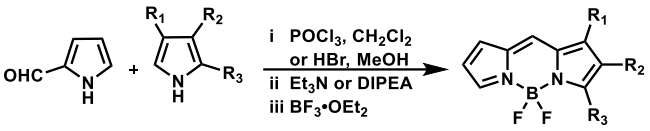

Scheme 3 synthesis of unsymmetrical BODIPYs 11, 12.

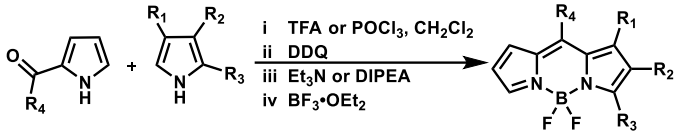

Scheme 4 synthesis of unsymmetrical BODIPYs 11, 13, 14, 15.

Simple BODIPYs show remarkable photophysical properties, such as very good photostability and high fluorescence quantum yields (typically φ_f > 50%, mainly in organic solvents). Their typical absorption/ emission wavelengths typically range between 470 and 530 nm[13]. The photophysical properties of simple BODIPYs are displayed in Table 1. Figure 3a depicts TD-DFT calculated HOMO/ LUMO levels for BODIPY **1**[14]. Generally, the HOMOs are built upon on the π-systems located on the pyrrole rings. Concurrently, the LUMOs are partially located on the meso-position accompanied by a depletion of the pyrrole π-systems relative to that found for the HOMOs. There are relatively minor differences in the reported UV absorption, fluorescence emission and quantum yields of these compounds, and these should not be over-interpreted because small calibration errors are common in these types of experiments. If BODIPY **5-7** are included in the comparison, an unambiguous trend toward red-shifted absorption and emission maxima with increased substitution becomes apparent. Alkylation at the meso position has blue-shift effect on the absorption and emission wavelengths (compare **11** with **15**, and **13** with **14**).

Table 1 Photophysical properties of simple BODIPYs.

Simple BODIPY	λ_{abs} / nm	λ_{em} / nm	φ_f
1	497	505	96 % in MeOH
2	507	520	81 % in EtOH
3		not reported	
4		not reported	
5	505	516	80 % in EtOH
6	528	535	56 % in EtOH
7	517	546	70 % in EtOH
8	494	503	100% in MeOH
9		not reported	
10		not reported	
11	499	509	70 % in EtOH
12	510	520	40 % in EtOH
13	506	512	100 % in MeOH
14	494	502	100% in MeOH
15	486	497	101 % in MeOH

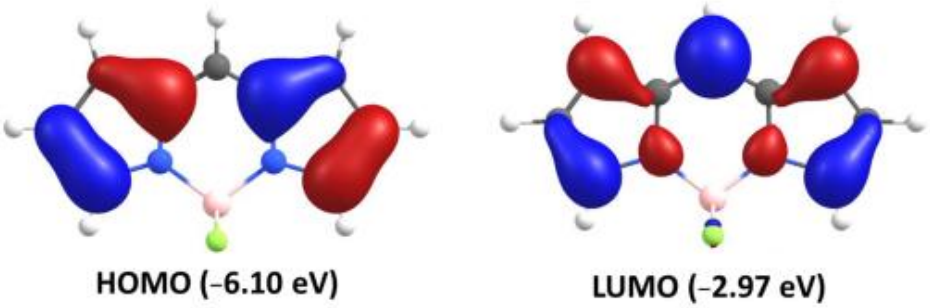

Figure 3a HOMO/ LUMO levels for BODIPY 1.

1.1.2 Modifications on the BODIPY core

The emission wavelengths of conventional simple BODIPYs' typically range between 480 and 530 nm but some applications such as biological imaging generally require dyes that absorb and emit at longer wavelengths, in the far-red or NIR region. To reach this objective, various structural modifications can be made to the BODIPY core. Meso arylated or alkylated BODIPY are relatively easy to prepare via condensation of acyl chlorides with pyrroles (Scheme 2)[15]. For some unsubstituted pyrroles, a condensation between aldehydes and pyrroles is a better method to choose (Scheme 5). For instance, BODIPYs **16**-**18**[16-17] could be prepared via the method in both Scheme 2 and Scheme 5 but BODIPY **19**[18] could only be synthesised via Scheme 5 from a unsubstituted pyrrole and an aromatic aldehyde. However, it is unusual to use alkyl aldehydes to prepare BODIPY in this reaction[4].

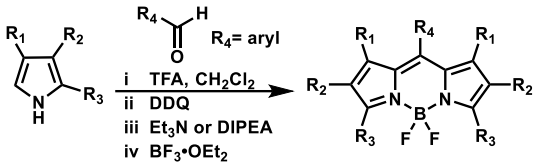

Scheme 5 synthesis of BODIPYs from aryl aldehyde and pyrroles.

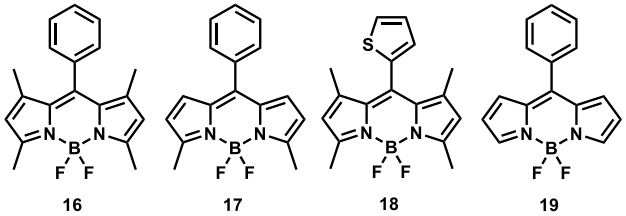

Figure 4 meso-aromatic BODIPY 16-19.

Condensations of pyrroles with acid chlorides or with benzaldehyde derivatives, as outlined above, are direct and convenient methods to access symmetrically substituted BODIPY dyes. However, another approach is required to form unsymmetrical analogs. Generally, this is achieved via preparations of 2-ketopyrrole intermediates, followed by a Lewis acid mediated condensation of these with a second pyrrole fragment. A series of approaches to 2-ketopyrrole (Figure 5) are shown in Scheme 6-8.

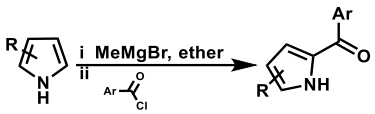

Scheme 6 synthesis of ketopyrrole from acyl chlorides and pyrroles [19-20].

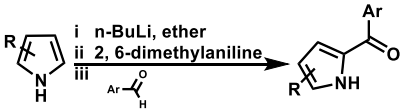

Scheme 7 synthesis of ketopyrrole from aryl aldehydes and pyrroles [21-22].

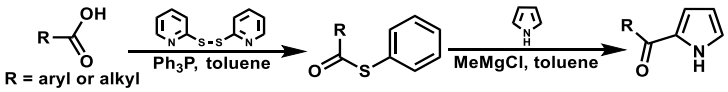

Scheme 8 synthesis of ketopyrrole from aryl acids and pyrroles [23].

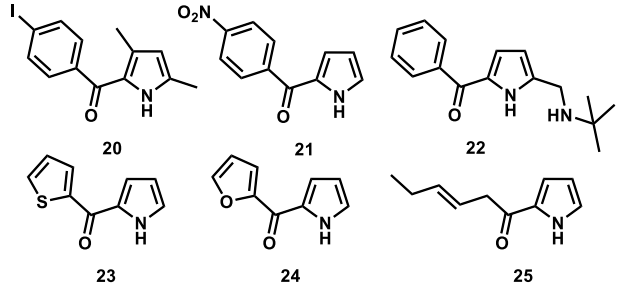

Figure 5 2-ketopyrroles 20-25.

The 2,-6-positions of the BODIPY core bear the least positive charge, so are the most susceptible to electrophilic attack. The 2-/2,6 nitrosubstituted BODIPY dye **26**-**27** could be obtained via nitration with nitric acid at 0 °C[24]. The synthesis condition can be easily controlled using dilute (42%) or concentrated HNO_3 (70%) to obtain 2-nitro BODIPY **26** and 2,6-dinitro BODIPY **27** exclusively. Significantly, introduction of the nitro groups drastically reduces the fluorescence quantum yield[25].

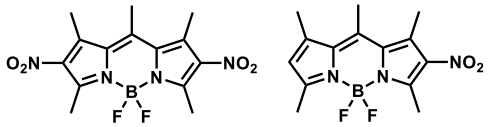

26 67% 27 82%

Figure 6 6 2-/2,6-position Nitrosubstituted BODIPY 26-27.

Halogenated BODIPYs can be easily applied to the further functionalization of BODIPY via substitution or coupling reactions. Direct halogenation methods normally generate 2,6-(β-) halogenated BODIPYs. Bromination of the unsubstituted meso-aromatic BODIPY occurs preferentially at the β-position. For example, 2,6-bromo BODIPYs **28** were developed via bromination with Br_2[26] or NBS[27]. A mild and selective bromination of the 1,3,5,7-tetramethyl-substituted BODIPY (Scheme 9) gave bromination products **29**-**30** by using $CuBr_2$ as the bromination reagent[28]. The selectivity for mono- or dibromination depends on the additives of the reactions. To prepare the dibrominated product, the use of 2.5 equivalents of $CuBr_2$ and oxygen atmosphere is required. Whilst monobromination is achieved using 3.0 equivalents of K_2CO_3 and 1.5 equivalents of $CuBr_2$ without oxygen. The reaction proceeds in good yield for both electron-rich and electron-deficient aromatic groups at the meso-position.

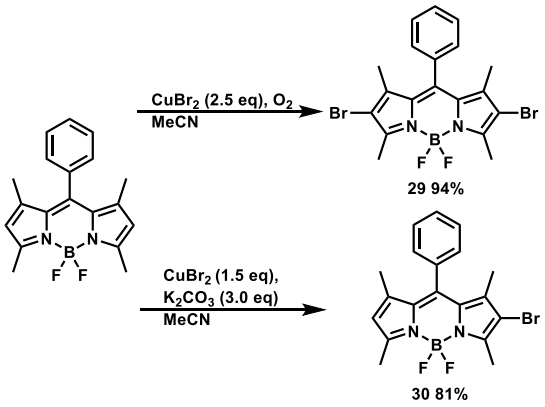

Scheme 9 Bromination of BODIPY.

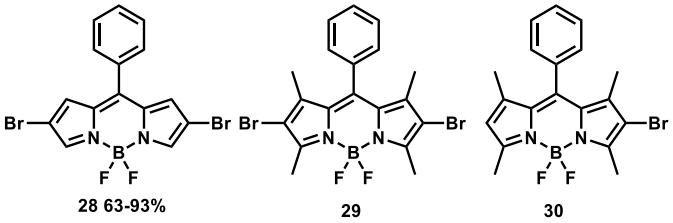

Figure 7 2-/2,6-position bromosubstituted BODIPY 28-30.

Iodination at the 2-/2,6- position of BODIPY (Scheme 10) gave the mono- or diiodination products **31**-**33**[29]. The synthesis conditions of 2,6-diiodo BODIPYs **31**-**32** are treated with excess equivalent of NIS or iodine and iodic acid[30]. The mono iodosubstituted BODIPY dye could be obtained via iodination with $CaCO_3$ and $BTEA{\cdot}ICl_2$[31] or with 0.5 equiv of $PhI(OAc)_2$[32].

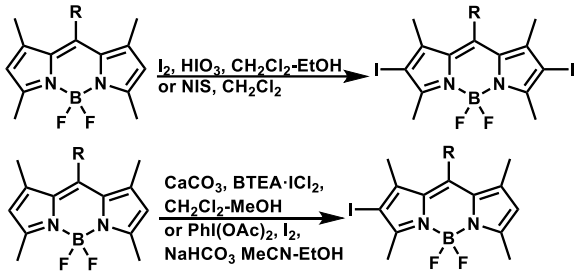

Scheme 10 Iodination on BODIPYs.

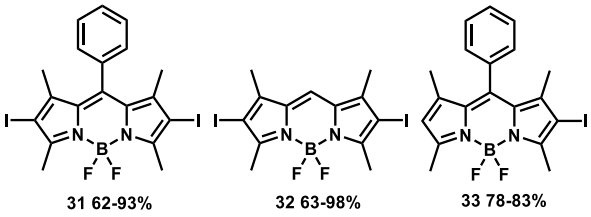

Figure 8 2-/2,6-position iodosubstituted BODIPY 31-33.

Chlorination of the unsubstituted meso-aromatic BODIPY occurs preferentially at the β-position via the treatment of NCS to achieve 2,6-chloro BODIPY (e.g. BODIPY **34**)[33]. The 3- and/or 5-(α)chloro BODIPYs **35**-**37** were first developed via chlorination of dipyrromethane[34] or pyrrole precursors[35] using NCS at -78 °C. Recently a highly regioselective α-chlorination of the BODIPY core with $CuCl_2$ in CH_3CN with good versatility for various meso-aryl, meso-H, and meso-alkyl BODIPYs **35**-**37** was reported[36].

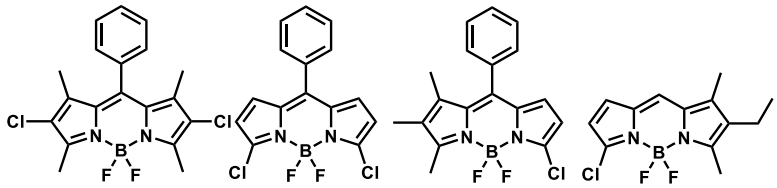

Figure 9 3-/3,5-position chlorosubstituted BODIPY 34-37.

Vilsmeier-Haack formylation of BODIPY is commonly used to further functionalize the BODIPY core on the 2,6-(β-) position. The mono-(2-) or diformyl(2,6-) BODIPY **38**-**39** can be obtained upon treatment with $POCl_3$ and DMF[37-38]. The selectivity of mono- or diformyl depends on the equivalent of Vilsmeier-Haack reagent in the reactions.

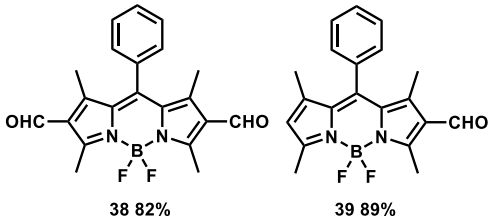

Figure 10 Formyl BODIPY 38-39.

The major drawback of BODIPY derivatives is their high hydrophobicity leading to low water solubility. This hinders their application in certain conditions such as living organisms and most operate only in aqueous media containing organic co-solvents and/or surfactants. Sulfonation of BODIPYs can make the hydrophobic dyes more water-soluble, enabling them to be dissolved in aqueous media for coupling to various water-soluble biomolecules. A variety of conditions can be used to synthesis mono or disulfonated BODIPYs (Scheme 11). Water-soluble BODIPY dyes **40**-**41**, bearing sulfonate groups at the 2- and 6-positions and chlorine group at the 3- and 5-positions, was prepared via sulfonation with chlorosulfonic acid[39]. The sulfonate containing BODIPY **42** was prepared effectively by electrophilic sulfonation with the sulfur trioxide-pyridine complex[40].

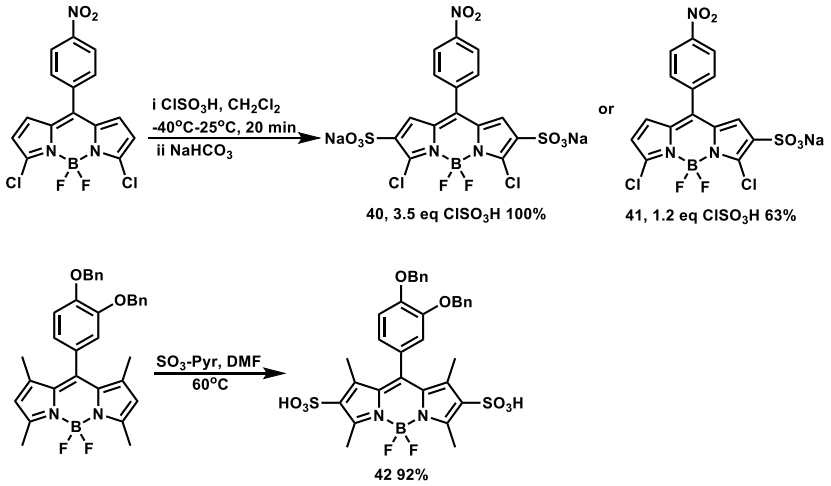

Scheme 11 Sulfonation on BODIPYs 40-42.

1.1.3 Bioimaging probes based on BODIPYs

The cytoplasm of the cells contains myriad ions, small molecules, and bio-molecules that are continuously interacting with each other in a dynamic environment[41]. It is highly important to track ongoing cellular processes at molecular-level in living cells in order to understand and clarify the biological roles and significance of these intracellular players. Towards this end, fluorescence imaging is an ideal technique to visualize living cells in their native environment, because it offers spatial and temporal resolution, high selectivity and sensitivity as well as enabling real-time investigations[42]. Accordingly, most synthetic fluorescent probes contain a binding site and a signaling core, which are linked or integrated to each other with a rapid communication in-between. The selective interaction of a probe with a target analyte yields measurable optical changes in the signaling core (in the form of altered emission wavelength/ intensity or lifetime). Due to their excellent photophysical characteristics, BODIPY derivatives are important components in the design of many fluorescent sensors.

Michael addition type chemodosimeters have been extensively applied as thiol selective fluorescent probes[43-44] (Scheme 12). In this context, BODIPY based probes **43**-**45** carrying a nitroalkene group, acting as a Michael acceptor, were reported. Nucleophilic attack of bio-thiols to the Nitroalkene breaks the conjugation and stops intramolecular charge transfer (ICT), which causes a blue shift in the absorption spectra. The addition reaction also alters the excited state dynamics of the probes and blocks photoinduced electron transfer (PET). In probes **43**-**44**, gallic acid derived units were incorporated in order to improve the water solubility of the probes. Probe **43** has an absorption maximum at 525 nm, while probe **44** has red-shifted absorption at 623 nm because of the extended π-conjugation[45]. The response of **43**-**44** to CYS

is much faster than to GSH. In another work, selective detection of GSH was achieved using aza-crown moiety at the meso position of BODIPY **45**[46] as an additional recognition side for the N-terminal ammonium group of GSH.

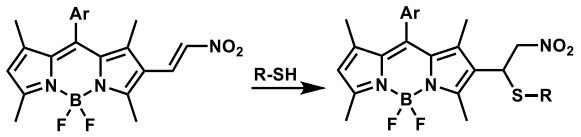

Scheme 12 Michael addition-based detection of bio-thiols.

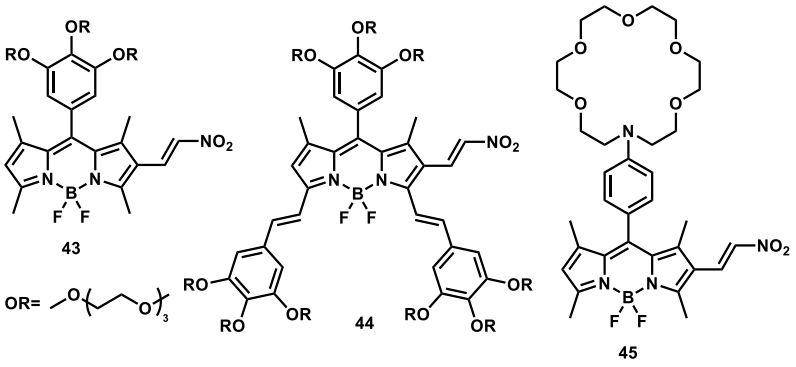

Figure 11 Thiol selective BODIPY probes 43-45.

Hypochlorous acid (HOCl) is an example of reactive oxygen species (ROS) which is closely linked with the induction of several diseases, including atherogenesis, cardiovascular disease, rheumatoid arthritis, neurodegenerative diseases, and cancer[47]. Using the strong oxidizing capacity of HOCl, a water-soluble BODIPY based fluorescent probe **46** that contains meso-catechol unit as a selective reaction site for OCl^- was reported[40]. The sulfonate groups at the 2- and 6-positions provide water solubility. The detection mechanism involves the oxidation of the catechol to quinone in the presence of NaOCl, which results in an emission intensity increase (Scheme 13). The probe fluorescence was modulated by a PET mechanism and it is non-emissive prior to oxidation. Another highly selective HOCl probe is BODIPY **47** bearing an organoselenium group at the meso position (Scheme 14)[48]. The probe is non-emissive because of PET from selenium moiety to the electron acceptor BODIPY core. HOCl-induced oxidation of selenium blocks PET and results in a highly emissive probe emitting at 526 nm.

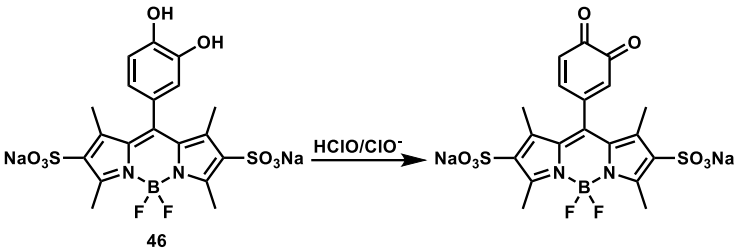

46

Scheme 13 Molecular structures of HOCl-selective probe 46 and the detection mechanism.

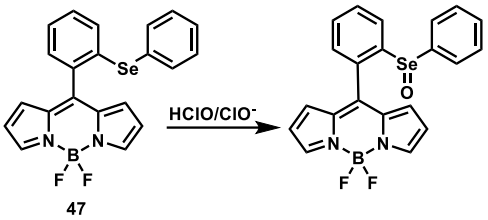

47

Scheme 14 Selenium oxidation for the detection of HOCl.

Nitrogen-based analogs of ROS are known as reactive nitrogen species (RNS) and include nitric oxide (NO), peroxynitrite ($ONOO^-$), nitrogen dioxide (NO_2), and nitroxyl (HNO)[49]. Probe **48** based on the BODIPY chromophore is a highly sensitive fluorescence probe for nitric oxide. It has a low fluorescence quantum yield of 0.002, whereas its triazole derivative (Scheme 15), the product of the reaction with NO, fluoresced strongly (φ_f =0.74)[50]. The change of the fluorescence intensity was found to be controlled by an intramolecular PET mechanism. The water-soluble BODIPY probe **49** can image the extracellular NO released from the living cells[51]. Probe **50** shows an expanded Stokes shift[52] and can react with NO in only 2 min to form the triazole with a φ_f of 0.32. Moreover, an excellent linear relationship was observed in the range of NO concentration from 0.5 mM to 4 mM with a detection limit of 1 nM.

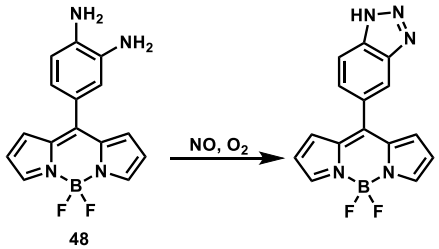

48

Scheme 15 Phenylenediamine substituted BODIPY based probes for selective detection of NO.

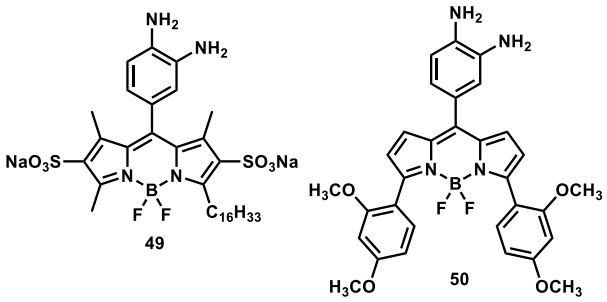

Figure 12 Phenylenediamine substituted BODIPY based probes 49-50.

1.2 Peroxisomes

1.2.1 Structure and functions of peroxisomes

Peroxisomes, one of the last major cellular organelles to be discovered[53], are multifunctional single-membrane subcellular vesicles present in virtually all eukaryotic cells[54]. They are probably the major sites of intracellular hydrogen peroxide (H_2O_2) production[55]. Peroxisomes in different tissues vary greatly in shape and size, ranging from 0.1-0.5 μm in diameter.. Peroxisomes in most, but not all, cell types contain a dense crystalline core of more than 50 enzymes, including H_2O_2-producing flavin oxidases but no DNA or ribosomes (Figure 13)[56]. In addition to being ubiquitous, they are also highly plastic, responding rapidly to cellular or environmental cues by modifying their size, number, morphology, and function[57].

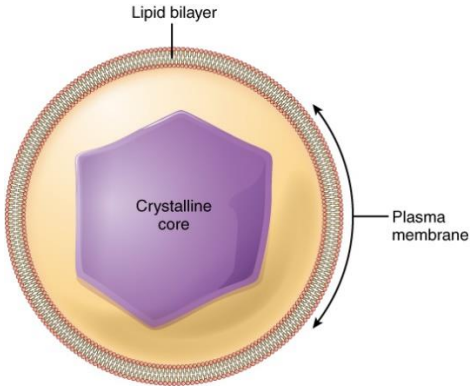

Figure 13 Structure of peroxisome.

Peroxisomes contain digestive enzymes for breaking down toxic materials in the cell and oxidative enzymes for metabolic activity, playing important roles in metabolic functions in lipid metabolism[58], metabolism of reactive oxygen species (ROS)[59], as well as some biosynthetic processes (biosynthesis of the phytohormones auxin, jasmonates and salicylates)[60]. A general characteristic of peroxisomes is that they contain as basic enzymatic constituents catalase and hydrogen peroxide (H_2O_2)-producing flavin oxidases[61]. The main metabolic functions of peroxisomes in mammalian cells, as shown in Figure 14, include β-oxidation of very long chain fatty acids (VLCFA), β-oxidation of branched chain fatty acids, synthesis of cholesterol, dolichol, bile acids and ether-linked phospholipids and removal of reactive oxygen species [56]. In plants, peroxisomes are essential for the glyoxylate cycle and photorespiration[62]. Interestingly, plant peroxisomal proteins are essential for synthesis and delivery of antifungal compounds outside the cell at the site of fungal infections[63]. The use of transcriptomic and

proteomic approaches has identified new functions for peroxisomes[64]. Table 2 shows some of the main functions that have been described so far for peroxisomes in plant cells[59].

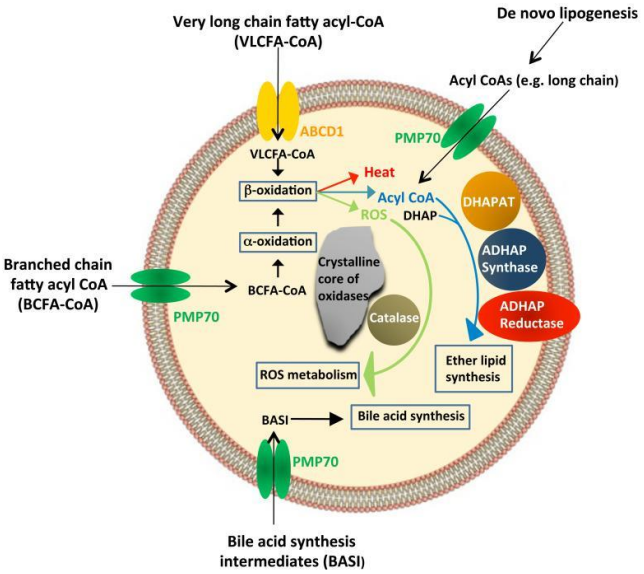

Figure 14 Structure and functions of peroxisomes in mammalian cells[56].

Table 2 Main functions reported for peroxisomes in plant cell[59].

Function
β-oxidation of fatty acids
Photorespiration
Glyoxylate cycle
Metabolism of ureides
Purine catabolism
Sulfur metabolism
Polyamine catabolism
Metabolism of reactive oxygen and Nitrogen species (ROS and RNS)
Metabolism of reactive sulfur species (RSS)
Biosynthesis of phytohormones (auxin, jasmonic acid, salicylic acid)
Photomorphogenesis
Leaf senescence
Plant defense against fungal infection
Protection against herbivores

1.2.2 Labelling of peroxisomes

There is a continuing need for bioprobes that are target-specific and combine speed of delivery with maintenance of normal cell behaviour. Most knowledge of peroxisomes has been gathered from electron microscopy, cytochemical techniques and protein characterization on isolated organelles[65]. Despite our extensive knowledge about the biochemical properties of the

peroxisome, relatively little was known about their biophysical properties and *in vivo* function until the peroxisomal targeting signal type 1 (PTS1) and type 2 (PTS2) were found[66]. These are short peptide motifs found at either the carboxy-terminal or amino-terminal (PTS1 or PTS2, respectively) of peroxisomal matrix proteins. Most peroxisomal matrix proteins carry a PTS1, which comprises a C-terminal tripeptide with the recognized sequence (C/A/S)-(K/R/H)-(L/I)-COOH[67]. The PTS2 is more complex and is located near the N-terminus with the recognized sequence (R/K)-L-X5-(Q/K)-L[68]. The majority of peroxisomal matrix proteins contain such a PTS1 and very few proteins contain an N-terminal PTS2[69]. Exploring this, a series of green fluorescent protein (GFP) fusion proteins were developed[70], through translational fusions with PTS1 or PTS2. For example, GFP-SKL fusion protein (peroxisome-specific carboxyl-terminal targeting sequence fluorescent proteins; SKL: C-terminal tripeptide, Ser-Lys-Leu) is a versatile reporter for the peroxisomal compartment, with many applications in studies involving peroxisomal import and biogenesis[71].

However, the use of GFP is limited, notably the need for ectopic expression and the potential for the relatively large size (>20 kD) of the fluorescent protein and/or the fusion to interfere with the biological role of the target molecule[72]. Therefore some fluorophores conjugated with the PTS1-peptide were developed. These peptide-based reporters combine the sensitivity of fluorescence detection with the information specificity of amino acid sequences. For instance, a BODIPY-PTS1 probe **51** containing heptapeptide (acetyl-CKGGAKL) was reported to internalize to peroxisomes of human hepatoma cells at 37 ^{o}C[65]. In another case, a nonapeptide (HLKPLQSKL)-based two-photon fluorescent probe **52**, for detecting peroxisomal $ONOO^-$ in the liver cells of mice, was constructed[73]. HLKPLQSKL amino acids serve as the peroxisome-targeting group because a peroxisomal membrane protein (PAS8p) binds to it with high affinity and transports it into peroxisomes[74].

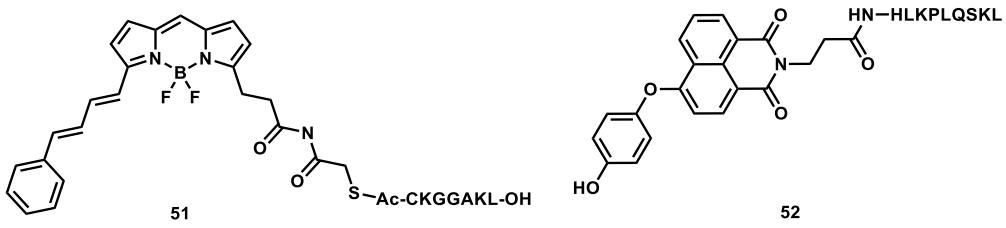

Figure 15 Peptide-based fluorescence probe 51-52.

Although the size of peptide-based fluorescence probes are much smaller than GFP probes, their molecular weight is still huge. While for small fluorophores, achieving selective localization within the cell remains a significant challenge. Consequently, there is a continuing

need for small probes of cellular function that combine ease of preparation and membrane permeability with precise cellular localization. In this context, a small nitro-BODIPY probe **53** (developed by our group) selectively identifies peroxisomes in plant cells, as verified by co-localization with an SKL-FP construct[72, 75]. This simple dye exhibits specific co-localization with a fluorescent protein fused to SKL (PTS1) that is known to label the peroxisome in plants. More details about this probe will be discussed in Section 2.

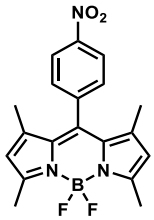

53

Figure 16 Nitro-BODIPY probe 53 for plant peroxisome.

1.3 Photoaffinity labelling

1.3.1 Design and process of photoaffinity labelling

First introduced in the early 1960s[76], photoaffinity labelling (PAL) has a longstanding history as a valuable biochemical technique in target identification, revolutionizing research in the life sciences. In recent years various kinds of possible interactions have been targeted successfully, such as protein-ligand (drug, inhibitor), protein-protein, protein-nucleic acid; and protein-cofactor[77]. The process of photoaffinity labelling has evolved over the past decade principally due to its coupling with bioorthogonal/click chemistry reactions. As shown in Figure 17, a targeting ligand is covalently modified with a photoaffinity groups (PRG) that can be irradiated with UV light (hv) upon reversible or irreversible complexation with a biological target. Under photoirradiation, PRG groups decompose to a highly reactive intermediate, typically a nitrene, carbene, or diradical, which undergo insertion reactions to bind the ligand to its target macromolecules[78-79]. In order to detect the targeted proteins, this usually requires labelling with a fluorophore or another entity to make the conjugates conspicuous[79]. However, fluorophores incorporated before the photodecomposition step can impact binding of the targeting ligand to the protein. The nature of most reporter tags and the commonly used linker chains generally makes photoaffinity probes large and cell impermeable. Even without fluorophores, addition of PRG-groups to targeting ligands can also impact how they bind proteins[80]. It is often advantageous to click chemistry[81] to couple the fluorophore after photodecomposition so that fluorophore-protein interactions have no impact on the recognition or coupling step, but after click the covalent conjugates can be readily detected. After covalent modification the desired protein can be ideally detected and is then usually purified by chromatography and characterized using spectroscopic methods.

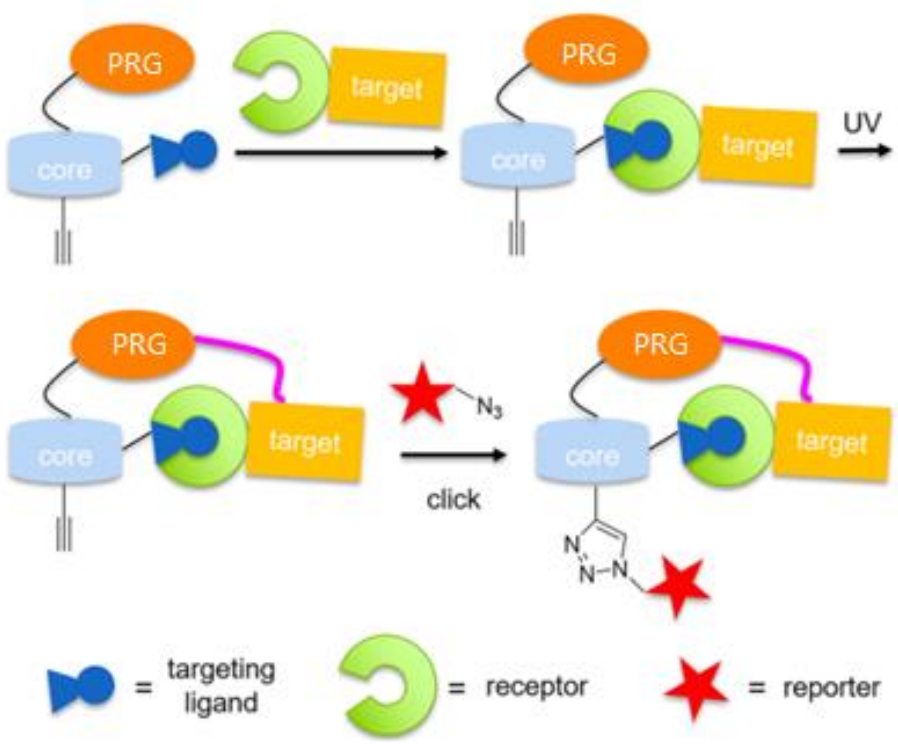

Figure 17 Typical process of PAL [78].

1.3.2 Photoaffinity groups and reporter tags

Three major types of PRGs are commonly used in PAL: benzophenones, arylazides and aryldiazirines (Figure 18), where the reactive intermediates formed on irradiation with specifc wavelengths of light are a diradical, a nitrene and a carbene, respectively[82]. Benzophenones form a reactive triplet diradical when irradiated with light and are activated by a long wavelength (350-360 nm), which lowers the risk of damaging biomolecules. The disadvantages of benzophenones include nonspecifc labelling[83] with the bulky group affecting the interaction between the affnity agent and the target protein[84]. In contrast to benzophenones, azides require shorter wavelengths (250-350 nm) to excite which can cause damage to biological molecules and decrease photoaffinity yields[85]. This may also reflect the fact that nitrenes are less reactive than carbenes. Nitrenes can also rearrange to form benzazirines and dehydroazepines/ ketenimines as undesired side products[86]. Substituted arylazides such as tetrafluorophenylazide have been developed and are reported to prevent rearrangement of nitrenes to ketenimines. Aryldiazirines are the most commonly used photoaffinity group, particularly the trifluoromethyl derivative, which is favored due to its excellent chemical stability. They require a high wavelength (350-380 nm) to be activated which reduces the potential damage to biological molecules. The carbene intermediate is extremely reactive and has a short half-life,

which is beneficial as it rapidly forms covalent cross-links to biomolecules. However, due to this high reactivity, the carbene is often quickly quenched by water.

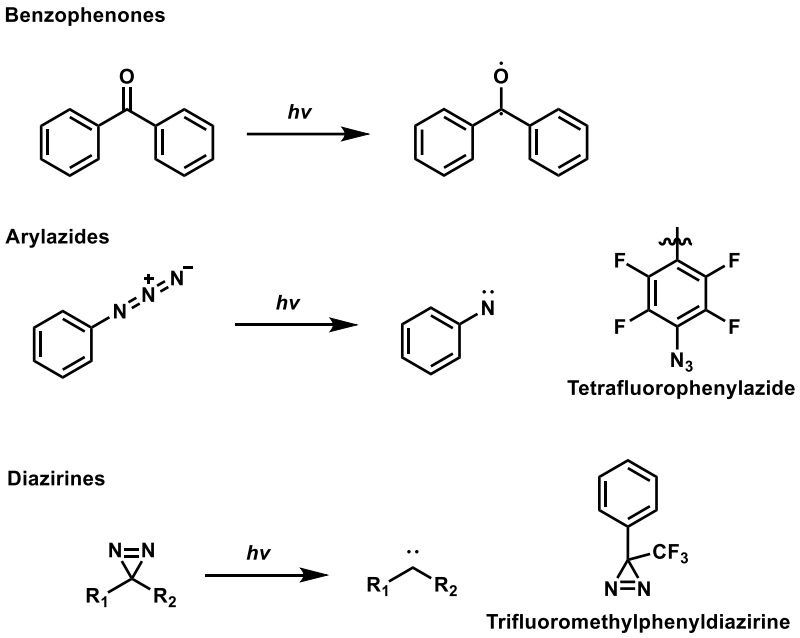

Figure 18 Types of PRGs.

In order to ascertain and facilitate the isolation of photolabeled products, reporter groups such as radioactive isotopes (^{125}I, ^{3}H), biotin, epitope tags (FLAG peptide), or fluorophores are often directly incorporated into the structure of the photoprobe. Radiolabels are preferentially used for profiling known targets because they cannot provide a direct means to isolate labeled proteins from the rest of the proteome[82]. Biotin, epitope tags, and fluorophores allow easy enrichment, isolation, and/or detection of photolabeled products, but they can be relatively large in size, cell impermeable, and may negatively affect biological activity by sterically disrupting key interactions between the biological target and the photoprobe[79].

2 MAIN OBJECTIVE

2.1 Preliminary work in the group

Previous work in the our group generated a small set of BODIPY fluorophores[72], including one, nitro-BODIPY **53** (1,3,5,7-tetramethyl-8-(4-Nitrophenyl)-BODIPY, Figure 19), that is intrinsically non-fluorescent but fluorescent but upon incubation of cells with this compound, fluorescence is observed at the target site. The target site in plant cells was identified as peroxisomes, as verified by co-localization with an SKL-FP construct (peroxisome-specific carboxyl-terminal targeting sequence fluorescent proteins). Interestingly, in mammalian cells, whilst discrete punctae could be seen, indicative of a discrete localisation event, co-localization with the mammalian peroxisomal marker SelectFXTM was not observed. These data suggest fundamental differences in peroxisome composition, development or function between plant and animal cells. Using the nitro-BODIPY probe, which, in vivo, fluoresces selectively inside peroxisomes enabled a simple technique for quantifying peroxisome abundance[75]. The physiological relevance of this technique was demonstrated using salinity as a known inducer of peroxisome proliferation. While significant peroxisome proliferation was observed in wildtype Arabidopsis leaves following 5-hour exposure to NaCl, no proliferation was detected in the salt susceptible mutants fry1-6, sos1-14, and sos1-15. It was also found that nitro-BODIPY detects aggregation of peroxisomes during final stages of programmed cell death and can be used as a marker of this stage. It was also found that fluorescence of nitro-BODIPY is specifically activated not only in peroxisomes of living cells but also in total protein extracts. This technique enables quantification of peroxisomes in plant material at various physiological settings with potential applications including the identification of genes controlling peroxisome homeostasis and capturing stress-tolerant genotypes.

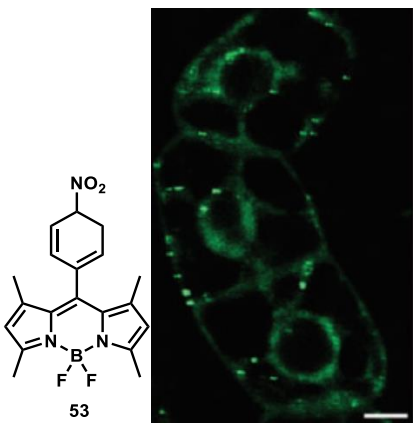

Figure 19 Nitro-BODIPY probe 53 and its localisation at plant peroxisomes.

2.2 Project plan

Based on these preliminary studies nitro-BODIPY **53** exhibited a specific localisation process and it is key to future applications to be able to understand how this is occurring at a molecular level. As indicated above these objectives are challenged by a lack of knowledge of its protein target and the physicochemical profile of nitro-BODIPY. This leads to the specific aims of this project which are: 1. To develop a 'toolbox' of analogues that enable multicolour visualisation. 2. To confirm the nature of the binding process between nitro-BODIPY and the target protein and to determine its reversibility. 3. To identify the target protein of nitro-BODIPY in plant peroxisomes.

The key points to be addressed are how the bioprobe localises and the specific structure of the target protein. Exploiting the modular nature of BODIPY synthesis, this will be achieved by preparing modified BODIPY probes conjugated to a photoaffinity labelling agent. Application of these modified probes will lead to a fluorescently tagged target protein that can be isolated and identified by gel electrophoresis coupled with MS proteomics. Importantly, these photoaffinity agents all have absorption energies at wavelengths considerably different from those observed for the BODIPY core. It is of interest to generate a toolbox of probes to provide a range of emission frequencies enabling multicolour analyses to allow the use of these probes with other markers e.g. the various fluorescent proteins in routine use. This will be achieved by simple variation of the substituents around the fluorophore core. Importantly, for such an approach, the synthesis of BODIPY probes is highly modular.

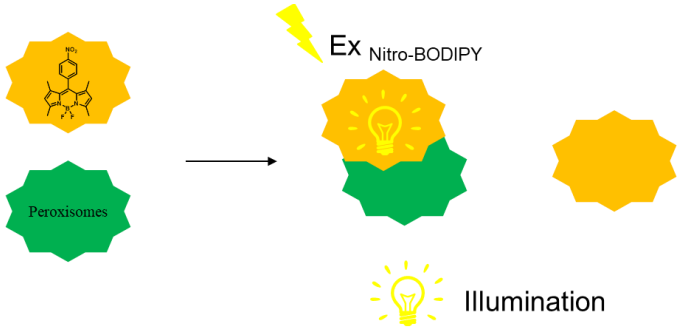

Figure 20 Nitro-BODIPY 's localization at plant peroxisomes.

The process of nitro-BODIPY's localization at plant peroxisomes is shown in Fig 20. On radiation of excitation wavelength for nitro-BODIPY (508 nm), the probe bound to peroxisome will illuminate at 528 nm while the rest probe outside of peroxisomes will be silent. The

complexing of peroxisome restrains the quenching process of nitro-BODIPY and enables the probe to emit fluorescence. Based on direct observation, quenched nitro-BODIPY cannot be found, which poses a challenge for determining whether the probe localizes on peroxisomes exclusively or not.

In order to explore nitro-BODIPY's physiological behaviours outside of peroxisomes, two sets of dual-fluorophore probes were designed. The first set of probes are assembled by nitro-BODIPY structure coupled to a fluorophor (Rodamine B, Cy 5 etc) whose excitation/emission wavelength is more red-shifted than nitro-BODIPY. In parallel, the second set of probe is assembled with the second fluorophor such as NBD (4-chloro-7-nitrobenzofurazan) and Dansyl (5-(dimethylamino)naphthalene-1-sulfonyl chloride) whose excitation/emission wavelength is more blue-shifted than nitro-BODIPY. For a molecule containing two different fluorophores, Förster resonance energy transfer (FRET) processes sometimes happen. Depending on whether FRET happens, these two sets of dual-fluorophore probes will exhibit different visual results.

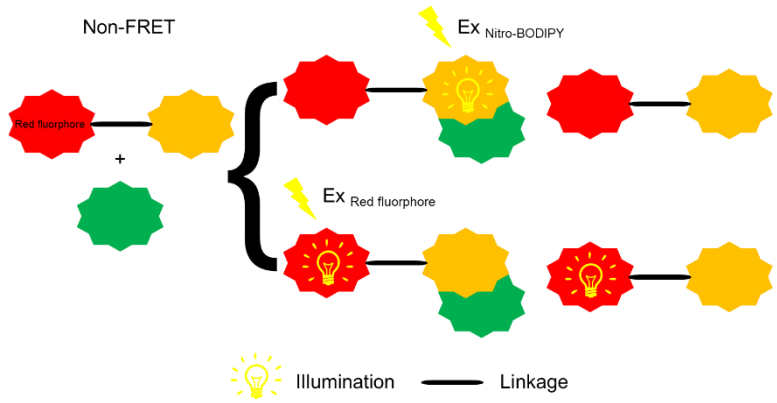

Figure 21 Non-FRET red-shifted fluorophore-nitro-BODIPY probes' localization at plant peroxisomes.

For the first set of probes, in the absence of FRET, the hypothetic visual results are shown in Fig 21. For peroxisome bound probe, on excitation of the nitro-BODIPY, the nitro-BODIPY moiety will emit and the red-shifted fluorophor part will be silent. In contrast probes outside of peroxisomes will be silent. On excitation of the 'red-shifted' fluorophor, the nitro-BODIPY component of a peroxisomal localised probe will be silent and emission for the red-shifted fluorophore will be observed for both peroxisomal bound and free probe.

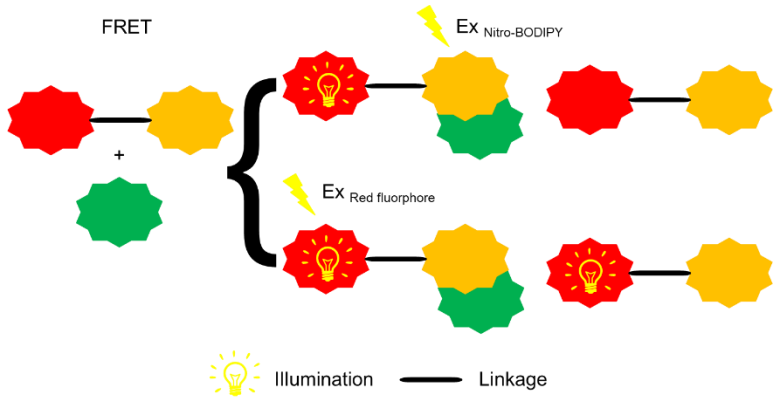

Figure 22 FRET red-shifted fluorophore-nitro-BODIPY probes' localization at plant peroxisomes.

If FRET happens, the hypothetic visual results is shown in Fig 22. On excitation of the nitro-BODIPY, the nitro-BODIPY unit of a peroxisome bound probe will be excited and FRET to the red-shifted fluorophor will occur. Meanwhile probes outside of peroxisomes will remain silent. On the excitation of the red-shifted fluorophor, both bound and unbound probes will show the emission of red-shifted fluorophor.

In consideration of the non-ideal results of red-shifted fluorophor-nitro-BODIPY probes in plant imaging experiments, we could shift the way of molecular assembly which combines nitro-BODIPY with another 'blue-shift' fluorophor (Dansyl, NBD etc) whose excitation/emission wavelength is more blue-shifted than nitro-BODIPY.

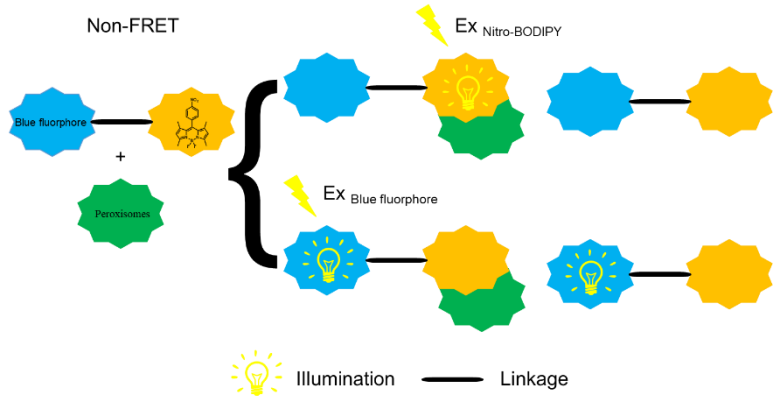

Figure 23 Non-FRET blue-shift fluorophore-nitro-BODIPY probes' localization at plant peroxisomes.

For the non-FRET Blue-shift fluorophor-nitro-BODIPY probes, the hypothetic visual result is shown in Fig 23. On excitation of nitro-BODIPY's wavelength, the nitro-BODIPY unit bound with peroxisomes will illuminate whilst the blue-shift fluorophor part will be silent. Meanwhile

unbound probes outside of peroxisomes will be silent. On excitation of blue-shift fluorophor's wavelength, the bound nitro-BODIPY part will be silent and all the probes will illuminate the fluorescence of blue-shift fluorophor and show a fluorescent background.

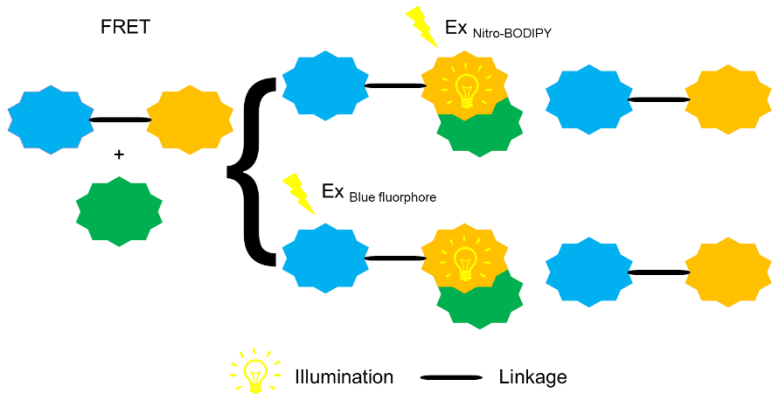

Figure 24 FRET blue-shift fluorophore-nitro-BODIPY probes' localization at plant peroxisomes.

If FRET occurs, the hypothetic visual results is shown in Fig 24. On excitation of blue-shift fluorophor, the blue-shift fluorophor part of a peroxisome bound probe will be excited and FRET to the nitro-BODIPY will occur. Meanwhile probes outside of peroxisomes will remain silent. On the excitation of the nitro-BODIPY, the nitro-BODIPY part of a peroxisome bound probe will illuminate and unbinded probes outside of peroxisomes will be silent.

3 RESULTS

3.1 Synthesis of nitro-BODIPY analogues and probes

As discussed before (Section 2.1), the nitro-BODIPY **53** (1,3,5,7-tetramethyl-8-(4-nitrophenyl)-BODIPY) was observed to localise in the peroxisome of plant cells and become emissive[72]. It was of interest to determine whether this reflected a specific localisation of the nitro-BODIPY and to identify the molecular basis for this localisation. The molecular basis for binding could be explored by developing an analogue of nitro-BODIPY probes conjugated to a photoaffinity agent (e.g. benzophenone, arylazide or aryldiazirine) to identify the target protein of nitro-BODIPY and a purification tag (reporter tag, e.g. biotin) to aid isolation. It is possible that nitro-BODIPY localizes at multiple points but that it can only be observed in the peroxisome because of fluorescence quenching elsewhere. To address this, it was proposed that a dual Nitro-BODIPY with second fluorophore conjugated probe could be used to determine whether Nitro-BODIPY only localizes at peroxisome or somewhere else.

3.1.1 Synthesis of pyrrole precursors and nitro-BODIPY analogues

One aim of the project was to couple the nitro-BODIPY unit with a reporter group, either a photoaffinity label or a second fluorophore. In order to avoid interfering with BODIPY-target protein engagement, this would need to be separated from the BODIPY by a linker/ spacer unit. Consequently, the initial objective of the synthetic work was to introduce a linker group into the nitro-BODIPY structure that does not affect its localisation.

The most direct route to introduce a linker group appeared to be the introduction of suitable functional groups onto a preformed nitro-BODIPY. Two potential options were either halogenation followed by Suzuki Miyaura cross coupling[87-88] or formylation followed by reductive amination[89]. Significantly, precedents exist for both of these transformations (Scheme 12). In order to explore these options, an efficient route to the parent nitro-BODIPY was required. Consequently this became the first objective.

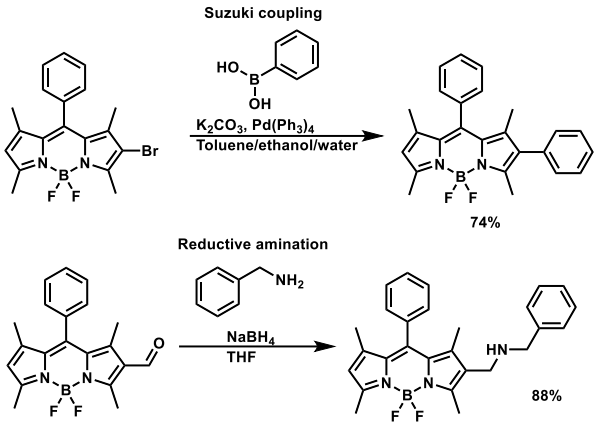

Scheme 12 Precedents of Suzuki Miyaura cross coupling and reductive amination of BODIPY.

Many procedures have been reported for the synthesis of 4-aryl-BODIPYs. The easiest way is a one-pot reaction[90-91] involving condensation of 2,4-dimethypyrrole and 4-nitrobenzaldehyde in the presence of TFA followed by treatment with TEA and $BF_3{\cdot}Et_2O$. However, all attempts to reproduce this were challenged by the aggressive conditions which led to low yields. In order to improve the yields, alternative stepwise approaches (Scheme 13) were explored involving initial formation of 2-pyrroleketone **S1** derivatives[22]. Following this strategy, reaction of magnesiated 2,4-dimethyl-1H-pyrrole with 4-Nitrobenzoyl chloride afforded ketopyrrole **S1** (64 % yield) as evidenced by a C=O signal at δ= 182.7 in ^{13}C-NMR spectrum. Subsequently in a second step, this was then condensed with 2,4-dimethyl-1H-pyrrole in the presence of $POCl_3$ before complexation with base and $BF_3{\cdot}Et_2O$ to give nitro-BODIPY (**S2**, 32 % yield) as evidenced by a peak in the LCMS spectrum of m/z of 370.2 $[M+H]^+$. Milder reaction conditions[92], replacing the $POCl_3$ with $BF_3{\cdot}Et_2O$ and carrying out the reaction at room temperature, led to a higher yield of nitro-BODIPY (**S2**, 60 % yield).

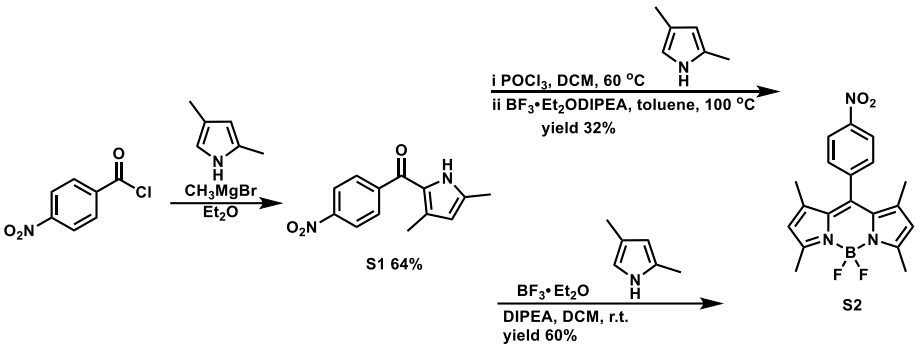

Scheme 13 Synthesis of nitro-BODIPY S2.

Having established an efficient route to the nitro-BODIPY, attention turned to the selective functionalisation. As discussed above, halogenation was considered a practical way to modify

the BODIPY framework. Consequently, selective brominations on nitro-BODIPY **S2** were then attempted. Following reported procedures[28], the dibrominated product **S3** (Scheme 14) was prepared selectively on treatment with $CuBr_2$ and oxygen (yield 34%) as evidenced by the disappearance of a 2-H signal at δ= 6.0 in ^{1}H-NMR spectrum. Alternatively, in the presence of K_2CO_3 and $CuBr_2$, the monobrominated product **S4** was obtained in a yield of 18% as evidenced by signals of 447.3 (^{79}Br) and 449.4 (^{81}Br) $[M+H]^+$ in LCMS. However, this second reaction was complicated by both low conversion and the competing formation of the dibrominated product **S3**. Consequently, it was very hard to isolate pure nitro-BODIPY **S4**. With these difficulties and given that similar selectivity issues had been reported for formylation of BODIPYs[93], attempts to directly funtionalise the BODIPY core were abandoned and attention turned to introducing the linker into a BODIPY precursor.

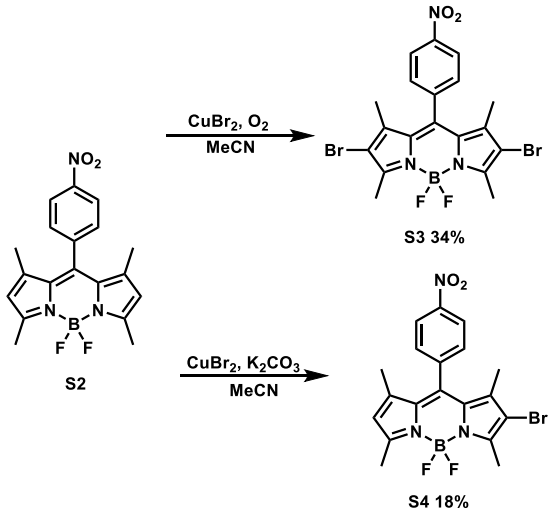

Scheme 14 Brominations of nitro-BODIPY.

For this approach it was envisaged that an ester group would enable a number of linker coupling strategies. For example, the ester could be hydrolysed to an acid which is easy to condense with amines or alternatively reduced to terminal alcohols to enable etherification (Scheme 15).

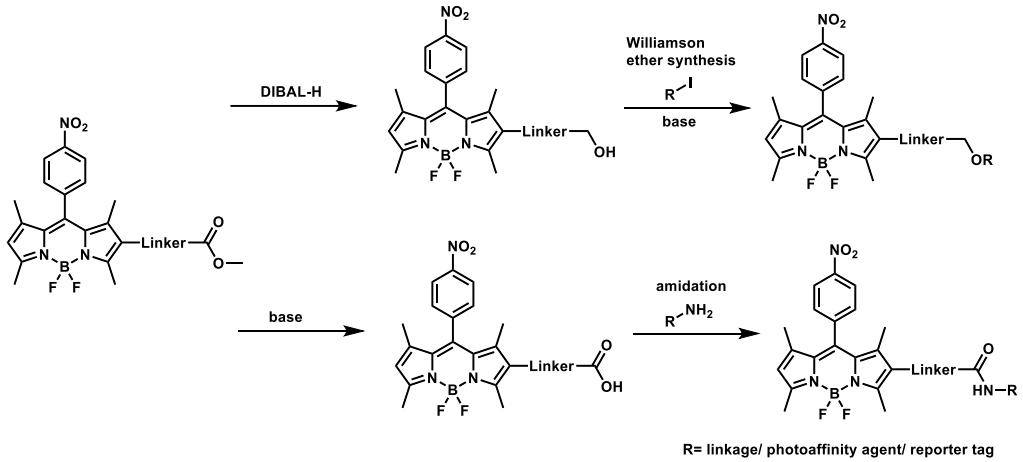

Scheme 15 Strategies to attach a linker on nitro-BODIPY.

With this strategy the first goal was the preparation of suitable pyrrole-esters. A survey of the literature revealed that these pyrroles could be prepared via a Knorr pyrrole synthesis. Following this reported procedure[94], tert-butyl acetoacetate was treated with $NaNO_2$, zinc and AcOH then a condensation with ethyl acetoacetate gave pyrrole **S5** in a moderate yield of 48% (Scheme 16) as evidenced by the appearance of two C=O signals at δ= 165.6 and 161.1 in ^{13}C-NMR spectrum. Subsequently, pyrrole **S5** was treated with HCl leading to the selective decarboxylation of the tert-butyl ester to give the required pyrrole **S6** in a yield of 70% as supported by the disappearence of one C=O signal at δ= 161.1 in ^{13}C-NMR spectrum, and appearance of a α-H signal at δ= 6.38 in the ^{1}H-NMR spectrum. Then following the same procedure as used for **S2**, pyrrole **S6** was condensed with ketopyrrole **S1** in the presence of $POCl_3$ before complexation with base and $BF_3{\cdot}Et_2O$ to give the unsymmetrically substituted nitro-BODIPY-ester **S7** in a yield of 27%.

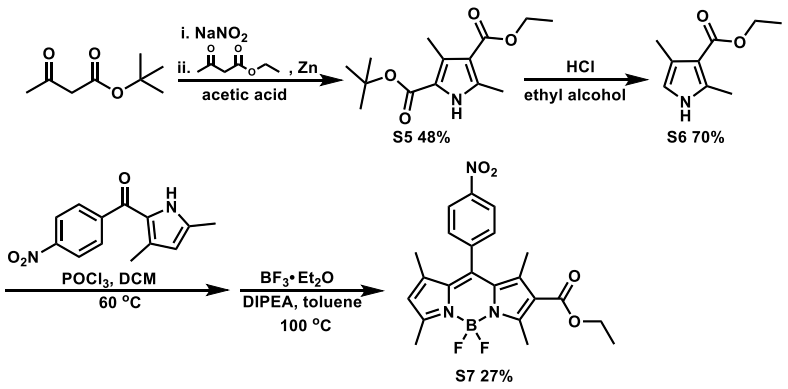

Scheme 16 Synthesis of nitro-BODIPY-ester S7.

Reflecting the fact that the length of the linker could affect the binding between probe and target protein, as shown in Scheme 17, pyrrole **S9** with a longer chain was then synthesised in

a similar route to **S6**. As neither hydrochloric acid and trifluoroacetic acid were effective in promoting the decarboxylation of the α-ethyl carboxylate in pyrrole **S8**, phosphoric acid was used as both the catalyst and the solvent for this reaction[95]. Although the preparation of pyrrole-ester **S9** was achieved, as evidenced by one C-H singlet signal at δ= 6.4 in ^{1}H-NMR spectrum, partial hydrolysis of the propionyl ester occurred which led to a lower yield and complicated purification.

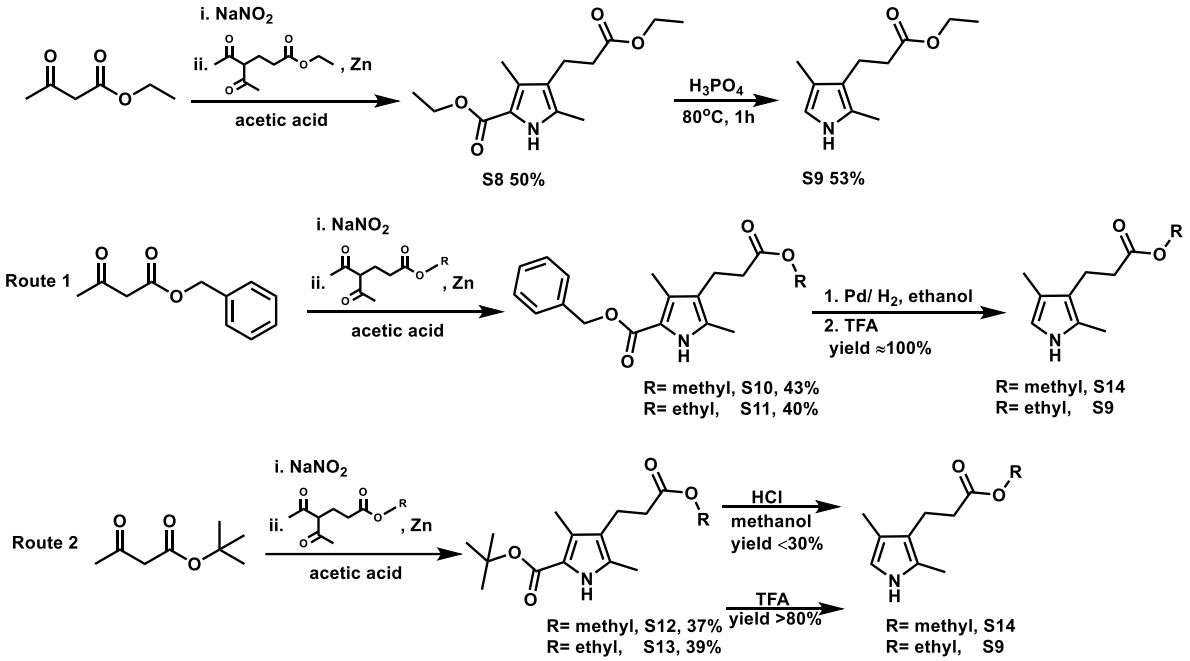

Scheme 17 Synthesis of pyrrole-esters.

In order to achieve a better yield of pyrrole **S9**, two different routes were developed to provide milder selective α-ester hydrolysis steps (Scheme 17). α-Benzyl carboxylate pyrrole **S10-11** and α- tert-butyl carboxylate pyrrole **S12-13** were synthesised through analogous Knorr pyrrole synthesis. For decarboxylation of tert-butyl analogues **S12-13** (Route 2), either hydrochloric acid or trifluoroacetic acid could be used, with the latter giving better yields (> 80%). However, even better yields could be obtained following route 1 in which hydrogenolysis (using Pd/C and hydrogen) of α-benzyl carboxylate pyrrole **S10-11** efficiently gave pyrrolecarboxylic acid which on the treatment with trifluoroacetic acid (Route 1) gave the pyrrole-ester **S9** and **S14** in excellent crude yield (≈100%). For reasons that were not obvious, these trialkyl pyrrole derivatives exhibited some instability and were prone to decomposition on storage.

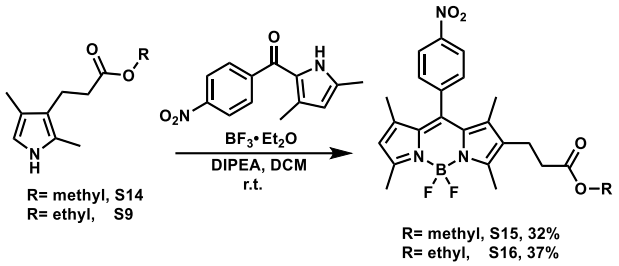

Scheme 18 Synthesis of nitro-BODIPY-esters.

Having developed an efficient route to pyrrole-esters **S9** and **S14**, the next stage was to synthesis the corresponding nitro-BODIPYs with a terminal ester. As shown in Scheme 18, following the previously established procedure, nitro-BODIPY-esters **S15** and **S16** were then prepared in 32% and 37% yield. The lower yields when compared to **S2** could be attributed to the lower stablity of pyrrole precursor **S14** and **S9**.

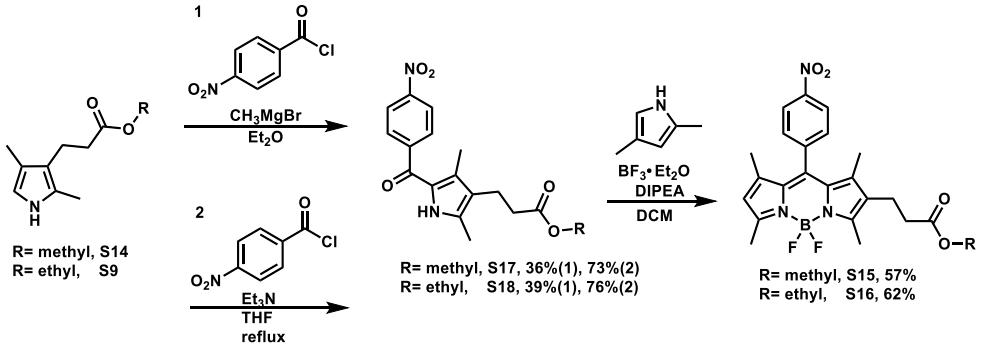

Scheme 19 Synthesis of nitro-BODIPY-esters.

To enhance the yield of BODIPY synthesis, the order of the synthesis was changed. In the first step, analogues of ketopyrrole ester **S17** and **S18** were synthesised first from **S9** and **S14**. These intermediates could then be converted, on reaction with 2,4-dimethyl pyrrole, into the desired nitro-BODIPY-esters **S15** and **S16** in better yields.

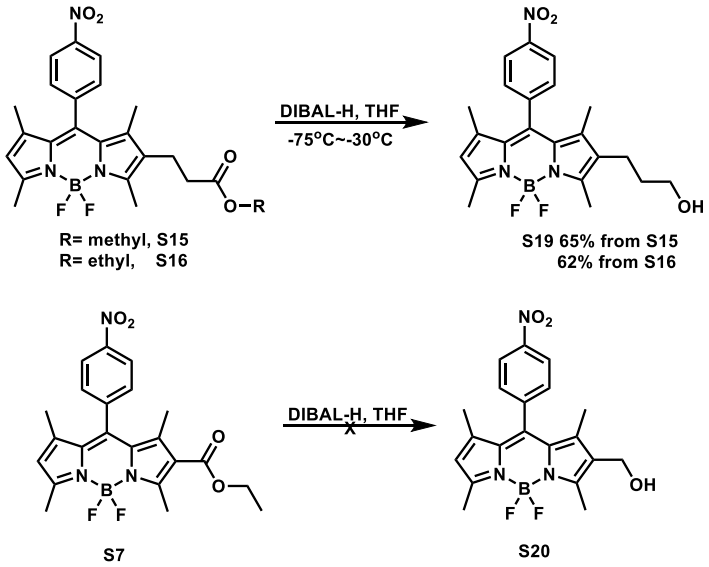

Scheme 20 Reduction of nitro-BODIPY-esters.

With nitro-BODIPY-esters **S7**, **S15** and **S16** prepared, the next goal was to attatch the second fluorophore. The first approach considered that this could be achieved by a click reaction of a fluorophore azide with a bodipy-alkyne. This required conversion of the ester linker moiety into a terminal alkyne. With this in mind, two routes were designed to extend the terminal ester on BODIPYs to a longer chain containing a terminal alkyne. The first route was based on etherification (Scheme 20). Consequently, the nitro-BODIPY-esters were reduced to the corresponding alcohol **S19** and **S20**. In order to avoid the reduction of the nitro group, DIBAL-H was chosen as the reductant because it is milder than $LiAlH_4$ or $NaBH_4$. Initially, DIBAL-H (> 2 equivalents) was added at -75 ^oC to reduce the ester to aldehyde before raising the reaction temperature to 0 ^oC or room temperature to complete the reduction from aldehyde to alcohol. Unexpectedly, the BODIPY framwork proved very fragile to DIBAL-H if the reaction temperature rose above -20 ^oC. Subsequently, it was found that maintaining the temperature below -30 ^oC gave alcohol **S19** in an acceptable yield as evidenced by disappearance of a C=O signal at δ=172.0 in ^{13}C-NMR spectrum. Unfortunately, all attempt to reduce pyrrole-ester **S7** failed with no reaction being observed below -30 ˚C and extensive decomposition being seen at -20 ˚C. This possibly reflected the steric hindrance of the aromatic ester which blocks the attack from DIBAL-H.

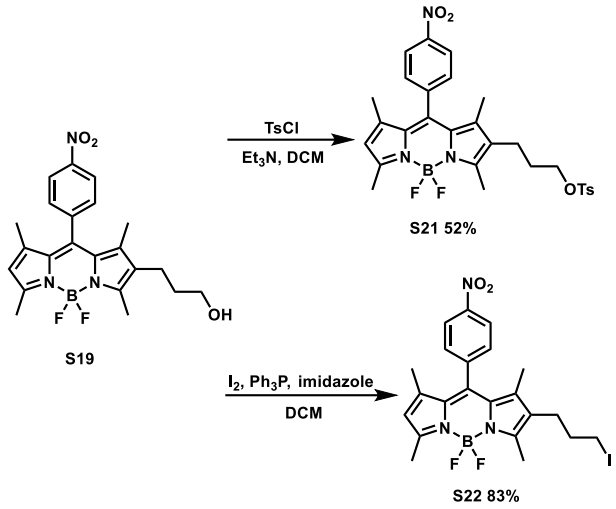

Scheme 21 Tosylation and iodination of nitro-BODIPY-alcohol.

Tosylate and iodide are appropriate leaving groups for etherification. Consequently, following the reported method[96], as shown in Scheme 21, a base-catalysed esterification between nitro-BODIPY-alcohol **S19** and 4-toluenesulfonyl chloride generated nitro-BODIPY-OTs **S21** effectively in a yield of 52% as evidenced by a methyl singlet signal at δ=2.46 in ^{1}H-NMR spectrum. In the second reaction, following the reported procedure[97], the hydroxyl group was transformed into the iodide by reaction with iodine in the precence of PPh_3 and imidazole to achieve nitro-BODIPY-I S22 in a yield of 83%.

With tosyl ester **S21** and iodide **S22** in hand, etherification was attempted following the reported procedure[98], using NaH as the base (Scheme 22). Disappointingly, neither the starting material nor the product could be found in the reaction mixture by LCMS. Weaker bases, NaOH and K_2CO_3, were then tried, however only starting materials could be observed. In conclusion, this route to synthesis an ether link on nitro-BODIPY failed because of the unexpected decomposition of nitro-BODIPY structure.

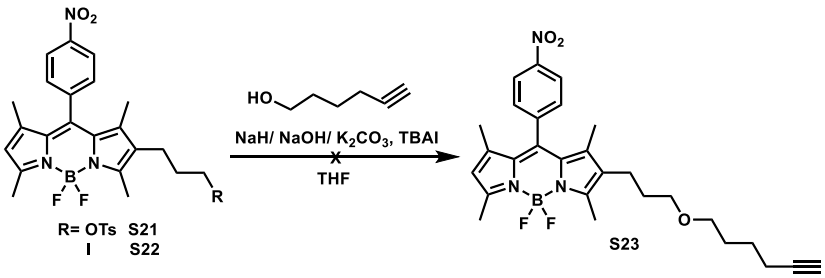

Scheme 22 Etherification of nitro-BODIPYs.

Given the difficulties in synthesizing the ether link on nitro-BODIPY, it was decided to attempt etherification on the pyrrole precursors. In consideration of the high reactivity of pyrroles and

the harsh conditions of etherification (using NaH as the base), it was proposed that pyrrole **S12** could be protected using a Boc group. As DIBAL-H could potentially reduce N-Boc or tert-butoxy carbonyl, two Boc-protected pyrroles **S24** and **S25** were synthesised to explore the selectivity of DIBAL-H reduction (Scheme 23).

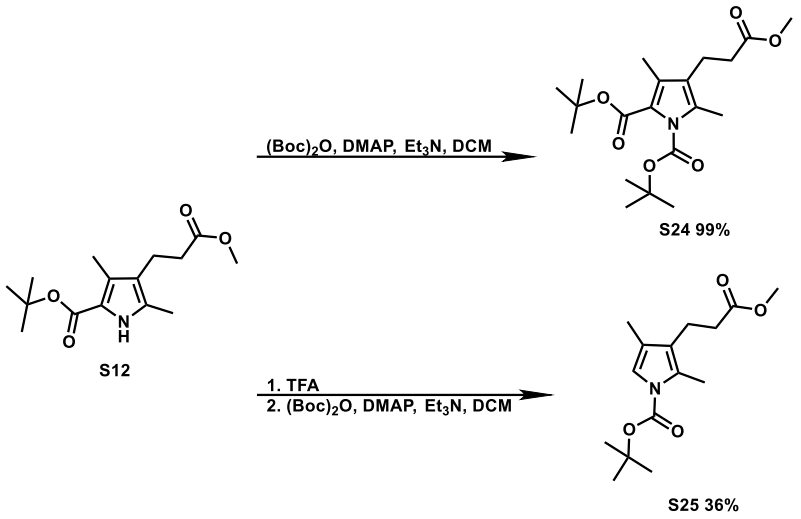

Scheme 23 Boc-protection of pyrroles.

As shown in Scheme 24, following the same procedures for DIBAL-H reduction and iodination as described above, pyrrole-alcohol intermediates **S26**-**28** and pyrrole-iodide intermediates **S29**-**31** were obtained in good yields. Pleasingly as anticipated, DIBAL-H selectively reduced the less hindered 3-methoxy-oxopropyl group leaving both N-Boc and t-Butoxy carbonyl groups unreduced. Compared with the other analogues, the yields of Pyrrole **S27** and **S31** were lower, reflecting the lower stability of the α-H pyrroles.

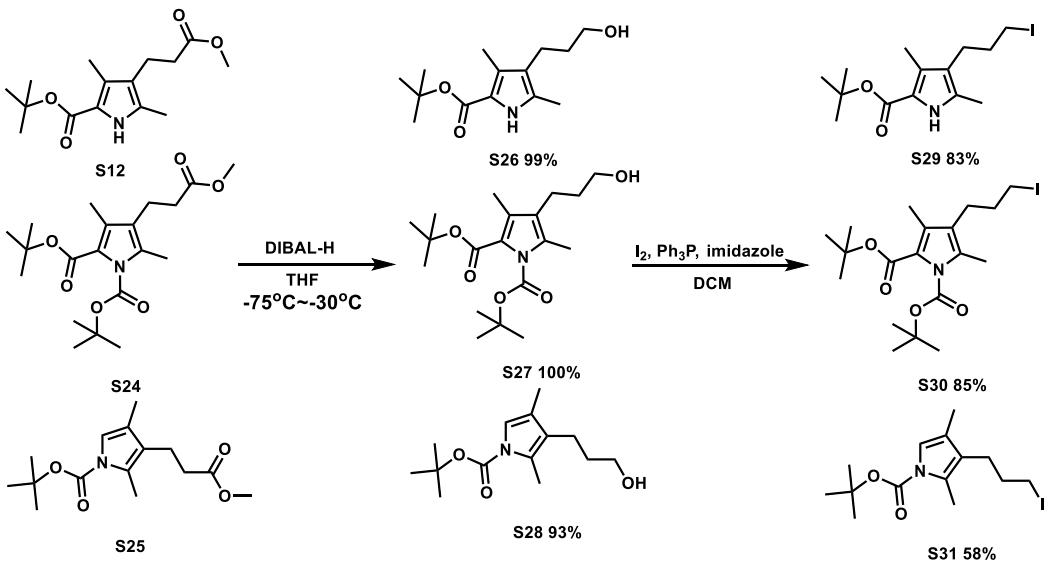

Scheme 24 Selective reduction on pyrrole-esters and iodination of pyrrole-alcohols.

Having successfully obtained pyrrole-iodide intermediates **S29-31**, the next step was etherification. As shown in Scheme 25, the products **S32-34** formed in the three respective reactions could be detected by LCMS (peaks of 334.5, 434.5, 334.5 respectively) but the signals were very weak. Moreover, many spots were observed by TLC which indicated these reactions were unselective and impractical to purify. As with the nitro-BODIPY analogues **S21** and **S22**, the pyrrole analogues were not stable under strongly basic conditions. As a result, the etherification route to pyrrole-ether precursors for BODIPY was abandoned.

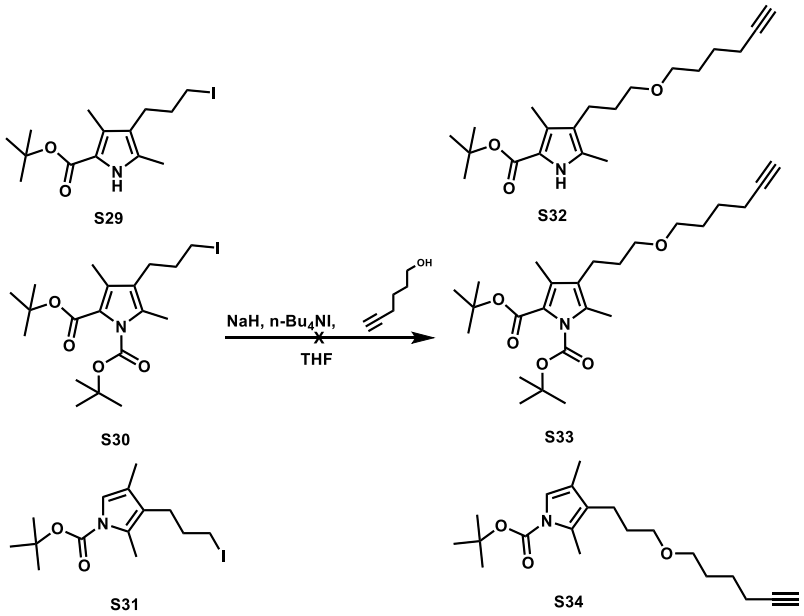

Scheme 25 Etherification of pyrrole-iodides.

Given the challenge to prepare BODIPY-ether intermediates via etherification, attention switched to the second route for amide synthesis. As the BODIPY framework was fragile and readily decomposed under strongly basic conditions, it was important to find mild and efficient conditions. As shown in Scheme 26, following the reported procedure[99], nitro-BODIPY **S15** and **S16** could be hydrolysed successfully with only a small portion of decomposed byproducts as evidenced by a carboxyl singlet signal at δ=12.18 in ^{1}H-NMR spectrum. However, under the same conditions, the hydrolysis of nitro-BODIPY-ester **S7** failed, giving unchanged starting materials. With the nitro-BODIPY acid **S36** in hand, following the reported procedure[100], the nitro-BODIPYs with terminal alkyne **S38** and with terminal azide **S39** could be accessed via amidation in high yield as evidenced by N-H's signals at δ=5.44/ 5.64 in ^{1}H-NMR spectrum.

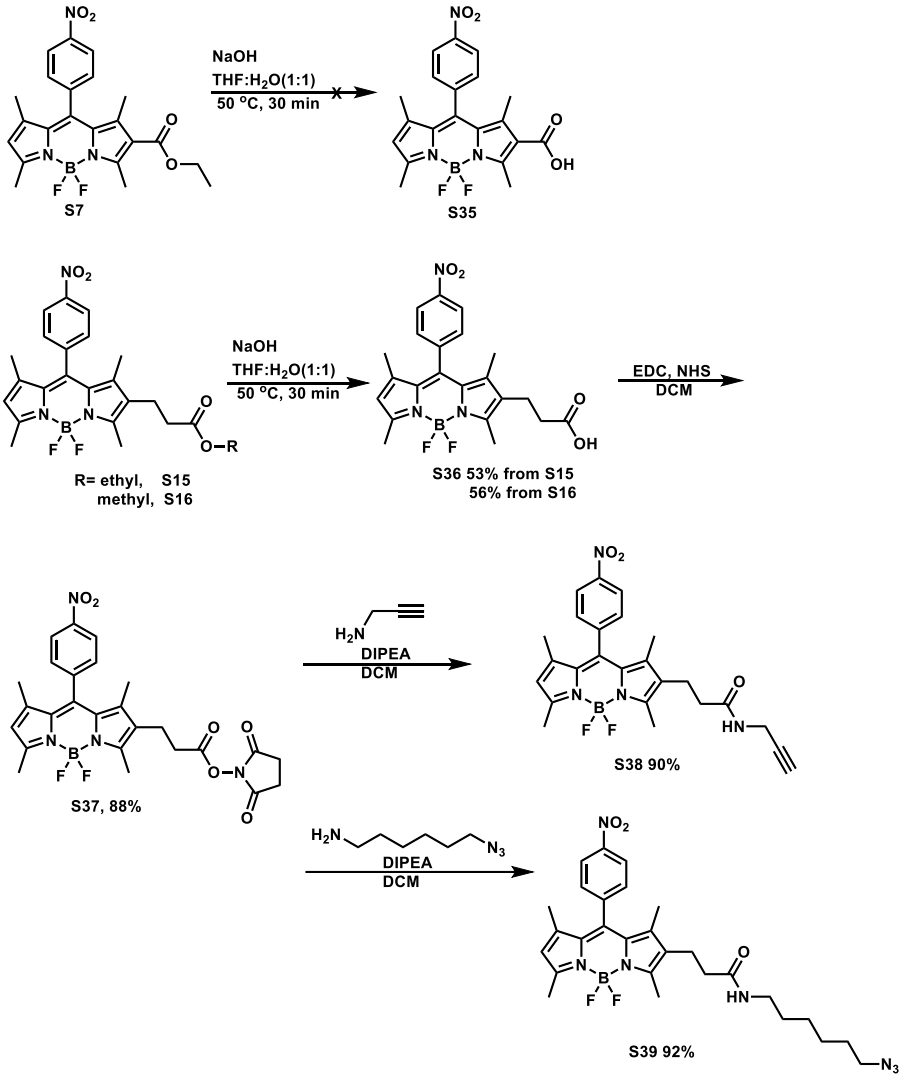

Scheme 26 Synthesis of nitro-BODIPYs with terminal alkyne or azide.

Although azide and alkyne linked BODIPYs **S38-39** could be prepared, it was still of interest to synthesis a conjugated BODIPY amide as it was hypothesised that this might lead to a red shift for BODIPY structure. As shown in Scheme 27, a route was designed to synthesis nitro-BODIPY **S45** via initial coupling of a pyrrole with a terminal alkyne. Following the Knorr pyrrole synthesis used above **S43** could be obtained in a 4 step sequence. Coupling with 4-nitrobenzoyl chloride in the presence of Et_3N failed, whilst reaction with MeMgBr successfully led to ketone **S44** in a yield of 35%. However, the subsequent reaction with 2,4-dimethyl-1H-pyrrole failed under all conditions with MS analysis showing that most starting material remained unchanged. With this disappointing results, all attempts to prepare **S45** were abandoned.

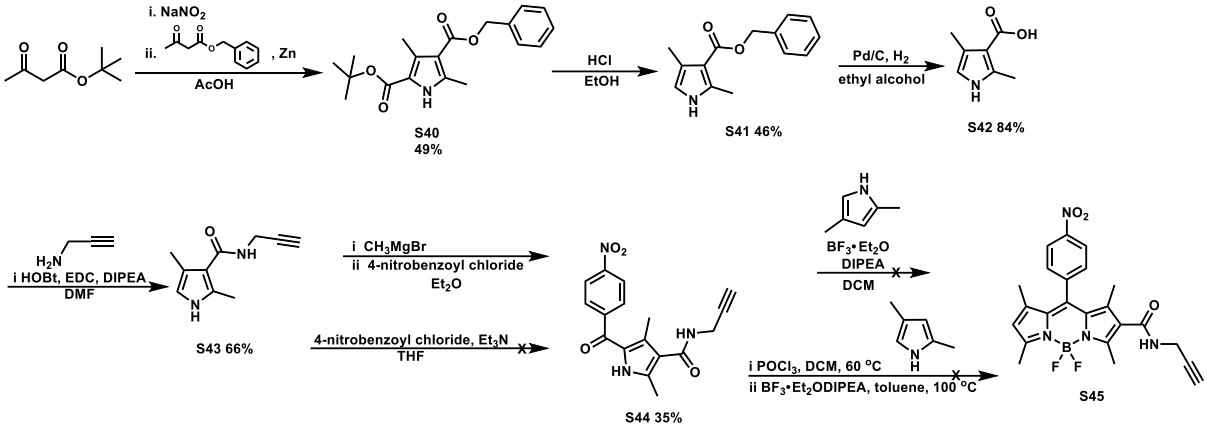

Scheme 27 Synthesis of nitro-BODIPYs with terminal alkyne.

It was of interest to move nitro-BODIPY's emission wavelength towards the red end of the spectrum to satisfy its further applications on plant materials. Consequently, modifications to the nitro-BODIPY framework, which could expand its conjugation and lead to red-shifted emission, were explored. The methyl (C-3 and C-7 groups) on a 1,3,5,7-tetramethyl BODIPY have been shown to undergo a condensation reaction with aldehydes via catalysis with piperidine and AcOH under reflux[101] or microwave[102](Scheme 28). This reaction was deemed an appropriate method to expand conjugation. However, selectivity could be a challenge as nitro-BODIPY **S2** contains two symmetrical active methyl groups. To avoid this, routes to prepare unsymmetrical nitro-BODIPYs for later condensation reactions were designed.

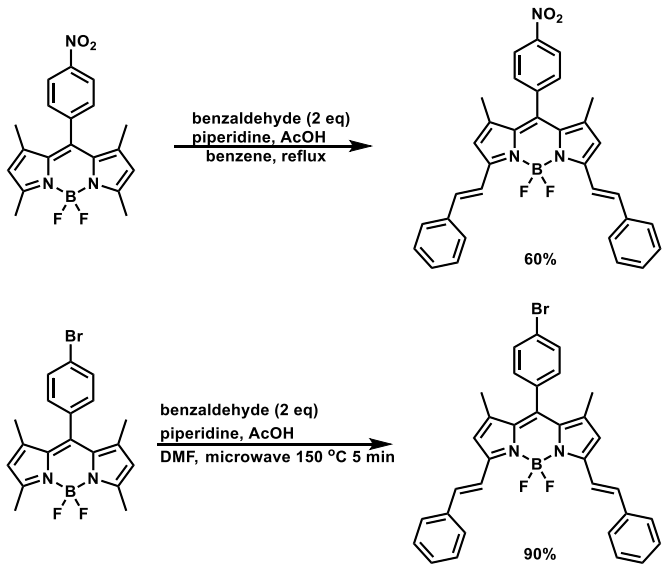

Scheme 28 Precedents of condensation reaction between 1,3,5,7-tetramethyl BODIPY and aldehydes.

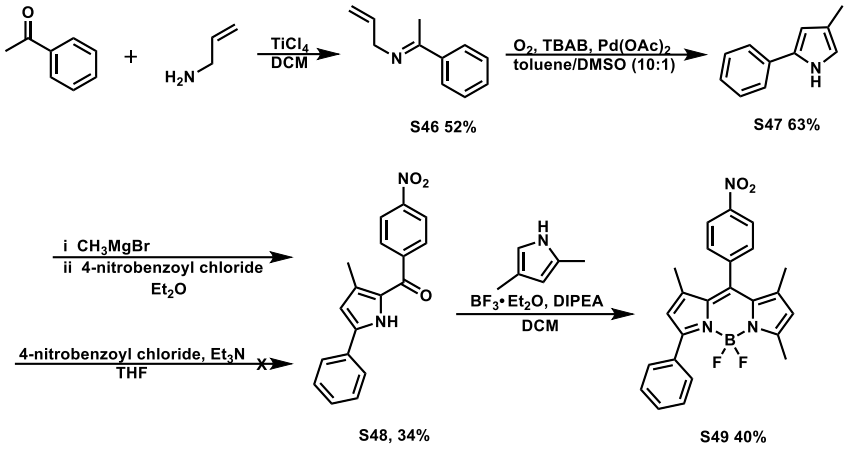

Scheme 29 Synthesis of nitro-BODIPYs S49.

As shown in Scheme 29, the route aimed to prepare the unsymmetrical mono-arylated-BODIPY **S49**. Following a reported procedure[103-104], the synthesis started with the condition of acetophenone, prop-2-en-1-amine and $TiCl_4$, to give intermediate **S46** in a yield of 52% as evidenced by intermediate signal of 160.35 $[M+H]^+$ in LCMS. Then a $Pd(OAc)_2/O_2$ catalyzed ring closing reaction led to phenyl-pyrrole **S47** in a yield of 63% as evidenced by N-H signal at δ=8.17 in ^{1}H-NMR spectrum. Whilst the Et_3N/ THF conditions did not work, base (Grignard) mediated coupling with the acid chloride gave nitro-phenyl-pyrrol-methanone intermediates **S48** as product in a yield of 34%, as evidencd by C=O signal at δ=183.8 in ^{13}C-NMR spectrum. Finally, coupling between **S48** and 2,4-dimethyl-1H-pyrrole followed by complexation with BF_3•Et_2O afforded 1,3,7-trimethyl-5-phenyl-8-(4-nitrophenyl)-BODIPY S49 in a yield of 40%.

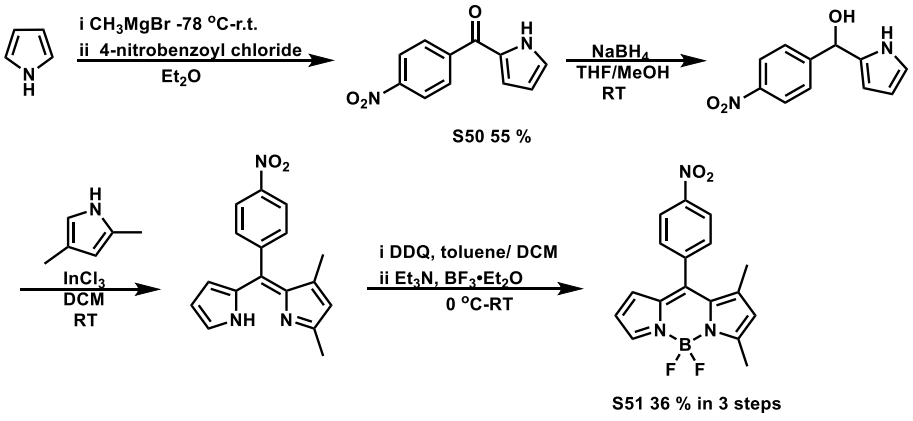

Scheme 30 Synthesis of nitro-BODIPYs S51.

Guided by similar design thoughts, 1,3-dimethyl-8-(4-nitrophenyl)-BODIPY S51 was prepared in four steps, following the reported procedure[105-106]. As shown in Scheme 30, the synthesis started with the coupling of pyrrole and 4-nitrobenzoyl chloride to give the ketone intermediate

S50 in a yield of 55%. Following $NaBH_4$ reduction, a $InCl_3$ catalyzed coupling and a complexation with BF_3•Et_2O afforded product **S51** in a yield of 36% in three steps as evidenced by signal of 340.1 $[M-H]^-$ in LCMS.

In summary, with readily prepared nitro-BODIPY **S38**, **S39**, **S49** and **S51**, we could connect them with another fluorophore via click reaction or condensation to prepare a dual-fluorophore probe.

3.1.2 Synthesis of linkers

In consideration of how different lengths and properties of the linkers in probes affect the process of how probes go through cell membrane and localize to the target, we designed and prepared a group of linkers with a terminal alkyne or azide. These linkers could be easily attatched to nitro-BODIPYs or other fluorophores via a click reaction.

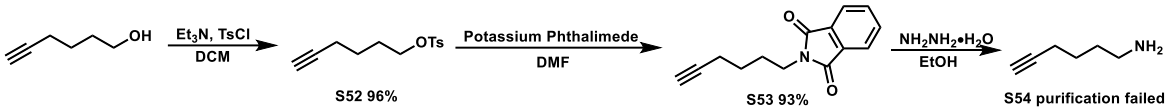

Scheme 31 Synthesis of NH_2-alkyne linker S54.

Initial attempts to prepare NH_2-alkyne linkers started with commercially available hex-5-yn-1-ol (Scheme 31). Following tosylation, reaction with phthalimide[107] afforded intermediate **S53** in an overall yield of 89% as evidenced by a C=O signal at δ=168.4 in ^{13}C-NMR spectrum. Unfortunately, the purification of the subsequent aminolysis was not possible because of the similar polarities of product **S54** and byproduct phthalimide. To address this challenge, another route avoiding phthalimide was tried (Scheme 32). In this, commercial 6-aminohexan-1-ol was N-Boc-protected and converted to the iodide **S56** in an overall yield of 85% as evidence by signal of 328.1 (^{126}I) and 329.2 (^{127}I) $[M+H]^+$ in LCMS. Etherification then connected **S56** and commercially available hex-5-yn-1-ol to give **S57** in a yield of 52%. Finally Boc-protected amine was deprotected under acidic condition to give the desired long chain NH_2-alkyne linker **S58**.

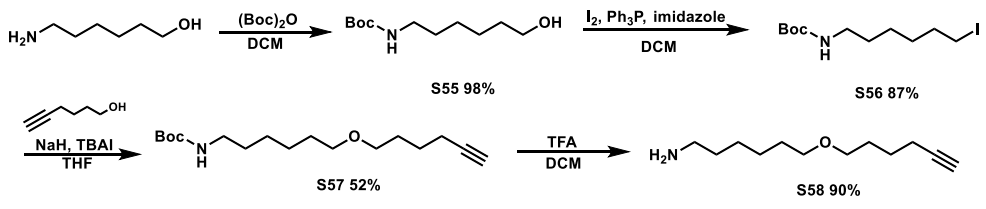

Scheme 32 Synthesis of NH_2-alkyne linker S58.

A second group of NH_2-azide linkers were also required to enable different click reaction conditions. As shown in Scheme 33, following a reported procedure[108], azidation of 1,6-dibromohexane gave 1,6-diazidohexane **S59** in a yield of 76% as evidenced by a signal of 168.1 $[M+H]^+$ in LCMS. Selective reduction of one azide group by Staudinger reaction then gave NH_2-azide linker **S60** in a yield of 70% as evidenced by a signal of 143.4 $[M+H]^+$ in LCMS. Identically, a mesylated tetraethylene glycol went through the same two steps to give an elongated NH_2-azide linker **S63** sucessfully, as evidenced by a signal of 245.1 $[M+H]^+$ in LCMS.

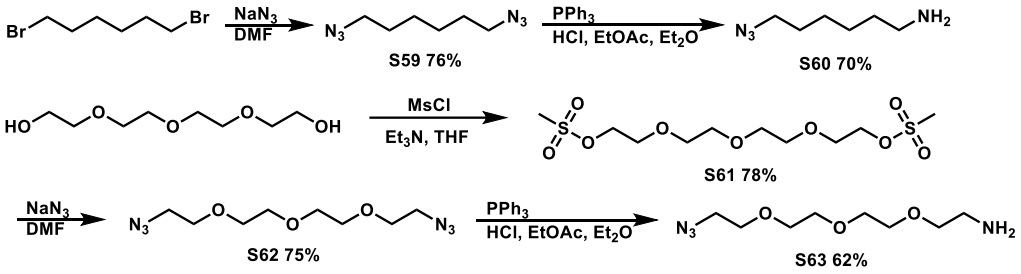

Scheme 33 Synthesis of NH_2-azide linkers.

3.1.3 Synthesis of red-shifted and water-soluble nitro-BODIPYs

As mentioned above (Section 3.1.1), the methyl groups on BODIPYs can be condensed with aldehydes via catalysis with piperidine and AcOH. To explore this, the reactions of nitro-BODIPY **S2** with different kinds of aldehydes were then explored to expand the probes' conjugation and to enhance their red-shifted emission. As shown in Scheme 34, following a reported procedure[101], **S2** was condensed with different equivalent of benzaldehyde in a Dean-Stark apparatus. Using 2 equivalent of benzaldehyde, bis-styryl-nitro-BODIPY **S64** could be prepared in a low yield of 18% after purification as evidenced by disappearance of two methyl signals in ^{1}H-NMR spectrum. No starting materials and intermediate **S65** could be detected by Mass-spec. Surprisingly, using only 1 equivalent of benzaldehyde, no mono-styryl-nitro-BODIPY **S65** could be observed with the only product identified as bis-styryl-nitro-BODIPY **S64**. This suggested that the condensation between mono-styryl-nitro-BODIPY **S65** and benzaldehyde is much faster than the initial reaction with **S2**. The different reactivities between **S65** and **S2** could be caused by their solubility in benzene. The reaction mixture cannot dissolve starting material **S2** well, while the product **S64** was soluble in benzene. This indicateds that

intermediate **S65** is more soluble than **S2** in the reaction so **S65** will react faster than **S2** in this reaction mixture.

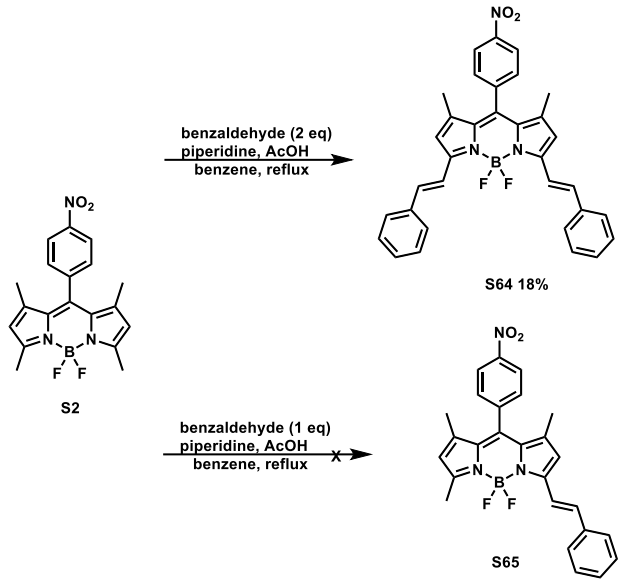

Scheme 34 Condensation reaction of nitro-BODIPY S2.

Although its yield and selectivity are not high, the condensation reaction between nitro-BODIPY and benzaldehyde was an effective and simple method to prepare the conjugated BODIPYs. Aldehyde analogues could expand conjugation of nitro-BODIPYs and lead to a red-shifted emission. Moreover PEG chains and morpholine are known to be hydrophilic which could help to increase water-solubility of nitro-BODIPY probes. To expand the family of red-shifted nitro-BODIPYs, a group of aldehyde analogues were then designed. With the method in Scheme 35, the benzaldehyde with PEG **S67** was prepared in a yield of 62% from a tosylated triethylene glycol monomethyl ether and 4-hydroxybenzaldehyde through an etherification. Similarly, the 4-morpholinobenzaldehyde **S68** (57% yield) and 1-methyl-1H-indole-5-carbaldehyde **S69** (86% yield) were prepared from commercial starting materials.

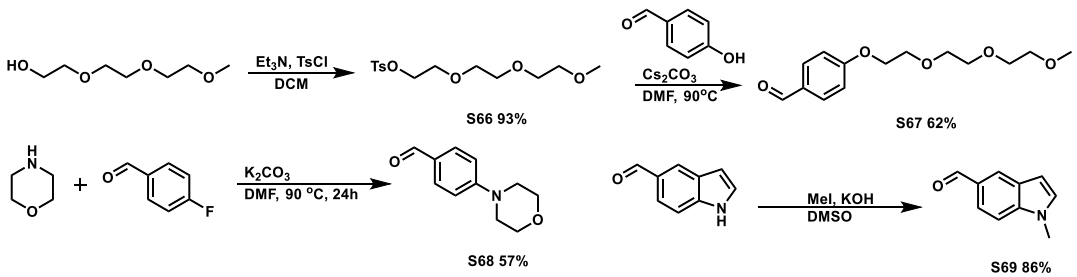

Scheme 35 Preparation of aldehyde precursors.

With the available aldehydes **S67**-**69** and commercial starting material 4-methoxybenzaldehyde in hand, the next step was to condense them with nitro-BODIPYs **S2**, **S49** and **S51**. As shown in Scheme 36, these reactions gave red-shifted nitro-BODIPYs **S70**-**75** in acceptable yields whilst nitro-BODIPY **S2** and aldehyde **S65** afforded the mono and bis PEGylated nitro-BODIPY **S76**, **S77** in lower or moderate yields, repectively. In contrast to **S2** and **S51**, the condensation reaction yields of **S49** were higher because products from **S49** are more stable than those products from **S2** and **S51** under reflux reaction mixture or at high temperature. A lot of products could be collected from the reflux reactions of **S49** after longer than 48h but almost no products could be detected in the reactions of **S2** and **S51** under reflux for 48h.

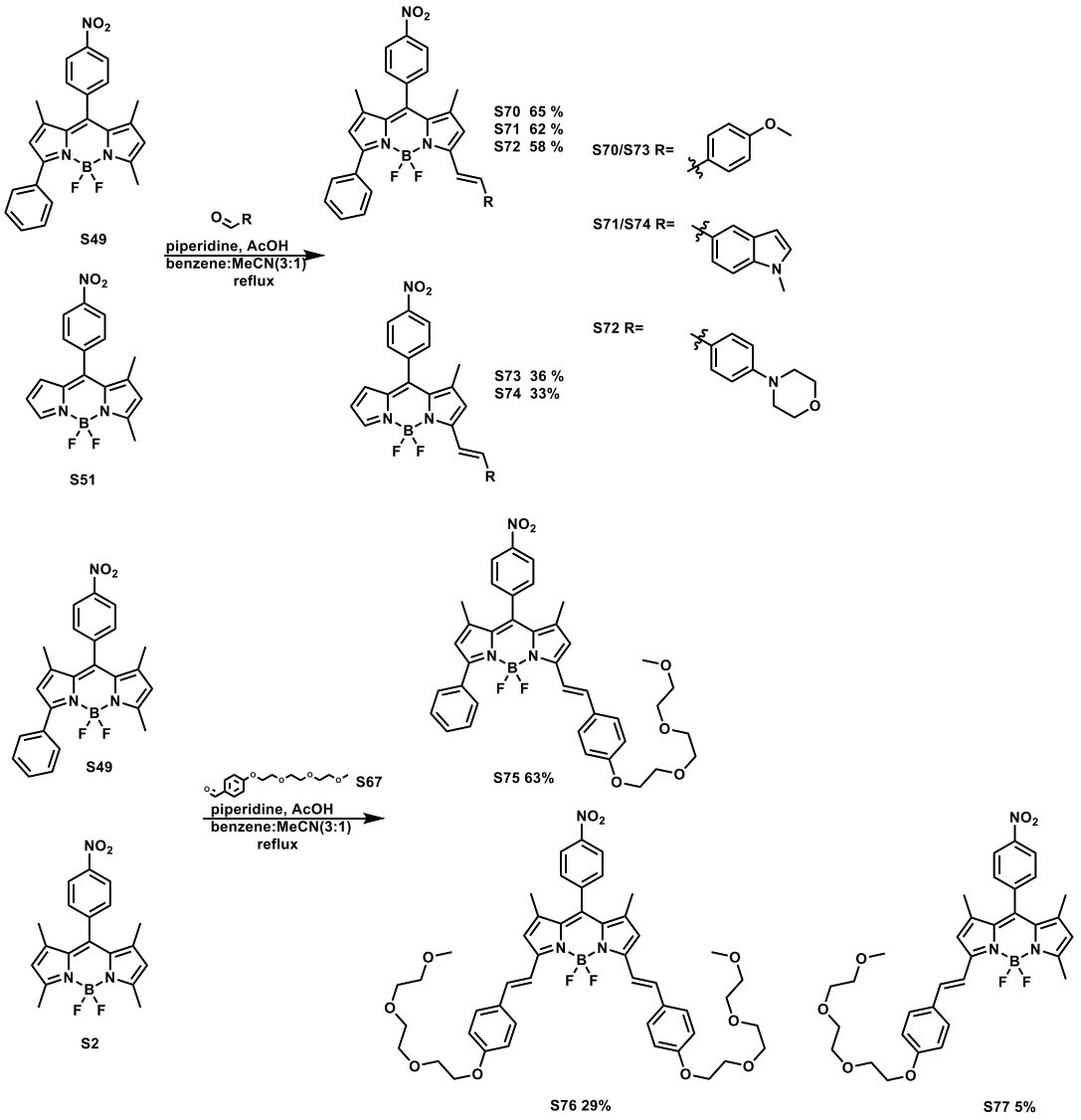

Scheme 36 Condensation reaction of nitro-BODIPYs.

Having prepared a series of red-shifted nitro-BODIPYs, attentions then turned to enhance the probes' water-solubility. The sulfonic acid group is one of the most hydrophilic groups in organic compound. Consequently, it was of interest to attempt the selective sulfonation on nitro-BODIPY S2 as a method to enhance water solubility. As shown in Scheme 37, following the reported procedure[39], nitro-BODIPY **S2** was sulfonated using different equivalents of chlorosulfonic acid under low temperature. With 1 equivalent of $ClSO_3H$, as observed by LCMS (448.4 $[M-H]^-$), most of product was mono-sulfonic nitro-BODIPY **S78** and with 2 equivalent of $ClSO_3H$, the majority was bis-sulfonic nitro-BODIPY **S79** (263.5 $[M-2H]/2^-$ in LCMS). Although these reactions were selective and efficient, purification proved to be very challenging. Ultimately, following reversed-phase chromatography, pure **S79** could be isolated in a low yield of 9% but unfortunately it was not possible to isolate **S78**.

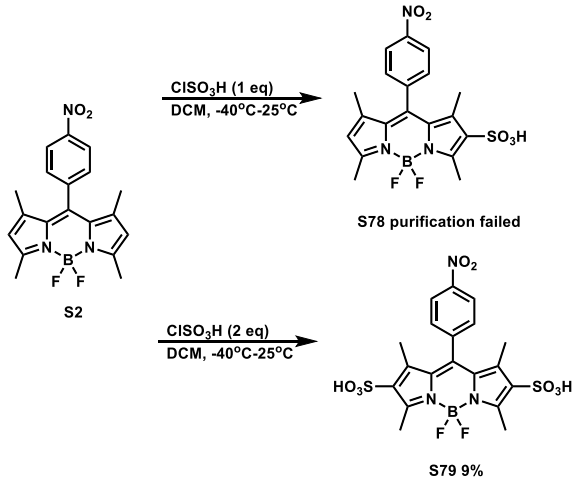

Scheme 37 Sulfonation of nitro-BODIPY S2.

3.1.4 Synthesis of meso-phenyl-BODIPYs

As mentioned in Section 2.1, nitro-BODIPY (S2) is intrinsically non-fluorescent but on incubation with plant cells becomes fluorescent at peroxisomes. To explore how the nitro group affacts localization phenomenon, a control group of meso-phenyl-BODIPYs were prepared (Scheme 38). Starting with readily prepared pyrroles **S9** and **S14**, Phenyl-BODIPYs **S80**, **S83** and **S84** were synthesised following the same procedures previously described.

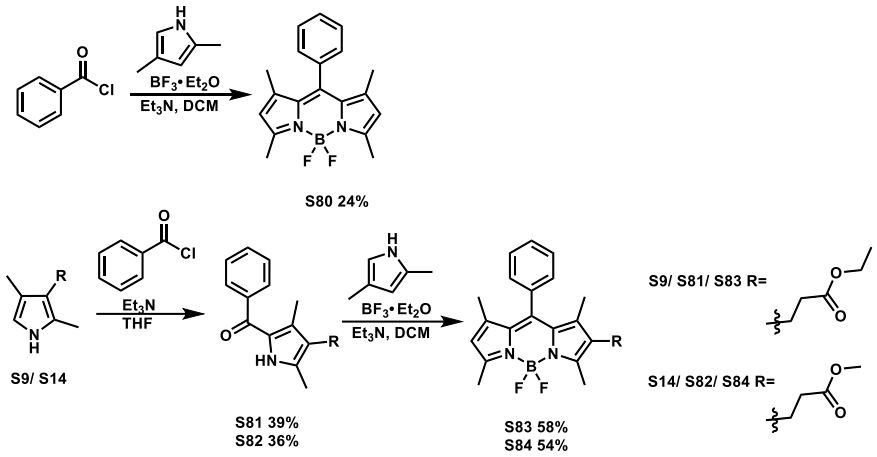

Scheme 38 Synthesis of meso-phenyl-BODIPYs.

3.1.5 Synthesis of reporter tags

As mentioned in Section 2.2, two sets of dual-fluorophore probes were designed to explore nitro-BODIPY's physiological behaviours outside of peroxisomes. In order to attach different fluorescent reporters on nitro-BODIPYs, a group of reporter tags with linkages were synthesised. NBD analogues were first prepared because of their stable fluorescence and small size. As shown in Scheme 39, NBD-Cl was connected with 6-aminohexan-1-ol via an aminolysis to give the NBD-alcohol **S85** in a yield of 61% as evidenced by a signal of 280.1 $[M+H]^+$ in LCMS. Iodination with I_2 the gave the NBD-iodide **S86** in a yield of 78% as evidenced by signals of 291.0 (^{126}I) and 392.0 (^{127}I) $[M+H]^+$ in LCMS. In the last step, reporter tags **S87** and **S88** were generated from **S86** through a etherification with 4-hydroxybenzaldehyde or an aminolysis with 1H-indole-5-carbaldehyde respectively.

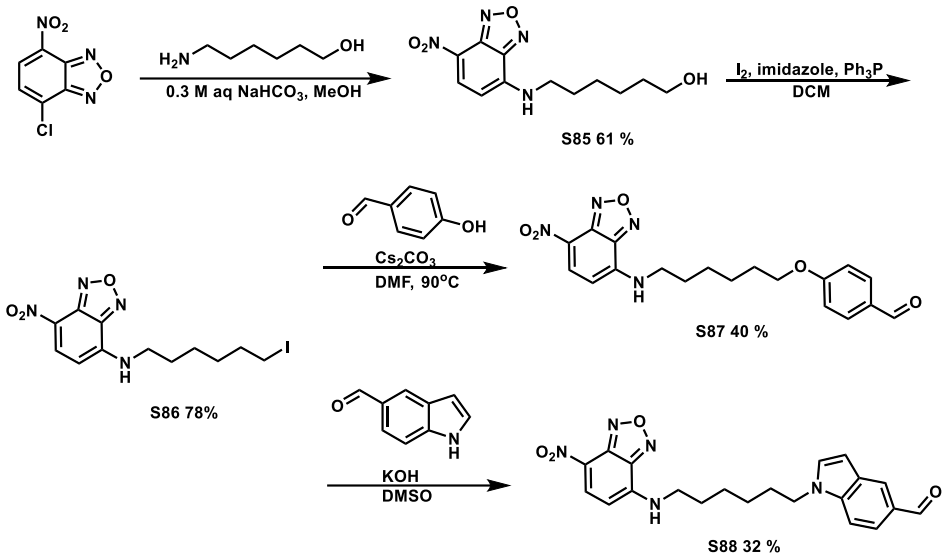

Scheme 39 Synthesis of NBD reporters.

With 'blue-shift' NBD reporter tags in hand, it was also of interest to prepare several 'red-shifted' reporter tags. Rhodamine B is known as a commercially available fluorochrome emiting at around 610 nm. Moreover, the Rhodamine B structure contains a carboxyl which makes it easier to modify. As shown in Scheme 40, we designed and synthesised two Rhodamine reporter tags with terminal azide **S90** and **S91** via amidation. Initially, the commercial starting material Rhodamine B was treated with EDC and NHS to generate the Rhodamine-NHS ester **S89** in a yield of 69% as evidenced by a NHS singlet signal at δ=2.75 in ^{1}H-NMR spectrum. Then a coupling of Rhodamine-NHS ester **S89** with the previously prepared linkages **S60** or **S63** gave Rhodamine reporter tags with terminal azide **S90** and **S91** in yield of 53% and 43% respectively.

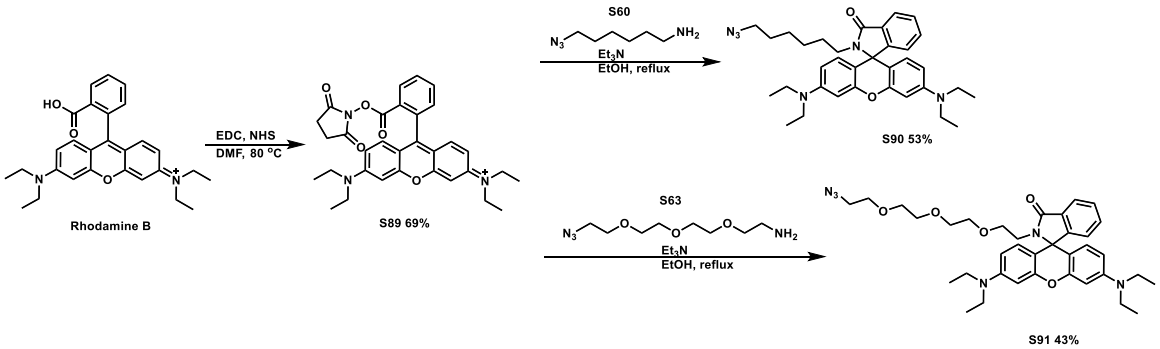

Scheme 40 Synthesis of Rhodamine B reporters.

Cy5 analogues are known as a group of dyes with outstanding red-shifted emission spectrum (λ_{em} >650 nm or within the near infrared region[109]) and commercially available as well. But the

price of Cy5 was too expensive to work on scale so it was decided to synthesis Cy5 from a cheap starting material 2,3,3-trimethyl-3H-indole. As shown in Scheme 41, following the reported procedure[110], 2,3,3-trimethyl-3H-indole was converted by alkylation to give two intermediates **S92** and **S93** in yield of 55% and 70% respectively. Condensation catalyzed by pyridine and acetic anhydride then gave Cy5 (**S94**) in a low yield of 5% because the reaction was not selective and generated a lot of byproducts. With Cy5 (**S94**) in hand, it was coupled with EDC and NHS to achieve a Cy5-NHS ester (**S95**, yield 67%, as evidenced by by a NHS's singlet signal at δ=2.89 in ^{1}H-NMR spectrum) and then with azide-amine linkage **S60** to give terminal azide (**S96**). The polarities of **S96** and starting materials **S60**, **S95** were similar, making purification challenging. Consequently, the synthesis **S96** was repeated using lower amounts of **S60** (<1 equivalent) providing material of sufficient quality that enabled its use without further purificition.

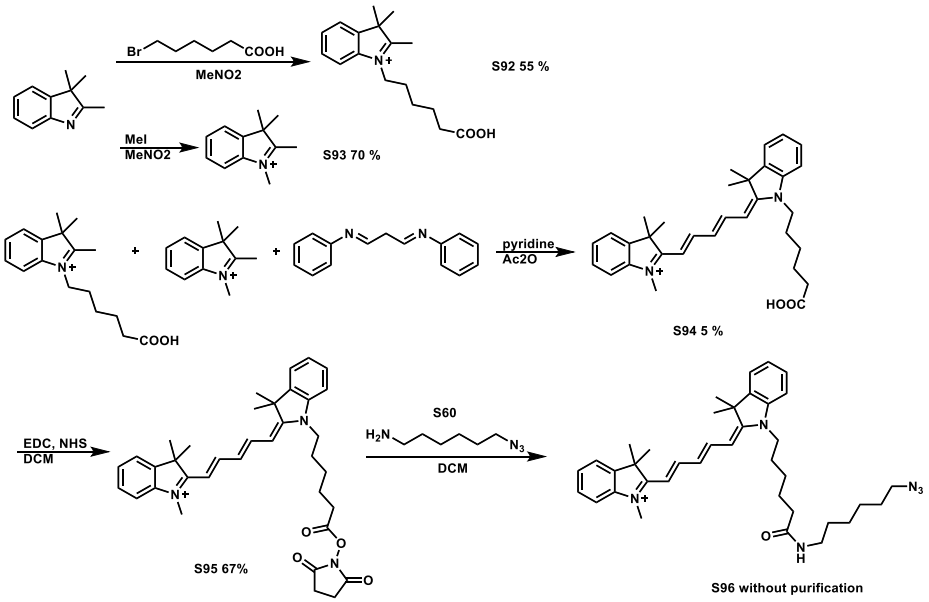

Scheme 41 Synthesis of Cy5 reporters.

3.1.6 Synthesis of dual-fluorophore probes

With different reporter tags and BODIPY cores now available in hand, attentions then turned to the coupling to give the desired dual-fluorophore probes. As shown in Table 3, the BODIPY-alkyne **S38** was connected with reporter tags containing terminal azide via a standard click reaction. The click reaction gave dual-fluorophore probes **S99-103** selectively and efficiently in acceptable yields.

Table 3 Click reaction to prepare dual-fluorophore probes.

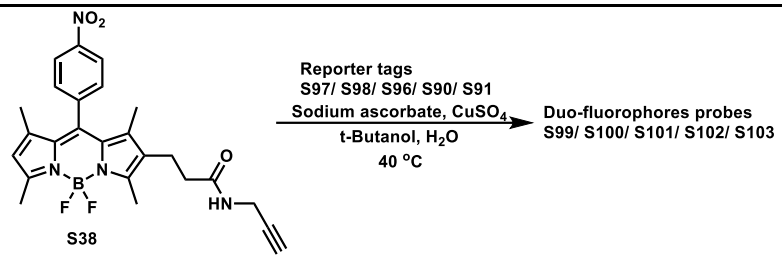

Reporter tags	Dual-fluorophore probes	Yield
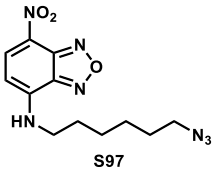 S97	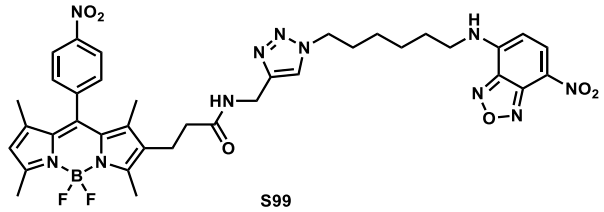 S99	45%
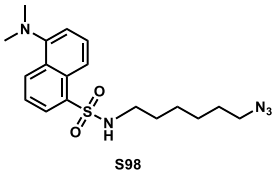 S98	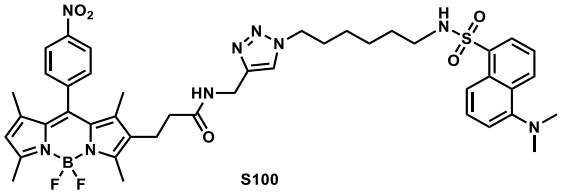 S100	36%
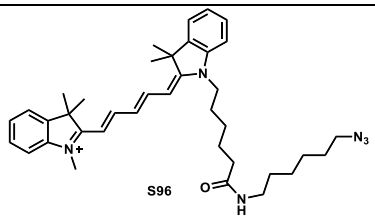 S96	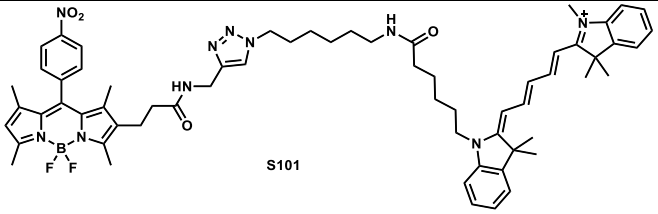 S101	16%
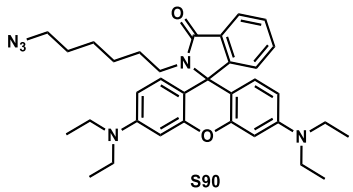 S90	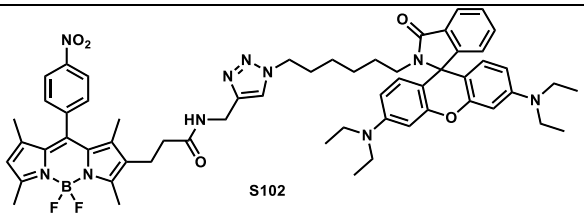 S102	42%
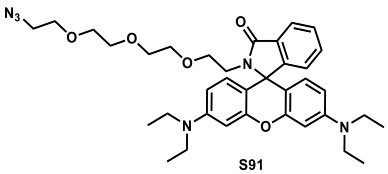 S91	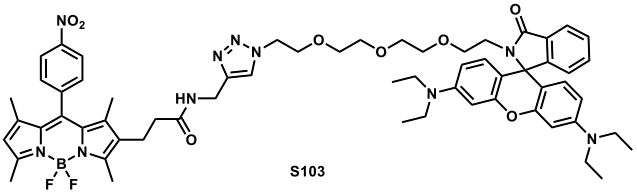 S103	39%

In a complementary approach, nitro-BODIPYs **S51** and **S49** were condensed with aldehyde analogues **S87** and **S88** via catalysis with piperidine and AcOH. The condensation gave dual-fluorophore probes **S104**-**107** selectively and efficiently in acceptable yields (Table 4).

Table 4 Condensation reaction to prepare dual-fluorophore probes.

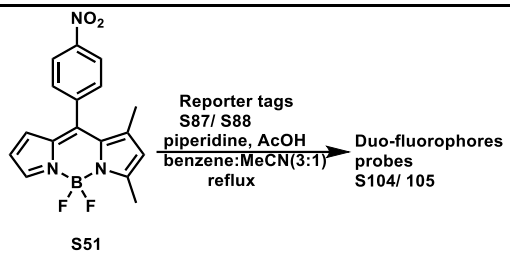

Reporter tags	Dual-fluorophore probes	Yield
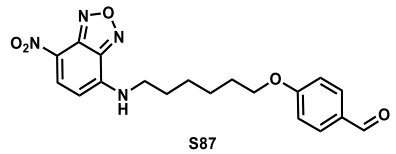 S87	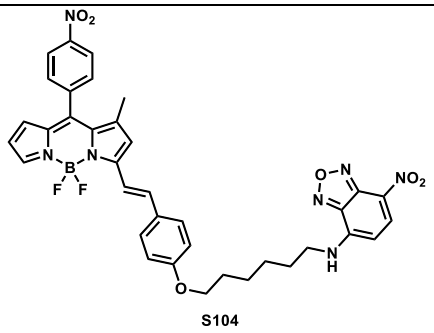 S104	35%
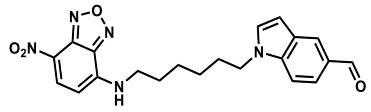 S88	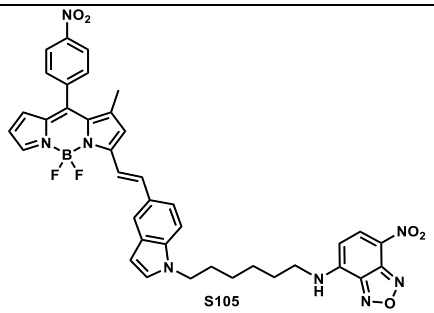 S105	37%
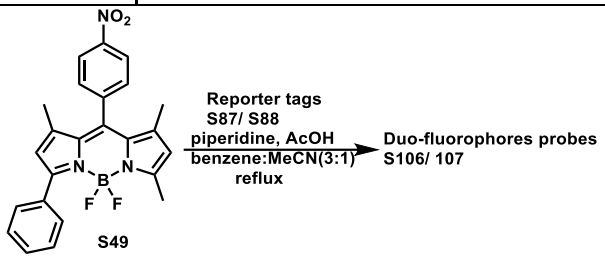 Reporter tags S87/ S88 piperidine, AcOH benzene:MeCN(3:1) reflux Duo-fluorophores probes S106/ 107 S49		
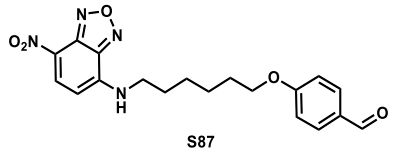 S87	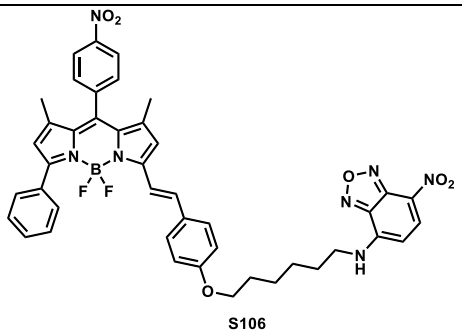 S106	43%

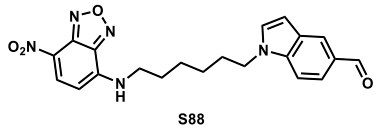 S88	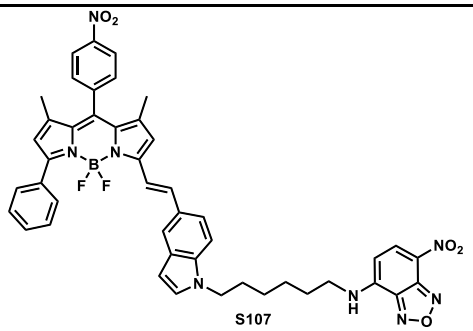 S107	42%

3.1.7 Synthesis of photoaffinity labelling probe

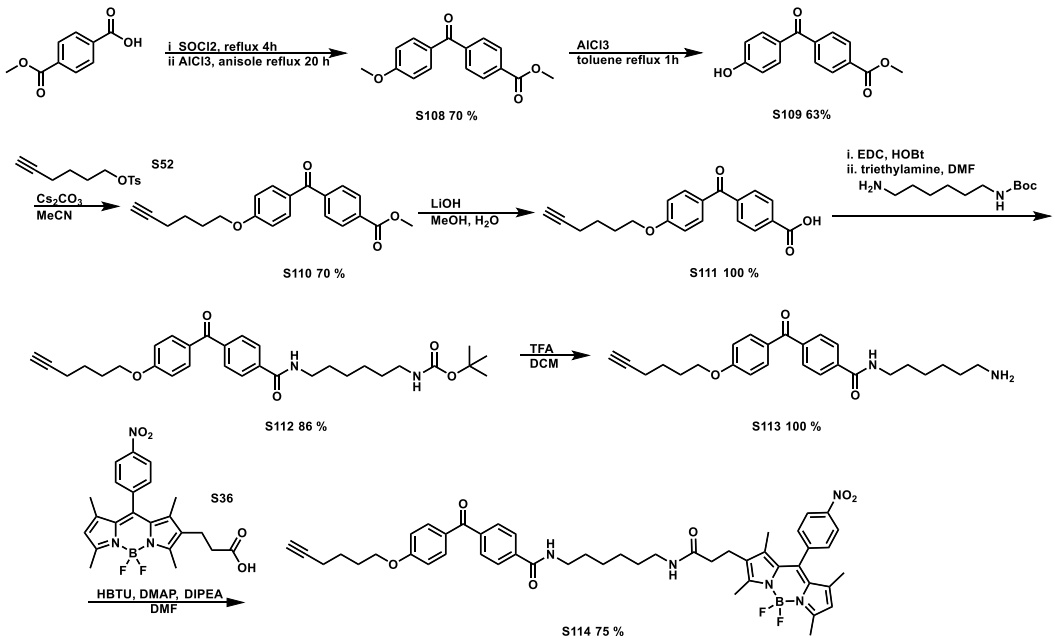

Scheme 42 Synthesis of photoaffinity labelling probe S114.

As discussed in Section 2.2, in order to identify the protein targets of nitro-BODIPY, it was necessary to attatch a photoaffinity group to the nitro-BODIPY core. The photoaffinity labelling probe will contain three basic components: a photoaffinity agent, a reporter unit and a protein labelling group (nitro-BODIPY). Benzophenone was chosen as the photoaffinity group in the probe because it could be activated by a long wavelength (350-360 nm), which lowers the risk of damaging biomolecules. As the nitro-BODIPY becomes fluorescent when it localizes to the target, it was assumed to function as both the reporter group and the labelling group.

As shown in Scheme 42, 4-(methoxycarbonyl)benzoic acid was treated with $SOCl_2$ to give the acyl chloride, a Friedel-Crafts acylation[111] with anisole then gave methyl 4-(4-

methoxybenzoyl)benzoate **S108** in a yield of 70% as evidenced by two methyl singlet signals at δ=3.98 and 3.91 in ^{1}H-NMR spectrum. Following a demethylation of the methyl ether, methyl 4-(4-hydroxybenzoyl)benzoate **S109** was achieved in a yield of 63%. An etherification using linkage **S52** gave **S110** in a yield of 70% as evidenced by a C≡CH signal at δ=2.00 in ^{1}H-NMR spectrum. The ester group of **S110** was then hydrolyzed by LiOH to give a benzophenone carboxylic acid **S111** in a yield of 100% without purification. Subsequently, amidation between **S111** and Boc-protected hexane-1,6-diamine gave benzophenone intermediate **S112** in a yield of 86% as evidenced by a singlet signal of tert-butyl at δ=1.45 in ^{1}H-NMR spectrum. After this, a Boc deprotection gave the benzophenone **S113** with terminal amine and terminal alkyne in a yield of 100% without purification. Finally, amide coupling of nitro-BODIPY-acid **S36** and benzophenone **S113** gave the desired photoaffinity labelling probe **S114** in a yield of 75% as evidenced by a signal of 844.4 $[M+H]^{+}$ in LCMS.

3.2 Photophysical properties and plant cell imaging of probes

3.2.1 Nitro-BODIPY probes

As discussed in Section 2.1, nitro-BODIPY **P1**/ **S2** was intrinsically non-fluorescent but upon incubation of cells with this compound, fluorescence is observed at the target site. Fluorescence measurement in different solvents showed **P1** is quenched in polar solutions such as water and ethanol but is emissive in toluene. Therefore, toluene and water were chosen as solvents under 25 ^{o}C to measure optical properties of the prepared nitro-BODIPY probes.

Initially, as shown in Fig 25, a subset of these probes (**P1**-**P10**, equal to **S2**, **S7**, **S16**, **S15**, **S36**, **S19**, **S4**, **S3**, **S79** and **S51** in Section 3.1) were studied to explore SAR affects. All the primary solutions of the probes were prepared in DMSO and then diluted to corresponding toluene or water solutions (final DMSO concentration <10%) for measurements Fig 26 and Table 5.

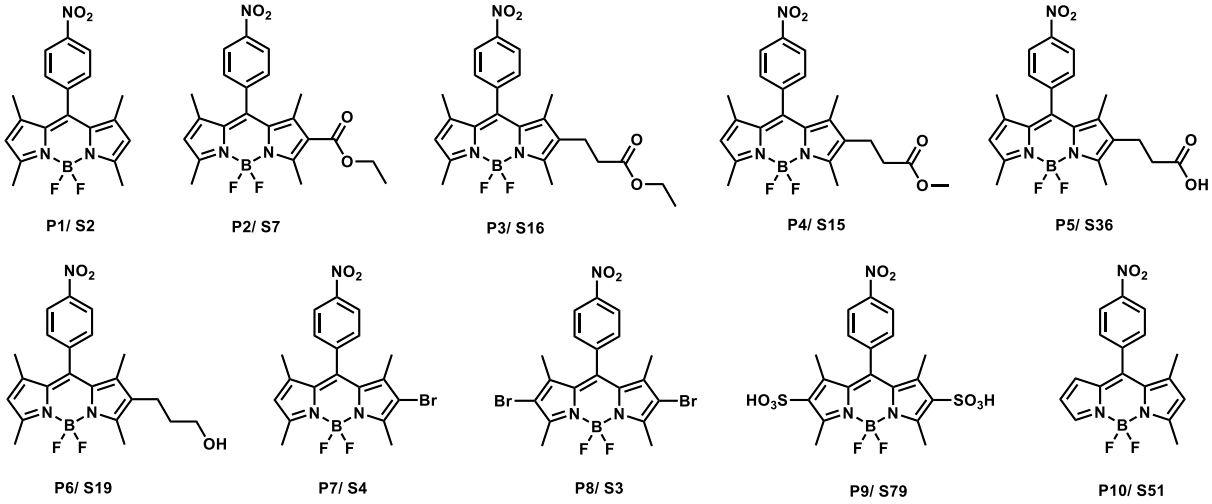

Figure 25 Nitro-BODIPY probes P1-10.

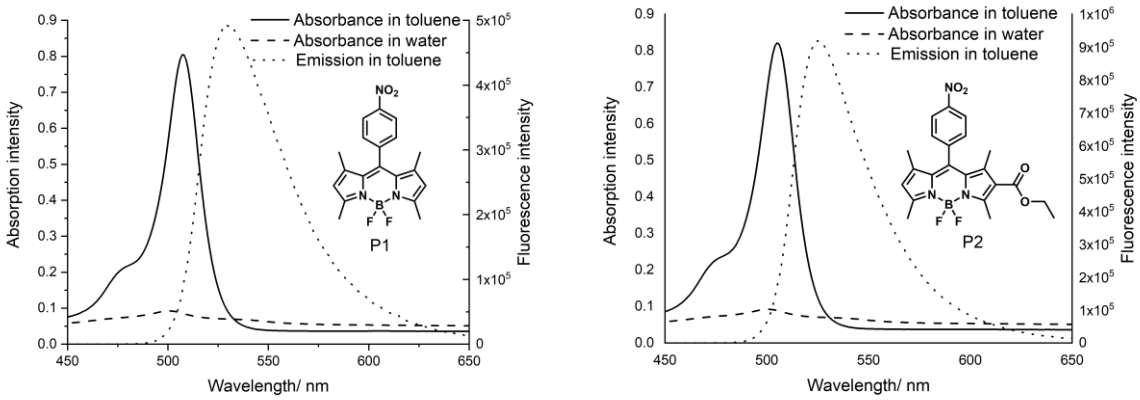

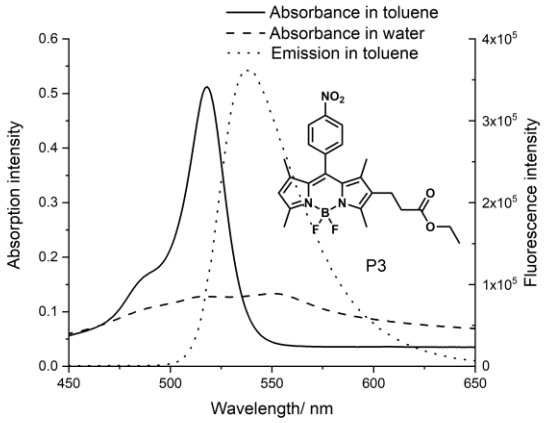
Absorbance in toluene
Absorbance in water
Emission in toluene
Absorption intensity
Fluorescence intensity
Wavelength/ nm
P3

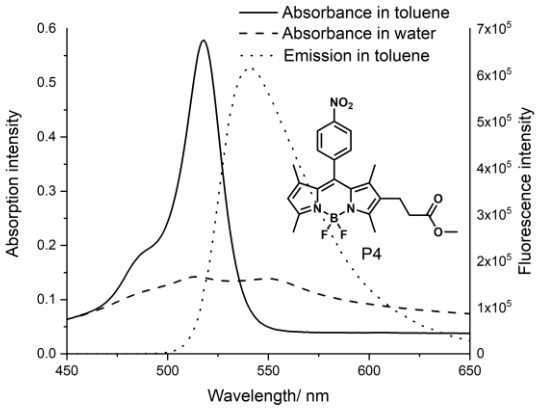
Absorbance in toluene
Absorbance in water
Emission in toluene
Absorption intensity
Fluorescence intensity
Wavelength/ nm
P4

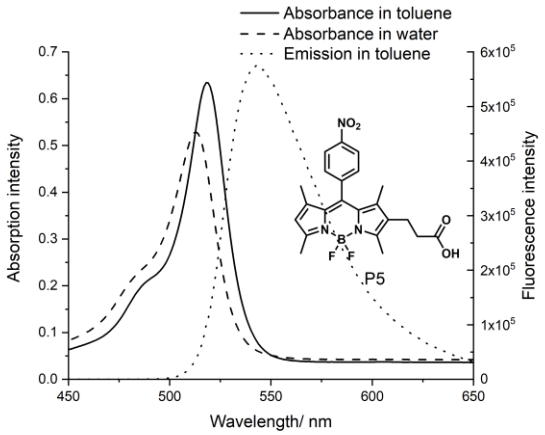
Absorbance in toluene
Absorbance in water
Emission in toluene
Absorption intensity
Fluorescence intensity
Wavelength/ nm
P5

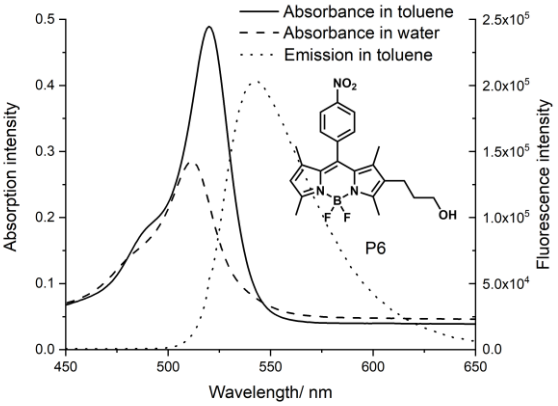
Absorbance in toluene
Absorbance in water
Emission in toluene
Absorption intensity
Fluorescence intensity
Wavelength/ nm
P6

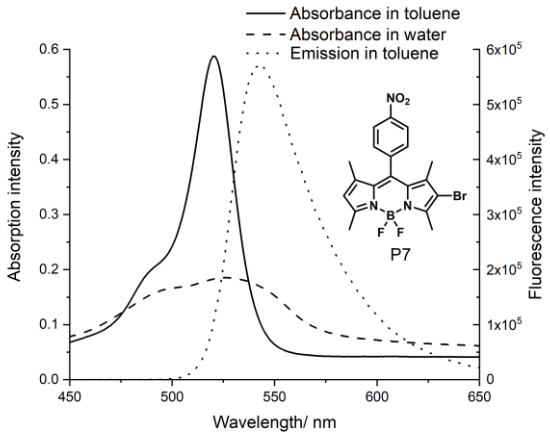
Absorbance in toluene
Absorbance in water
Emission in toluene
Absorption intensity
Fluorescence intensity
Wavelength/ nm
P7

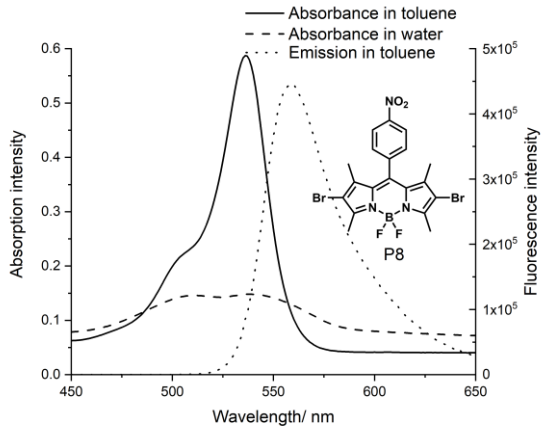
Absorbance in toluene
Absorbance in water
Emission in toluene
Absorption intensity
Fluorescence intensity
Wavelength/ nm
P8

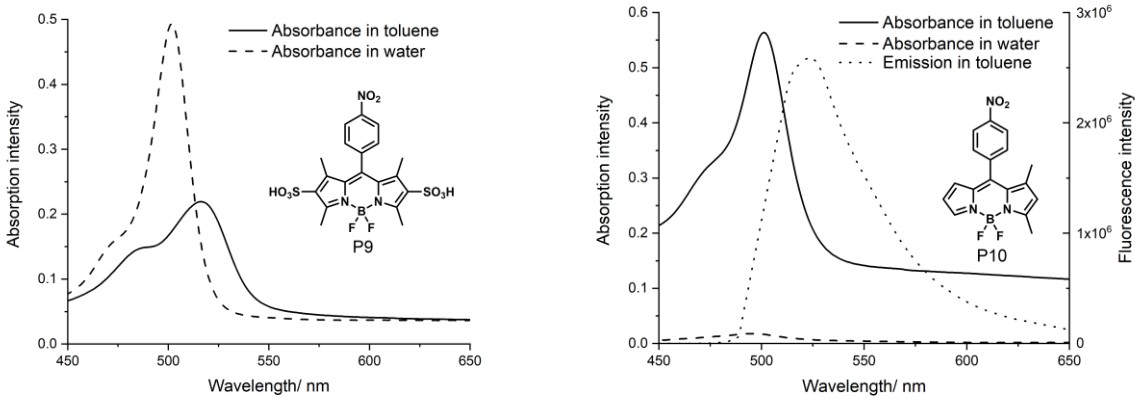

Figure 26 Absorption and emission spectra of nitro-BODIPY probes P1-10.

Table 5 Photophysical properties of nitro-BODIPY probes P1-10.

Probes	λ_{abs} in toluene	λ_{em} in toluene	λ_{abs} in water	λ_{em} in water
P1	508 nm	528 nm	501 nm	quench
P2	505 nm	526 nm	500 nm	quench
P3	518 nm	539 nm	517 nm	quench
P4	518 nm	541 nm	515 nm	quench
P5	518 nm	544 nm	514 nm	quench
P6	520 nm	543 nm	513 nm	quench
P7	521 nm	543 nm	527 nm	quench
P8	536 nm	561 nm	541 nm	quench
P9	517 nm	quench	502 nm	quench
P10	501 nm	524 nm	498 nm	quench

All the probes (**P1-10**) were quenched in water solution and with the exception of P9 emissive in toluene. By contrast, the meso-phenyl-BODIPYs **P21-23** (will be discussed later in Chapter 3.2.3) exhibits fluorescence in water. A hypothesis is proposed that the nitro group leads to BODIPY's quenching in water. As nitro group could accept proton in hydrogen bonding so this quenching can be a result of nitro-BODIPY-water hydrogen bond breaking in the excited state[112]. Interestingly probes **P5**, **P6** and **P9** contain carboxyl, hydroxyl or sulfonic acid which lead to the probes being more water-soluble because their absorption intensity in water looks much higher than the other probes. Probes containing the electron donating substituents (alkyl and halogen) **P3-P8** showed red-shifted in both absorbance and emission spectra. Significantly for future applications as a linker the presence of an ester linker on the position 2 of nitro-BODIPY did not affect the spectral properties of the probe (**P2-4**). **P9** displays extremely weak

fluorescence owing to weaker electron density on BODIPY core caused by sulfonic acid groups' electron-withdrawing effect.

Table 6 Images of plant cells incubated with nitro-BODIPY probes P1-P9.

Probe	Structure	Image
P1	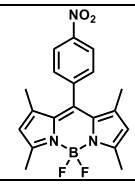	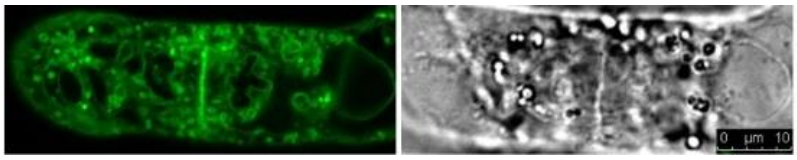
P2	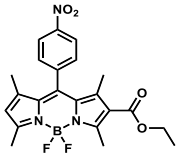	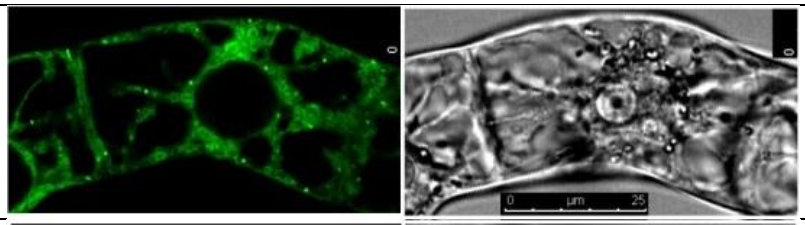
P3	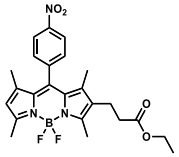	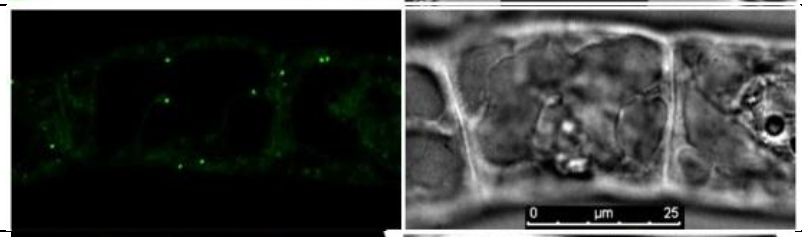
P4	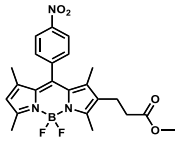	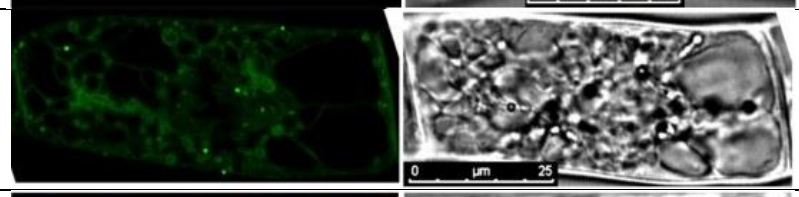
P5	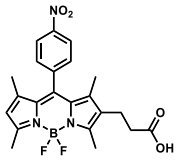	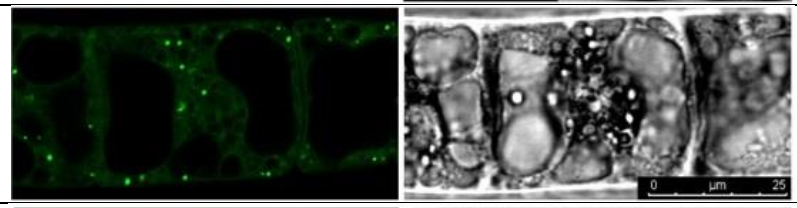
P6	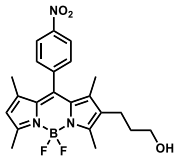	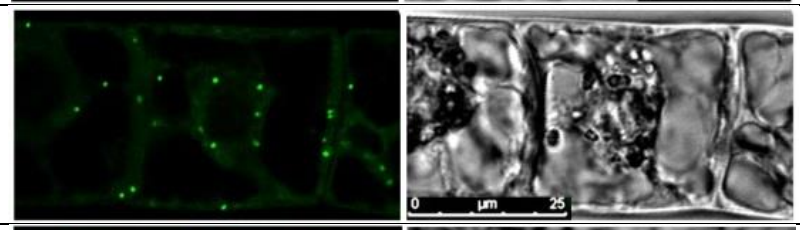
P7	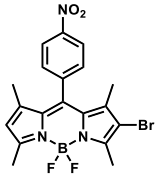	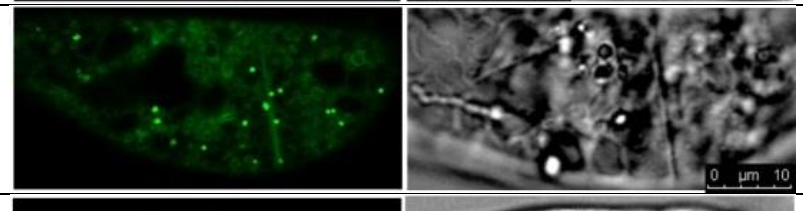
P8	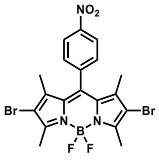	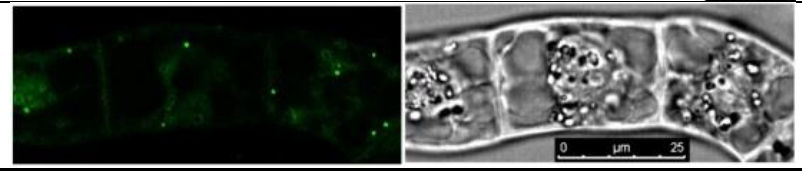

P9	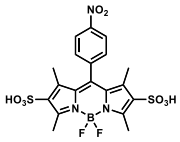		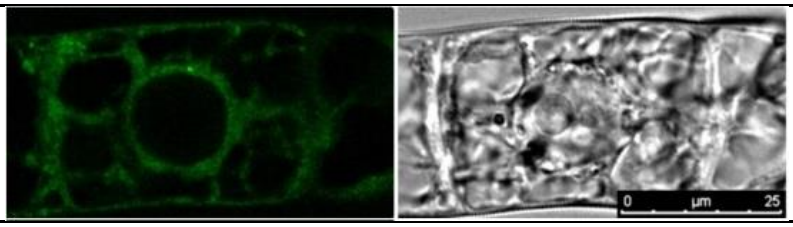

The plant cell images of the nitro-BODIPY probes **P1**-**P9** are collected in Table 6. All probes were applied at the same concentration (10 uM) on arabidopsis bright yellow-2 (BY-2) tissue culture cells. Exhilaratingly, bright fluorescent spots could be observed from most photographs (exclude **P9**'s). As discussed in section 2.1, on the basis of the previous results obtained in the group, it is assumed that these bright fluorescent spots represent nitro-BODIPY probes localized with peroxisomes.

Although probes **P1**-**P8** could localize to peroxisomes selectively and emit effectively, the peroxisome signals in some photographs were compromised by background fluorescence. There are several possible reasons for this which included the possibility that the probes undergo more efficient diffusion through the membrane and/ or have higher quantum efficiency (probes bound with membrane will exhibit stronger fluorescence). Therefore, decreasing the concentration of probes could be a feasible way to lower background noise in future plant cell imaging experiments. In comparison with **P1**, probes **P2**-**P8** gave similar outputs which indicates that the presence of the linker or halogen at position 2 of nitro-BODIPY does not affect the function of the probes. This result supported the feasibility of the planned dual-fluorophore probes (Section 2.2) because the second fluorophore will be attached through a linker at this position. In conclusion, probes **P1**-**P8** are practical probes able to label peroxisomes in plant cells.

3.2.2 Red-shifted nitro-BODIPY probes

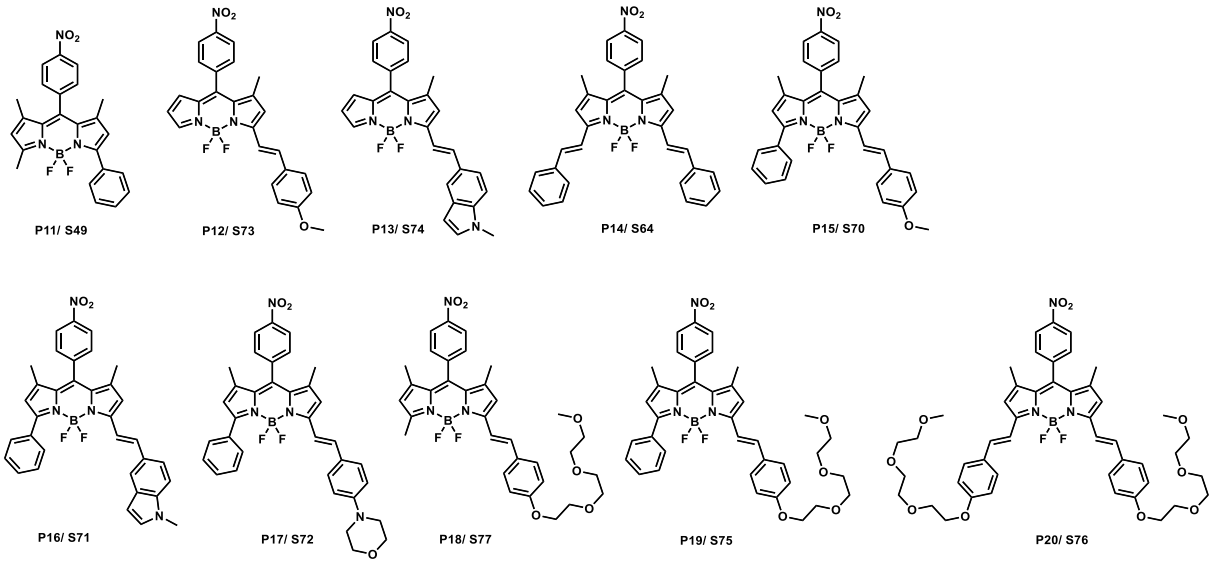

Figure 27 Red-shifted nitro-BODIPY probes P11-20.

To enhance a red-shifted in the emission of the probes, nitro-BODIPYs could be condensed with different aldehydes to extend the probe conjugation. As shown in Fig 27, a family of red-shifted nitro-BODIPY probes (**P11**-**P20**, equal to **S49**, **S73**, **S74**, **S64**, **S70**, **S71**, **S72**, **S77**, **S75** and **S76** in Section 3.1) for peroxisomes were prepared. As before, by including hydrophilic groups (morpholine and PEG chains) as seen in probes **P11**-**P20**, it was possible to improve probe water solubility. The photophysical properties of the red-shifted nitro-BODIPY probes **P11**-**P20** were measured and are collected in Fig 28 and Table 7.

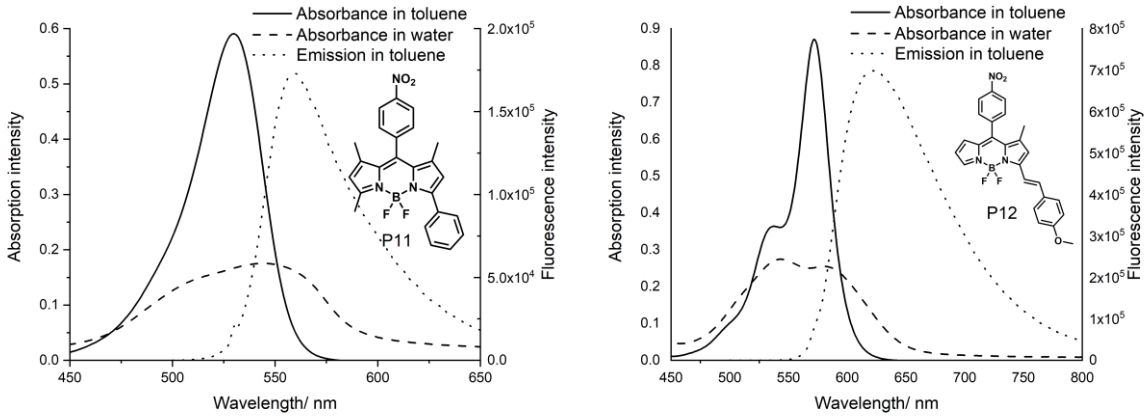

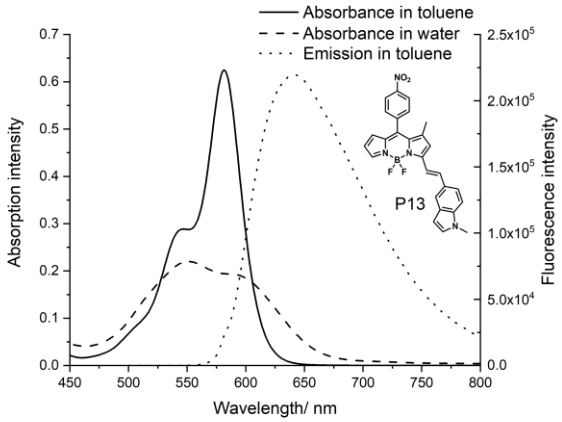
Absorbance in toluene
Absorbance in water
Emission in toluene
P13
Absorption intensity
Fluorescence intensity
Wavelength/ nm

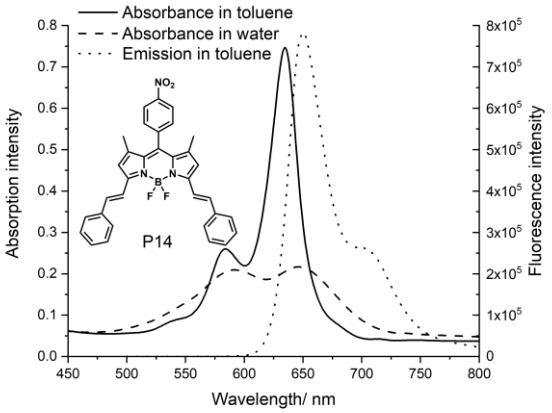
Absorbance in toluene
Absorbance in water
Emission in toluene
P14
Absorption intensity
Fluorescence intensity
Wavelength/ nm

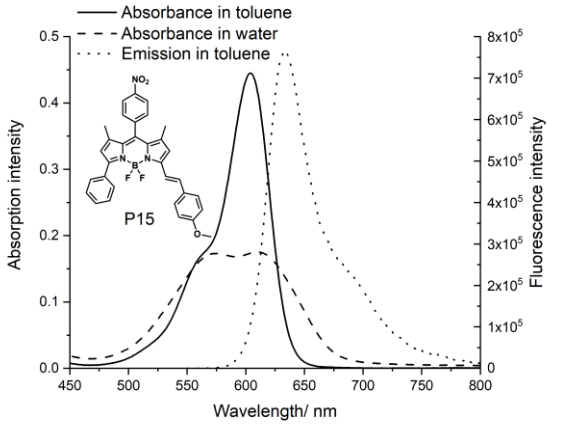
Absorbance in toluene
Absorbance in water
Emission in toluene
P15
Absorption intensity
Fluorescence intensity
Wavelength/ nm

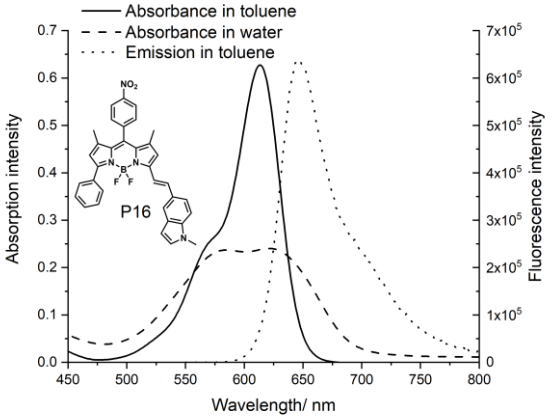
Absorbance in toluene
Absorbance in water
Emission in toluene
P16
Absorption intensity
Fluorescence intensity
Wavelength/ nm

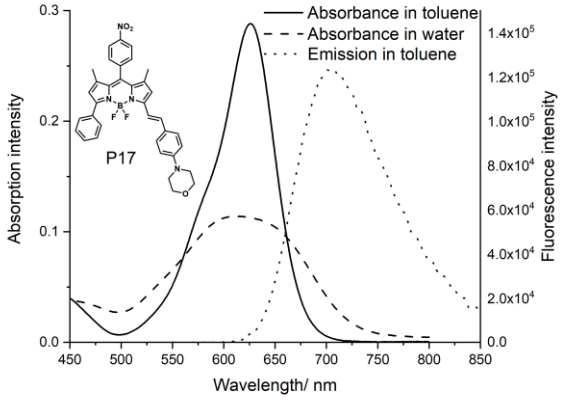
Absorbance in toluene
Absorbance in water
Emission in toluene
P17
Absorption intensity
Fluorescence intensity
Wavelength/ nm

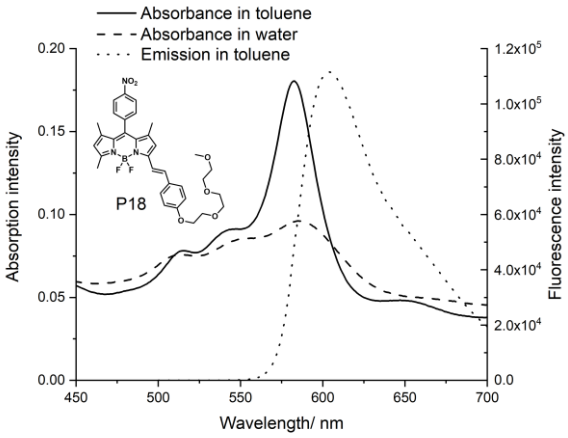
Absorbance in toluene
Absorbance in water
Emission in toluene
P18
Absorption intensity
Fluorescence intensity
Wavelength/ nm

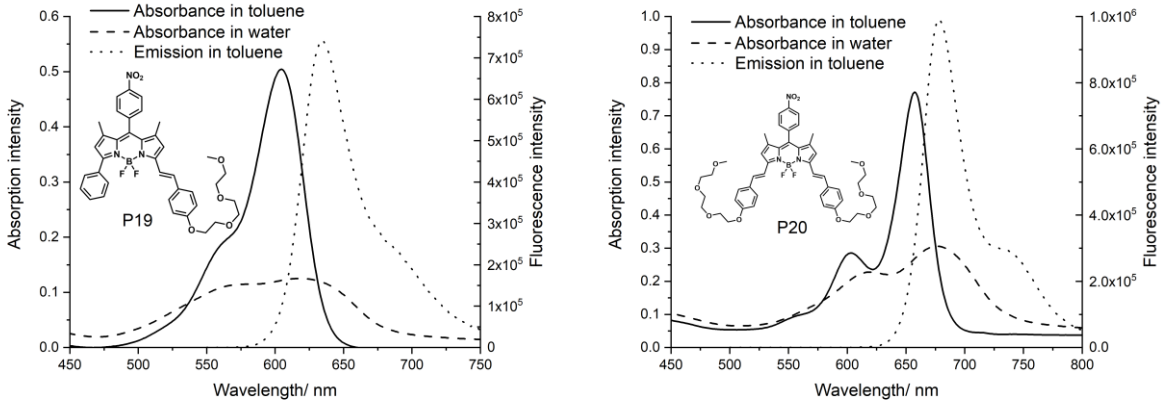

Figure 28 Absorption and emission spectra of nitro-BODIPY probes P11-20.

Table 7 Photophysical properties of nitro-BODIPY probes P11-20.

Probes	λ_{abs} in toluene	λ_{em} in toluene	λ_{abs} in water	λ_{em} in water
P11	530 nm	559 nm	547 nm	quench
P12	573 nm	622 nm	584nm	quench
P13	581nm	642 nm	595 nm	quench
P14	634 nm	650 nm	645 nm	quench
P15	604 nm	634 nm	613 nm	quench
P16	613 nm	646 nm	625 nm	quench
P17	625 nm	703 nm	617 nm	quench
P18	583nm	604 nm	585 nm	quench
P19	604 nm	635 nm	621 nm	quench
P20	657 nm	679 nm	675 nm	quench

As with the probes **P1**-**P10**, all the probes were quenched in water and were emissive in toluene solution. Significantly, their absorption and emission spectra exhibited enhanced red-shifted compared with probes **P1**-**P10** which indicates that, as predicted, the expanded conjugated structure does enhance this response. In comparison to probes **P11**-**P13**, the absorption spectra and emission spectra of **P12** and **P13** exhibit a stronger red-shifted than that of **P11** because the double bond linkage plays an important role in extending the conjugated structure. Similarly, probe **P14** exhibited stronger red-shifted than **P15** and **P16** because **P14** contains two conjugated double bonds to connect the BODIPY core and the auxochromic group.

Table 8 Images of plant cells incubated with nitro-BODIPY probes P11-P20.

Probe	Structure	Image
P11	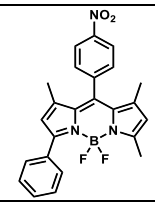	Ex 530 nm, Em540-575 nm 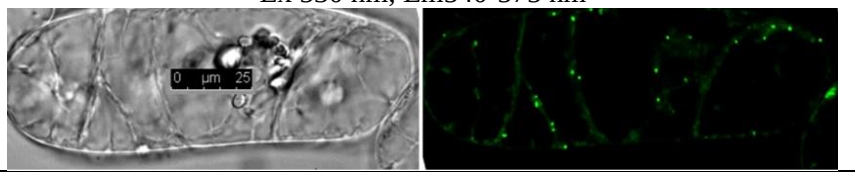
P12	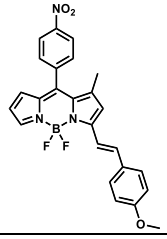	Ex 580 nm, Em610-630 nm 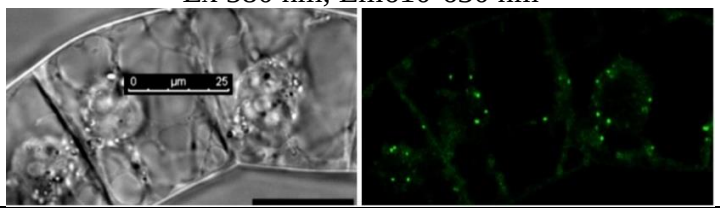
P13	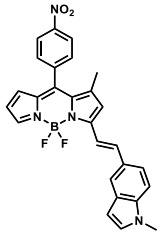	Ex 580 nm, Em 590-656 nm 
P14	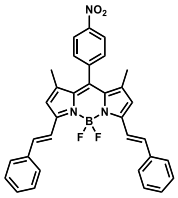	Ex 561 nm 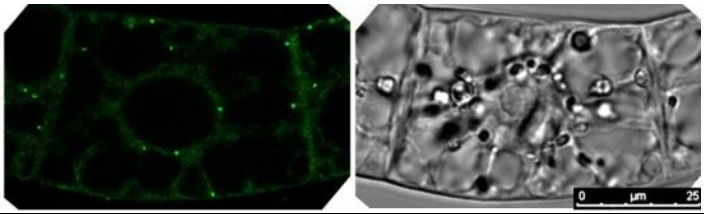
P15	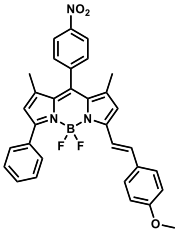	Ex 530 nm, Em 540-590 nm 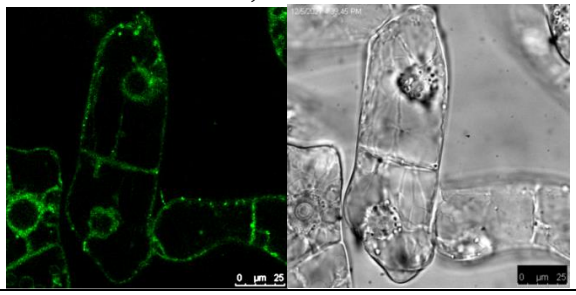
P16	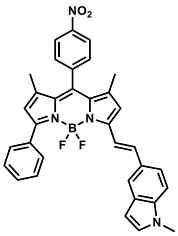	Ex 610 nm, Em 620-665 nm 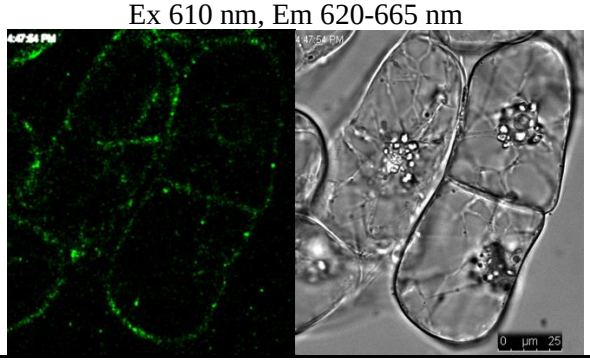

P17	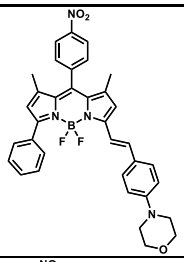	Ex 630 nm, Em 640-670 nm 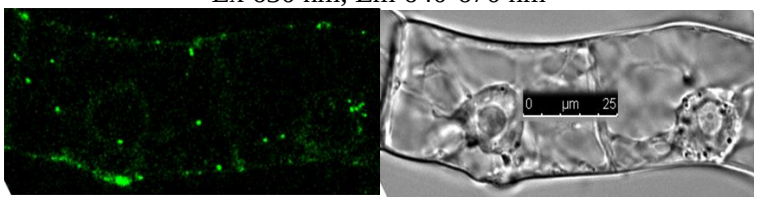
P18	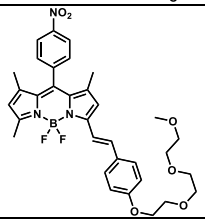	Ex 561 nm 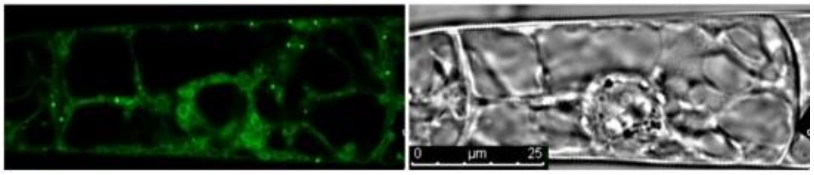
P19	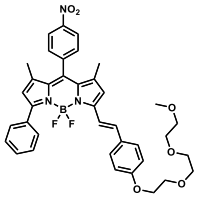	Ex 630 nm, Em 640-670 nm 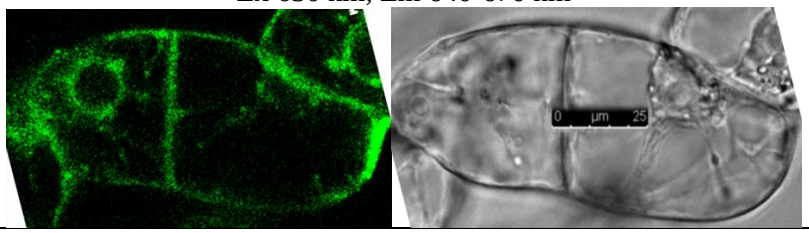
P20	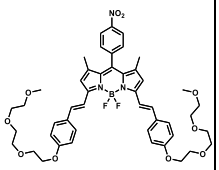	Ex 594 nm 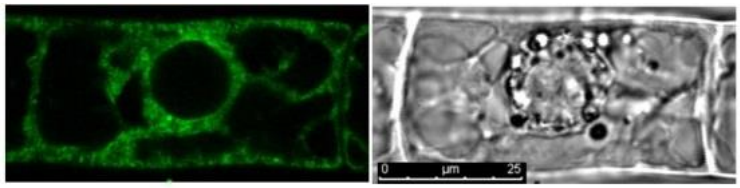

The plant cell images of the nitro-BODIPY probes **P11-20** are collected in Table 8. For this group of probes, because of their different excitation wavelengths different wavelengths were used to excite them. From the images of **P11-14**, bright fluorescent spots could be distinguished, indicating that these probes could localize to peroxisomes and that the substituent groups on position 3 of nitro-BODIPY does not affect this function.

From the images of **P15-17**, bright fluorescent spots corresponding to the peroxisomes could be observed. In addition, some smaller bright fluorescent spots were observed as well. The sharp discrete nature of these other spots suggested that these were not random background. Moreover, the size being much smaller than the spots attributed to peroxisomes led to the conclusion that **P15-17** potentially localize to somewhere else besides peroxisomes. This phenomenon might be caused by their bulky structure which enable probes **P15-17** to bind to other unknown targets.

Of the PEG based nitro-BODIPY probes (**P18-20**), **P18** could target peroxisomes selectively and be easily observed in contrast to **P19** and **P20** for which it was difficult to distinguish

peroxisome labelling from fluorescent background. In the image for **P19**, a large amount of small bright fluorescent spots similar to that seen for **P15-17** were found. This is potentially accounted for by the fact that **P19** contains an additional PEG chain suggesting that PEG chains enhance background noise by enabling more efficient transport through the membrane.

In summary, red-shifted nitro-BODIPY probes **P11-14** and **P18** fit the requirements as plant cell peroxisomes probes. Probes **P15-17** could detect peroxisomes, but with lower selectivity and higher background noise and probes **P18-19** cannot label peroxisomes.

3.2.3 Meso-phenyl-BODIPY probes

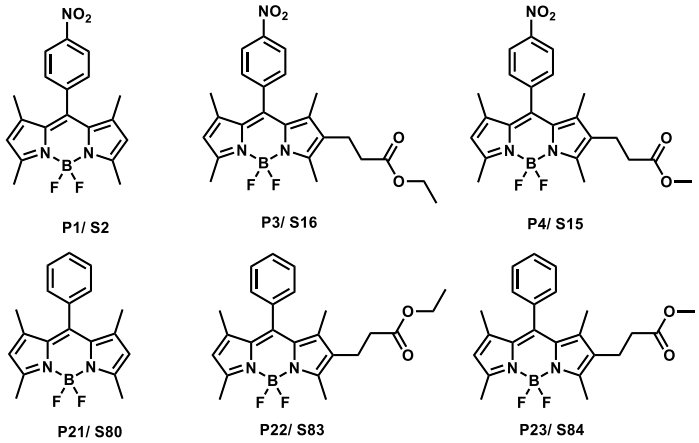

Figure 29 Meso-phenyl-BODIPY probes P21-23.

As mentioned in Section 3.1.4, nitro-BODIPYs are intrinsically non-fluorescent but on incubation with plant cells become fluorescent at peroxisomes. To explore how the nitro group affects localization phenomenon, a control group of meso-phenyl-BODIPYs (**P21**-**P23**, equal to **S80**, **S83** and **S84** in Section 3.1) without a nitro group were prepared and analysed as before. The photophysical properties of BODIPY probes **P21**-**23** were measured and are collected in Fig 30 and Table 9.

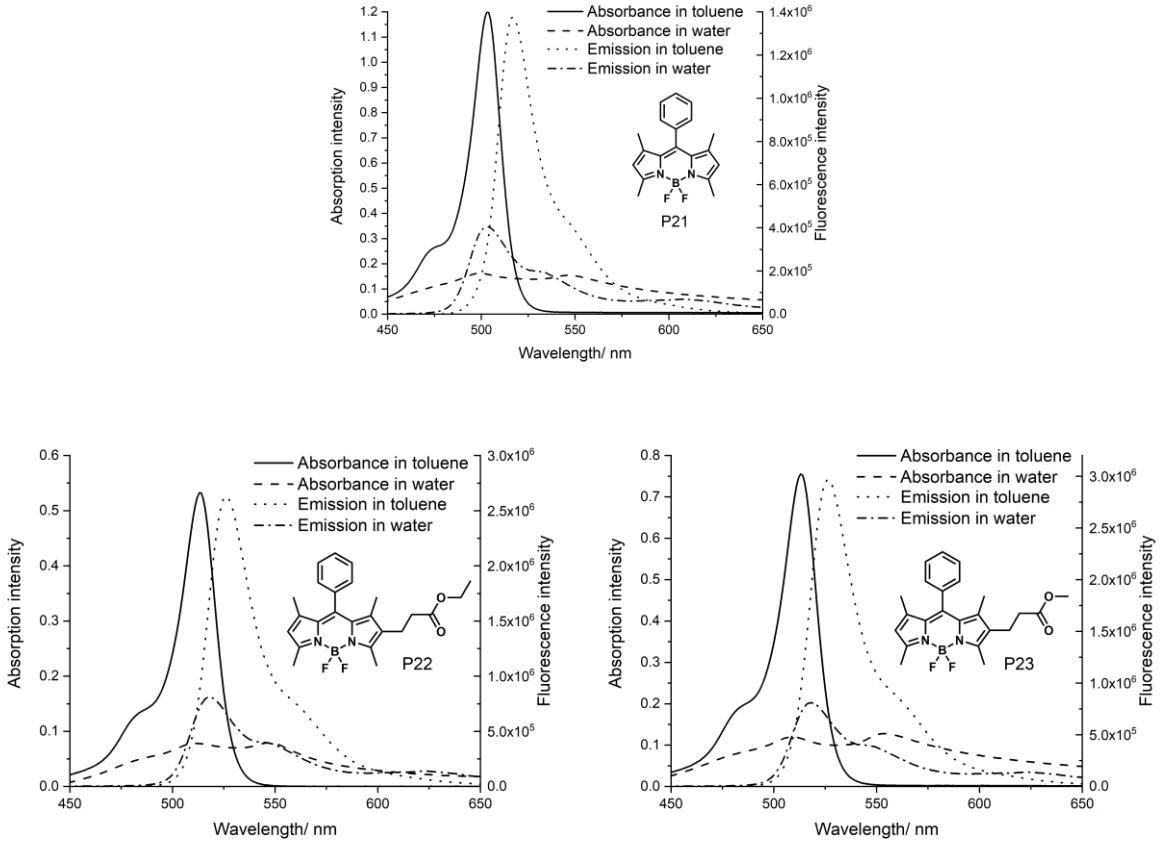

Figure 30 Absorption and emission spectra of BODIPY probes P21-23.

Table 9 Photophysical properties of BODIPY probes P21-23 and their control probes.

Probes	λ_{abs} in toluene	λ_{em} in toluene	λ_{abs} in water	λ_{em} in water
P21	504 nm	518 nm	500 nm	504 nm
P22	513 nm	527 nm	509nm	518 nm
P23	513 nm	527 nm	509 nm	518 nm
P1	508 nm	528 nm	501 nm	quench
P3	518 nm	539 nm	517 nm	quench
P4	518 nm	541 nm	515 nm	quench
P5	518 nm	544 nm	514 nm	quench

In comparison to nitro-BODIPY probes (**P1**, **P3-5**), this control group of probes (**P21-23**) exhibited similar absorption and emission spectra in toluene but were not quenched in water solution. Therefore, this control group of probes could illuminate somewhere else they localise in a plant cell besides peroxisomes. Given the structural similarities to nitro-BODIPY probes **P1** and **P3-5**, their plant cell imaging could possibly expose potential localization targets of nitro-BODIPY besides peroxisomes.

Table 10 Images of plant cells incubated with BODIPY probes P21-P23 and their control probes.

Probe	Structure	Image
P1	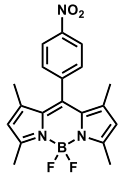	Ex 488 nm 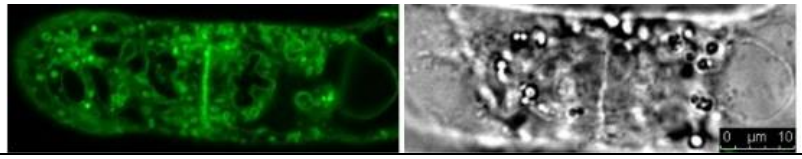
P3	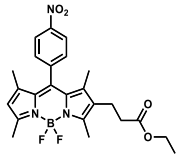	Ex 488 nm 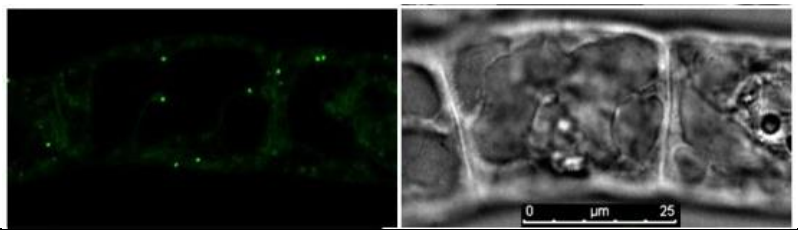
P4	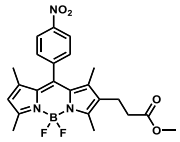	Ex 488 nm 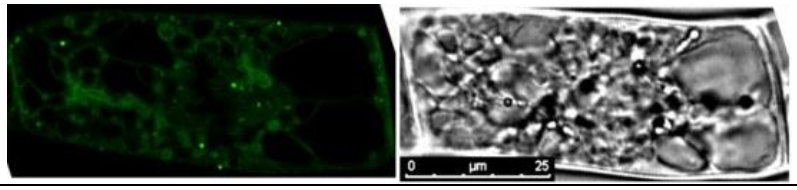
P5	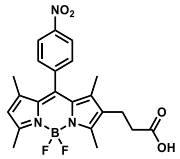	Ex 488 nm 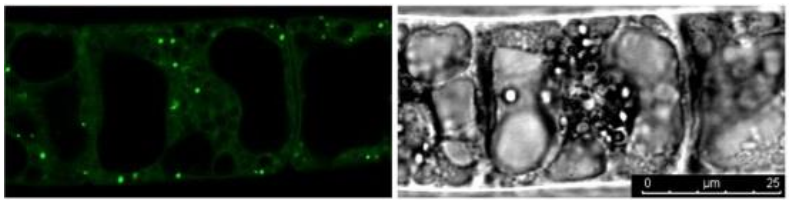
P21	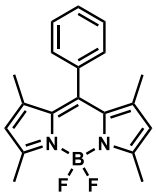	Ex 510 nm 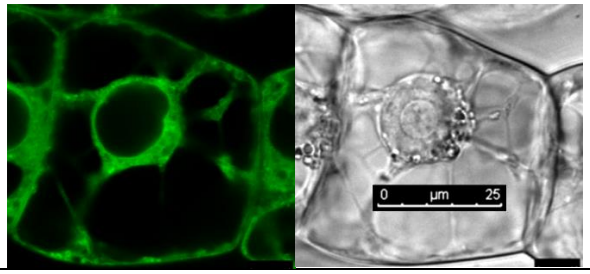
P22	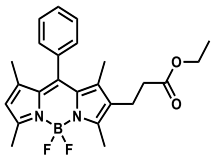	Ex 510 nm 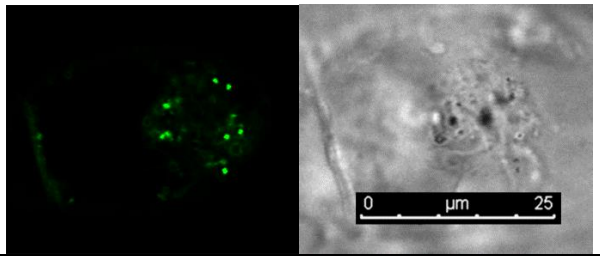
P23	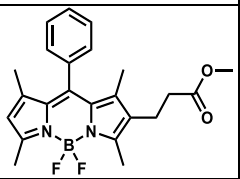	Ex 510 nm

			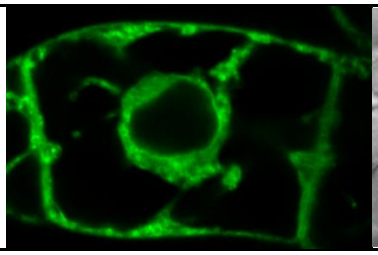	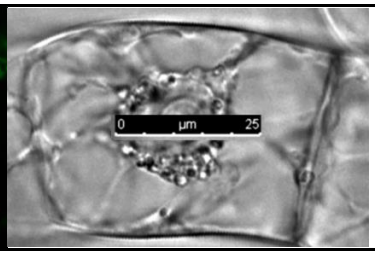

The plant cell images following incubation with BODIPY probes **P21-23** are collected in Table 10. From images obtained using **P21** and **P23**, it was difficult to distinguish peroxisomes labelling from the bright background. Consequently, it was not possible to conclude they label peroxisomes or not. Unexpectedly, probe **P22** labelled peroxisomes selectively with a clear background, which was quite different from the original prediction. This probe showed sharp bright fluorescence when it localized in peroxisomes and was quenched everywhere in plant cell, indicating that a BODIPY without a nitro group might bind and selectively report peroxisomes. To further understand probe **P22**, this result was compared with results from **P1** and **P3-5**. It was surprising to find that probe **P3** gave a clearer background than the others. The only difference between **P3** and **P22** is a nitro group which has previously been shown to play a role in quenching BODIPY fluorescence. These observations together with the background fluorescence observed with the free acid and methyl ester analogies suggests that the ethyl ester linker at position 2 of BODIPY uniquely contribute to localisation in the peroxisomes. Whilst this conclusion is difficult to rationalise on a structural basis such aryl-BODIPYs containing this ethyl propanoyl ester linkers show promise to become another family of interesting probes for peroxisomes.

3.2.4 Red-shifted fluorophore-nitro-BODIPY probes

As discussed in Section 2.2, a dual nitro-BODIPY with second fluorophore could be used to determine whether nitro-BODIPY only localizes at peroxisome or somewhere else. In order to explore nitro-BODIPY's physiological behaviours outside of peroxisomes, two sets of dual-fluorophore probes were designed. The first set of probes are assembled by nitro-BODIPY structure coupled to a fluorophor (Rodamine B, Cy 5 etc) whose excitation/emission wavelength is more red-shifted than nitro-BODIPY. In parallel, the second set of probe is assembled with the second fluorophor (NBD, Dansyl etc) whose excitation/emission wavelength is more blue-shifted than nitro-BODIPY. For a molecule containing two different fluorophores, Förster resonance energy transfer (FRET) processes sometimes happens. Depending on whether FRET happens, these two sets of dual-fluorophore probes will exhibit different visual results.

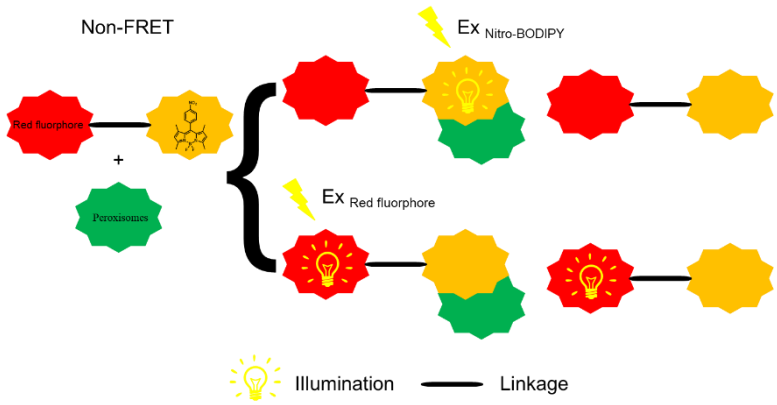

Figure 31 Non-FRET red-shifted fluorophore-nitro-BODIPY probes' localization at plant peroxisomes.

For the first set of probes, in the absence of FRET, the hypothetic visual results is shown on Fig 31. For peroxisome bound probe, on excitation of the nitro-BODIPY, the nitro-BODIPY moiety will emit and the red-shifted fluorophore part will be silent. In contrast probes outside of peroxisomes will be silent. On excitation of the 'red-shifted' fluorophore, the nitro-BODIPY component of a peroxisomal localised probe will be silent and emission for the red-shifted fluorophore will be observed for both peroxisomal bound and free probe.

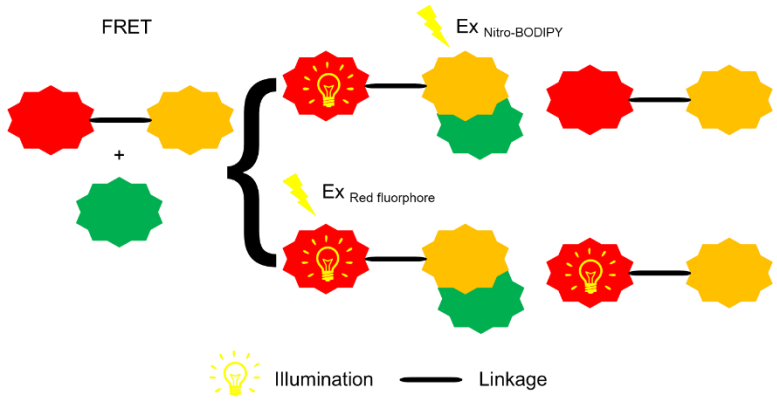

Figure 32 FRET red-shifted fluorophore-nitro-BODIPY probes' localization at plant peroxisomes.

If FRET happens, the hypothetic visual results is shown in Fig 32. On excitation of the nitro-BODIPY, the nitro-BODIPY unit of a peroxisome bound probe will be excited and FRET to the red-shifted fluorophor will occur. Meanwhile probes outside of peroxisomes will remain silent. On the excitation of the red-shifted fluorophor, both bound and unbound probes will show the emission of red-shifted fluorophor.

In the beginning, two nitro-BODIPY-Rhodamine B probes **P24-25** (equal to **S102** and **S103** in Section 3.1) and two Rhodamine B reporters **P26-27** (equal to **S90** and **S91** in Section 3.1) as a comparison were prepared as shown in Fig 33.

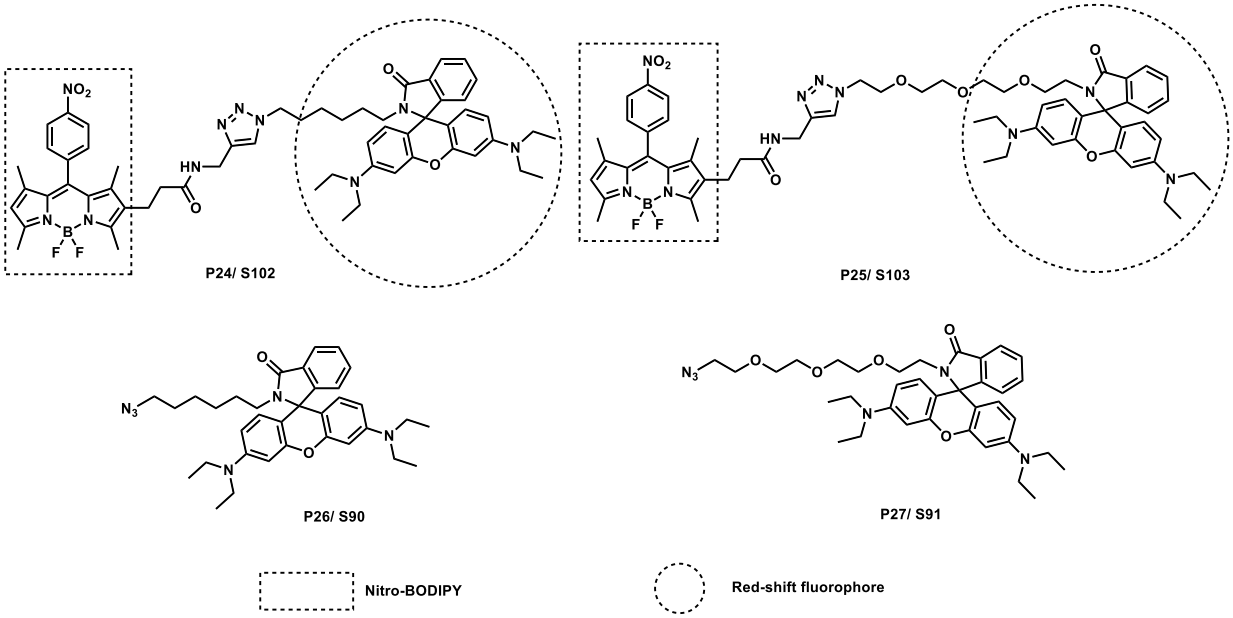

Figure 33 Dual-fluorophore probes P24-25 and Rhodamine B analogs P26-27.

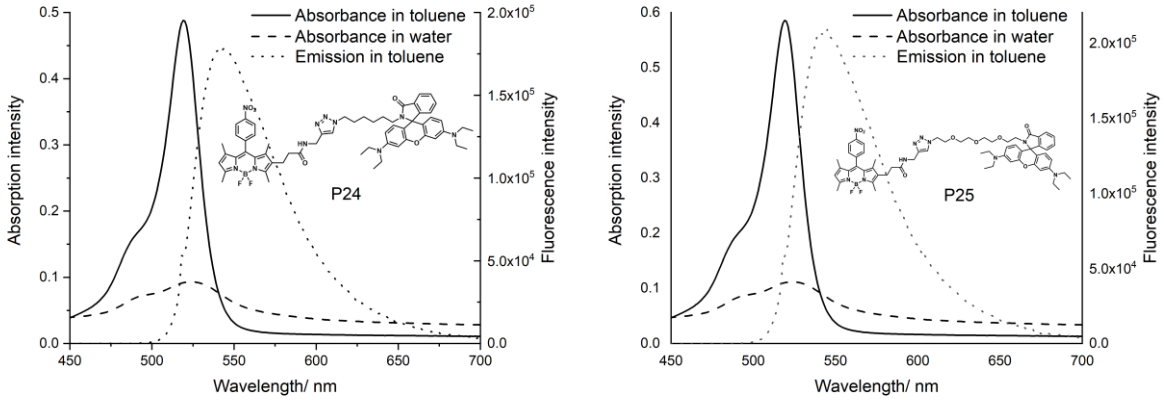

Figure 34 Absorption and emission spectra of dual-fluorophore probes P24-25.

Table 11 Photophysical properties of dual-fluorophore probes P24-25.

Probes	λ_{abs} in toluene	λ_{em} in toluene	λ_{abs} in water	λ_{em} in water
P24	519 nm	545 nm	526 nm	quench
P25	519 nm	545 nm	526nm	quench

In the absorption spectra of **P24** and **P25**, Fig 34 and Table 11, one strong signal of nitro-BODIPY at 519 nm in toluene solution and another signal for nitro-BODIPY at 526 nm in water solution could be found but the expected absorption peak of Rhodamine at around 540-550 nm disappeared. From the emission spectra in toluene, an emission peak of nitro-BODIPY at 542 nm could be observed. However, no evidence of Rhodamine B's signal at around 560-570 nm could be seen. Moreover, both probes **P24** and **P25** were quenched in water solution regardless of irradiation frequency (excited by 526 nm (λ_{ex} of nitro-BODIPY) or 550 nm (λ_{ex} of Rhodamine B). These spectra indicates that all absorption and emission signals of Rhodamine B disappeared because cyanamide on the rhodamine spirolactam framework shows a reversible ring-opening/ring-closure process in response to the solution pH, which exhibits an 'ON/OFF' switching in its fluorescence and absorption[113], as shown in Scheme 43.

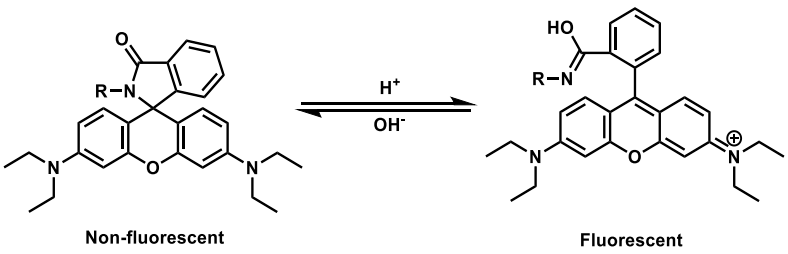

Scheme 43 Reversible ring-opening/ring-closure switching of Rhodamine.

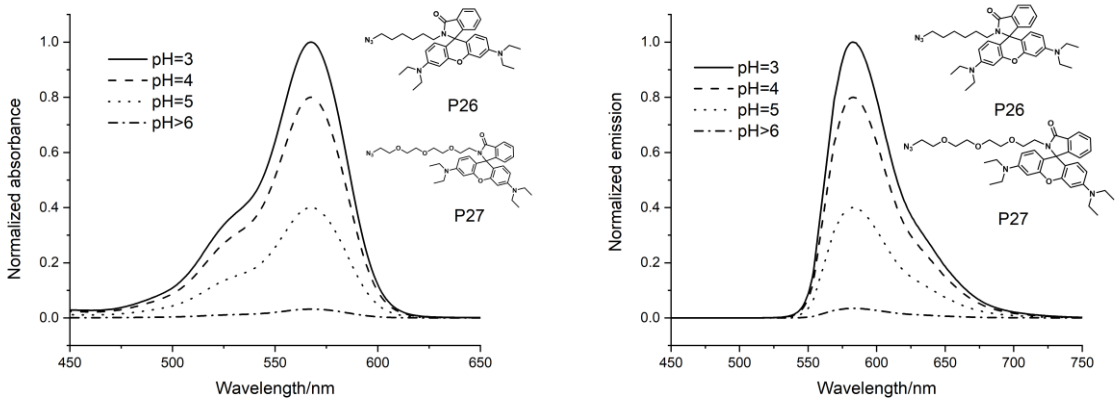

Figure 35 pH response of Rhodamine B analogs P26-27.

In order to verify the fluorescence of Rhodamine B in probes **P24** and **P25** were turned off, photophysical properties of control probes **P26** and **P27** were measured at progressively higher pH values leading to a corresponding decrease in intensity of their absorption and emission spectra (Fig 35). In conclusion, fluorescence of Rhodamine B in probes **P24-27** could be turned off when pH>5 so these probes cannot show signals of Rhodamine B in plant cell imaging experiments and therefore these two probes cannot fit our requirements for dual fluor plant cell imaging experiments.

Table 12 Images of plant cells incubated with dual-fluorophore probes P24-25.

Probe	Structure	Image
P24	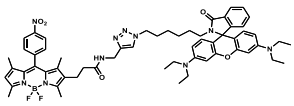	Ex 514 nm 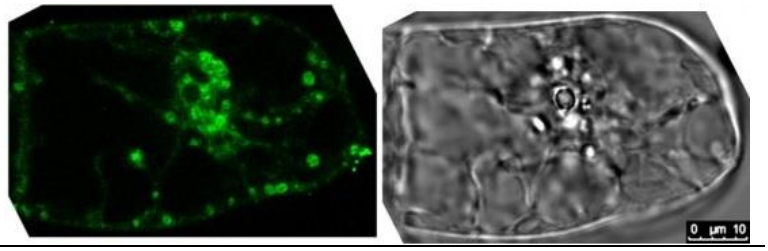
P25	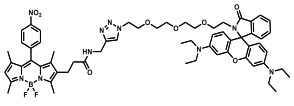	Ex514 nm 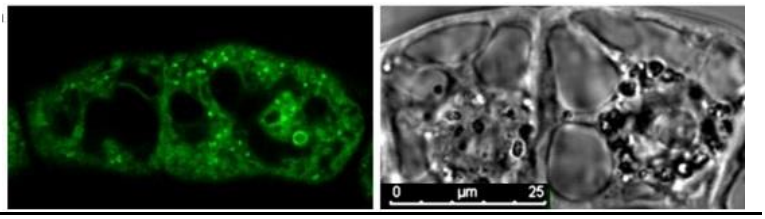

Although the Rhodamine B fluorophore in probes **P24-25** are not active under neutral condition, it was still of interest to observe their plant cell behaviour (Table 12). Both probes were membrane permeable and labelled peroxisomes successfully which indicates that the presence

of the linker and a second bulky fluorophore doesn't affect nitro-BODIPY selectivity and ability to report on peroxisomes. Although probe **P24**-**25** cannot be used to explore other localization of NITRO-BODIPY outside of the peroxisome, these results demonstrated that the modular molecular design of Dual-fluorophore probes is viable.

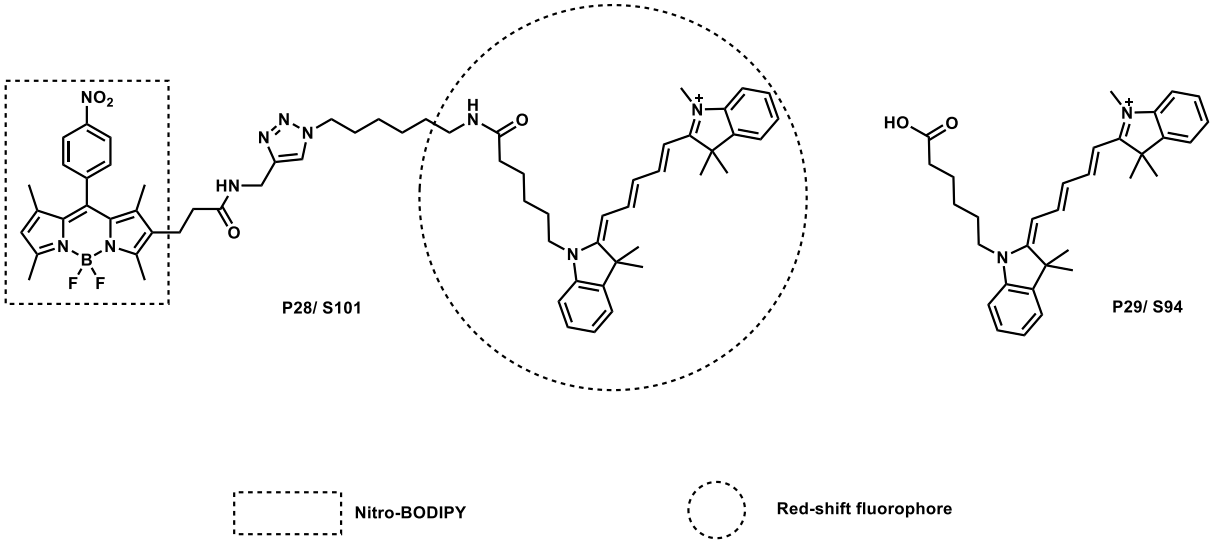

Figure 36 Dual-fluorophore probe P28 and control probe P29.

As **P24** and **P25** with an N linked Rhodamine B could not be used to determine other localizations of nitro-BODIPY an alternative "red" dual-fluorophore probe **P28** (equal to **S101** in Section 3.1) which contains nitro-BODIPY and Cy5 was prepared (Fig 36). The parent Cy5 linker (**P29**, equal to **S94** in Section 3.1) was also measured as a control probe (Fig 37 and Table 13).

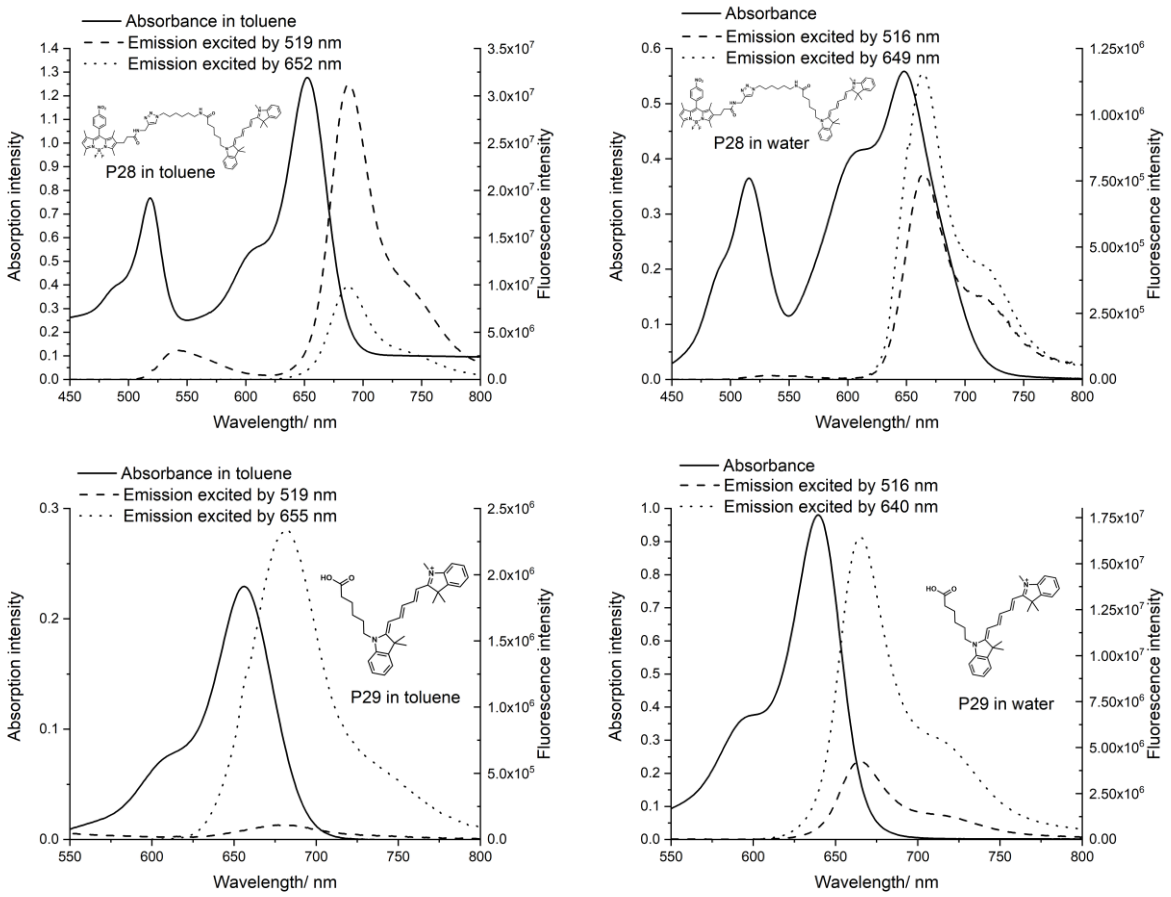

Figure 37 Absorption and emission spectra of dual-fluorophore probe P28 and control probe P29.

Table 13 Photophysical properties of dual-fluorophore probe P28 and control probe P29.

Probes	λ_{abs} in toluene	λ_{em} in toluene	λ_{abs} in water	λ_{em} in water
P28	519 nm/ 652 nm	543 nm & 689 nm (excited by 519 nm) 689 nm (excited by 652 nm)	516 nm/ 649 nm	666 nm (excited by 516 nm) 666 nm (excited by 649 nm)
P29	655 nm	681 nm (excited by 519 nm) 681 nm (excited by 655 nm)	640nm	665 nm (excited by 516 nm) 665 nm (excited by 640 nm)

In toluene solution, probe **P28** exhibited two absorption signals, 519 nm for nitro-BODIPY and 652 nm for Cy5. On excitation at 652 nm, **P28** only exhibited one fluorescence signal corresponding to that of Cy 5 at 689 nm. In contrast, on excitation at 519 nm, the probe emitted a weak fluorescence signal of nitro-BODIPY at 543 nm and a strong one of Cy 5 at 689 nm , which suggested that partial FRET occurs with **P28**. In water solution, **P28** showed an absorption signal of nitro-BODIPY at 516 nm and another one of Cy 5 at 649 nm. It was expected that, as a FRET probe, in water solution, **P28** should be quenched on excitation at

516 nm but be emissive on excitation at 649 nm. However, a fluorescence signal of Cy 5 at 666 nm was observed at both excitation wavelengths. It was not obvious why FRET effects could be observed in both toluene and water. To understand this, the photophysical properties of control probe **P29** in both toluene and water solution were then measured. This revealed that the absorption profile for Probe **P29** was broad with excitation possible at both 655 and 519 nm in toluene and 640 nm and 516 nm in water. With this observation it was not possible to assign the emission at 665-689 nm as arising from FRET from BODIPY to Cy5 which challenges the use of this probe to explore peroxisome localization as planned.

Table 14 Images of plant cells incubated with dual-fluorophore probe P28 and control probe P29.

Probe	Structure	Image
P28	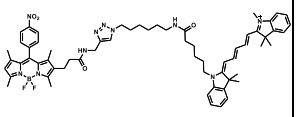	Ex 512 nm, no fluorescence around Em 550 nm Em 640-660 nm 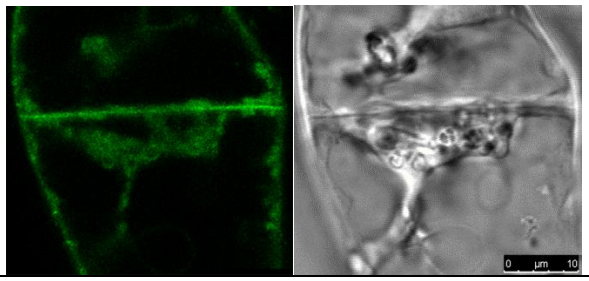
P29	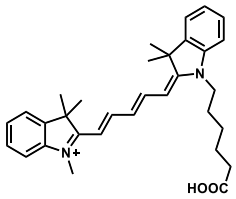	Ex 651 nm, Ex 660-680 nm 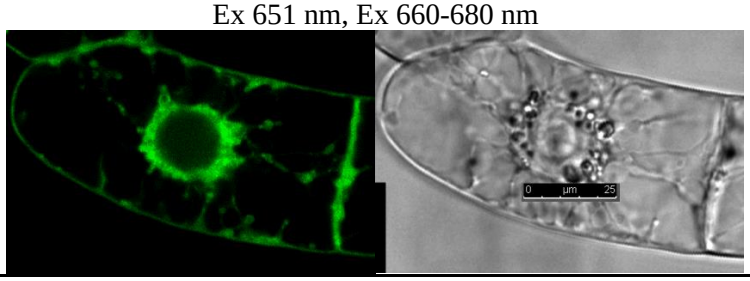

Concurrent with the fluorescence studies, the localisation of probes **P28** and its control probe **P29** (Cy5) were studied (Table 14). Initially plant cells incubated with probe **P28** were excited at 512 nm. When using an optical filter at 550 nm, no fluorescence was observed whilst , when using a filter at 650 nm, non specific fluorescence could be observed without any obvious labelling of peroxisomes. Similarly the control probe **P29** stained the whole cell with no apparent selectivity. In conclusion, probe **P28** did not show any selectivity towards peroxisomes so alternative dual-fluorophore probes with a different wavelength combination were required.

3.2.5 Blue-shift fluorophore-nitro-BODIPY-probes

In consideration of the non-ideal results of 'red' fluorophor-nitro-BODIPY probes **P25-26** and **P28** in plant imaging experiments, a molecular assembly of nitro-BODIPY with a fluorophor (Dansyl or NBD) whose excitation/emission wavelength is more blue-shift than nitro-BODIPY was then explored.

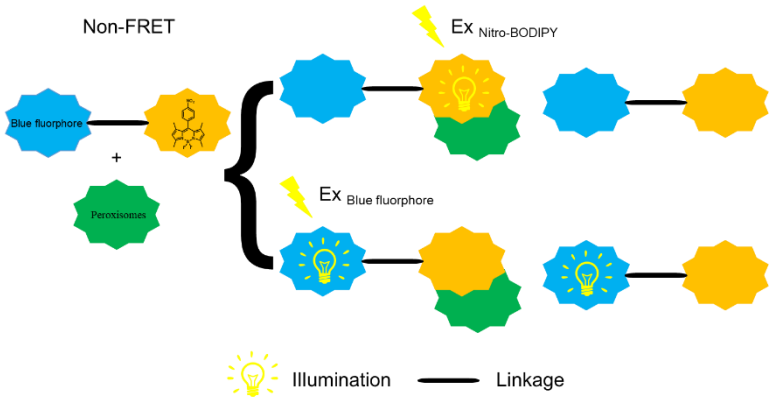

Figure 38 Non-FRET blue-shift fluorophore-nitro-BODIPY probes' localization at plant peroxisomes.

For the non-FRET Blue-shift fluorophor-nitro-BODIPY probes, the hypothetic visual results is shown on Fig 38. On excitation of nitro-BODIPY's wavelength, the nitro-BODIPY unit bound with peroxisomes will illuminate whilst the blue-shift fluorophor part will be silent. Meanwhile unbinded probes outside of peroxisomes will be silent. On excitation of blue-shift fluorophor's wavelength, the bound nitro-BODIPY part will be silent and all the probes will illuminate the fluorescence of blue-shift fluorophor and show a fluorescent background.

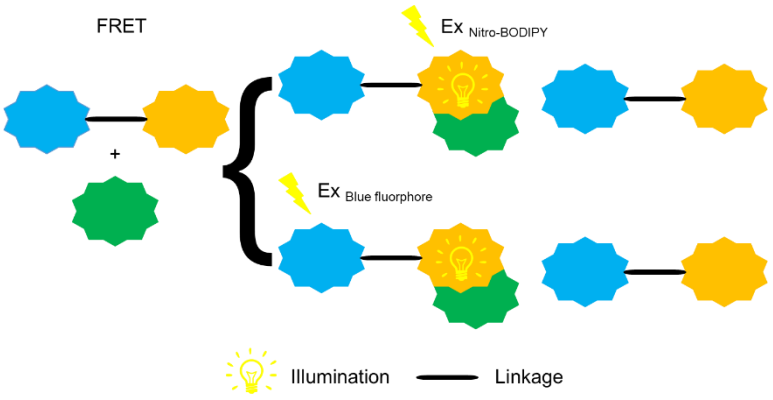

Figure 39 Non-FRET blue-shift fluorophore-nitro-BODIPY probes' localization at plant peroxisomes.

If FRET occurs, the hypothetic visual results is shown on Fig 39. On excitation of blue-shift fluorophore, the blue-shift fluorophore part of a peroxisome bound probe will be excited and FRET to the nitro-BODIPY will occur. Meanwhile probes outside of peroxisomes will remain silent. On the excitation of the nitro-BODIPY, the nitro-BODIPY part of a peroxisome bound probe will illuminate and unbinded probes outside of peroxisomes will be silent.

As shown in Fig 40, at first, we designed and synthesised dual-fluorophore probe **P30** (equal to **S100** in Section 3.1) which contains nitro-BODIPY and Dansyl as two different fluorophores. A simple dansyl probe (**P31**, equal to **S98** in Section 3.1) was also measured as a control probe (Fig 41 and Table 15).

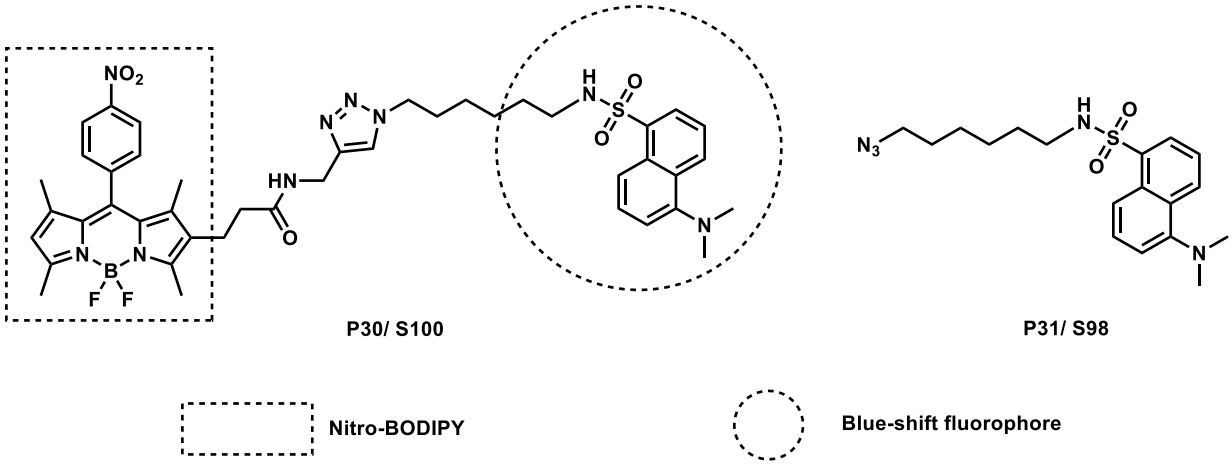

Figure 40 Dual-fluorophore probe P30 and control probe P31.

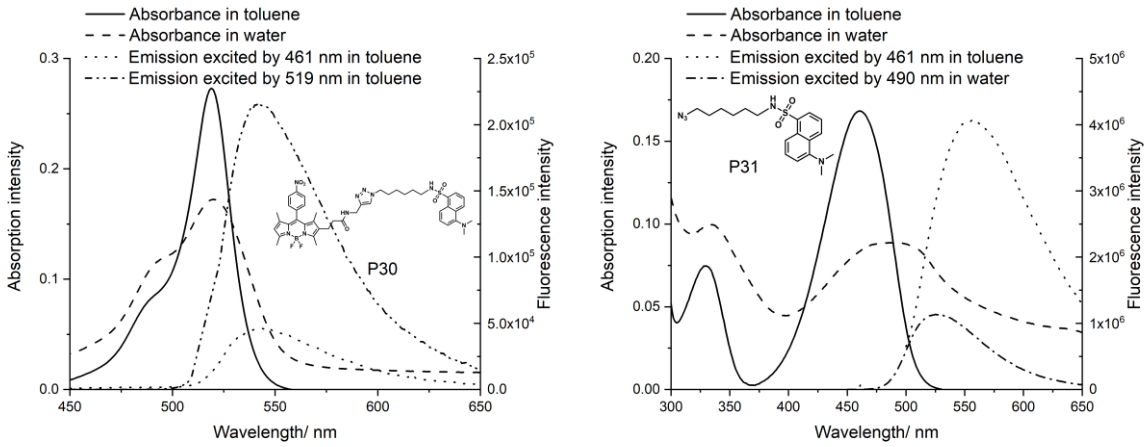

Figure 41 Absorption and emission spectra of dual-fluorophore probe P30 and control probe P31.

Table 15 Photophysical properties of dual-fluorophore probe P30 and control probe P31.

Probes	λ_{abs} in toluene	λ_{em} in toluene	λ_{abs} in water	λ_{em} in water
P30	519 nm	543 nm (excited by 461 nm) 543 nm (excited by 519 nm)	520 nm	quench
P31	461 nm	556 nm	490 nm	527 nm

Dansyl probe **P31** illuminated a fluorescence signal at 556 nm on excitation at 461 nm in toluene solution and at 527 nm on excitation at 490 nm in water solution. On excitation at 461 nm or 519 nm in toluene, Dual-fluorophore probe **P30** only exhibited a fluorescence response due to the nitro-BODIPY at 543 nm with no signal arising from the dansyl part. In addition, probe **P30** was quenched in water on excitation at either 490 nm or 520 nm indicating that **P30** is a FRET probe.

Based on these observations it was predicted that the illuminating model in plant cell imaging experiments of Dual-fluorophore probe **P30** is shown in Fig 41a. However, no discrete fluorescent spots consistent with selective labelling of the peroxisome were observed on incubation of **P30** in plant cell (Table 16). So this probe cannot localize to peroxisomes because the dansyl part will affect nitro-BODIPY's labelling selectivity to peroxisomes.

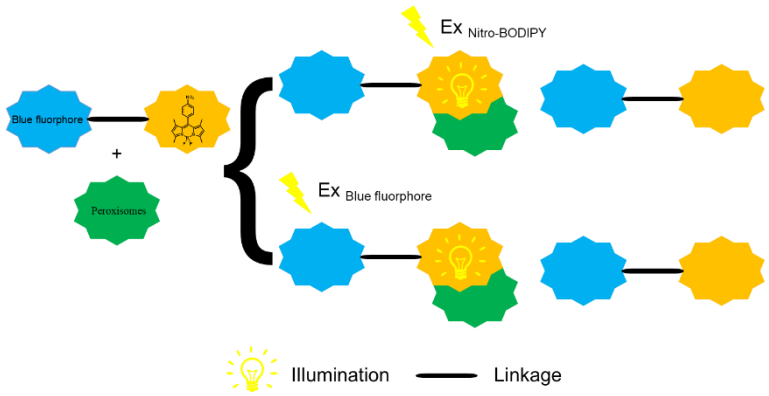

Figure 41a Predicted illuminating behaviors of dual-fluorophore probe P30 in plant cells.

Table 16 Images of plant cells incubated with dual-fluorophore probe P30.

Probe	Structure	Image
P30	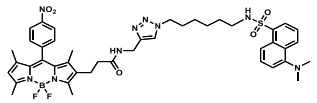	Ex 514 nm 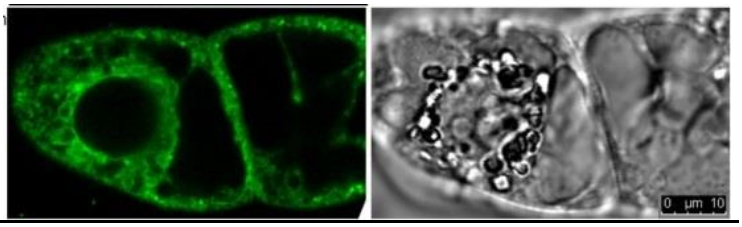

As FRET between the two fluors proved problematic we then wanted to explore probes in which FRET did not occur. Many factors can influence FRET efficiency, since several primary conditions must be satisfied for FRET to occur. The donor and acceptor molecules must be in close proximity to one another, typically 10-100 Å (1-10 nm). FRET efficiency (E) is defined by the equation $E = R_0^6/(R_0^6 + r^6)$, where R_0 is the Förster radius, and r is the actual distance between the donor and acceptor molecules. The Förster radius is the distance at which 50% of the excitation energy is transferred from the donor to the acceptor, and the R_0 value usually lies between 10-100 Å. FRET pairs with an R_0 value towards the higher end of this range are often preferred due to the increased likelihood of FRET occurrence. The absorption or excitation spectrum of the acceptor must overlap the fluorescence emission spectrum of the donor (Fig 42). The degree to which they overlap is referred to as the spectral overlap integral (grey shaded region). The greater the degree of grey shaded region, the greater the likelihood FRET is to occur.

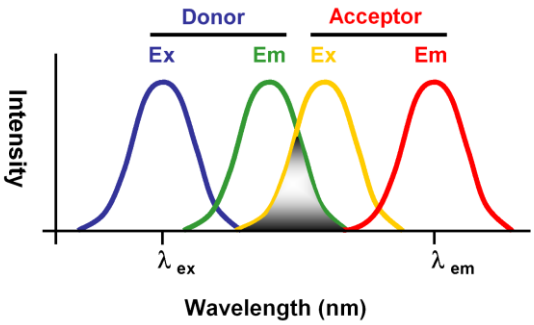

Figure 42 Schematic representation of the FRET spectral overlap integral (shown in gray shadow).

Two methods could potentially prevent FRET in these dual-fluorophorese probes. One is to increase the distance between the donor and acceptor molecules by lengthening the linkage between nitro-BODIPY and blue-shift fluorophore to greater distances than 100 Å. However,

as seen with Probe **P28**, longer aliphatic linkages can impede probe molecule transport across membranes. Consequently, to improve cytomembrane transport it was proposed to replace the aliphatic linkage by hydrophilic PEG chains. However, it was recognised that these PEG chains could affect probe localization. For instance, PEG containing Probes **P18**-**20** and **P25** localised to peroxisomes but this was accompanied by significant background illumination.

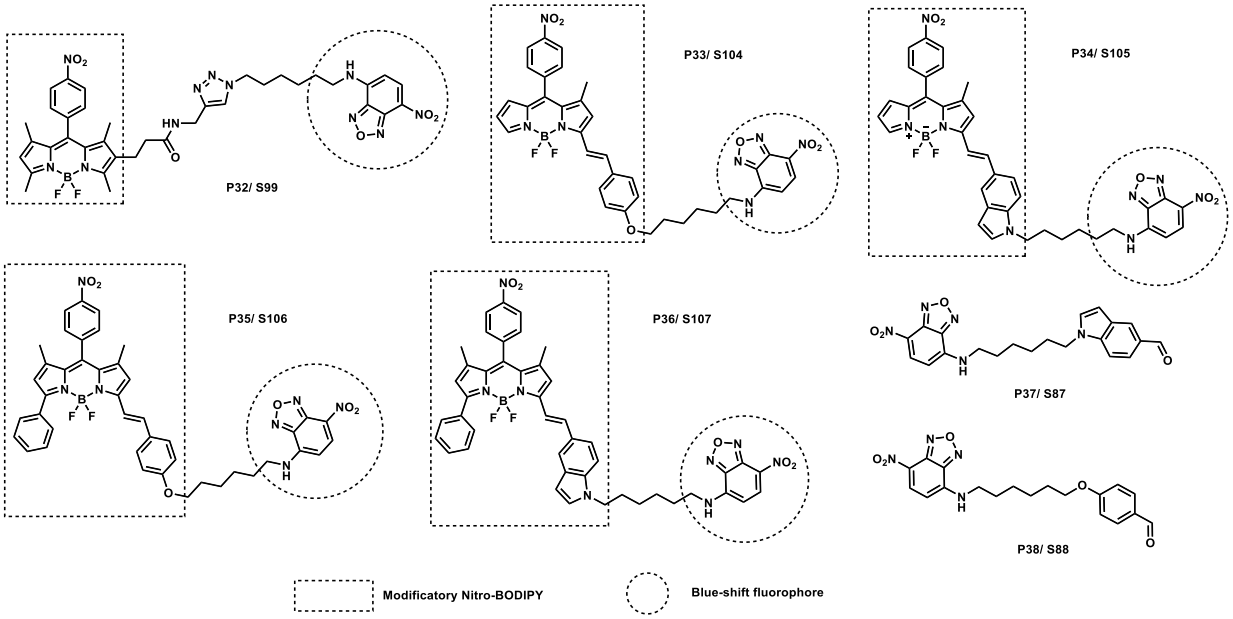

Figure 43 Dual-fluorophore probes P32-36 and control probes P37-38.

The alternative strategy is to modify the profile of the BODIPY to give better separation between the absorption and emission spectra of the donor and acceptor fluorophores respectively. As discussed in Section 3.2.2, a family of red-shifted nitro-BODIPYs including **P11**-**20** whose absorption and emission spectrum are much more red-shifted than the original nitro-BODIPY core had been prepared. It was hypothesised that, connecting these with blue-shifted fluorophore could address the problem of internal FRET. From the plant cell imaging of Probe **P30**, dansyl fluorophores potentially affect the localization selectivity of probe so another blue-shift fluorophore NBD was chosen. On this basis, dual-fluorophore probes **P32**-**36** (equal to **S99**, **S104**, **S105**, **S106** and **S107** in Section 3.1) which contains nitro-BODIPY and NBD as the two different fluorochromes were constructed and analysed with the two NBD analogues (**P37**-**38**, equal to **S87** and **S88** in Section 3.1) used as control probes (Fig 43).

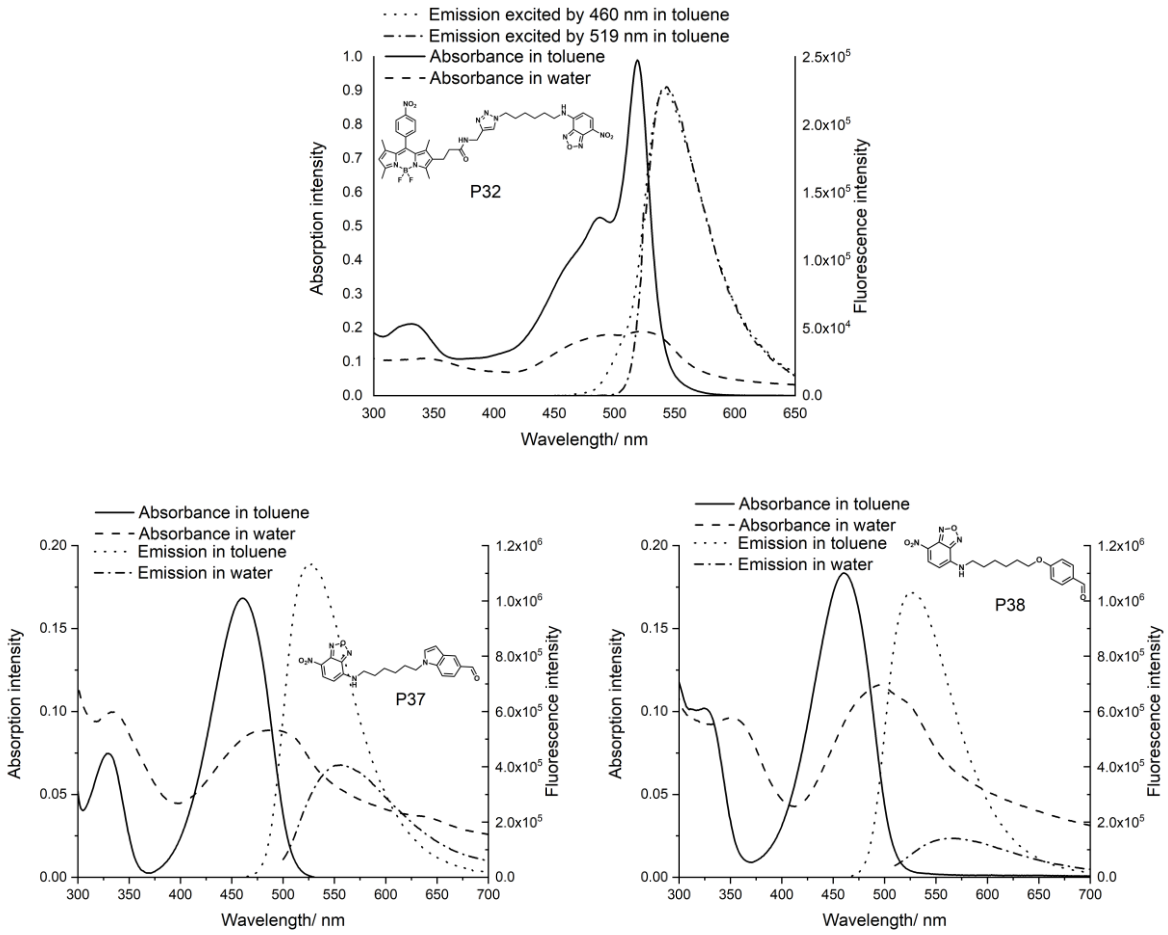

Figure 44 Absorption and emission spectra of dual-fluorophore probe P32 and control probes P37-38.

Table 17 Photophysical properties of dual-fluorophore probe P32 and control probes P37-38.

Probes	λ_{abs} in toluene	λ_{em} in toluene	λ_{abs} in water	λ_{em} in water
P32	519 nm	543 nm (excited by 460 nm) 543 nm (excited by 519 nm)	527 nm	quench
P37	460 nm	525 nm	489 nm	556 nm
P38	460 nm	530 nm	496 nm	565 nm

As shown in Fig 44 and Table 17, on excitation of 460 nm (NBD) or 519 nm (nitro-BODIPY) in toluene, dual-fluorophore probe **P32** only exhibited one fluorescence signal of nitro-BODIPY at 543 nm and were quenched in water on excitation of both 489 nm (NBD) and 527 nm (nitro-BODIPY) so it is a FRET probe similar to probe **P30**. The plant cell imagings of the dual-fluorophore probe **P32** and its control probe **P37-38** are collected in Table 18. Exploring this NBD probe in a plant cell revealed that the NBD unit did not affect localisation (verified

by ‘NBD only’ control probes 37 and 38) and this probe showed selective labelling of the peroxisome.

Table 18 Images of plant cells incubated with dual-fluorophore probe P32 and control probes P37-38.

Probe	Structure	Image
P32	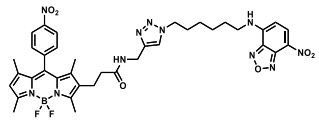	Ex 514 nm 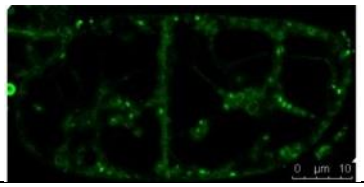
P37	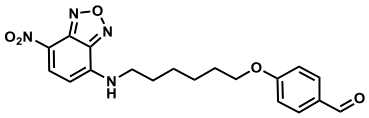	Ex 480 nm, Em 545-565 nm 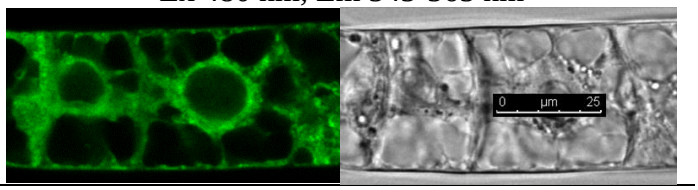
P38	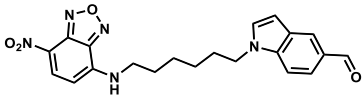	Ex 480 nm, Em 545-565 nm 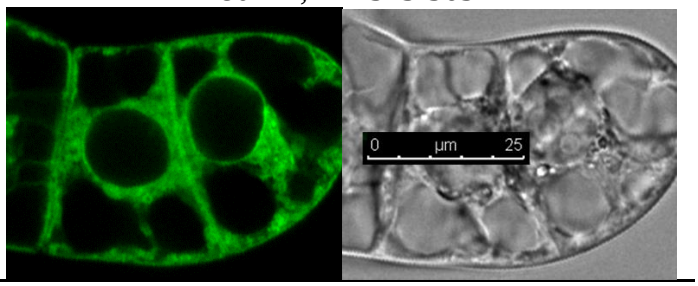

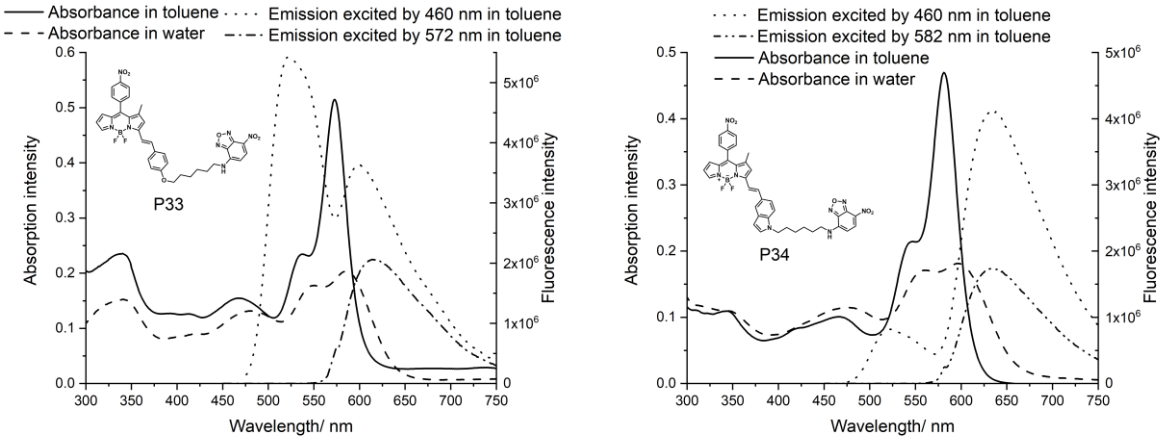

Figure 45 Absorption and emission spectra of dual-fluorophore probes P33-34.

Table 19 Photophysical properties of dual-fluorophore probes P33-34.

Probes	λ_{abs} in toluene	λ_{em} in toluene	λ_{abs} in water	λ_{em} in water
P33	460 nm/ 572 nm	525 & 601 nm (excited by 460 nm) 601 nm (excited by 572 nm)	475 nm/ 586 nm	quench
P34	460 nm/ 582 nm	518 nm & 636 nm (excited by 460 nm) 636 nm (excited by 582 nm)	478 nm/ 592 nm	quench

In contrast to **P32**, on excitation at 460 nm in toluene, probe **P33** exhibited two fluorescent signals, one due to the red-shifted Nitro-BODIPY at around 601 nm and one due to the NBD moiety at around 525 nm indicating that partial FRET occurs with this probe potentially (Fig 45, Table 19). Whilst a similar photophysical output was seen with P34. However, Probe **P33** and **P34** were fully quenched in water at all excitation wavelengths, suggesting that efficient FRET occurs in water solution. For these partial FRET probes **P33-34**, the predicted illumination model for a plant cell is shown in Fig 46. **P33** and **P34** potentially fit the requirement for plant peroxisomal imaging experiments because on excitation at 460nm (NBD), they will exhibit fluorescence signals of its two fluorophores which could be distinguished via an optical filter.

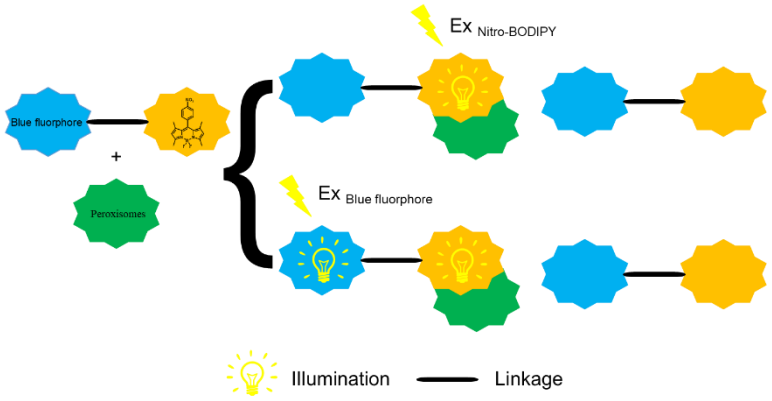

Figure 46 Predicted illuminating behaviors of dual-fluorophore probes P33-34 in plant cells.

Table 20 Images of plant cells incubated with dual-fluorophore probes P33-34 and control probes P12-13.

Probe	Structure	Image
P12	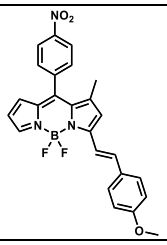	Ex 580 nm, Em610-630 nm 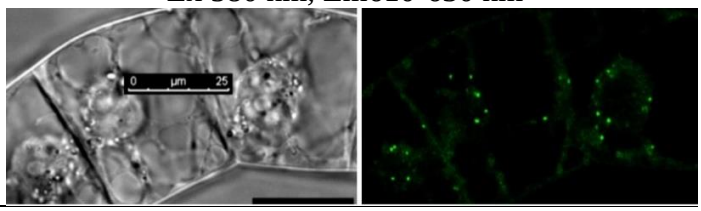
P13	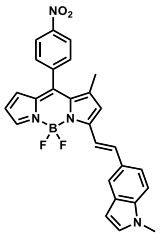	Ex 580 nm, Em 590-656 nm 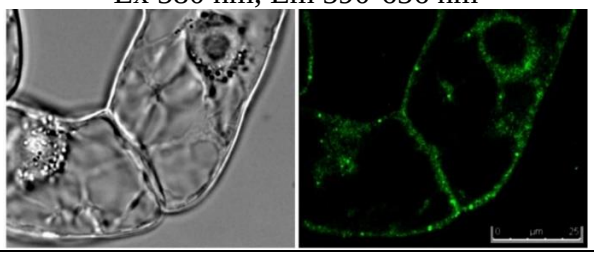
P33	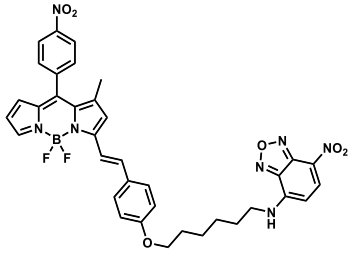	Ex 512 nm, Em 540-560 nm 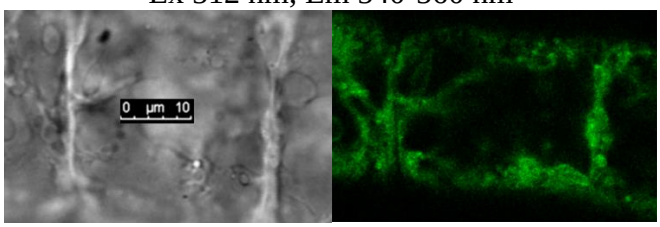 Ex 512 nm, Em 590-610 nm 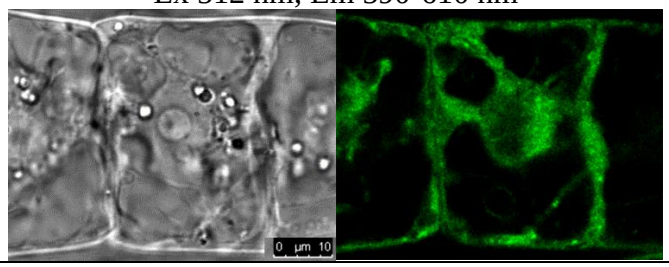
P34	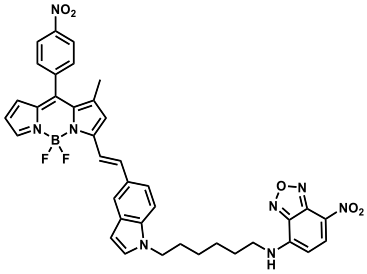	Ex 480 nm, Em 600-620 nm 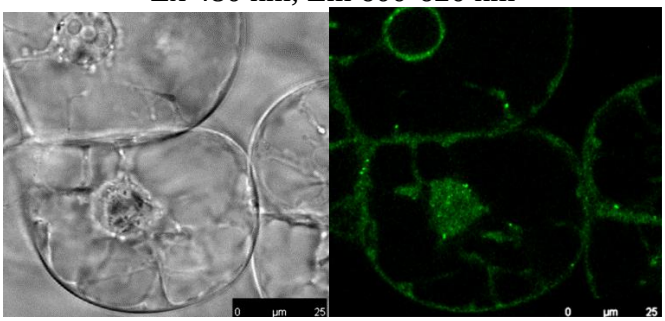 Ex 585 nm, Em 610-630 nm 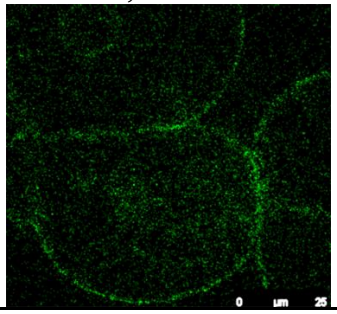

On excitation of the NBD chromophore, probe **P33** stained the whole plant cell but did not label peroxisomes no matter which optical filters (540-560 nm for NBD's emission, 590-610 nm for red-shifted nitro-BODIPY's emission) were used (Table 20). In contrast, probe **P34** containing an indole unity instead of the anisyl linker showed localisation to peroxisomes. The reasons for this structural dependency are not obvious as control probes **P12** and **P13** both show some selectivity towards peroxisomal labelling. Moreover, on excitation at 585 nm this probe identified a lot of tiny fluorescent spots were observed throughout the cell. This localisation or lack of thereof coupled with the much smaller size indicates that these are not peroxisomes and are an as yet unidentified cell component.

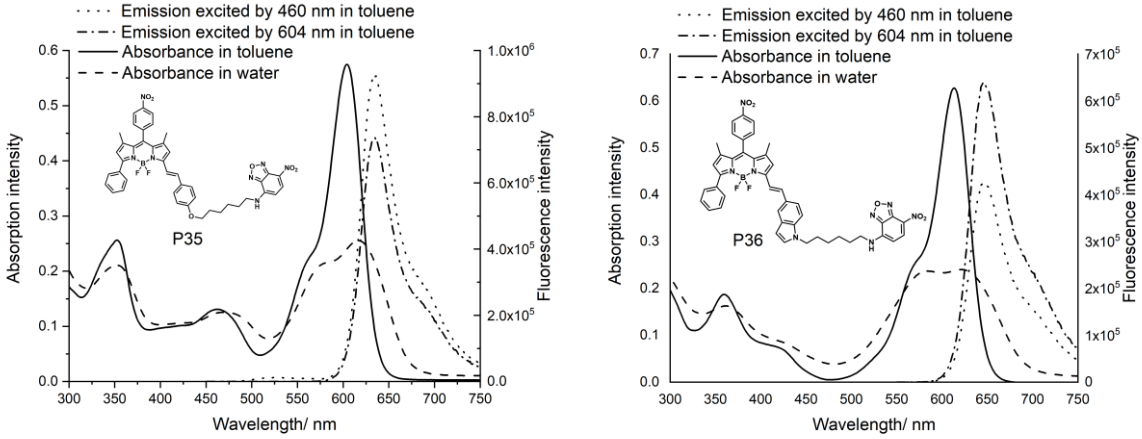

Figure 47 Absorption and emission spectra of dual-fluorophore probes P35-36.

Table 21 Photophysical properties of dual-fluorophore probes P35-36.

Probes	λ_{abs} in toluene	λ_{em} in toluene	λ_{abs} in water	λ_{em} in water
P35	460 nm/ 604 nm	634 nm (excited by 460 nm) 634 nm (excited by 604 nm)	477 nm/ 616 nm	quench
P36	460 nm/ 604 nm	646 nm (excited by 460 nm) 646 nm (excited by 604 nm)	625 nm	quench

A clearer FRET response (Fig 47, Table 21) was obtained with Probe **P35** and **P36** with longer BODIPY emission wavelengths. These probes exhibited only one fluorescence signal of red-shifted Nitro-BODIPY (on excited by 460 nm or 604 nm) in toluene solution and were, again, quenched in water solution suggesting these probes could be a family of red-shifted FRET probes for peroxisomes enable to be excited by blue-shift wavelength. For these FRET probes **P35-36**, the predicted illumination model for a plant cell is shown in Fig 48.

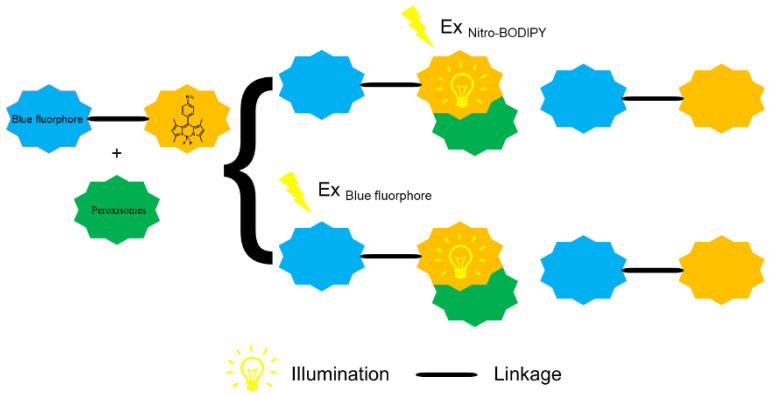

Figure 48 Predicted illuminating behaviors of dual-fluorophore probes P35-36 in plant cells.

Incorporating a Phenyl group at C-8 (**P15**,**16**,**35**,**36**) showed further unexpected divergence in labelling (Table 22). Nitro-BODIPYs **P15** and **P16**, as with **P12** and **P13**, label peroxisomes but show increased background staining. Similarly on excitation at 488 nm (NBD) both probes **P35** and **P36** could label peroxisomes whereas at 615 nm (red-shifted Nitro-BODIPY), many fluorescent spots were observed via a 670-690 nm optical filter. The origins of this latter output remain to be ascertained.

Table 22 Images of plant cells incubated with dual-fluorophore probes P35-36 and control probes P15-16.

Probe	Structure	Image
P15	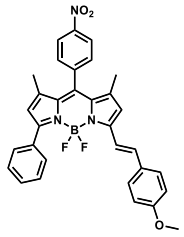	Ex 530 nm, Em 540-590 nm 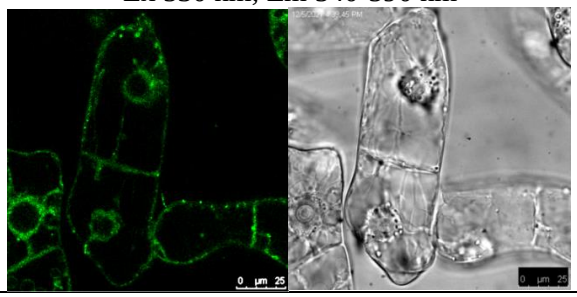
P16	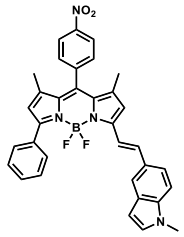	Ex 610 nm, Em 620-665 nm 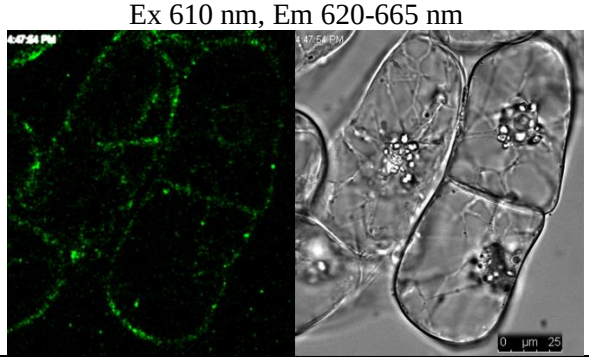
P35	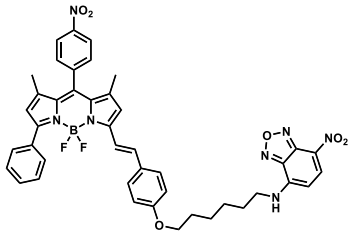	Ex 480 nm, Em 540-560 nm 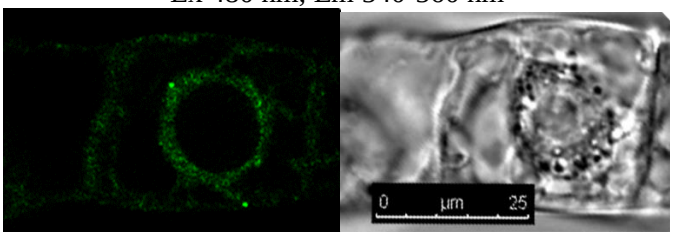 Ex 615 nm, Em 670-690 nm 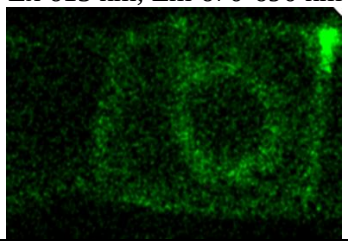
P36	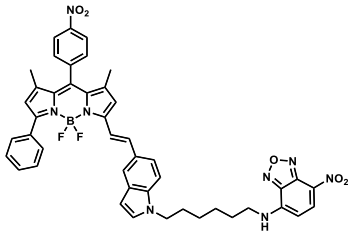	Ex 480 nm, Ex 540-560 nm 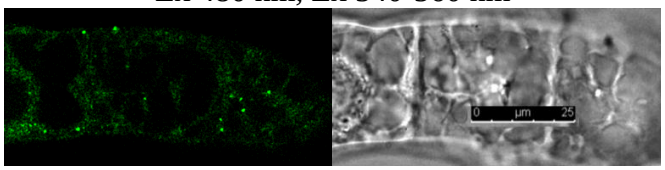 Ex 615 nm, Em 670-690 nm 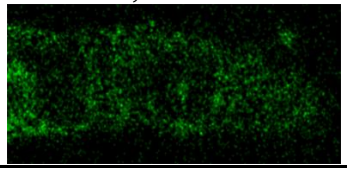

3.3 Photoaffinity probe cross-links with proteins

In order to identify the protein targets of nitro-BODIPY on peroxisomes, a photoaffinity labelling probe (**P39**, equal to **S114** in Section 3.1.7) based on nitro-BODIPY was designed (Fig 49). The photophysical properties of Photoaffinity labelling probe **P39** and control probe **P3** were measured and collected in Fig 50 and Table 23. As would be expected the spectra are quite similar, with both probes being quenched in water solution and emissive at 540 nm in toluene indicating that the benzophenone moiety and the linker do not affect the photophysical properties of nitro-BODIPY group.

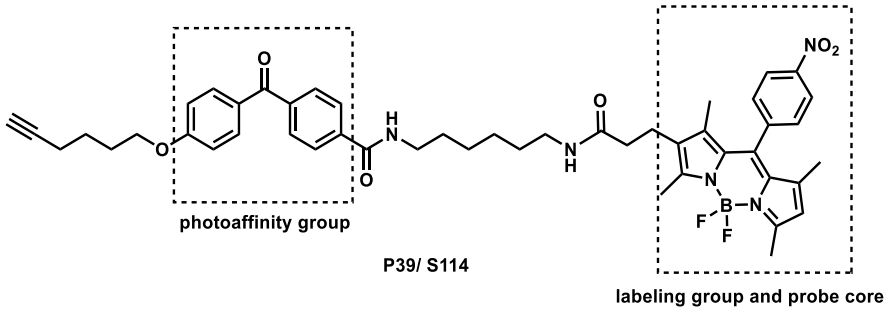

Figure 49 Photoaffinity labelling probe P39.

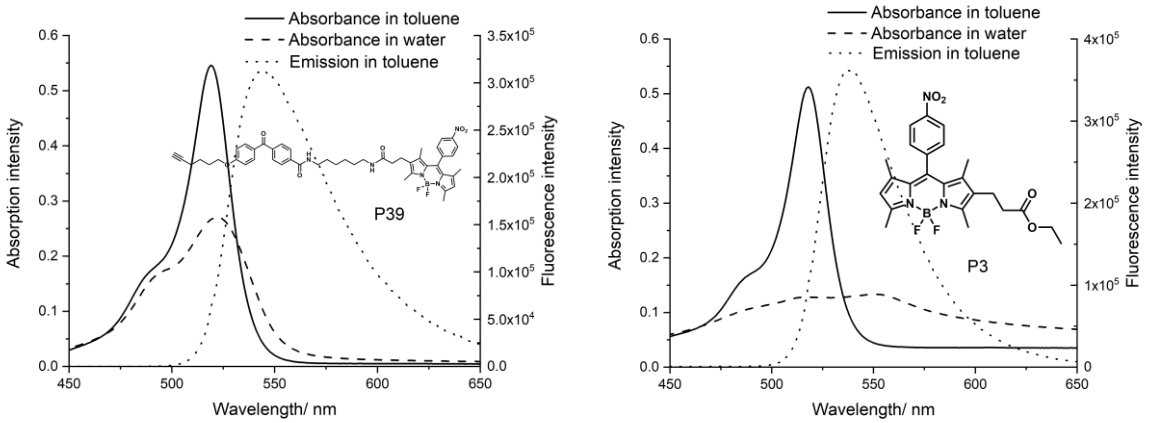

Figure 50 Absorption and emission spectra of photoaffinity labelling probe P39 and control probe P3.

Table 23 Photophysical properties of photoaffinity labelling probe P39 and control probe P3.

Probes	λ_{abs} in toluene	λ_{em} in toluene	λ_{abs} in water	λ_{em} in water
P39	519 nm	544 nm	522 nm	quench
P3	518 nm	539 nm	517 nm	quench

To verifiy that this photoaffinity labelling probe showed similar localisation in plant cells, it was incubated with plant cells (Table 24). This revealed that **P39** easily went through

membrane and illuminated peroxisomes albeit with some increased background staining when compared with **P3**.

Table 24 Images of plant cells incubated with photoaffinity labelling probe P39 and control probe P3.

Probe	Structure	Image
P39	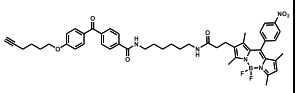	Ex 518 nm 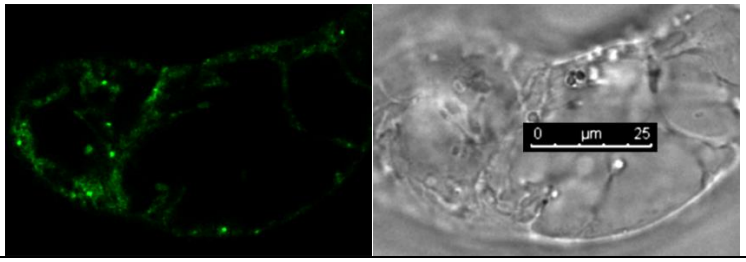
P3	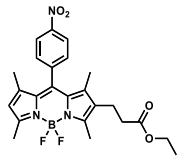	Ex 488 nm 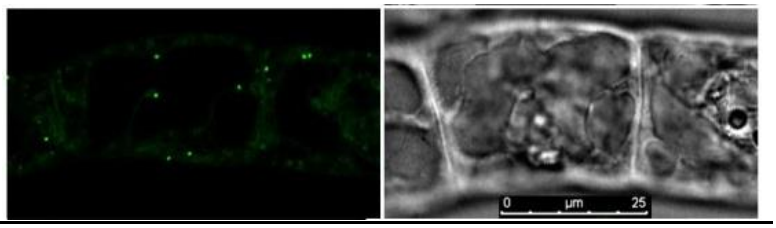

With the probe **P39** in hand the initial requirement was to verify cross-linking effectiveness between P39 and proteins. To do this three commercially available proteins albumin, α-chymotrypsin and glucose oxidase were selected as simple non specific model substrates. Each protein solution (5 mg/ mL) was incubated with probe **P39** (1 mM) under three different irradation conditions for 5 min and then analysed by SDS-PAGE. The irradiation conditions were: a positive control (365nm) that should lead to activation of the benzophenone with control experimetns under dark (no activation) and an exposure at natural light (background residual activation) After irradiation, saturated urea solution (8M) was added to the reaction mixture to eliminate non-covalent binding between probe and proteins. The proteins were then treated using a mixture of LDS sample buffer and 2-mercaptoethanol (95:5) before loading on the gels.

The fluorescence signals and comassie blue stain images are shown in Fig 51. Coomassie blue dyes are a family of dyes commonly used to stain proteins in SDS-PAGE gels. This treatment allows the visualization of proteins as blue bands on a clear background. The stronger signals were observed for all proteins upon irradiation at 365 nm (Lanes 3,6,9) with weaker signals also being detected on iraditation under ‘natural’ light conditions and no output being detected under dark conditions indicating that cross-linking between photoaffinity function group and proteins requires irradiation. This was most strongly apparent for albumin potentially reflecting

the greater lipophilicity of this protein as it is established that nitro-BODIPY is quenched in water and emits fluorescent signals when it localizes to hydrophobic targets (even non-specific targets). Collectively these results suggested that, albumin was an appropriate protein model to use in subseqent optimisation experiments.

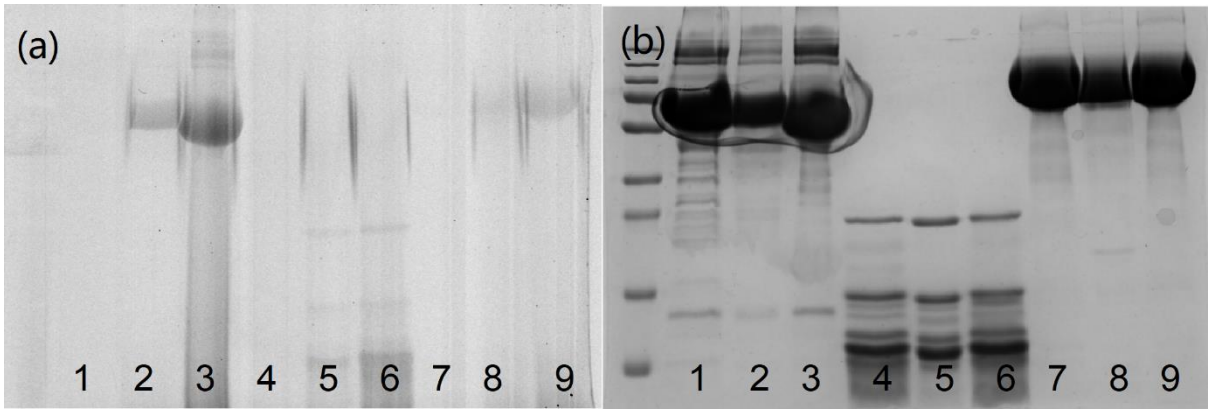

Figure 51 Photoaffinity labelling probe P39 binding on different proteins by SDS-PAGE. Proteins (5 mg/mL) pre-incubated with P39 (1000 µM) for 1 h at RT and then irradiated on ice at the wavelength indicated for 5 min (a) fluorescence signals detected by Gel Doc imager; (b) proteins stained with comassie blue. L1- Albumin under dark condition, L2- Albumin under natural light, L3- Albumin under 365 nm irradiation, L4- α-Chymotrypsin under dark condition, L5- α-Chymotrypsin under natural light, L6- α-Chymotrypsin under 365 nm irradiation, L7- Glucose oxidase under dark condition, L8- Glucose oxidase under natural light, L9- Glucose oxidase under 365 nm irradiation.

With Albumin selected as a model, the next objective was to determine the optimum time of irradaition with probe **P39** to be used in further experiments. Consequently, albumin (5 mg/ mL in water) was incubated with probe **P39** (1mM) for 1 h at RT and then irradiated for increasing time periods up to 60 minutes and then analysed as described above. The gel images are shown in Fig 52. The degree of labelling as indicated by the fluorescence intensity increased from 5 to 35 minutes (L3 to L9) and plateaued thereafter (L9-L14). From this it was concluded that 35min represented the optimum irradiating time for exploration of plant protein extracts with probe **P39**.

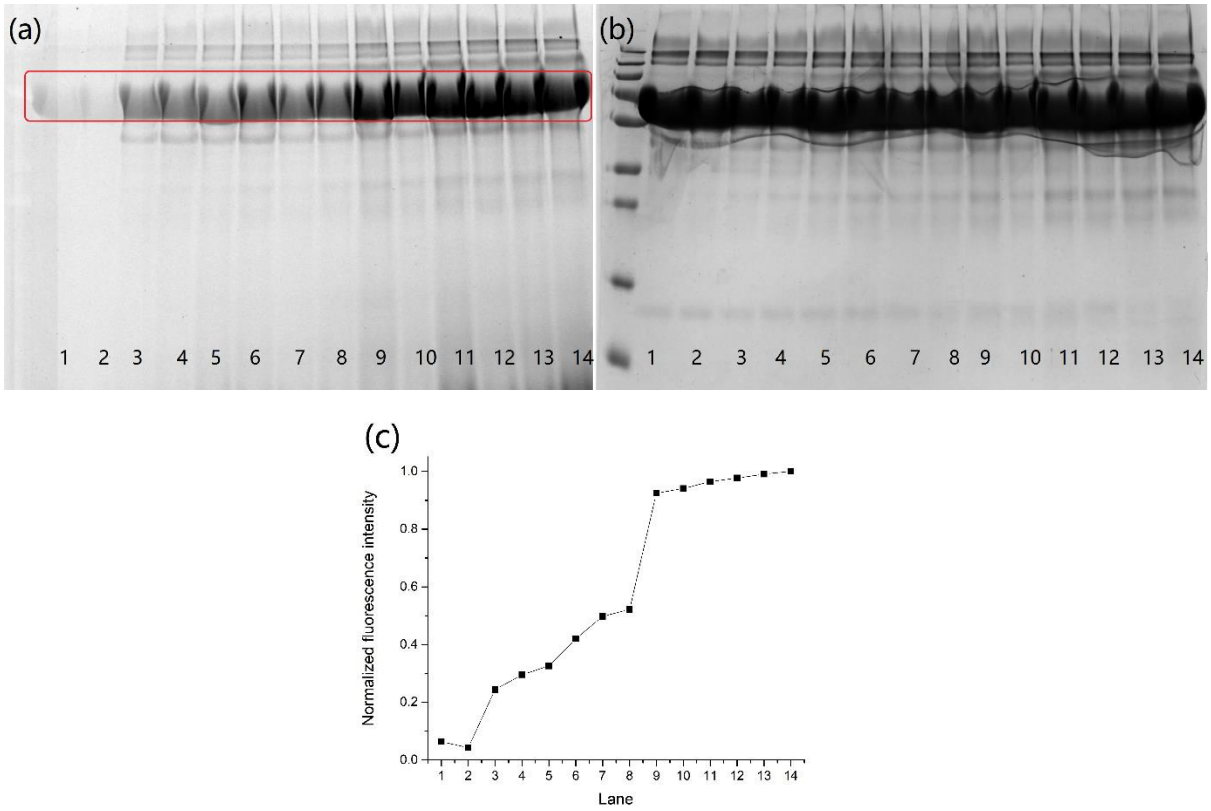

Figure 52 Photoaffinity labelling probe P39 binding on albumin by SDS-PAGE. Albumin (5 mg/mL) pre-incubated with P39 (1000 µM) for 1 h at RT. (a) fluorescence signals detected by Gel Doc imager; (b) proteins stained with comassie blue. L1- natural light, L2- dark condition, L3-14- 365 nm irradiating for 5, 10, 15, 20, 25, 30, 35, 40, 45, 50, 55, 60 min; (c) Normalized fluorescence intensity of highted bands.

Having identified a set of labelling conditions, the attention then turned to identifying the target of nitro-BODIPY in plant peroxisomes. In order to develop a suitable protocol, commercially available spinach was selected as a simple plant material due to a high level of peroxisomes. A protein solution was prepared with buffer from freezed dried leaves then was diluted to prapare it to different concentrations (1 mg/ mL to 20 mg/ mL) as determined by Bradford assay (Pierce™ Rapid Gold BCA Protein Assay Kit). Each plant protein extract was then incubated with probe **P39** (1000 uM) for 1 h at r.t. and irradiated with 365 nm light for 35 min. The results for fluorescence scanner and signals (detected by Gel Doc imager) and comassie blue stain image were showed in Fig 53. A concentration of 10 mg/ mL (Lane 3) was found to provide the clearest image and was selected as an appropriate concentration of all subsequent plant protein extract experiments.

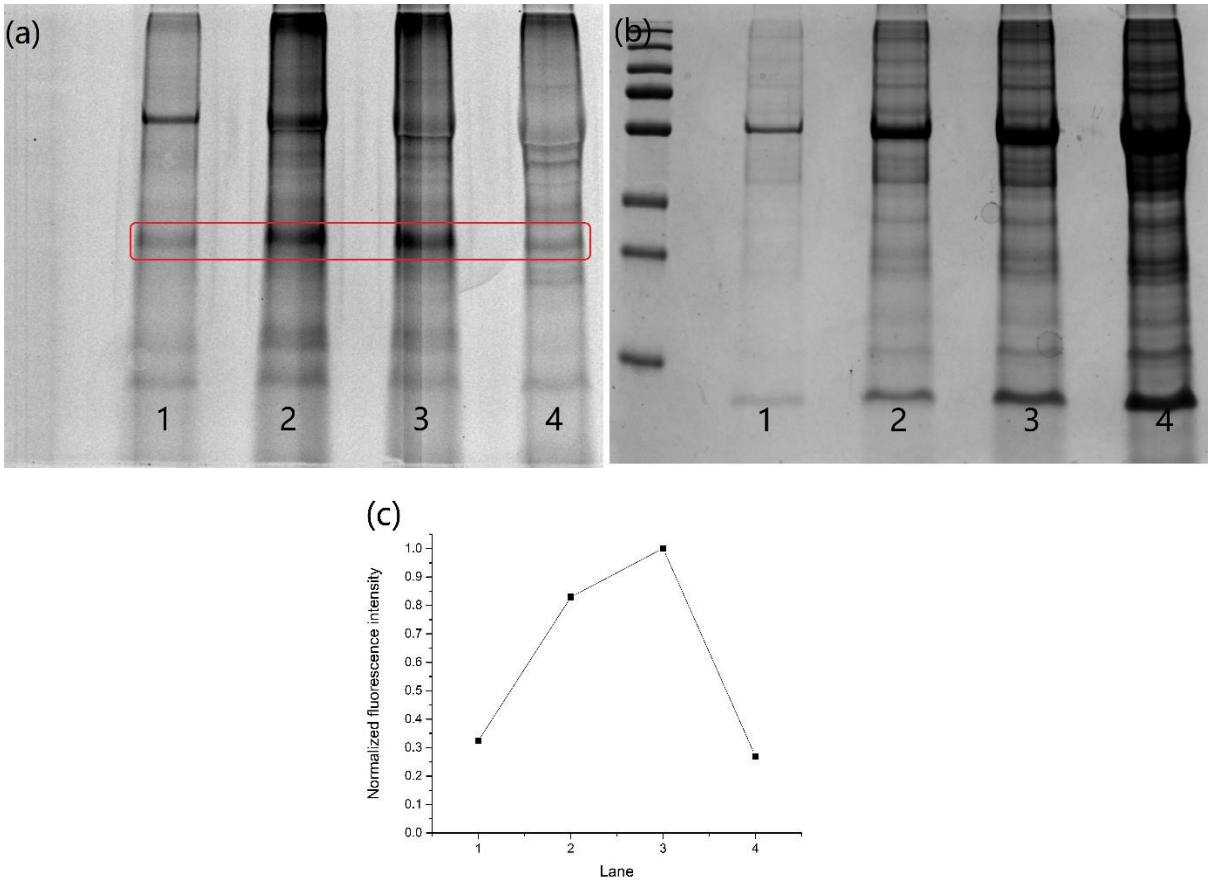

Figure 53 Photoaffinity labelling probe P39 binding on spinach leaves proteins by SDS-PAGE. Protein extraction pre-incubated with P39 (1000 µM) for 1 h at RT, then 365 nm irradiating for 35 min in ice bath. (a) fluorescence signals detected by Gel Doc imager; (b) proteins stained with comassie blue. L1- 1 mg/ mL of protein extraction, L2- 5 mg/ mL of protein extraction, L3-10 mg/ mL of protein extraction, L4- 20 mg/ mL of protein extraction; (c) Normalized fluorescence intensity of highted bands.

In all the SDS-PAGE experiments to date, it was seen that probe **P39** could cross-link with multiple plant proteins suggesting that the cross-linking reaction could probably occur without specific binding. Consequently, some fluorescent bands detected by Gel Doc imager do not represent target proteins of nitro-BODIPY. In these experiments, in order to ensure a strong signal, extracts had been treated with an excess amount of photoaffinity labelling probe **P39** (1000 uM) . However this leads to higher levels of background labelling and would also challenge future competitive labelling experiments (see later). Therefore the labelling experiment was then repeated at different concentrations of **P39** (100 uM-1000 uM). The fluorescence signals (detected by Gel Doc imager) and comassie blue stain image were showed in Fig 54. From this it was identified that 200 uM (Fig 4, lane 4) was an appropriate concentration of probe **P39** for SDS-PAGE. Interestingly, comparing two groups of lanes

(Lane 1, 3, 5, 7 and Lane 2, 4, 6, 8), we found that the treatment of the samples with urea reduces resolution and was deemed unnecessary in future experiments.

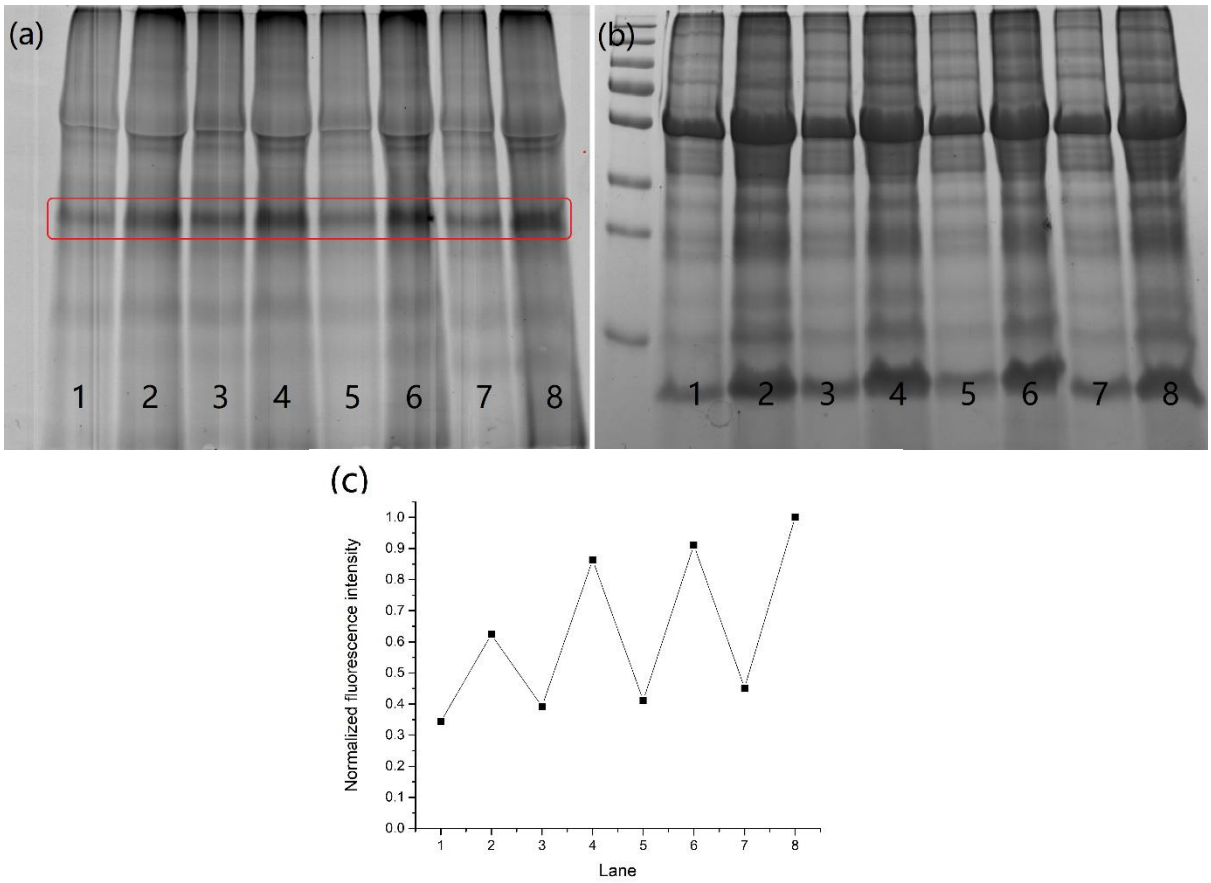

Figure 54 Photoaffinity labelling probe P39 binding on spinach leaves proteins by SDS-PAGE. Protein extraction (10 mg/mL) pre-incubated with P39 for 1 h at RT, then 365 nm irradiating for 35 min in ice bath. (a) fluorescence signals detected by Gel Doc imager; (b) proteins stained with comassie blue. L1-2- P39 (100 uM), L3-4- P39 (200 uM), L5-6- P39 (500 uM), L7-8- P39 (1000 uM), L1, 3, 5, 7 treated with urea, L2, 4, 6, 8 treated without urea; (c) Normalized fluorescence intensity of highted bands.

Alhtough the studies with albumin had identifed that 35 min was the optimum irradiation time there was concern that this level of high-energy light could alter important plant proteins. Consequently, we conducted an irradiation time experiment for spinach protein extraction. Following the same procedure as used for albumin it was possible to conclude that shortest irradiating time for photoaffinity labelling probe **P39** (200 uM) and spinach protein extraction (10 mg/ mL) is 25 min (Figure 55, Lane 7).

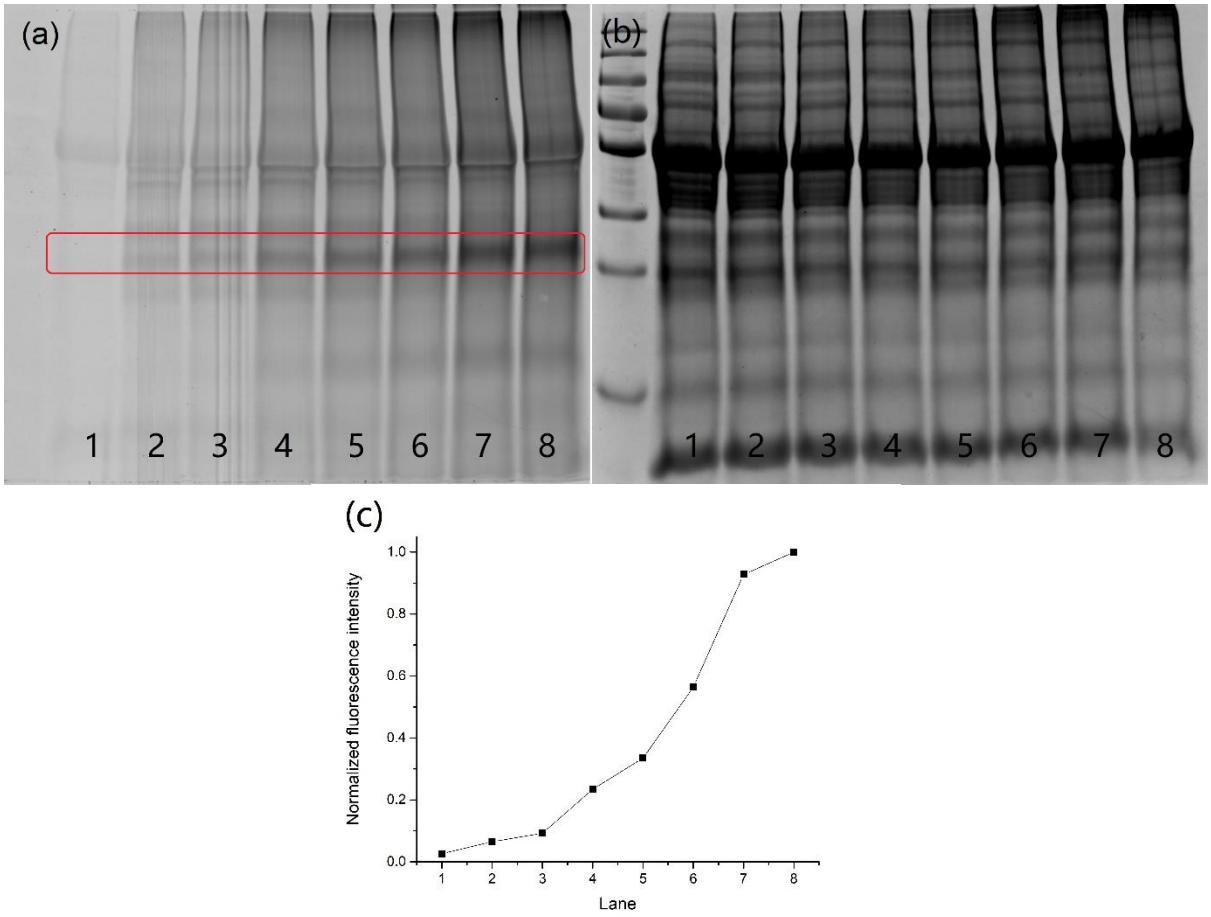

Figure 55 Photoaffinity labelling probe P39 binding on spinach leaves proteins by SDS-PAGE. Protein extraction (10 mg/mL) pre-incubated with P39 (200 uM) for 1 h at RT. (a) fluorescence signals detected by Gel Doc imager; (b) proteins stained with comassie blue. L1- natural light, L2-8- 365 nm irradiating for 2, 5, 10, 15, 20, 25, 30 min; (c) Normalized fluorescence intensity of highted bands.

Even with these refined labelling conditions, multiple protein bands were apparent in the gels. To better identify those corresponding to nitro-BODIPY a competitive experiment was designed. The extracts were incubated with different concentration (0-2000 uM) of nitro-BODIPY (P1) for 1 h at RT before being treated with probe **P39** (200 uM) for 1 h at RT. After incubation, the lysate was irradiated by 365 nm for 25 min as previously described and then analysed by SDS-PAGE (Fig 56). Excitingly, a number of protein bands at around 40 (Band 1), 25 (Band 2) and 15 KDa (Band 3) showed progressive reduction in intensity with the increasing amount of nitro-BODIPY (P1). The Band 2 showed the greatest change and represents the principal target for future investigations as discused in Chapter 4.

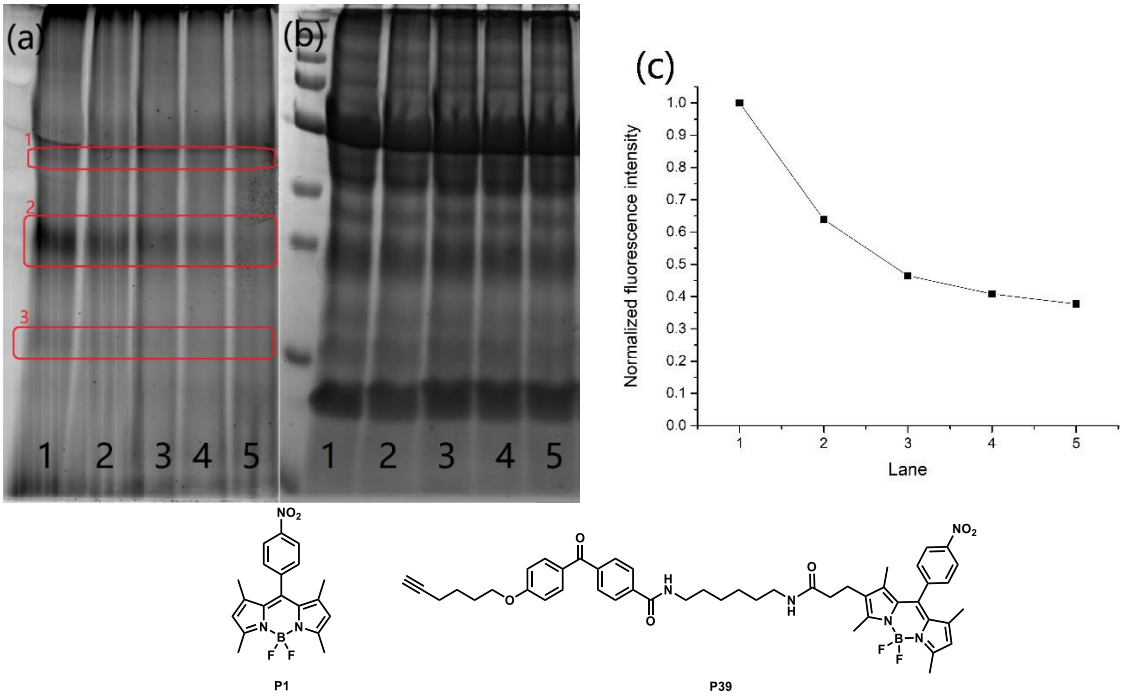

Figure 56 Photoaffinity labelling probe P39 binding on spinach leaves proteins by SDS-PAGE. Protein extraction (10 mg/mL) pre-incubated with P39 (200 uM) for 1 h at RT, then 365 nm irradiating for 25 min in ice bath. (a) fluorescence signals detected by Gel Doc imager; (b) proteins stained with comassie blue. L1- P1:P39= 0:1, L2- P1:P39= 1:1, L3- P1:P39= 2:1, L4- P1:P39= 5:1, L5- P1:P39= 10:1; (c) Normalized fluorescence intensity of highted bands 2.

4 CONCLUSION AND FUTURE WORK

As discussed in Section 2.1, the specific aims of this project were: 1. To develop a 'toolbox' of analogues that enable multicolour visualisation. 2. To confirm the nature of the binding process between nitro-BODIPY and the target protein and to determine its reversibility. 3. To identify the target protein of nitro-BODIPY in plant peroxisomes.

For the first aim, a family of red-shifted nitro-BODIPY probes (**P11**-**20**) were synthesised with the highest emission wavelength reachng a maximum of around 700nm (Section 3.1.3 and 3.2.2). Importantly, most retained selective localisation towards plant peroxisome. In addition, two water-soluble probes **P5** and **P6** were prepared and proved to exhibit water solubility and selective labelling towards plant peroxisomes (Section 3.1.3 and 3.2.1).

Towards the second aim, a group of dual-fluorophore probes (nitro-BODIPY probes with a second fluorophore) were developed (Section 3.1.6). Although several probes showed selective labelling of the peroxisome, the reporter function of the second fluorophore in all probes were challenged by various degrees of FRET (Section 3.2.4 and 3.2.5). Surprisingly, probes **P33**-**36** exhibited specific localisation towards unidentified targets in plant cell. More work is required to ascertain this result. In addition, to overcome the effects of FRET in thses probes, the research on non-FRET dual-fluorophore probes can be carried out. To address this, two methods could potentially prevent FRET in dual-fluorophorese probes. One is to increase the distance between the donor and acceptor molecules by lengthening the linkage between intramolecular fluorophores to greater distances than 100 Å. The alternative startegy is to choose a appropriate fluorophores whose absorption and excitation spectra do not overlap with nitro-BODIPY's spectrum.

For the third aim, several potential protein targets of nitro-BODIPY in plant peroxisomes were detected by the photoaffinity labelling probe **P39** via a competitive labelling experiment using SDS-PAGE techniques (Section 3.1.7 and 3.3). To determine the target proteins, protein enrichment and analysis remain to be completed. This will be achieved by protein isolation and enrichment by SDS-PAGE and protein mass spectrometry analysis.

5 GENERAL CHEMICAL EXPERIMENTAL DETAILS

5.1 IUPAC nomenclature

The IUPAC names and atom numbering were obtained using ChemDraw Ultra (v15.0) CambridgeSoft. For fluorophores used in this work, for simplicity shorter common names have been used throughout. For example, nitro-BODIPY is formally named as 5,5-difluoro-1,3,7,9-tetramethyl-10-(4-nitrophenyl)-5H-4l4,5l4-dipyrrolo[1,2-c:2',1'-f][1,3,2]diazaborinine.

5.2 Solvents and reagents

All chemicals were purchased from commercial suppliers and used without further purification. All used solvents THF, DCM, MeCN, EtOAc, MeOH, DMF and $CDCl_3$ were obtained dry and stored under argon.

5.3 Reaction conditions

All reactions were performed in round-bottom flasks, with stirring, under argon atmosphere unless otherwise stated. Reactions under microwave irradiation conditions were performed using monomodal EmrysTM Optimizer from Personal Chemistry, in sealed microwave process vials under argon atmosphere. The reaction progress was followed by thin layer chromatography (TLC) using Merck aluminium precoated plates (silica gel 60 Å F254). Compounds were visualized by UV radiation (λmax = 254 nm and 365 nm) followed by staining with the appropriate reagent and heating. Purification were conducted by flash chromatography using CombiFlash EZ Prep system with RediSep normal-phase silica flash columns (Teledyne Isco).

5.4 Spectroscopic analysis

Infrared: IR spectra were documented using a Perkin-Elmer Spectrum 1000 FT-IR Spectrometer with a ATR module, and absorption maxima νmax were reported as wavenumbers (cm^{-1}).

Nuclear magnetic resonance: ^{1}H and ^{13}C NMR spectra were acquired on Varian VNMRS 700 (^{1}H at 700 MHz, ^{13}C at 176 MHz) or Varian VNMRS 600 (^{1}H at 600 MHz, ^{13}C at 151 MHz), $CDCl_3$ was used as solvent and the chemical shifts (δH or δC) reported in parts per million (ppm), number of protons, multiplicity (s, singlet; d, doublet; t, triplet; m, multiplet), coupling

constants (J) and assignment. The assignment was performed with COSY, HSQC, HMBC and NOESY experiments.

Mass spectrometry: Low resolution mass spectra (LRMS) were recorded via electrospray ionisation (ESI), using a Waters TQD spectrometer equipped with an Acquity UPLC or by matrix-assisted laser desorption/ionization (MALDI) Autoflex II ToF/ToF (Bruker). High resolution mass spectra (HRMS) were obtained using Waters LCT Premier XE by Durham University Mass Spectroscopy service. Mass to charge ratios (m/z) are reported in Daltons with the corresponding fragment ion.

5.5 Analogues and probe synthesis

(3,5-Dimethyl-1H-pyrrol-2-yl)(4-nitrophenyl)methanone (S1)

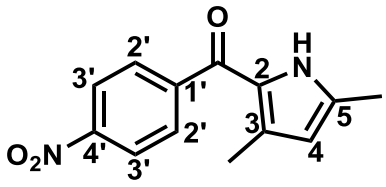

Procedure: Methylmagnesium bromide 3M in ether (13.3 mL, 39.40 mmol, 1.0 eq) was added to a solution of 2,4-dimethypyrrole (3.75g, 39.40 mmol, 1.0eq) in 100 mL ether and then under refluxing at 50 °C for 30 min. 4-nitrobenzoyl chloride (7.32 g, 39.40 mmol, 1.0 eq) in ether 100mL was then added to the solution and stirring was continued for 24 h at room temperature. The mixture was then poured into 500 mL saturated aqueous NH_4Cl, and the resultant mixture extracted with dichloromethane (200 mL × 3). The organic layer was washed with water, dried over $MgSO_4$ and concentrated under vacuum. The compound was purified using column chromatography (ethyl acetate : hexane = 20%-40%) to afford (3,5-dimethyl-1H-pyrrol-2-yl)(4-nitrophenyl)methanone as a bright yellow solid (6.16 g, 25.3 mmol, 64 % yield).

Characteristics: Melting point 157-160 °C; υ_{max} (ATR) 3278 (N-H), 1720 (C=O), 1608, 1572 (N=O), 1526, 1501, 1440, 1370, 1348 (N=O), 1319, 1286, 1227, 1143, 1108 cm^{-1}; δ_H (400 MHz, DMSO-d_6) 11.40 (s, 1H, N-H), 8.33 (d, J = 8.8 Hz, 2H, 3'-H), 7.79 (d, J = 8.8 Hz, 2H, 2'-H), 5.90 (s, 1H, 4-H), 2.21 (s, 3H, 5-CH_3), 1.91 (s, 3H, 3-CH_3); δ_C (101 MHz, DMSO-d_6) 182.7 (C=O), 148.8 (C-4'), 146.8 (C-1'), 137.5 (C-5), 131.2 (C-3), 129.5 (C-2'), 127.1 (C-2), 124.1 (C-3'), 113.3 (C-4), 14.2 (5-CH_3), 13.1 (3-CH_3); m/z (LCMS ES+) r_t 2.47 min, 245.18 $[M+H]^+$.

1,3,5,7-Tetramethyl-8-(4-nitrophenyl)-BODIPY (S2)

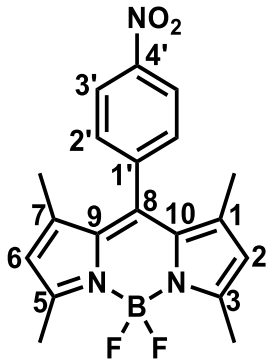

Procedure 1: To a solution of S1 (1.00 g, 4.09 mmol, 1.0 eq) in dichloromethane (5.0 mL) was added 2,4-dimethypyrrole (0.39 g, 4.09 mmol, 1.0 eq) and phosphorus oxychloride (0.45 mL, 4.91 mmol, 1.2 eq). The reaction mixture compound was heated at 60 ºC for 30 min, during which it turned red-purple, the reaction mixture was then concentrated and toluene (5.0 mL) added. The mixture was then treated with N,N-diisopropylethylamine (1.40 mL, 8.19 mmol, 12.0 eq) and boron trifluoride diethyl etherate (1.00 mL, 8.19 mmol, 2.0 eq). The remaining mixture was then heated at 100 ºC for 30 min after which the crude product was then filtered through a plug of celite. The residue was purified by flash column chromatography eluting with ethyl acetate : hexane = 1 : 4 to yield the product S2 as an orange solid (0.48 g, 1.31 mmol, 32 % yield).

Procedure 2: To a solution of 2-(4'-nitrophenyl)-3,5-dimethylpyrrole (100 mg, 0.41 mmol, 1.0 eq) in dry dichloromethane (2.5 mL) was added 2,4-dimethypyrrole (40 mg, 0.41 mmol, 1.0 eq) and $BF_3{\cdot}OEt_2$ (0.41 mL, 3.28mmol, 8.0 eq) and the resulting solution stirred at room temperature for 30 min. After the mixture turned red-purple, the reaction was neutralized with N,N-diisopropylethylamine (0.38 mL, 2.46 mmol, 6.0 eq) and then stirred at room temperature for 1 h. The resulting orange crude product was purified by column chromatography (ethyl acetate : hexane = 1 : 4) to give S2 as an orange solid (91 mg, 0.25 mmol, 60 % yield).

Characteristics: Melting point 274-275 ºC; υ_{max} (ATR) 3109, 2954, 2260, 1719, 1603, 1553 (N=O), 1522,1473, 1444, 1415, 1372, 1348 (N=O), 1319, 1286, 1263, 1227, 1204,1162, 1122, 1093, 1081, 1047 cm^{-1}; δ_H (400 MHz, Chloroform-d) 8.41 (d, J = 8.7 Hz, 2H, 3'-H), 7.56 (d, J = 8.7 Hz, 2H, 2'-H), 6.04 (s, 2H, 2,6-H), 2.59 (s, 6H, 3,5-CH_3), 1.38 (s, 6H, 1,7-CH_3); δ_C (101 MHz, Chloroform-d) 156.7 (C-3), 148.4 (C-4'), 142.6 (C-9, C-10), 142.0 (C-8), 138.4 (C-1'), 130.7 (C-1, C-7), 129.7 (C-2'), 124.4 (C-3'), 121.9 (C-2, C-6), 14.7 (1-CH_3, 3-CH_3, 5-CH_3, 7-CH_3); m/z (LCMS ES+) r_t 3.50 min, 370.20 $[M+H]^+$.

1,3,5,7-Tetramethyl-2,6-dibromo-8-(4-nitrophenyl)-BODIPY (S3)

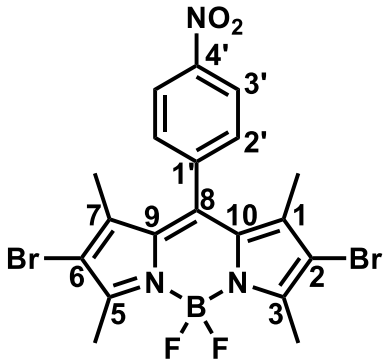

Procedure: To a solution of the S2 (50 mg, 0.14 mmol, 1.0 eq) in anhydrous acetonitrile (10 mL) was slowly added a solution of $CuBr_2$ (90 mg, 0.42 mmol, 3.0 eq) in acetonitrile (15 mL). The mixture was stirred under O_2 atmosphere at room temperature for 24 h. The residue obtained after the removal of the solvent by rotary evaporation was extracted with EtOAc (3 × 20 mL), washed with water (3 × 15 mL), dried (anhyd Na_2SO_4), and concentrated under reduced pressure. The crude product was further purified using column chromatography (EtOAc/hexane = 1:4) afforded S3 (24 mg, 0.05 mmol, 34 % yield).

Characteristics: Melting point 279-280 ºC; υ_{max} (ATR) 3105, 2954, 2259, 1718, 1602, 1554 (N=O), 1524, 1448, 1403, 1362, 1346 (N=O), 1288, 1264, 1228, 1201, 1147, 1091, 1061 cm^{-1}; δ_H (400 MHz, Chloroform-d) 8.45 (d, J = 8.3 Hz, 2H, 3'-H), 7.55 (d, J = 8.3 Hz, 2H, 2'-H), 2.65 (s, 6H, 3,5-CH_3), 1.38 (s, 6H, 1,7-CH_3); δ_C (101 MHz, Chloroform-d) 155.3 (C-3, C-5), 148.7 (C-4'), 141.2 (C-9, C-10), 140.0 (C-8), 138.6 (C-1'), 129.7 (C-1, C-7), 129.6 (C-2'), 124.7 (C-3'), 112.6 (C-2, C-6), 14.1 (1,7-CH_3), 13.9 (3,5-CH_3); m/z (LCMS ES+) r_t 3.94 min, 525.00, 527.46 and 528.35 $[M+H]^+$.

1,3,5,7-Tetramethyl-2-bromo-8-(4-nitrophenyl)-BODIPY (S4)

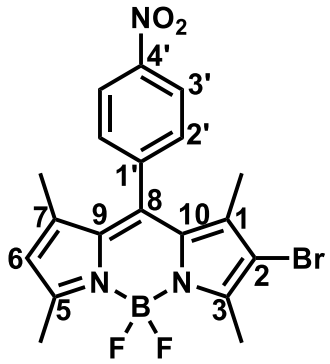

Procedure: To a solution of S2 (50 mg, 0.14 mmol, 1.0 eq) and K_2CO_3 (56 mg, 0.41 mmol, 3.0 eq) in anhydrous acetonitrile (10 mL) was slowly added a solution of $CuBr_2$ (45 mg, 0.20 mmol, 1.5 eq) in acetonitrile (15 mL). The mixture was stirred under O_2 atmosphere at room temperature for 24 h. The residue obtained after the removal of the solvent by rotary evaporation was extracted with EtOAc (3 × 20 mL), washed with water (3 × 15 mL), dried (anhyd Na_2SO_4), and concentrated under reduced pressure. The crude product was further purified using column chromatography (EtOAc/hexane = 1:4) afforded S4 as a red solid (11 mg, 0.03 mmol, 18 % yield).

Characteristics: Melting point 263-264 ºC; υ_{max} (ATR) 3105, 2954, 2259, 1718, 1609, 1550 (N=O), 1468, 1445, 1410, 1353 (N=O), 1312, 1264, 1227, 1193, 1124, 1089, 1061 cm^{-1}; δ_H (400 MHz, Chloroform-d) 8.43 (d, J = 8.7 Hz, 2H, 3'-H), 7.56 (d, J = 8.7 Hz, 2H, 2'-H), 6.10 (s, 1H, 6-H), 2.63 (s, 3H, 5-CH_3), 2.60 (s, 3H, 3-CH_3), 1.39 (s, 3H, 7-CH_3), 1.38 (s, 3H, 1-CH_3); δ_C (101 MHz, Chloroform-d) 159.2 (C-5), 152.8 (C-10), 148.5 (C-4'), 144.4 (C-7), 141.6 (C-8), 138.4 (C-3), 138.2 (C-1'), 131.3 (C-9), 129.6 (C-2'), 129.0 (C-1, C-2), 124.5 (C-3'), 122.8 (C-6), 14.9 (7-CH_3), 14.9 (5-CH_3), 13.8 (3-CH_3), 13.6 (1-CH_3); m/z (LCMS ES+) r_t 3.60 min, 448.83 and 450.462 $[M+H]^+$.

2-Tert-butyl-4-ethyl-3,5-dimethyl-1H-pyrrole-2,4-dicarboxylate (S5)

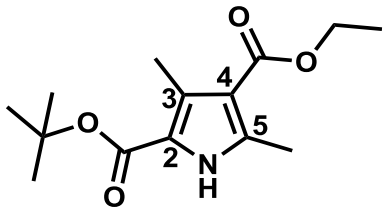

Procedure: To an ice-cooled mixture of tert-butyl acetoacetate (10.0 g, 63.21 mmol, 1.0 eq) and glacial acetic acid (10 mL) was slowly added an aqueous solution of $NaNO_2$ (3 M, 10 mL, 63.21 mmol, 1.0 eq). The resulting solution was warmed to room temperature and stirring was continued at this temperature for 4 h. A solution of ethyl acetoacetate (8.22 g, 63.21 mmol, 1.0 eq) in glacial acetic acid (20 mL) was added in one portion to the mixture. The resulting solution was then heated to 65°C. Zinc dust (3.13 g, 63.21 mmol, 1.0 eq) was then added to the warm solution in small portions. The mixture was stirred at 65°C for 2 h and subsequently poured into 500 mL of cold water and stirred for 30 min. The resulting precipitate was collected by filtration, washed with water and dried under vacuum. The resulting crude product was purified by column chromatography (ethyl acetate : hexane = 1 : 4) to S5 as a white solid (8.13 g, 30.41 mmol, 48% yield).

Characteristics: Melting point 129-130 ºC; υ_{max} (ATR) 3306 (N-H), 3013, 2987, 2940, 1713 (C=O), 1519, 1458, 1428, 1396, 1370, 1331, 1285, 1254, 1172 (C-O), 1096, 1053, 1010 cm^{-1}; δ_H (400 MHz, Chloroform-d) 8.86 (s, 1H, N-H), 4.21 (q, J = 7.1 Hz, 2H, O$\underline{C}H_2CH_3$), 2.46 (s, 3H, 5-CH_3), 2.43 (s, 3H, 3-CH_3), 1.50 (s, 9H, tert-butyl), 1.29 (t, J = 7.1 Hz, 3H, $OCH_2C\underline{H}_3$); δ_C (101 MHz, Chloroform-d) 165.6 (4-C=O), 161.1 (2-C=O), 138.2 (C-5), 130.0 (C-3), 119.1 (C-2), 113.4 (C-4), 81.2 ($\underline{C}(CH_3)_3$), 59.5 ($\underline{C}H_2CH_3$), 28.5 ($C(\underline{C}H_3)_3$), 14.5 (5-CH_3), 14.4 ($CH_2\underline{C}H_3$), 12.0 (3-CH_3); m/z (LCMS ES+) r_t 2.95 min, 268.24 $[M+H]^+$.

Ethyl 2,4-dimethyl-1H-pyrrole-3-carboxylate (S6)

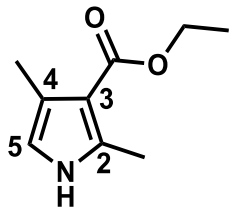

Procedure: To a stirred solution of S5 (7.0 g, 26.19 mmol, 1.0 eq) in ethanol (230 mL) at 0°C was added slowly HCl (12 M, 10.9 mL, 130.93 mmol, 5.0 eq). The reaction mixture was then stirred at 65°C for 4 h. After cooling to room temperature the mixture was poured into ice water (800 mL) and was extracted with dichloromethane (3 × 200 mL). The combined organic extracts were washed with brine (200 mL) and water (200 mL), dried over anhydrous $MgSO_4$, filtered off and concentrated in vacuum. The crude product was further purified using column chromatography (ethyl acetate : hexane = 1 : 4) afforded S6 as a white solid (3.05 g, 18.24 mmol, 70% yield).

Characteristics: Melting point 71-72 ºC; υ_{max} (ATR) 3298 (N-H), 2985, 2938, 1720, 1700, 1667 (C=O), 1565, 1518, 1483, 1453, 1431, 1391, 1369, 1274, 1227, 1204 (C-O), 1230, 1111, 1094, 1028 cm^{-1}; δ_H (400 MHz, Chloroform-d) 7.97 (s, 1H, N-H), 6.38 (d, J = 1.1 Hz, 1H, 5-H), 4.29 (q, J = 7.1 Hz, 2H, O-C$\underline{H_2}CH_3$), 2.51 (s, 3H, 2-CH_3), 2.26 (s, 3H, 4-CH_3), 1.37 (t, J = 7.1 Hz, 3H, O-$CH_2C\underline{H_3}$); δ_C (101 MHz, Chloroform-d) 166.5 (C=O), 136.0 (C-2), 121.6 (C-4), 114.3 (C-5), 110.7 (C-3), 59.1 (O-CH_2), 14.5 (2-CH_3), 14.1 ($CH_2\underline{C}H_3$), 12.6 (4-CH_3); m/z (LCMS ES+) r_t 2.20 min, 168.15 $[M+H]^+$.

1,3,5,7-Tetramethyl-2-ethyl carboxylate-8-(4-nitrophenyl)-BODIPY (S7)

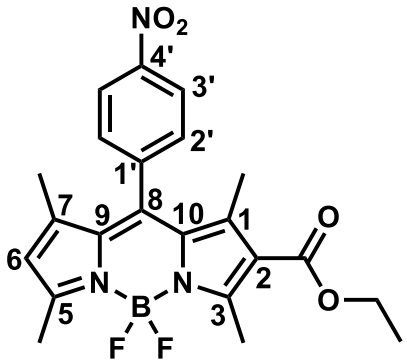

Procedure: following the same procedure 1 as described for S2.

S1 (2.92 g, 11.96 mmol, 1.0 eq) in dichloromethane (8.0 mL), S6 (2.00 g, 11.96 mmol, 1.0 eq), phosphorus oxychloride (1.1 mL, 11.96 mmol, 1.0 eq), toluene (16.0 mL), triethylamine (3.2 mL, 23.92 mmol, 2.0 eq) and boron trifluoride diethyl etherate (3.0 mL, 23.92 mmol) were converted to S7 (chromatography ethyl acetate/ hexane = 20%) as an orange solid (1.40 g, 3.17 mmol, 27 % yield).

Characteristics: Melting point 203-204 ºC; υ_{max} (ATR) 3113, 2923, 2857, 2300, 2259, 1707 (C=O), 1602, 1547 (N=O), 1518, 1448, 1378, 1352 (N=O), 1317, 1323, 1274, 1194 (C-O), 1150, 1123, 1097, 1044 cm^{-1}; δ_H (700 MHz, Chloroform-d) 8.44 (d, J = 8.4 Hz, 2H, 3'-H), 7.57 (d, J = 8.4 Hz, 2H, 2'-H), 6.16 (s, 1H, 6-H), 4.29 (q, J = 7.1 Hz, 2H, O-CH_2), 2.83 (s, 3H, 5-CH_3), 2.63 (s, 3H, 3-CH_3), 1.65 (s, 3H, 7-CH_3), 1.40 (s, 3H, 1-CH_3), 1.34 (t, J = 7.1 Hz, 3H, $CH_2C\underline{H_3}$); δ_C (176 MHz, Chloroform-d) 164.5 (C=O), 160.8 (C-5), 157.3 (C-3), 148.5 (C-4'), 145.3 (C-1), 143.7 (C-7), 141.5 (C-8), 139.9 (C-1'), 132.4 (C-1), 129.6 (C-2'), 129.1 (C-9), 124.5 (C-3'), 123.9 (C-6), 121.2 (C-10), 60.1 ($\underline{C}H_2CH_3$), 15.1 (5-CH_3), 15.0 (3-CH_3), 14.7 (1-CH_3), 14.3 ($CH_2\underline{C}H_3$), 13.6 (7-CH_3); m/z (LCMS ES+) r_t 3.67 min, 442.37 $[M+H]^+$; HRMS (ES+) found $[M+H]^+$ 442.1763, $C_{22}H_{22}BF_2N_3O_4$ requires M 442.1671.

Ethyl 4-(3-ethoxy-3-oxopropyl)-3,5-dimethyl-1H-pyrrole-2-carboxylate (S8)

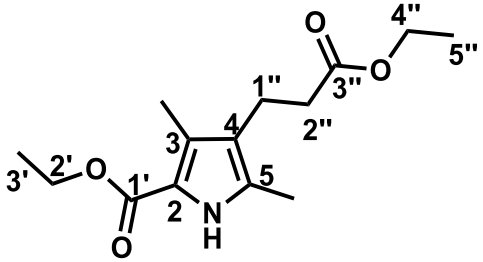

Procedure: To a solution of ethyl acetoacetate (6.51 g, 50.02 mmol, 1.25 eq) in glacial acetic acid (25 mL), $NaNO_2$ (4.55 g, 65.92 mmol, 1.65 eq) in water (10 mL) was added dropwise under 0 °C. When all the $NaNO_2$ was added, the mixture was stirred for 4 h at room temperature, during which time it slowly turned orange. Ethyl 4-acetyl-5-oxohexanoate (8.00 g, 39.95 mmol) was added all at once followed by zinc dust (8.62 g, 131.85 mmol, 3.3 eq) in portions. Zinc was added only in the absence of foaming and only when previous additions were dissolved. After all the zinc was added, the mixture was heated under reflux for 2 h. The reaction was quenched by adding the hot solution to ice/water 500 mL and stirring for 30 min. The resulting precipitate was filted and washed with water and dried under vacuum to afford a pale yellow solid. The filtration liquor was extracted with dichloromethane and concentrated in vacuo to a brown oil. The brown oil was taken up in ethanol (10 mL) and water was added until the solution remained turbid. Then the solution was cooled in an ice bath and filted to afford a brown solid. The brown solid and the above pale yellow solid was dissolved together, purified by flash column chromatography eluting with ethyl acetate : hexane = 1:9 to obtain S8 as a pale yellow solid (5.33 g, 50 % yield).

Characteristics: Melting point 72-73 °C; υ_{max} (ATR) 3319(N-H), 2985 (C-H), 2940 (C-H), 2876 (C-H), 1733 (C=O), 1665 (C=O), 1587, 1510, 1445, 1379, 1343, 1271 (C-O), 1220, 1175 (C-O), 1097, 1061, 1028 cm^{-1}; δ_H (400 MHz, Chloroform-d) 8.81 (s, 1H, N-H), 4.31 (q, J = 6.3 Hz, 2H, 2'-H), 4.13 (q, J = 6.4 Hz, 2H, 4''-H), 2.84-2.63 (m, 2H, 1''-H), 2.53-2.37 (m, 2H, 2''-H), 2.29 (s, 3H, 5-CH3), 2.23 (s, 3H, 3-CH3), 1.36 (t, J = 6.5 Hz, 3H, 3'-H), 1.26 (t, J = 6.5 Hz, 3H, 5''-H); δ_C (101 MHz, Chloroform-d) 173.2 (C-3''), 161.8 (C-1'), 129.9 (C-5), 127.0 (C-3), 120.1 (C-4), 117.0 (C-2), 60.4 (C-2'), 59.7 (C-4''), 35.2 (C-2''), 19.6 (C-1''), 14.6 (C-5''), 14.2 (C-3'), 11.5 (4-CH_3), 10.6 (2-CH_3); m/z (LCMS ES+) r_t 2.64 min, 268.39 $[M+H]^+$.

Ethyl 3-(2,4-dimethyl-1H-pyrrol-3-yl) propanoate (S9)

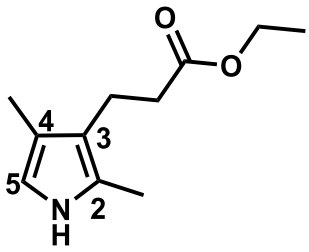

Procedure 1: S8 (6.50 g, 24.32 mmol) in 30.0 ml 85% phosphoric acid was heated to 80 ºC under a nitrogen atmosphere. After heating the reaction mixture an additional hour at 80 ºC, it was cooled to room temperature and 100 ml of distilled water was added. This was partially neutralized to pH=7 by the slow addition of 2M sodium hydroxide while the mixture was stirred vigorously in an ice bath. Extraction of the aqueous phase with three 100 ml portions of chloroform, followed by drying of the organic phase with anhydrous sodium sulfate and evaporation of the solvent under reduced pressure gave S9 as a slightly yellow oil (2.50 g, 12.80 mmol, 53 % yield).

Procedure 2: To a stirred solution of S13 (100 mg, 0.34 mmol, 1.0 eq) in methanol (3.6 mL) at 0°C was added slowly HCl (12 M, 0.14 mL, 1.70 mmol, 5.0 eq). The reaction mixture was then stirred at 65°C for 4 h. After cooling to room temperature the mixture was poured into ice water and was extracted with dichloromethane. The combined organic extracts were washed with brine and water, dried over anhydrous $MgSO_4$, filtered off and concentrated in vacuo to afford S9 as a slightly yellow oil (15 mg, 0.08 mmol, 23 % yield).

Procedure 3: S13 (100 mg, 0.34 mmol) was immediately dissolved in 1 mL trifluoroacetic acid and stirred under an Ar atmosphere at ambient temperature for 10 min. 10 mL of dichloromethane was then added and the resulting solution was washed with water and 1 M NaHCO3 aq., dried over anhydrous sodium sulfate, filtered and evaporated, affording S9 as a slightly yellow oil (56 mg, 0.29 mmol, 85% yield).

Procedure 4: S11 (100 mg, 0.30 mmol) was dissolved in 10 mL of ethanol containing 10% palladium-carbon (10 mg). The resulting solution was stirred under H_2 at ambient temperature for 12 h. The reaction solution was then filtered and evaporated. The residue was immediately dissolved in 1 mL of trifluoroacetic acid and stirred under an Ar atmosphere at ambient temperature for 10 min. 10 mL of dichloromethane was then added and the resulting solution was washed with water and 1 M $NaHCO_3$ aq., dried over anhydrous sodium sulfate, filtered and evaporated, affording S9 as a slightly yellow oil (58 mg, 0.29 mmol, 98 % yield).

Characteristics: δ_H (400 MHz, Chloroform-d) 7.62 (s, 1H, N-H), 6.41 (s, 1H, 5-H), 4.16 (q, J

= 7.1 Hz, 2H, OC$\underline{H_2}$CH$_3$), 2.78-2.72 (m, 2H, 3-C$\underline{H_2}$CH$_2$), 2.50-2.44 (m, 2H, 3-CH$_2$C$\underline{H_2}$), 2.21 (s, 3H, 2-CH$_3$), 2.07 (s, 3H, 4-CH$_3$), 1.29 (t, J = 7.1 Hz, 3H, OCH$_2$C$\underline{H_3}$); δ_C (101 MHz, Chloroform-d) 113.0 (C=O), 60.3 (O$\underline{C}$H$_2$CH$_3$), 35.6 (C-2), 32.0 (C-3), 29.7 (C-4), 29.4 (C-5), 22.7 (3-CH$_2$$\underline{C}H_2$), 19.9 (3-$\underline{C}H_2CH_2$), 14.3 (OCH$_2$$\underline{C}H_3$), 11.3 (2-CH$_3$), 10.4 (4-CH$_3$); m/z (LCMS ES+) r_t 2.37 min,196.31 $[M+H]^+$.

Benzyl 4-(3-methoxy-3-oxopropyl)-3,5-dimethyl-1H-pyrrole-2-carboxylate (S10)

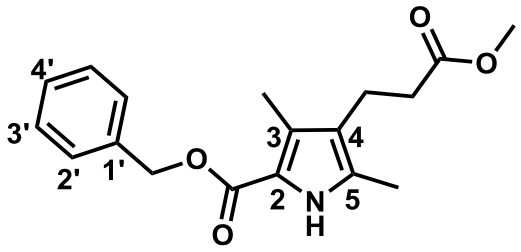

Procedure: following the same procedure as described for S8.

Benzyl acetoacetate (1.14 g, 5.91 mmol, 1.1 eq) in glacial acetic acid (2.4 mL), $NaNO_2$ (0.54 g, 7.79 mmol, 1.45 eq) in water (1.0 mL), methyl 4-acetyl-5-oxohexanoate (1.0 g, 5.37 mol, 1.0 eq) and zinc dust (0.98 g, 15.04 mmol, 2.9 eq) was converted to Benzyl 4-(3-methoxy-3-oxopropyl)-3,5-dimethyl-1H-pyrrole-2-carboxylate (purified by chromatography ethyl acetate/ hexane = 20%-40%) as a pale yellow solid (0.72 g, 2.28 mmol, 43 % yield).

Characteristics: Melting point 100-101 ^oC; υ_{max} (ATR) 3313 (N-H), 3073 (C-H), 3038 (C-H), 2958 (C-H), 2928 (C-H), 2865 (C-H), 1738 (C=O), 1665 (C=O), 1589, 1504, 1439, 1383, 1367, 1335, 1267 (C-O), 1218, 1164 (C-O), 1094, 1077, 1058, 1032 cm^{-1}; δ_H (400 MHz, Chloroform-d) 8.82 (s, 1H, N-H), 7.39 (m, 5H, Ar-H), 5.31 (s, 2H, Ar-O-CH_2), 3.68 (s, 3H, O-CH_3), 2.73 (t, J = 7.8 Hz, 2H, 4-C$\underline{H_2}$$CH_2$), 2.49 – 2.41 (m, 2H, 4-CH_2C$\underline{H_2}$), 2.31 (s, 3H, 5-C$\underline{H_3}$), 2.22 (s, 3H, 3-C$\underline{H_3}$); δ_C (101 MHz, Chloroform-d) 173.6 (4-C=O), 161.3 (2-C=O), 136.6 (C-1'), 130.3 (C-5), 128.6 (C-3'), 128.1 (C-2'), 128.0 (C-4'), 127.6 (C-3), 120.2 (C-4), 116.6 (C-2), 65.5 (Ar-CH_2-O), 51.6 (O-CH_3), 34.9 (4-CH2$\underline{C}$H2), 19.6 (4-$\underline{C}$H2CH2), 11.5 (5-CH_3), 10.7 (3-CH_3); m/z (LCMS ES+) r_t 2.82 min, 316.39 $[M+H]^+$.

Benzyl 4-(3-ethoxy-3-oxopropyl)-3,5-dimethyl-1H-pyrrole-2-carboxylate (S11)

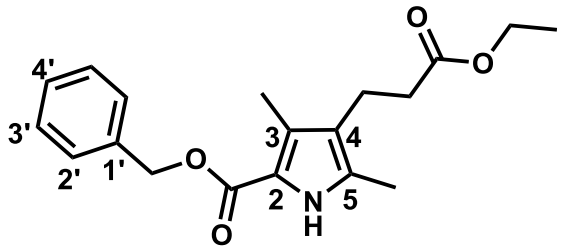

Procedure: following the same procedure as described for S8.

Benzyl acetoacetate (1.06 g, 5.49 mmol, 1.1 eq) in glacial acetic acid (2.2 mL), $NaNO_2$ (0.50 g, 7.24 mmol, 1.45 eq) in water (1.0 mL), ethyl 4-acetyl-5-oxohexanoate (1.00 g, 4.99 mmol, 1.0 eq) and zinc dust (0.95 g, 14.48 mmol, 2.9 eq) was converted to benzyl 4-(3-ethoxy-3-oxopropyl)-3,5-dimethyl-1H-pyrrole-2-carboxylate (purified by chromatography ethyl acetate/ hexane = 1:9) as a pale yellow solid (0.65 g, 1.97 mmol, 40 % yield).

Characteristics: Melting point 78-79 ºC; υ_{max} (ATR) 3319 (N-H), 3072 (C-H), 3039 (C-H), 2988 (C-H), 2933 (C-H), 2864 (C-H), 1735 (C=O), 1665 (C=O), 1589, 1504, 1440, 1376, 1339, 1269 (C-O), 1218, 1162 (C-O), 1092, 1075, 1059, 1033 cm^{-1}; δ_H (400 MHz, Chloroform-d) 9.03 (s, 1H, N-H), 7.39 (m, 5H, Ar-H), 5.32 (s, 2H, Ar-O-CH_2), 4.14 (q, J = 7.1 Hz, 2H, OC$\underline{H_2}$$CH_3$), 2.76-2.69 (m, 2H, 4-$CH_2C\underline{H_2}$), 2.47-2.41 (m, 2H, 4-$CH_2C\underline{H_2}$), 2.32 (s, 3H, 5-$CH_3$), 2.22 (s, 3H, 3-$CH_3$), 1.27 (t, J = 7.1 Hz, 3H, $OCH_2C\underline{H_3}$); δ_C (101 MHz, Chloroform-d) 173.2 (4-C=O), 161.5 (2-C=O), 136.6 (C-1'), 130.5 (C-5), 128.6 (C-3'), 128.0 (C-2', C-4'), 127.6 (C-3), 120.2 (C-4), 116.6 (C-2), 65.5 (Ar-CH_2-O), 60.4 ($\underline{C}H_2CH_3$), 35.2 (4-$CH_2\underline{C}H_2$), 19.6 (4-$\underline{C}H_2CH_2$), 14.2 ($CH_2\underline{C}H_3$), 11.4 (4-CH_3), 10.8 (2-CH_3); m/z (LCMS ES+) r_t 3.05 min, 330.37 $[M+H]^+$.

Tert-butyl 4-(3-methoxy-3-oxopropyl)-3,5-dimethyl-1H-pyrrole-2-carboxylate (S12)

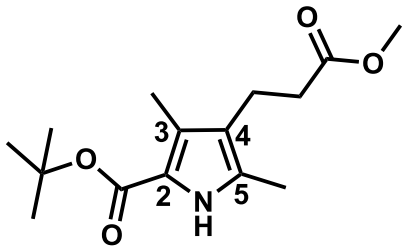

Procedure: following the same procedure as described for S8.

Tert-butyl acetoacetate (18.69 g, 118.15 mmol, 1.1 eq) in glacial acetic acid (50.0 mL), $NaNO_2$ (10.75 g, 155.74 mmol, 1.45 eq) in water (20.0 mL), methyl 4-acetyl-5-oxohexanoate (20.00 g, 107.41 mmol, 1.0 eq) and zinc dust (20.37 g, 311.48 mmol, 2.9 eq) was converted to tert-butyl 4-(3-methoxy-3-oxopropyl)-3,5-dimethyl-1H-pyrrole-2-carboxylate (purified by chromatography ethyl acetate/ hexane = 1:9) as a pale yellow solid (11.20 g, 39.81 mmol, 37 % yield).

Characteristics: Melting point 97-98 ºC; υ_{max} (ATR) 3326 (N-H), 2985 (C-H), 2934 (C-H), 2865 (C-H), 1737 (C=O), 1684, 1660 (C=O), 1587, 1506, 1482, 1440, 1396, 1371, 1283 (C-O), 1258, 1225, 1161 (C-O), 1131, 1098, 1080, 1061 cm^{-1}; δ_H (400 MHz, Chloroform-d) 8.78 (s, 1H, N-H), 3.68 (s, 3H, O-CH_3), 2.76-2.68 (m, 2H, 4-C$\underline{H_2}CH_2$), 2.49-2.40 (m, 2H, 4-$CH_2C\underline{H_2}$), 2.26 (s, 3H, 5-CH_3), 2.23 (s, 3H, 3-CH_3), 1.57 (s, 9H, tert-butyl); δ_C (101 MHz, Chloroform-d) 173.6 (4-C=O), 161.3 (2-C=O), 129.2 (C-5), 126.0 (C-3), 119.8 (C-4), 118.3 (C-2), 80.2 ($\underline{C}(CH_3)_3$), 51.6 (O-CH_3), 35.0 (4-$CH_2\underline{C}H_2$), 28.6 ($C(\underline{C}H_3)_3$), 19.6 (4-$\underline{C}H_2CH_2$), 11.4 (5-CH_3), 10.6 (3-CH_3); m/z (LCMS ES+) r_t 2.78 min, 282.38 $[M+H]^+$.

Tert-butyl 4-(3-ethoxy-3-oxopropyl)-3,5-dimethyl-1H-pyrrole-2-carboxylate (S13)

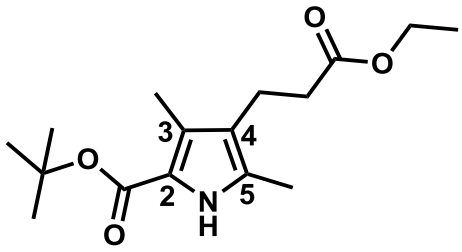

Procedure: followed the same procedure as described for S8.

Tert-butyl acetoacetate (0.87 g, 5.49 mmol, 1.1 eq) in glacial acetic acid (2.2 mL), $NaNO_2$ (0.50 g, 7.24 mmol, 1.45 eq) in water (1.0 mL), ethyl 4-acetyl-5-oxohexanoate (1.00 g, 4.99 mmol, 1.0 eq) and zinc dust (0.95 g, 14.48 mmol, 2.9 eq) were reacted to give tert-butyl 4-(3-ethoxy-3-oxopropyl)-3,5-dimethyl-1H-pyrrole-2-carboxylate (purified by chromatography ethyl acetate/ hexane = 1:9) as a pale yellow solid (0.57 g, 1.93 mmol, 39 % yield).

Characteristics: Melting point 68-69 °C; υ_{max} (ATR) 3326 (N-H), 2985 (C-H), 2937 (C-H), 2870 (C-H), 1737 (C=O), 1661 (C=O), 1587, 1506, 1482, 1440, 1396, 1371, 1283 (C-O), 1258, 1225, 1160 (C-O), 1131, 1098, 1080, 1062 cm^{-1}; δ_H (400 MHz, Chloroform-d) 8.90 (s, 1H, N-H), 4.13 (q, J = 7.1 Hz, 2H, $OC\underline{H_2}CH_3$), 2.73-2.67 (m, 2H, 4-$C\underline{H_2}CH_2$), 2.47-2.38 (m, 2H, 4-$CH_2C\underline{H_2}$), 2.26 (s, 3H, 5-CH_3), 2.23 (s, 3H, 3-CH_3), 1.57 (s, 9H, tert-butyl), 1.26 (t, J = 7.1 Hz, 3H, $OCH_2C\underline{H_3}$); δ_C (101 MHz, Chloroform-d) 173.2 (4-C=O), 161.2 (2-C=O), 129.0 (C-5), 126.1 (C-3), 119.9 (C-4), 118.2 (C-2), 80.2 ($\underline{C}(CH_3)_3$), 60.4 ($\underline{C}H_2CH_3$), 35.2 (4-CH2$\underline{C}$H2), 28.6 ($C(\underline{C}H_3)_3$), 19.6 (4-$\underline{C}H_2CH_2$), 14.2 ($CH_2\underline{C}H_3$), 11.5 (5-CH_3), 10.6 (3-CH_3); m/z (LCMS ES+) r_t 2.82 min, 296.36 $[M+H]^+$.

Methyl 3-(2,4-dimethyl-1H-pyrrol-3-yl) propanoate (S14)

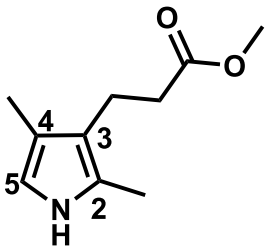

Procedure 1: following the same procedure 2 as described for S9.

S12 (100 mg, 0.36 mmol) in methanol (3.6 mL) and HCl (12 M, 0.14 mL, 1.70 mmol, 5.0 eq) was converted to S14 (16 mg, 0.09 mmol, 25 % yield).

Procedure 2: following the same procedure 3 as described for S9.

S12 (100 mg, 0.36 mmol) in trifluoroacetic acid (1 mL) was converted to methyl S14 (55 mg, 0.31 mmol, 85 % yield).

Procedure 3: following the same procedure 4 as described for S9.

S12 (100 mg, 0.36 mmol) in (1) 10 mL of ethanol containing 10% palladium-carbon (10 mg) and (2) trifluoroacetic acid (1 mL) was converted to S14 (65 mg, 0.36 mmol, 100 % yield).

Characteristics: δ_H (400 MHz, Chloroform-d) 7.59 (s, 1H, N-H), 6.41 (s, 1H, 5-H), 3.70 (s, 3H, OCH_3), 2.78-2.71 (m, 2H, 3-$C\underline{H}_2CH_2$), 2.52-2.45 (m, 2H, 3-$CH_2C\underline{H}_2$), 2.20 (s, 3H, 2-CH_3), 2.06 (s, 3H, 4-CH_3). δ_C (101 MHz, Chloroform-d) 174.5(C=O), 123.6(C-2), 116.1(C-4), 115.4(C-3), 112.8(C-5), 50.5($O\underline{C}H_3$), 35.1 (3-$CH_2\underline{C}H_2$), 19.7(3-$\underline{C}H_2CH_2$), 9.7(2-$\underline{C}H_3$), 9.2(4-$\underline{C}H_3$); m/z (LCMS ES+) r_t 2.37 min, 182.49 $[M+H]^+$.

1,3,5,7-Tetramethyl-2-methyl propanoate-8-(4-nitrophenyl)-BODIPY (S15)

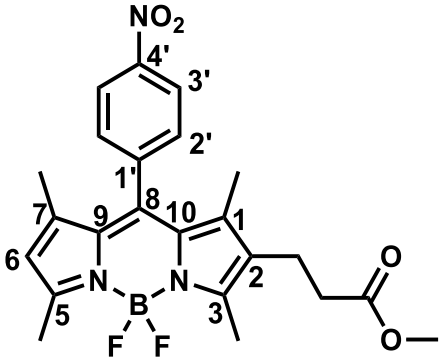

Procedure 1: following the same procedure 2 as described for S2.

S1 (2.97 g, 12.14 mmol, 1.0 eq) in dichloromethane (7.0 mL), S14 (2.20 g, 12.14 mmol, 1.0 eq), N,N-diisopropylethylamine (4.3 mL, 24.28 mmol, 2.0 eq) and boron trifluoride diethyl etherate (12.0 mL, 97.1 mmol, 8.0 eq) was converted to S15 (chromatography ethyl acetate/ hexane = 20%) as an orange solid (1.76 g, 3.87 mmol, 32 % yield).

Procedure 2: following the same procedure 2 as described for S2.

S17 (500 mg, 1.51 mmol, 1.0 eq) in dry DCM (7.0 mL), 2,4-dimethypyrrole (144 mg, 1.51 mmol, 1.0 eq), $BF_3{\cdot}OEt_2$ (1.5 mL, 12.11 mmol, 8.0 eq) and N,N-diisopropylethylamine (1.6 mL, 9.08 mmol, 6.0 eq) was converted to S15 as an orange solid (395 mg, 0.87 mmol, 57%).

Characteristics: Melting point 168-169 ^oC; υ_{max} (ATR) 3109, 2960, 2262, 1739 (C=O), 1604, 1548 (N=O), 1524, 1480, 1442, 1406, 1351 (N=O), 1316, 1268, 1247, 1198, 1164 (C-O), 1118, 1073, 1046, 1018 cm^{-1}; δ_H (700 MHz, Chloroform-d) 8.41 (d, J = 8.7 Hz, 2H, 3'-H), 7.55 (d, J = 8.7 Hz, 2H, 2'-H), 6.02 (s, 1H, 6-H), 3.68 (s, 3H, $OC\underline{H}_3$), 2.69-2.64 (m, 2H, 2-$C\underline{H}_2CH_2$), 2.59 (s, 3H, 5-CH_3), 2.58 (s, 3H, 3-CH_3), 2.41-2.35 (m, 2H, 2-$CH_2C\underline{H}_2$), 1.36 (s, 3H, 7-CH_3), 1.32 (s, 3H, 1-CH_3); δ_C (176 MHz, Chloroform-d) 172.9 (C=O), 156.2 (C-5), 156.0 (C-10), 148.3 (C-4'), 142.2 (C-7), 142.2 (C-8), 139.1 (C-3), 137.9 (C-1'), 130.5 (C-9), 130.3 (C-1), 130.2 (C-2), 129.7 (C-2'), 124.4 (C-3'), 121.7 (C-6), 51.8 ($O\underline{C}H_3$), 34.1 (2-$CH_2\underline{C}H_2$), 19.3 (2-$\underline{C}H_2CH_2$), 14.7 (7-CH_3), 14.7 (5-CH_3), 12.8 (3-CH_3), 12.2 (1-CH_3); m/z (LCMS ES-) r_t 3.31 min, 454.33 $[M-H]^-$; HRMS (ES-) found $[M-H]^-$ 454.1756, $C_{24}H_{26}BF_2N_3O_4$ requires M 454.1828.

1,3,5,7-tetramethyl-2-ethyl propanoate-8-(4-nitrophenyl)-BODIPY (S16)

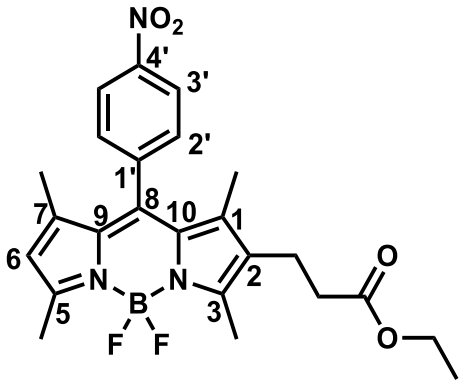

Procedure 1: following the same procedure 2 as described for S2.

S1 (3.13 g, 12.80 mmol, 1.0 eq) in dichloromethane (8.6 mL), S9 (2.50 g, 12.80 mmol, 1.0 eq), N,N-diisopropylethylamine (4.5 mL, 25.61 mmol, 2.0 eq) and boron trifluoride diethyl etherate (3.2 mL, 25.61 mmol, 2.0 eq) was converted to S16 (chromatography ethyl acetate/ hexane = 20%) as an orange solid (2.20 g, 4.69 mmol, 37 % yield).

Procedure 2: following the same procedure 2 as described for S2.

S18 (500 mg, 1.45 mmol, 1.0 eq) in dry DCM (7.0 mL), 2,4-dimethypyrrole (138 mg, 1.45 mmol, 1.0 eq), $BF_3 \cdot OEt_2$ (1.4 mL, 11.62 mmol, 8.0 eq) and N,N-diisopropylethylamine (1.5 mL, 8.71 mmol, 6.0 eq) was converted to S16 as an orange solid (420 mg, 0.90 mmol, 62%).

Characteristics: Melting point 134-135 ºC; υ_{max} (ATR) 3282, 2955, 2260, 1719 (C=O), 1577 (N=O), 1550, 1527, 1502, 1483, 1442, 1374, 1350 (N=O), 1316, 1288, 1199, 1164 (C-O), 1104, 1074, 1042, 1015 cm^{-1}; δ_H (700 MHz, Chloroform-d) 8.41 (d, J = 8.7 Hz, 2H, 3'-H), 7.55 (d, J = 8.7 Hz, 2H, 2'-H), 6.02 (s, 1H, 6-H), 4.13 (q, J = 7.1 Hz, 2H, $OC\underline{H_2}CH_3$), 2.72-2.62 (m, 2H, 2-$C\underline{H_2}CH_2$), 2.59 (s, 3H, 5-CH_3), 2.58 (s, 3H, 3-CH_3), 2.37 (t, J = 7.8 Hz, 2H, 2-$CH_2C\underline{H_2}$), 1.36 (s, 3H, 7-CH_3), 1.32 (s, 3H, 1-CH_3), 1.26 (t, J = 7.1 Hz, 3H, $OCH_2C\underline{H_3}$); δ_C (176 MHz, Chloroform-d) 172.4 (C=O), 156.0 (C-5), 156.0 (C-10), 148.3 (C-4'), 142.2 (C-7), 142.1 (C-8), 139.2 (C-3), 137.9 (C-1'), 130.4 (C-9), 130.3 (C-1,2), 129.7 (C-2'), 124.4 (C-3'), 121.6 (C-6), 60.6 ($\underline{C}H_2CH_3$), 34.3 (2-$CH_2\underline{C}H_2$), 19.2 (2-$\underline{C}H_2CH_2$), 14.7 (7-CH_3), 14.6 (5-CH_3), 14.2 ($CH_2\underline{C}H_3$), 12.8 (3-CH_3), 12.2 (1-CH_3); m/z (LCMS ES-) rt 3.38 min, 468.29 $[M-H]^-$; HRMS (ES+) found $[M+H]^+$ 470.2012, $C_{24}H_{26}BF_2N_3O_4$ requires M 470.1984.

Methyl 3-(2,4-dimethyl-5-(4-nitrobenzoyl)-1H-pyrrol-3-yl)propanoate (S17)

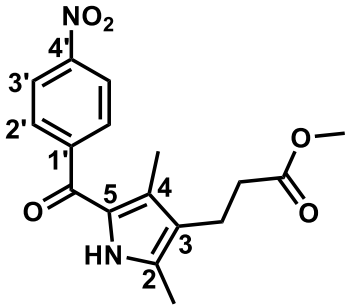

Procedure 1: following the same **procedure** as described for S1.

S14 (1.0 g, 5.52 mmol, 1.0 eq) and methylmagnesium bromide 3M in ether (1.8 mL, 5.52 mmol, 1.0 eq) in ether (50 mL) and 4-nitrobenzoyl chloride (1.02 g, 5.52 mmol, 1.0 eq) in ether (50 mL) was converted to S17 (purified by chromatography ethyl acetate/ hexane = 20%-40%) as bright yellow solid (0.66 g, 2.00 mmol, 36% yield).

Procedure 2: To a solution of S14 (1.00 g, 5.52 mmol, 1.0 eq) and Et_3N (1.9 mL, 5.63 mmol, 1.1 eq) in THF (50 mL) at room temperature was added 4-nitrobenzoyl chloride (1.02 g, 5.52 mmol, 1.0 eq) over few minutes. Thereafter the mixture was heated under reflux for 6 h and then cooled to room temperature. The triethylamine hydrochloride precipitate was removed by filtration and was washed with THF. From the combined filtrate and washings the volatiles were removed in vacuo (trap condensation) and the solid residue was purified by chromatography (ethyl acetate/ hexane = 20%-40%) to obtain S17 as a bright yellow solid (1.34 g, 3.89 mmol, 76% yield).

Characteristics: Melting point °C; υ_{max} (ATR) 3255 (N-H), 1750 (C=O) cm^{-1}; δ_H (400 MHz, DMSO-d_6) 9.39 (s, 1H, N-H), 8.33 (d, J = 8.6 Hz, 2H, 3'-H), 7.77 (d, J = 8.5 Hz, 2H, 2'-H), 3.69 (s, 3H, OC$\underline{H}_3$), 2.72 (t, J = 7.7 Hz, 2H, 3-$CH_2C\underline{H}_2$), 2.46 (t, J = 7.7 Hz, 2H, 3-$C\underline{H}_2CH_2$), 2.32 (s, 3H, 2-C$\underline{H}_3$), 1.85 (s, 3H, 4-C$\underline{H}_3$); δ_C (101 MHz, DMSO-d_6) 182.84(C=O ketone), 173.26(C=O ester), 149.01(C-4'), 146.07(C-1'), 135.30(C-2), 129.40(C-4), 129.03(C-2'), 126.71(C-5), 123.70(C-3'), 122.24(C-3), 51.71(O$\underline{C}H_3$), 34.54(3-$CH_2\underline{C}H_2$), 19.47(3-$\underline{C}H_2CH_2$), 11.92(2-$\underline{C}H_3$), 11.76(4-$\underline{C}H_3$); m/z (LCMS ES+) r_t 2.60 min, 331,13 $[M+H]^+$. HRMS (ES+) found $[M+H]^+$ 331.13, $C_{17}H_{18}N_2O_5$ requires M 331.1216.

Ethyl 3-(2,4-dimethyl-5-(4-nitrobenzoyl)-1H-pyrrol-3-yl)propanoate (S18)

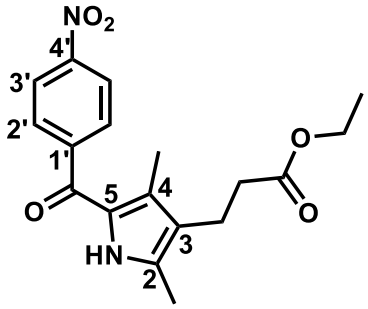

Procedure 1: following the same procedure as described for S1.

S9 (1.00 g, 5.12 mmol, 1.0 eq) and methylmagnesium bromide 3M in ether (1.7 mL, 5.12 mmol, 1.0 eq) in ether (25 mL) and 4-nitrobenzoyl chloride (0.95 g, 5.12 mmol, 1.0 eq) in ether (25 mL) was converted to S18 (purified by chromatography ethyl acetate/ hexane = 20%-40%) as bright yellow solid (0.68 g, 1.98 mmol, 39% yield).

Procedure 2: following the same procedure 2 as described for S17.

S9 (1.0 g, 5.12 mmol, 1.0 eq), 4-nitrobenzoyl chloride (0.95 g, 5.12 mmol, 1.0 eq) and Et_3N (1.9 mL, 5.63 mmol, 1.1 eq) in THF (50 mL) was converted to S18 as a bright yellow solid (1.34 g, 3.89 mmol, 76% yield).

Characteristics: Melting point °C; υ_{max} (ATR) 3270 (N-H), 1725 (C=O) cm^{-1}; δ_H (400 MHz, DMSO-d_6) 9.91 (s, 1H, N-H), 8.31 (d, J = 8.3 Hz, 2H, 3'-H), 7.76 (d, J = 8.4 Hz, 2H, 2'-H), 4.12 (q, J = 7.1 Hz, 2H, $OC\underline{H_2}CH_3$), 2.71 (t, J = 7.8 Hz, 2H, 3-$CH_2C\underline{H_2}$), 2.43 (t, J = 7.7 Hz, 2H, 3-$C\underline{H_2}CH_2$), 2.31 (s, 3H, 2-$C\underline{H_3}$), 1.83 (s, 3H, 4-$C\underline{H_3}$), 1.25 (t, J = 7.1 Hz, 3H, $OCH_2C\underline{H_3}$); δ_C (101 MHz, DMSO-d_6) 182.81(C=O ketone), 172.9(C=O ester), 149.0(C-4'), 146.2(C-1'), 135.9(C-2), 129.7(C-4), 129.1(C-2'), 126.7(C-5), 123.7(C-3'), 122.4(C-3), 60.5($O\underline{C}H_2CH_3$), 34.8(3-$CH_2\underline{C}H_2$), 19.5(3-$\underline{C}H_2CH_2$), 14.2($OCH_2\underline{C}H_3$), 12.0(2-$\underline{C}H_3$), 11.7(4-$\underline{C}H_3$); m/z (LCMS ES+) r_t 1.37 min, 345.39 $[M+H]^+$. HRMS (ES+) found $[M+H]^+$ 345.14, $C_{18}H_{20}N_2O_5$ requires M 345.1372.

1,3,5,7-Tetramethyl-2-propanol-8-(4-nitrophenyl)-BODIPY (S19)

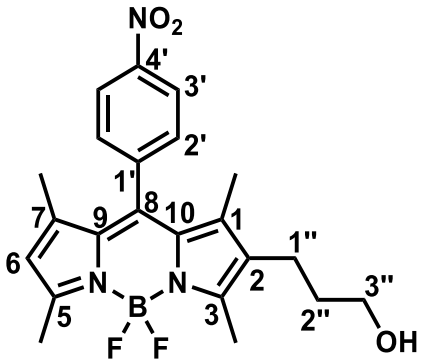

Procedure 1: To a solution of S16 (500 mg, 1.07 mmol, 1.0 equiv) in THF (25 mL) at -78 °C DIBAL-H (1M solution in toluene, 3.2 mL, 3.0 equiv) was added portionwise. After 2 h (monitored by TLC) stirring at -30 °C, methanol (1.0 mL, >24.0 equiv) and water (0.1 mL, >3.0 equiv) were added dropwise. The reaction mixture was then filtered through a plug of celite, dried over anhydrous sodium sulphate and evaporated in a rotavapor. The residue was purified by flash column chromatography eluting with ethyl acetate : hexane = 1:1 to yield S19 as a red solid (280 mg, 0.66 mmol, 62% yield).

Procedure 2: following the same procedure 1 as described for S19.

S15 (500 mg, 1.10 mmol, 1.0 equiv) in THF (25 mL) and DIBAL-H (1M solution in toluene, 3.3 mL, 3.0 equiv) was was converted to S19 as a red solid (305 mg, 0.72 mmol, 65% yield).

Characteristics: Melting point 125-126 ºC; υ_{max} (ATR) 3105, 2958, 2927, 2873, 1717, 1604, 1550 (N=O), 1523, 1478, 1440, 1407, 1366, 1352 (N=O), 1316, 1287, 1267, 1226, 1200, 1165, 1119, 1054 (C-O) cm^{-1}; δ_H (700 MHz, Chloroform-d) 8.37 (d, J = 8.6 Hz, 2H, 3'-H), 7.52 (d, J = 8.5 Hz, 2H, 2'-H), 5.97 (s, 1H, 6-H), 3.60 (t, J = 6.2 Hz, 2H, 3''-H), 2.55 (s, 3H, 5-CH_3), 2.54 (s, 3H, 3-CH_3), 2.40 (t, J = 7.3 Hz, 2H, 1''-H), 1.61 (dt, J = 13.7, 6.6 Hz, 2H, 2''-H), 1.33 (s, 3H, 7-CH_3), 1.29 (s, 3H, 1-CH_3); δ_C (176 MHz, Chloroform-d) 156.6 (C-5), 155.5 (C-10), 148.3 (C-4'), 142.3 (C-8), 141.6 (C-7), 139.0 (C-3), 137.6 (C-1'), 131.8 (C-2), 130.4 (C-1), 130.2 (C-9), 129.8 (C-2'), 124.3 (C-3'), 121.4 (C-6), 61.9 (C-3''), 32.7 (C-2''), 19.9 (C-1''), 14.6 (7-CH_3), 14.5 (5-CH_3), 12.8 (3-CH_3), 12.2 (1-CH_3); m/z (LCMS ES-) r_t 2.93 min, 426.29 $[M-H]^-$; HRMS (ES-) found $[M-H]^-$ 426.1801, $C_{22}H_{24}BF_2N_3O_3$ requires M 426.1879.

1,3,5,7-Tetramethyl-2-(4-methylbenzenesulfonate)-propyl-8-(4-nitrophenyl)-BODIPY (S21)

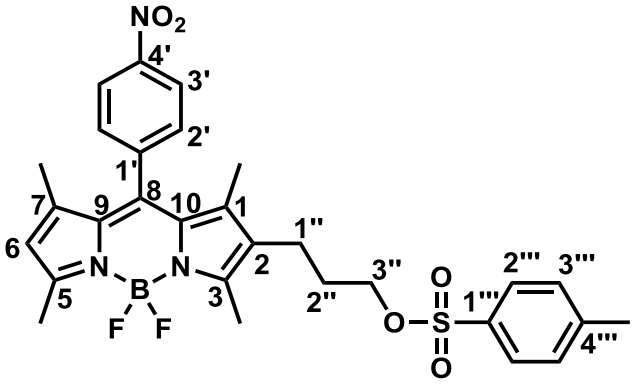

Procedure: Toluene-4-sulfonyl chloride (161 mg, 0.84 mmol, 1.2 eq) and triethylamine (0.25 mL, 2.5 eq) were added to a stirred solution of S19 (300 mg, 0.70 mmol, 1 mmol) in DCM (7.0 mL) at 0 °C. The solution was stirred at 0 °C for 4 h. The mixture was then poured into satd. $NaHCO_3$ (20 mL) and extracted with DCM (3 × 20 mL). The organic layers were washed with HCl (2 M, 3 × 20 mL) and water (20 mL). The combined organic layer were dried by $MgSO_4$, and the solvent removed under reduced pressure. The residue was purified by flash column chromatography eluting with 10%-20% ethyl acetate / hexane to yield S21 as a red solid (206 mg, 0.36 mmol, 52% yield).

Characteristics: Melting point 76-77 °C; υ_{max} (ATR) 3593, 3008, 2951, 2298, 2259, 2161, 2025, 1603, 1550 (N=O), 1524, 1479, 1445, 1410, 1378, 1352 (N=O), 1316, 1289, 1268, 1194 (S=O), 1179 (C-O), 1074, 1055 cm^{-1}; δ_H (700 MHz, Chloroform-d) 8.40 (d, J = 8.7 Hz, 2H, 3'-H), 7.78 (d, J = 8.3 Hz, 2H, 2'''-H), 7.53 (d, J = 8.7 Hz, 2H, 2'-H), 7.36 (d, J = 8.0 Hz, 2H, 3'''-H), 6.02 (s, 1H, 6-H), 4.01 (t, J = 6.0 Hz, 2H, 3''-H), 2.57 (s, 3H, 5-CH_3), 2.49 (s, 3H, 3-CH_3), 2.46 (s, 3H, 4'''-CH_3), 2.42 – 2.35 (m, 2H, 1''-H), 1.71 (dt, J = 12.6, 6.2 Hz, 3H, 2''-H), 1.36 (s, 3H, 7-CH_3), 1.27 (s, 3H, 1-CH_3); δ_C (176 MHz, Chloroform-d) 156.1 (C-5), 155.8 (C-10), 148.3 (C-4'), 144.9 (C-1'''), 142.2 (C-7), 142.1 (C-8), 139.0 (C-3), 137.9 (C-1'), 133.0 (C-4'''), 130.5 (C-2), 130.2 (C-1), 130.2 (C-9), 129.9 (C-3'''), 129.7 (C-2'), 127.8 (C-2'''), 124.4 (C-3'), 121.7 (C-6), 69.4 (C-3''), 29.2 (C-2''), 21.6 (4'''-CH_3), 19.8 (C-1''), 14.7 (7-CH_3), 14.6 (5-CH_3), 12.7 (3-CH_3), 12.2 (1-CH_3); m/z (LCMS ES+) r_t 3.60 min, 582.37 $[M+H]^+$; HRMS (ES+) found $[M+H]^+$ 581.1973, $C_{29}H_{30}BF_2N_3O_5S$ requires M 581.1967.

1,3,5,7-Tetramethyl-2-iodopropyl-8-(4-nitrophenyl)-BODIPY (S22)

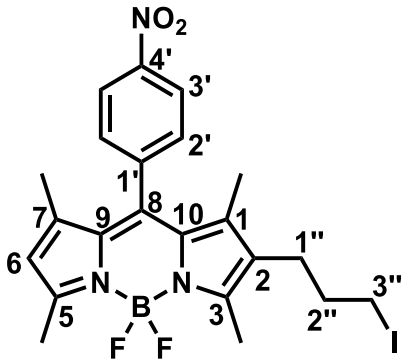

Procedure: A round bottom flask was charged with PPh_3 (46 mg, 0.18 mmol, 1.5 eq) and 1 mL dichloromethane. Iodine (45 mg, 0.18 mmol, 1.5 eq) was added in small portions under N_2 at room temperature and the reaction was stirred for 10 minutes. Imidazole (20 mg, 0.29 mmol, 2.5 eq) was added to the solution in small portions and the reaction was allowed to stir for a furyher 10 minutes. S19 (50 mg, 0.12 mmol, 1.0 eq) in dichloromethane (1 mL) was added to the suspension dropwise in 5 minutes and the reaction was stirred for 1 hour at room temperature. 10 mL saturated $Na_2S_2O_5$ was added to the reaction mixture and the aqueous layer was extracted with dichloromethane twice. The organic layer was dried over $MgSO_4$ and concentrated. The residue was purified by flash column chromatography eluting with 10% ethyl acetate / hexane to yield S22 as a red solid (52 mg, 0.10 mmol 83% yield).

Characteristics: Melting point 163-164 ºC; υ_{max} (ATR) 3105, 2954, 2927, 2862, 2300, 2257, 1712, 1604, 1549 (N=O), 1524, 1479, 1445, 1406, 1350 (N=O), 1316, 1266, 1228, 1199, 1165, 1116, 1073, 1016 cm^{-1}; δ_H (700 MHz, Chloroform-d) 8.41 (d, J = 8.7 Hz, 2H, 3'-H), 7.56 (d, J = 8.7 Hz, 2H, 2'-H), 6.02 (s, 1H, 6-H), 3.17 (t, J = 6.7 Hz, 2H, 3''-H), 2.59 (s, 3H, 5-CH_3), 2.58 (s, 3H, 3-CH_3), 2.50-2.41 (m, 2H, 1''-H), 1.90 (p, J = 6.7 Hz, 2H, 2''-H), 1.37 (s, 3H, 7-CH_3), 1.33 (s, 3H, 1-CH_3); m/z (LCMS ES+) r_t 3.74 min, 538.29 $[M+H]^+$; HRMS (ES+) found $[M+H]^+$ 538.0930, $C_{22}H_{23}BF_2IN_3O_2$ requires M 538.0896.

1,2-Di-tert-butyl-4-(3-methoxy-3-oxopropyl)-3,5-dimethyl-1H-pyrrole-1,2-dicarboxylate (S24)

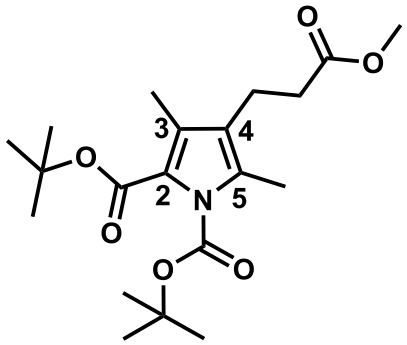

Procedure: S12 (2.5 g, 8.89 mmol, 1.0 eq) was dissolved in 30 mL of dichloromethane. A solution of triethylamine (5.9 mL, 44.43 mmol, 5.0 eq), di-*tert*-butyldicarbonate (2.33 g, 10.66 mmol, 1.2 eq) and 4-dimethylaminopyridine (0.11 g, 0.89 mmol, 0.1 eq) in 30 mL dichloromethane was added immediately. The resulting mixture was refluxed overnight. The reaction mixture was subjected to flash chromatography over silica gel using with 10% ethyl acetate / hexane leading to S24 as a colourless oil (3.35 g, 8.78 mmol, 99% yield).

Characteristics: υ_{max} (ATR) 3009, 2985, 2958, 2937, 2257, 1743, 1701 (C=O), 1606 (C=O), 1516, 1482, 1459, 1438, 1426, 1392, 1371, 1326, 1294, 1261, 1239 (C-O), 1156 (C-O), 1106, 1069, 1050, 1036, 1019 cm^{-1}; δ_H (400 MHz, Chloroform-d) 3.68 (s, 3H, OCH_3), 2.68 (t, J = 7.9 Hz, 2H, 4-C$\underline{H_2}CH_2$), 2.40 (t, J = 7.8 Hz, 2H, 4-C$\underline{H_2}CH_2$), 2.28 (s, 3H, 5-CH_3), 2.17 (s, 3H, 3-CH_3), 1.57 (s, 18H, tert-butyl); δ_C (101 MHz, Chloroform-d) 173.3 (4-C=O), 160.8 (2-C=O), 149.9 (N-C=O), 131.9 (C-5), 128.4 (C-3), 122.1 (C-4), 120.7 (C-2), 84.1 (2-$\underline{C}(CH_3)_3$), 80.8 (N-$\underline{C}(CH_3)_3$), 51.6 (OCH_3), 34.6 (4-$CH_2\underline{C}H_2$), 28.5 (2-C($\underline{C}H_3)_3$), 27.7 (N-C($\underline{C}H_3)_3$), 19.5 (4-$\underline{C}H_2CH_2$), 11.6 (5-CH_3), 10.5 (3-CH_3); m/z (LCMS ES+) r_t 4.01 min, 382.47 $[M+H]^+$.

Tert-butyl 3-(3-methoxy-3-oxopropyl)-2,4-dimethyl-1H-pyrrole-1-carboxylate (S25)

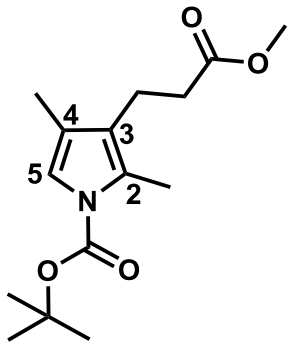

Procedure: S12 (500 mg, 1.78 mmol, 1.0 eq) was immediately dissolved in 1 mL of TFA and stirred under an Ar atmosphere at ambient temperature for 10 min. The reaction was then diluted with 50 mL dichloromethane and washed with water and 1 M $NaHCO_3$ aq., dried over anhydrous sodium sulfate, filtered, and evaporated, affording methyl 3-(2,4-dimethyl-1H-pyrrol-3-yl) propanoate as a slightly yellow oil. The oil was dissolved in 4 mL of dichloromethane and then di-tert-butyldicarbonate (465 mg, 2.13 mmol, 1.2 eq) and 4-dimethylaminopyridine (19 mg, 0.18 mmol, 0.1 eq) in 2 mL dichloromethane were added. The resulting mixture was stirred overnight at room temperature. The reaction mixture was subjected to flash chromatography over silica gel using with 5% ethyl acetate / hexane leading to S25 as a colourless oil (180 mg, 0.64 mmol, 36% yield).

Characteristics: υ_{max} (ATR) 3012, 2991, 2959, 2935, 2865, 2299, 2257, 1740 (C=O), 1553, 1480, 1459, 1441, 1416, 1391, 1370, 1362, 1257 (C-O), 1196, 1161 (C-O), 1120, 1083, 1062, 1040 cm^{-1}; δ_H (400 MHz, Chloroform-d) 6.94 (s, 1H, 5-H), 3.69 (s, 3H, OCH_3), 2.72-2.65 (m, 2H, 3-C$\underline{H_2}CH_2$), 2.47-2.40 (m, 2H, 3-$CH_2C\underline{H_2}$), 2.36 (s, 3H, 2-CH_3), 1.99 (d, J = 1.2 Hz, 3H, 4-CH_3), 1.58 (s, 9H, tert-butyl); δ_C (101 MHz, Chloroform-d) 173.5 (3-C=O), 149.6 (N-C=O), 127.6 (C-2), 122.5 (C-4), 120.2 (C-3), 117.0 (C-5), 82.7 ($\underline{C}(CH_3)_3$), 51.6 (OCH_3), 34.8 (3-$CH_2\underline{C}H_2$), 28.1 ($C(\underline{C}H_3)_3$), 19.8 (3-$\underline{C}H_2CH_2$), 12.7 (2-CH_3), 10.2 (4-CH_3); m/z (LCMS ES+) r_t 3.57 min, 282.42 $[M+H]^+$.

Tert-butyl 4-(3-hydroxypropyl)-3,5-dimethyl-1H-pyrrole-2-carboxylate (S26)

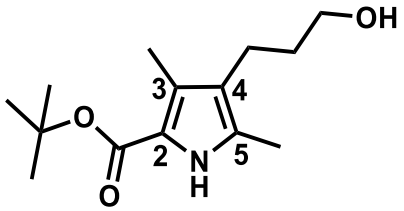

Procedure: following the same procedure as described for S19.

S12 (150 mg, 0.53 mmol, 1.0 equiv) in THF (25 mL) and DIBAL-H (1M solution on toluene, 1.6 mL, 3.0 equiv) was converted to S26 (purified by chromatography ethyl acetate/ hexane = 1:4) as a colourless oil (133 mg, 0.53 mmol, 99% yield).

Characteristics: υ_{max} (ATR) 3322 (N-H, O-H), 2981, 2935, 2869, 2296, 2257, 1654 (C=O), 1585, 1505, 1482, 1438, 1395, 1381, 1369, 1333, 1281, 1258, 1223, 1161 (C-O), 1102, 1066, 1038 cm^{-1}; δ_H (400 MHz, Chloroform-d) 8.94 (s, 1H, N-H), 3.65 (t, J = 6.4 Hz, 2H, $C\underline{H_2}OH$), 2.46 (t, J = 7.5 Hz, 2H, 4-$C\underline{H_2}CH_2$), 2.26 (s, 3H, 5-CH_3), 2.22 (s, 3H, 3-CH_3), 1.71 (dt, J = 13.7, 6.6 Hz, 2H, 4-$CH_2C\underline{H_2}$), 1.57 (s, 9H, tert-butyl); δ_C (101 MHz, Chloroform-d) 161.5 (C=O), 129.1 (C-5), 126.2 (C-3), 121.0 (C-4), 118.1 (C-2), 80.1 ($\underline{C}(CH_3)_3$), 62.4 (CH_2OH), 33.6 (4-$CH_2\underline{C}H_2$), 28.6 ($C(\underline{C}H_3)_3$), 20.2 (4-$\underline{C}H_2CH_2$), 11.4 (5-CH_3), 10.7 (3-CH_3); m/z (LCMS ES+) r_t 2.95 min, 254.45 $[M+H]^+$.

1,2-Di-tert-butyl 4-(3-hydroxypropyl)-3,5-dimethyl-1H-pyrrole-1,2-dicarboxylate (S27)

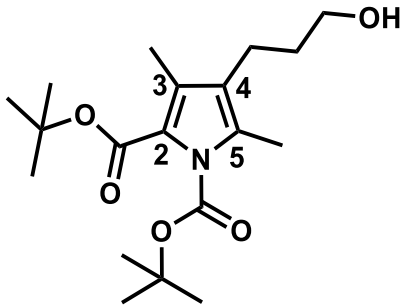

Procedure: following the same procedure as described for S19.

S24 (3.0 g, 7.86 mmol, 1.0 equiv) in THF (180 mL) and DIBAL-H (1M solution on toluene, 23.6 mL, 3.0 equiv) was converted to S27 (purified by chromatography ethyl acetate/ hexane = 1:4) as a colourless oil (3.11 g, 7.86 mmol, 100% yield).

Characteristics: υ_{max} (ATR) 3493 (O-H), 3013, 2984, 2939, 2873, 2300, 2258, 1748 (C=O), 1698 (C=O), 1600, 1518, 1481, 1458, 1425, 1392, 1371, 1322, 1298, 1239 (C-O), 1158 (C-O), 1106, 1048 cm^{-1}; δ_H (400 MHz, Chloroform-d) 3.58 (t, J = 6.3 Hz, 2H, $C\underline{H_2}OH$), 2.38 (t, J = 7.4 Hz, 2H, 4-$C\underline{H_2}CH_2$), 2.24 (s, 3H, 5-CH_3), 2.13 (s, 3H, 3-CH_3), 1.62 (q, J = 6.9 Hz, 2H, 4-$CH_2C\underline{H_2}$), 1.54 (s, 18H, tert-butyl); δ_C (101 MHz, Chloroform-d) 160.9 (2-C=O), 150.0 (N-C=O), 131.6 (C-5), 128.8 (C-3), 122.2 (C-4), 122.0 (C-2), 83.9 (2-$\underline{C}(CH_3)_3$), 80.7 (N-$\underline{C}(CH_3)_3$), 61.9 ($\underline{C}H_2OH$), 33.1 (4-$CH_2\underline{C}H_2$), 28.4 (2-$C(\underline{C}H_3)_3$), 27.6 (N-$C(\underline{C}H_3)_3$), 20.1 (4-$\underline{C}H_2CH_2$), 11.6 (5-CH_3), 10.5 (3-CH_3); m/z (LCMS ES+) r_t 3.29 min, 354.43 $[M+H]^+$.

Tert-butyl 3-(3-hydroxypropyl)-2,4-dimethyl-1H-pyrrole-1-carboxylate (S28)

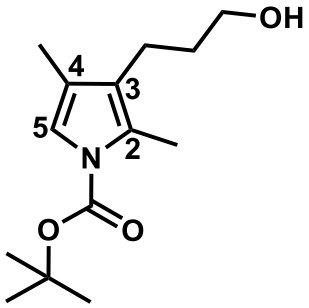

Procedure: following the same procedure as described for S19.

S25 (150 mg, 0.53 mmol, 1.0 equiv) in THF (25 mL) and DIBAL-H (1M solution on toluene, 1.6 mL, 3.0 equiv) was converted to S28 (purified by chromatography ethyl acetate/ hexane = 1:9) as a colourless oil (126 mg, 0.50 mmol, 93% yield).

Characteristics: υ_{max} (ATR) 3430 (O-H), 2981, 2935, 2873, 2296, 2257, 2161, 2037, 1983, 1769, 1731 (C=O), 1619, 1552, 1480, 1460, 1412, 1390, 1363, 1330, 1256 (C-O), 1194, 1160, 1098, 1070, 1042 cm^{-1}; δ_H (400 MHz, Chloroform-d) 6.94 (s, 1H, 5-H), 3.66 (t, J = 6.4 Hz, 2H, $C\underline{H_2}OH$), 2.47-2.40 (m, 2H, 3-$C\underline{H_2}CH_2$), 2.36 (s, 3H, 2-CH_3), 1.99 (d, J = 1.2 Hz, 3H, 4-CH_3), 1.71 (dt, J = 13.8, 6.5 Hz, 2H, 3-$CH_2C\underline{H_2}$), 1.58 (s, 9H, tert-butyl); δ_C (101 MHz, Chloroform-d) 149.7 (C=O), 127.2 (C-2), 123.8 (C-4), 120.5 (C-3), 116.9 (C-5), 82.6 ($\underline{C}(CH_3)_3$), 62.4 (CH_2OH), 33.3 (3-$CH_2\underline{C}H_2$), 28.1 ($C(\underline{C}H_3)_3$), 20.4 (3-$\underline{C}H_2CH_2$), 12.7 (2-CH_3), 10.3 (4-CH_3); m/z (LCMS ES+) r_t 2.71 min, 254.71 $[M+H]^+$.

Tert-butyl 4-(3-iodopropyl)-3,5-dimethyl-1H-pyrrole-2-carboxylate (S29)

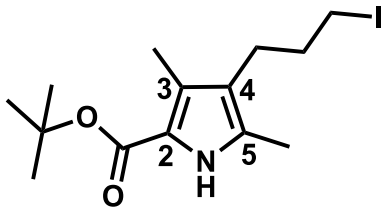

Procedure: following the same procedure as described for S22.

PPh_3 (186 mg, 0.71 mmol, 1.5 eq) in 2 mL dichloromethane, iodine (180 mg, 0.71 mmol, 1.5 eq), imidazole (81 mg, 1.18 mmol, 2.5 eq) and S26 (120 mg, 0.47 mmol, 1.0 eq) was converted to S29 (purified by chromatography ethyl acetate/ hexane = 1:4) as a colourless oil (142 mg, 0.39 mmol, 83% yield).

Characteristics: υ_{max} (ATR) 3342 (N-H), 3017, 2976, 2925, 2861, 2259, 1660 (C=O), 1503, 1479, 1456, 1442, 1391, 1377, 1367, 1279, 1256, 1226, 1218, 1187, 1164 (C-O), 1137, 1092, 1039, 1024 cm^{-1}; δ_H (400 MHz, Chloroform-d) 8.58 (s, 1H, N-H), 3.19 (t, J = 6.8 Hz, 2H, CH_2I), 2.49 (t, J = 7.3 Hz, 2H, 4-$C\underline{H_2}CH_2$), 2.27 (s, 3H, 5-CH_3), 2.25 (s, 3H, 3-CH_3), 1.98 (p, J = 6.9 Hz, 2H, 4-$CH_2C\underline{H_2}$), 1.58 (s, 9H, tert-butyl); δ_C (101 MHz, Chloroform-d) 161.2 (C=O), 129.0 (C-5), 126.2 (C-3), 119.9 (C-4), 118.3 (C-2), 80.2 ($\underline{C}(CH_3)_3$), 34.6 (4-$CH_2\underline{C}H_2$), 28.6 ($C(\underline{C}H_3)_3$), 24.7 (4-$\underline{C}H_2CH_2$), 11.7 (5-CH_3), 10.8 (3-CH_3), 6.6 (CH_2I); m/z (LCMS ES+) r_t 3.53 min, 364.35 $[M+H]^+$.

Tert-butyl 3-(3-iodopropyl)-2,4-dimethyl-1H-pyrrole-1-carboxylate (S31)

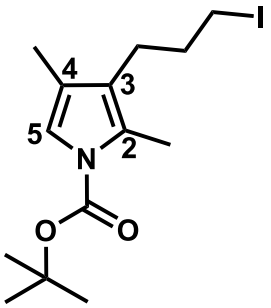

Procedure: following the same procedure as described for S22.

PPh_3 (186 mg, 0.71 mmol, 1.5 eq) in 2 mL dichloromethane, iodine (180 mg, 0.71 mmol, 1.5 eq), imidazole (81 mg, 1.18 mmol, 2.5 eq) and S28 (120 mg, 0.47 mmol, 1.0 eq) was converted to S31 (purified by chromatography ethyl acetate/ hexane = 1:4) as a colourless oil (100 mg, 0.28 mmol, 58% yield).

Characteristics: υ_{max} (ATR) 3011, 2984, 2936, 2900, 2865, 2296, 2258, 1737 (C=O), 1618, 1551, 1480, 1459, 1415, 1390, 1362, 1347, 1333, 1255, 1224, 1194, 1161 (C-O), 1135, 1079, 1039, 1024 cm^{-1}; δ_H (400 MHz, Chloroform-d) 6.95 (s, 1H, 5-H), 3.20 (t, J = 6.9 Hz, 2H, CH_2I), 2.46 (t, J = 7.4 Hz, 2H, 3-C$\underline{H_2}CH_2$), 2.38 (s, 3H, 2-CH_3), 1.99 (m, 5H, 3-$CH_2C\underline{H_2}$, 5-CH_3), 1.59 (s, 9H, tert-butyl); δ_C (101 MHz, Chloroform-d) 149.6 (C=O), 127.6 (C-2), 122.6 (C-4), 120.4 (C-3), 117.0 (C-5), 82.7 ($\underline{C}(CH_3)_3$), 34.4 (3-$CH_2\underline{C}H_2$), 28.1 ($C(\underline{C}H_3)_3$), 24.9 (3-$\underline{C}H_2CH_2$), 13.0 (2-CH_3), 10.4 (4-CH_3), 6.5 (CH_2I); m/z (LCMS ES+) r_t 4.04 min, 364.58 $[M+H]^+$.

1,3,5,7-Tetramethyl-2-propanoic acid-8-(4-nitrophenyl)-BODIPY (S36)

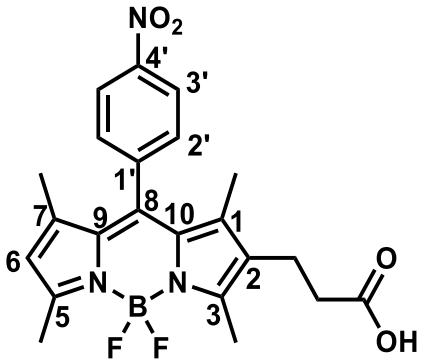

Procedure 1: An aqueous solution of NaOH (0.06 M, 40 mL) was slowly added to a solution of S16 (100 mg, 0.22 mmol, 1.0 eq) in 40 mL THF and the reaction mixture was stirred at 50 °C for 30 min. When the reaction was completed, AcOH in water (0.5 M) was added until reaching pH 3 and the aqueous layer was extracted with DCM (3 × 20 mL). The organic extracts were dried over $MgSO_4$, filtered and evaporated under reduced pressure. The crude compound was purified by column chromatography over silica gel (ethyl acetate : AcOH = 99:1) to afford S36 as a red solid (54 mg, 0.12 mmol, 56 % yield).

Procedure 2: following the same procedure 1 as described for S36.

Aqueous solution of NaOH (0.06 M, 40 mL), S15 (100 mg, 0.21 mmol, 1.0 eq) in 40 mL THF was converted to S36 as a red solid (50 mg, 0.11 mmol, 53 % yield).

Characteristics: υ_{max} (ATR) 2923, 2854, 1708(C=O), 1548 (N=O), 1524, 1475, 1406, 1347 (N=O), 1310, 1196, 1165 cm^{-1}; δ_H (700 MHz, DMSO-d_6) 12.18 (s, 1H, COO<u>H</u>), 8.41 (d, J = 8.6 Hz, 2H, 3'-H), 7.74 (d, J = 8.6 Hz, 2H, 2'-H), 6.18 (s, 1H, 6-H), 2.56 (t, J = 7.5 Hz, 2H, 2-C<u>H</u>$_2$CH$_2$), 2.49 (s, 3H, 5-CH_3), 2.45 (s, 3H, 3-CH_3), 2.29 (t, J = 7.4 Hz, 2H, 2-CH$_2$C<u>H</u>$_2$), 1.31 (s, 3H, 7-CH_3), 1.29 (s, 3H, 1-CH_3); δ_C (176 MHz, DMSO-d_6) 174.12(C=O), 156.45(C-5), 154.91(C-10), 148.50(C-4'), 142.15 (C-7), 141.57(C-8), 140.00(C-3), 139.09(C-1'), 131.23(C-9), 130.50(C-2'), 130.15(C-1), 130.10(C-2), 124.87(C-3'), 121.83(C-6), 34.17(2-CH$_2$<u>C</u>H$_2$), 19.22(2-<u>C</u>H$_2$CH$_2$), 14.73(7-CH_3), 14.66(5-CH_3), 13.04(3-CH_3), 12.38(1-CH_3); m/z (LCMS ES+) r_t 3.34 min, 440.12 $[M-H]^-$; HRMS (ES+) found $[M+H]^+$ 442.1754, $C_{22}H_{22}BF_2N_3O_4$ requires M 442.1671.

1,3,5,7-Tetramethyl-2-N-(prop-2-yn-1-yl)propanate NHS ester-8-(4-nitrophenyl)-BODIPY (S37)

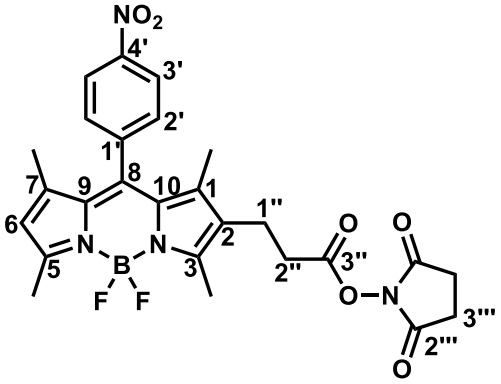

Procedure: EDC (196 mg, 1.02 mmol, 1.5 eq) was added to a solution of S36 (300 mg, 0.68 mmol, 1.0 eq) in dichloromethane (5.5 mL). The mixture was stirred for 10 min and N-hydroxysuccinimide (172 mg, 1.50 mmol, 2.2 eq) was added. The reaction was stirred overnight until no starting material was left. The crude mixture was diluted with dichloromethane (100 mL) and washed with water (3 x 50 mL). The organic extracts were dried over $MgSO_4$, filtered and evaporated under reduced pressure. The crude compound was purified by column chromatography over silica gel (ethyl acetate : hexane = 50%) to afford S37 as a red solid (320 mg, 0.60 mmol, 88% yield).

Characteristics: δ_H (700 MHz, Chloroform-d) 8.40 (d, J = 8.2 Hz, 2H, 3'-H), 7.57 (d, J = 8.3 Hz, 2H, 2'-H), 6.02 (s, 1H, 6-H), 2.84 (s, 4H, 3'''-H), 2.77 (t, J = 7.6 Hz, 2H, 1''-H), 2.66 (t, J = 7.2 Hz, 2H, 2''-H), 2.57 (d, J = 6.2 Hz, 6H, 3-CH_3, 5-CH_3), 1.34 (d, J = 15.5 Hz, 6H, 1-CH_3, 7-CH_3); δ_C (101 MHz, Chloroform-d) 169.01 (C-2'''), 167.59 (C-3''), 156.72 (C-5), 155.26 (C-10), 148.35 (C-4'), 142.64 (C-7), 142.07 (C-8), 139.13 (C-3), 138.21 (C-1'), 130.71 (C-9), 130.14 (C-1), 129.75 (C-2'), 128.63 (C-2), 124.42 (C-3'), 121.92 (C-6), 31.09 (C-2''), 25.57 (C-3'''), 18.94 (C-1''), 14.75 (5-CH_3), 14.66 (7-CH_3), 12.79 (3-CH_3), 12.31 (1-CH_3); m/z (LCMS ES-) r_t 3.06 min, 537.43 $[M-H]^-$; HRMS (ES-) found $[M-H]^-$ 537.18, $C_{26}H_{25}BF_2N_4O_6$ requires M 538.18.

1,3,5,7-Tetramethyl-2-N-(prop-2-yn-1-yl)propanamide-8-(4-nitrophenyl)-BODIPY (S38)

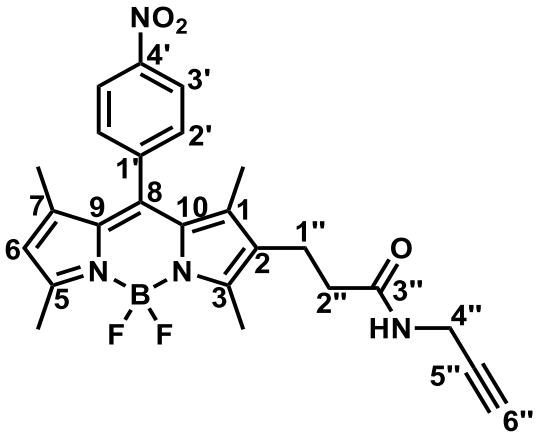

Procedure: Propargylamine (7 mg, 0.11 mmol, 1.2 eq) and DIPEA (24 mg, 0.18 mmol, 2.0 eq) was added to a solution of S37 (50 mg, 0.09 mmol, 1.0 eq) in DCM (0.6 mL). The reaction was stirred overnight until no starting material was left. Then, was added. After 1 h, the crude mixture was diluted with dichloromethane (10 mL) and washed with water (3 x 10 mL). The organic extracts were dried over $MgSO_4$, filtered and evaporated under reduced pressure. The crude compound was purified by column chromatography over silica gel (ethyl acetate : hexane = 1:1) to afford S38 as a red solid (37 mg, 0.08 mmol, 90 % yield).

Characteristics: Melting point 96-97 ºC; υ_{max} (ATR) 3437 (N-H), 3308 (C≡C-H), 2991, 2957, 2929, 2875, 2856, 1741, 1712, 1659 (C=O), 1605, 1548 (N-H), 1524, 1479, 1456, 1441, 1405, 1370, 1353, 1311, 1269, 1237, 1224, 1196, 1163, 1098, 1075, 1031 cm^{-1}; δ_H (700 MHz, Chloroform-d) 8.36 (d, J = 8.7 Hz, 2H, 3'-H), 7.51 (d, J = 8.7 Hz, 2H, 2'-H), 5.98 (s, 1H, 6-H), 5.64 (s, 1H, N-H), 3.98 (d, J = 5.2, 2.5 Hz, 2H, 4''-H), 2.69-2.63 (m, 2H, 1''-H), 2.53 (s, 6H, 3-CH_3, 5-CH_3), 2.24-2.17 (m, 3H, 2''-H, 6''-H), 1.32 (s, 3H, 7-CH_3), 1.28 (s, 3H, 1-CH_3); δ_C (176 MHz, Chloroform-d) 171.1 (C=O), 156.1 (C-5), 155.9 (C-10), 148.3 (C-4'), 142.2 (C-7), 142.1 (C-8), 139.1 (C-3), 137.9 (C-1'), 130.5 (C-2), 130.4 (C-1), 130.3 (C-9), 129.7 (C-2'), 124.4 (C-3'), 121.7 (C-6), 79.3 (C-5''), 71.7 (C-6''), 36.2 (C-2''), 29.2 (C-4''), 19.5 (C-1''), 14.7 (7-CH_3), 14.6 (5-CH_3), 12.8 (3-CH_3), 12.2 (1-CH_3); m/z (LCMS ES-) r_t 3.67 min, 477.34 $[M-H]^-$; HRMS (ES-) found $[M-H]^-$ 477.1908, $C_{25}H_{25}BF_2N_4O_3$ requires M 477.1988.

1,3,5,7-Tetramethyl-2-N-(6-azidohexyl) propanamide-8-(4-nitrophenyl)-BODIPY (S39)

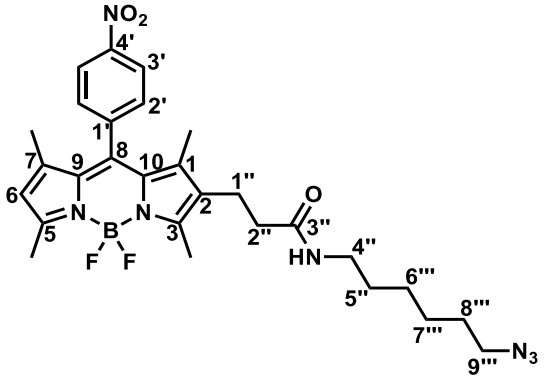

Procedure: EDC (26 mg, 0.14 mmol, 1.2 eq) was added to a solution of S36 (50 mg, 0.11 mmol, 1.0 eq) in DMF (0.6 mL). The mixture was stirred for 10 min and HOBt (18 mg, 0.14 mmol, 1.2 eq) and DIPEA (29 mg, 0.23 mmol, 2.0 eq) was added. After 30 min stirring, a solution of 6-azidohexan-1-amine (19 mg, 0.14 mmol, 1.2 eq) in DMF (0.6 mL) was added. The reaction was stirred overnight until no starting material was left. The crude mixture was diluted with dichloromethane (10 mL) and washed with water (3 x 10 mL). The organic extracts were dried over $MgSO_4$, filtered and evaporated under reduced pressure. The crude compound was purified by column chromatography over silica gel (ethyl acetate : hexane = 1:1) to afford 1,3,5,7-tetramethyl-2-N-(6-azidohexyl) propanamide-8-(4-nitrophenyl)-BODIPY as a red solid (60 mg, 0.10 mmol, 92% yield).

Characteristics: δ_H (700 MHz, Chloroform-*d*) δ 8.40 (d, *J* = 8.7 Hz, 2H, 3'-H), 7.53 (d, *J* = 8.7 Hz, 2H, 2'-H), 6.01 (s, 1H), 5.44 (t, *J* = 5.4 Hz, 1H, N-H), 3.23 (dt, *J* = 12.8, 6.5 Hz, 4H, 1'',4''-H), 2.67 (t, *J* = 7.7 Hz, 2H, 2''-H), 2.56 (s, 6H, 3,5-CH_3), 2.23-2.14 (m, 2H, CH_2), 1.58 (m, 2H, CH_2), 1.48 (m, 2H, CH_2), 1.42-1.28 (m, 10H, 1,7-CH_3, CH_2, CH_2); δ_C (176 MHz, Chloroform-d) ^{13}C NMR (101 MHz, $CDCl_3$) δ 171.47 (C=O), 156.14 (C-5), 156.00 (C-10), 148.32 (C-4'), 142.17 (C-8), 142.14 (C-7), 139.12 (C-3), 137.85 (C-1'), 130.76 (C-2), 130.42 (C-1), 130.29 (C-9), 129.70 (C-2'), 124.41 (C-3'), 121.65 (C-6), 51.32 ($\underline{C}H_2$), 39.48 ($\underline{C}H_2$), 36.58 (C-2''), 29.49 ($\underline{C}H_2$), 28.70 ($\underline{C}H_2$), 26.42 ($\underline{C}H_2$), 26.39 ($\underline{C}H_2$), 19.78 (C-1''), 14.70 (5-CH_3), 14.61 (7-CH_3), 12.85 (3-CH_3), 12.26 (1-CH_3); m/z (LCMS ES-) r_t 3.24 min, 564.44 [M-H]$^-$; HRMS (ES-) found [M-H]$^-$ 564.28, $C_{28}H_{34}BF_2N_7O_3$ requires M 565.28.

4-Benzyl 2-(tert-butyl) 3,5-dimethyl-1H-pyrrole-2,4-dicarboxylate (S40)

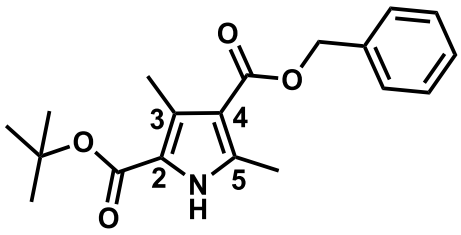

Procedure: following the same procedure as described for S8.

Tert-butyl acetoacetate (2.0 g, 12.64 mmol, 1.0 eq) in glacial acetic acid (17.0 mL), $NaNO_2$ (3 M, 5.5 mL, 15.17 mmol, 1.2 eq), benzyl acetoacetate (2.43 g, 12.64 mmol, 1.0 eq) and zinc dust (1.98 g, 30.34 mmol, 2.4 eq) was converted to S40 (purified by column chromatography, ethyl acetate : hexane = 5%) as a white solid (2.03 g, 6.16 mmol, 49 % yield).

Characteristics: υ_{max} (ATR) 3305 (N-H), 2978, 1706 (C=O), 1681 (C=O), 1660, 1571, 1428, 1367, 1286, 1256, 1164, 1110, 1083 cm^{-1}; δ_H (400 MHz, Chloroform-d) 9.24 (s, 1H, N-H), 7.47-7.31 (m, 5H, C_6H_5), 5.32 (s, 2H, 4-CH_2), 2.56 (s, 3H, 3-CH_3), 2.51 (s, 3H, 5-CH_3), 1.59 (s, 9H, tert-butyl); δ_C (101 MHz, Chloroform-d) 165.36 (4-C=O), 161.42 (2-C=O), 138.91 (C-5), 136.68 (C-3), 130.13 (benzyl), 128.54 (benzyl), 128.06 (benzyl), 127.96 (benzyl), 119.32 (C-4), 113.00 (C-2), 81.28 ($\underline{C}(CH_3)_3$), 65.43 (4-CH_2), 28.48 ($C(\underline{C}H_3)_3$), 14.50 (5-CH_3), 12.21 (3-CH_3); m/z (LCMS ES+) r_t 3.33 min, 330.20 $[M+H]^+$; HRMS (ES+) found $[M+H]^+$ 330.17, $C_{19}H_{23}NO_4$ requires M 329.16.

Benzyl 2,4-dimethyl-1H-pyrrole-3-carboxylate (S41)

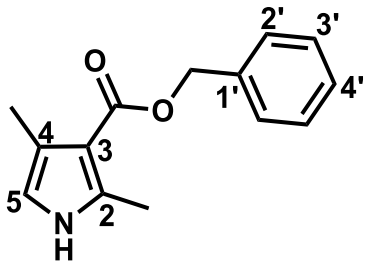

Procedure: following the same procedure as described for Ethyl S6.

S40 (10.0 g, 30.36 mmol, 1.0 eq) in ethanol (270 mL), HCl (12 M, 12.6 mL, 151.79 mmol, 5.0 eq) was converted S41 (purified by column chromatography, ethyl acetate : hexane = 25%) as a white solid (3.21 g, 14.00 mmol, 46% yield).

Characteristics: υ_{max} (ATR) 1676 (C=O), 1263 cm^{-1}; δ_H (400 MHz, Chloroform-d) 8.34 (s, 1H, N-H), 7.52- 7.31 (m, 5H, C_5H_6), 6.37 (s, 1H, 5-H), 5.33 (s, 2H, 3-CH_2), 2.50 (s, 3H, 2-CH_3), 2.29 (s, 3H, 4-CH_3); δ_C (101 MHz, Chloroform-d) 166.21 (C=O), 137.04 (C-1'), 136.47 (C-2), 128.50 (C-3'), 127.94 (C-2'), 127.83 (C-4'), 121.68, 114.47 (C-5), 110.35 (C-3), 65.13 (3-CH_2), 14.27 (2-CH_3), 12.85 (4-CH_3); m/z (LCMS ES+) r_t 3.16 min, 230.14 $[M+H]^+$; HRMS (ES+) found $[M+H]^+$ 230.12, $C_{14}H_{15}NO_2$ requires M 229.11.

2,4-Dimethyl-1H-pyrrole-3-carboxylic acid (S42)

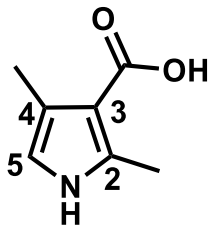

Procedure: S41 (3.0 g, 13.08 mmol, 1.0 eq) was dissolved in 360 mL of ethanol containing 10% palladium-carbon (0.42 g, 3.93 mmol, 0.3 eq). The resulting solution was stirred under H_2 at ambient temperature for 12 hr. The reaction solution was then filtered and evaporated, affording a slightly brown solid. The solid was purified by flash column chromatography eluting with ethyl acetate / hexane = 50% to yield S42 as a pale yellow solid (1.52 g, 10.92 mmol, 84%).

Characteristics: υ_{max} (ATR) 3364, 1649 (C=O), 1579, 1481, 1448, 1324, 1280, 1138 cm^{-1}; δ_H (400 MHz, Chloroform-d) 9.20 (s, 1H, N-H), 6.32-6.27 (m, 1H, 5-H), 2.43 (s, 3H, 2-CH_3), 2.19 (s, 3H, 4-CH_3); δ_C (101 MHz, Chloroform-d) 169.55 (C=O), 137.20 (C-2), 121.75 (C-4), 114.51 (C-5), 109.78 (C-3), 13.80 (2-CH_3), 12.38 (4-CH_3); m/z (LCMS ES+) r_t 1.42 min, 140.31 $[M+H]^+$; HRMS (ES-) found $[M-H]^-$ 138.05, $C_7H_9NO_2$ requires M 139.06.

2,4-Dimethyl-N-(prop-2-yn-1-yl)-1H-pyrrole-3-carboxamide (S43)

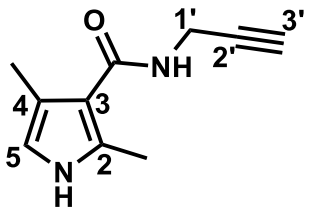

Procedure: S42 (500 mg, 3.59 mmol, 1.0 eq), EDC (827 mg, 4.31 mmol, 1.2 eq), HOBt (583 mg, 4.31 mmol, 1.2 eq) was added in DMF (3.0 mL) and DIPEA (0.9 mL). After stirring for 1 h, propylamine (0.28 mL, 4.31 mmol, 1.2 eq) was added and the reaction solution stirred for 3 h. Water was added and and was extracted with dichloromethane (3 × 50 mL). The combined organic extracts were washed with brine (50 mL) and water (50 mL), dried over anhydrous MgSO4, filtered off and concentrated in vacuum. The crude product was further purified using column chromatography (ethyl acetate : hexane = 1 : 1) afforded S43 as a pale yellow solid (420 mg, 2.38 mmol, 66% yield).

Characteristics: δ_H (400 MHz, Chloroform-d) 8.50 (s, 1H, pyrrole N-H), 6.38 (s, 1H, 5-H), 5.80 (s, 1H, amide N-H), 4.22 (d, J = 5.2, 2.6 Hz, 2H, CH_2), 2.47 (s, 3H, 2-CH_3), 2.26 (m, 4H, 4-CH_3, alkyne-H); δ_C (101 MHz, Chloroform-d) 166.46 (C=O), 133.36 (C-2), 117.15 (C-4), 115.70 (C-5), 112.94 (C-5), 80.88 (C-2'), 70.21 (C-3'), 30.09 (C-1'), 15.40 (2-CH_3), 12.60 (4-CH_3); m/z (LCMS ES+) r_t 1.14 min, 177.10 $[M+H]^+$; HRMS (ES-) found $[M-H]^-$ 177.10, $C_{10}H_{12}N_2O$ requires M 176.10.

2,4-Dimethyl-5-(4-nitrobenzoyl)-N-(prop-2-yn-1-yl)-1H-pyrrole-3-carboxamide (S44)

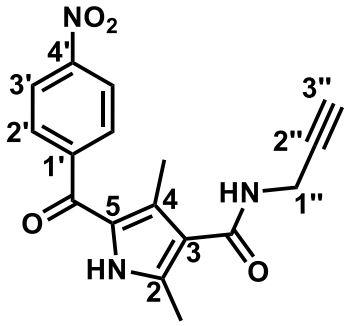

Procedure: following the same procedure as described for S1.

S43 (50 mg, 0.28 mmol, 1.0 eq) and methylmagnesium bromide 3M in ether (0.1 mL, 0.30 mmol, 1.0 eq) in ether (5 mL) and 4-nitrobenzoyl chloride (52 mg, 0.28 mmol, 1.0 eq) in ether (3.0 mL) was converted to S44 (purified by chromatography ethyl acetate/ hexane = 20%-40%) as a light yellow solid (32 mg, 0.10 mmol, 35% yield).

Characteristics: δ_H (400 MHz, MeOD) 8.38 (d, J = 8.7 Hz, 2H, 3'-H), 7.84 (d, J = 8.7 Hz, 2H, 2'-H), 4.13 (m, 2H, amide N-H, pyrrole N-H), 3.36-3.29 (m, 2H, 1''-H), 2.62 (t, J = 2.5 Hz, 1H, alkyne-H), 2.41 (s, 3H, 4-CH_3), 2.13 (s, 3H, 2-CH_3); δ_C (101 MHz, MeOD) 184.44 (C=O ketone), 166.61 (C=O amide), 149.37 (C-4'), 145.51 (C-1'), 137.78 (C-2), 129.90 (C-4), 129.07 (C-2'), 126.73 (C-5), 123.38 (C-3'), 119.86 (C-3), 79.51 (C-2''), 70.57 (C-3''), 28.12 (C-1''), 11.35 (2-$\underline{C}H_3$), 10.94 (4-$\underline{C}H_3$); m/z (LCMS ES+) r_t 2.22 min, 326.28 $[M+H]^+$; HRMS (ES+) found $[M+H]^+$ 326.12, $C_{17}H_{15}N_3O_4$ requires M 325.11.

(E)-N-allyl-1-phenylethan-1-imine (S46)

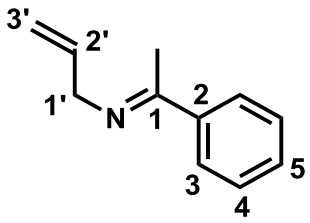

Procedure: A solution of acetophenone (5.00 g, 4.9 mL, 41.6 mmol, 1.0 eq) and allylamine (11.88 g, 15.6 mL, 208.1 mmol, 5.0 eq) in DCM (120 mL) was cooled to 0 °C. $TiCl_4$ (1 M in DCM) solution (41.6 mL, 41.6 mmol, 1.0 eq) was added dropwise over 40 min. The reaction mixture was then stirred at room temperature for 2 h and the resultant precipitate filtered. The filtrate was washed with sat. NaCl (250 mL), dried (MgSO4), filtered and concentrated to give S46 as an orange liquid (3.43 g, 21.6 mmol, 52 % yield).

Characteristics: δ_H (400 MHz, Chloroform-*d*) 7.87-7.79 (m, 2H, 3-H), 7.41 (m, 3H, 4-H, 5-H), 6.15 (ddt, J = 17.3, 10.5, 5.4 Hz, 1H, 2'-H), 5.34-5.15 (m, 2H, 3'-H), 4.21 (d, J = 5.1 Hz, 2H, 1'-H), 2.27 (s, 3H, 1-CH_3); δ_C (101 MHz, Chloroform-*d*) 166.29 (C-1), 141.15 (C-2), 136.07 (C-2'), 129.58 (C-5), 128.24 (C-4), 126.67 (C-3), 115.18 (C-3'), 54.63 (C-1'), 15.64 (1-CH_3); m/z (LCMS ES+) r_t 0.71 min, 160.35 $[M+H]^+$; HRMS (ES+) found $[M+H]^+$ 160.11, $C_{11}H_{13}N$ requires M 159.10.

4-Methyl-2-phenyl-1H-pyrrole (S47)

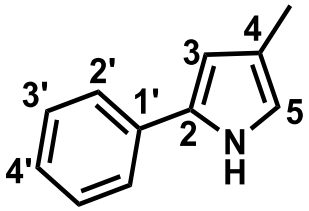

Procedure: S46 (5.00 g, 31.4 mmol, 1.0 eq.) was placed in a round bottomed flask with a stirrer bar and the flask flushed with O_2. Toluene (40 mL) and DMSO (4 mL) were added followed by Bu4NBr (10.12 g, 31.4 mmol, 1.0 eq.) and $Pd(OAc)_2$ (0.71 g, 3.14 mmol, 0.1 eq.). The flask was flushed a few times with O_2 and then the flask was sealed with a suba seal and a balloon of O_2 put in place. The reaction was stirred at 35 °C for 14 h. Water (200 mL) was added to the reaction and the mixture extracted with Et2O (3 × 200 mL). The combined organic phases were dried ($MgSO_4$), filtered, and concentrated to give the crude product. Purification by column chromatography (9:1 hexane:EtOAc) gave S47 as a pink solid (3.11 g, 19.8 mmol, 63 % yield). **Characteristics:** δ_H (400 MHz, Chloroform-*d*) 8.17 (s, 1H, N-H), 7.48 (d, J = 6.9 Hz, 2H, 2'-H), 7.38 (t, J = 7.9 Hz, 2H, 3'-H), 7.24 (t, J = 7.4 Hz, 1H, 4'-H), 6.65 (s, 1H, 5-H), 6.43 (s, 1H, 3-H), 2.22 (s, 3H, 4-CH_3); δ_C (101 MHz, Chloroform-*d*) 132.91 (C-1'), 132.04 (C-2), 128.89 (C-3'), 126.06 (C-4'), 123.69 (C-2'), 120.69 (C-4), 116.84 (C-5), 107.52 (C-3), 12.01 (4-CH_3); m/z (LCMS ES+) r_t 2.58 min, 158.26 $[M+H]^+$; HRMS (ES+) found $[M+H]^+$ 158.10, $C_{11}H_{11}N$ requires M 157.09.

(3-Methyl-5-phenyl-1H-pyrrol-2-yl)(4-nitrophenyl)methanone (S48)

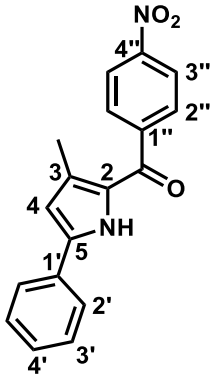

Procedure: following the same procedure as described for S1.

S47 (500 mg, 3.18 mmol, 1.0 eq), methylmagnesium bromide 3M in ether (1.1 mL, 3.18 mmol, 1.0 eq) in 16 mL ether and 4-nitrobenzoyl chloride (590 mg, 3.18 mmol, 1.0 eq) in ether 16 mL was converted to S48 (purified by chromatography hexane:EtOAc = 10%-20%) as a yellow solid (331 mg, 1.08 mmol, 34% yield).

Characteristics: δ_H (400 MHz, Chloroform-*d*) 9.74 (s, 1H, N-H), 8.36 (d, *J* = 8.7 Hz, 2H, 3''-H), 7.83 (d, *J* = 8.7 Hz, 2H, 2''-H), 7.65 (d, *J* = 7.0 Hz, 2H, 2'-H), 7.45 (t, *J* = 7.4 Hz, 2H, 3'-H), 7.38 (t, *J* = 7.3 Hz, 1H, 4'-H), 6.50 (d, *J* = 2.9 Hz, 1H, 4-H), 1.96 (s, 3H, 3-CH_3); δ_C (101 MHz, Chloroform-*d*) 183.75 (C=O), 149.19 (C-4''), 145.65 (C-1''), 139.14 (C-5), 131.78 (C-1'), 130.34 (C-3), 129.17 (C-3'), 129.08 (C-2''), 128.86 (C-2), 128.76 (C-4'), 125.23 (C-2'), 123.75 (C-3''), 112.16 (C-4)), 14.32 (3-CH_3); m/z (LCMS ES+) r_t 3.48 min, 307.43 $[M+H]^+$; HRMS (ES+) found $[M+H]^+$ 307.11, $C_{18}H_{14}N_2O_3$ requires M 306.10.

1,3,7-Trimethyl-5-phenyl-8-(4-nitrophenyl)-BODIPY (S49)

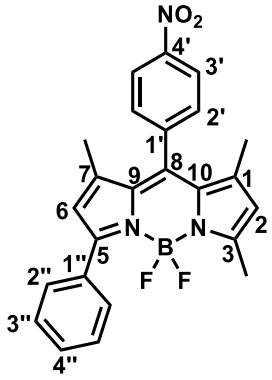

Procedure: following the same procedure 2 as described for S2.

S48 (300 mg, 0.98 mmol, 1.0 eq) in dry DCM (5.0 mL), 2,4-dimethypyrrole (93 mg, 0.98 mmol, 1.0 eq), $BF_3 \cdot OEt_2$ (0.97 mL, 7.84 mmol, 6.0 eq) and N,N-diisopropylethylamine was converted to S49 (purified by chromatography ethyl acetate : hexane = 1 : 9) as a purple solid (169 mg, 0.39 mmol, 40% yield).

Characteristics: δ_H (400 MHz, Chloroform-*d*) 8.44 (d, *J* = 8.7 Hz, 2H, 3'-H), 7.88 (d, *J* = 5.9 Hz, 2H, 2''-H), 7.61 (d, *J* = 8.7 Hz, 2H, 2''-H), 7.53-7.41 (m, 3H, 3''-H, 4''-H), 6.35 (s, 1H, 6-H)), 6.09 (s, 1H, 2-H)), 2.56 (s, 3H, 7-CH_3), 1.44 (d, *J* = 14.6 Hz, 6H, 1-CH_3, 3-CH_3); δ_C (101 MHz, Chloroform-*d*) 158.81, 156.06, 148.43, 143.72, 141.98, 141.56, 139.17, 132.66, 131.64, 131.40, 129.78 (2''-H), 129.41 (4''-H), 129.28 2'-H), 128.16 (3'-H), 124.48 (3'-H), 122.95 (C-6), 122.48 (C-2), 15.02 (1,3-CH_3), 14.87 (7-CH_3); m/z (LCMS ES-) r_t 3.67 min, 430.41 $[M-H]^-$; HRMS (ES-) found $[M-H]^-$ 430.15, $C_{24}H_{20}BF_2N_3O_2$ requires M 431.16.

(4-Nitrophenyl)(1H-pyrrol-2-yl)methanone (S50)

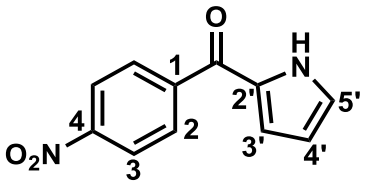

Procedure: CH_3MgBr (3 M) in diethylether (5.0 mL, 14.9 mmol, 1.0 eq) was added by dropwise to the solution of pyrrole (1.0 g, 14.9 mmol, 1.0 eq) in THF (23 mL) at -78 ℃ and continued for 1h at room temperature. 4-Nitrobenzoyl chloride (2.77 g, 14.9 mmol, 1.0 eq) in THF (30 mL) was added by dropwise to the solution and stirring was continued for 3 hours at room temperature. The mixture was poured into saturated aqueous NH_4Cl and extracted with EtOAc. The organic layer was washed with water, dried over $MgSO_4$ and concentrated under vacuum to give an oily product. The crude was isolated by chromatography on silica gel flash column twice (1^{st} ethylacetate/ hexane = 1:4, 2^{nd} DCM/ hexane = 20%-100%) to furnish S50 as a light yellow solid (1.77 g, 8.20 mmol, 55% yield).

Characteristics: δ_H (400 MHz, Chloroform-*d*) 9.96 (s, 1H, N-H), 8.36 (d, *J* = 8.8 Hz, 2H, 2-H), 8.05 (d, *J* = 8.8 Hz, 2H, 3-H), 7.26 (s, 1H, 5'-H), 6.89 (s, 1H, 3'-H), 6.42 (s, 1H, 4'-H); δ_C (101 MHz, Chloroform-*d*) 182.55 (C=O), 149.65 (C-4), 143.65 (C-1), 130.61 (C-2'), 129.80 (C-2), 126.71 (C-5'), 123.61 (C-3), 120.39 (C-4'), 111.75 (C-3'); m/z (LCMS ES+) r_t 3.09 min, 217.20 $[M+H]^+$; HRMS (ES+) found $[M+H^+$ 217.06, $C_{11}H_8N_2O_3$ requires M 216.05.

1,3-Dimethyl-8-(4-nitrophenyl)-BODIPY (S51)

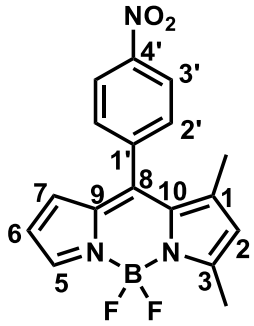

Procedure: A solution of S50 (862 mg , 4.0 mmol, 1 eq) in THF/methanol (MeOH) (11 mL, 10:1) was treated with $NaBH_4$ (285 mg, 8.0 mmol, 2 eq) at room temperature for 1 hour. The reaction mixture was poured in a mixture of saturated aqueous NH_4Cl (10 mL) and EtOAc (20 mL). The organic phase was separated, washed with water, dried (Na_2SO_4), and concentrated to dryness, affording crude yellow oil. The crude reduced alcohol product was used directly without purification due to the instability. A mixture of the resulting residue and 2,4-dimethylpyrrole(0.4 mL, 4.0 mmol, 1 eq) was dissolved in DCM (10 mL) and treated with $InCl_3$ (9 mg, 0.4 mmol, 0.1 eq) at room temperature. After 3 hours, the reaction mixture was quenched with triethylamine (55 µL, 0.4 mmol, 0.1 eq). The organic layer was concentrated, and silica gel filtered with DCM, affording crude compound of coupled dipyrrole, which was used directly in next step. To a solution of dipyrrole in toluene (10 mL) was added DDQ (273 mg, 1.2 mmol, 0.3 eq) in DCM (2 mL). The mixture was stirred for 15 min at room temperature. A solution of reaction mixture was cooled under N_2 to 0 °C. Triethylamine (1.7 mL, 12.0 mmol, 3 eq) was added for neutralization. After 2 min of stirring, $BF_3{\cdot}OEt_2$ (2.5 mL, 20.0 mmol, 5 eq) was added dropwise, during 10 min. Thereafter, the mixture was stirred for 8 hrs at r.t. The combined organic phases were dried ($MgSO_4$), filtered, The reaction solution was filtered through short panel of silica-gel with DCM-Hexane (1:2) solution and concentrated to give the crude product. Purification by column chromatography (9:1 hexane:EtOAc) gave S51 as a red solid (491 mg, 1.44 mmol, 36 % yield).

Characteristics: δ_H (400 MHz, Chloroform-*d*) 8.40 (d, J = 8.7 Hz, 2H, 3'-H), 7.74 (s, 1H, 5-H), 7.61 (d, J = 8.7 Hz, 2H, 2'-H), 6.42 (dd, J = 4.1, 2.1 Hz, 1H, 6-H), 6.33 (d, J = 4.0 Hz, 1H, 7-H), 6.20 (s, 1H, 2-H), 2.67 (s, 3H, 3-CH_3), 1.56 (s, 3H, 1-CH_3); δ_C (101 MHz, Chloroform-*d*) 163.62 (C-5), 148.54 (C-1'), 146.45 (C-4'), 140.64 (C-7), 139.84 (C-9), 139.68 (C-8), 133.77 (C-3), 133.03 (C-1), 130.08 (C-2'), 126.71 (C-10), 123.98 (C-6), 123.79 (C-3'), 116.69 (C-2), 15.33 (3-C), 15.24 (1-C); HRMS (ES-) found $[M-H]^-$ 340.10, $C_{17}H_{14}BF_2N_3O_2$ requires M 341.12.

Hex-5-yn-1-yl 4-methylbenzene-1-sulfonate (S52)

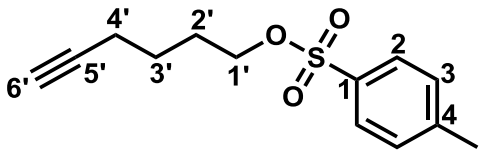

Procedure: Toluene-4-sulfonyl chloride (4.66 g, 24.45 mmol, 1.2 eq.) and triethylamine (6.8 mL, 50.95 mmol, 2.5 eq.) was added to a stirred solution of 5-Hexyn-1-ol (2 g, 20.38 mmol, 1.0 eq.) in dichloromethane (20.0 mL) at 0 ºC. The solution was stirred at room temperature overnight. After, the mixture was poured into satd. $NaHCO_3$ (20 mL) and extracted with dichloromethane (3 × 20 mL). The organic layers were washed with HCl (2 M, 3 × 20 mL) and water (20 mL). The combined organics were dried ($MgSO_4$), and the solvent removed under reduced pressure to yield S52 as a light yellow oil (4.92 g, 23.47 mmol, 96% yield).

Characteristics: υ_{max} (ATR) 3297 (C≡C-H), 2955, 2875, 2849, 2301, 2258 (C≡C), 2165, 2120, 1713, 1602, 1498, 1473, 1459, 1438, 1359, 1310, 1294, 1261, 1215, 1191, 1176 (S=O), 1122, 1101, 1045, 1021, 1014 cm^{-1}; δ_H (400 MHz, Chloroform-d) 7.74 (d, J = 8.3 Hz, 2H, 2-H), 7.32 (d, J = 9.1 Hz, 2H, 3-H), 4.01 (t, J = 6.3 Hz, 2H, 1'-H), 2.41 (s, 3H, CH_3), 2.12 (td, J = 7.0, 2.7 Hz, 2H, 4'-H), 1.91 (t, J = 2.7 Hz, 1H, 6'-H), 1.80 – 1.68 (m, 2H, 3'-H), 1.51 (p, J = 7.1 Hz, 2H, 2'-H); δ_C (101 MHz, Chloroform-d) 144.8 (C-1), 133.0 (C-4), 129.9 (C-3), 127.8 (C-2), 83.4 (C-5'), 70.0 (C-1'), 69.0 (C-6'), 27.7 (C-2'), 24.2 (C-3'), 21.6 (CH_3), 17.7 (C-4'); m/z (LCMS ES+) r_t 2.99 min, 253.307 $[M+H]^+$; HRMS (ES+) found $[M+H]^+$ 253.0903, $C_{13}H_{16}O_3S$ requires M 253.0820.

2-(Hex-5-yn-1-yl)isoindoline-1,3-dione (S53)

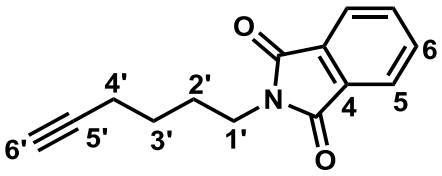

Procedure: Potassium phtalimide (0.55 g, 2.97 mmol, 1.5 equiv) was added to a solution of S52 (0.50 g, 1.98 mmol, 1.0 equiv) in DMF (5.0 mL). After stirring for 1 hour at 70°C, the solvent was removed in *vacuo.* The solid residue was suspended in dichloromethane and filtered through a layer of silica gel. The filtrate was evaporated and purified by column chromatography over silica gel (Hexane / EtOAc, 4:1) to afford S53 as an colourless oil (0.42 g, 2.76 mmol, yield 93%).

Characteristics: υ_{max} (ATR) 3285(C≡C-H), 2950, 2871, 1774, 1707 (C=O), 1618, 1470, 1440, 1400, 1376, 1340, 1238, 1220, 1190, 1175, 1157, 1120, 1090, 1072, 1039 cm^{-1}; δ_H (400 MHz, Chloroform-d) 7.80 (m, J = 5.3, 3.2 Hz, 2H, 6-H), 7.68 (m, J = 5.4, 3.1 Hz, 2H, 5-H), 3.67 (t, J = 7.1 Hz, 2H, 1'-H), 2.21 (td, J = 7.0, 2.5 Hz, 2H, 4'-H), 1.93 (t, J = 2.5 Hz, 1H, 6'-H), 1.77 (p, J = 7.2 Hz, 2H, 2'-H), 1.54 (p, J = 7.1 Hz, 2H, 3'-H); δ_C (101 MHz, Chloroform-d) 168.36 (C=O), 133.91 (C-6), 132.04 (C-4), 123.17 (C-5), 83.76 (C-5'), 68.86 (C-6'), 37.38 (C-1'), 27.62 (C-2'), 25.60 (C-3'), 17.96 (C-4'); m/z (LCMS ES+) r_t 2.58 min, 228.23 $[M+H]^+$; HRMS (ES+) found $[M+H]^+$ 228.10, $C_{14}H_{13}NO_2$ requires M 227.10.

Tert-butyl (6-hydroxyhexyl)carbamate (S55)

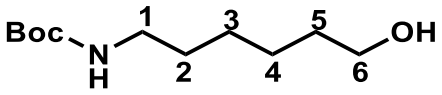

Procedure: 6-aminohexan-1-ol (2.00 g, 17.1 mmol, 1.0 eq) was dissolved in 20 mL CH_2Cl_2 and cooled to 0°C in an ice bath. Solid Boc_2O (4.10 g, 18.8 mmol, 1.1 eq) was added and the reaction mixture was stirred overnight (15 hr) at room temperature. Solvent was reduced by rotary evaporation and crude product was extracted with EtOAc from 10 % aqueous citric acid, saturated $NaHCO_3$, and brine. The organic phase was dried over Na_2SO_4 and concentrated by rotary evaporation to yield S55 quantitatively as a clear viscous oil (3.65 g, 16.8 mmol, yield 98%).

Characteristics: υ_{max} (ATR) 3356 (OH), 2978, 2936 (N-H), 2860, 1686 (C=O), 1530, 1456, 1393, 1366, 1276, 1252, 1170, 1033 cm^{-1}; δ_H (400 MHz, Chloroform-d) 4.62 (s, 1H, N-H), 3.66-3.57 (m, 2H, 6-H), 3.11 (q, J = 5.8, 4.8 Hz, 2H, 1-H), 1.60-1.53 (m, 2H, 2-H), 1.48 (t, J = 6.8 Hz, 2H, 4-H), 1.43 (s, 9H, tert-butyl), 1.41-1.29 (m, 4H, 3-H, 5-H); δ_C (101 MHz, Chloroform-d) 156.10 (C=O), 79.07 ($\underline{C}(CH_3)_3$), 62.58 (C-6), 40.35 (C-1), 32.57 (C-5), 30.05 (C-2), 28.42 ($C(\underline{C}H_3)_3$), 26.39 (C-3), 25.28 (C-4); m/z (LCMS ES+) r_t 2.58 min, 218.25 $[M+H]^+$; HRMS (ES+) found $[M+H]^+$ 218.18, $C_{11}H_{23}NO_3$ requires M 217.18.

Tert-butyl (6-iodohexyl)carbamate (S56)

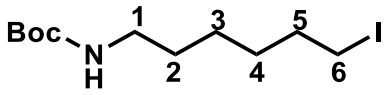

Procedure: A round bottom flask was charged with PPh_3 (3.62 g, 13.81 mmol, 1.5 eq) and 35 mL dichloromethane. Iodine (3.50 g, 13.81 mmol, 1.5 eq) was added in small portions under N_2 at room temperature and the reaction was stirred for 10 minutes. Imidazole (1.57 g, 23.00 mmol, 2.5 eq) was added to the solution in small portions and the reaction was allowed to stir for a further 10 minutes. S55 (2.00 g, 9.20 mmol, 1.0 eq) in 35 mL dichloromethane was added to the suspension dropwise in 5 minutes and the reaction was stirred for 1 hour at room temperature. Saturated $Na_2S_2O_5$ was added to quench the reaction mixture and the aqueous layer was extracted with dichloromethane twice. The organic layer was dried over $MgSO_4$ and concentrated. The residue was purified by flash column chromatography eluting with 10% ethyl acetate / hexane to yield S56 as a clear viscous oil (2.63 g, 8.04 mmol 87% yield).

Characteristics: υ_{max} (ATR) 3345, 2974, 2930 (N-H), 2857, 1686 (C=O), 1514, 1454, 1390, 1365, 1271, 1248, 1166 cm^{-1}; δ_H (400 MHz, Chloroform-d) 4.65 (s, 1H, N-H), 3.14 (t, J = 6.9 Hz, 2H, 6-H), 3.11-3.00 (m, 2H, 1-H), 1.78 (p, J = 7.8, 7.2 Hz, 2H, 5-H), 1.48-1.26 (m, 17H, 2-H, 3-H, 4-H, tert-butyl); δ_C (101 MHz, Chloroform-d) 155.96 (C=O), 78.93 ($\underline{C}(CH_3)_3$), 40.40 (C-1), 33.34 (C-5), 30.12 (C-4), 28.43 ($C(\underline{C}H_3)_3$), 27.78 (C-2), 25.70 (C-3), 7.02 (C-6); m/z (LCMS ES+) r_t 3.53 min, 328.14, 329.21 $[M+H]^+$.

Tert-butyl (6-(hex-5-yn-1-yloxy)hexyl)carbamate (S57)

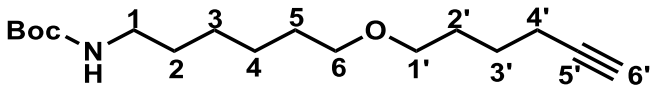

Procedure: To a stirred solution of NaH (0.27 g, 6.73 mmol, 1.1 equiv) in 30 mL dry THF, 5-hexyn-1-ol (0.60 g, 6.11 mmol, 1.0 equiv) was added and the mixture was let to react for 30 min. Subsequently, S56 (2.20 g, 6.73 mmol, 1.1 equiv) and TBAI (0.22 g, 0.61 mmol, 0.1 equiv) were added. And the reaction was stirred at r.t. overnight. Afterwards it was concentrated, dissolved with EtOAc, washed with water, dried with MgSO4, purified by flash column chromatography eluting with 10% ethyl acetate / hexane to yield S57 a clear viscous oil (0.94 g, 3.17 mmol 52% yield).

Characteristics: δ_H (400 MHz, Chloroform-d) 4.59 (s, 1H, N-H), 3.38 (dt, J = 12.0, 6.4 Hz, 4H, 6-H, 1'-H), 3.09 (q, J = 6.2 Hz, 2H, 1-H), 2.20 (td, J = 6.9, 2.6 Hz, 2H, 4'-H), 1.93 (t, J = 2.6 Hz, 1H, 6'-H), 1.72-1.44 (m, 10H, 2-H, 5-H, 2'-H, 3'-H), 1.42 (s, 9H, tert-butyl), 1.38-1.24 (m, 4H, 3-H, 4-H); δ_C (101 MHz, Chloroform-d) 155.97 (C=O), 84.34 (C-5'), 78.92 ($\underline{C}(CH_3)_3$), 70.76 (C-6), 70.18 (C-1'), 68.40 (C-6'), 40.51 (C-1), 30.02 (C-5), 29.64 (C-2'), 28.74 (C-3), 28.41 ($C(\underline{C}H_3)_3$), 26.63 (C-2), 25.89 (C-4), 25.23 (C-3'), 18.20 (C-4'); m/z (LCMS ES+) r_t 3.50 min, 298.31 $[M+H]^+$; HRMS (ES+) found $[M+H]^+$ 298.24, $C_{17}H_{31}NO_3$ requires M 297.23.

6-(Hex-5-yn-1-yloxy)hexan-1-amine (S58)

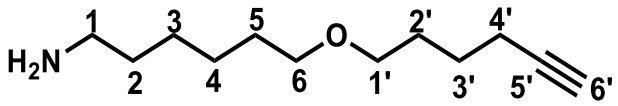

Procedure: S57 (100 mg, 0.34 mmol) was immediately dissolved in 1 mL trifluoroacetic acid and stirred under an Ar atmosphere at ambient temperature for 10 min, then evaporated to afford S58 as a yellow oil (61 mg, 0.30 mmol, yield 90 %).

Characteristics: υ_{max} (ATR) 3309 (C≡C-H), 2932, 2855, 1661, 1575, 1455, 1432, 1370, 1310, 1238, 1113 (C-O) cm^{-1}; δ_H (400 MHz, Chloroform-d) 3.40 (dt, J = 9.4, 6.4 Hz, 4H, 6-H, 1'-H), 3.19 (t, J = 7.3 Hz, 2H, 1-H), 2.21 (td, J = 7.0, 2.7 Hz, 2H, 4'-H), 2.00 (t, J = 1.4 Hz, 3H, NH_2), 1.94 (t, J = 2.7 Hz, 1H, 6'-H), 1.72- 1.52 (m, 8H, 2-H, 5-H, 2'-H, 3'-H), 1.41-1.31 (m, 4H, 3-H, 4-H); δ_C (101 MHz, Chloroform-d) 84.38 (5'-C), 70.91 (5-C), 70.15 (1'-C), 68.34 (6'-C), 51.50 (1-C), 30.86 (2-C), 29.74 (5-C), 28.77 (2'-C), 27.50 (3-C), 26.12 (4-C), 25.25 (3'-C), 18.22 (4'-C); m/z (LCMS ES+) r_t 1.52 min, 198.49 $[M+H]^+$; HRMS (ES+) found $[M+H]^+$ 198.19, $C_{12}H_{23}NO$ requires M 197.18.

1,6-Diazidohexane (S59)

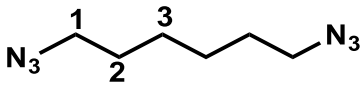

Procedure : 1,6-Dibromohexane (2.0 g, 8.20 mmol, 1.0 eq) and sodium azide (1.17 g, 18.04 mmol, 2.2 eq) were added to 30 mL of DMF. The mixture was heated to 60 °C for 10 h. Water (100 mL) was added and the crude product was extracted with (3 x 50 mL) portions of ether. The organic layers were combined, dried over magnesium sulfate, gravity filtered and concentrated *in vacuo* and purified by chromatography on silica gel (5-10% ethyl acetate/hexane) to afford the pure S59 as a colorless oil (1.05 g, 6.24 mmol, 76% yield).

Characteristics: υ_{max} (ATR) 2935, 2860, 2085(azide), 1456, 1345, 1250 cm^{-1}; δ_H (700 MHz, Chloroform-d) 3.31 (t, J = 6.9 Hz, 4H, 1-H), 1.63 (m, 4H, 2-H), 1.44 (m, 4H, 3-H); δ_C (176 MHz, Chloroform-d) 51.32(C-1), 28.75(C-2), 26.32(C-3); m/z (LCMS ES-) r_t 1.01 min, 143.126 $[M+H]^+$.

6-Azidohexan-1-amine (S60)

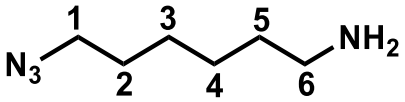

Procedure : To a solution of S59 (1.0 g, 5.95 mmol, 1.0 eq) in 2.0 M aq. HCl/EtOAc/Et_2O (3/4/4, v/v, 30 mL), PPh3 (1.56 g, 5.95 mmol, 1.0 eq) was added on ice, and the mixture was stirred at room temperature overnight. Then 30 mL 2.0 M aq. HCl was added to the mixture, washed by Et_2O (3 x 30 mL). The aqueous layer was basified with 1.0 M NaOH, then extracted with Et_2O (3 x 30 mL). The organic layer was dried over $MgSO_4$ and concentrated to afford S60 as a colorless oil (0.59 g, 4.15 mmol, 70% yield).

Characteristics: δ_H (700 MHz, Chloroform-d) 3.07 (t, J = 6.9 Hz, 2H, 6-H), 2.49 (t, J = 6.9 Hz, 2H, 1-H), 1.42 (p, J = 6.9 Hz, 2H, 5-H), 1.31-1.10 (m, 6H, 2,3,4-H), 0.85 (s, 2H, N-H); m/z (LCMS ES-) r_t 0.49 min, 143.354 $[M+H]^+$.

2-(2-{2-[2-(Methanesulfonyloxy)ethoxy]ethoxy}ethoxy)ethyl methanesulfonate (S61)

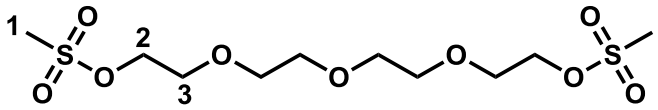

Procedure : NEt_3 (10.0 mL, 74.1 mmol, 2.2 eq) in dry THF (10.0 ml) was added dropwise at 0 ˚C to a solution of tetraethylene glycol (6.5 g, 33.7 mmol, 1 eq) and methanesulfonyl chloride (5.7 mL, 74.1 mmol, 2.2 eq) in dry THF (20.0 ml) under Ar. The reaction was stirred for 1 hr at 0 ˚C, and then a further 3 hrs at RT. The THF was then removed in vacuo and the residue was re-dissolved in EtOAc (25.0 mL) and washed with H_2O (30.0 mL x 3), dried ($MgSO_4$) and concentrated. Purification by column chromatography (SiO_2, hexane: EtOAc 0-100 %) gave S61 as a colourless oil (9.3 g, 26.3 mmol, 78 % yield).

Characteristics: ν_{max} (ATR) 3034, 3005-2741, 1460, 1347, 1252, 1175; δ_H (700 MHz, Chloroform-d) 4.35-4.34 (4H, m, 2-H), 3.75-3.73 (4H, m, 3-H), 3.65-3.60 (8H, m, O-CH_2CH_2-O), 3.05 (6H, s, CH_3); δ_C (176 MHz, Chloroform-d) 70.7 (O-$\underline{C}H_2\underline{C}H_2$-O), 70.5 (O-$\underline{C}H_2\underline{C}H_2$-O), 69.4 (C-2), 69.1 (C-3), 37.7 (CH_3); m/z (LC-MS ES^+) 351.079 [$M+H^+$].

1-Azido-2-(2-(2-(2-azidoethoxy)ethoxy)ethoxy)ethane (S62)

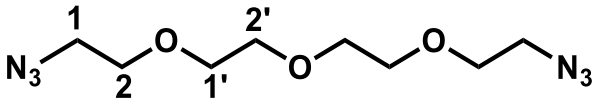

Procedure : $NaHCO_3$ (1.2 g, 13.8 mmol, 0.54 eq) and NaN_3 (3.7 g, 56.2 mmol, 2.2 eq) were dissolved in 10 ml H_2O, and this solution was added dropwise to S61 (8.9 g, 25.5 mmol, 1 eq). The resulting solution was heated under reflux at 80 ˚C for 12 hrs. The product was then extracted with DCM (20 ml x 5), dried ($MgSO_4$) and concentrated affording S62 as a colourless oil (4.7 g, 19.1 mmol, 75 % yield).

Characteristics: ν_{max} (ATR) 2103 (-N=N^+=N^-), 2103, 1450, 1351, 1288, 1121; δ_H (700 MHz, Chloroform-d) 3.70-3.63 (12H, m, O-CH_2), 3.38 (4H, t, J = 5.1 Hz, N_3-CH_2); δ_C (176 MHz, Chloroform-d) 70.8 (O-CH_2), 70.1 ($\underline{C}H_2\underline{C}H_2$-$N_3$), 50.8 ($\underline{C}H_2\underline{C}H_2$-$N_3$); m/z (LC-MS ES^+) 245.138 [$M+H^+$].

2-(2-(2-(2-Azidoethoxy)ethoxy)ethoxy)ethan-1-amine (S63)

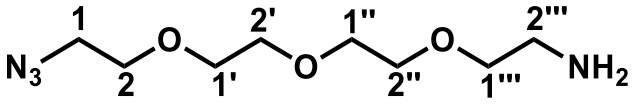

Procedure : Triphenylphosphine (1.8 g, 6.9 mmol, 0.86 eq) dissolved in dry Et_2O (16.0 ml) was added dropwise to a solution of S62 (2.0 g, 8.1 mmol, 1 eq) dissolved in 0.65 M aqueous phosphoric acid (160. mL) cooled to 0 ˚C. The reaction was stirred for 1 hr at 0 ˚C, then at RT for 18 hrs. The aqueous layer was washed with Et_2O (20 ml x 3) and then adjusted to pH 10 by the addition of KOH pellets, and extracted with DCM (15 ml x 4). The combined DCM extracts were concentrated in vacuo, dried ($MgSO_4$) and the resultant oil triturated in Et_2O. Following trituration to remove the triphenylphosphine oxide, the filtrate was concentrated and the residue purified using column chromatography (SiO_2, 0-30 % $CHCl_3$: MeOH), to afford S63 as a colourless oil (1.2 g, 5.0 mmol, 62 %).

Characteristics: ν_{max} (ATR) 3725-3086 (N-H), 3017-2745, 2109 (-N=N^+=N^-), 1460, 1291, 1126 (C-O); δ_H (700 MHz, Chloroform-d) 3.72 (2H, m, C$\underline{H}_2$-NH_2), 3.69-3.65 (10H, m, O-CH_2 1'-1$'''$), 3.61 (2H, t, J = 4.5, 2-H), 3.39 (2H, t, J = 5.0 Hz, CH_2-N_3); δ_C (176 MHz, Chloroform-d) 72.6 (C-2), 70.9 (O-CH_2), 70.8 (O-CH_2), 70.8 (O-CH_2), 70.5 (O-CH_2), 70.2 (O-CH_2), 61.9 (CH_2-NH_2), 50.8 (CH_2-N_3); m/z (LC-MS ES^+) 245.138 [M+H^+].

1,7-Dimethyl-3,5-styryl-8-(4-nitrophenyl)-BODIPY (S64)

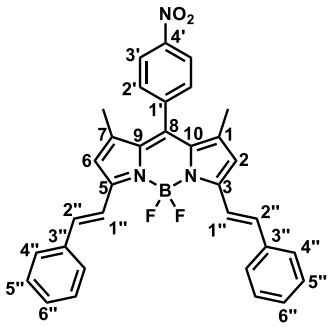

Procedure: S2(30 mg, 0.08mmol, 1.0 eq) and benzaldehyde(18 mg, 0.16 mmol, 2.0 eq) were dissolved in 0.7 mL benzene and 0.2 mL acetonitrile, into which piperidine(55 mg, 0.65 mmol, 8.0 eq) and acetic acid(59 mg, 0.98 mmol, 12.0 eq) were added. The mixture was heated under reflux for 24 h. The solvent was then removed under vacuum and purification was performed by silica-gel column chromatography (eluant: 1st EtOAc / Hexane = 0~50%, 2nd DCM/ Hexane = 0~100% then EtOAc/ DCM = 0~20%) to obtain S64 as a blue powder (8 mg, 0.015 mmol, 18 % yield).

Characteristics: δ_H (400 MHz, Chloroform-*d*) 8.44 (d, *J* = 8.6 Hz, 2H, 3'-H), 7.77 (d, *J* = 16.4 Hz, 2H, 2''-H), 7.67 (d, *J* = 7.3 Hz, 4H, 4''-H), 7.63 (d, *J* = 8.6 Hz, 2H, 2'-H), 7.44 (dd, *J* = 8.3, 6.7 Hz, 4H, 5''-H), 7.40-7.29 (m, 4H, 4'', 6''-H), 6.71 (s, 2H, 2,6-H), 1.47 (s, 6H, 1,7-CH_3); HRMS (ES+) found $[M+H]^+$ 546.37, $C_{33}H_{26}BF_2N_3O_2$ requires M 545.21.

2-(2-(2-Methoxyethoxy)ethoxy)ethyl 4-methylbenzenesulfonate (S66)

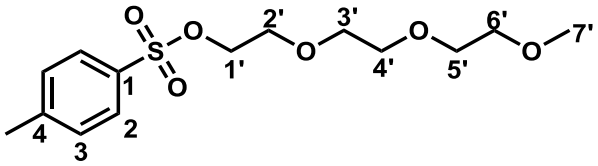

Procedure: following the same procedure as described for S52.

Toluene-4-sulfonyl chloride (2.78 g, 14.62 mmol, 1.2 eq.) and triethylamine (4.0 mL, 30.45 mmol, 2.5 eq.) and triethylene glycol monomethyl ether (2.00 g, 12.18 mmol, 1.0 eq.) in DCM (12.0 mL) was converted to S66 as a light yellow oil (3.62 g, 11.36 mmol, 93% yield, purified by chromatography on silica gel 0-20% ethyl acetate/hexane).

Characteristics: δ_H (400 MHz, Chloroform-d) 7.78 (d, J = 8.3 Hz, 2H, 2-H), 7.33 (d, J = 8.2 Hz, 2H, 3-H), 4.18-4.11 (m, 2H), 3.70-3.65 (m, 2H), 3.62-3.55 (m, 6H), 3.54-3.49 (m, 2H), 3.35 (s, 3H, 7'-H), 2.43 (s, 3H, 4-CH_3); δ_C (101 MHz, Chloroform-*d*) 144.82 (C-1), 132.94 (C-4), 129.83 (C-3), 127.95 (C-2), 71.87, 70.70, 70.53, 70.51, 69.26, 68.63, 59.00(C-7'), 21.62(4-CH_3); m/z (LC-MS ES^+) 319.24 [$M+H^+$].

4-(2-(2-(2-Methoxyethoxy)ethoxy)ethoxy)benzaldehyde (S67)

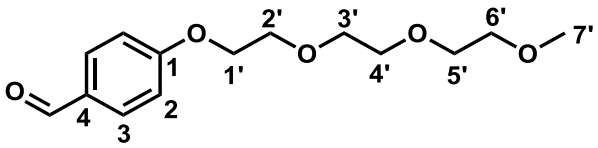

Procedure: Cesium carbonate (2.67 g, 8.19 mmol, 2.0 equiv) was added to a solution of S66 (0.50 g, 4.10 mmol, 1.0 equiv) and 4-Hydroxybenzaldehyde (1.37 g, 4.30 mmol, 1.05 equiv) in DMF (5.0 mL). After stirring overnight at 90°C, the mixture was then poured into saturated aqueous NaCl, and then resultant mixture extracted with EtOAc.). The organic layer was washed with water, dried over Mg_2SO_4 and concentrated under vacuum. The compound was purified by column chromatography over silica gel (Hexane/ EtOAc, 1:1) to afford S67 as a light yellow oil (0.68 g, 2.54 mmol, 62% yield).

Characteristics: δ_H (400 MHz, Chloroform-*d*) 9.85 (s, 1H, CHO), 7.80 (d, *J* = 8.8 Hz, 2H, 3-H), 6.99 (d, *J* = 8.7 Hz, 2H, 2-H), 4.22-4.15 (m, 2H), 3.90-3.81 (m, 2H), 3.75-3.68 (m, 2H), 3.69-3.59 (m, 4H), 3.52 (m, 2H), 3.34 (s, 3H, 7'-H); δ_C (101 MHz, Chloroform-*d*) 190.79 (C=O), 163.84 (C-1), 131.91 (C-3), 129.98 C-4), 114.86 (C-2), 71.88, 70.85, 70.61, 70.54, 69.43, 67.74, 59.00 (C-7'); m/z (LC-MS ES^+) 269.23 [$M+H^+$].

4-Morpholinobenzaldehyde (S68)

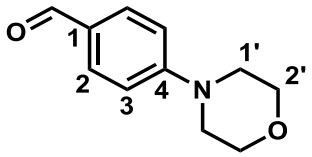

Procedure: A mixture of 4-fluorobenzaldehyde (1.00 g, 8.06 mmol, 1.0 eq), morpholine (1.05 g, 12.09 mmol, 1.5 eq) and anhydrous potassium carbonate (1.67 g, 12.09 mmol, 1.5 eq) was stirred in DMF (20 mL) for 24 h at 80 °C. The mixture was concentrated under low pressure and left to cool. The mixture was then poured into ice water and extracted with EtOAc, washed with water. The combined organics were dried ($MgSO_4$), and purification was performed by silica-gel column chromatography (eluant: EtOAc/ Hexane = 0~50%) to obtain S68 as a white solid (0.88 g, 5.59 mmol, 57 % yield).

Characteristics: δ_H (400 MHz, Chloroform-*d*) 9.77 (s, 1H, CHO), 7.75 (d, *J* = 8.6 Hz, 2H, 2-H), 6.91 (d, *J* = 8.6 Hz, 2H, 3-H), 3.97-3.71 (m, 4H, 2'-H), 3.45-3.22 (m, 4H, 1'-H); δ_C (101 MHz, Chloroform-*d*) 190.55 (C=O), 155.15 (C-4), 131.82 (C-2), 127.56 (C-1), 113.43 (C-3), 66.49 (C-1'), 47.23 (C-2'); HRMS (ES+) found $[M+H]^+$ 192.10, $C_{11}H_{13}NO_2$ requires M 191.10.

1-Methyl-1H-indole-5-carbaldehyde (S69)

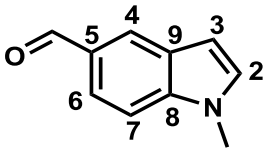

Procedure: Iodomethane (0.50 mL, 7.58 mmol, 1.1 equiv) was slowly added to a solution of 1H-indole-5-carbaldehyde (1.0 g, 6.89 mmol, 1.0 equiv) and KOH (0.58 g, 10.33 mmol, 1.5 equiv) in DMSO (6.7 mL). The mixture was stirred overnight at room temperature, and then added water and extracted with dichloromethane. The organic layer was washed with water, dried over Mg_2SO_4 and concentrated under vacuum. The compound was purified by column chromatography over silica gel (Hexane/ EtOAc, 1:4) to afford S69 as a white solid (942 mg, 5.92 mmol, 86 % yield).

Characteristics: δ_H (400 MHz, Chloroform-*d*) 10.02 (s, 1H, CHO), 8.13 (s, 1H, 4-H), 7.79 (d, *J* = 10.1 Hz, 1H, 7-H), 7.37 (d, *J* = 8.6 Hz, 1H, 6-H), 7.14 (d, *J* = 3.2 Hz, 1H, 2-H), 6.64 (d, *J* = 3.3 Hz, 1H, 3-H), 3.79 (s, 3H, N-CH_3); δ_C (101 MHz, Chloroform-*d*) 192.57 (C=O), 139.93, 130.87, 129.22, 128.22, 126.42, 121.74, 109.84, 103.21, 33.10 (N-CH_3); HRMS (ES+) found $[M+H]^+$ 160.08, $C_{10}H_9NO$ requires M 159.07.

1,7-Dimethyl-3-phenyl-5-methoxystyryl-8-(4-nitrophenyl)-BODIPY (S70)

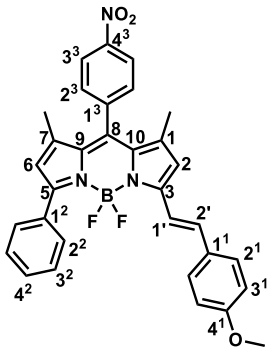

Procedure: following the same procedure as described for S64.

S49 (25 mg, 0.06 mmol, 1.0 eq), 4-methoxybenzaldehyde (8 mg, 0.06 mmol, 1.0 eq), piperidine (40 mg, 0.47 mmol, 8.0 eq) and acetic acid (42 mg, 0.70 mmol, 12.0 eq) in 0.6 mL benzene and 0.2 mL acetonitrile were converted to S70 as a blue solid (21 mg, 0.039 mmol, 65 % yield). Purification was performed by silica-gel column chromatography (eluant: 1st EtOAc / Hexane = 0~50%, 2nd DCM/ Hexane = 0~100% then EtOAc/ DCM = 0~20%).

Characteristics: δ_H (400 MHz, Chloroform-*d*) 8.44 (d, *J* = 8.6 Hz, 2H), 7.91 (dd, *J* = 8.0, 1.5 Hz, 2H), 7.64 (d, *J* = 8.6 Hz, 2H), 7.53 (dq, *J* = 15.9, 8.4 Hz, 6H), 7.28 (d, *J* = 16.2 Hz, 2H), 6.91 (d, *J* = 8.8 Hz, 2H), 6.70 (s, 1H), 6.35 (s, 1H), 3.86 (s, 3H), 1.47 (s, 6H); δ_C (101 MHz, Chloroform-*d*) 160.97, 156.14, 154.88, 148.39, 142.89, 142.29, 140.22, 138.61, 136.90, 132.94, 131.82, 130.12, 129.55, 129.33, 129.29, 129.24, 128.91, 128.17, 124.37, 122.33, 119.19, 116.59, 114.32, 55.41, 15.14, 14.97; HRMS (ES+) found $[M+H]^+$ 550.21, $C_{32}H_{26}BF_2N_3O_3$ requires M 549.20.

1,7-Dimethyl-3-phenyl-5-(2-(1-methyl-1H-indol-5-yl)vinyl)-8-(4-nitrophenyl)-BODIPY (S71)

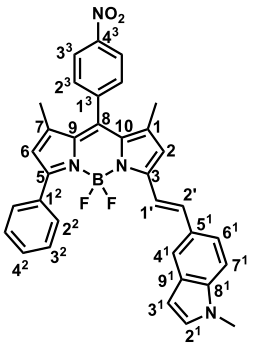

Procedure: following the same procedure as described for S64.

S49 (25 mg, 0.06 mmol, 1.0 eq), S69 (9 mg, 0.06 mmol, 1.0 eq), piperidine (40 mg, 0.47 mmol, 8.0 eq) and acetic acid (42 mg, 0.70 mmol, 12.0 eq) in 0.6 mL benzene and 0.2 mL acetonitrile were converted to S71 as a blue solid (22 mg, 0.037 mmol, 62 % yield). Purification was performed by silica-gel column chromatography (eluant: 1st EtOAc / Hexane = 0~50%, 2nd DCM/ Hexane = 0~100% then EtOAc/ DCM = 0~20%).

Characteristics: δ_H (400 MHz, Chloroform-*d*) 8.43 (d, *J* = 8.6 Hz, 2H), 7.93 (dd, *J* = 8.1, 1.4 Hz, 2H), 7.82 (s, 1H), 7.71 – 7.59 (m, 3H), 7.58-7.44 (m, 5H), 7.31 (d, *J* = 8.6 Hz, 1H), 7.07 (d, *J* = 3.1 Hz, 1H), 6.75 (s, 1H), 6.53 (d, *J* = 3.0 Hz, 1H), 6.34 (s, 1H), 3.81 (s, 3H), 1.47 (d, *J* = 3.6 Hz, 6H); δ_C (101 MHz, Chloroform-*d*) 157.02, 154.08, 148.35, 143.03, 142.45, 141.49, 139.74, 139.46, 137.71, 136.34, 133.15, 131.58, 130.20, 129.95, 129.76, 129.34, 129.09, 128.79, 128.15, 127.75, 124.32, 122.29, 122.05, 121.55, 119.42, 115.78, 115.50, 115.24, 109.77, 102.11, 33.03, 15.19, 14.91; HRMS (ES+) found $[M+H]^+$ 573.22, $C_{34}H_{27}BF_2N_4O_2$ requires M 572.22.

1,7-Dimethyl-3-phenyl-5-yl)vinyl)phenyl)morpholine-8-(4-nitrophenyl)-BODIPY (S72)

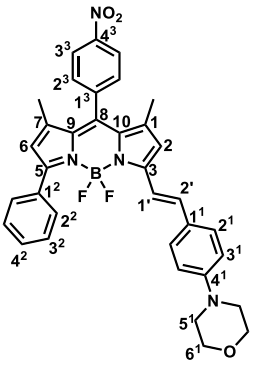

Procedure: following the same procedure as described for S64.

S49 (25 mg, 0.06 mmol, 1.0 eq), S68 (12 mg, 0.06 mmol, 1.0 eq), piperidine (40 mg, 0.47 mmol, 8.0 eq) and acetic acid (42 mg, 0.70 mmol, 12.0 eq) in 0.6 mL benzene and 0.2 mL acetonitrile were converted to S72 as a blue solid (20 mg, 0.033 mmol, 58 % yield). Purification was performed by silica-gel column chromatography (eluant: 1st EtOAc / Hexane = 0~50%, 2nd DCM/ Hexane = 0~100% then EtOAc/ DCM = 0~20%).

Characteristics: δ_H (400 MHz, Chloroform-*d*) 8.43 (d, *J* = 8.4 Hz, 2H), 7.92 (d, *J* = 9.3 Hz, 2H), 7.62 (d, *J* = 8.6 Hz, 2H), 7.57-7.43 (m, 6H), 7.28 (s, 1H), 6.87 (d, *J* = 8.8 Hz, 2H), 6.70 (s, 1H), 6.34 (s, 1H), 3.91-3.83 (m, 4H), 3.31-3.19 (m, 4H), 1.46 (s, 6H); δ_C (101 MHz, Chloroform-*d*) 156.65, 154.17, 152.06, 148.35, 142.93, 142.40, 139.57, 139.21, 136.29, 133.10, 131.64, 130.19, 129.53, 129.32, 129.10, 128.14, 127.22, 124.33, 122.10, 119.36, 115.57, 114.66, 66.68, 48.08, 15.16, 14.92; HRMS (ES+) found $[M+H]^+$ 605.25, $C_{35}H_{31}BF_2N_4O_3$ requires M 604.25.

1-Methyl-3-methoxystyryl-8-(4-nitrophenyl)-BODIPY (S73)

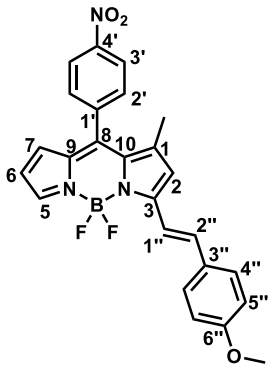

Procedure: following the same procedure as described for S64.

S51 (20 mg, 0.06 mmol, 1.0 eq), 4-methoxybenzaldehyde (8 mg, 0.06 mmol, 1.0 eq), piperidine (40 mg, 0.47 mmol, 8.0 eq) and acetic acid (42 mg, 0.70 mmol, 12.0 eq) in 0.6 mL benzene and 0.2 mL acetonitrile were converted to S73 as a purple solid (10 mg, 0.022 mmol, 36 % yield). Purification was performed by silica-gel column chromatography (eluant: 1st EtOAc / Hexane = 0~50%, 2nd DCM/ Hexane = 0~100% then EtOAc/ DCM = 0~20%).

Characteristics: δ_H (400 MHz, Chloroform-*d*) 8.40 (d, J = 8.6 Hz, 2H), 7.74 (s, 1H), 7.62 (d, J = 8.6 Hz, 5H), 7.41 (d, J = 16.2 Hz, 1H), 6.96 (d, J = 8.7 Hz, 2H), 6.78 (s, 1H), 6.43 (dd, J = 3.9, 2.1 Hz, 1H), 6.29 (d, J = 3.7 Hz, 1H), 3.89 (s, 3H), 1.60 (s, 3H); δ_C (101 MHz, Chloroform-*d*) 161.58, 159.81, 148.45, 145.21, 141.12, 141.08, 138.26, 137.21, 134.47, 134.00, 130.36, 129.95, 128.52, 125.24, 123.72, 119.93, 116.32, 116.19, 114.54, 55.49, 15.47; HRMS (ES+) found $[M+H]^+$ 460.16, $C_{25}H_{20}BF_2N_3O_3$ requires M 459.16.

1-Methyl-3-(2-(1-methyl-1H-indol-5-yl)vinyl)-8-(4-nitrophenyl)-BODIPY (S74)

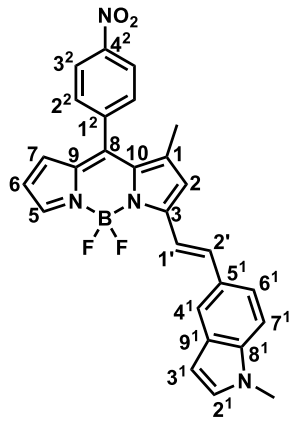

Procedure: following the same procedure as described for S64.

S51 (20 mg, 0.06 mmol, 1.0 eq), S69 (9 mg, 0.06 mmol, 1.0 eq), piperidine (40 mg, 0.47 mmol, 8.0 eq) and acetic acid (42 mg, 0.70 mmol, 12.0 eq) in 0.6 mL benzene and 0.2 mL acetonitrile were converted to S74 as a purple solid (9 mg, 0.020 mmol, 33 % yield). Purification was performed by silica-gel column chromatography (eluant: 1st EtOAc / Hexane = 0~50%, 2nd DCM/ Hexane = 0~100% then EtOAc/ DCM = 0~20%).

Characteristics: δ_H (400 MHz, Chloroform-*d*) 8.40 (d, *J* = 8.6 Hz, 2H), 7.90 (s, 1H), 7.75 (d, *J* = 16.5 Hz, 2H), 7.63 (d, *J* = 8.5 Hz, 4H), 7.37 (d, *J* = 8.6 Hz, 1H), 7.11 (d, *J* = 3.1 Hz, 1H), 6.84 (s, 1H), 6.57 (d, *J* = 2.9 Hz, 1H), 6.42 (dd, *J* = 3.7, 2.1 Hz, 1H), 6.26 (d, *J* = 3.6 Hz, 1H), 3.85 (s, 3H), 1.28 (s, 4H); δ_C (101 MHz, Chloroform-*d*) 148.41, 145.16, 143.97, 141.27, 138.08, 137.52, 136.46, 130.42, 130.22, 128.91, 127.41, 124.55, 123.70, 122.91, 121.65, 120.13, 115.98, 115.47, 110.01, 102.34, 33.09, 15.50; HRMS (ES+) found $[M+H]^+$ 483.18, $C_{27}H_{21}BF_2N_4O_2$ requires M 482.17.

1,7-Dimethyl-3-phenyl-(4-(2-(2-(2-methoxyethoxy)ethoxy)ethoxy)styryl)-8-(4-nitrophenyl)-BODIPY (S75)

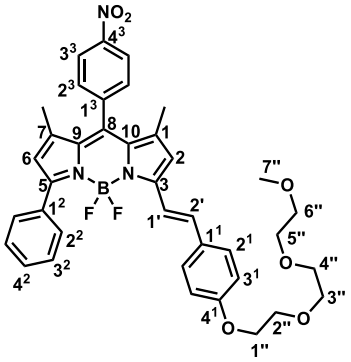

Procedure: following the same procedure as described for S64.

S49 (25 mg, 0.06 mmol, 1.0 eq), S67 (16 mg, 0.06 mmol, 1.0 eq), piperidine (40 mg, 0.47 mmol, 8.0 eq) and acetic acid (42 mg, 0.70 mmol, 12.0 eq) in 0.6 mL benzene and 0.2 mL acetonitrile were converted to S75 as a blue solid (26 mg, 0.038 mmol, 63 % yield). Purification was performed by silica-gel column chromatography (eluant: 1st EtOAc / Hexane = 0~50%, 2nd DCM/ Hexane = 0~100% then EtOAc/ DCM = 0~20%).

Characteristics: δ_H (400 MHz, Chloroform-*d*) 8.44 (d, *J* = 8.6 Hz, 2H), 7.91 (dd, *J* = 8.0, 1.5 Hz, 2H), 7.63 (d, *J* = 8.5 Hz, 2H), 7.59-7.43 (m, 6H), 7.28 (s, 1H), 6.92 (d, *J* = 8.8 Hz, 2H), 6.69 (s, 1H), 6.35 (s, 1H), 4.23-4.12 (m, 2H), 3.94-3.85 (m, 2H), 3.77 (dd, *J* = 6.4, 3.7 Hz, 2H), 3.74-3.64 (m, 4H), 3.58 (dd, *J* = 5.6, 3.6 Hz, 2H), 3.40 (s, 3H), 1.46 (s, 6H); δ_C (101 MHz, Chloroform-*d*) 160.19, 156.12, 154.88, 148.39, 142.90, 142.28, 140.23, 138.60, 136.91, 132.93, 131.82, 130.11, 129.51, 129.32, 129.24, 129.03, 128.16, 124.37, 122.34, 119.19, 116.61, 115.27, 114.95, 71.94, 70.87, 70.67, 70.59, 69.64, 67.52, 59.07, 15.14, 14.97; HRMS (ES+) found $[M+H]^+$ 682.29, $C_{38}H_{38}BF_2N_3O_6$ requires M 681.28.

1,7-Dimethyl-3,5-bis(4-(2-(2-(2-methoxyethoxy)ethoxy)ethoxy)styryl)-8-(4-nitrophenyl)-BODIPY (S76)

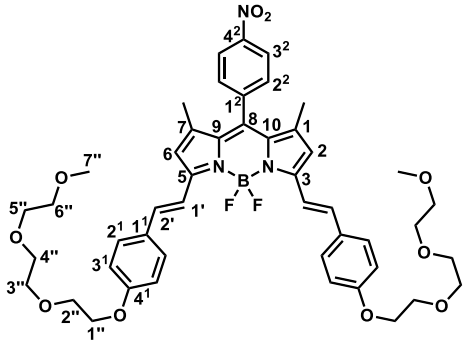

Procedure: following the same procedure as described for S64.

S2 (22 mg, 0.06 mmol, 1.0 eq), S67 (32 mg, 0.12 mmol, 2.0 eq), piperidine (40 mg, 0.47 mmol, 8.0 eq) and acetic acid (42 mg, 0.70 mmol, 12.0 eq) in 0.6 mL benzene and 0.2 mL acetonitrile were converted to S76 as a blue solid (15 mg, 0.018 mmol, 29 % yield). Purification was performed by silica-gel column chromatography (eluant: 1st EtOAc / Hexane = 0~50%, 2nd DCM/ Hexane = 0~100% then EtOAc/ DCM = 0~20%).

Characteristics: δ_H (400 MHz, Chloroform-*d*) 8.44 (d, *J* = 8.2 Hz, 2H), 7.64 (t, *J* = 10.9 Hz, 8H), 7.31 (d, *J* = 6.0 Hz, 2H), 7.00 (d, *J* = 8.3 Hz, 4H), 6.69 (s, 2H), 4.23 (t, *J* = 4.8 Hz, 4H), 3.94 (t, *J* = 4.9 Hz, 4H), 3.81 (d, *J* = 5.0 Hz, 4H), 3.78-3.69 (m, 9H), 3.62 (t, *J* = 4.7 Hz, 4H), 3.44 (s, 6H), 1.46 (s, 6H); δ_C (101 MHz, Chloroform-*d*) 159.87, 153.48, 148.29, 142.42, 140.93, 136.70, 134.40, 132.38, 130.27, 129.46, 129.19, 128.83, 124.23, 118.11, 116.93, 114.98, 114.30, 71.95, 70.88, 70.68, 70.60, 69.69, 67.52, 59.08, 14.99; HRMS (ES+) found $[M+H]^+$ 870.39, $C_{47}H_{54}BF_2N_3O_{10}$ requires M 869.39.

1,5,7-Trimethyl-3-(4-(2-(2-(2-methoxyethoxy)ethoxy)ethoxy)styryl)-8-(4-nitrophenyl)-BODIPY (S77)

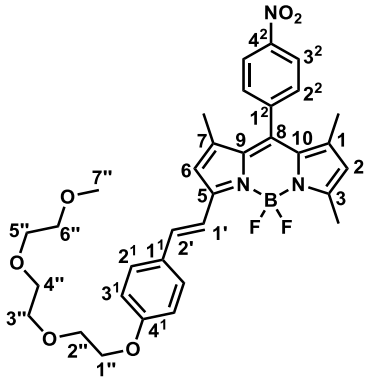

Procedure: following the same procedure as described for S64.

S2 (22 mg, 0.06 mmol, 1.0 eq), S67 (18 mg, 0.06 mmol, 1.0 eq), piperidine (40 mg, 0.47 mmol, 8.0 eq) and acetic acid (42 mg, 0.70 mmol, 12.0 eq) in 0.6 mL benzene and 0.2 mL acetonitrile were converted to S77 as a purple solid (2 mg, 0.003 mmol, 5 % yield). Purification was performed by silica-gel column chromatography (eluant: 1st EtOAc / Hexane = 0~50%, 2nd DCM/ Hexane = 0~100% then EtOAc/ DCM = 0~20%).

Characteristics: δ_H (400 MHz, Chloroform-*d*) 8.42 (d, *J* = 8.7 Hz, 2H), 7.65 – 7.51 (m, 5H), 7.25 (d, *J* = 16.6 Hz, 1H), 6.95 (d, *J* = 8.8 Hz, 2H), 6.65 (s, 1H), 6.05 (s, 1H), 4.23 – 4.17 (m, 2H), 3.94 – 3.88 (m, 2H), 3.78 (dd, *J* = 6.1, 3.5 Hz, 2H), 3.75 – 3.66 (m, 4H), 3.58 (dd, *J* = 5.6, 3.6 Hz, 2H), 3.41 (s, 3H), 2.62 (s, 3H), 1.44 (s, 3H), 1.40 (s, 3H); HRMS (ES-) found $[M-H]^-$ 618.27, $C_{33}H_{36}BF_2N_3O_6$ requires M 619.27.

1,3,5,7-Tetramethyl-2,6-disulfonic acid-8-(4-nitrophenyl)-BODIPY (S79)

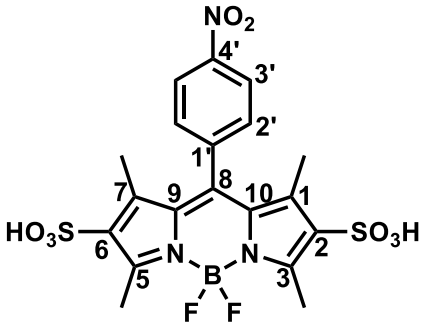

Procedure: A solution of chlorosulfonic acid (33 mg, 0.284 mmol, 2.1 eq) in 2 mL dry DCM was added dropwise to a solution of S2 (50 mg, 0.135 mmol, 1.0 eq) in 5 mL dry DCM over 10 min under N_2 at -40 °C. Then the resulting solution was slowly warmed to room temperature. After 20 min, TLC showed all of the starting material was consumed, and then 1 mL water was added to quench chlorosulfonic acid, and the products were separated from the DCM into the aqueous layer. The aqueous layer was purified by reverse phase column chromatography (1st methanol : water = 0%-20%, 2nd acetonitrile : water = 0%-20%) to afford S79 as a red solid (7 mg, 0.012 mmol, 9 % yield).

Characteristics: δ_H (400 MHz, MeOD) 8.49 (d, J = 8.6 Hz, 2H), 7.74 (d, J = 8.6 Hz, 2H), 2.82 (s, 6H), 1.69 (s, 6H); δ_C (101 MHz, MeOD) 156.18, 148.75, 142.43, 141.53, 141.19, 134.97, 129.90, 129.70, 124.43, 13.16, 12.33; HRMS (ES-) found [M-2H]/2$^-$ 263.52, $C_{19}H_{18}BF_2N_3O_8S_2$ requires M 529.06.

1,3,5,7-Tetramethyl-8-phenyl-BODIPY (S80)

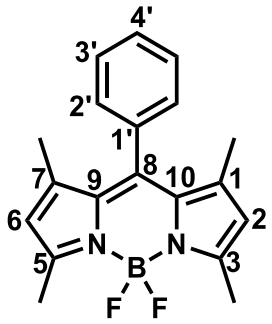

Procedure: Benzoyl chloride (1.0 g, 7.11 mmol, 1.0 eq) and 2, 4-dimethylpyrrole (1.5 mL, 14.23 mmol, 2.0 eq) were added into 100 mL DCM under Ar atmosphere. N,N-diisopropylethylamine (12.4 mL, 71.14 mmol, 10.0 eq) and $BF_3 \cdot OEt_2$ (9.7 mL, 78.26 mmol, 11.0 eq) were drop added in an ice-water bath, and the mixture was stirred until the completed reaction, monitored by thin-layer chromatography (TLC). The solvent was removed under reduced pressure to obtain a residue, which was dissolved in DCM and washed with saturated Na_2CO_3 solution and water. The organic layers were dried over anhydrous Na_2SO_4 and evaporated under reduced pressure. The crude product was purified by column chromatography (silica gel, ethyl acetate : hexane = 10-20 %, v/v) to obtain S80 as an orange powder(0.55 g, 1.70 mmol, 24 %).

Characteristics: δ_H (400 MHz, Chloroform-*d*) 7.49 (s, 3H), 7.29 (s, 2H), 6.00 (s, 2H), 2.58 (s, 6H), 1.40 (s, 7H); δ_C (101 MHz, Chloroform-*d*) 155.43, 143.18, 141.77, 134.99, 131.44, 129.15, 128.97, 127.94, 121.25, 14.59, 14.34; HRMS (ES+) found $[M+H]^+$ 325.17, $C_{19}H_{19}BF_2N_2$ requires M 324.16.

Ethyl 3-(5-benzoyl-2,4-dimethyl-1H-pyrrol-3-yl)propanoate (S81)

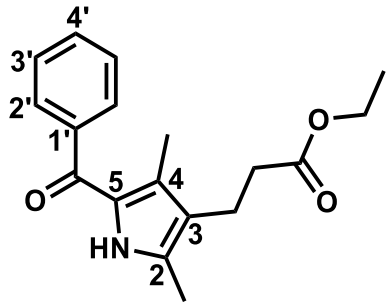

Procedure: following the same procedure 2 as described for S17.

S9 (2.00 g, 10.24 mmol, 1.0 eq) and Et_3N (3.8 mL, 11.27 mmol, 1.1 eq) in THF (100 mL) and benzoyl chloride (1.44 g, 10.24 mmol, 1.0 eq) was converted to S81 as pale yellow oil (1.19 g, 3.98 mmol, 39% yield). Purification was performed by silica-gel column chromatography (eluant: Hexane/ EtOAC= 10-50%).

Characteristics: δ_H (400 MHz, Chloroform-*d*) 9.88 (s, 1H), 7.67-7.58 (m, 2H), 7.53-7.40 (m, 3H), 4.12 (q, J = 7.1 Hz, 2H), 2.71 (dd, J = 8.8, 6.9 Hz, 2H), 2.43 (dd, J = 8.8, 6.9 Hz, 2H), 2.28 (s, 3H), 1.89 (s, 3H), 1.24 (t, J = 7.1 Hz, 3H); δ_C (101 MHz, Chloroform-*d*) 185.67, 173.12, 140.36, 133.97, 130.86, 128.57, 128.30, 128.24, 127.10, 121.46, 60.43, 34.94, 19.60, 14.23, 11.88, 11.59; HRMS (ES+) found $[M+H]^+$ 325.17, $C_{18}H_{21}NO_3$ requires M 299.15.

Methyl 3-(5-benzoyl-2,4-dimethyl-1H-pyrrol-3-yl)propanoate (S82)

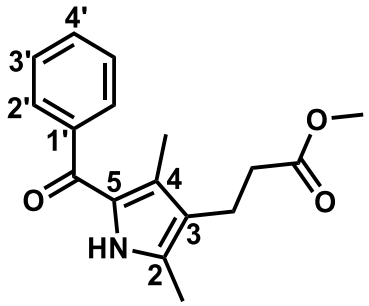

Procedure: following the same procedure 2 as described for S17.

S14 (200 mg, 1.10 mmol, 1.0 eq) and Et_3N (0.41 mL, 1.21 mmol, 1.1 eq) in THF (11 mL) and benzoyl chloride (155 mg, 1.10 mmol, 1.0 eq) was converted to S82 as pale yellow oil (114 mg, 0.40 mmol, 36% yield). Purification was performed by silica-gel column chromatography (eluant: Hexane/ EtOAC= 10-50%).

Characteristics: δ_H (400 MHz, Chloroform-*d*) 10.00 (s, 1H), 7.66-7.60 (m, 2H), 7.53-7.41 (m, 3H), 3.67 (s, 3H), 2.75-2.66 (m, 2H), 2.44 (t, J = 7.8 Hz, 2H), 2.28 (s, 3H), 1.89 (s, 3H); δ_C (101 MHz, Chloroform-*d*) 185.70, 173.53, 140.37, 134.09, 130.88, 128.56, 128.32, 128.25, 127.14, 121.37, 51.65, 34.73, 19.62, 11.87, 11.55; HRMS (ES+) found $[M+H]^+$ 286.15, $C_{17}H_{19}NO_3$ requires M 285.14.

1,3,5,7-Tetramethyl-2-ethyl propanoate-8-(4-nitrophenyl)-BODIPY (S83)

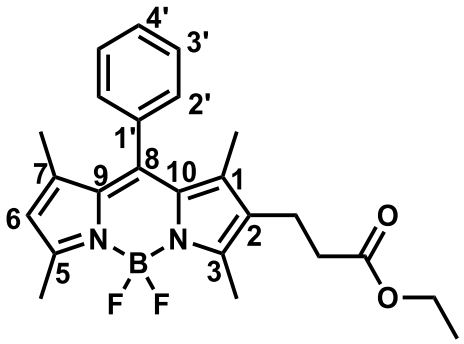

Procedure : following the same procedure 2 as described for S2.

S81 (200 mg, 0.67 mmol, 1.0 eq), 2,4-dimethypyrrole (640mg, 0.67 mmol, 1.0 eq), $BF_3 \cdot OEt_2$ (0.66 mL, 5.35 mmol, 8.0 eq) and N,N-diisopropylethylamine (0.70 mL, 4.01 mmol, 6.0 eq) in dry DCM (3.3 mL) were converted to S83 as an orange solid (165 mg, 0.39 mmol, 58% yield). Purification was performed by silica-gel column chromatography (eluant: Hexane/ EtOAC= 10-20 %).

Characteristics: δ_H (400 MHz, Chloroform-*d*) 7.50 (dd, *J* = 5.0, 1.8 Hz, 3H), 7.32-7.25 (m, 2H), 5.98 (s, 1H), 4.13 (q, *J* = 7.1 Hz, 2H), 2.71-2.61 (m, 2H), 2.57 (d, *J* = 6.0 Hz, 6H), 2.42-2.32 (m, 2H), 1.37 (s, 3H), 1.33 (s, 3H), 1.25 (t, *J* = 7.1 Hz, 4H); δ_C (101 MHz, Chloroform-*d*) 172.67, 154.89, 154.64, 142.78, 141.29, 139.77, 135.22, 131.29, 131.02, 129.47, 129.15, 128.95, 128.01, 121.01, 60.54, 34.43, 19.32, 14.55, 14.34, 14.19, 12.68, 11.85; HRMS (ES+) found $[M+H]^+$ 425.22, $C_{24}H_{27}BF_2N_2O_2$ requires M 424.21.

1,3,5,7-Tetramethyl-2-ethyl propanoate-8-(4-nitrophenyl)-BODIPY (S84)

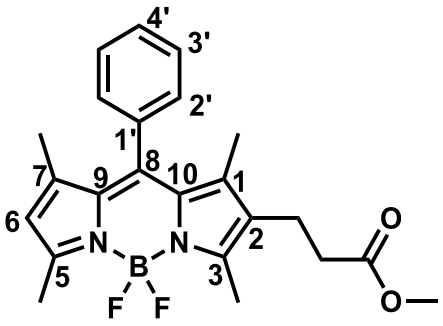

Procedure : following the same procedure 2 as described for S2.

S82 (100 mg, 0.35 mmol, 1.0 eq), 2,4-dimethypyrrole (33 mg, 0.35 mmol, 1.0 eq), $BF_3 \cdot OEt_2$ (0.35 mL, 2.80 mmol, 8.0 eq) and N,N-diisopropylethylamine (0.37 mL, 2.10 mmol, 6.0 eq) in dry DCM (1.8 mL) were converted to S84 as an orange solid (78 mg, 0.19 mmol, 54% yield). Purification was performed by silica-gel column chromatography (eluant: Hexane/ EtOAC= 10-20 %).

Characteristics: δ_H (400 MHz, Chloroform-*d*) 7.48 (dt, *J* = 4.4, 2.0 Hz, 3H), 7.32-7.22 (m, 2H), 5.96 (s, 1H), 3.65 (s, 3H), 2.7-2.59 (m, 2H), 2.55 (d, *J* = 2.4 Hz, 6H), 2.41-2.31 (m, 2H), 1.35 (s, 3H), 1.31 (s, 3H); δ_C (101 MHz, Chloroform-*d*) 173.03, 154.96, 154.50, 142.82, 141.29, 139.69, 135.19, 131.30, 130.98, 129.32, 129.12, 128.92, 127.99, 121.01, 51.64, 34.16, 19.30, 14.52, 14.30, 12.60, 11.78; HRMS (ES+) found $[M+H]^+$ 411.21, $C_{23}H_{25}BF_2N_2O_2$ requires M 410.20.

6-((7-Nitrobenzo[c][1,2,5]oxadiazol-4-yl)amino)hexan-1-ol (S85)

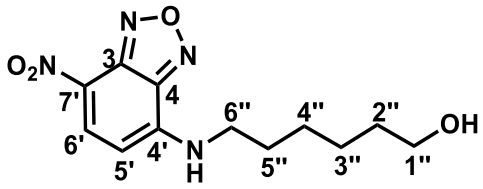

Procedure: To a solution of 6-amino-1-hexanol (310 mg, 2.57 mmol) in 0.3 M aq $NaHCO_3$ (10 mL) was added a solution of 4-chloro-7-nitro-2,1,3-benzoxadiazole (497 mg, 2.49 mmol) in MeOH (20 mL) and the reaction mixture was stirred overnight at room temperature. The solvent was evaporated under diminished pressure. The residue was purified by column chromatography with a mixture EtOAC/ Hexane (0-100%) to afford S85 as a red solid (419 mg, 1.47 mmol, 61%).

Characteristics: δ_H (400 MHz, Chloroform-*d*) 8.51-8.42 (m, 1H), 6.76 (d, J = 6.0 Hz, 1H), 6.18 (d, J = 8.7 Hz, 1H), 3.69 (t, J = 6.3 Hz, 2H), 3.52 (p, J = 6.0, 5.2 Hz, 2H), 1.85 (p, J = 7.5 Hz, 3H), 1.63 (dt, J = 13.5, 6.4 Hz, 2H), 1.58-1.43 (m, 4H); δ_C (101 MHz, Chloroform-*d*) 144.25, 144.08, 143.93, 136.71, 123.60, 98.60, 62.68, 43.96, 32.22, 28.28, 26.64, 25.45; HRMS (ES+) found $[M+H]^+$ 281.13, $C_{12}H_{16}N_4O_4$ requires M 280.12.

N-(6-iodohexyl)-7-nitrobenzo[c][1,2,5]oxadiazol-4-amine (S86)

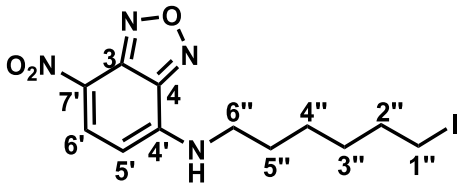

Procedure: A round bottom flask was charged with PPh_3 (280 mg, 1.07 mmol, 1.5 eq.) and 3 mL dichloromethane. Iodine (272 mg, 1.01 mmol, 1.5 eq.) was added in small portions under N_2 at room temperature. The reaction was stirred for 10 minutes. Imidazole (121 mg, 1.78 mmol, 2.5 eq.) was added to the solution in small portions and the reaction was allowed to stir for 10 more minutes. A solution of S85 (200 mg, 0.71 mmol, 1.0 eq.) in 2 mL DCM was added to the suspension dropwise in 5 minutes and the reaction was stirred for 1 hour at room temperature. Then the solvent was removed in *vacuo* and the solid residue was purified by flash column chromatography eluting with 50% ethyl acetate / hexane to yield S86 as a red solid(216 mg, 0.55 mmol, 78 % yield).

Characteristics: δ_H (400 MHz, Chloroform-*d*) 8.49 (d, J = 8.6 Hz, 1H), 6.39 (s, 1H), 6.21 (d, J = 8.7 Hz, 1H), 3.55 (q, J = 6.7 Hz, 2H), 3.22 (t, J = 6.8 Hz, 2H), 1.94-1.79 (m, 4H), 1.53 (p, J = 3.5 Hz, 4H); δ_C (101 MHz, Chloroform-*d*) 144.26, 143.96, 143.90, 136.63, 123.84, 98.67, 43.90, 33.06, 30.01, 28.36, 25.87, 6.79; HRMS (ES+) found $[M+H]^+$ 391.03, $C_{12}H_{15}IN_4O_3$ requires M 390.02.

4-((6-((7-nitrobenzo[c][1,2,5]oxadiazol-4-yl)amino)hexyl)oxy)benzaldehyde (S87)

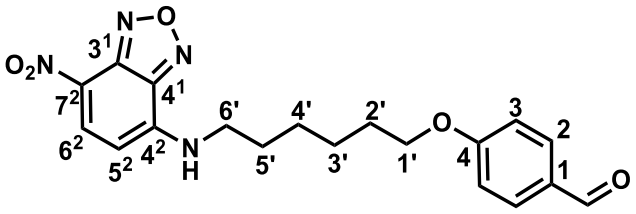

Procedure: Cesium carbonate (251 mg, 0.77 mmol, 2.0 equiv) was added to a solution of S86 (150 mg, 0.38 mmol, 1.0 equiv) and 4-Hydroxybenzaldehyde (56 mg, 0.46 mmol, 1.2 equiv) in DMF (1.0 mL). After stirring overnight at 90°C, the mixture was then poured into saturated aqueous NaCl, and then resultant mixture extracted with EtOAc.). The organic layer was washed with water, dried over Mg_2SO_4 and concentrated under vacuum. The compound was purified by column chromatography over silica gel (Hexane/ EtOAc, 1:1) to afford S87 as an orange solid (58 mg, 0.15 mmol, 40 % yield).

Characteristics: δ_H (400 MHz, Chloroform-*d*) 9.90 (s, 1H), 8.51 (d, J = 8.6 Hz, 1H), 7.85 (d, J = 8.6 Hz, 2H), 7.00 (d, J = 8.6 Hz, 2H), 6.29 (s, 1H), 6.20 (d, J = 8.6 Hz, 1H), 4.09 (t, J = 6.2 Hz, 2H), 3.55 (d, J = 6.4 Hz, 2H), 1.96-1.81 (m, 4H), 1.67-1.56 (m, 4H); δ_C (101 MHz, Chloroform-*d*) 190.81, 164.04, 144.28, 143.89, 143.78, 136.43, 132.02, 129.92, 124.14, 114.71, 98.54, 68.00, 43.88, 28.94, 28.53, 26.74, 25.79; HRMS (ES+) found $[M+H]^+$ 385.15, $C_{19}H_{20}N_4O5$ requires M 384.14.

1-(6-((7-nitrobenzo[c][1,2,5]oxadiazol-4-yl)amino)hexyl)-1H-indole-5-carbaldehyde (S88)

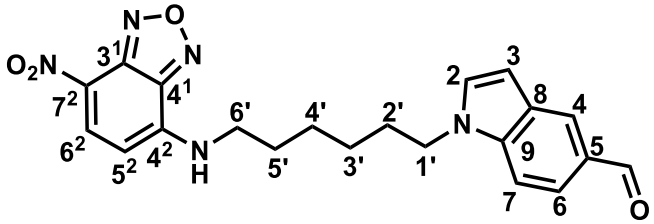

Procedure: To a solution of 1H-indole-5-carbaldehyde (100 mg, 0.69 mmol, 1.0 eq) and S86 (269 mg, 0.69 mmol, 1.0 eq) in DMSO (1.0 mL) was added KOH (58 mg, 1.03 mmol, 1.5 eq) at room temperature. The mixture was stirred overnight at room temperature, and then added water and extracted with dichloromethane. The organic layer was washed with water, dried over Mg_2SO_4 and concentrated under vacuum. The compound was purified by column chromatography over silica gel (Hexane/ EtOAc, 1:1) to afford S88 as an orange solid (91 mg, 0.22 mmol, 32 % yield).

Characteristics: δ_H (400 MHz, Chloroform-*d*) 10.04 (s, 1H), 8.46 (d, *J* = 8.6 Hz, 1H), 8.16 (d, *J* = 1.6 Hz, 1H), 7.79 (dd, *J* = 8.6, 1.6 Hz, 1H), 7.42 (d, *J* = 8.6 Hz, 1H), 7.21 (d, *J* = 3.3 Hz, 1H), 6.70-6.61 (m, 1H), 6.26 (t, *J* = 5.8 Hz, 1H), 6.12 (d, *J* = 8.6 Hz, 1H), 4.21 (t, *J* = 6.9 Hz, 2H), 3.46 (q, *J* = 6.7 Hz, 2H), 1.93 (p, *J* = 7.1 Hz, 2H), 1.80 (p, *J* = 7.3 Hz, 2H), 1.57-1.36 (m, 4H); δ_C (101 MHz, Chloroform-*d*) 192.47, 144.22, 143.85, 143.74, 139.25, 136.45, 129.68, 129.31, 128.30, 126.71, 124.04, 121.69, 109.86, 103.49, 98.54, 46.56, 43.76, 30.14, 28.40, 26.63; HRMS (ES+) found $[M+H]^+$ 408.17, $C_{21}H_{21}N_5O_4$ requires M 407.16.

N-(6-(diethylamino)-9-(2-(((2,5-dioxopyrrolidin-1-yl)oxy)carbonyl)phenyl)-3H-xanthen-3-ylidene)-N-ethylethanaminium (Rhodamine B-NHS ester) (S89)

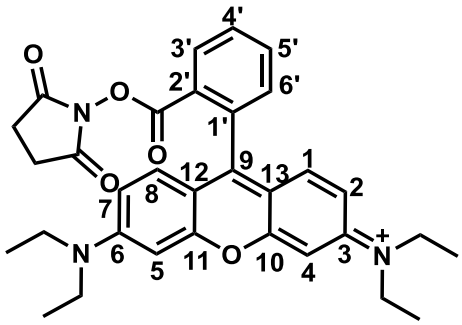

Procedure: EDC (1.76 g, 9.19 mmol, 2.2 eq) was added to a solution of Rhodamine B (2.00 g, 4.18 mmol, 1.0 eq) in DMF (35 mL). The mixture was stirred for 10 min and N-hydroxysuccinimide (0.72g, 6.26 mmol, 1.5 eq) was added. The reaction was stirred at 80 °C overnight until no starting material was left. The mixture was concentrated *in vacuo* and purified by chromatography on silica gel (5-10% MeOH/ DCM) to afford S89 as a red mud (1.65 g, 2.86 mmol, 69 % yield).

Characteristics: δ_H (400 MHz, MeOD) 8.47 (dd, J = 8.0, 0.9 Hz, 1H), 8.07 (td, J = 7.6, 1.3 Hz, 1H), 7.96 (td, J = 7.8, 1.3 Hz, 1H), 7.63 (dd, J = 7.7, 0.9 Hz, 1H), 7.17 (d, J = 9.5 Hz, 2H), 7.08 (dd, J = 9.6, 2.4 Hz, 2H), 6.98 (d, J = 2.4 Hz, 2H), 3.69 (q, J = 7.1 Hz, 8H), 2.75 (s, 4H), 1.31 (t, J = 7.1 Hz, 12H); m/z (LCMS ES+) r_t 2.78 min, 541.23 $[M+H]^+$, $C_{32}H_{34}N_3O_5$ requires M 540.25.

2-(6-Azidohexyl)-3',6'-bis(diethylamino)spiro[isoindoline-1,9'-xanthen]-3-one (S90)

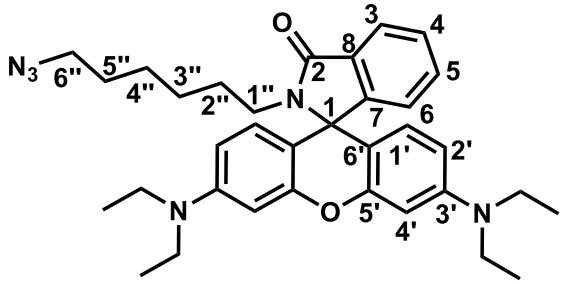

Procedure: To a solution of S89 (500 mg, 0.87 mmol, 1.0 eq) and S60 (123 mg, 0.87 mmol, 1.0 eq) in 17 mL ethanol, triethylamine (0.17 mL, 1.30 mmol, 1.5 eq) was added, and the mixture was reflux overnight. Then the mixture was concentrated *in vacuo* and purified by chromatography on silica gel (20% ethyl acetate/ hexane) to afford S90 as a colourless oil (260 mg, 0.46 mmol, 53 % yield).

Characteristics: δ_H (400 MHz, Chloroform-*d*) 7.92 (dd, *J* = 5.8, 2.5 Hz, 1H), 7.53-7.40 (m, 2H), 7.14-7.06 (m, 1H), 6.46 (s, 1H), 6.44 (s, 1H), 6.41 (d, *J* = 2.2 Hz, 2H), 6.30 (d, *J* = 2.3 Hz, 1H), 6.28 (d, *J* = 2.3 Hz, 1H), 3.36 (q, *J* = 6.9 Hz, 8H), 3.14 (q, *J* = 8.1, 7.6 Hz, 4H), 1.48-1.37 (m, 2H), 1.23-1.04 (m, 18H); δ_C (101 MHz, Chloroform-*d*) 168.02, 153.47, 153.37, 148.72, 132.19, 131.58, 129.02, 127.95, 123.74, 122.69, 107.97, 105.98, 97.65, 64.85, 51.37, 44.37, 40.13, 28.50, 27.99, 26.51, 26.16, 12.60; HRMS (ES+) found $[M+H]^+$ 567.34, $C_{34}H_{42}N_6O_2$ requires M 566.34.

2-(2-(2-(2-(2-Azidoethoxy)ethoxy)ethoxy)ethyl)-3',6'-bis(diethylamino)spiro [isoindoline-1,9'-xanthen]-3-one (S91)

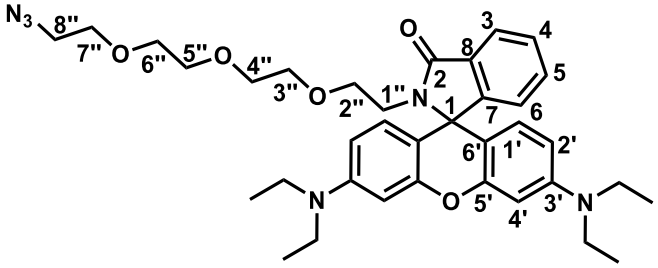

Procedure: following the same procedure as described for S90.

S89 (500 mg, 0.87 mmol, 1.0 eq), S63 (189 mg, 0.87 mmol, 1.0 eq) and triethylamine (0.17 mL, 1.30 mmol, 1.5 eq) in 17 mL ethanol were converted to S91 as a colourless oil (242 mg, 0.37 mmol, 43 % yield).

Characteristics: δ_H (400 MHz, Chloroform-*d*) 7.90 (dd, *J* = 5.6, 3.1 Hz, 1H), 7.43 (dd, *J* = 5.6, 3.1 Hz, 2H), 7.08 (dd, *J* = 5.6, 3.0 Hz, 1H), 6.45 (s, 1H), 6.43 (s, 1H), 6.38 (d, *J* = 2.6 Hz, 2H), 6.28 (d, *J* = 2.6 Hz, 1H), 6.26 (d, *J* = 2.6 Hz, 1H), 3.66-3.57 (m, 6H), 3.51 (dd, *J* = 5.8, 3.7 Hz, 2H), 3.40 (dd, *J* = 5.9, 3.8 Hz, 2H), 3.35 (q, *J* = 6.9 Hz, 12H), 3.18 (t, *J* = 7.4 Hz, 2H), 1.18 (t, *J* = 7.0 Hz, 12H); δ_C (101 MHz, Chloroform-*d*) 168.24, 153.79, 153.24, 148.73, 132.38, 130.98, 128.85, 127.95, 123.78, 122.73, 108.03, 105.47, 97.74, 70.64, 70.62, 70.49, 69.97, 67.78, 64.82, 50.64, 44.37, 39.24, 12.62; HRMS (ES+) found $[M+H]^+$ 643.36, $C_{36}H_{46}N_6O_5$ requires M 642.35.

1-(5-Carboxypentyl)-2,3,3-trimethyl-3*H*-indolium bromide (S92)

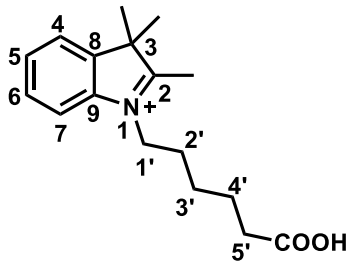

Procedure: 6-Bromohexanoic acid (1.23 g, 6.28 mmol, 1.0 eq) was added to a solution of 2,3,3-trimethylindolenine (1.0 g, 6.28 mmol, 1.0eq) in $MeNO_2$ (3.8 mL) in a cold water bath and then the reaction mixture was magnetically stirred for 6 h at 80 °C. After reaction, the cooled reaction mixture was triturated with diethyl ether (20 mL) and the precipitate was filtered off, then precipitated again with acetone: diethyl ether (1:5) and dried in vacuo to afford S92 as a pale pink solid (1.23 g, 3.47 mmol, 55 % yield).

Characteristics: δ_H (400 MHz, MeOD) 7.92 (dd, J = 6.0, 3.1 Hz, 1H), 7.81 (dd, J = 5.7, 3.1 Hz, 1H), 7.68 (dd, J = 5.8, 3.2 Hz, 2H), 4.55 (t, J = 7.8 Hz, 2H), 2.37 (t, J = 7.2 Hz, 2H), 2.18 (s, 3H), 2.01 (p, J = 7.8 Hz, 2H), 1.72 (p, J = 7.3 Hz, 2H), 1.64 (s, 6H), 1.56 (tt, J = 12.5, 6.2 Hz, 2H); δ_C (101 MHz, MeOD) 208.72, 196.51, 175.78, 142.01, 141.12, 129.78, 129.12, 123.28, 115.16, 54.55, 32.99, 29.33, 27.18, 25.67, 24.04, 21.38; HRMS (ES+) found $[M+H]^+$ 275.19, $C_{17}H_{24}NO_2$ requires M 274.18.

1,2,3,3-Tetramethyl-3*H*-indolium iodide (S93)

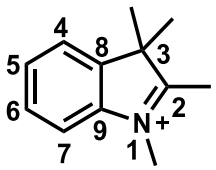

Procedure: Iodomethane (0.89 g, 6.28 mmol, 1.0 eq) was added to a solution of 2,3,3-trimethylindolenine (1.0 g, 6.28 mmol, 1.0eq) in $MeNO_2$ (3.8 mL) in a cold water bath and then the reaction mixture was magnetically stirred for 12 h at room temperature. After reaction, the cooled reaction mixture was triturated with diethyl ether (20 mL) and the precipitate was filtered off, then precipitated again with acetone: diethyl ether (1:5) and dried in vacuo to afford S93 as a pale pink solid (1.33 g, 4.41 mmol, 70 % yield).

Characteristics: δ_H (400 MHz, DMSO-d_6) 8.01-7.89 (m, 1H), 7.89-7.77 (m, 1H), 7.63 (q, J = 5.4, 3.9 Hz, 2H), 3.99 (s, 3H), 2.79 (s, 3H), 1.54 (s, 6H); δ_C (101 MHz, DMSO-d_6) 196.47, 142.59, 142.08, 129.78, 129.29, 123.80, 115.62, 54.41, 35.29, 22.19, 14.77; HRMS (ES+) found $[M+H]^+$ 175.13, $C_{12}H_{16}N$ requires M 174.13.

2-((1E,3E)-5-((E)-1-(5-carboxypentyl)-3,3-dimethylindolin-2-ylidene)penta-1,3-dien-1-yl)-1,3,3-trimethyl-3H-indol-1-ium chloride (S94)

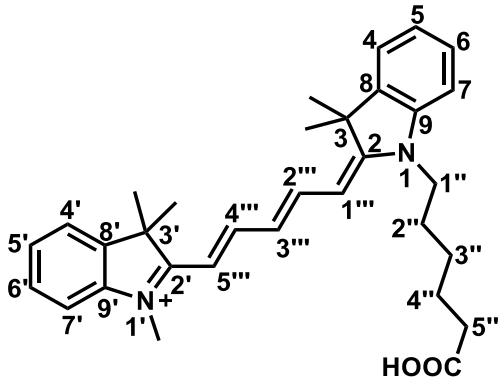

Procedure: S92 (2.0 g, 5.65 mmol, 1.00 eq), S93 (1.26 g, 5.65 mmol, 1.00 eq) and acetic anhydride (35 mL) were combined and allowed to stir at 120 °C for 0.5 h then cooled to room temperature. To the solution was added 1,2,3,3- tetramethyl-3*H*-indolium iodide (1.70 g, 5.65 mmol, 1.00 eq) and pyridine (35 mL) and the reaction mixture was allowed to stir at room temperature for a further 0.5 h then diluted with dichloromethane. The solution was washed with 1 M aqueous hydrochloric acid and brine and the organic layer was dried over anhydrous magnesium sulfate and concentrated under reduced pressure. The crude compound was purified by column chromatography over Al_2O_3 (MeOH : DCM = 0% to 20%) to afford S94 (Cy5) as a blue mud (148 mg, 0.29 mmol, 5 % yield).

Characteristics: δ_H (600 MHz, Chloroform-*d*) 8.05 (td, *J* = 13.0, 4.8 Hz, 2H), 7.36-7.30 (m, 4H), 7.22-7.15 (m, 2H), 7.09 (dd, *J* = 16.8, 8.0 Hz, 2H), 6.87 (t, *J* = 12.5 Hz, 1H), 6.37 (d, *J* = 13.6 Hz, 1H), 6.30 (d, *J* = 13.5 Hz, 1H), 4.04 (t, *J* = 7.6 Hz, 2H), 3.68 (s, 3H), 2.41 (t, *J* = 7.2 Hz, 2H), 1.81 (p, *J* = 7.9 Hz, 2H), 1.72 (m, 14H), 1.54 (p, *J* = 7.6 Hz, 2H); δ_C (151 MHz, Chloroform-*d*) 210.89, 207.03, 177.08, 173.37, 172.75, 153.48, 142.72, 141.95, 141.22, 140.97, 128.63, 126.53, 125.09, 122.27, 122.13, 110.52, 104.23, 103.75, 69.55, 53.77, 49.36, 49.26, 44.24, 34.01, 32.46, 31.73, 30.91, 29.66, 29.23, 28.17, 28.02, 26.89, 26.21, 24.32; HRMS (ES+) found $[M+H]^+$ 484.31, $C_{32}H_{39}N_2O_2$ requires M 483.30.

2-((1E,3E)-5-((E)-1-(6-((2,5-dioxopyrrolidin-1-yl)oxy)-6-oxohexyl)-3,3-dimethylindolin-2-ylidene)penta-1,3-dien-1-yl)-1,3,3-trimethyl-3H-indol-1-ium chloride (S95)

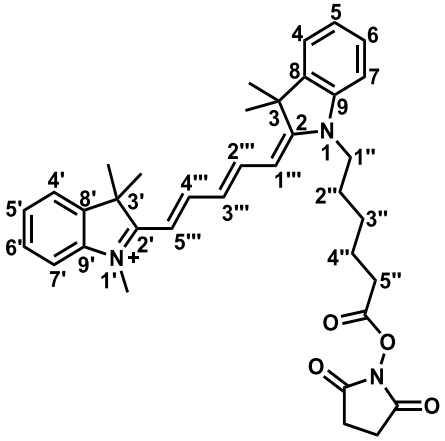

Procedure: EDC (112 mg, 0.59 mmol, 1.5 eq) was added to a solution of S94 (Cy5, 200 mg, 0.39 mmol, 1.0 eq) in dichloromethane (3 mL). The mixture was stirred for 10 min and N-hydroxysuccinimide (90 mg, 0.78 mmol, 2.0 eq) was added. The reaction was stirred overnight until no starting material was left. The crude compound was purified by column chromatography over Al_2O_3 (ethyl acetate : acetone = 0% to 100%) to afford S95 (Cy5-NHS ester) as a blue mud (165 mg, 0.26 mmol, 67 % yield).

Characteristics: δ_H (600 MHz, Chloroform-*d*) 8.13 (t, *J* = 13.0 Hz, 2H), 7.41-7.32 (m, 4H), 7.23 (t, *J* = 7.5 Hz, 2H), 7.12 (dd, *J* = 13.4, 7.9 Hz, 2H), 6.86 (t, *J* = 12.5 Hz, 1H), 6.35 (d, *J* = 13.6 Hz, 2H), 4.15-4.02 (m, 2H), 3.71 (s, 3H), 2.89 (s, 4H), 2.66 (t, *J* = 7.1 Hz, 2H), 1.94-1.57 (m, 18H); δ_C (151 MHz, Chloroform-*d*) 173.48, 172.82, 169.22, 168.40, 153.68, 142.71, 141.94, 141.29, 140.98, 128.59, 126.44, 125.15, 125.08, 122.30, 122.16, 110.50, 110.44, 104.10, 103.67, 49.40, 49.33, 44.12, 30.67, 28.19, 27.99, 26.84, 25.81, 25.76, 24.28; HRMS (ES+) found $[M+H]^+$ 581.32, $C_{36}H_{42}N_3O_4$ requires M 580.32.

2-((1E,3E)-5-((E)-1-(6-((6-azidohexyl)amino)-6-oxohexyl)-3,3-dimethylindolin-2-ylidene)penta-1,3-dien-1-yl)-1,3,3-trimethyl-3H-indol-1-ium chloride (S96)

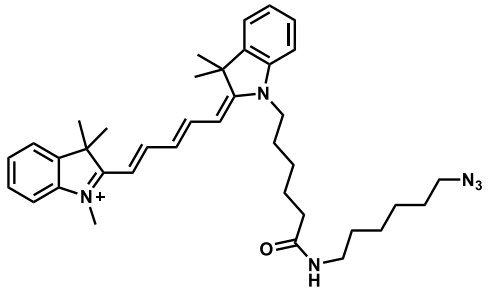

Procedure: S60 (22 mg, 0.15 mmol, 0.95 eq) was added to a solution of S95 (Cy5-NHS ester, 100 mg, 0.16 mmol, 1.0 eq) in dichloromethane (5 mL). The mixture was stirred overnight and then added water and extracted with dichloromethane. The organic layer was washed with water, dried over Mg_2SO_4 and concentrated under vacuum. The crude S96 was collected without further purificition as a blue mud (95 mg, 0.15 mmol crude).

Characteristics: HRMS (ES+) found $[M+H]^+$ 608.42, $C_{38}H_{51}N_6O$ requires M 607.41.

Nitro-BODIPY-NBD probe (S99)

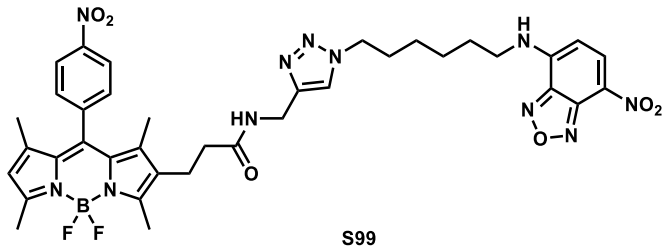

S99

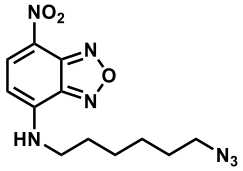

S97

Procedure: $CuSO_4 \cdot 5H_2O$ (1.7 mg, 0.01 mmol, 0.1 eq) and sodium ascorbate (8.3 mg, 0.04 mmol, 0.4eq) dissolved in 2.1 mL t-Butanol/ water (1:2) was stirred at room temperature. Then, a solution of S38 (50 mg, 0.11 mmol, 1.0 eq) and S97 (36 mg, 0.12 mmol, 1.1 eq) in 0.7 mL t-butanol was added. After 1h, the crude mixture was added into 20 mL water and extracted with DCM (3 × 10 mL), dried over Na_2SO_4, filtered, and evaporated. The crude compound was purified by column chromatography over silica gel (Hexane/ EtOAC= 0-100 %) to afford S99 as an orange powder (37 mg, 0.05 mmol, 45 % yield).

Characteristics: δ_H (600 MHz, Chloroform-*d*) 8.48 (d, *J* = 8.6 Hz, 1H), 8.40 (d, *J* = 8.5 Hz, 2H), 7.54 (d, *J* = 8.5 Hz, 3H), 6.71-6.62 (m, 1H), 6.52 (t, *J* = 5.3 Hz, 1H), 6.18 (d, *J* = 8.7 Hz, 1H), 6.01 (s, 1H), 4.45 (d, *J* = 5.5 Hz, 2H), 4.29 (t, *J* = 6.9 Hz, 2H), 3.57-3.44 (m, 2H), 2.66 (t, *J* = 7.5 Hz, 3H), 2.53 (d, *J* = 9.8 Hz, 6H), 2.26 (t, *J* = 7.4 Hz, 2H), 2.19 (d, *J* = 2.4 Hz, 3H), 1.91 (p, *J* = 7.1 Hz, 2H), 1.81 (dt, *J* = 14.4, 6.8 Hz, 3H), 1.51 (tt, *J* = 14.9, 6.9 Hz, 3H), 1.37 (d, *J* = 12.7 Hz, 6H), 1.25 (s, 3H); δ_C (151 MHz, Chloroform-*d*) 171.79, 155.84, 148.30, 144.61, 144.28, 143.90, 142.18, 142.04, 139.11, 137.93, 136.48, 130.43, 130.40, 130.24, 129.73, 124.40, 123.83, 122.28, 121.59, 69.51, 53.78, 49.88, 43.62, 36.31, 34.82, 31.72, 30.91, 29.90, 29.25, 28.15, 26.09, 25.88, 19.71, 14.67, 14.57, 12.77, 12.17; HRMS (ES+) found $[M+H]^+$ 784.33, $C_{37}H_{40}BF_2N_{11}O_6$ requires M 783.32.

Nitro-BODIPY-dansyl probe (S100)

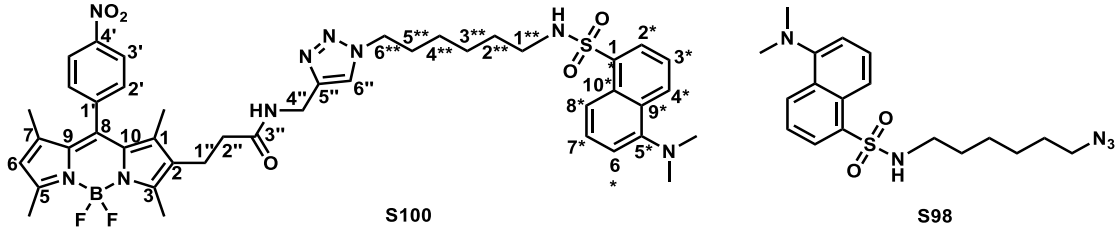

Procedure: following the same procedure as described for S99.

$CuSO_4 \cdot 5H_2O$ (1.7 mg, 0.01 mmol, 0.1 eq), sodium ascorbate (8.3 mg, 0.04 mmol, 0.4eq) in 2.1 mL t-Butanol/ water (1:2) and S38 (50 mg, 0.11 mmol, 1.0 eq) and S98 (45 mg, 0.12 mmol, 1.1 eq) in 0.7 mL t-Butanol was converted to S100 as an orange powder (33 mg, 0.04 mmol, 36% yield). Purification was performed by silica-gel column chromatography (eluant: Hexane/ EtOAC= 0-100 %).

Characteristics: δ_H (600 MHz, Chloroform-*d*) 8.52 (d, *J* = 8.4 Hz, 1H), 8.33 (d, *J* = 8.6 Hz, 2H), 8.25 (d, *J* = 8.7 Hz, 1H), 8.19 (dd, *J* = 7.3, 0.9 Hz, 1H), 7.53-7.49 (m, 2H), 7.47-7.42 (m, 3H), 7.16 (d, *J* = 7.6 Hz, 1H), 6.48 (t, *J* = 5.9 Hz, 1H), 5.97 (s, 1H), 5.14-5.06 (m, 1H), 4.45 (d, *J* = 5.8 Hz, 2H), 4.14 (t, *J* = 7.1 Hz, 2H), 2.86 (s, 6H), 2.82 (q, *J* = 6.7 Hz, 2H), 2.65-2.60 (m, 2H), 2.52 (d, *J* = 9.8 Hz, 6H), 2.21 (t, *J* = 7.6 Hz, 2H), 1.70 (p, *J* = 7.3 Hz, 2H), 1.35 (p, *J* = 6.8, 6.3 Hz, 2H), 1.31 (s, 3H), 1.21 (s, 3H), 1.18-1.08 (m, 4H); δ_C (176 MHz, Chloroform-*d*) 171.69, 156.51, 155.57, 152.04, 148.27, 144.53, 142.05, 141.88, 139.34, 137.85, 134.66, 130.61, 130.31, 129.85, 129.64, 129.57, 129.49, 124.41, 124.29, 121.44, 118.67, 118.53, 115.33, 115.00, 53.77, 49.93, 45.53, 45.22, 42.82, 36.25, 34.74, 30.86, 29.70, 29.06, 25.58, 25.43, 19.75, 14.67, 14.61, 12.21, 12.16; HRMS (ES+) found $[M+H]^+$ 854.38, $C_{43}H_{50}BF_2N_9O_5S$ requires M 853.37.

Nitro-BODIPY-Cy5 probe (S101)

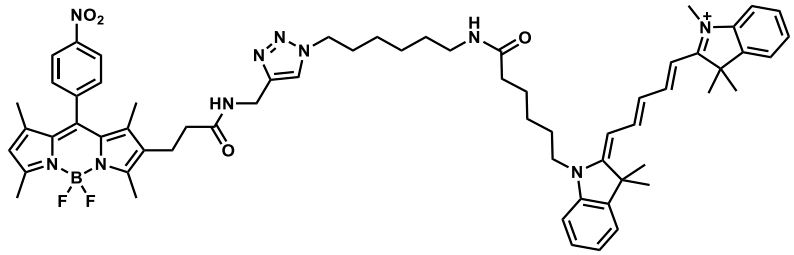

Procedure: following the same procedure as described for S99.

$CuSO_4 \cdot 5H_2O$ (1.7 mg, 0.01 mmol, 0.1 eq), sodium ascorbate (8.3 mg, 0.04 mmol, 0.4eq) in 2.1 mL t-Butanol/ water (1:2) and S38 (50 mg, 0.11 mmol, 1.0 eq) and S96 (crude, 77 mg, 0.12 mmol, 1.1 eq) in 0.7 mL t-Butanol was converted to S101 as a blue mud (19 mg, 0.018 mmol, 16% yield). Purification was performed by Al_2O_3 column chromatography (eluant: ethyl acetate: acetone = 0%-100%).

Characteristics: δ_H (600 MHz, Chloroform-*d*) 8.35 (d, *J* = 8.7 Hz, 2H), 7.83 (q, *J* = 13.5 Hz, 2H), 7.62 (s, 1H), 7.50 (d, *J* = 8.7 Hz, 2H), 7.39-7.31 (m, 4H), 7.21 (dt, *J* = 14.1, 7.2 Hz, 2H), 7.13 (d, *J* = 8.0 Hz, 1H), 7.09 – 7.04 (m, 3H), 6.95 (d, *J* = 25.1 Hz, 1H), 6.45 (d, *J* = 13.6 Hz, 1H), 6.29 (d, *J* = 13.5 Hz, 1H), 5.96 (s, 1H), 4.49 (d, *J* = 5.5 Hz, 2H), 4.23 (t, *J* = 6.8 Hz, 2H), 4.09-4.01 (m, 2H), 3.59 (s, 3H), 3.16 (q, *J* = 6.7 Hz, 2H), 2.66 (t, *J* = 7.6 Hz, 2H), 2.54 (s, 3H), 2.50 (s, 3H), 2.33 (t, *J* = 7.2 Hz, 4H), 1.81 (tt, *J* = 14.3, 7.4 Hz, 4H), 1.68 (d, *J* = 2.0 Hz, 12H), 1.51 (h, *J* = 7.3 Hz, 4H), 1.30 (d, *J* = 2.9 Hz, 10H); δ_C (151 MHz, Chloroform-*d*) 173.38, 173.12, 172.55, 171.89, 157.01, 155.11, 153.21, 152.45, 148.25, 144.77, 142.73, 142.06, 141.86, 141.57, 141.04, 140.63, 139.80, 137.82, 131.09, 130.46, 130.18, 129.87, 128.88, 128.70, 126.45, 125.46, 124.99, 124.36, 122.47, 122.11, 121.27, 111.05, 110.26, 104.49, 103.60, 49.98, 49.35, 48.95, 44.61, 38.71, 36.31, 36.25, 35.20, 30.90, 29.79, 29.67, 28.68, 28.07, 27.10, 26.43, 25.90, 25.65, 25.31, 19.89, 14.62, 14.52, 13.00, 12.55; HRMS (ES+) found $[M+H]^+$ 1086.61, $C_{63}H_{76}BF_2N_{10}O_4$ requires M 1085.61.

Nitro-BODIPY-C_6H_{12}-Rhodamine B probe (S102)

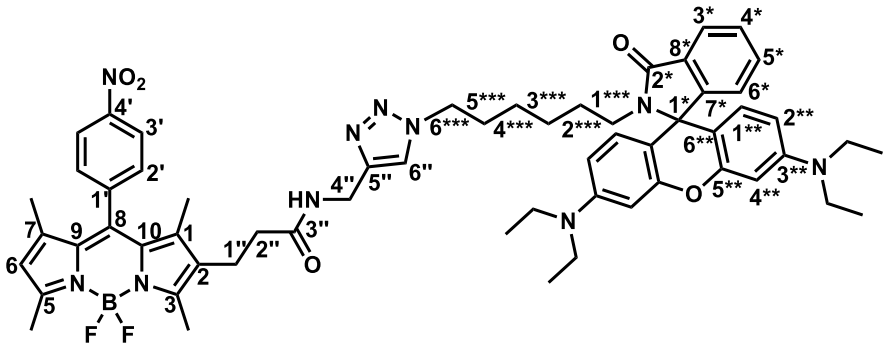

Procedure: following the same procedure as described for S99.

$CuSO_4 \cdot 5H_2O$ (1.7 mg, 0.01 mmol, 0.1 eq), sodium ascorbate (8.3 mg, 0.04 mmol, 0.4eq) in 2.1 mL t-Butanol/ water (1:2) and S38 (50 mg, 0.11 mmol, 1.0 eq) and S90 (68 mg, 0.12 mmol, 1.1 eq) in 0.7 mL t-Butanol was converted to S102 as an orange oil (46 mg, 0.04 mmol, 42 % yield). Purification was performed by silica-gel column chromatography (eluant: ethyl acetate: acetone = 0%-50%).

Characteristics: δ_H (600 MHz, Chloroform-*d*) 8.34 (d, *J* = 7.4 Hz, 2H), 7.85-7.78 (m, 1H), 7.64 (dd, *J* = 12.0, 8.1 Hz, 1H), 7.45 (d, *J* = 8.1 Hz, 2H), 7.39 (dd, *J* = 5.4, 3.0 Hz, 2H), 7.38 (s, 1H), 7.04 (dd, *J* = 5.0, 3.0 Hz, 1H), 6.49 (s, 1H), 6.40-6.33 (m, 4H), 6.24 (d, *J* = 9.9 Hz, 2H), 5.95 (s, 1H), 4.47-4.38 (m, 2H), 4.09 (t, *J* = 7.1 Hz, 2H), 3.31 (q, *J* = 7.0 Hz, 8H), 3.04 (t, *J* = 7.1 Hz, 2H), 2.65 (t, *J* = 7.5 Hz, 2H), 2.52 (d, *J* = 9.0 Hz, 6H), 2.24 (t, *J* = 7.5 Hz, 2H), 1.64 (p, *J* = 6.9 Hz, 2H), 1.23 (s, 6H), 1.13 (m, 12H), 1.06 (m, 4H); δ_C (151 MHz, Chloroform-*d*) 171.54, 168.10, 156.49, 155.67, 153.49, 153.29, 148.72, 148.27, 144.29, 142.07, 141.91, 139.22, 137.82, 132.79, 132.25, 132.09, 132.02, 131.94, 131.92, 131.28, 130.61, 130.30, 129.69, 128.89, 127.99, 124.35, 123.73, 122.55, 121.73, 121.51, 108.00, 105.80, 97.67, 69.48, 64.89, 53.79, 50.14, 44.32, 39.86, 36.22, 34.94, 31.70, 30.89, 29.76, 29.24, 27.81, 26.15, 25.87, 19.74, 14.61, 14.53, 12.80, 12.55, 12.23; HRMS (ES+) found $[M+H]^+$ 1045.55, $C_{59}H_{67}BF_2N_{10}O_5$ requires M 1044.54.

Nitro-BODIPY-PEG-Rhodamine B probe (S103)

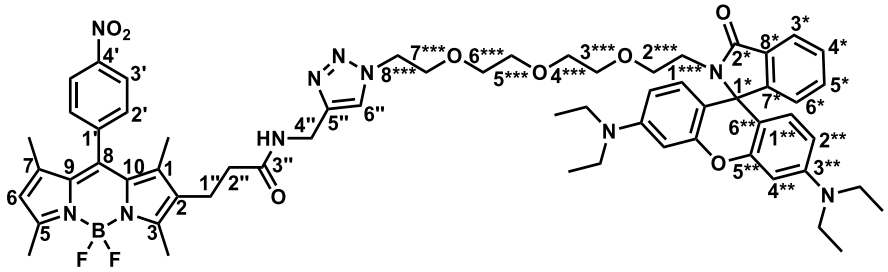

Procedure: following the same procedure as described for S99.

$CuSO_4 \cdot 5H_2O$ (1.7 mg, 0.01 mmol, 0.1 eq), sodium ascorbate (8.3 mg, 0.04 mmol, 0.4eq) in 2.1 mL t-Butanol/ water (1:2) and S38 (50 mg, 0.11 mmol, 1.0 eq) and S91 (74 mg, 0.12 mmol, 1.1 eq) in 0.7 mL t-Butanol was converted to S103 as an orange oil (46 mg, 0.04 mmol, 39 % yield). Purification was performed by silica-gel column chromatography (eluant: ethyl acetate: acetone = 0%-50%).

Characteristics: δ_H (600 MHz, Chloroform-*d*) 8.43-8.35 (m, 2H), 7.83 (dd, *J* = 4.8, 2.4 Hz, 1H), 7.66 (s, 1H), 7.53 (d, *J* = 8.7 Hz, 2H), 7.48-7.39 (m, 2H), 7.09 (dd, *J* = 5.3, 2.7 Hz, 1H), 6.61 (s, 1H), 6.47-6.35 (m, 4H), 6.28 (dd, *J* = 8.9, 2.5 Hz, 2H), 6.01 (s, 1H), 4.50 (d, *J* = 5.4 Hz, 2H), 4.42 (t, *J* = 4.9 Hz, 2H), 3.80 (t, *J* = 5.0 Hz, 2H), 3.45 (dd, *J* = 5.8, 3.5 Hz, 2H), 3.35 (q, *J* = 7.2 Hz, 14H), 3.14 (t, *J* = 7.2 Hz, 3H), 2.74-2.63 (m, 2H), 2.57 (d, *J* = 2.7 Hz, 6H), 2.33-2.23 (m, 2H), 1.27 (s, 6H), 1.18 (m, 12H); δ_C (151 MHz, Chloroform-*d*) 171.53, 168.24, 153.71, 153.22, 148.77, 148.29, 142.15, 141.84, 137.84, 132.44, 130.82, 129.74, 128.75, 128.00, 124.35, 123.79, 123.02, 122.61, 108.08, 105.38, 97.76, 70.52, 70.41, 70.33, 69.92, 69.31, 67.75, 64.88, 50.12, 44.33, 39.22, 36.21, 35.04, 31.90, 29.68, 29.25, 19.74, 14.63, 14.09, 12.82, 12.57, 12.24; HRMS (ES+) found $[M+H]^+$ 1121.56, $C_{61}H_{71}BF_2N_{10}O_8$ requires M 1120.55.

Nitro-BODIPY-NBD probe (S104)

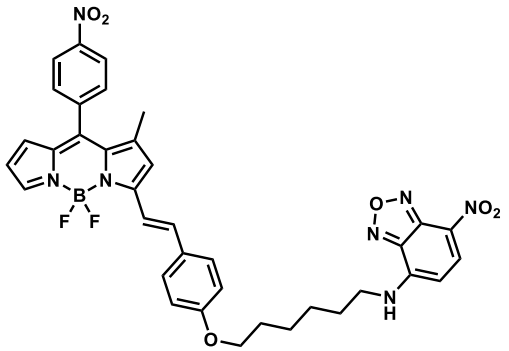

Procedure: following the same procedure as described for S64.

S51 (20 mg, 0.06 mmol, 1.0 eq), S87 (23 mg, 0.06 mmol, 1.0 eq), piperidine (40 mg, 0.47 mmol, 8.0 eq) and acetic acid (42 mg, 0.70 mmol, 12.0 eq) in 0.6 mL benzene and 0.2 mL acetonitrile were converted to S104 as a purple mud (15 mg, 0.02 mmol, 35 % yield). Purification was performed by silica-gel column chromatography (eluant: 1st EtOAc / Hexane = 0~50%, 2nd DCM/ Hexane = 0~100% then EtOAc/ DCM = 0~20%).

Characteristics: δ_H (600 MHz, Chloroform-*d*) 8.50 (dd, *J* = 8.6, 2.6 Hz, 1H), 8.40 (d, *J* = 8.5 Hz, 2H), 7.73 (s, 1H), 7.67-7.53 (m, 5H), 7.38 (d, *J* = 16.1 Hz, 1H), 6.93 (d, *J* = 8.6 Hz, 2H), 6.77 (s, 1H), 6.43 (dd, *J* = 3.8, 2.1 Hz, 1H), 6.29 (d, *J* = 3.5 Hz, 2H), 6.20 (d, *J* = 8.6 Hz, 1H), 4.05 (t, *J* = 6.1 Hz, 2H), 3.53 (q, *J* = 6.6 Hz, 2H), 1.93-1.82 (m, 4H), 1.60 (s, 7H); HRMS (ES+) found $[M+H]^+$ 708.26, $C_{36}H_{32}BF_2N_7O_6$ requires M 707.25.

Nitro-BODIPY-NBD probe (S105)

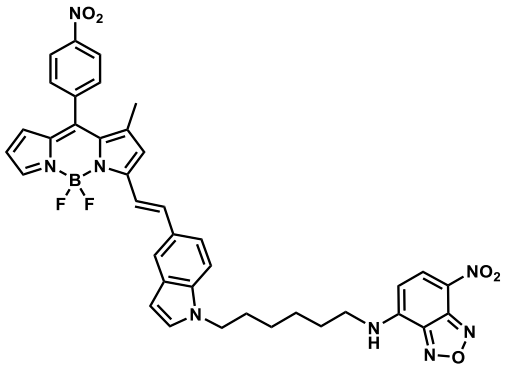

Procedure: following the same procedure as described for S64.

S51 (20 mg, 0.06 mmol, 1.0 eq), S88 (24 mg, 0.06 mmol, 1.0 eq), piperidine (40 mg, 0.47 mmol, 8.0 eq) and acetic acid (42 mg, 0.70 mmol, 12.0 eq) in 0.6 mL benzene and 0.2 mL acetonitrile were converted to S105 as a purple mud (15 mg, 0.02 mmol, 37 % yield). Purification was performed by silica-gel column chromatography (eluant: 1st EtOAc / Hexane = 0~50%, 2nd DCM/ Hexane = 0~100% then EtOAc/ DCM = 0~20%).

Characteristics: δ_H (600 MHz, Chloroform-*d*) 8.45 (d, *J* = 8.6 Hz, 1H), 8.39 (d, *J* = 8.3 Hz, 2H), 7.85 (s, 1H), 7.71 (d, *J* = 11.7 Hz, 2H), 7.66-7.52 (m, 4H), 7.35 (d, *J* = 8.6 Hz, 1H), 7.13 (d, *J* = 3.1 Hz, 1H), 6.82 (s, 1H), 6.56 (d, *J* = 3.1 Hz, 1H), 6.42 (dd, *J* = 3.9, 2.1 Hz, 1H), 6.27 (d, *J* = 3.7 Hz, 1H), 6.17 (s, 1H), 6.08 (d, *J* = 8.7 Hz, 1H), 4.18 (t, *J* = 6.6 Hz, 2H), 3.38 (q, *J* = 6.7 Hz, 2H), 1.91 (p, *J* = 6.7 Hz, 2H), 1.75 (p, *J* = 7.2 Hz, 2H), 1.61 (s, 3H), 1.43 (m, 4H); HRMS (ES+) found $[M+H]^+$ 731.26, $C_{38}H_{33}BF_2N_8O_5$ requires M 730.26.

Nitro-BODIPY-NBD probe (S106)

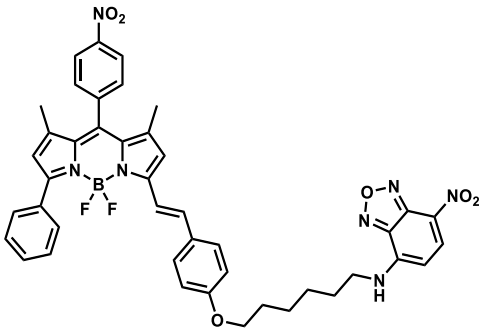

Procedure: following the same procedure as described for S64.

S49 (25 mg, 0.06 mmol, 1.0 eq), S87 (23 mg, 0.06 mmol, 1.0 eq), piperidine (40 mg, 0.47 mmol, 8.0 eq) and acetic acid (42 mg, 0.70 mmol, 12.0 eq) in 0.6 mL benzene and 0.2 mL acetonitrile were converted to S106 as a blue mud (21 mg, 0.026 mmol, 43 % yield). Purification was performed by silica-gel column chromatography (eluant: 1st EtOAc / Hexane = 0~50%, 2nd DCM/ Hexane = 0~100% then EtOAc/ DCM = 0~20%).

Characteristics: δ_H (600 MHz, Chloroform-*d*) 8.46 (d, *J* = 8.6 Hz, 1H), 8.42 (d, *J* = 8.2 Hz, 2H), 7.88 (d, *J* = 7.1 Hz, 2H), 7.62 (d, *J* = 8.3 Hz, 2H), 7.54-7.41 (m, 6H), 7.22 (d, *J* = 16.2 Hz, 1H), 6.84 (d, *J* = 8.6 Hz, 2H), 6.65 (s, 1H), 6.32 (s, 1H), 6.25 (t, *J* = 5.1 Hz, 1H), 6.14 (d, *J* = 8.6 Hz, 1H), 3.99 (t, *J* = 6.2 Hz, 2H), 3.47 (q, *J* = 6.5 Hz, 2H), 1.82 (p, *J* = 7.6, 7.0 Hz, 4H), 1.54 (m, 4H), 1.44 (s, 6H); δ_C (151 MHz, Chloroform-*d*) 160.31, 155.95, 154.91, 148.40, 144.23, 143.86, 143.81, 142.93, 142.20, 140.36, 138.36, 137.00, 136.45, 132.93, 131.84, 130.09, 129.47, 129.30, 129.20, 128.88, 128.12, 124.35, 123.98, 122.36, 119.11, 116.60, 114.76, 67.69, 53.42, 28.97, 28.46, 26.65, 25.73, 15.09, 14.94; HRMS (ES+) found $[M+H]^+$ 798.29, $C_{43}H_{38}BF_2N_7O_6$ requires M 797.29.

Nitro-BODIPY-NBD probe (S107)

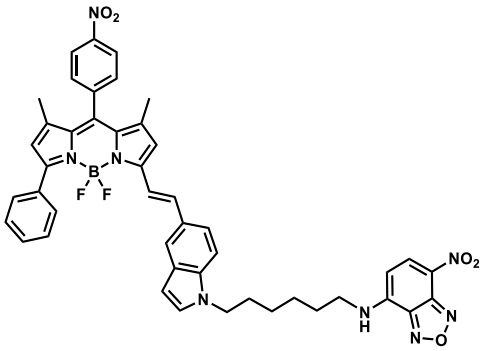

Procedure: following the same procedure as described for S64.

S49 (25 mg, 0.06 mmol, 1.0 eq), S88 (24 mg, 0.06 mmol, 1.0 eq), piperidine (40 mg, 0.47 mmol, 8.0 eq) and acetic acid (42 mg, 0.70 mmol, 12.0 eq) in 0.6 mL benzene and 0.2 mL acetonitrile were converted to S106 as a blue mud (20 mg, 0.025 mmol, 42 % yield). Purification was performed by silica-gel column chromatography (eluant: 1st EtOAc / Hexane = 0~50%, 2nd DCM/ Hexane = 0~100% then EtOAc/ DCM = 0~20%).

Characteristics: δ_H (600 MHz, Chloroform-*d*) 8.46-8.38 (m, 3H), 7.92 (d, *J* = 6.6 Hz, 2H), 7.76 (s, 1H), 7.68-7.57 (m, 3H), 7.54-7.36 (m, 5H), 7.25 (d, *J* = 8.7 Hz, 1H), 7.08 (d, *J* = 3.1 Hz, 1H), 6.72 (s, 1H), 6.51 (d, *J* = 3.1 Hz, 1H), 6.34 (s, 1H), 6.19 (t, *J* = 5.5 Hz, 1H), 6.04 (d, *J* = 8.7 Hz, 1H), 4.11 (t, *J* = 6.7 Hz, 2H), 3.33 (q, *J* = 6.5 Hz, 2H), 1.86 (p, *J* = 6.8 Hz, 2H), 1.69 (p, *J* = 7.3 Hz, 2H), 1.46 (d, *J* = 2.4 Hz, 6H), 1.37 (m, 4H); δ_C (151 MHz, Chloroform-*d*) 156.61, 154.20, 148.36, 144.16, 143.82, 143.74, 143.13, 142.29, 140.89, 139.77, 136.93, 136.58, 136.48, 133.13, 133.07, 131.66, 130.16, 129.32, 129.05, 128.85, 128.10, 127.79, 124.31, 123.80, 122.35, 122.14, 121.19, 119.28, 115.94, 109.84, 102.31, 98.57, 46.29, 43.65, 29.99, 29.69, 28.23, 26.40, 15.13, 14.89; HRMS (ES+) found $[M+H]^+$ 821.31, $C_{45}H_{39}BF_2N_8O_5$ requires M 820.31.

Methyl 4-(4-methoxybenzoyl)benzoate (S108)

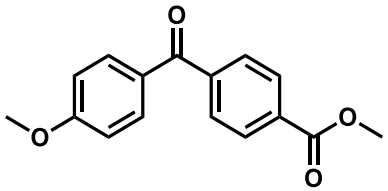

Procedure: $SOCl_2$ (4.80 mL, 66.6 mmol, 4.0 eq) was added to 4-(methoxycarbonyl)benzoic acid (3.00 g, 16.7 mmol, 1.0 eq) and the reaction mixture was refluxed overnight until a clear solution had formed. The solvent was reduced *in vacuo* and the resulting acid chloride dissolved in $CHCl_3$ (83 mL), and anisole (3.6 mL, 33.3 mmol, 2.0 eq) and $AlCl_3$ (2.22 g, 16.7 mmol, 1.0 eq) were added. The reaction mixture was then refluxed for 10 h, after which time another portion of $AlCl_3$ (2.22 g, 16.7 mmol, 1.0 eq) was added and the mixture refluxed for a further 10 h. Following this, the solution was cooled, quenched with H_2O (100 mL), and extracted with EtOAc (3 x 100 mL). The combined organic layers were washed with brine (100 mL), dried over MgSO4, and the solution was concentrated to 50 mL then precipitated by 300 mL hexane to obtain S108 as a white solid (3.12 g, 11.5 mmol, 70 % yield).

Characteristics: δ_H (400 MHz, Chloroform-*d*) 8.18-8.13 (m, 2H), 7.86-7.77 (m, 4H), 7.04-6.93 (m, 2H), 3.98 (s, 3H), 3.91 (s, 3H); δ_C (101 MHz, Chloroform-*d*) 194.78, 166.39, 163.62, 142.15, 132.76, 132.63, 129.55, 129.44, 113.75, 55.56, 52.44; HRMS (ES+) found $[M+H]^+$ 271.10, $C_{16}H_{14}O_4$ requires M 270.09.

Methyl 4-(4-hydroxybenzoyl)benzoate (S109)

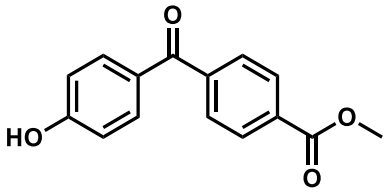

Procedure: $AlCl_3$ (8.88 g, 66.6 mmol, 6.0 eq) was added to a solution of S108 (3.00 g, 11.10 mmol, 1.0 eq) in toluene (45 mL) and the reaction mixture was stirred at r.t. for 30 min followed by 30 min at reflux. The reaction was then cooled to r.t. followed by further addition of $AlCl_3$ ((4.44 g, 33.3 mmol, 3.0 eq) and the reaction mixture was refluxed for another 30 min. The reaction mixture was then poured into an ice/water mixture, stirred for a further 30 min and extracted with EtOAc (3 x 50 mL). The combined organic layers were washed with brine, dried ($MgSO_4$), and concentrated *in vacuo*. After silica gel flash chromatography (eluting in EtOAc : DCM, 0%~ 20%), S109 was obtained as a white solid (1.8 g, 7.02 mmol, 63 % yield).

Characteristics: δ_H (400 MHz, MeOD) 8.20-8.11 (m, 2H), 7.83-7.70 (m, 4H), 6.95-6.86 (m, 2H), 3.97 (s, 3H); δ_C (101 MHz, MeOD) 195.20, 166.29, 162.81, 142.45, 132.71, 132.58, 129.04, 127.88, 114.94, 51.53; HRMS (ES+) found $[M+H]^+$ 257.08, $C_{15}H_{12}O_4$ requires M 256.07.

Methyl 4-(4-(hex-5-yn-1-yloxy)benzoyl)benzoate (S110)

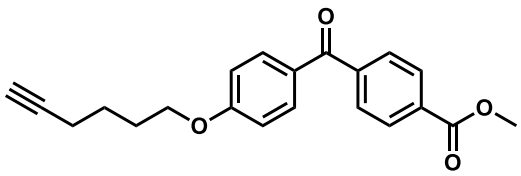

Procedure: To a solution of S109 (600 mg, 2.34 mmol, 1.0 eq) in dry acetonitrile (23 mL) was added Cs_2CO_3 (2.29 g, 7.02 mmol, 3.0 eq) and the reaction was stirred at r.t. for 30 min. Then S52 (590 mg, 2.34 mmol, 1.0 eq) and TBAI (86 mg, 0.23 mmol, 0.1 eq) was added and the reaction was stirred at 50 °C overnight. The reaction mixture was then cooled down, diluted with EtOAc and water (20 mL). The aqueous layer was extracted with EtOAc (2 x 30 mL) and the combined organic layers were dried with $MgSO_4$, filtered and the solvent removed *in vacuo*. After silica gel flash chromatography (eluting in DCM: hexane, 0%~ 100%), S110 was obtained as a white solid (553 mg, 1.64 mmol, 70 % yield).

Characteristics: δ_H (400 MHz, Chloroform-*d*) 8.16-8.11 (m, 2H), 7.83-7.75 (m, 4H), 6.99-6.93 (m, 2H), 4.08 (t, J = 6.2 Hz, 2H), 3.96 (s, 3H), 2.30 (td, J = 7.0, 2.7 Hz, 2H), 2.00 (t, J = 2.6 Hz, 1H), 1.98-1.91 (m, 2H), 1.79-1.69 (m, 2H); δ_C (101 MHz, Chloroform-*d*) 194.74, 166.38, 163.07, 142.16, 132.72, 132.63, 129.44, 129.41, 114.17, 83.90, 68.87, 67.63, 52.44, 28.08, 24.92, 18.13; HRMS (ES+) found $[M+H]^+$ 337.14, $C_{21}H_{20}O_4$ requires M 336.14.

4-(4-(Hex-5-yn-1-yloxy)benzoyl)benzoic acid (S111)

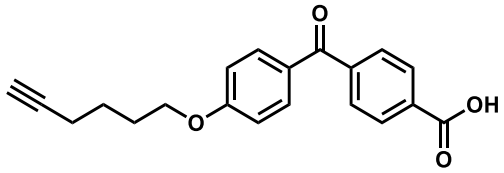

Procedure: To a stirred solution of S110 (400 mg, 1.19 mmol, 1.0 eq) in MeOH (3.2 mL) was added a solution of LiOH (285 mg, 11.89 mmol, 10.0 eq) in H_2O (10.7 mL). The mixture was stirred under 50 ºC overnight. The reaction was neutralized and precipitated by 100 mL 6 M HCl. The precipitate was filted and washed by water and diethyl ether to give S111 as a white solid (385 mg, 1.19 mmol, 100 % yield).

Characteristics: δ_H (400 MHz, DMSO-d_6) 13.33 (s, 1H), 8.09 (d, J = 8.1 Hz, 2H), 7.77 (dd, J = 8.6, 7.1 Hz, 4H), 7.10 (d, J = 8.7 Hz, 2H), 4.11 (t, J = 6.4 Hz, 2H), 2.82 (t, J = 2.7 Hz, 1H), 2.25 (td, J = 7.1, 2.7 Hz, 2H), 1.84 (dq, J = 11.8, 6.6 Hz, 2H), 1.63 (q, J = 7.3 Hz, 2H); δ_C (101 MHz, DMSO-d_6) 194.41, 167.17, 163.17, 141.95, 133.91, 132.80, 129.79, 129.72, 129.27, 114.94, 84.71, 71.96, 67.93, 28.08, 25.00, 17.87; HRMS (ES+) found $[M+H]^+$ 323.13, $C_{20}H_{18}O_4$ requires M 322.12.

Tert-butyl (6-(4-(4-(hex-5-yn-1-yloxy)benzoyl)benzamido)hexyl)carbamate (S112)

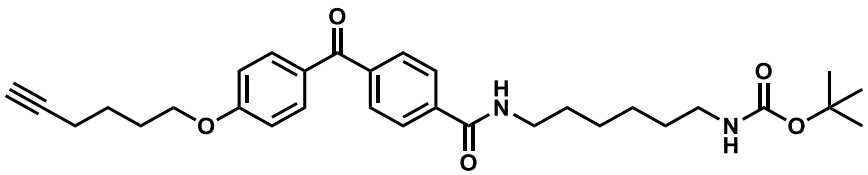

Procedure: EDC (89 mg, 0.47 mmol, 1.5 eq) was added to a solution of S111 (100 mg, 0.31 mmol, 1.0 eq) in DMF (30 mL). The mixture was stirred for 10 min and HOBt (63 mg, 0.47 mmol, 1.5 eq) was added. After 30 min stirring, tert-butyl (6-aminohexyl)carbamate (73 mg, 0.34 mmol, 1.1 eq) and triethylamine (47 mg, 0.47 mmol, 1.5 eq) was added. The mixture was stirred overnight. The reaction mixture was then diluted with EtOAc washed by brine and the combined organic layers were dried with $MgSO_4$, filtered and the solvent removed *in vacuo*. After silica gel flash chromatography (eluting in hexane: ethyl acetate = 1:1), S112 was obtained as a white solid (139 mg, 0.27 mmol, 86 % yield).

Characteristics: δ_H (400 MHz, Chloroform-*d*) 7.93 (d, J = 8.0 Hz, 2H), 7.84-7.76 (m, 4H), 6.99 – 6.94 (m, 2H), 6.69 (s, 1H), 4.61 (s, 1H), 4.10 (t, J = 6.2 Hz, 2H), 3.49 (q, J = 6.7 Hz, 2H), 3.15 (q, J = 6.6 Hz, 2H), 2.31 (td, J = 7.0, 2.7 Hz, 2H), 2.04-1.92 (m, 3H), 1.81-1.72 (m, 2H), 1.66 (p, J = 7.0 Hz, 2H), 1.54-1.35 (m, 15H); δ_C (101 MHz, Chloroform-*d*) 194.86, 166.71, 163.01, 156.22, 140.69, 137.59, 132.63, 129.77, 129.56, 126.89, 114.14, 83.92, 79.15, 68.84, 67.63, 39.90, 39.58, 30.11, 29.37, 28.43, 28.09, 25.94, 25.70, 24.93, 18.15; HRMS (ES+) found $[M+H]^+$ 521.30, $C_{31}H_{40}N_2O_5$ requires M 520.29.

N-(6-aminohexyl)-4-(4-(hex-5-yn-1-yloxy)benzoyl)benzamide (S113)

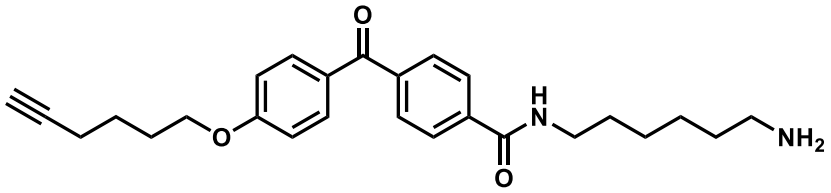

Procedure: Trifluoroacetic acid (2 mL) was added to a solution of S112 (100 mg, 0.19 mmol, 1.0 eq) in DCM (2 mL) and the mixture was stirred under an Ar atmosphere at ambient temperature for 1 h. Then the solvent was removed *in vacuo* and S113 was obtained as a white solid without purification(80 mg, 0.19 mmol, 100 % yield).

Characteristics: HRMS (ES+) found $[M+H]^+$ 421.25, $C_{26}H_{32}N_2O_3$ requires M 420.24.

Photoaffinity labelling probe (S114)

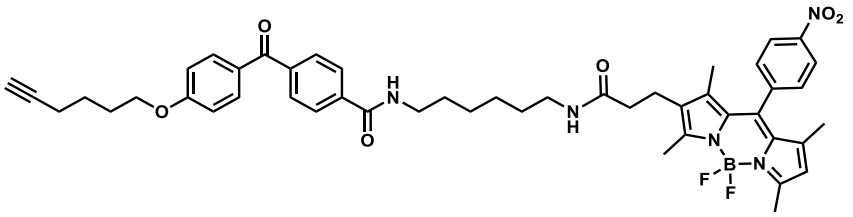

Procedure: HBTU (68 mg, 0.18 mmol, 1.5 eq) was added to a solution of S36 (53 mg, 0.12 mmol, 1.0 eq) in DMF (5 mL). After 30 min stirring, a solution of S113 (50 mg, 0.12 mmol, 1.0 eq), DIPEA (29 mg, 0.24 mmol, 2.0 eq) and DMAP (29 mg, 0.24 mmol, 2.0 eq) in DMF (5 mL) was added. The mixture was stirred overnight. The reaction mixture was then diluted with EtOAc washed by brine and the combined organic layers were dried with $MgSO_4$, filtered and the solvent removed *in vacuo*. The Nitro-BODIPY-Benzophenone-alkyne was obtained after silica gel flash chromatography (eluting in ethyl acetate/ hexane = 0-100%) as a red mud (76 mg, 0.09 mmol, 75 % yield).

Characteristics: δ_H (400 MHz, Chloroform-*d*) 8.39 (d, *J* = 8.6 Hz, 2H), 7.89 (d, *J* = 8.3 Hz, 2H), 7.84-7.73 (m, 4H), 7.51 (d, *J* = 8.6 Hz, 2H), 6.97 (d, *J* = 8.8 Hz, 2H), 6.61 (t, *J* = 5.7 Hz, 1H), 5.99 (s, 1H), 5.77 (t, *J* = 5.6 Hz, 1H), 4.09 (t, *J* = 6.2 Hz, 2H), 3.45 (q, *J* = 6.6 Hz, 2H), 3.22 (q, *J* = 6.6 Hz, 2H), 2.73 – 2.63 (m, 3H), 2.55 (d, *J* = 11.3 Hz, 6H), 2.31 (td, *J* = 7.0, 2.6 Hz, 2H), 2.23 (s, 2H), 2.03 – 1.92 (m, 3H), 1.76 (p, *J* = 7.1 Hz, 3H), 1.63 (q, *J* = 6.7 Hz, 2H), 1.49 (p, *J* = 6.8 Hz, 2H), 1.30-1.40 (m, 10H); δ_C (101 MHz, Chloroform-*d*) ^{13}C NMR (151 MHz, cdcl$_3$) δ 194.69, 171.65, 166.79, 163.03, 156.27, 155.81, 148.30, 142.11, 142.01, 140.77, 139.19, 137.81, 137.44, 132.57, 130.82, 130.35, 130.30, 129.66, 129.46, 126.79, 124.35, 121.57, 114.15, 83.86, 68.78, 67.63, 53.78, 39.49, 38.93, 36.54, 31.71, 30.89, 29.33, 29.25, 28.06, 25.70, 24.91, 19.83, 18.10, 14.64, 12.83, 12.24; HRMS (ES+) found $[M+H]^+$ 844.39, $C_{48}H_{52}BF_2N_5O_6$ requires M 843.40.

6 BIOLOGICAL EXPERIMENTAL DETAILS

6.1 Images of plant cells incubated with nitro-BODIPY probes

N. tabacum BY-2 cells were grown in Murashige and Skoog (MS) medium supplemented with 200 mg l^{-1} KH_2PO_4, 3% sucrose and 0.2 mg l^{-1} 2,4-dichlorophenoxyacetic acid (2.4-D), pH 5.8, at 25°C in the dark[114]. Cells were sub-cultured every 7 days by transferring 1 ml of old culture into 60 ml of fresh medium. The stock solutions of fluorescent probes were made in DMSO at the final concentration 1 mg/ml. One millilitre of 3-days old cells was transferred to a microfuge tube and incubated with a fluorescent probes at final concentration 1 mg/ml. After 10 minutes of staining, the cells were mounted on microscopy slides under No. 0 glass coverslips. The images were acquired using a Leica TCS SP8 X confocal laser-scanning microscope equipped with white light laser, 40x 1.3 NA oil immersion objective, and the LAS X software (Leica Microsystems, Wetzlar, Germany). The excitation wavelength was set up to match the excitation peak in water and the emitted light was collected using 40 nm window around the emission maxima.

6.2 Buffers

Details of the buffers, media components and concentrations used throughout this research are detailed in Table 25. All biological reagents were dissolved in biological grade DMSO (Fisher Bioreagents) before application, unless otherwise specified. Biological grade buffers and medias were prepared using biological grade water from a Milli-Q purification system. The sodium dodecyl sulfate (SDS) was purchased from Fisher Scientific.

Table 25 Buffer compositions used throughout.

Buffer	Ingredient	Final concentration
Plant protein extraction	Sucrose	250 mM
	HEPES-KOH (pH 7.5)	50 mM
	$Na_4P_2O_7$	50 mM
	Na_2MoO_4	1 mM
	NaF	25 mM
	Glycerol	5%
	Triton X-100	0.5%
	Sigma plant protease inhibitor cocktail	10 mg proteome per tablet
SDS electrophoresis buffer (X10, pH 8.3)	Tris base	25 mM
	Glycine	250 mM
	SDS	0.1 %

6.3 Plant whole protein extraction

1. Plant tissues (100-200 mg) were grinded in liquid nitrogen and then 300 ul of protein extraction buffer was add. Vortex and rock for 10 min.
2. Centrifuge at 14,000 g for 10 min in a table-top centrifuge.
3. Carefully transfer supernatant into a fresh microfuge tube (avoid picking up debris).
4. Dilute extract to required concentration before adding probes.

6.4 Crosslinking between photoaffinity probe and proteins

Each protein extraction (5-20 mg/ mL) was incubated with probe P39 (100-1000 uM) for 1 h and then treated under three different irradation conditions (dark condition, natural light, irradiation at 365nm for 0-60 min). After irradiation, saturated urea solution was added to the reaction mixture to final concentration of 8M. After 15 min, the protein extractions were then denatured for 15 min using a mixture of LDS sample buffer and 2-mercaptoethanol (95:5) and then analysed by SDS-PAGE gel.

6.5 Competitive labelling experiment

Protein extractions (10 mg/ mL) were incubated with probe S1 (0-2000 uM) for 1 h and then incubated with probe P39 (200 uM) for 1 h. After incubation, protein extractions were irradiated by 365 nm for 10 min. After irradiation, the protein extractions were denatured for 15 min using a mixture of LDS sample buffer and 2-mercaptoethanol (95:5) and then analysed by SDS-PAGE gel.

7 APPENDIX

(3,5-Dimethyl-1H-pyrrol-2-yl)(4-nitrophenyl)methanone (S1)

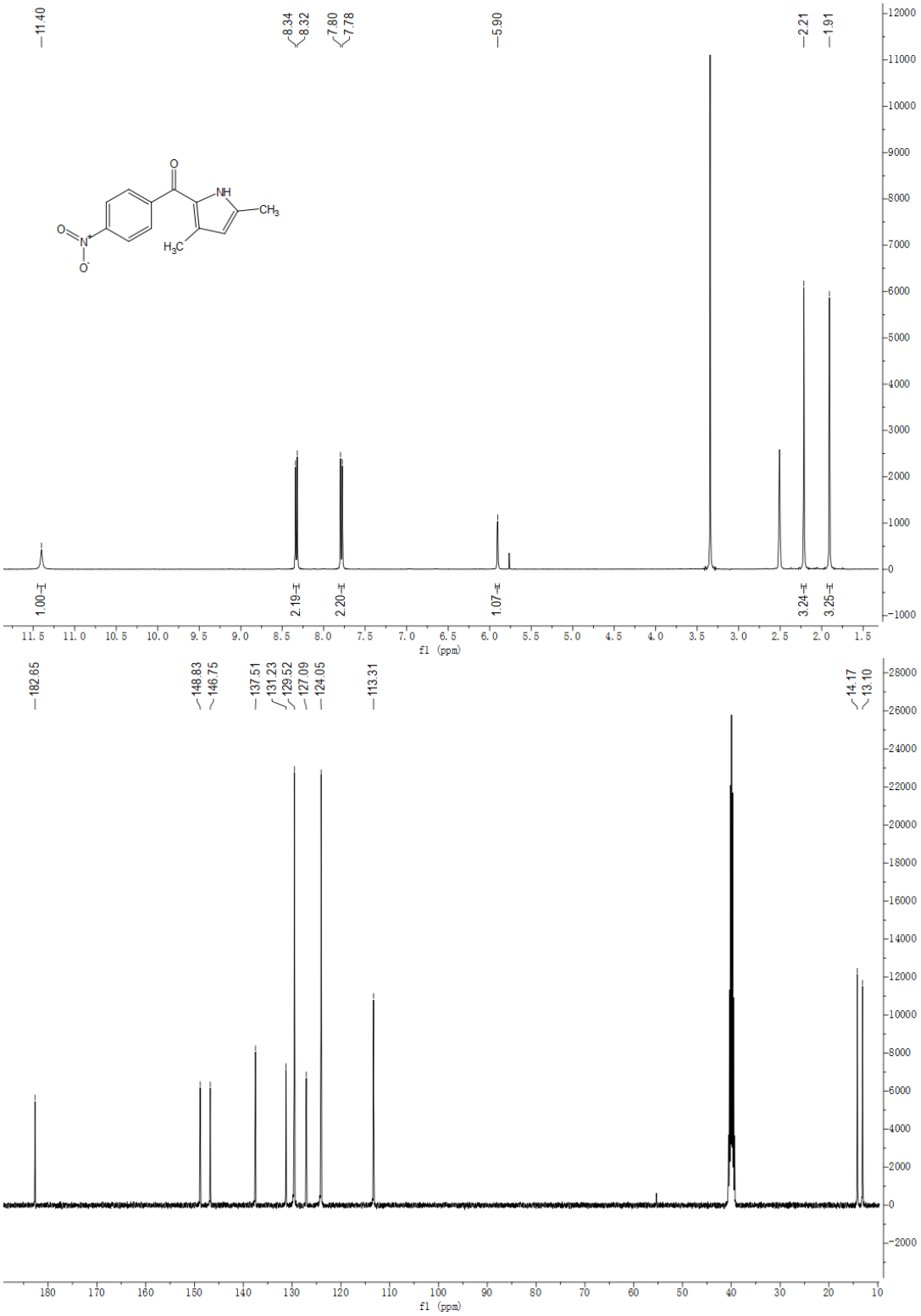

1,3,5,7-Tetramethyl-8-(4-nitrophenyl)-BODIPY (S2)

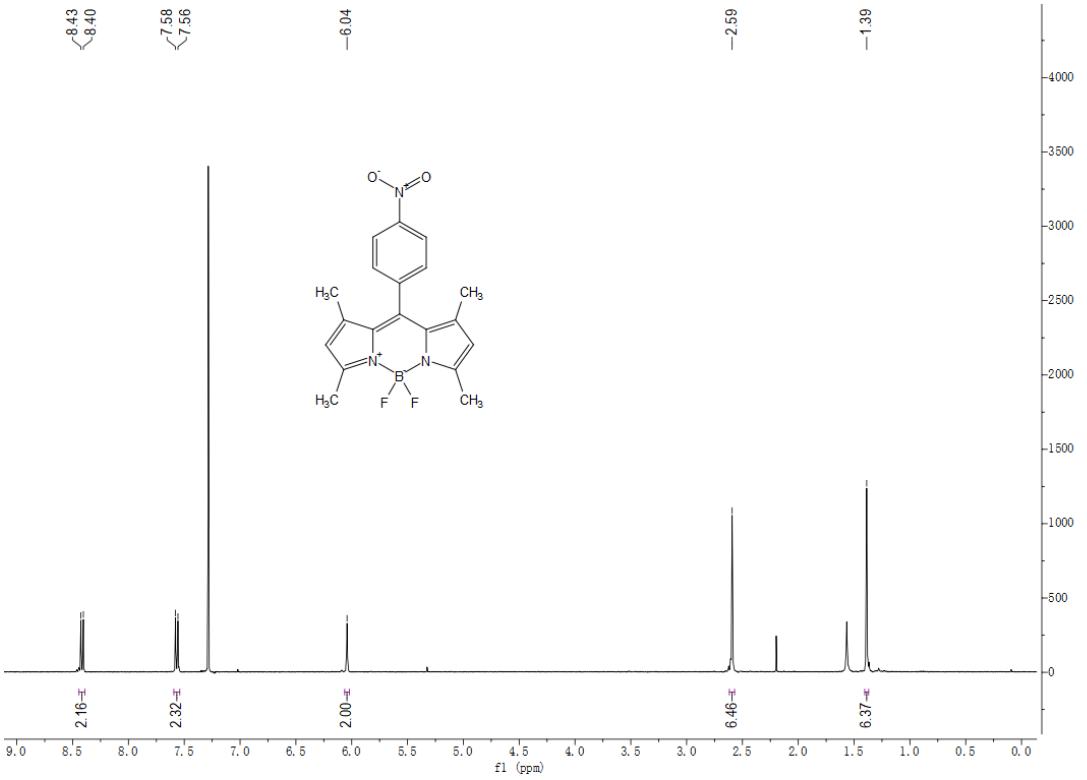

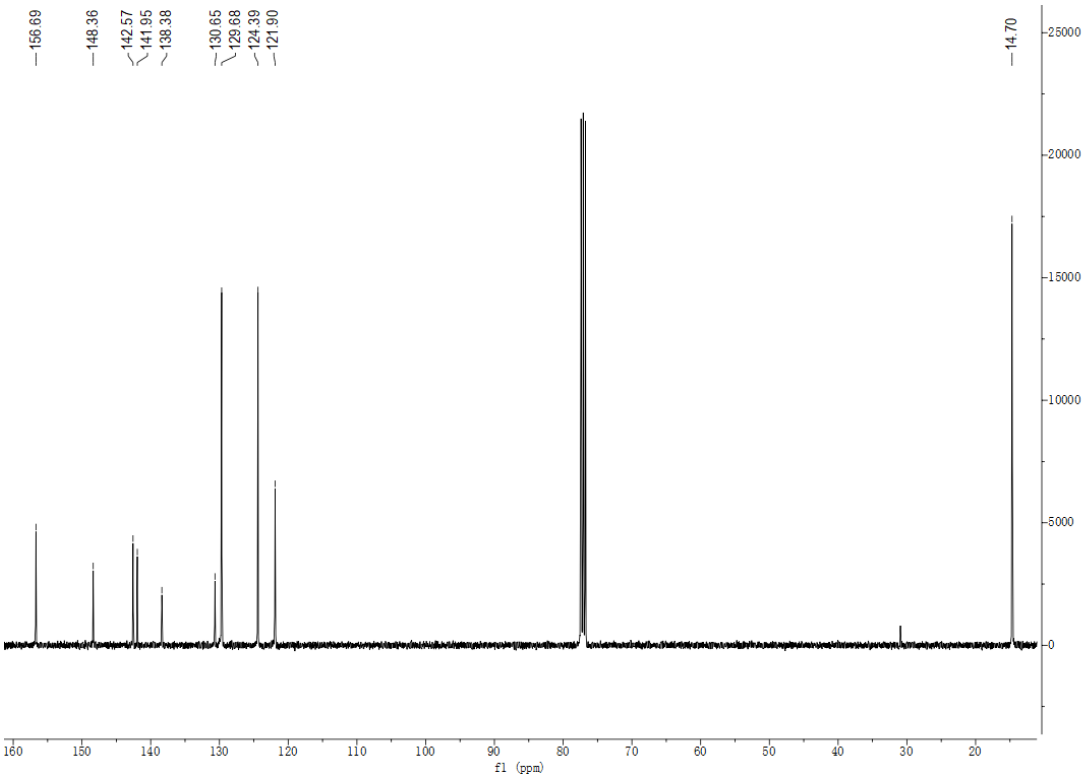

1,3,5,7-Tetramethyl-2,6-dibromo-8-(4-nitrophenyl)-BODIPY (S3)

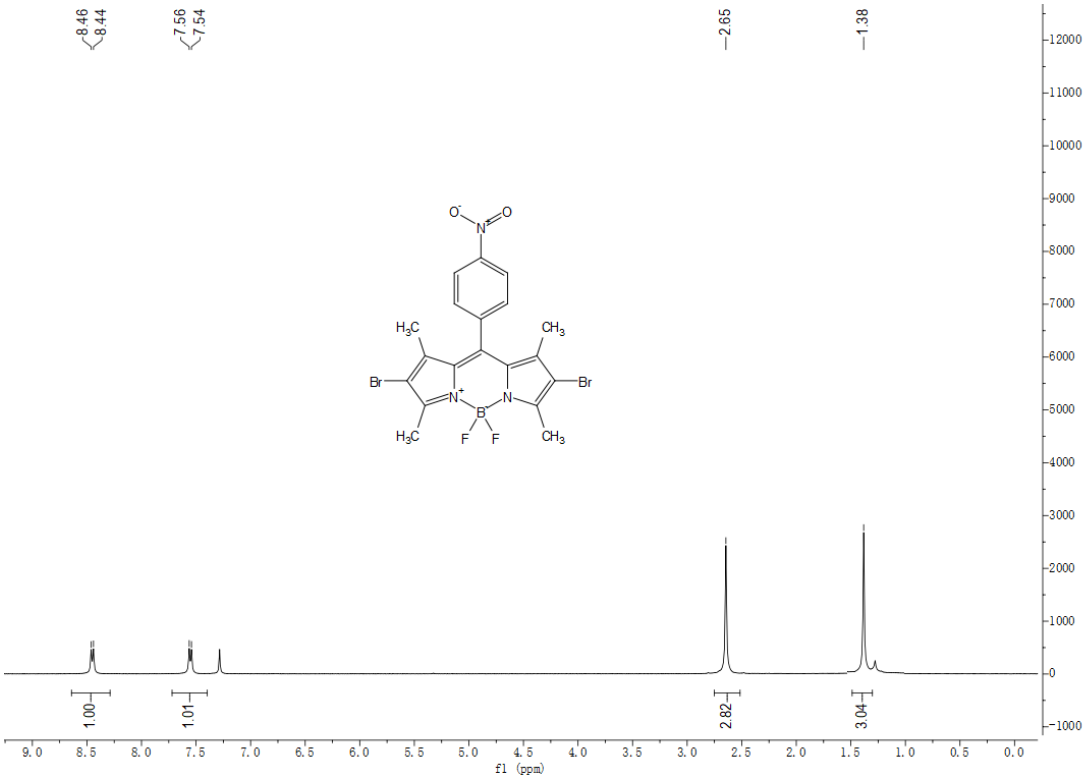

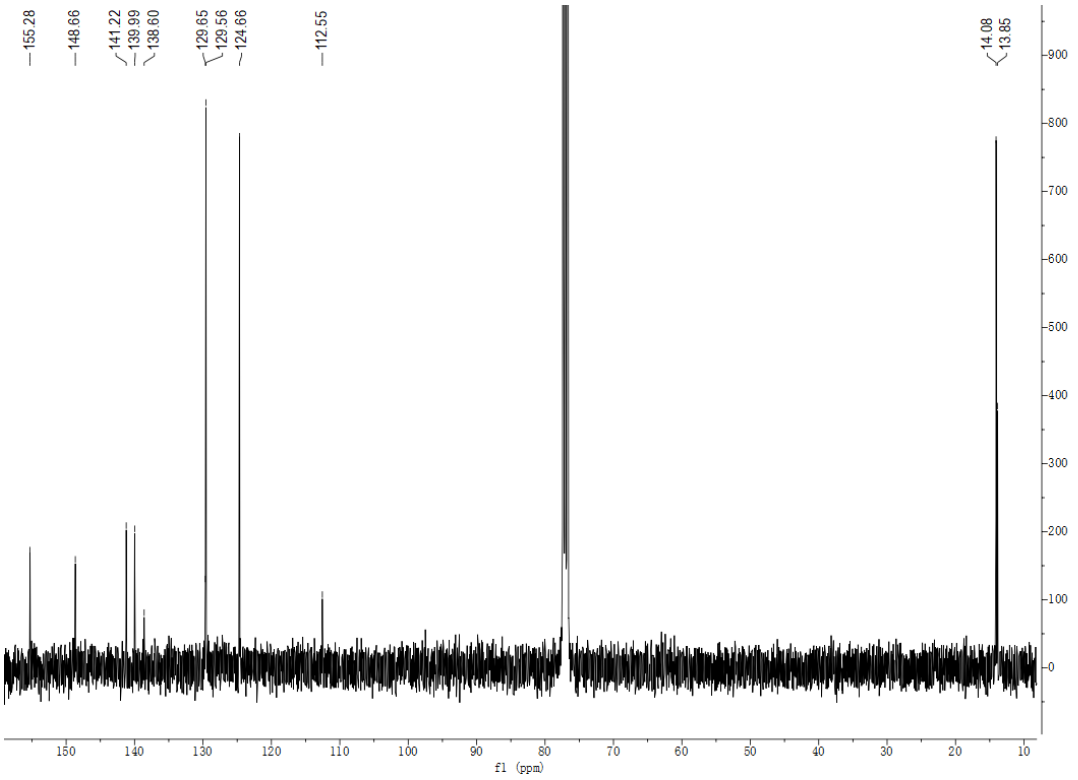

1,3,5,7-Tetramethyl-2-bromo-8-(4-nitrophenyl)-BODIPY (S4)

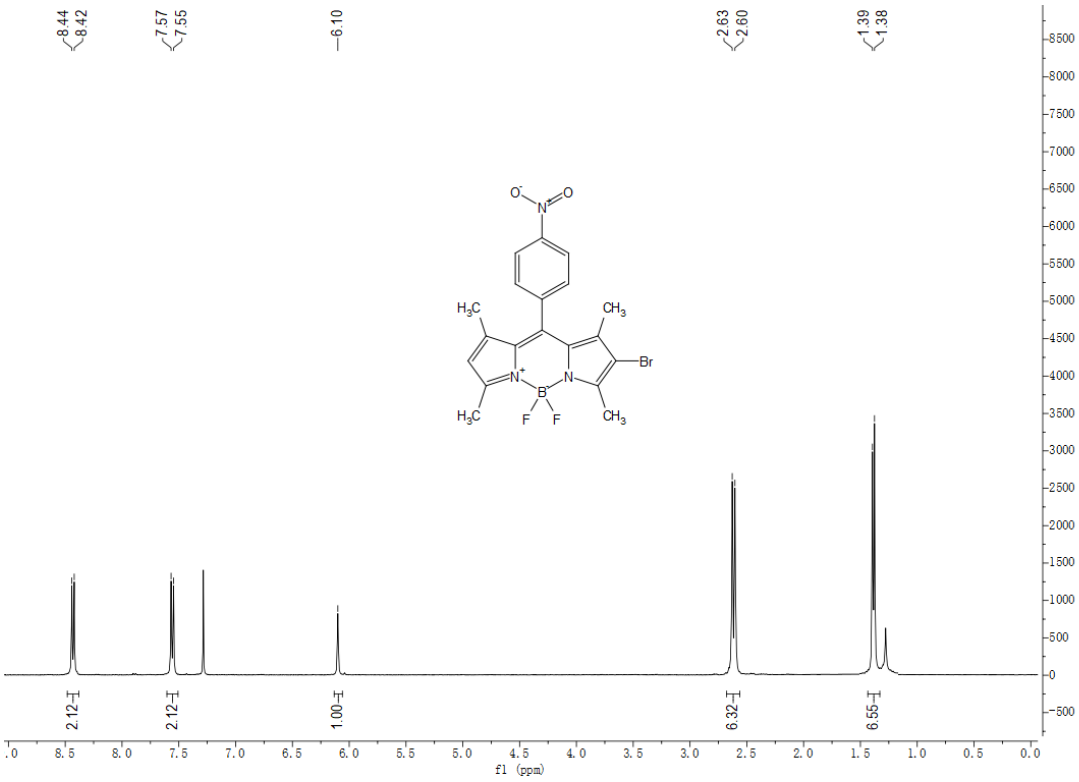

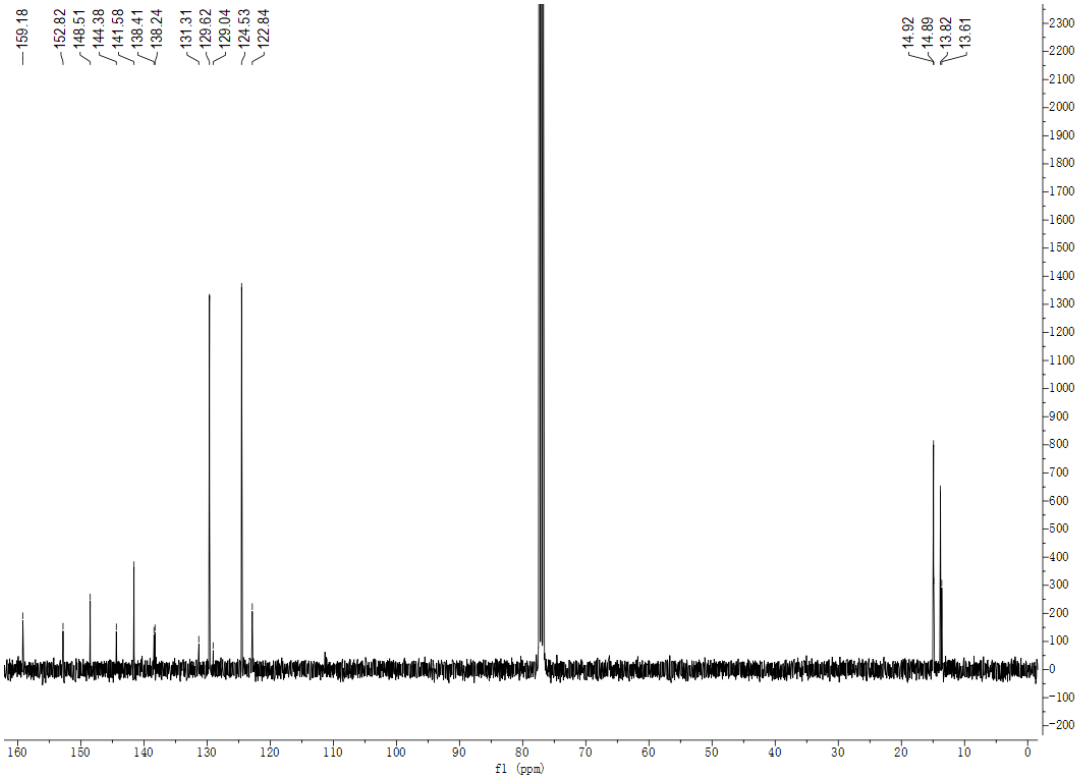

2-Tert-butyl-4-ethyl-3,5-dimethyl-1H-pyrrole-2,4-dicarboxylate (S5)

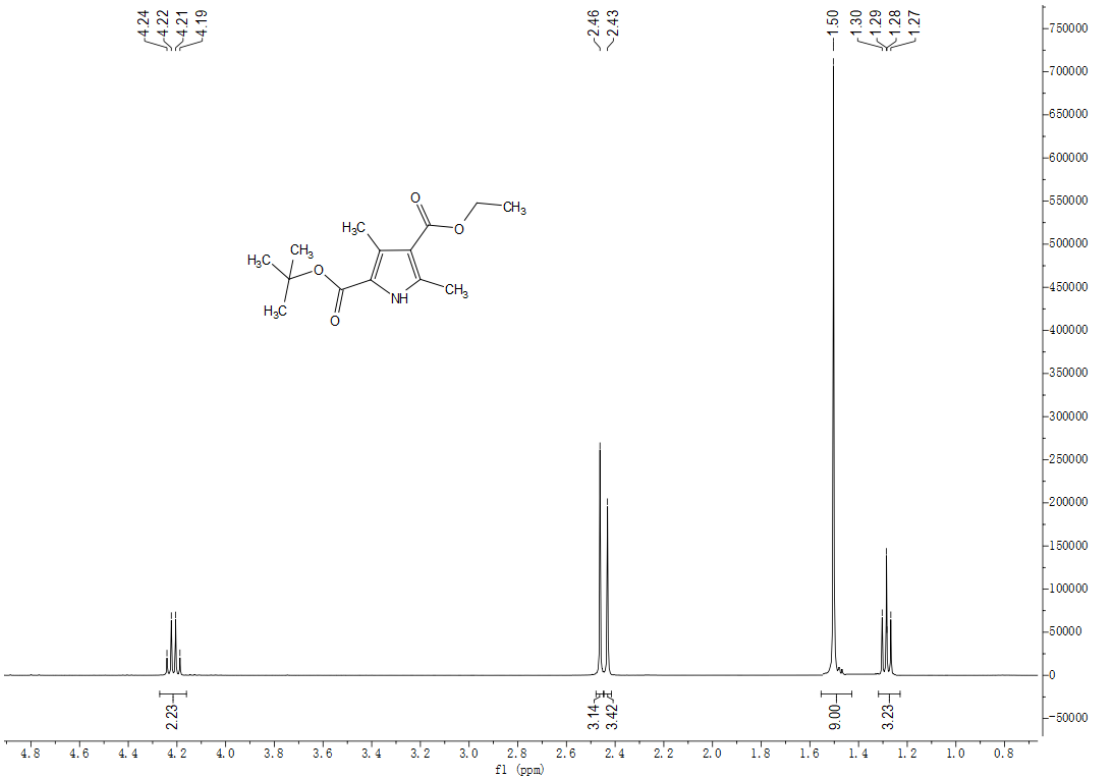

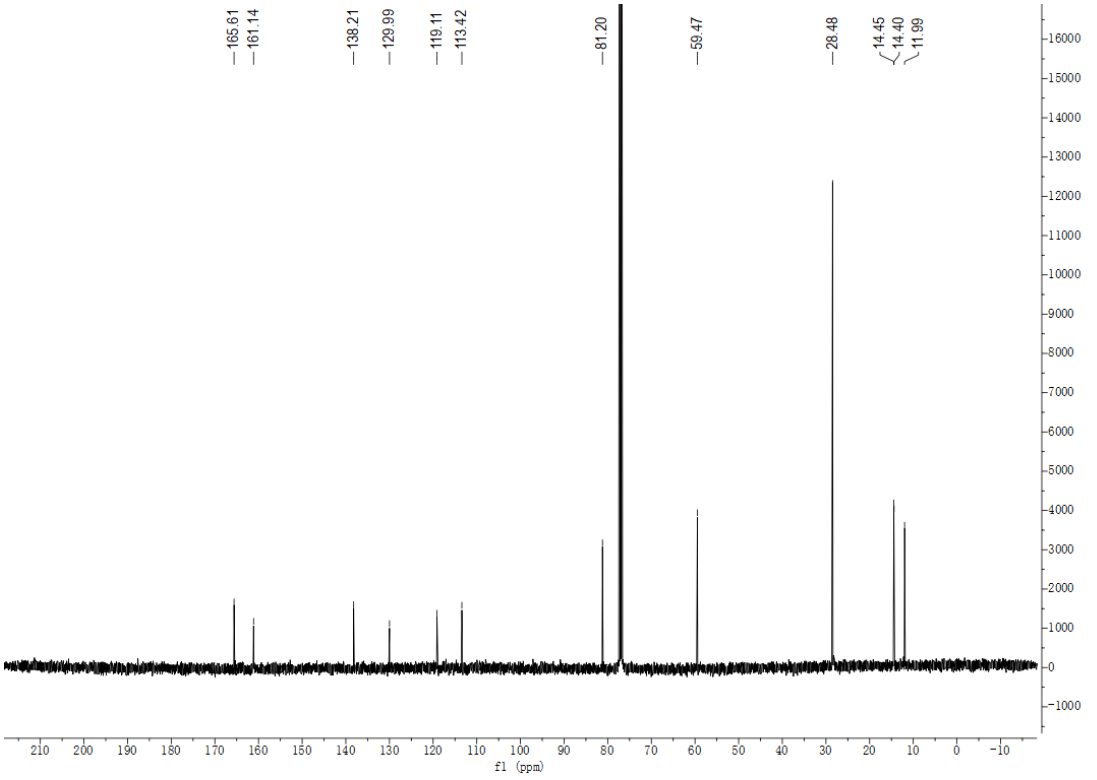

Ethyl 2,4-dimethyl-1H-pyrrole-3-carboxylate (S6)

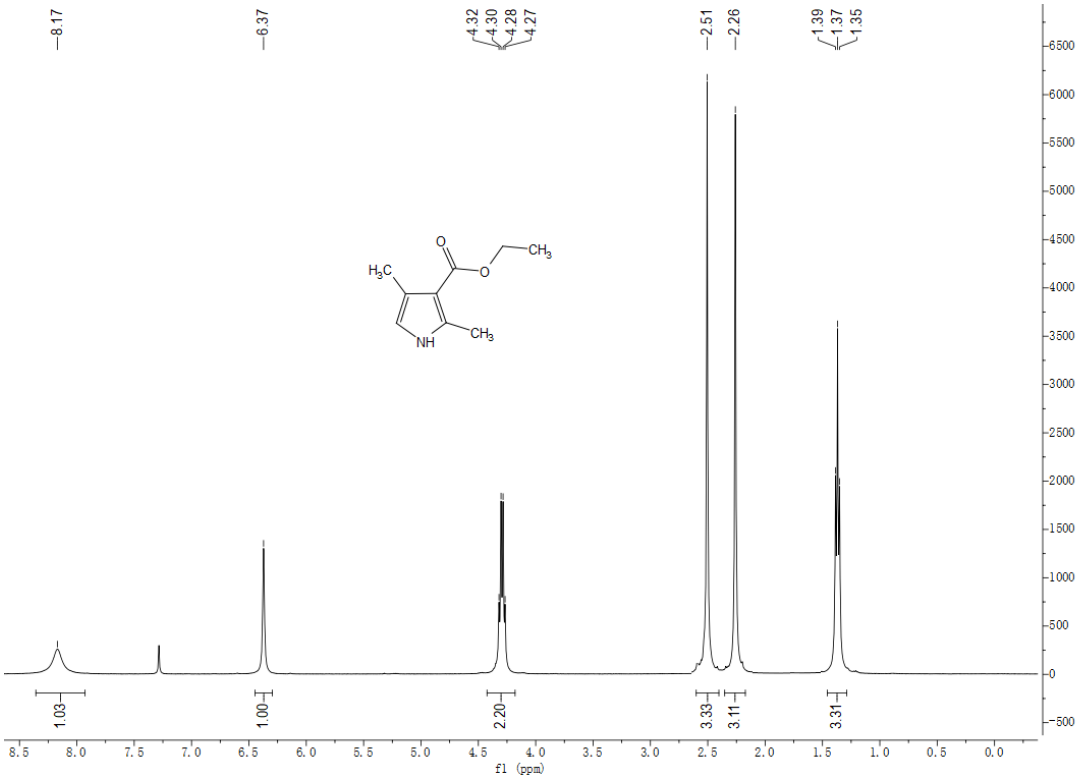

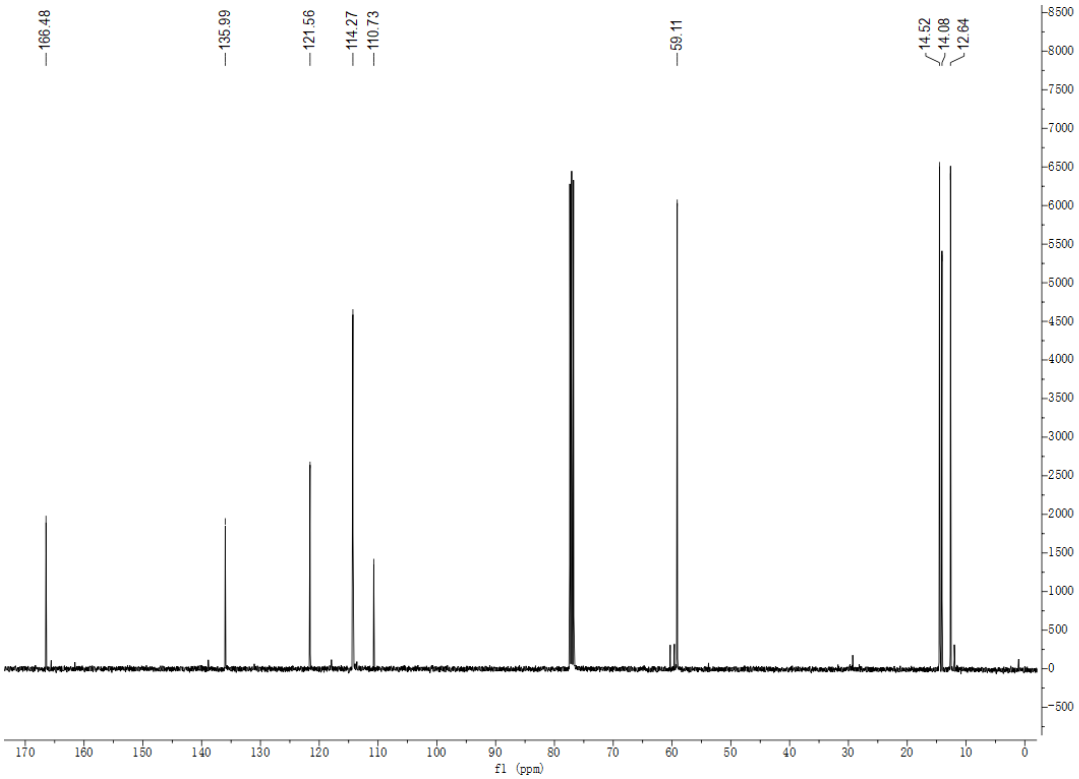

1,3,5,7-Tetramethyl-2-ethyl carboxylate-8-(4-nitrophenyl)-BODIPY (S7)

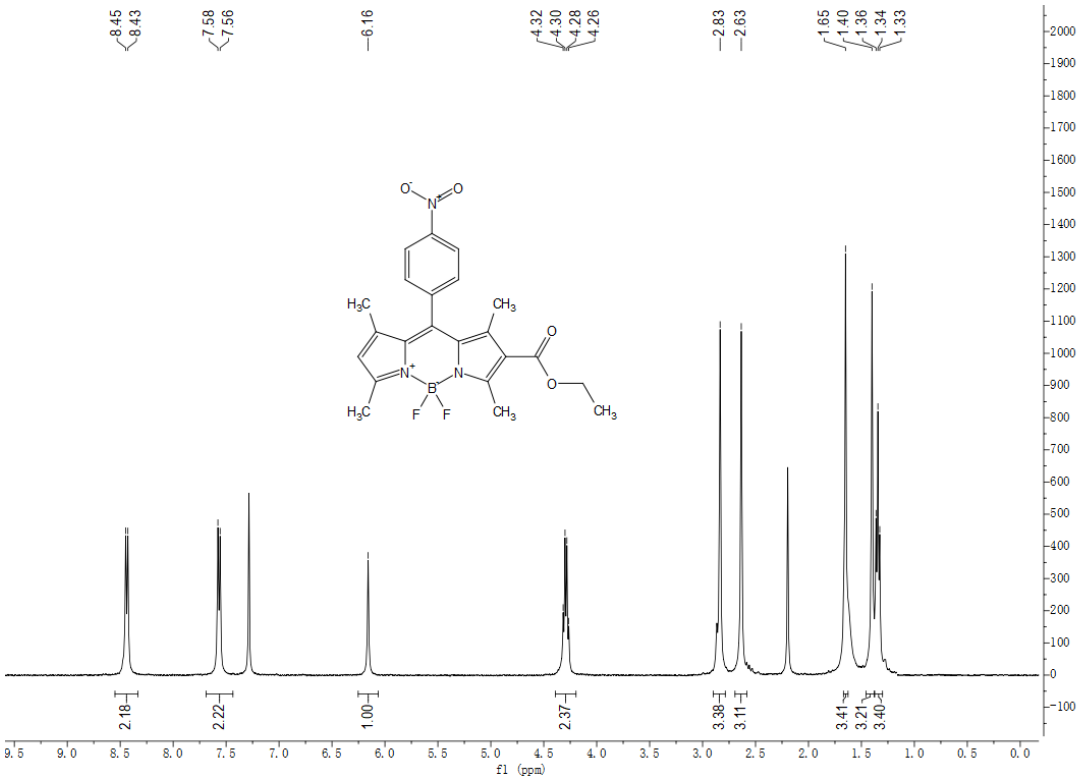

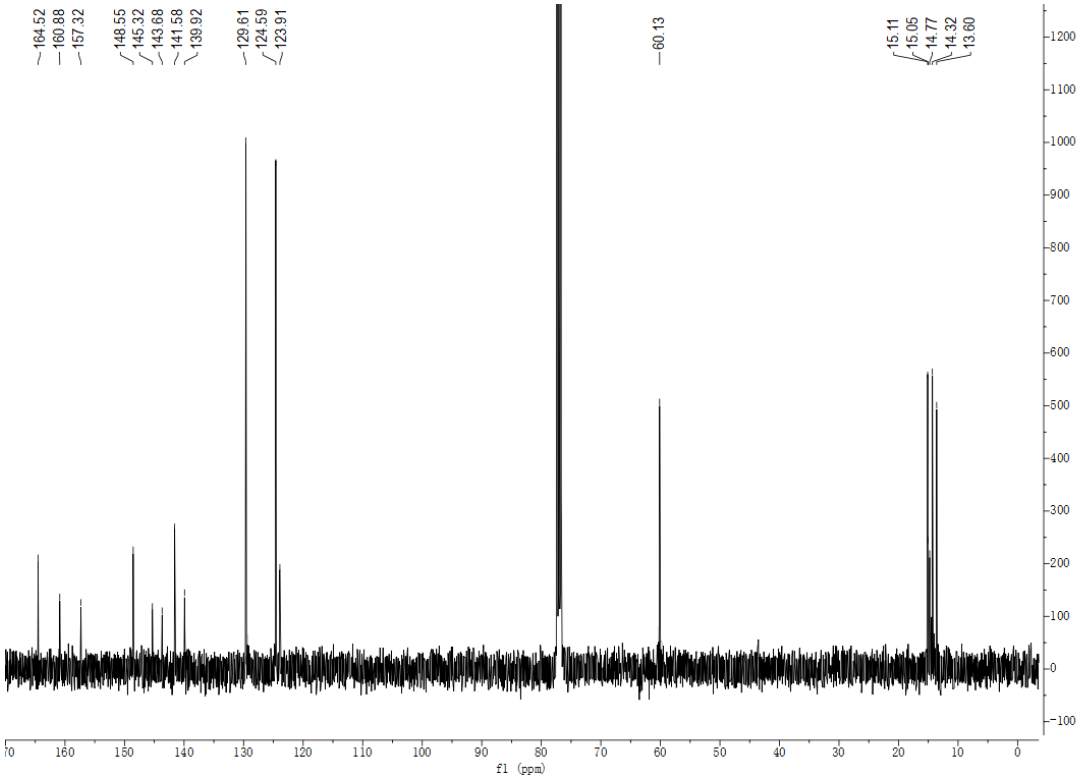

Ethyl 4-(3-ethoxy-3-oxopropyl)-3,5-dimethyl-1H-pyrrole-2-carboxylate (S8)

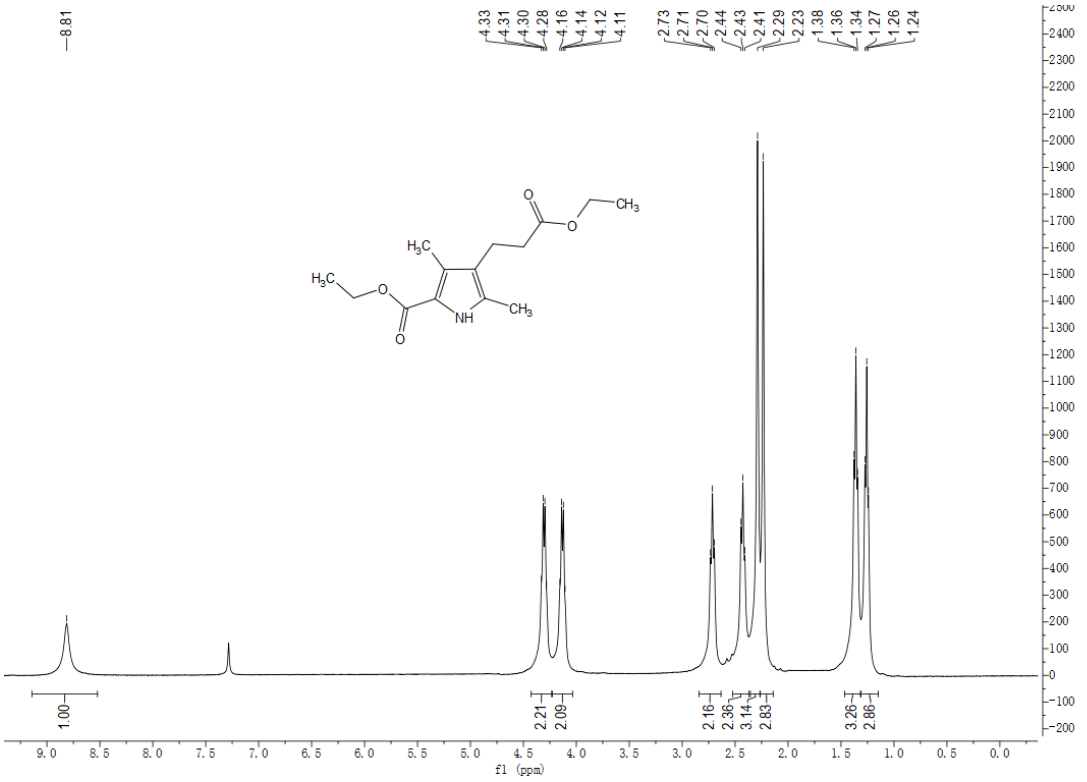

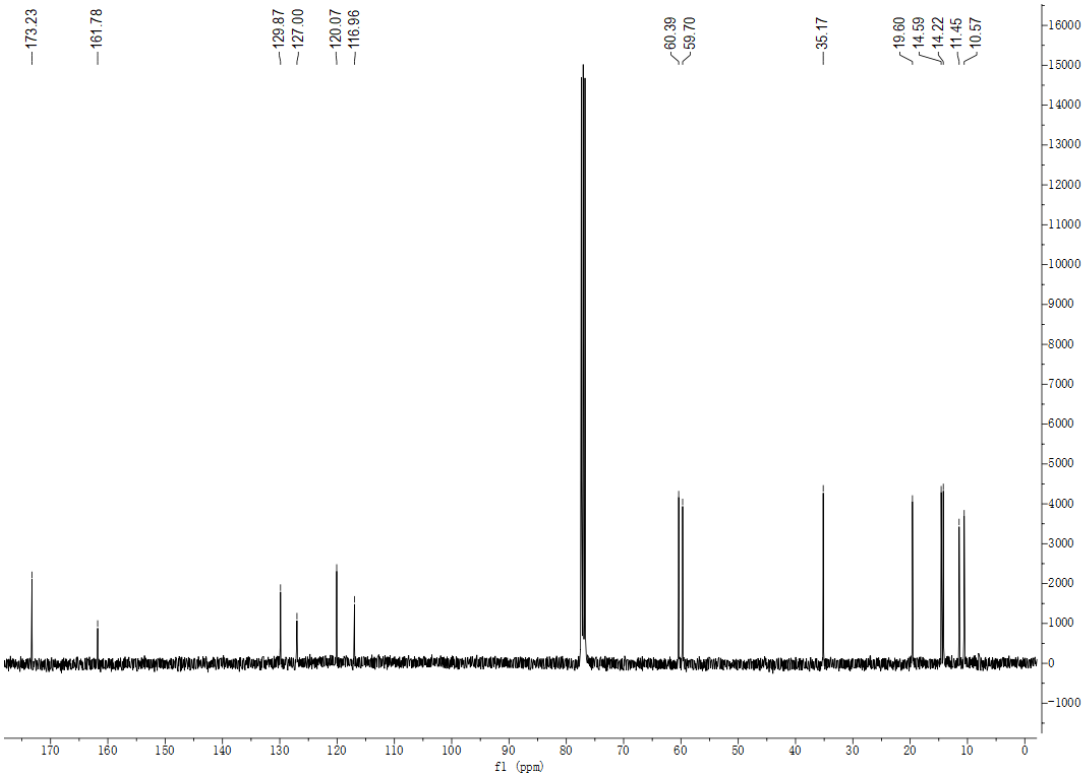

Ethyl 3-(2,4-dimethyl-1H-pyrrol-3-yl) propanoate (S9)

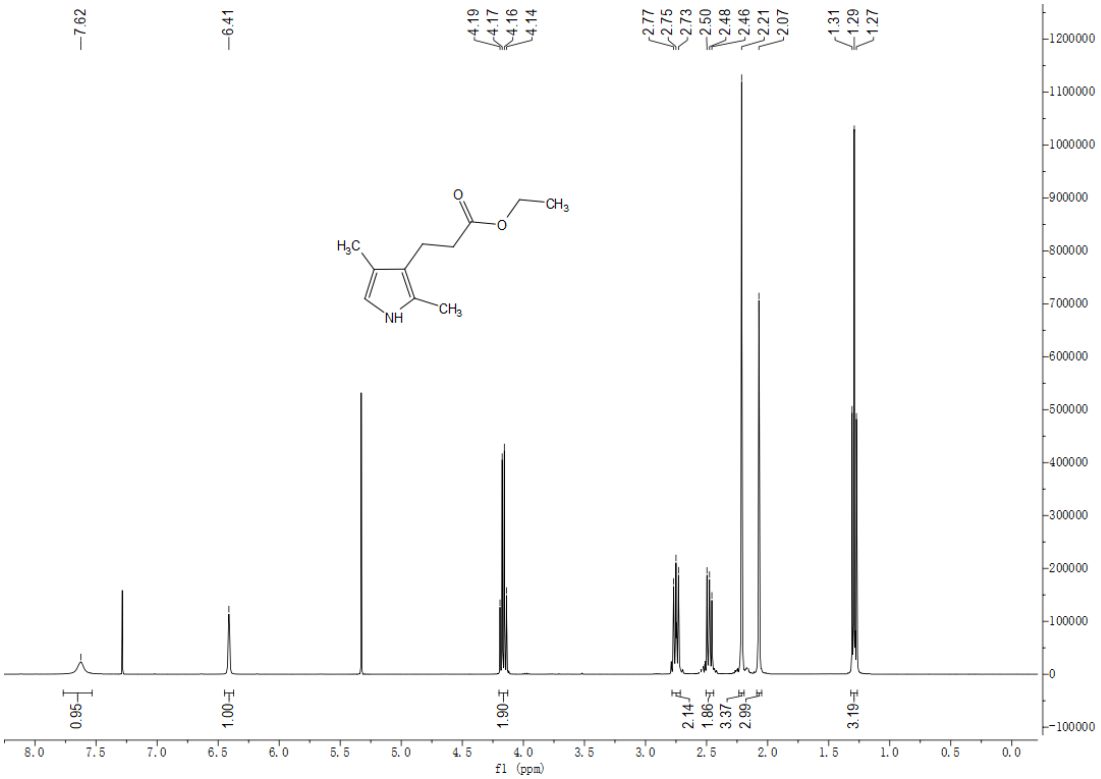

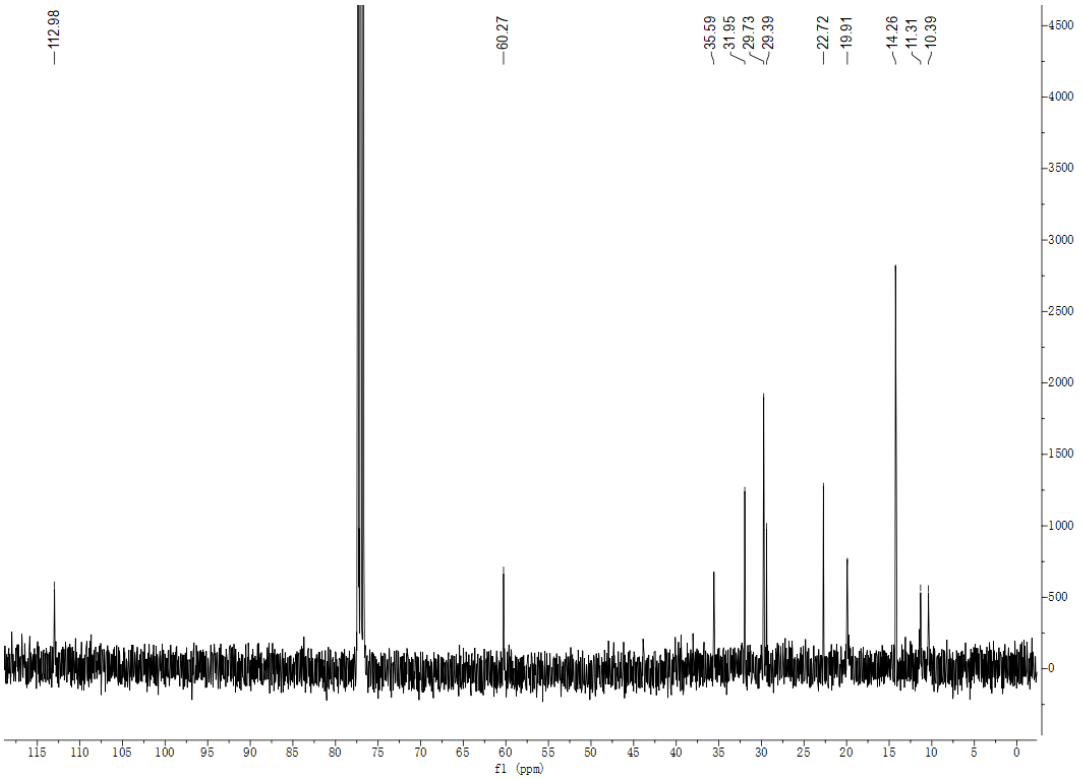

Benzyl 4-(3-methoxy-3-oxopropyl)-3,5-dimethyl-1H-pyrrole-2-carboxylate (S10)

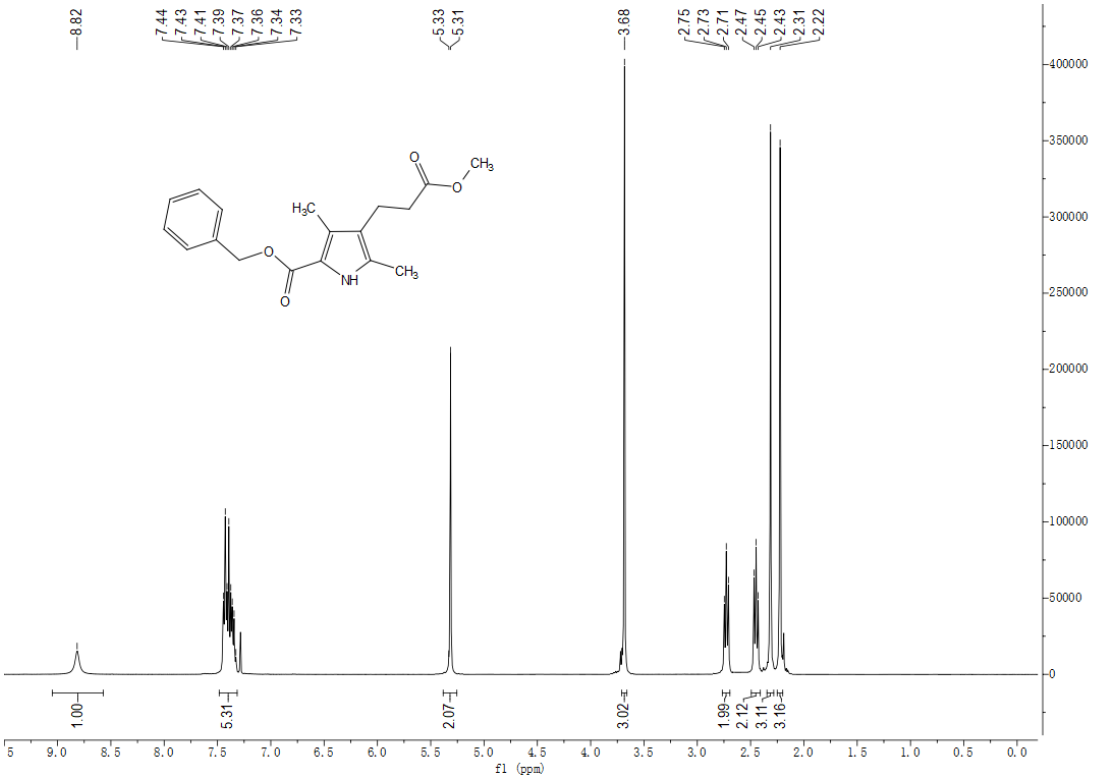

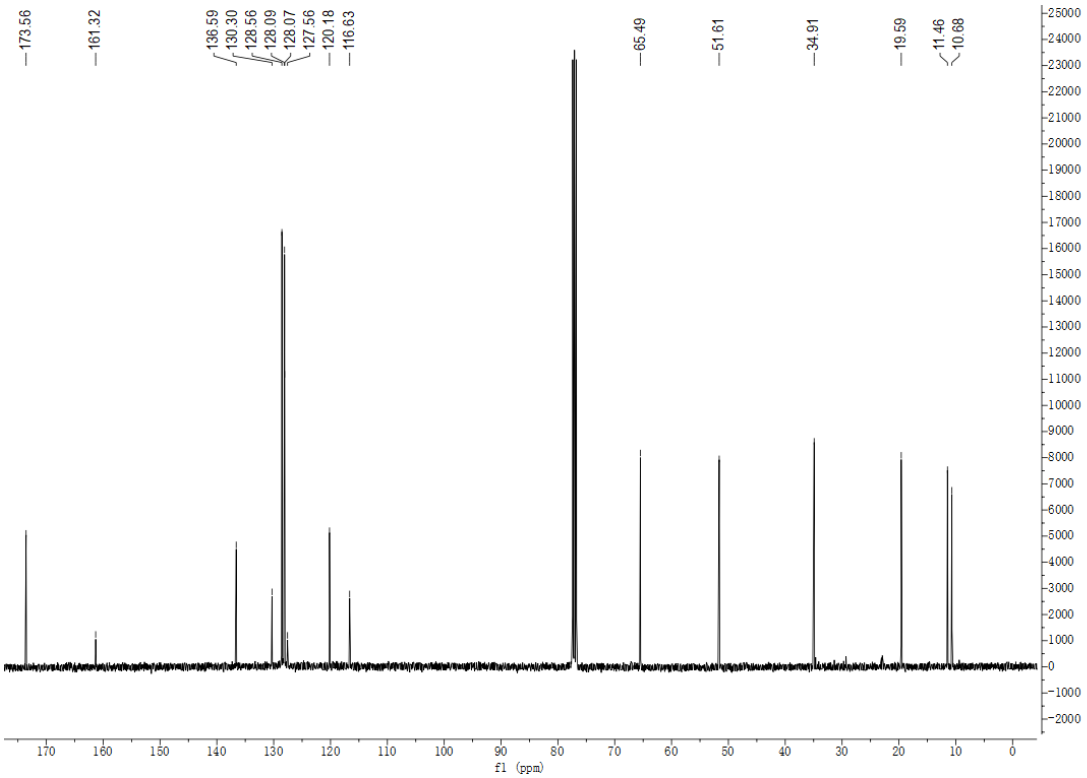

Benzyl 4-(3-ethoxy-3-oxopropyl)-3,5-dimethyl-1H-pyrrole-2-carboxylate (S11)

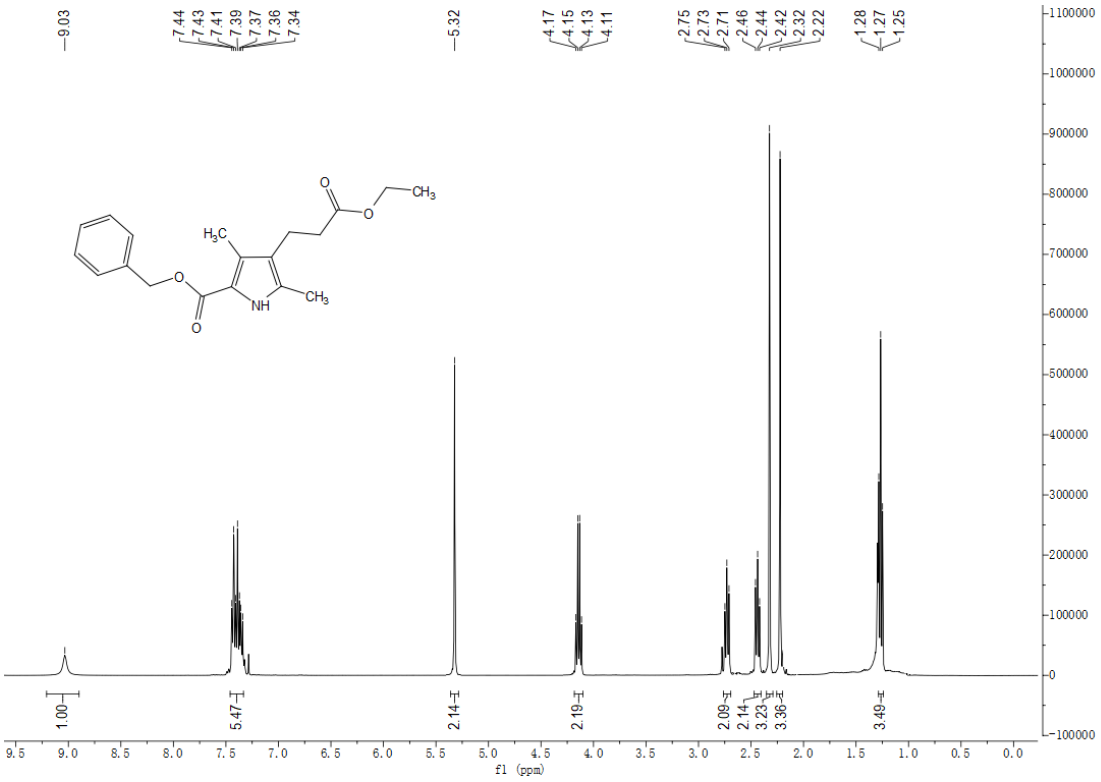

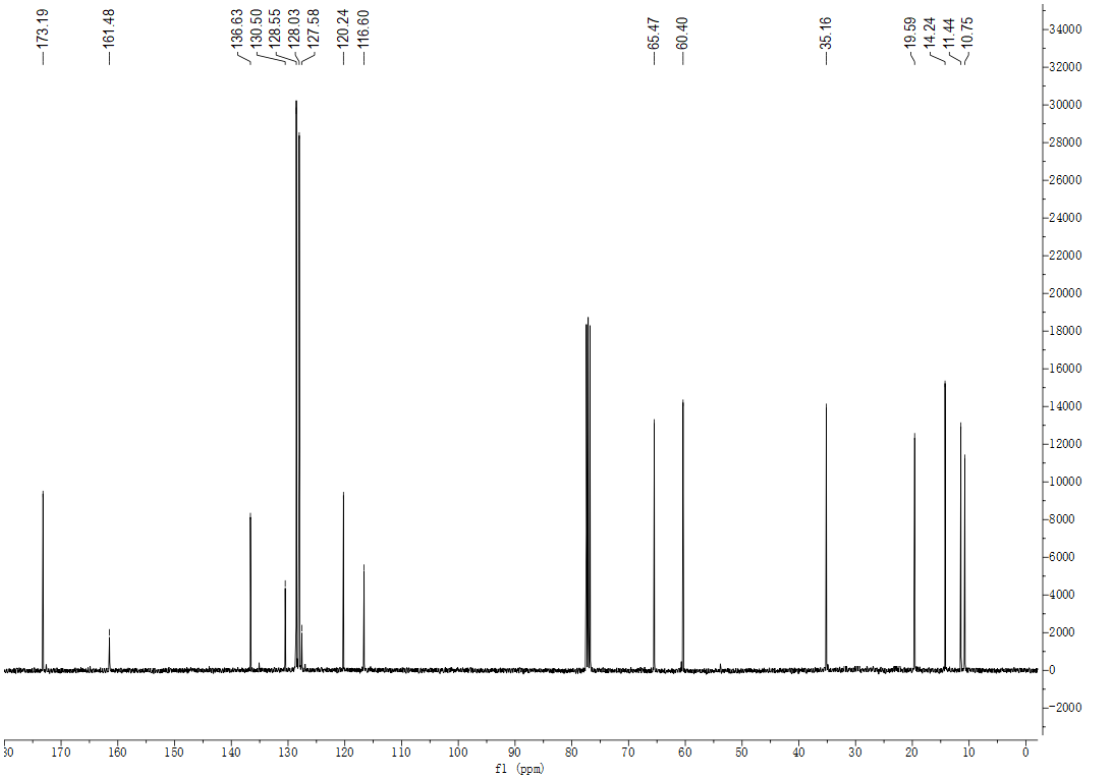

Tert-butyl 4-(3-methoxy-3-oxopropyl)-3,5-dimethyl-1H-pyrrole-2-carboxylate (S12)

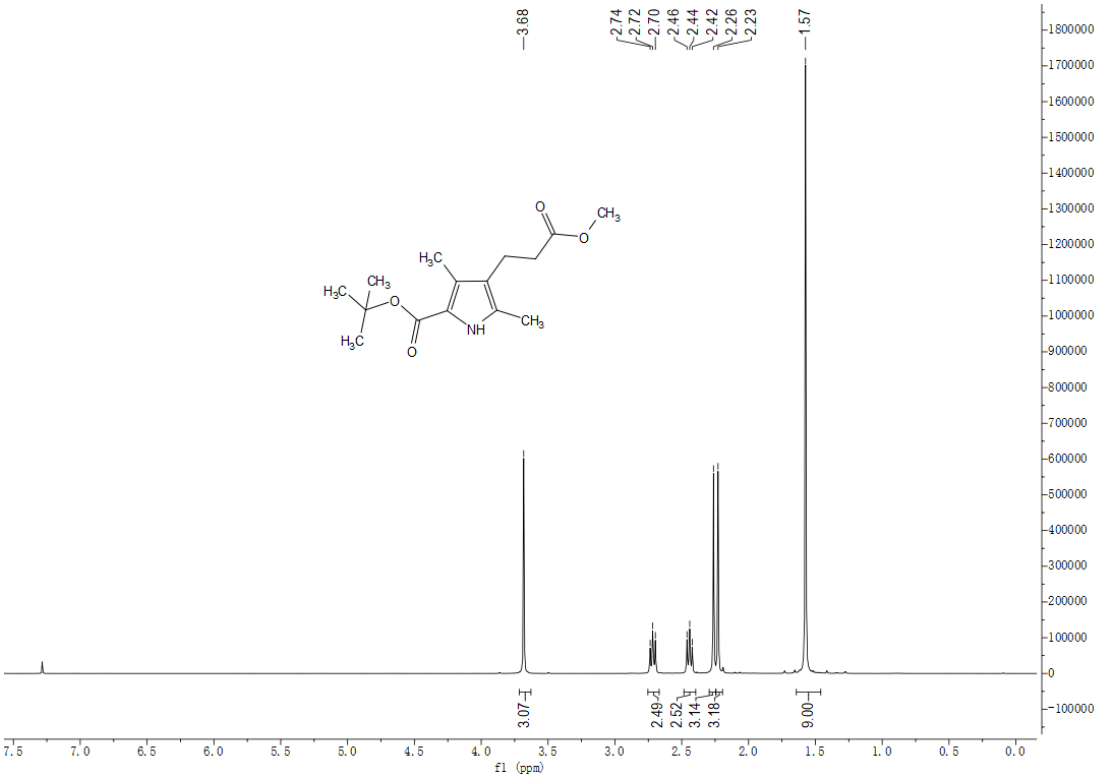

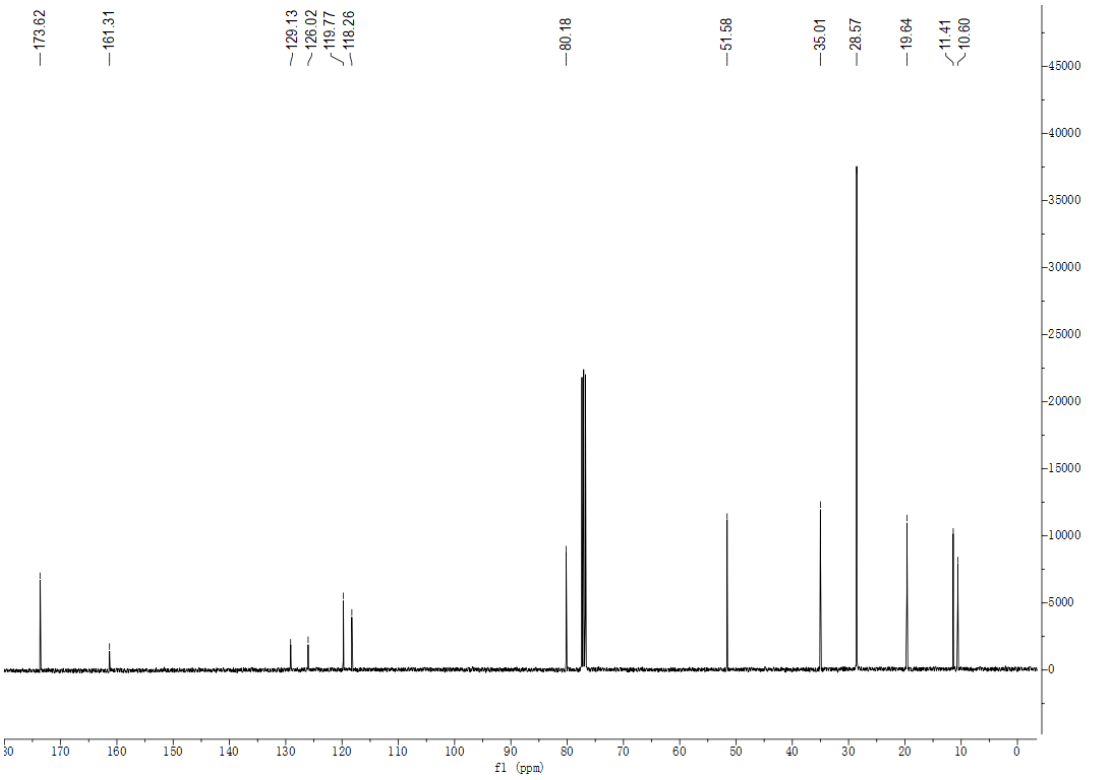

Tert-butyl 4-(3-ethoxy-3-oxopropyl)-3,5-dimethyl-1H-pyrrole-2-carboxylate (S13)

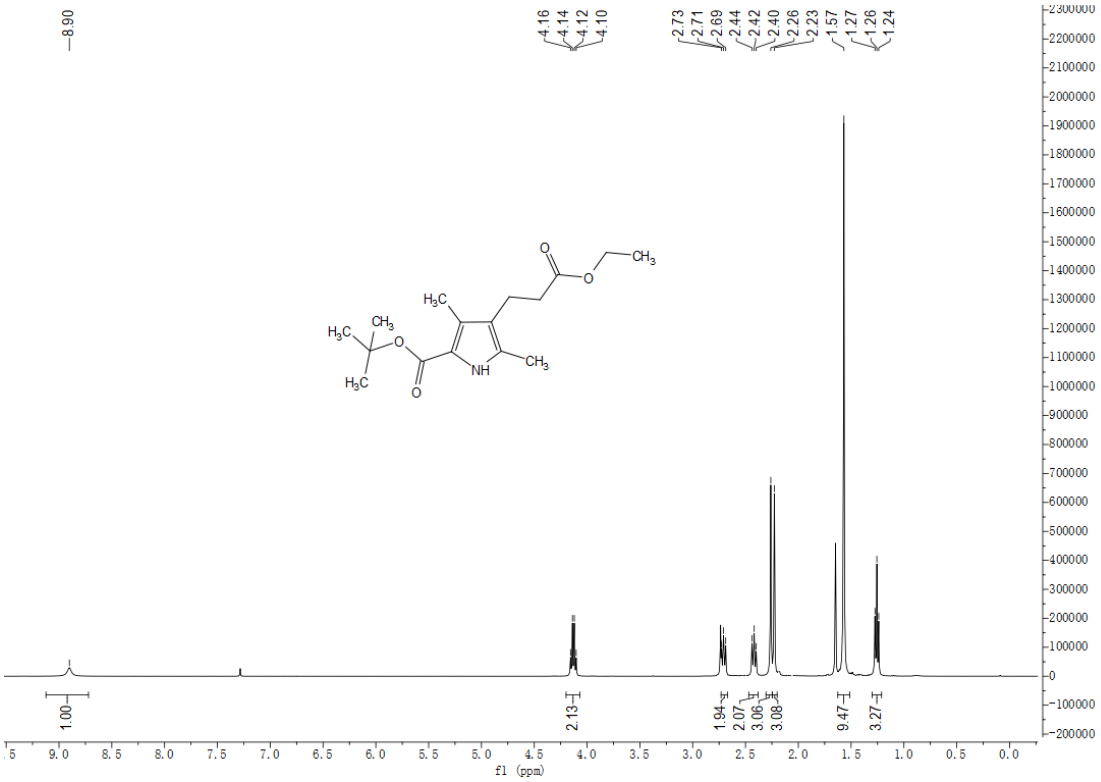

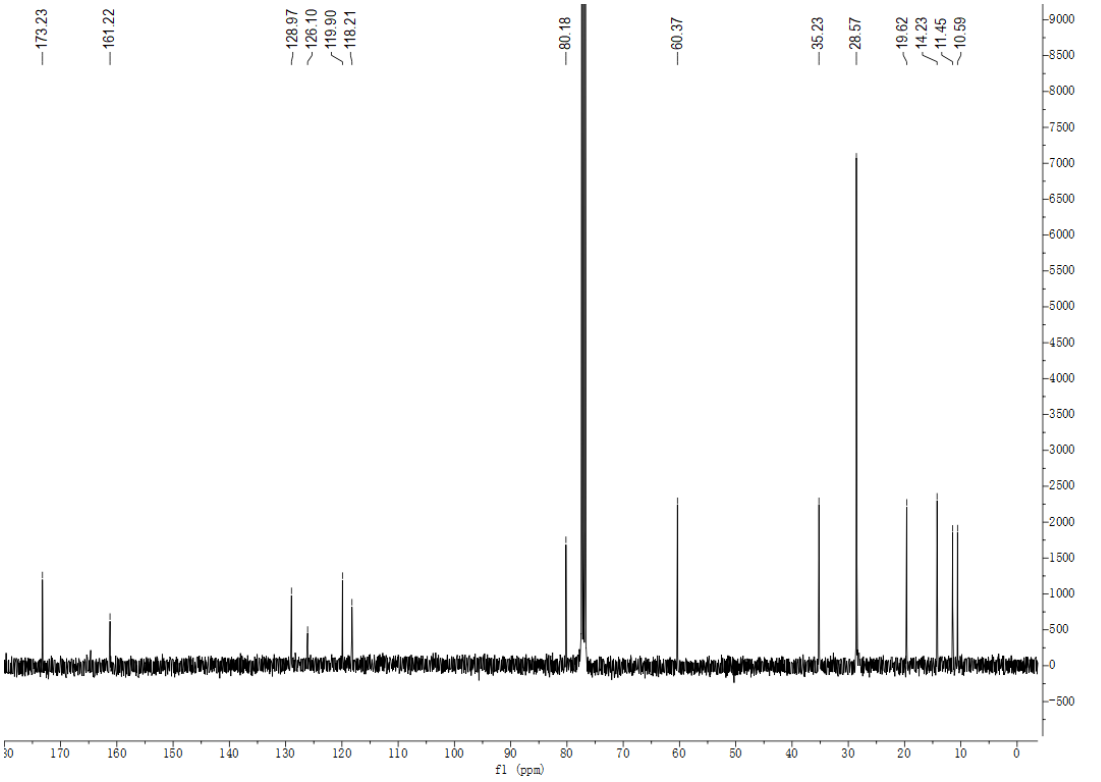

Methyl 3-(2,4-dimethyl-1H-pyrrol-3-yl) propanoate (S14)

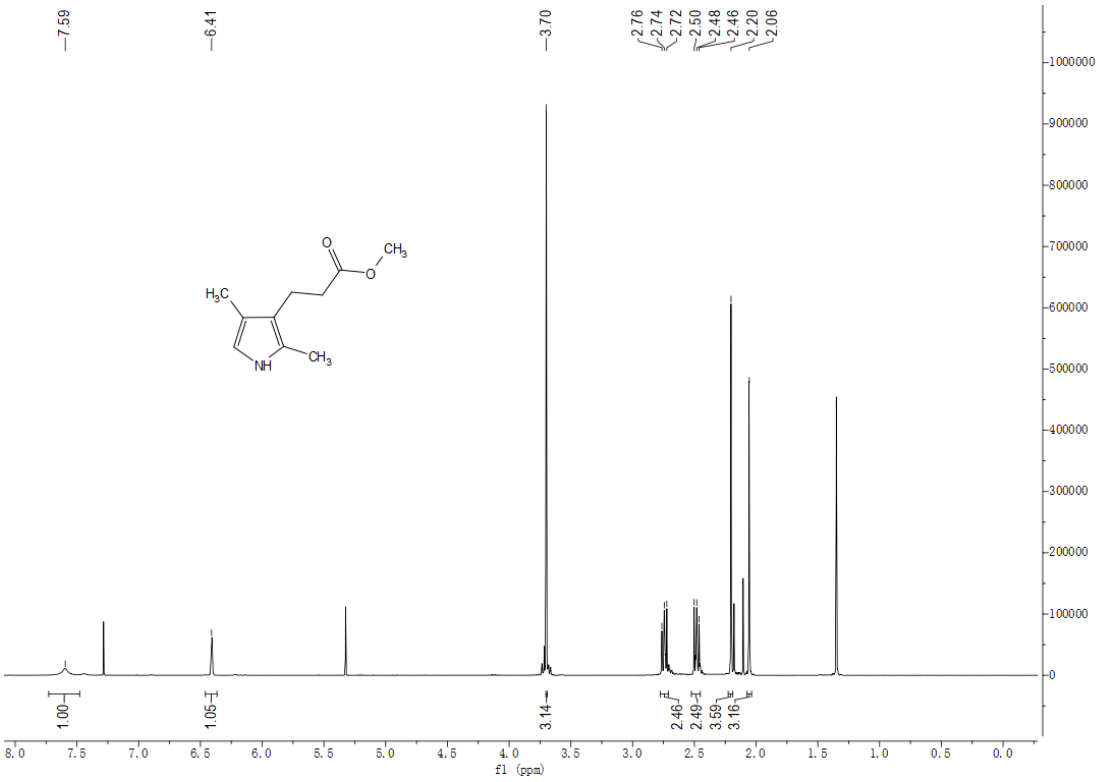

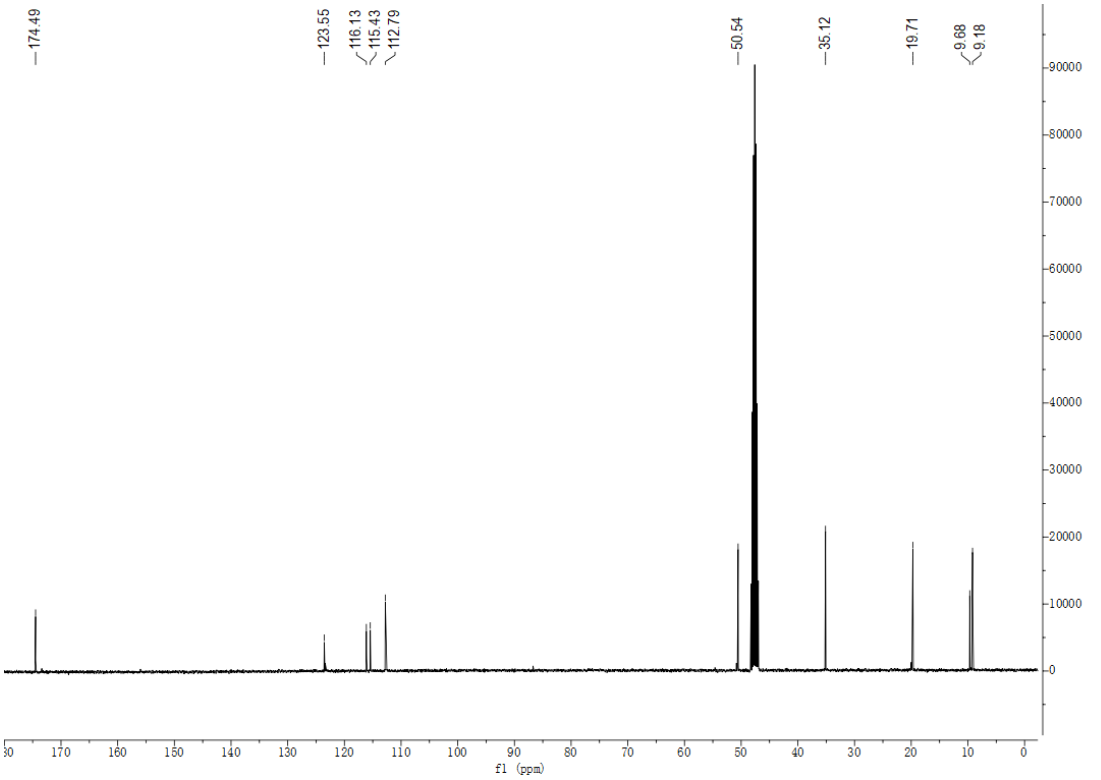

1,3,5,7-Tetramethyl-2-methyl propanoate-8-(4-nitrophenyl)-BODIPY (S15)

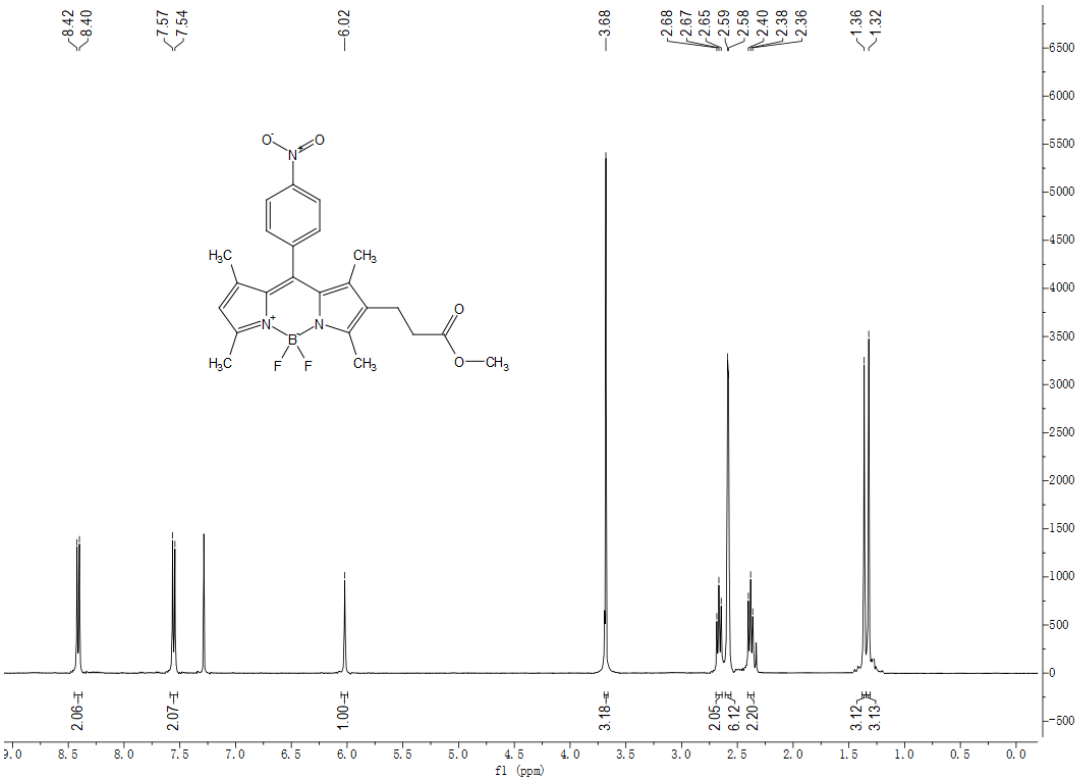

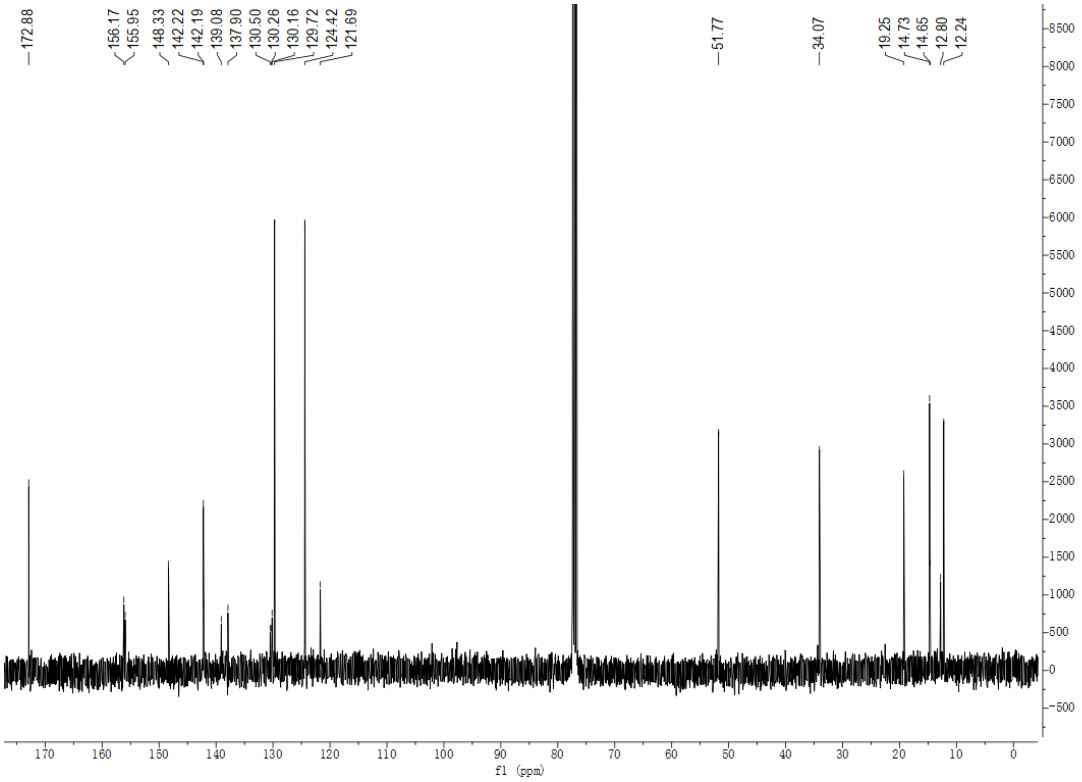

1,3,5,7-tetramethyl-2-ethyl propanoate-8-(4-nitrophenyl)-BODIPY (S16)

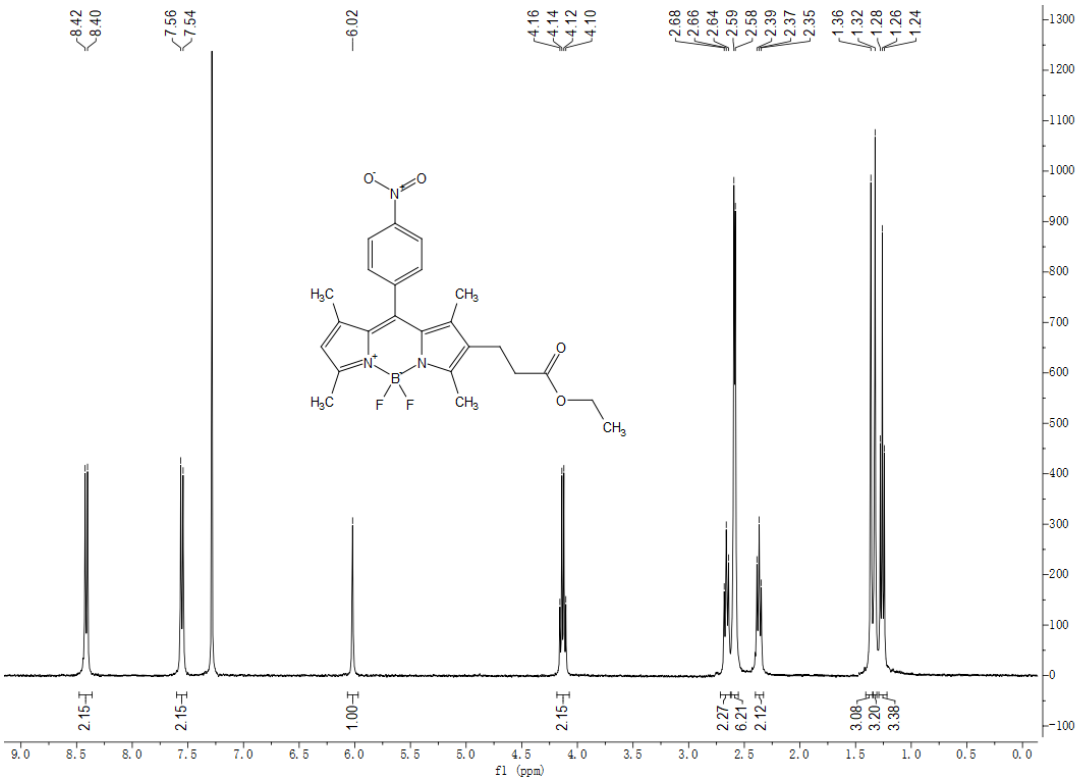

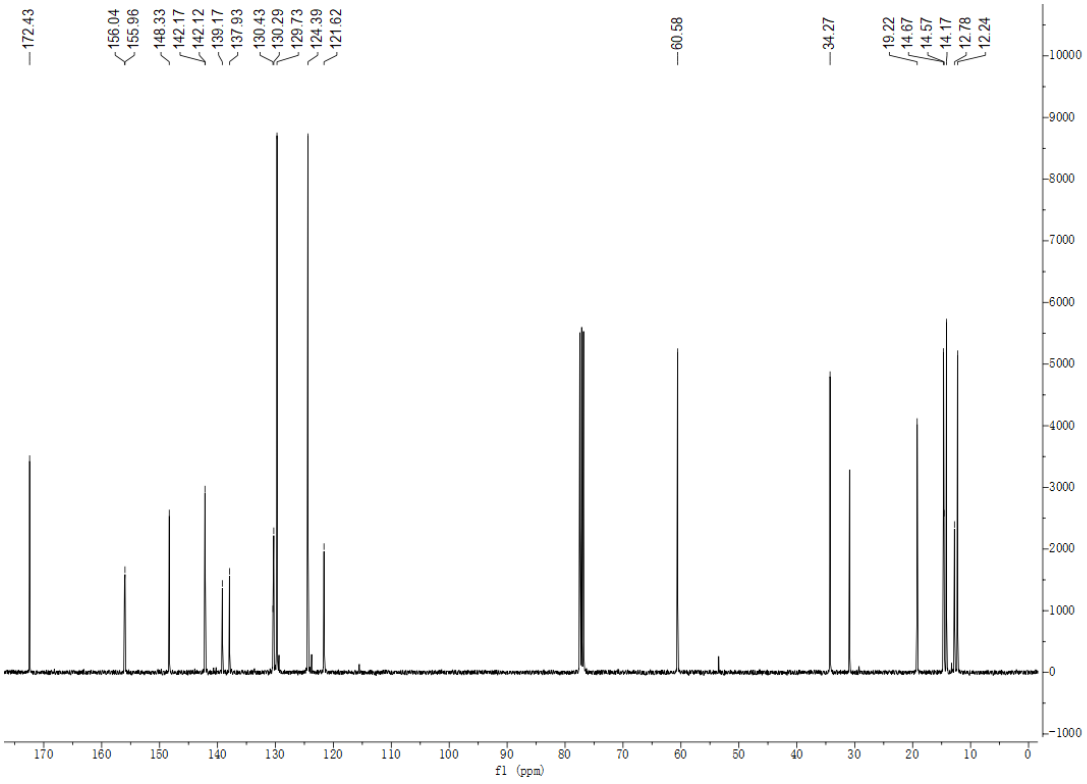

Methyl 3-(2,4-dimethyl-5-(4-nitrobenzoyl)-1H-pyrrol-3-yl)propanoate (S17)

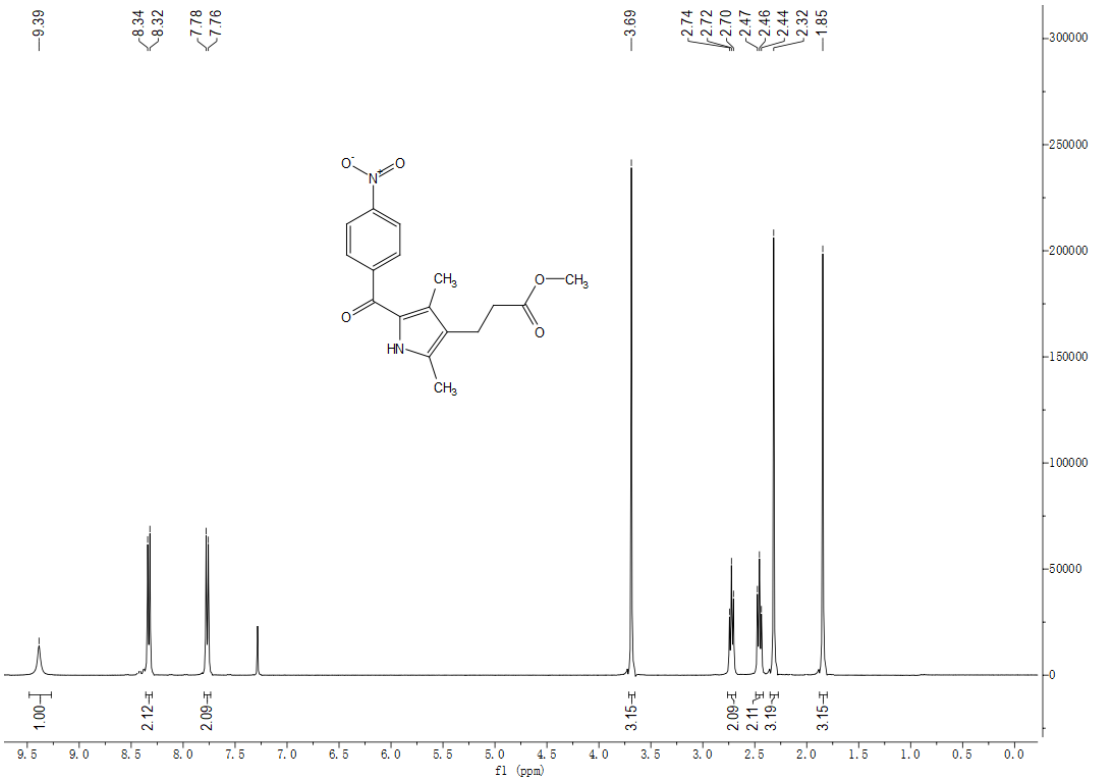

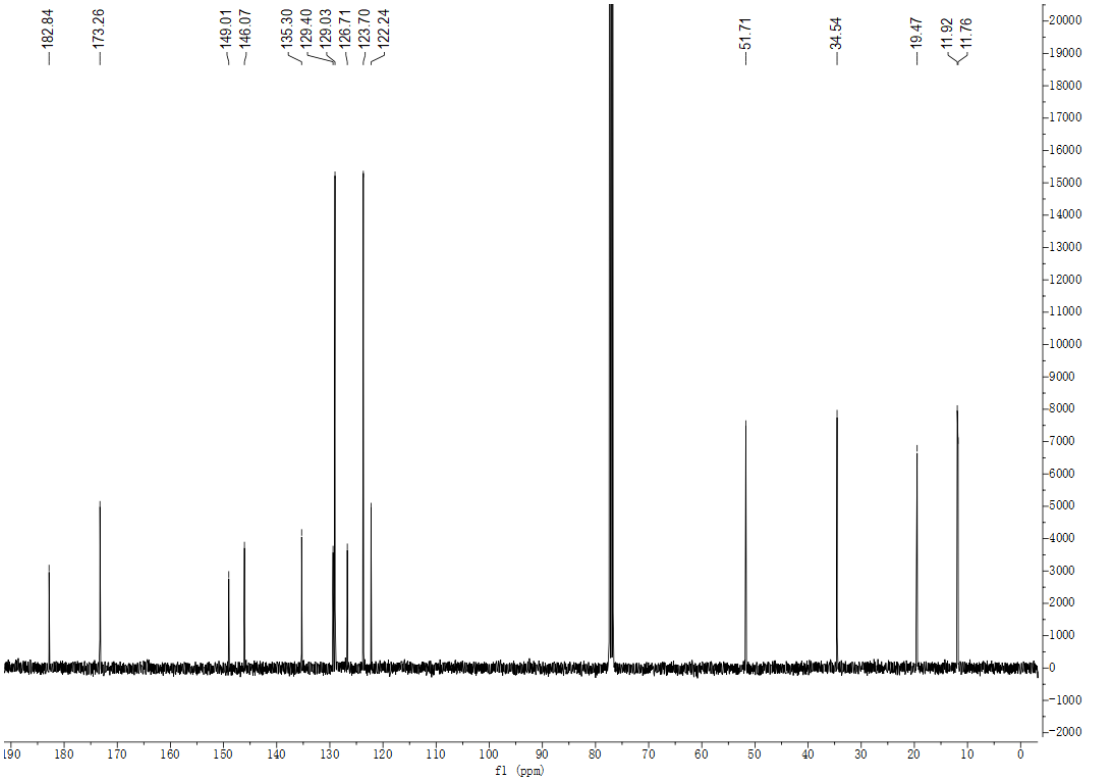

Ethyl 3-(2,4-dimethyl-5-(4-nitrobenzoyl)-1H-pyrrol-3-yl)propanoate (S18)

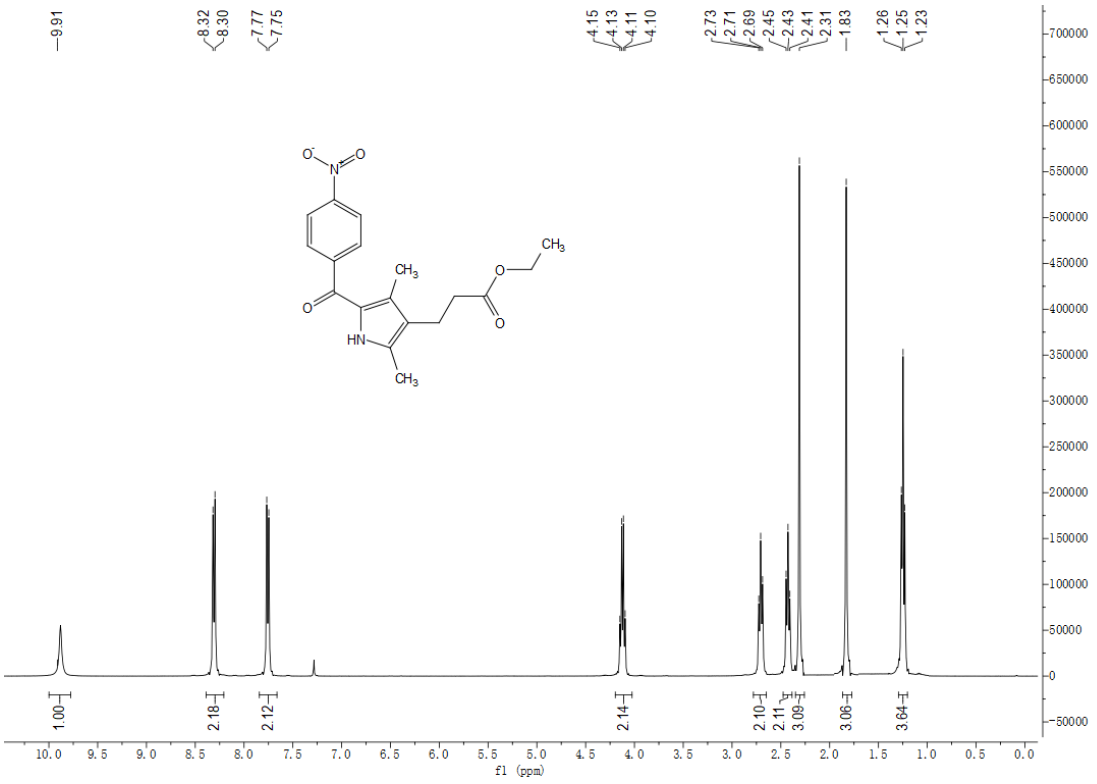

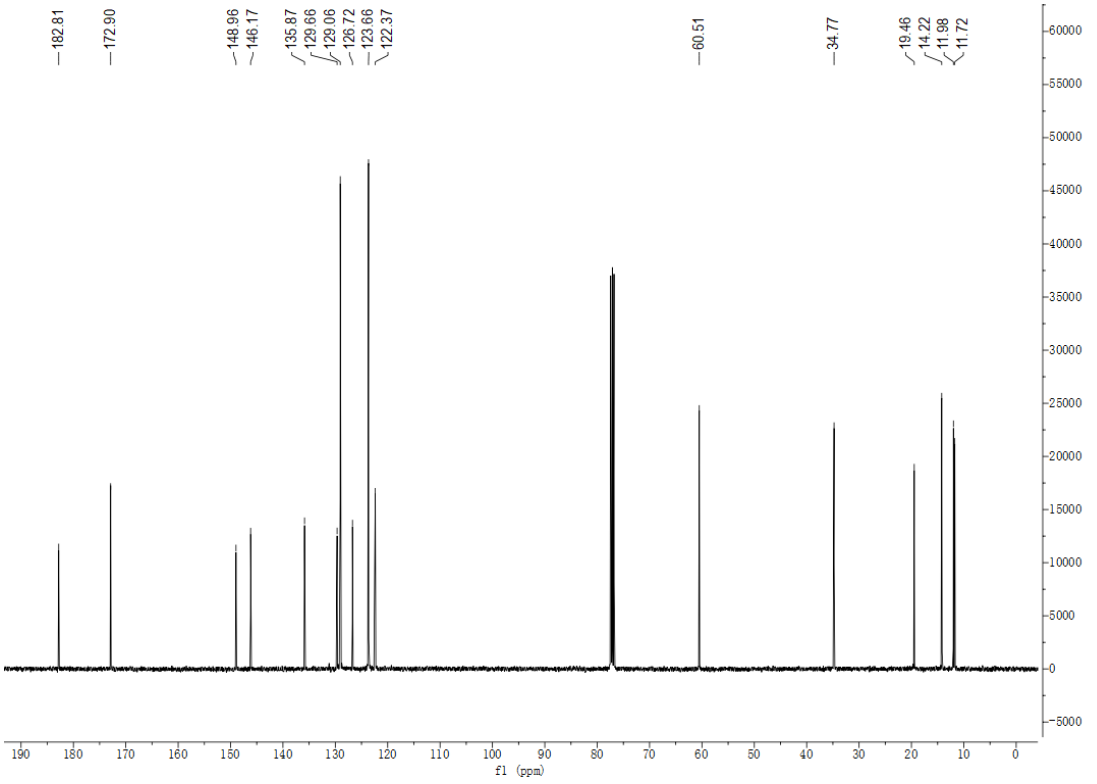

1,3,5,7-Tetramethyl-2-propanol-8-(4-nitrophenyl)-BODIPY (S19)

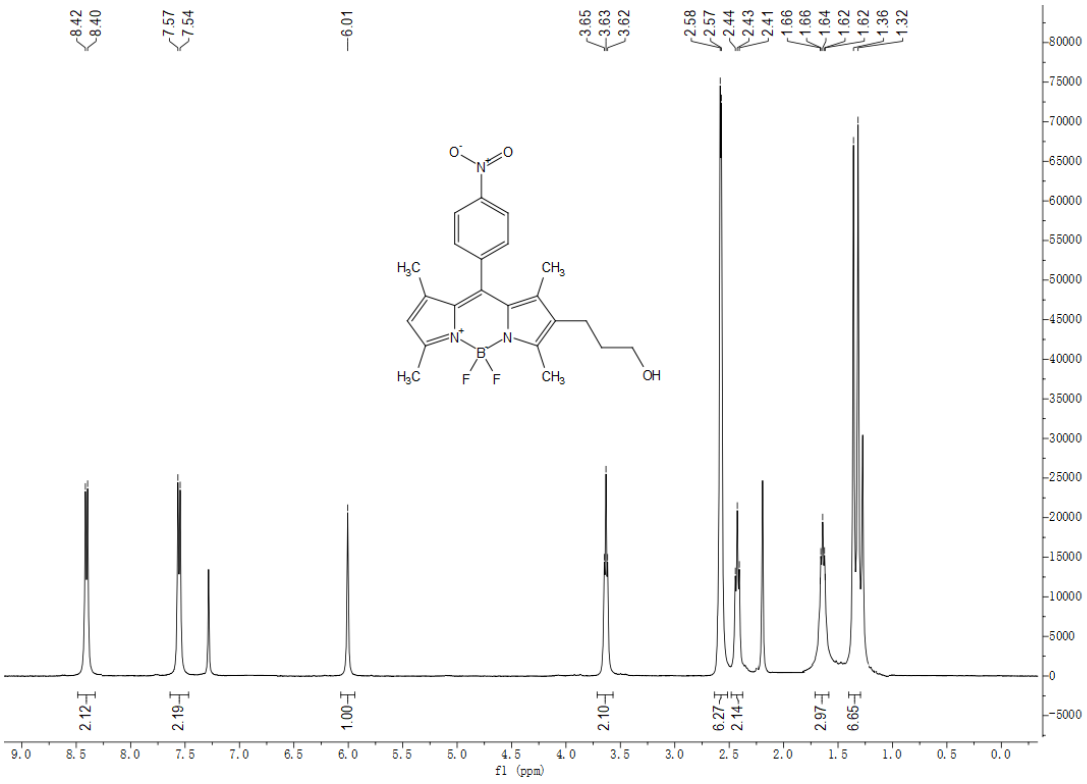

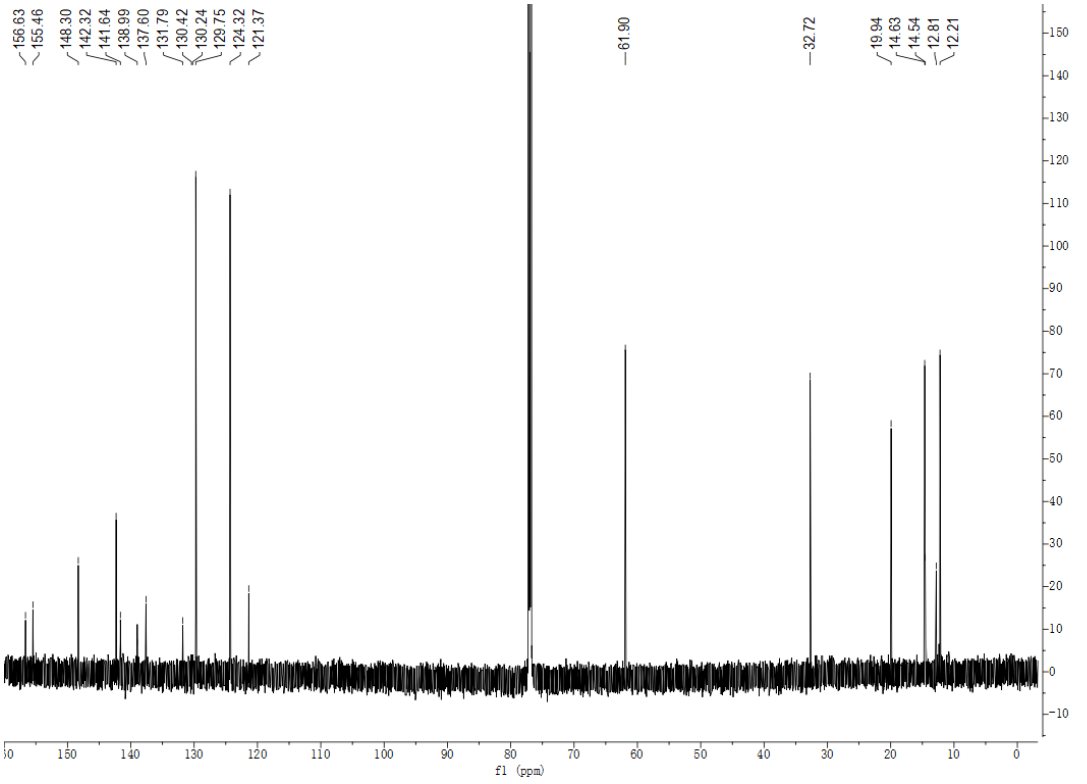

1,3,5,7-Tetramethyl-2-(4-methylbenzenesulfonate)-propyl-8-(4-nitrophenyl)-BODIPY (S21)

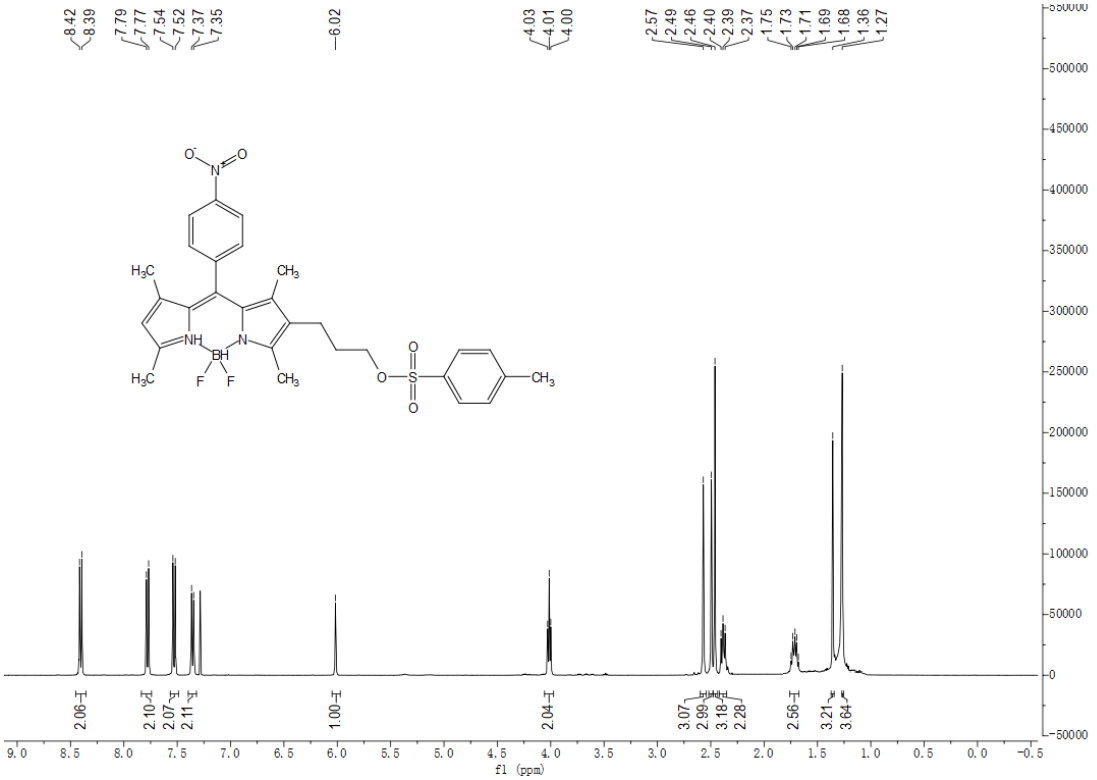

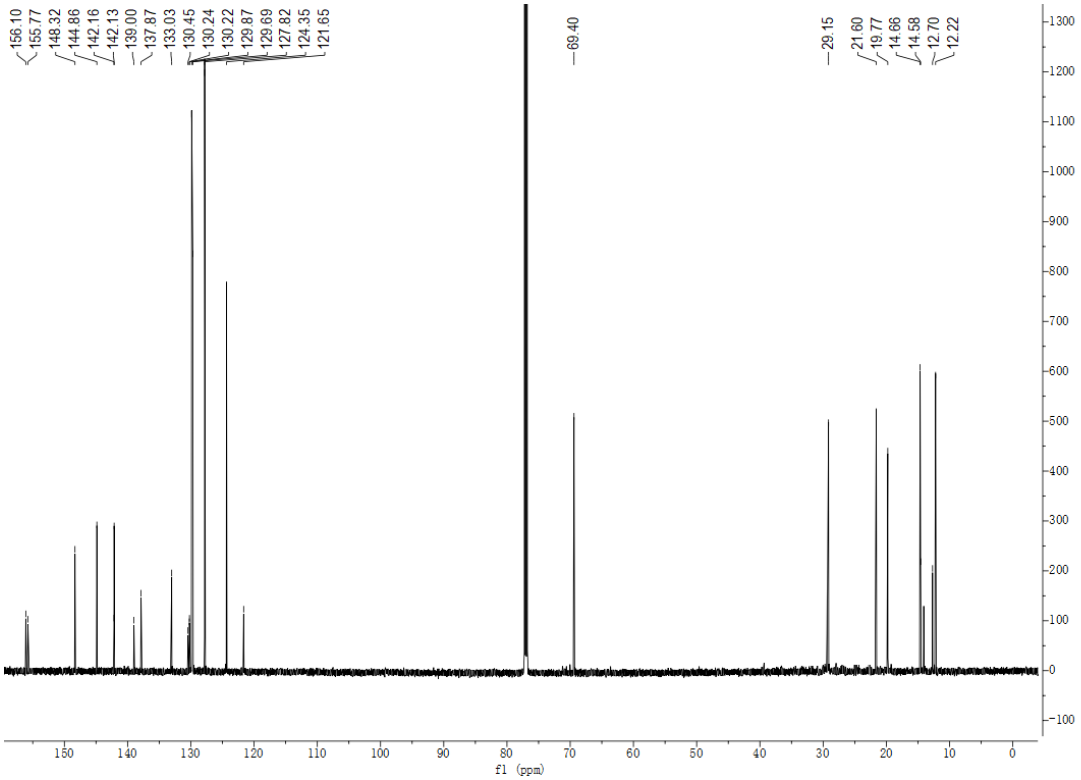

1,3,5,7-Tetramethyl-2-iodopropyl-8-(4-nitrophenyl)-BODIPY (S22)

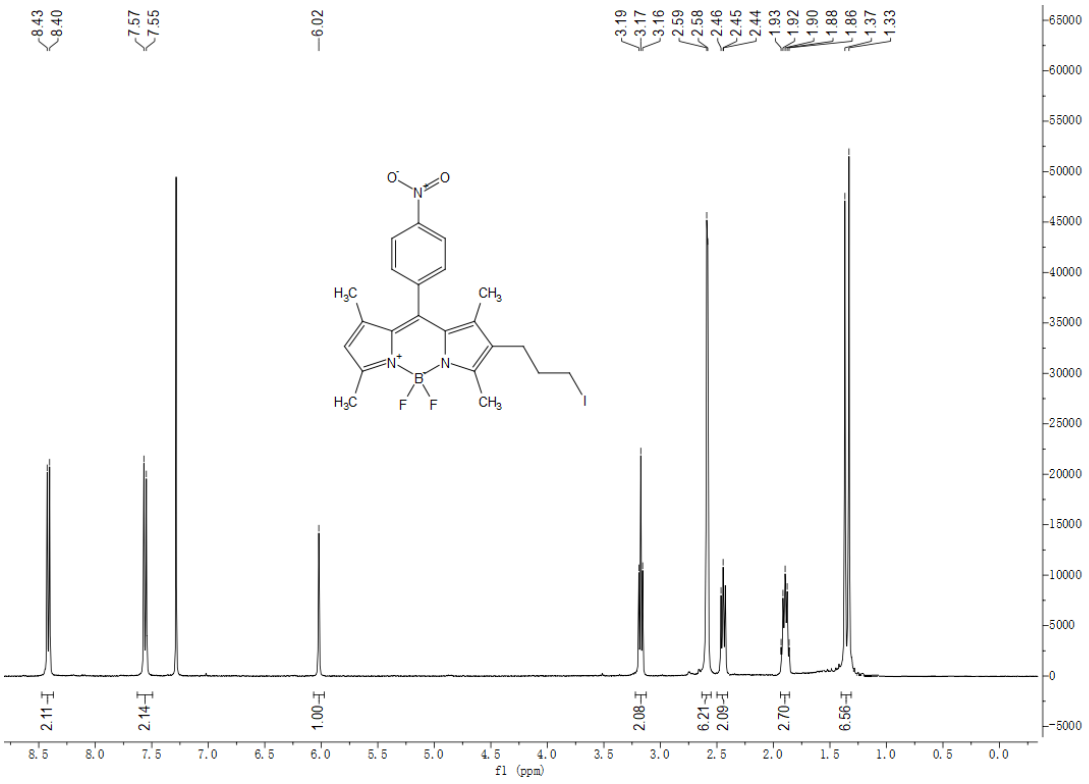

1,2-Di-tert-butyl-4-(3-methoxy-3-oxopropyl)-3,5-dimethyl-1H-pyrrole-1,2-dicarboxylate (S24)

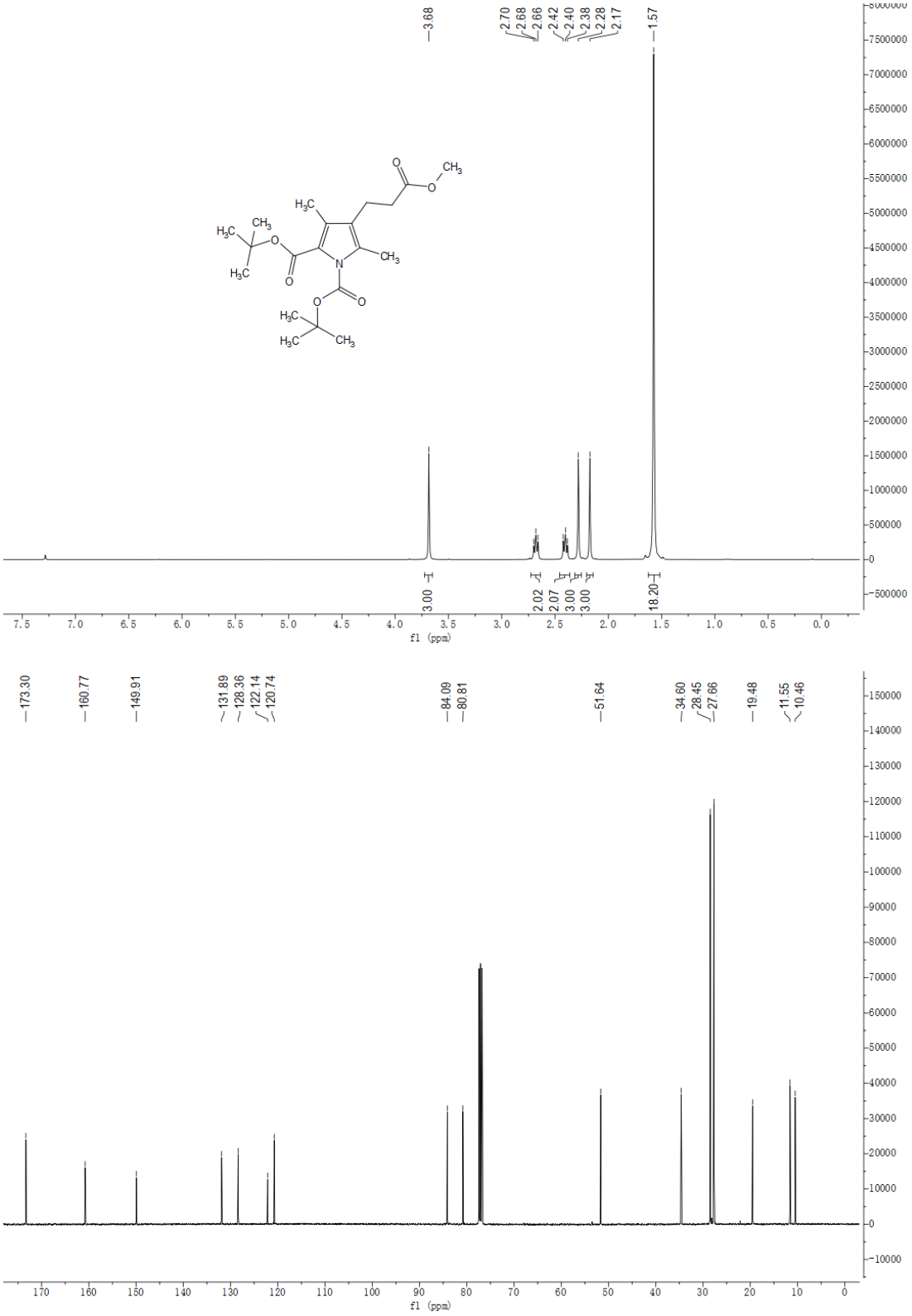

Tert-butyl 3-(3-methoxy-3-oxopropyl)-2,4-dimethyl-1H-pyrrole-1-carboxylate (S25)

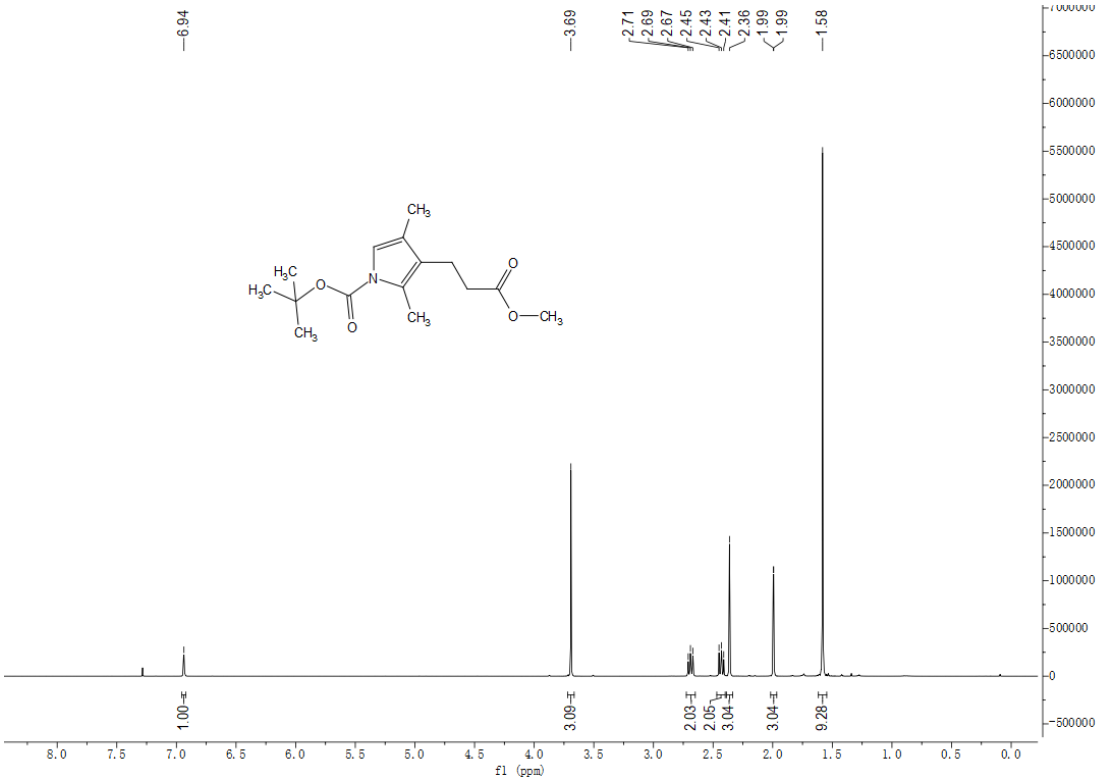

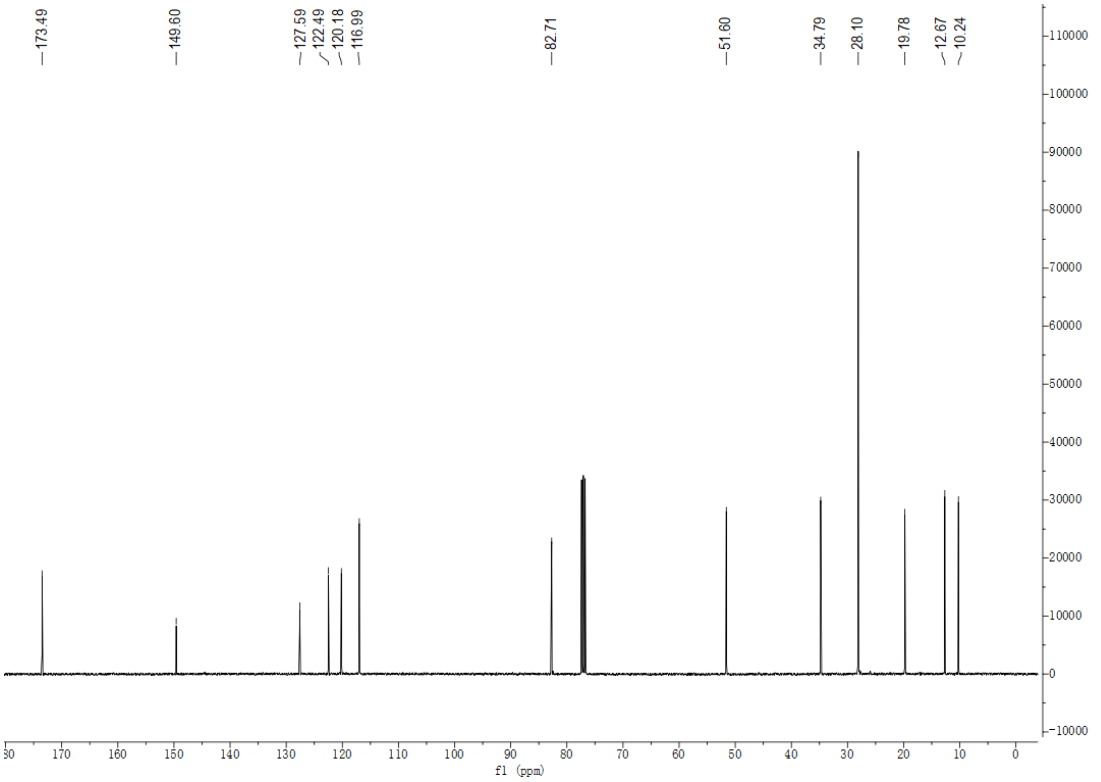

Tert-butyl 4-(3-hydroxypropyl)-3,5-dimethyl-1H-pyrrole-2-carboxylate (S26)

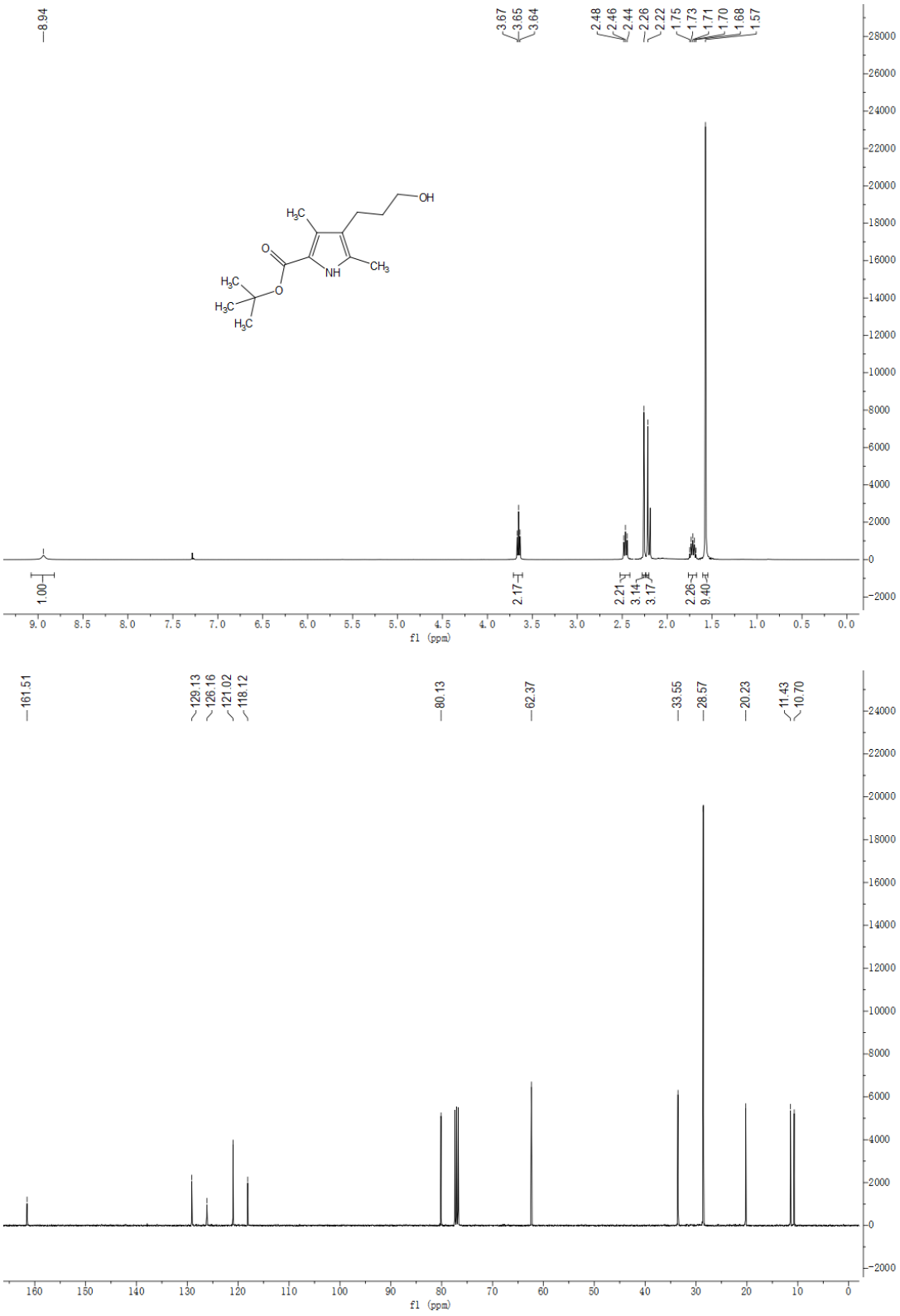

1,2-Di-tert-butyl 4-(3-hydroxypropyl)-3,5-dimethyl-1H-pyrrole-1,2-dicarboxylate (S27)

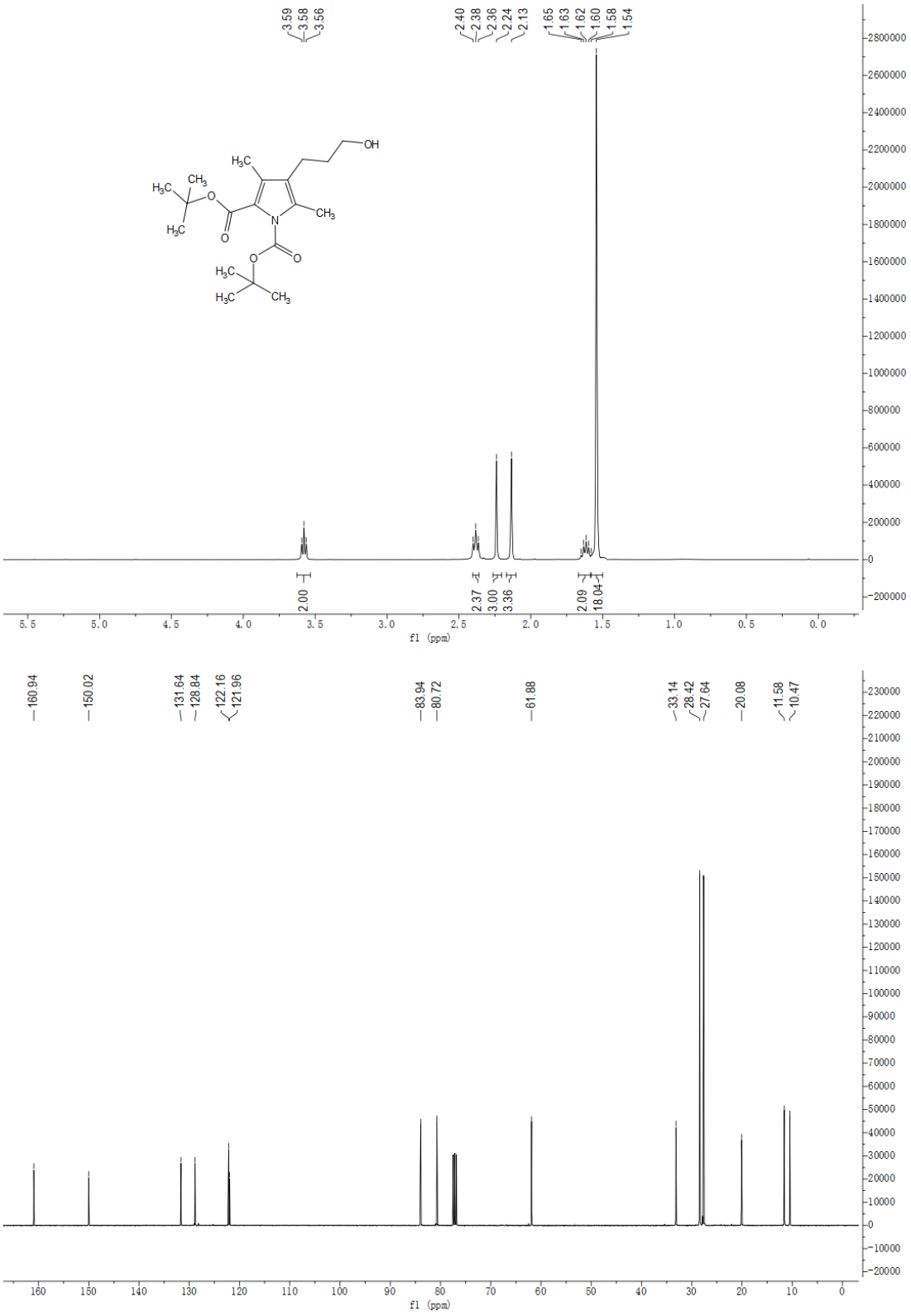

Tert-butyl 3-(3-hydroxypropyl)-2,4-dimethyl-1H-pyrrole-1-carboxylate (S28)

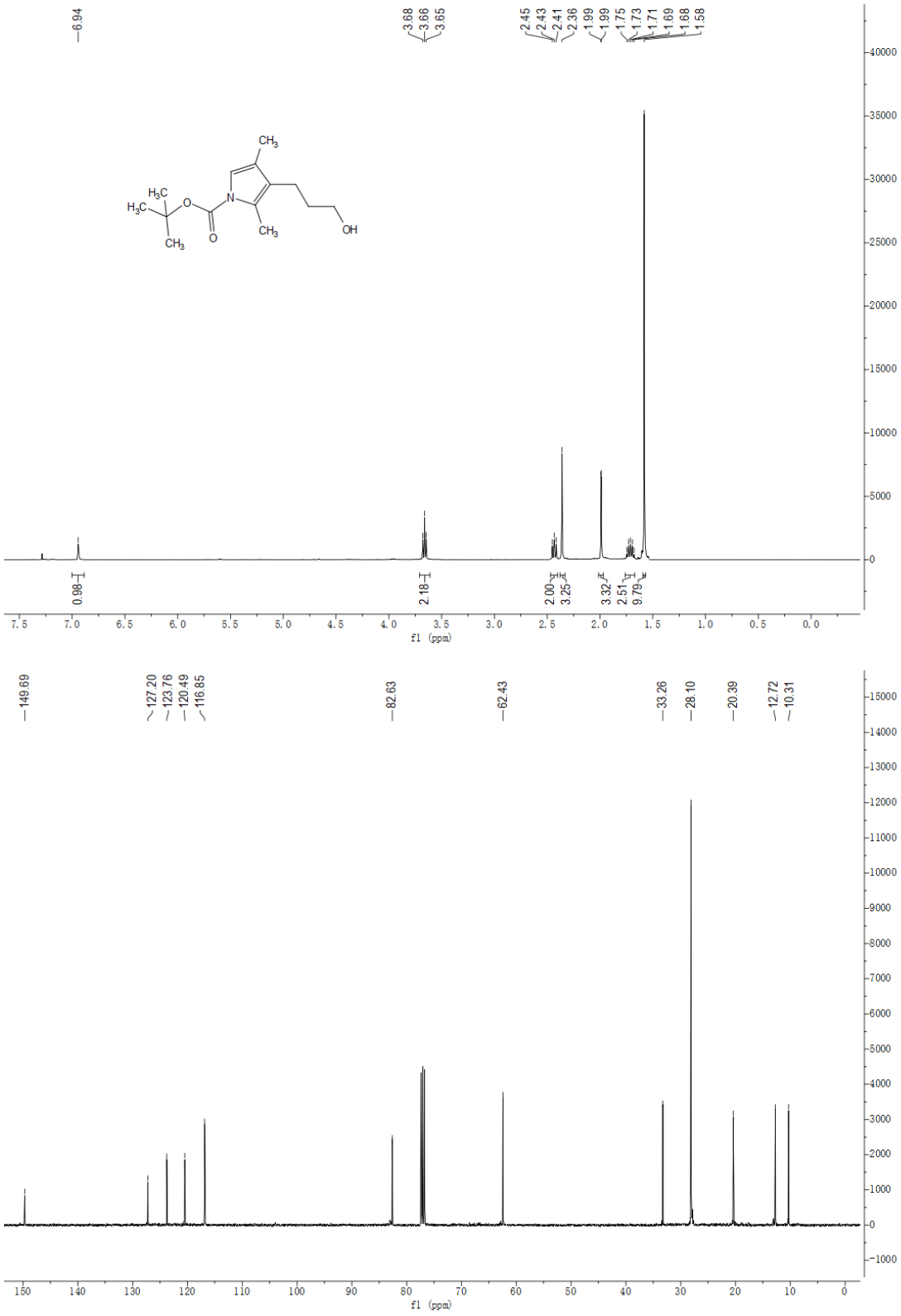

Tert-butyl 4-(3-iodopropyl)-3,5-dimethyl-1H-pyrrole-2-carboxylate (S29)

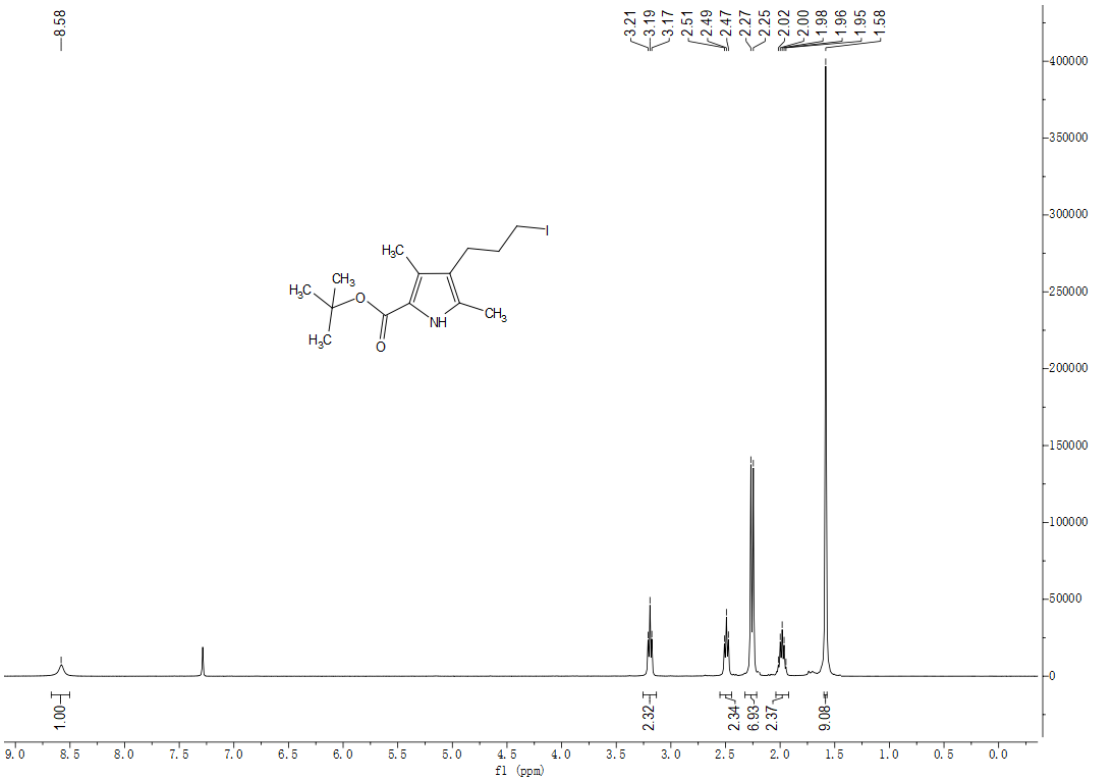

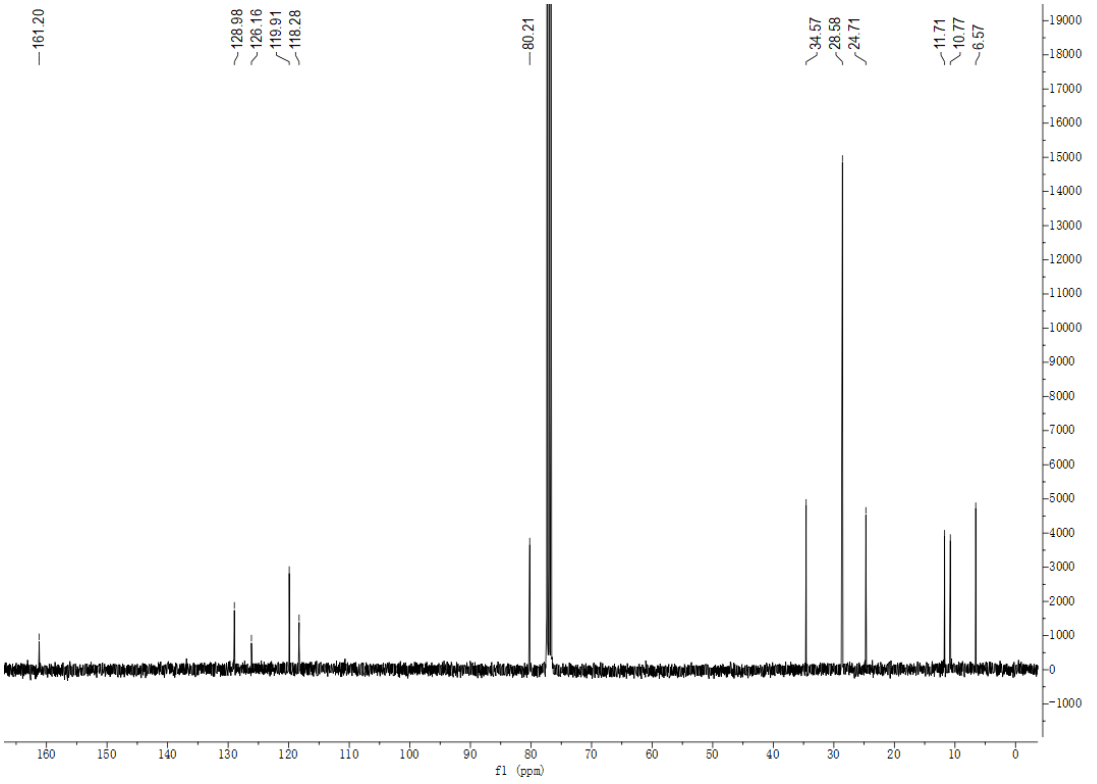

Tert-butyl 3-(3-iodopropyl)-2,4-dimethyl-1H-pyrrole-1-carboxylate (S31)

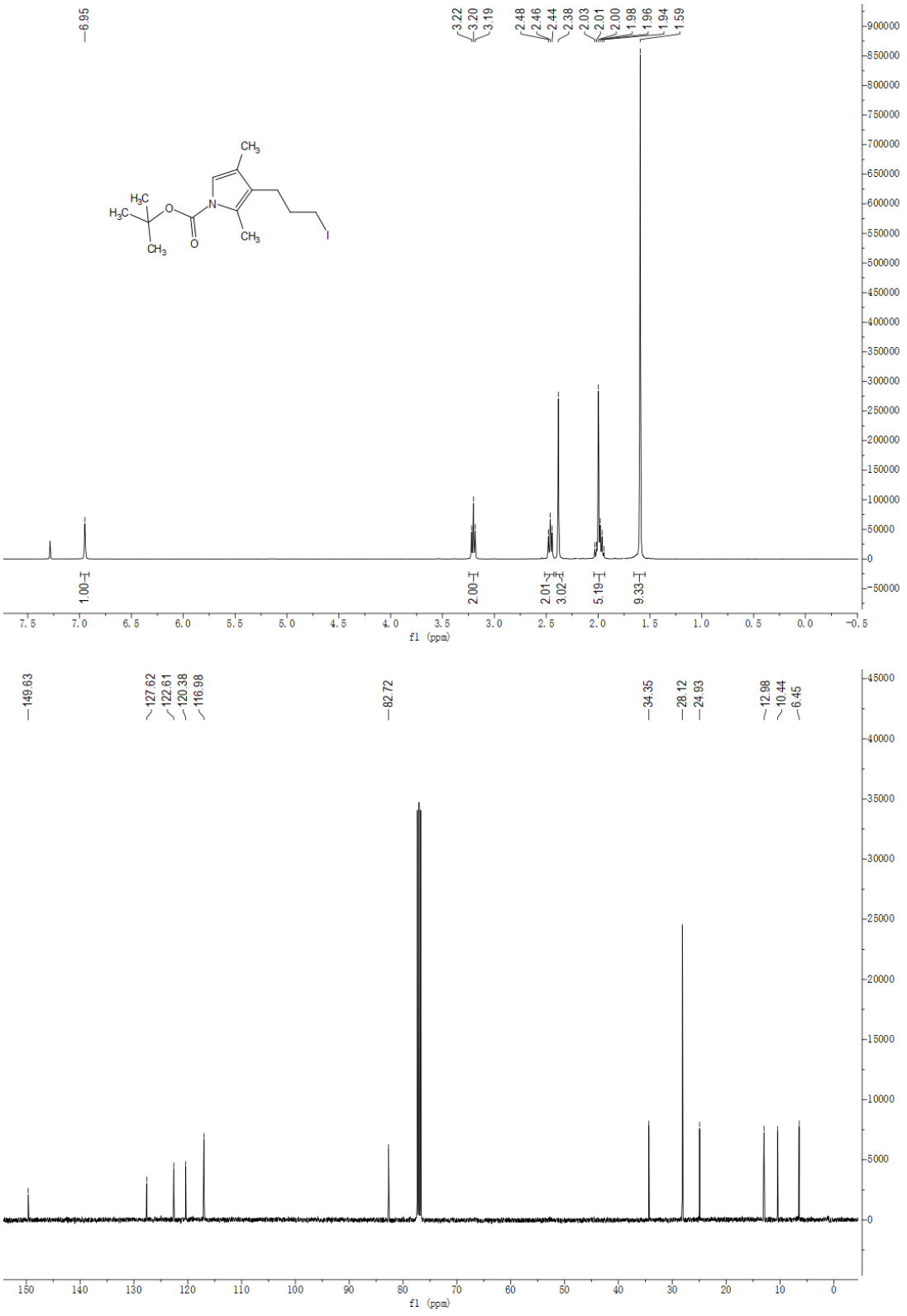

1,3,5,7-Tetramethyl-2-propanoic acid-8-(4-nitrophenyl)-BODIPY (S36)

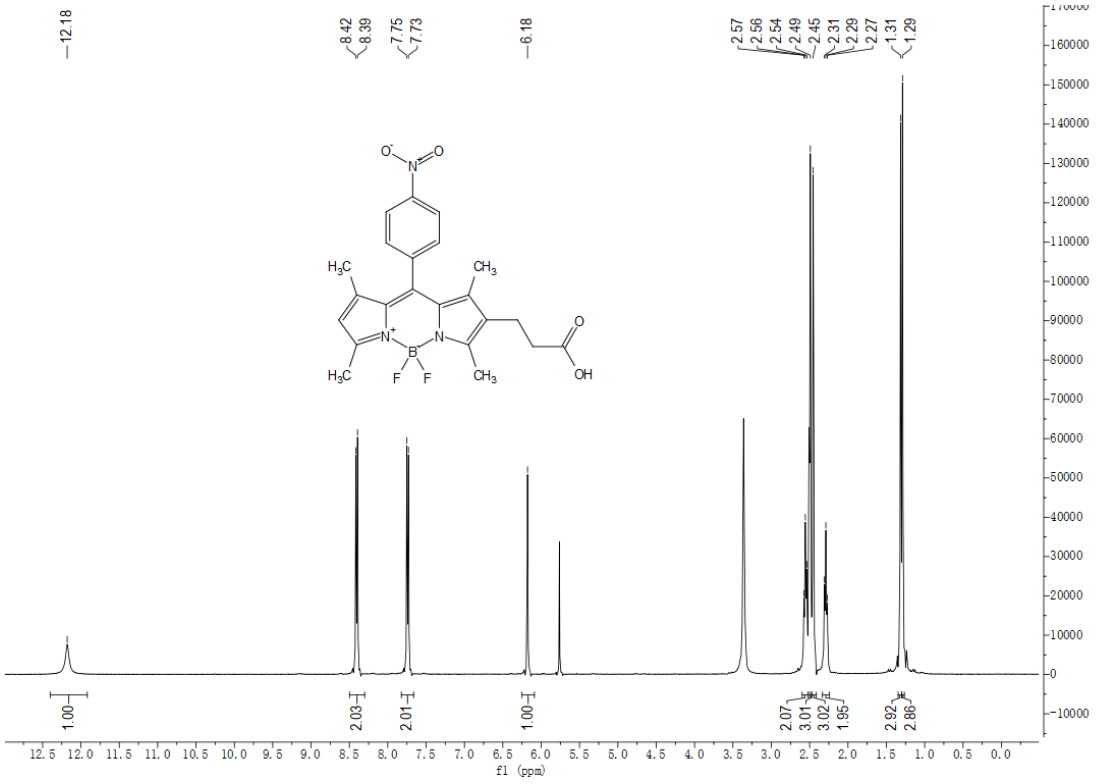

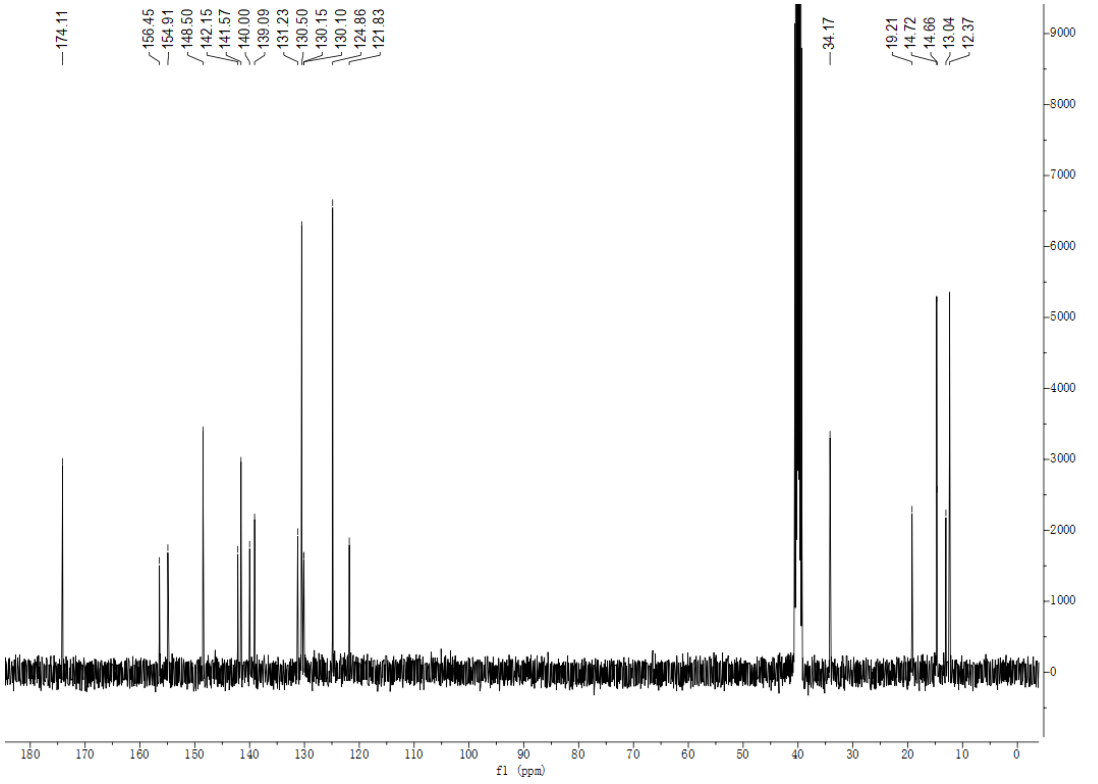

1,3,5,7-Tetramethyl-2-N-(prop-2-yn-1-yl)propanate NHS ester-8-(4-nitrophenyl)-BODIPY (S37)

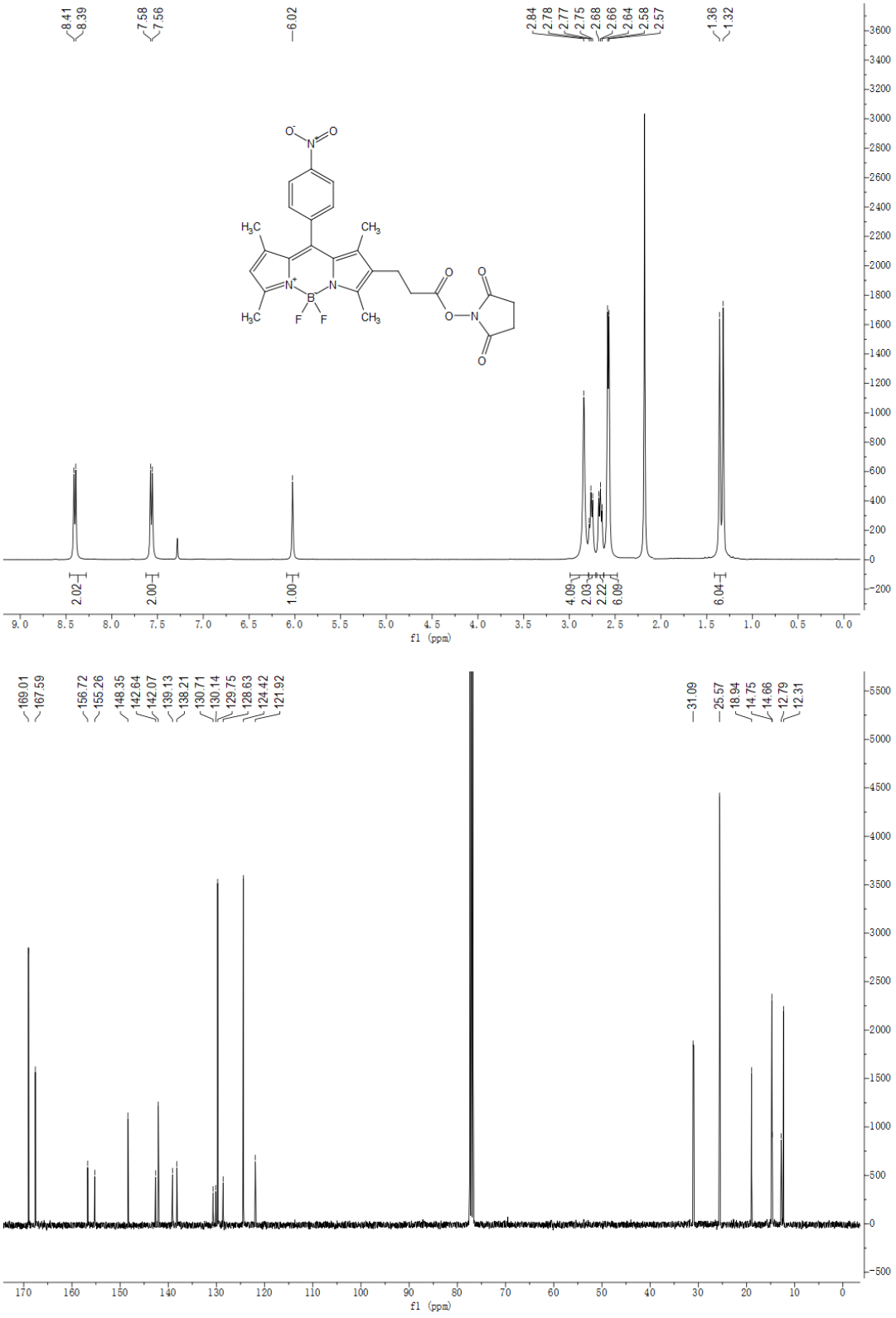

1,3,5,7-Tetramethyl-2-N-(prop-2-yn-1-yl)propanamide-8-(4-nitrophenyl)-BODIPY (S38)

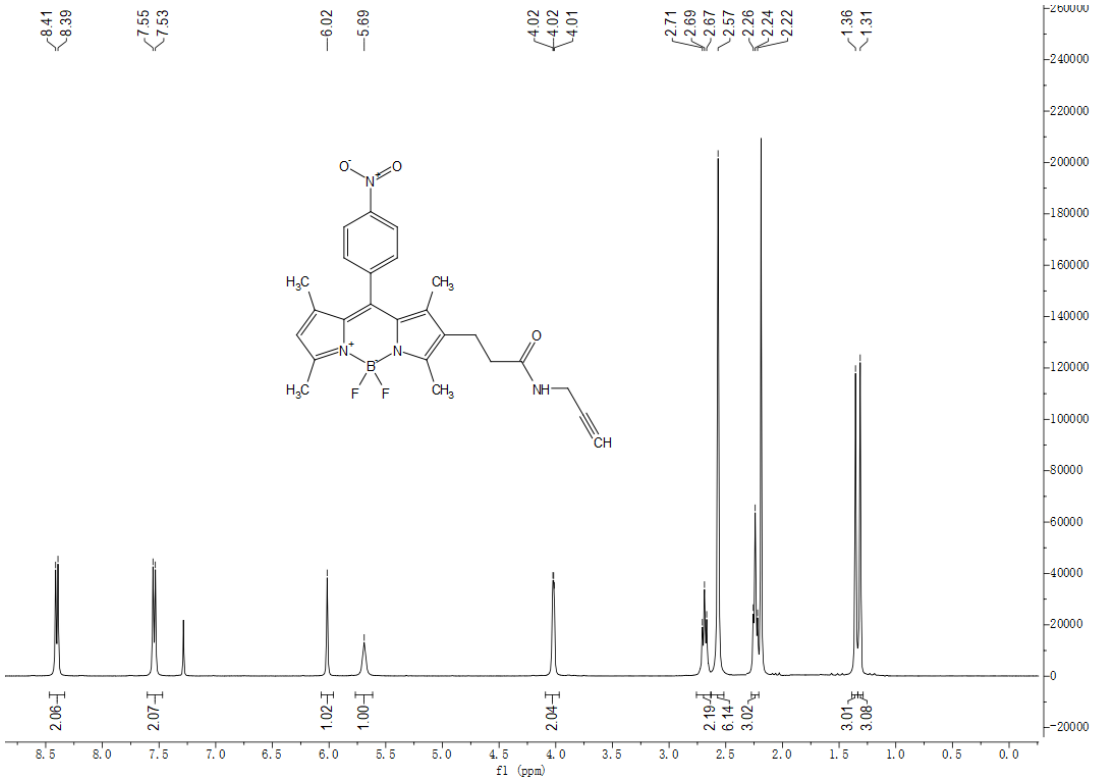

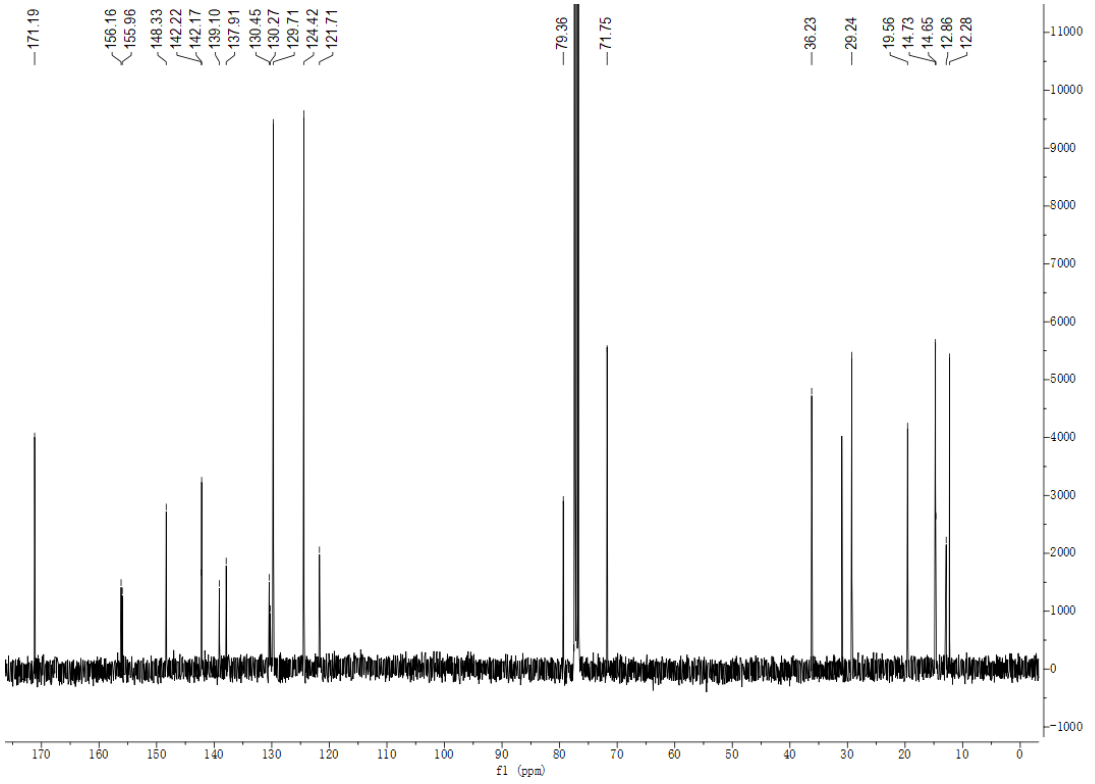

1,3,5,7-Tetramethyl-2-N-(6-azidohexyl) propanamide-8-(4-nitrophenyl)-BODIPY (S39)

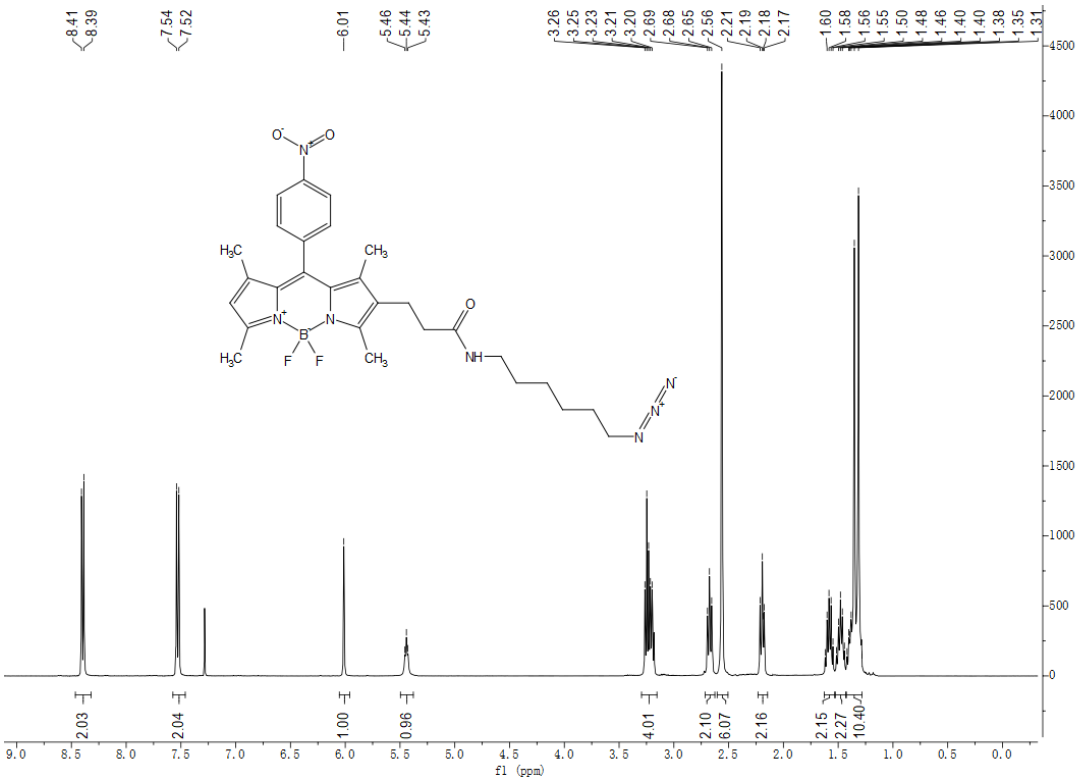

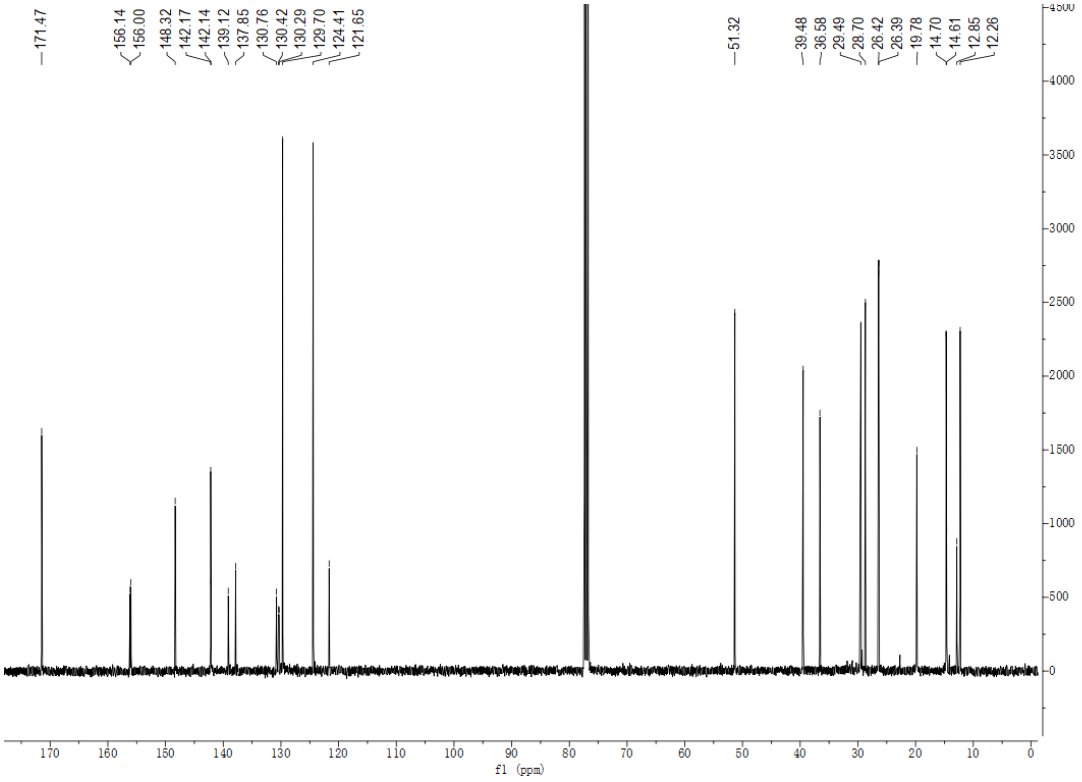

4-Benzyl 2-(tert-butyl) 3,5-dimethyl-1H-pyrrole-2,4-dicarboxylate (S40)

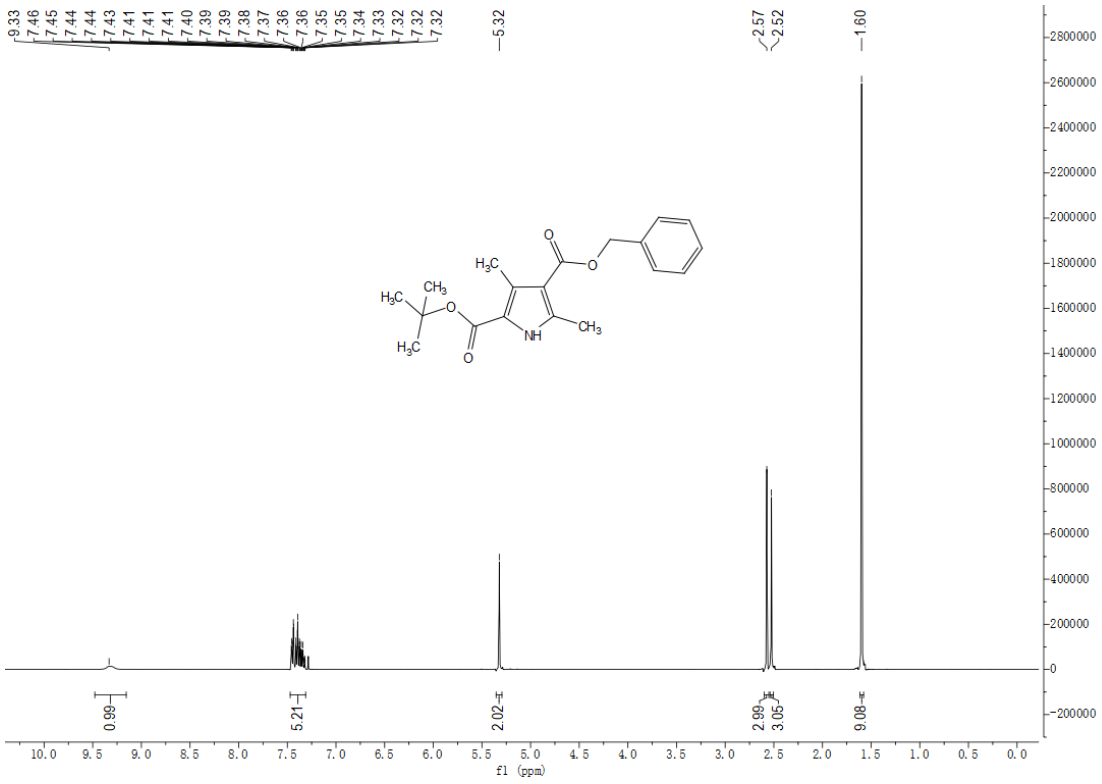

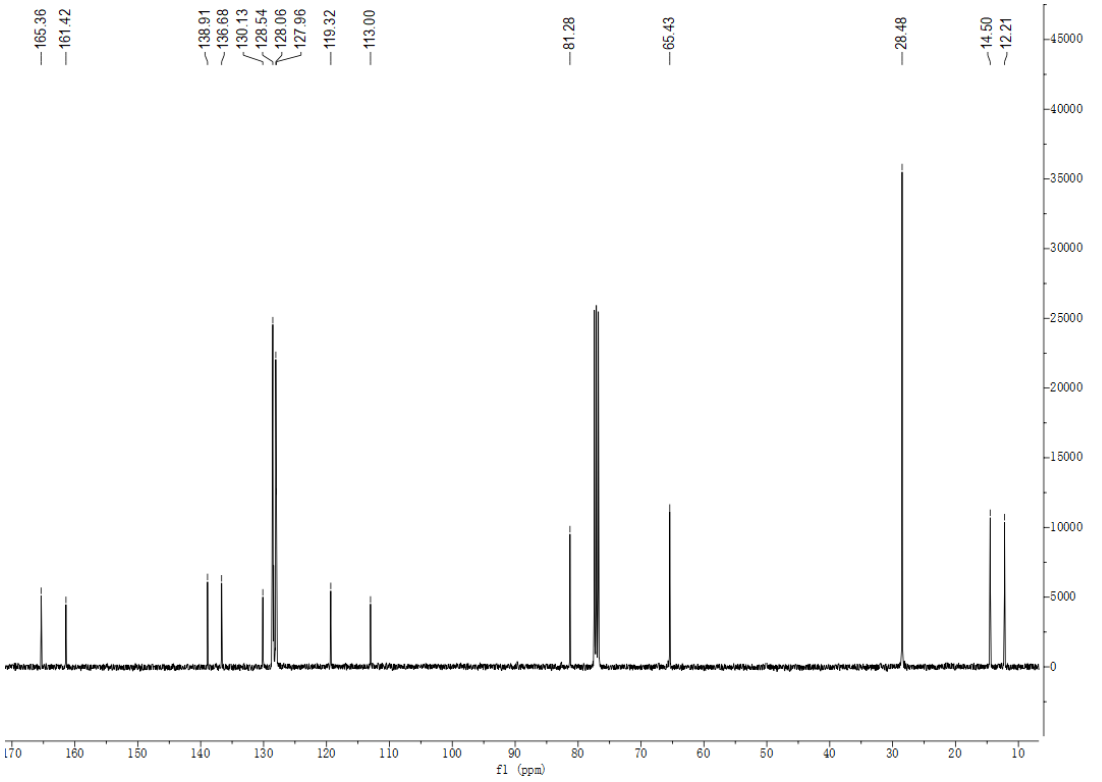

Benzyl 2,4-dimethyl-1H-pyrrole-3-carboxylate (S41)

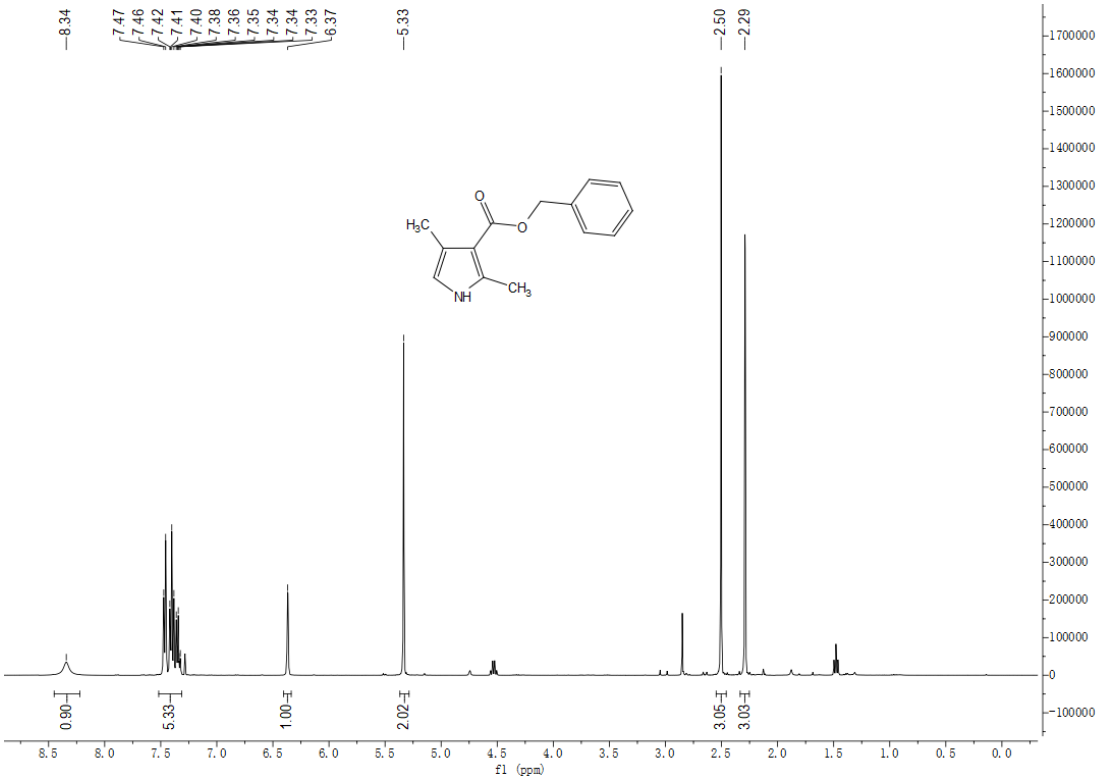

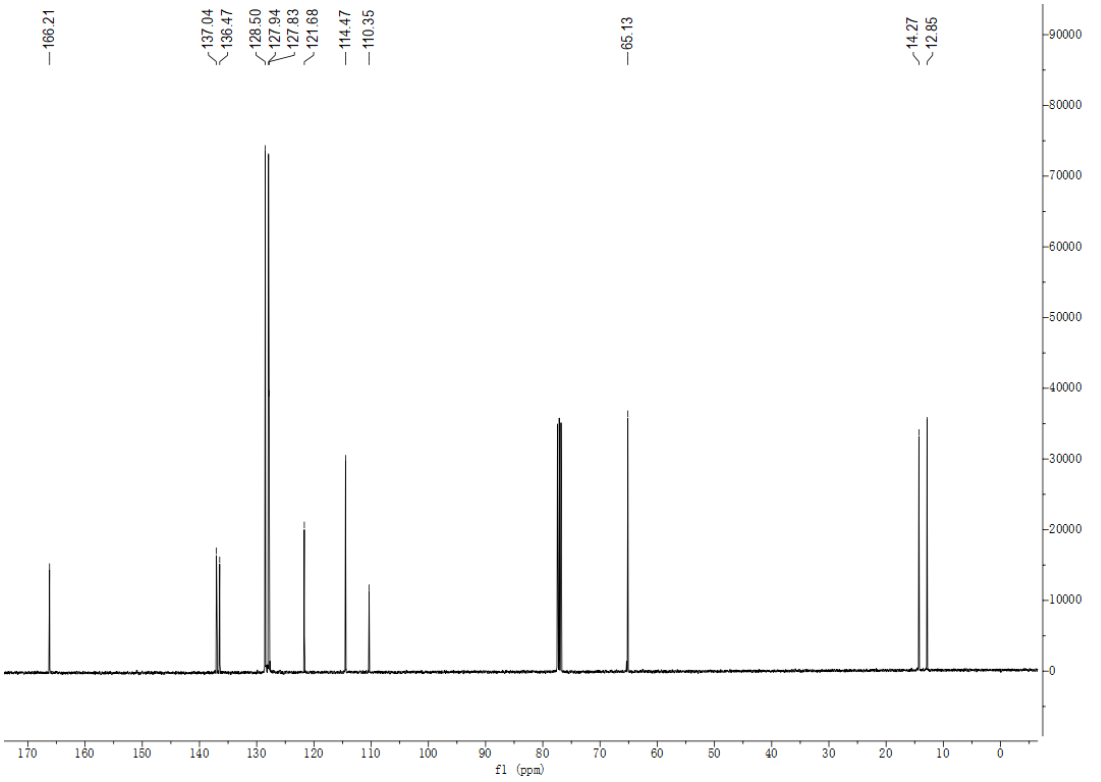

2,4-Dimethyl-1H-pyrrole-3-carboxylic acid (S42)

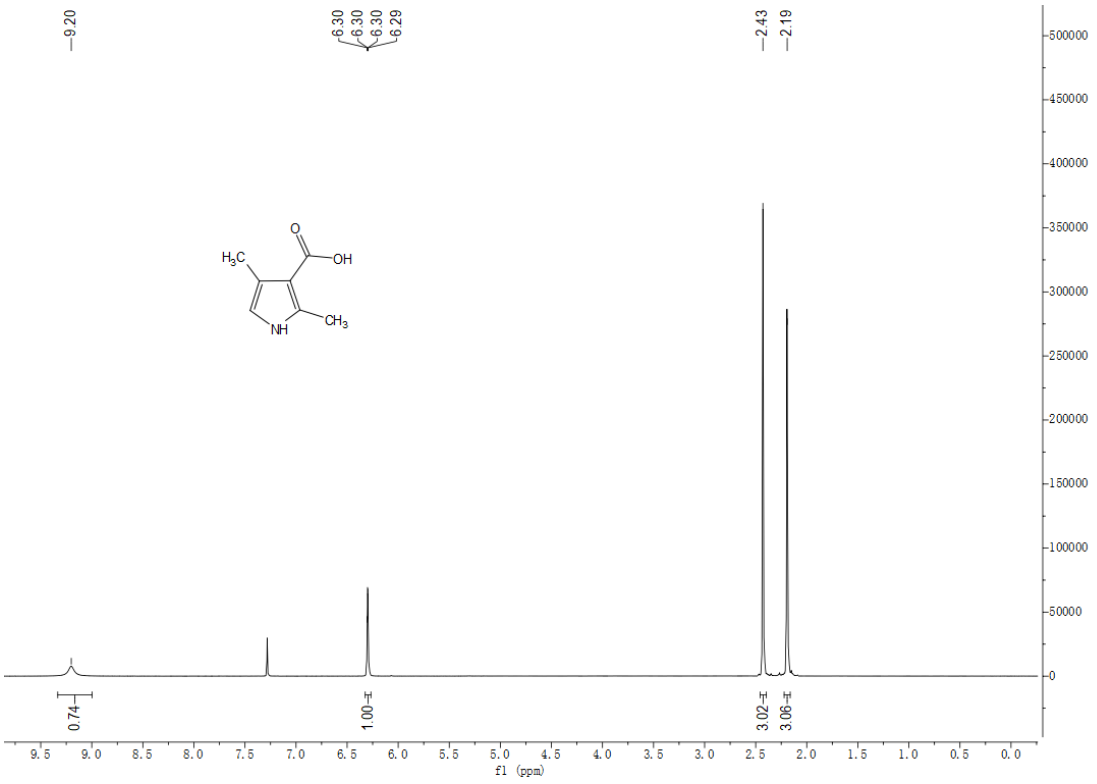

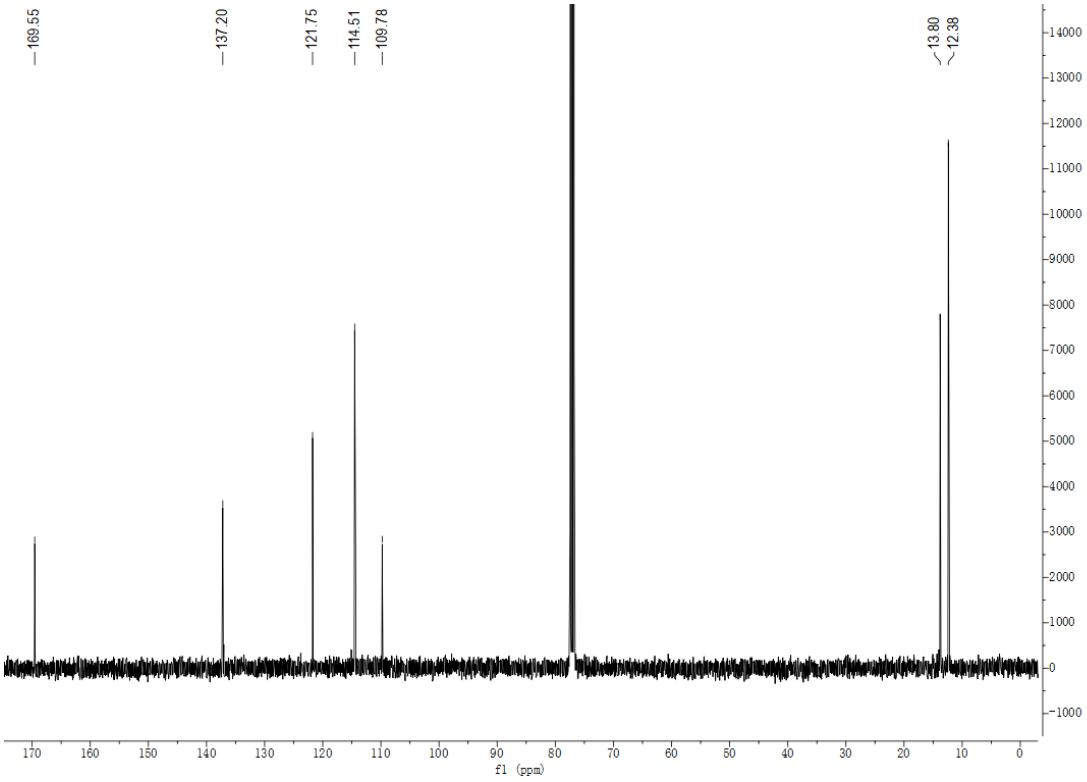

2,4-Dimethyl-N-(prop-2-yn-1-yl)-1H-pyrrole-3-carboxamide (S43)

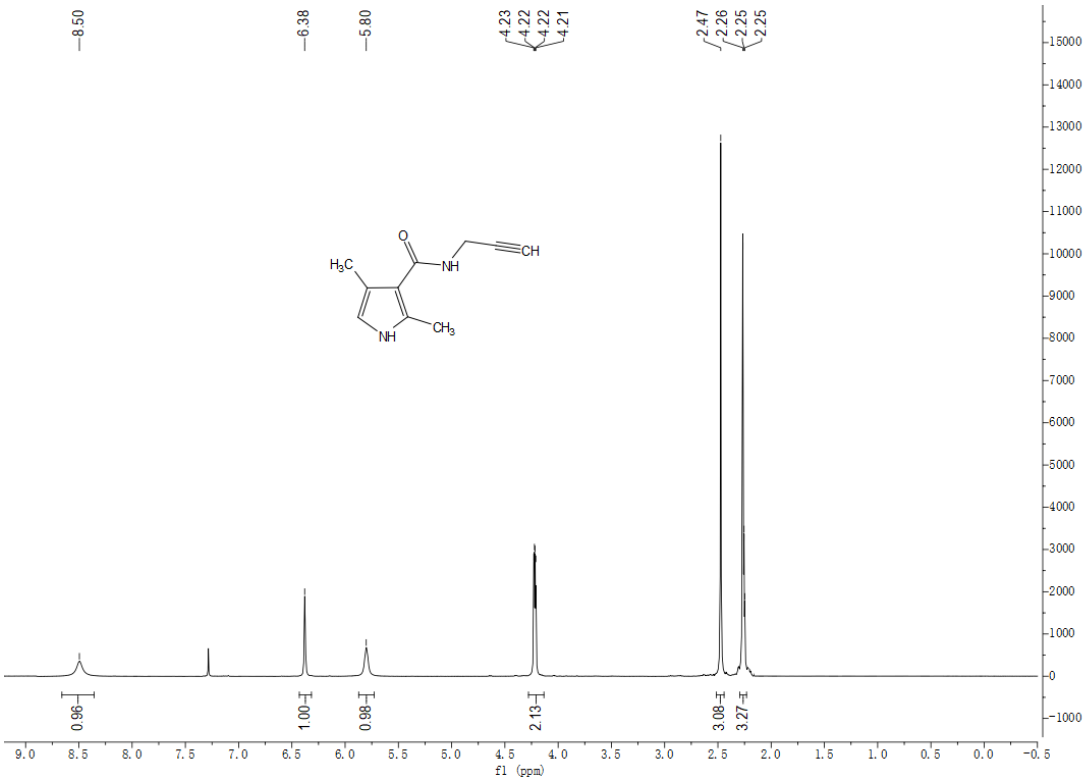

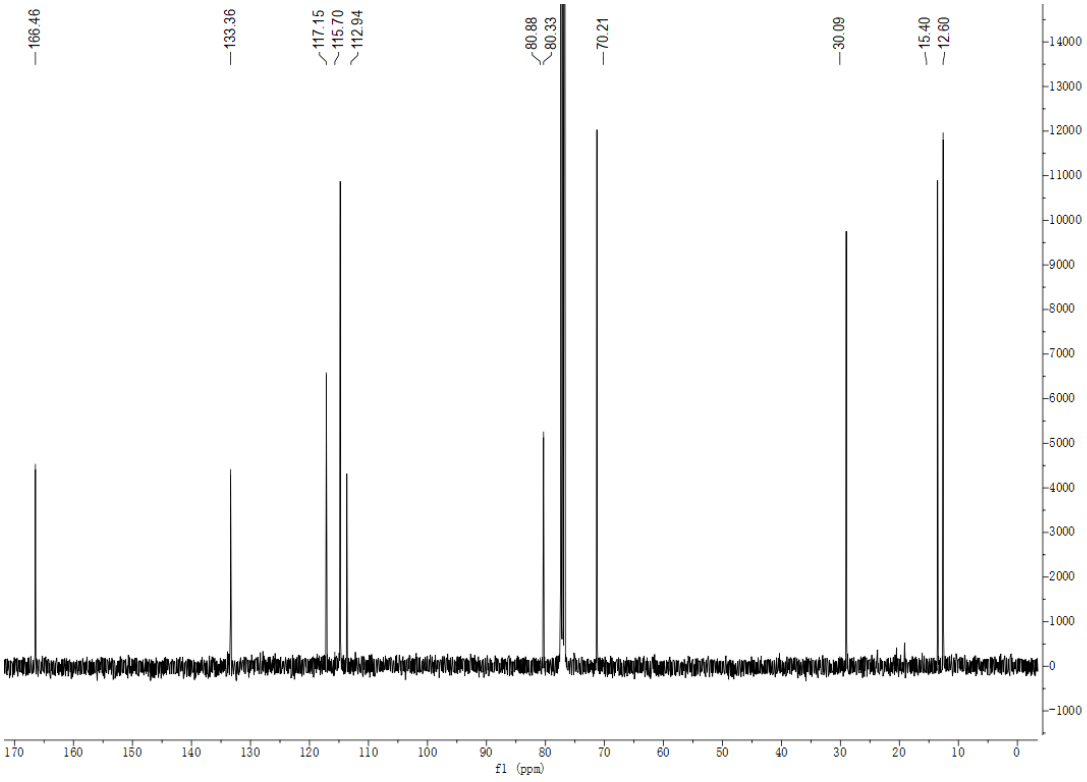

2,4-Dimethyl-5-(4-nitrobenzoyl)-N-(prop-2-yn-1-yl)-1H-pyrrole-3-carboxamide (S44)

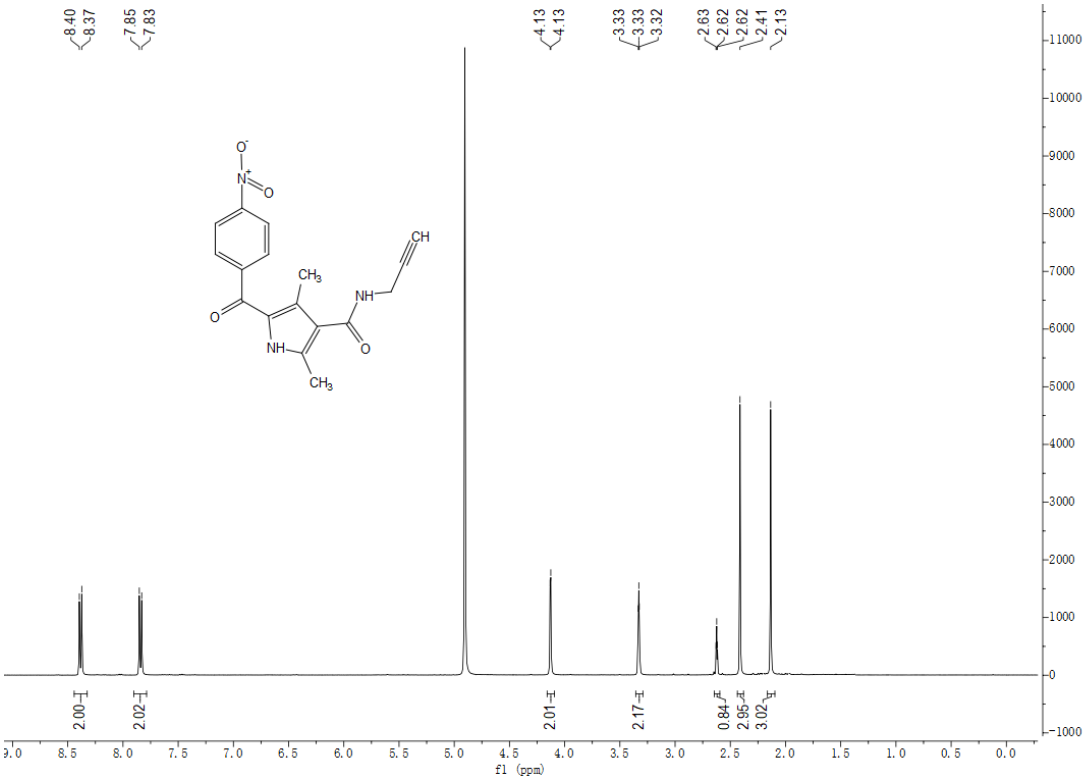

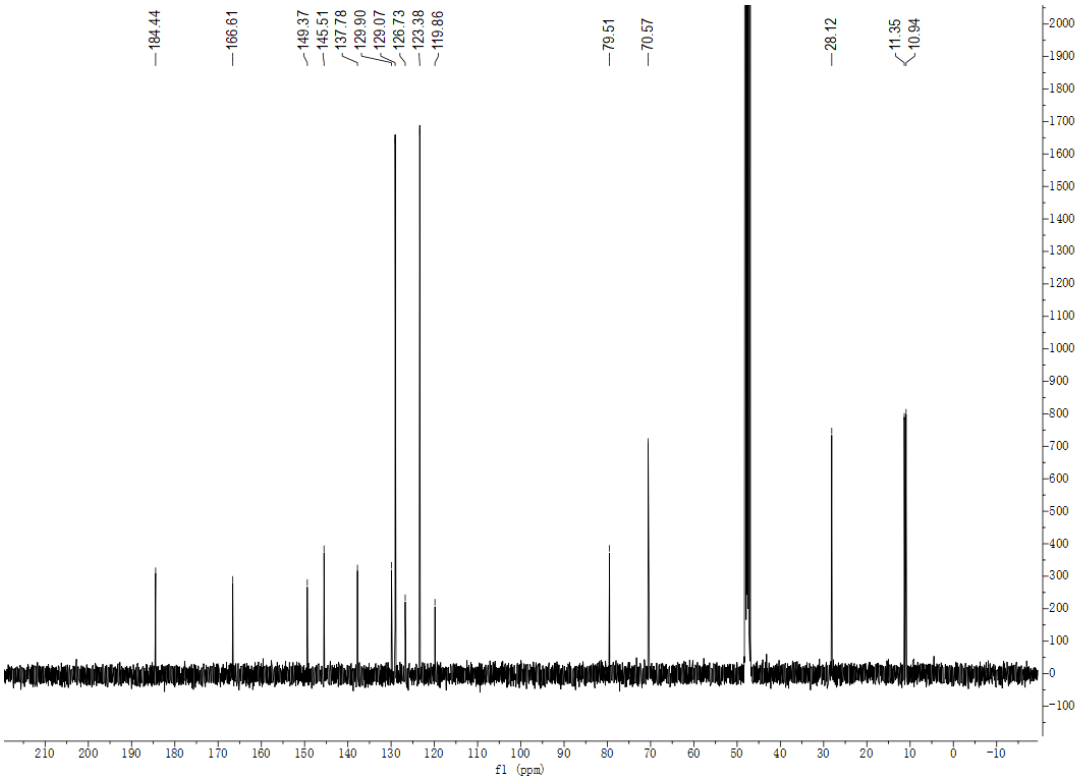

(E)-N-allyl-1-phenylethan-1-imine (S46)

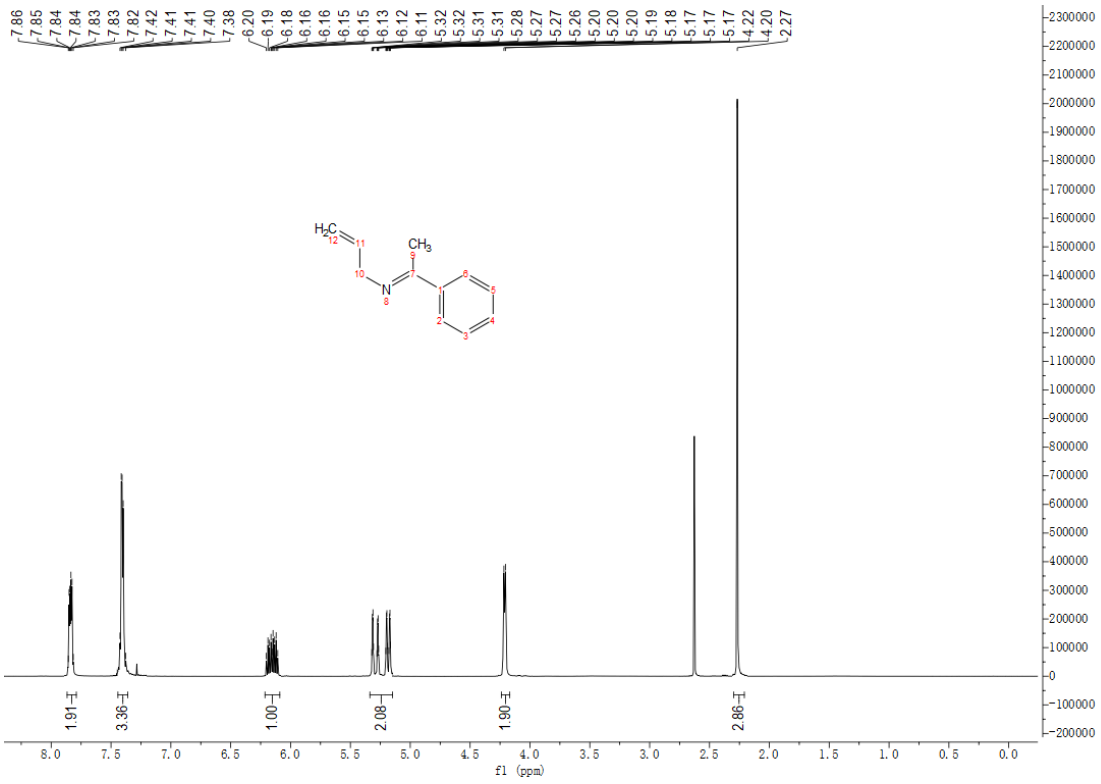

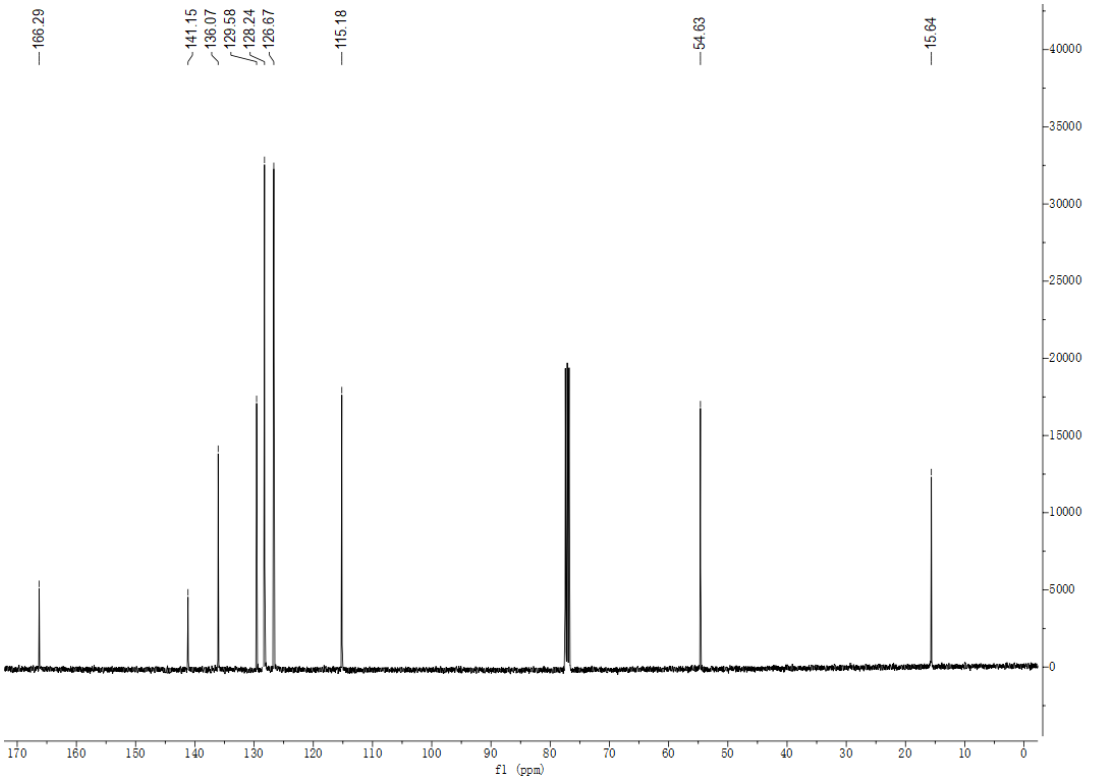

4-Methyl-2-phenyl-1H-pyrrole (S47)

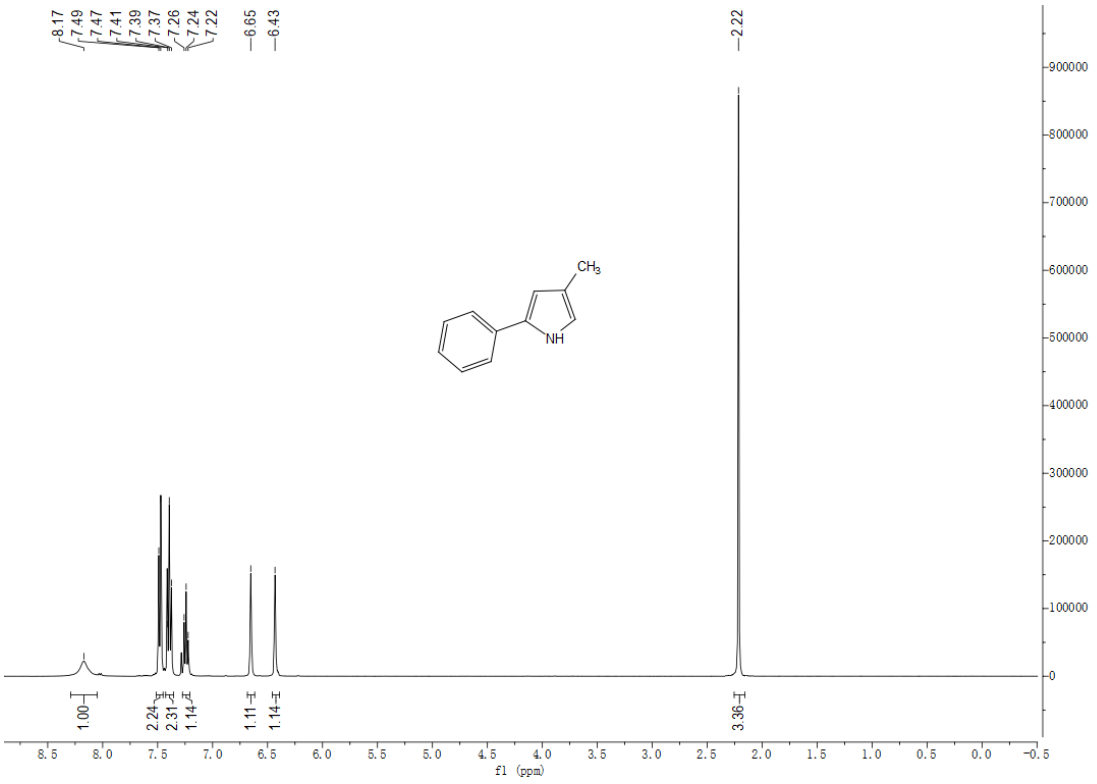

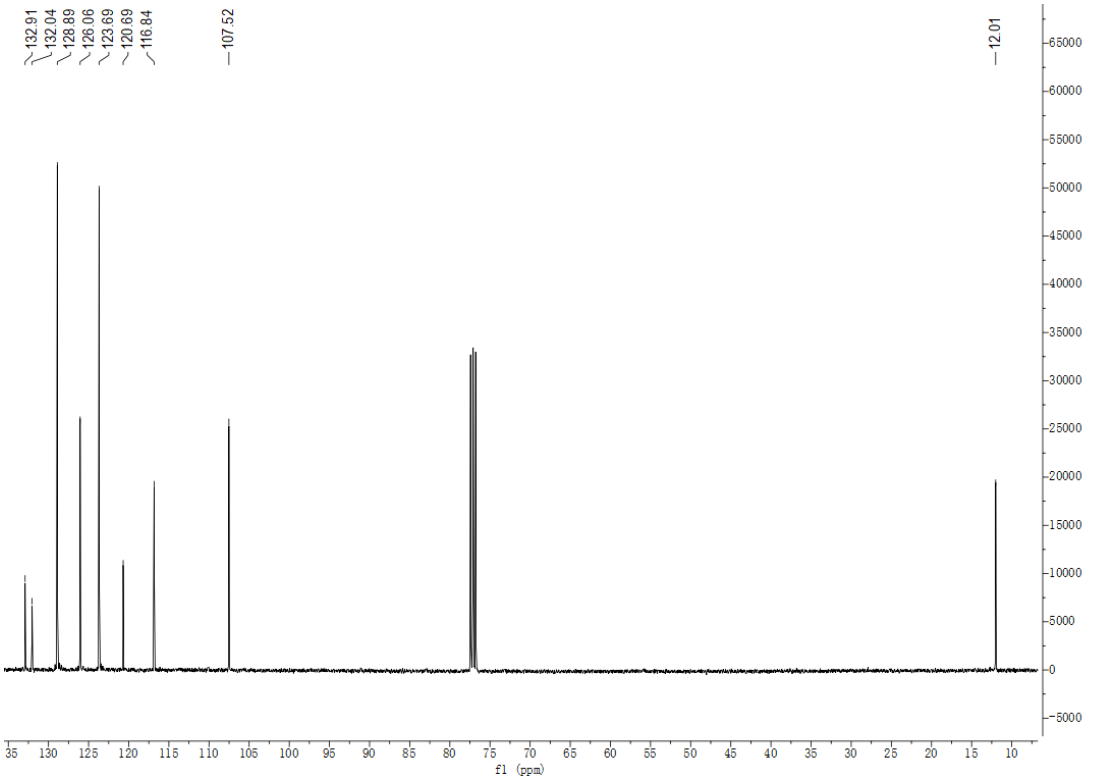

(3-Methyl-5-phenyl-1H-pyrrol-2-yl)(4-nitrophenyl)methanone (S48)

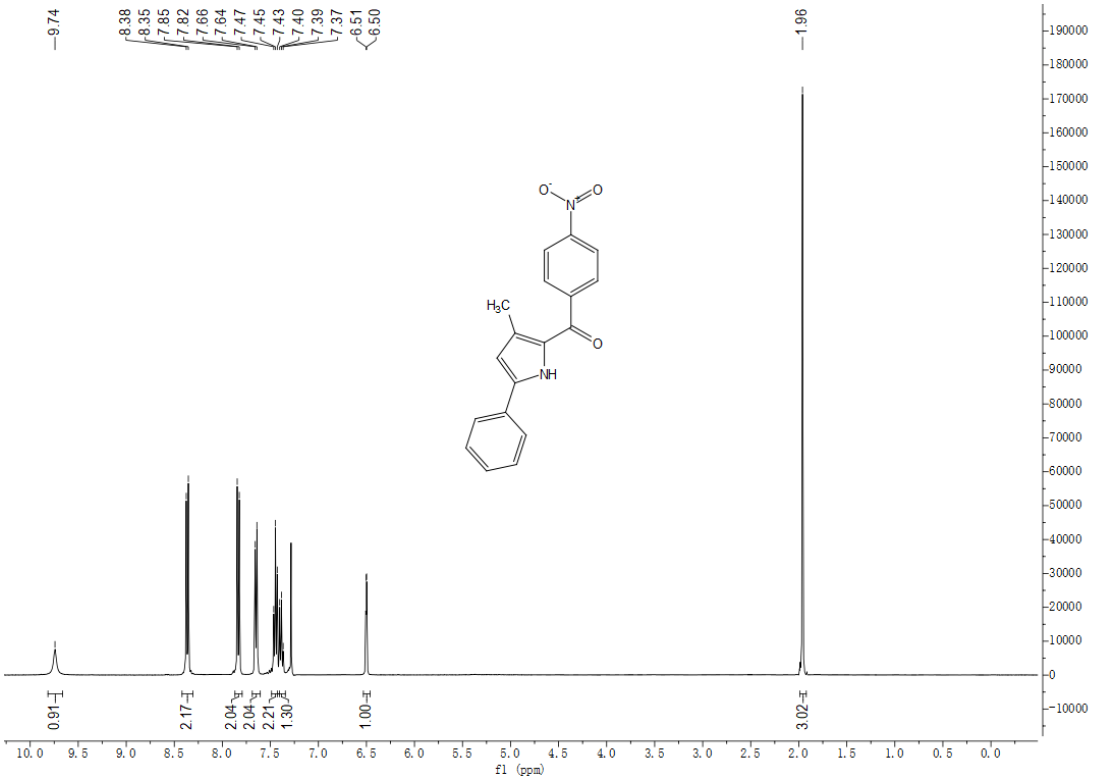

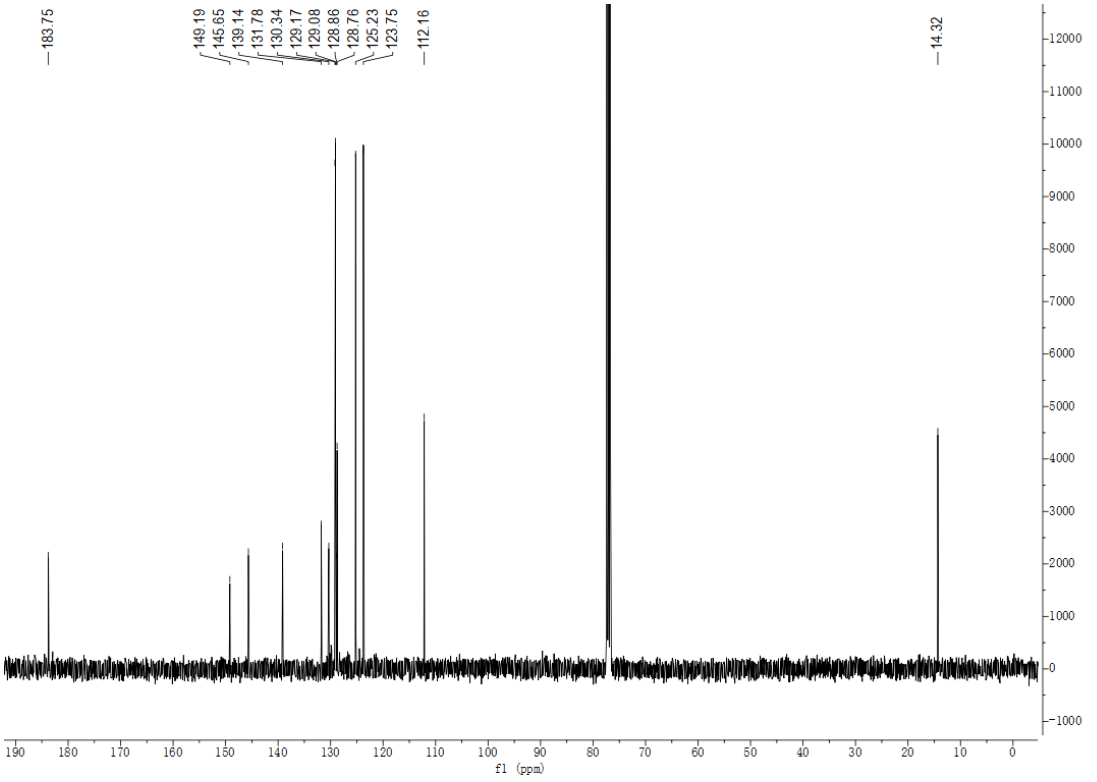

1,3,7-Trimethyl-5-phenyl-8-(4-nitrophenyl)-BODIPY (S49)

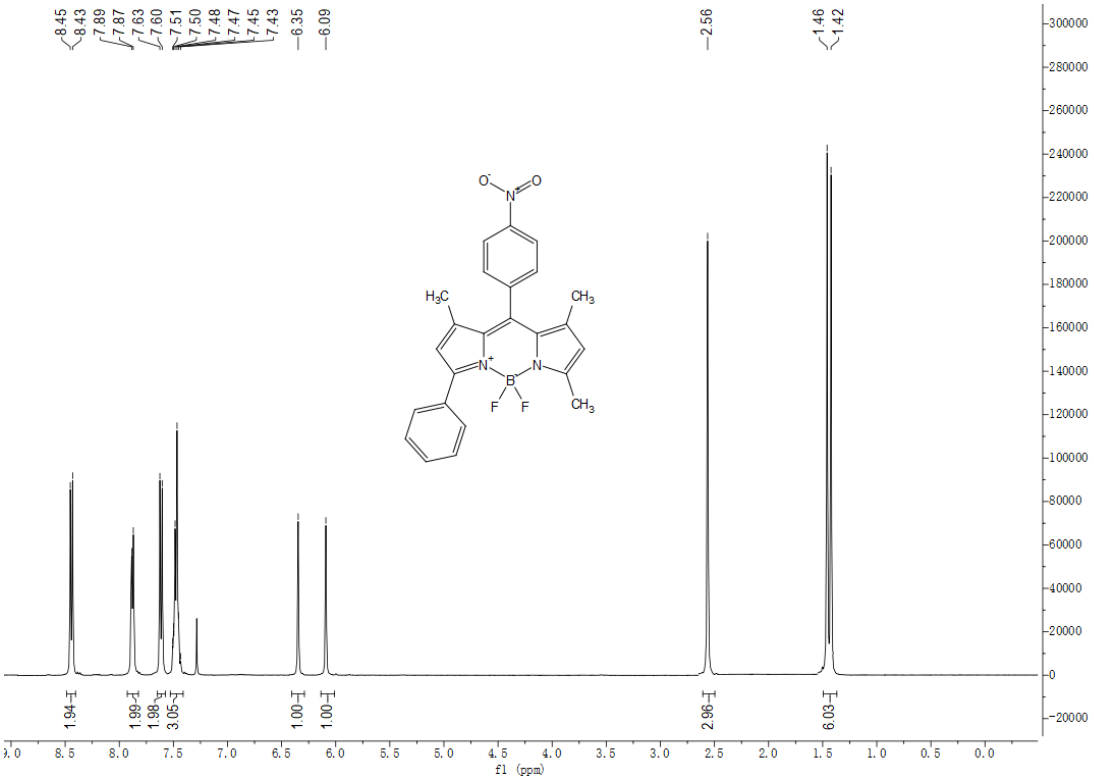

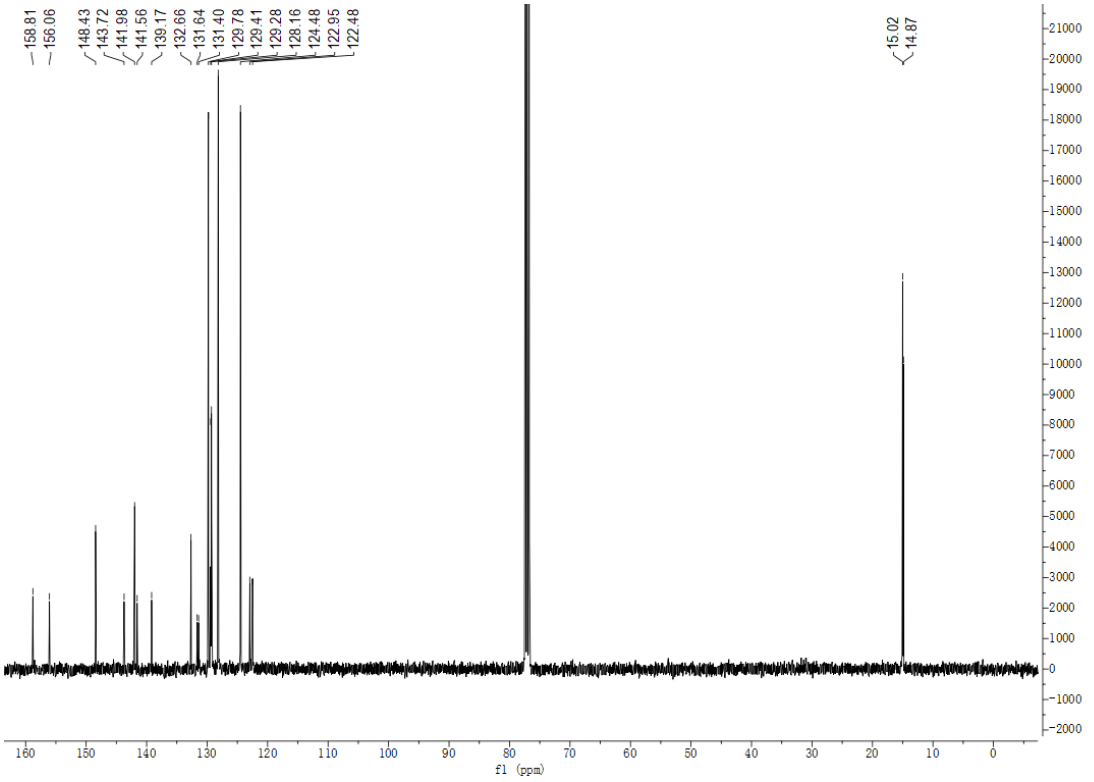

(4-Nitrophenyl)(1H-pyrrol-2-yl)methanone (S50)

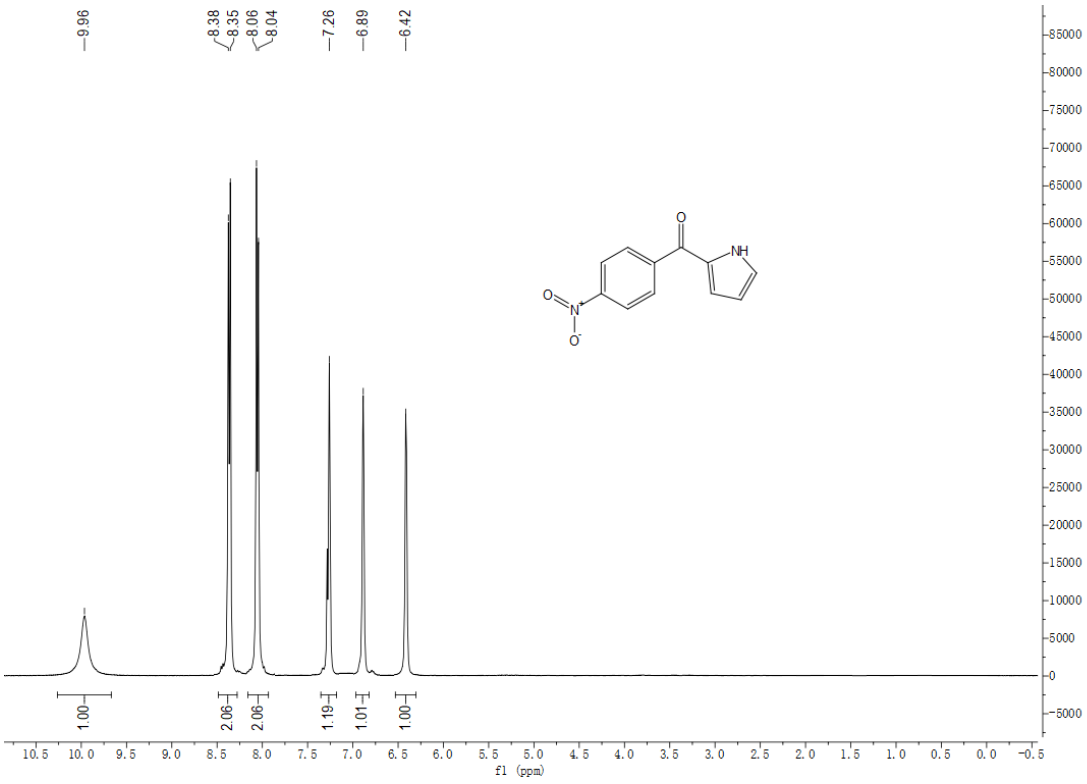

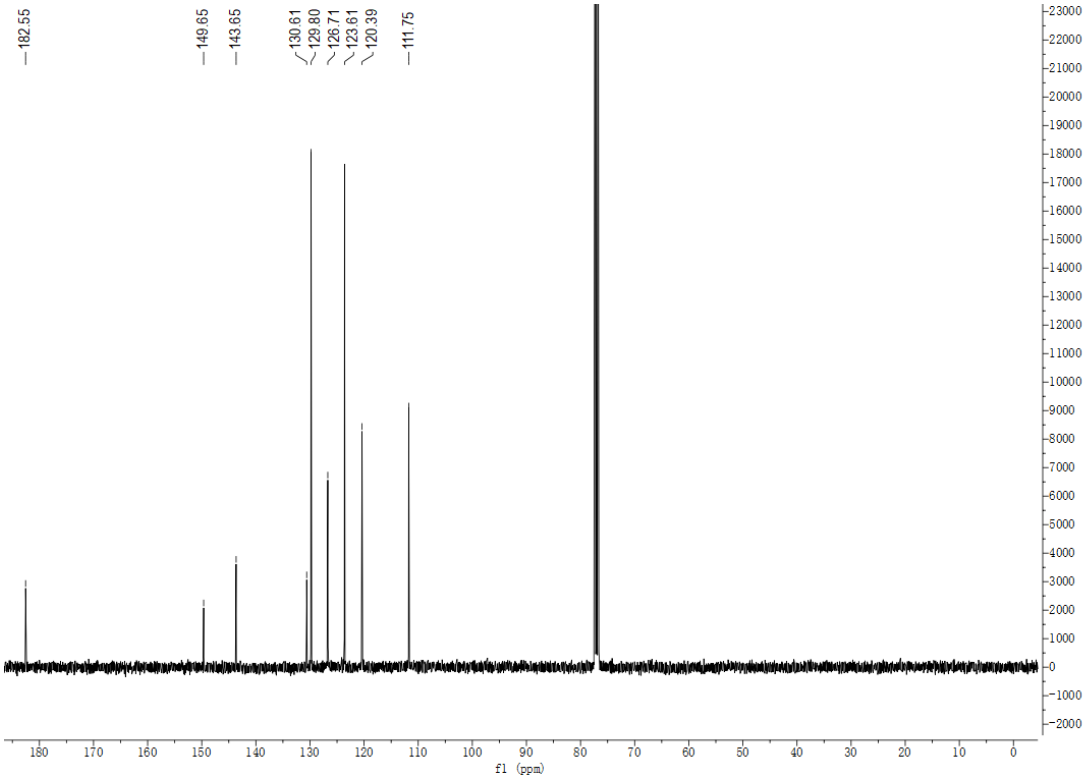

1,3-Dimethyl-8-(4-nitrophenyl)-BODIPY (S51)

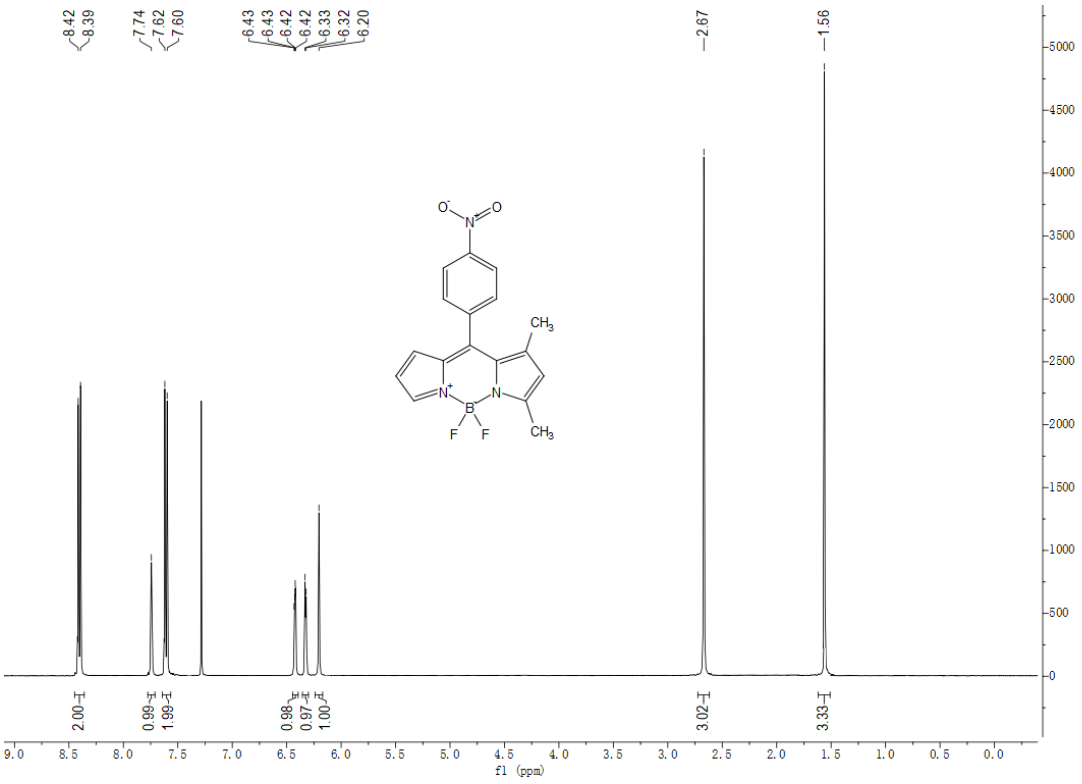

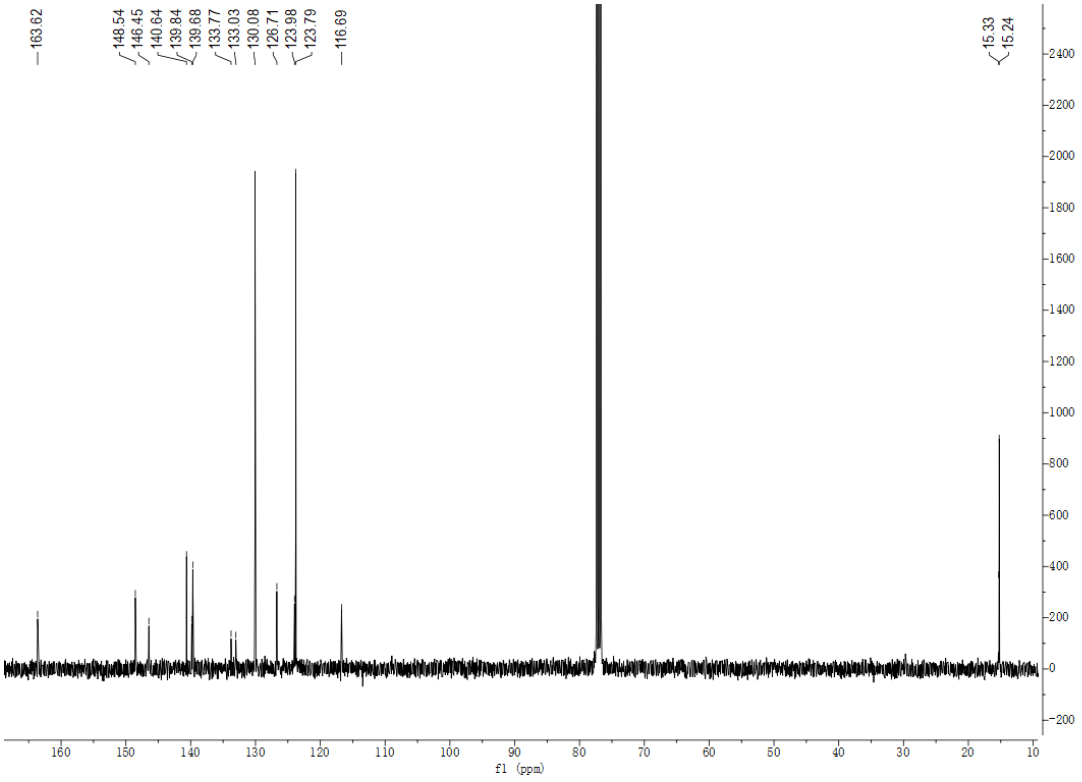

Hex-5-yn-1-yl 4-methylbenzene-1-sulfonate (S52)

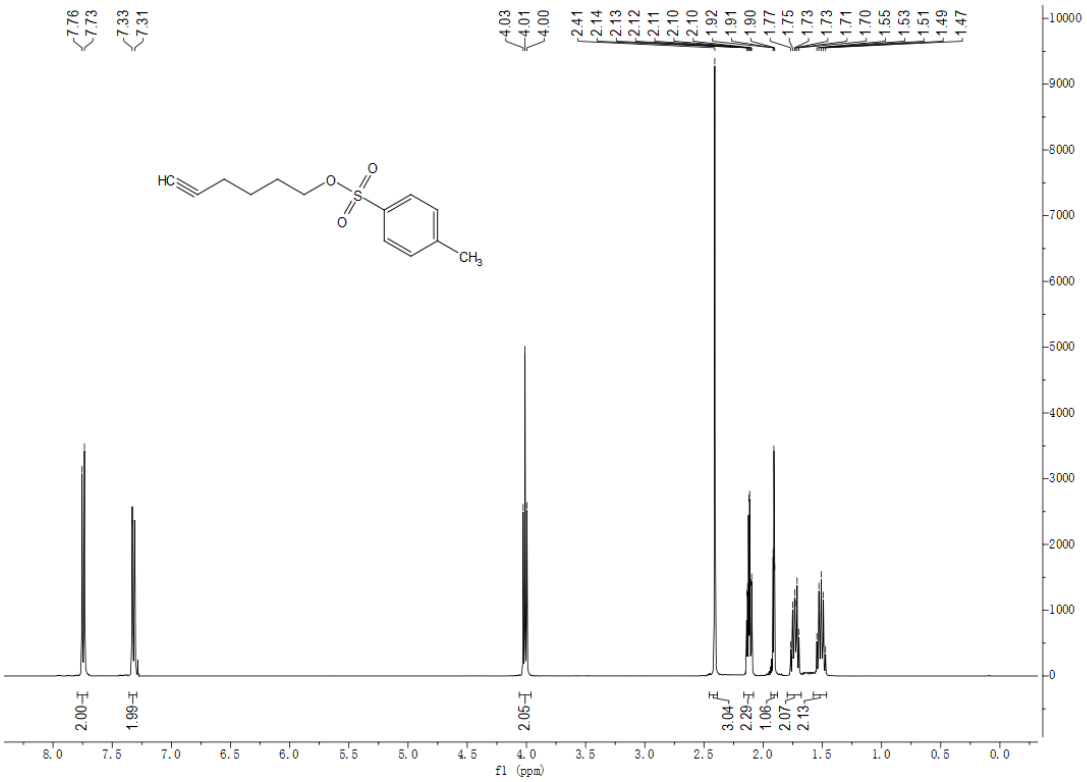

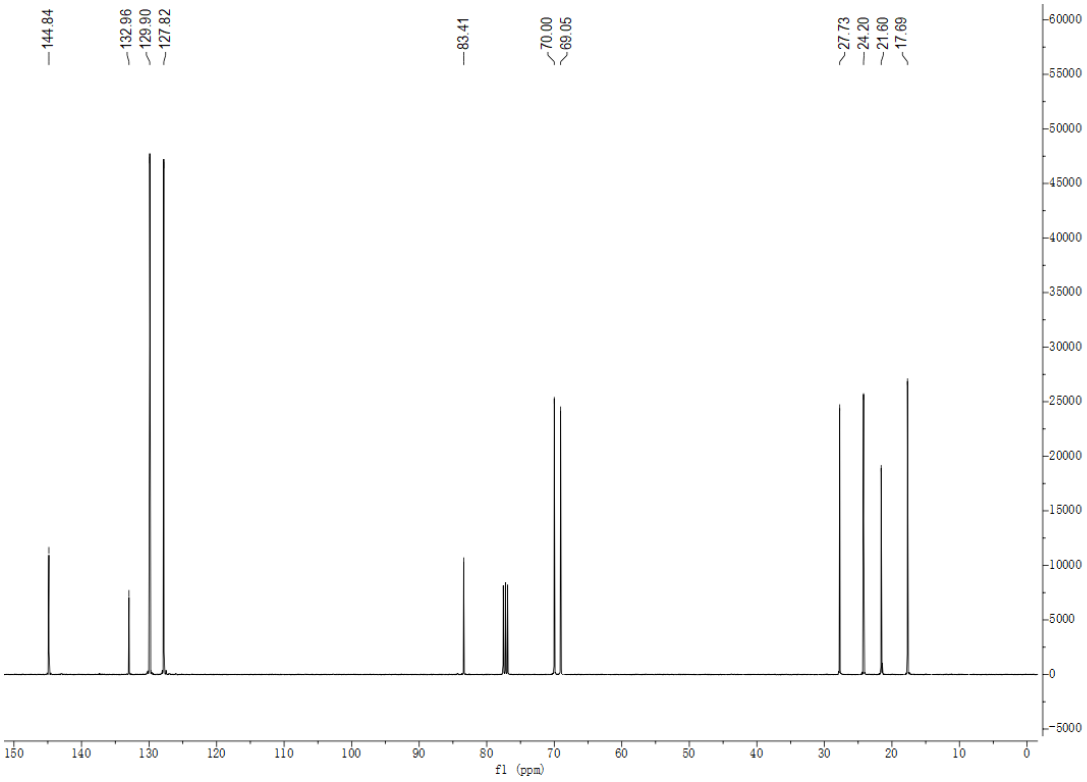

2-(Hex-5-yn-1-yl)isoindoline-1,3-dione (S53)

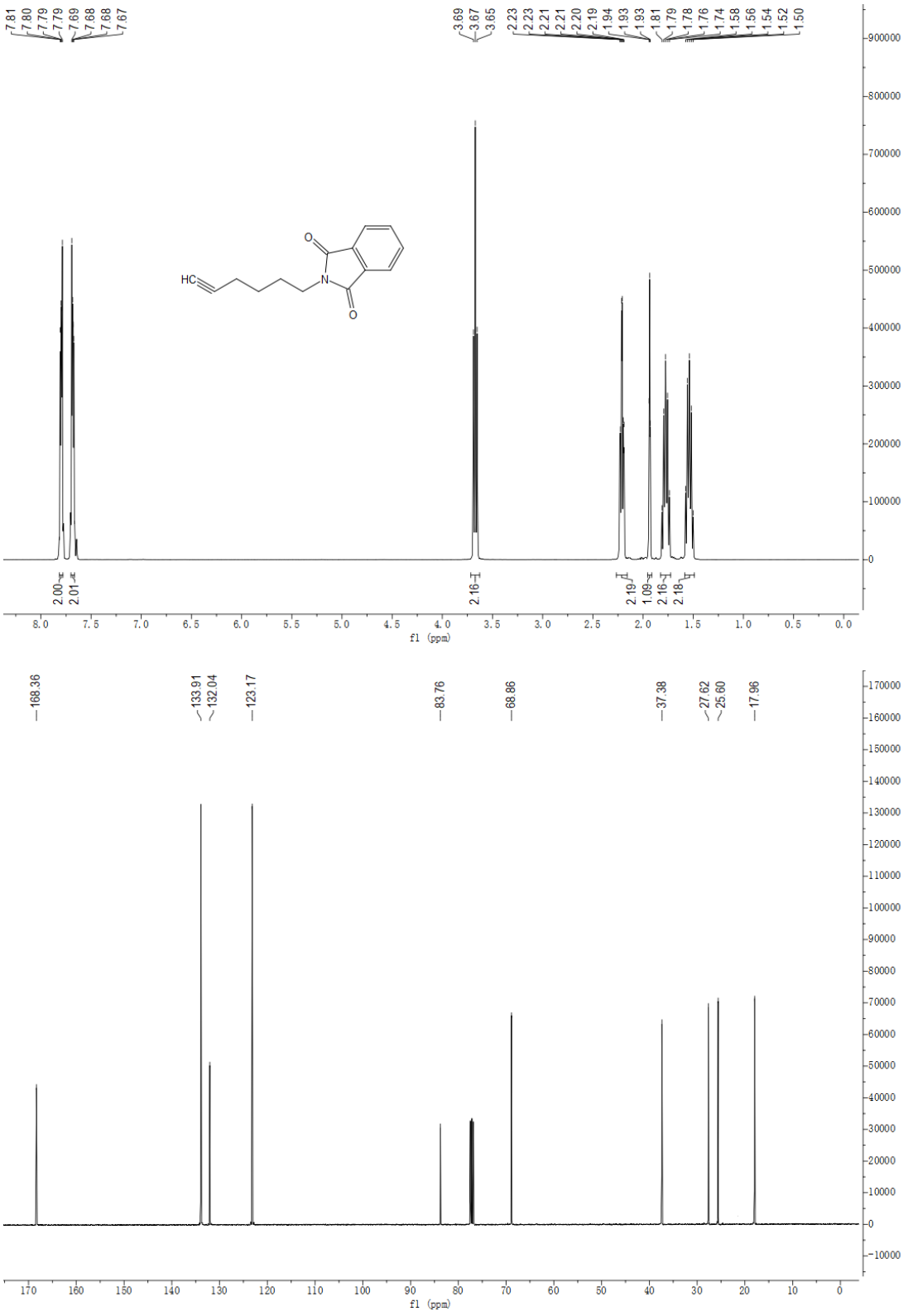

Tert-butyl (6-hydroxyhexyl)carbamate (S55)

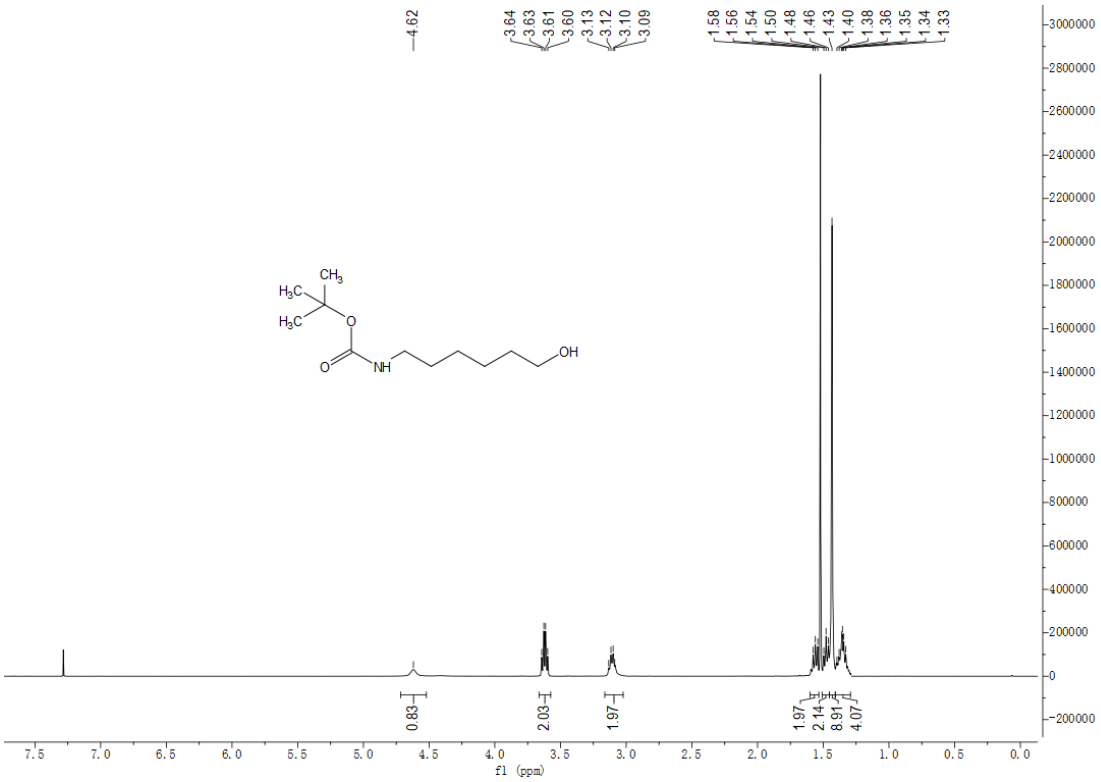

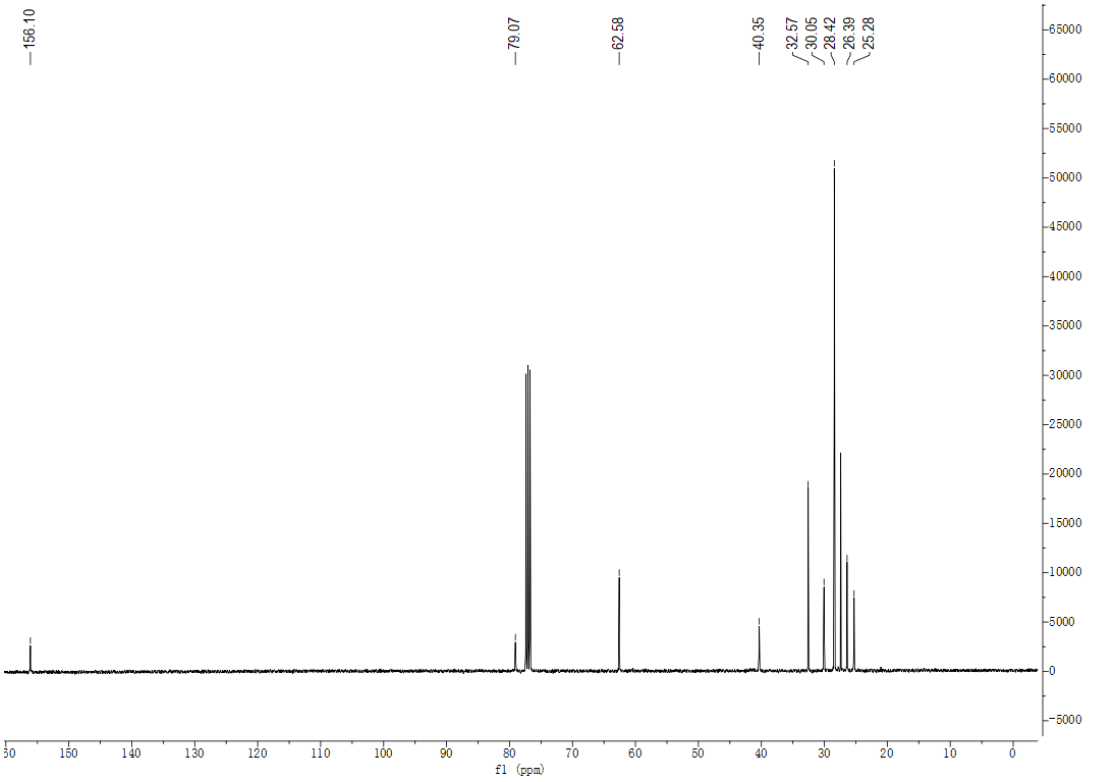

Tert-butyl (6-iodohexyl)carbamate (S56)

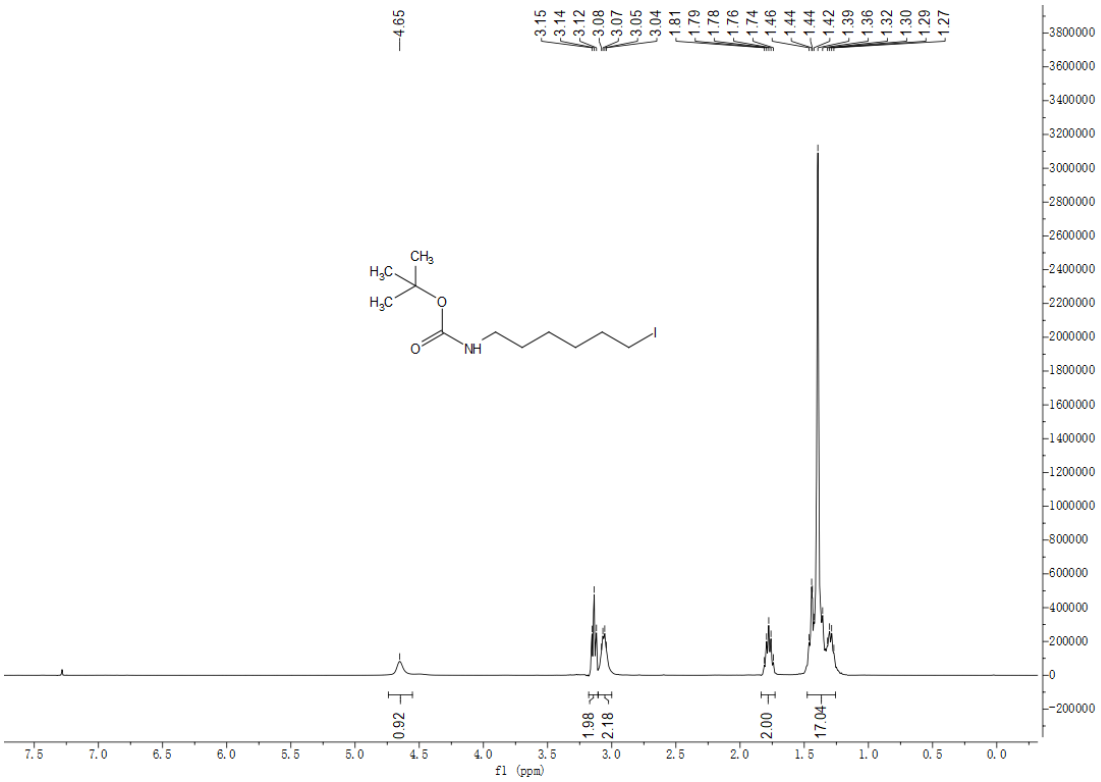

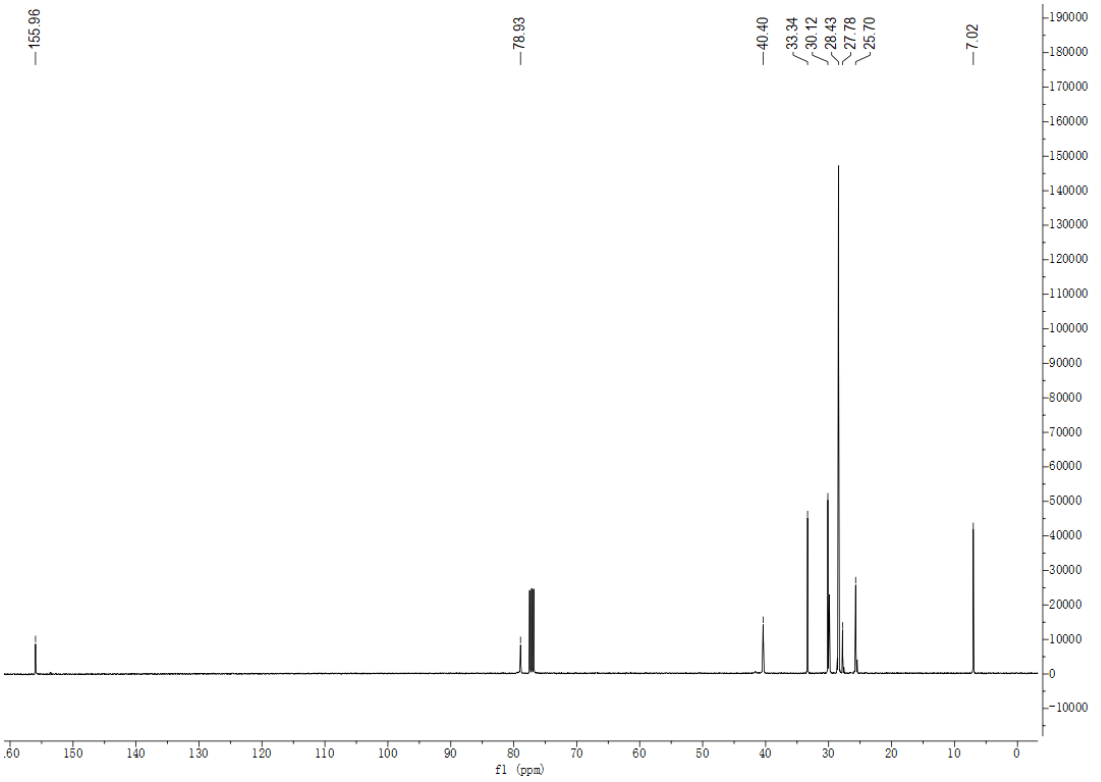

Tert-butyl (6-(hex-5-yn-1-yloxy)hexyl)carbamate (S57)

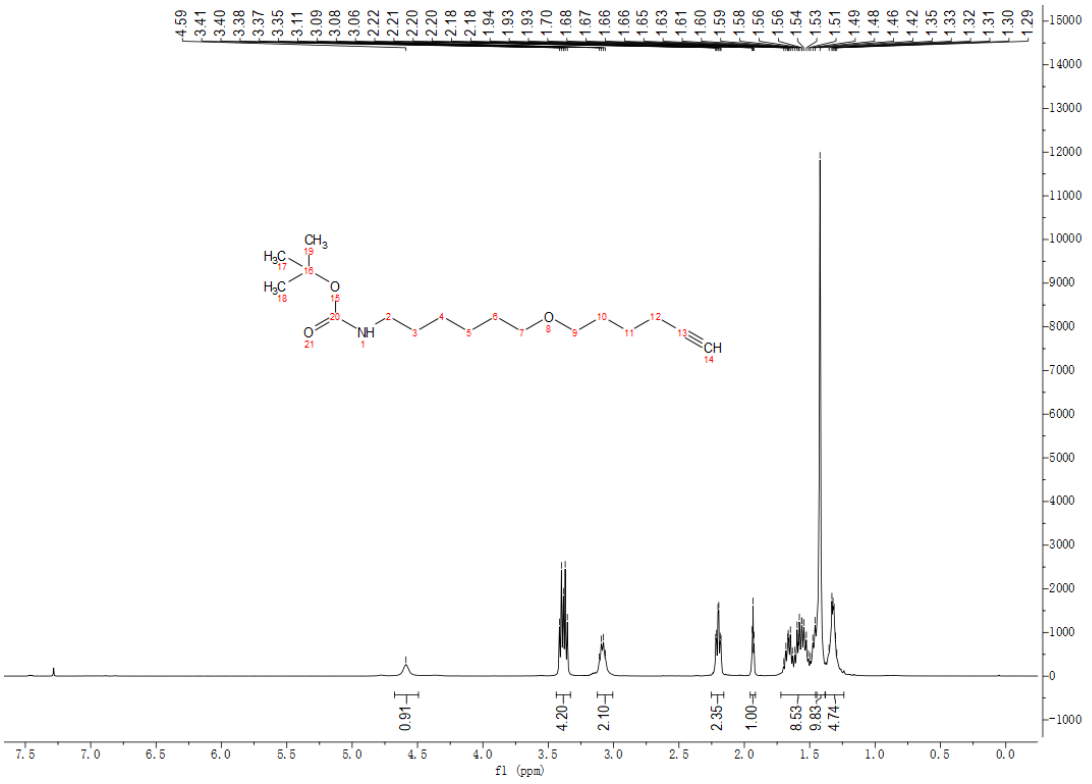

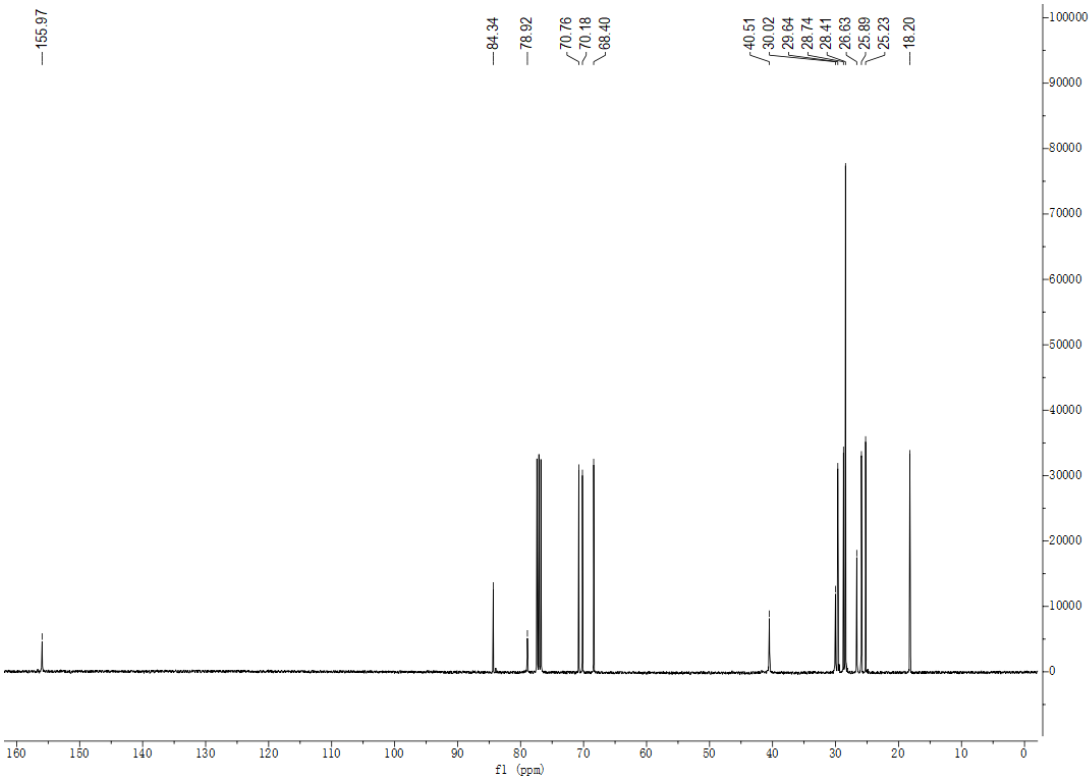

6-(Hex-5-yn-1-yloxy)hexan-1-amine (S58)

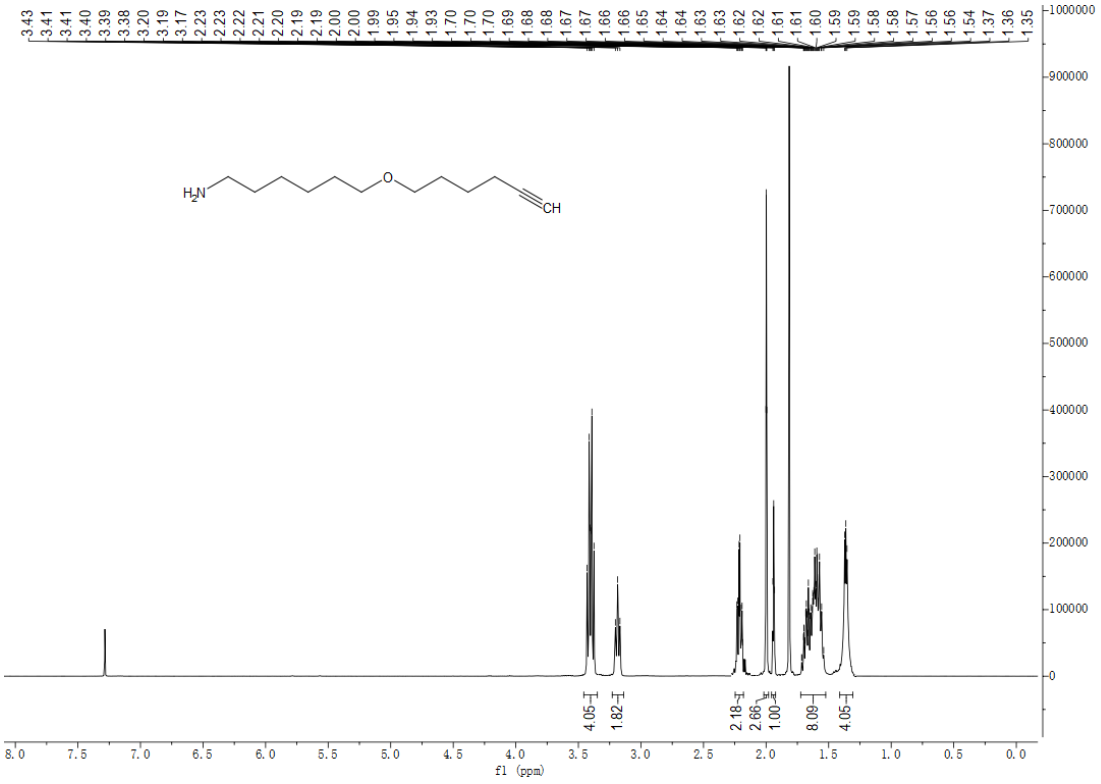

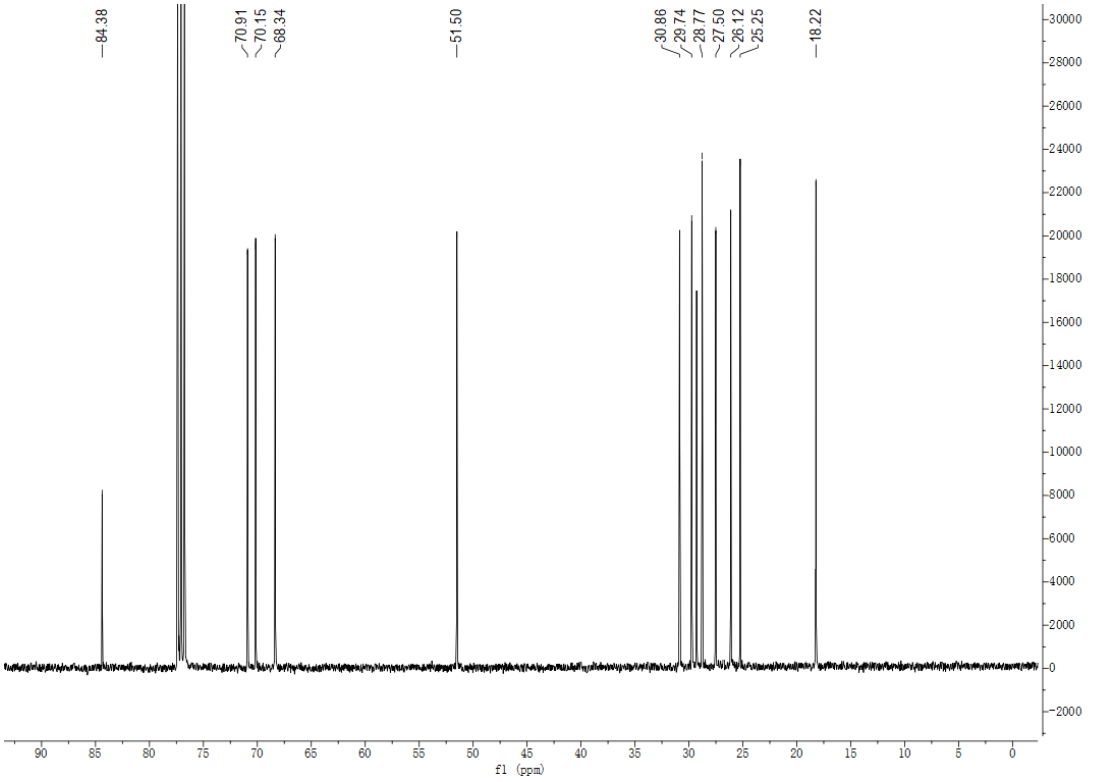

1,6-Diazidohexane (S59)

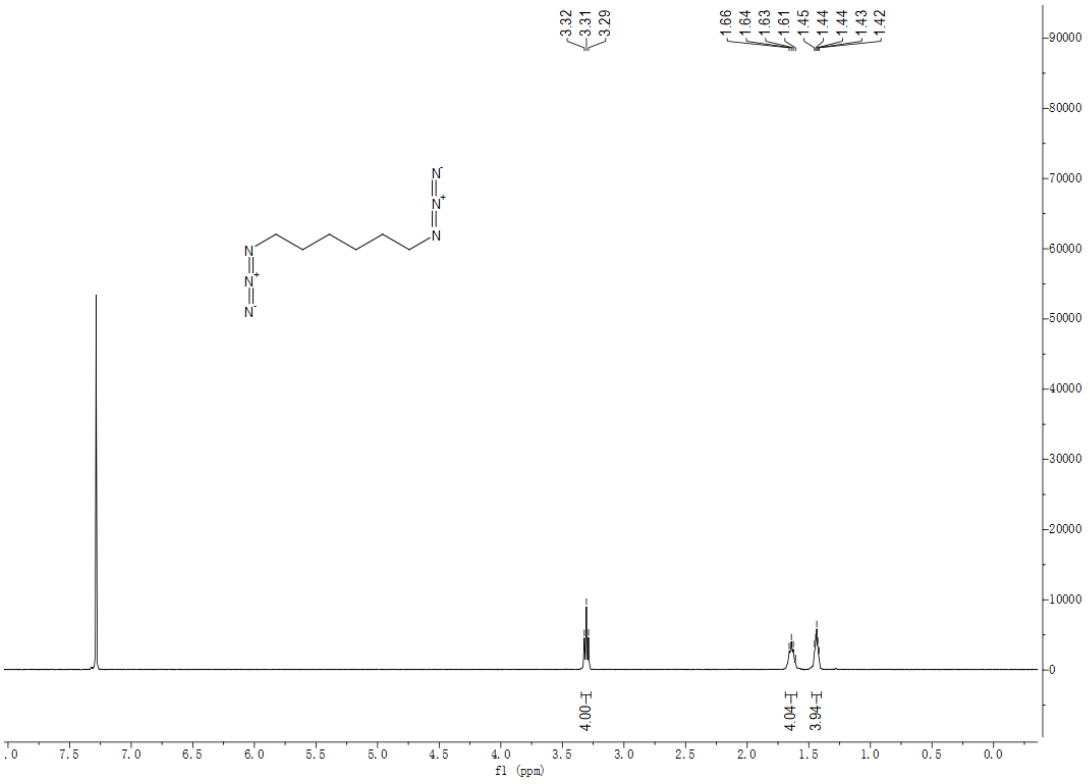

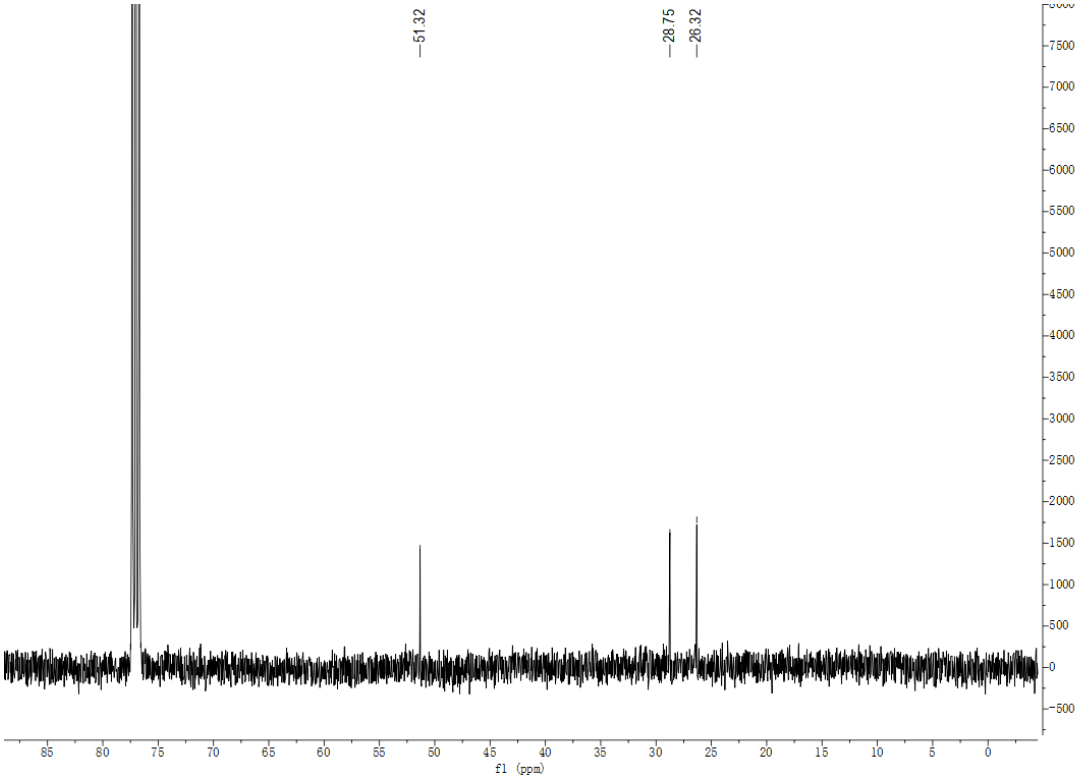

6-Azidohexan-1-amine (S60)

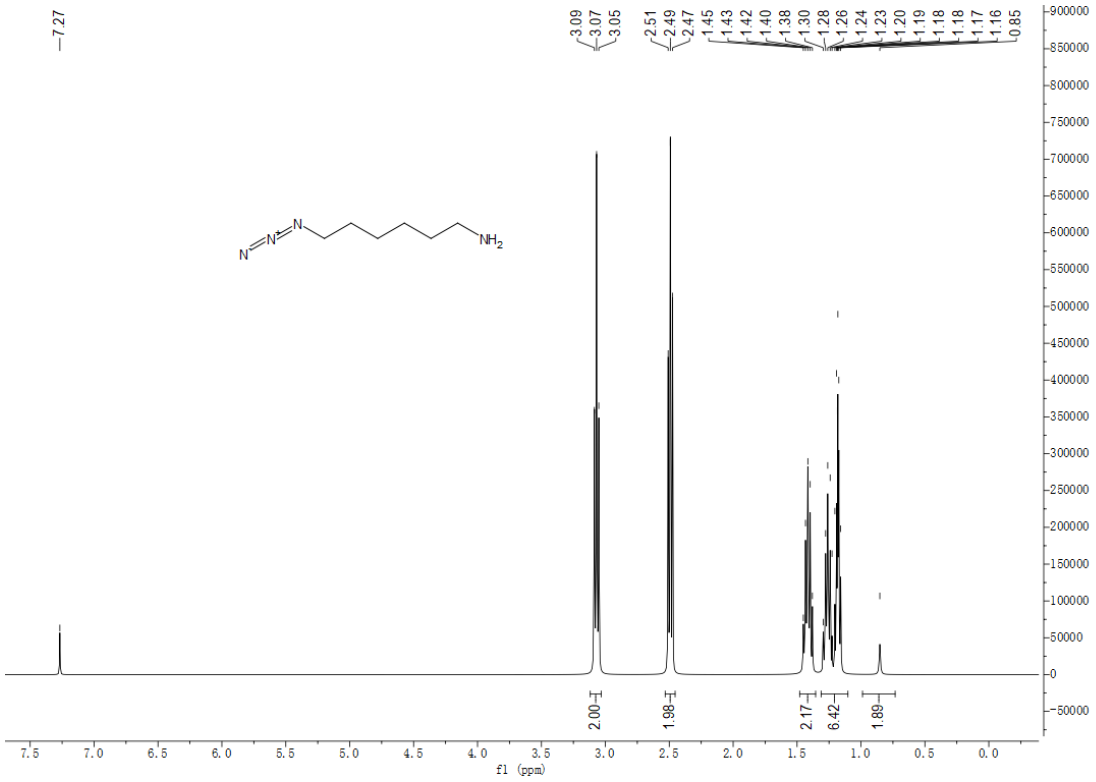

2-(2-{2-[2-(Methanesulfonyloxy)ethoxy]ethoxy}ethoxy)ethyl methanesulfonate (S61)

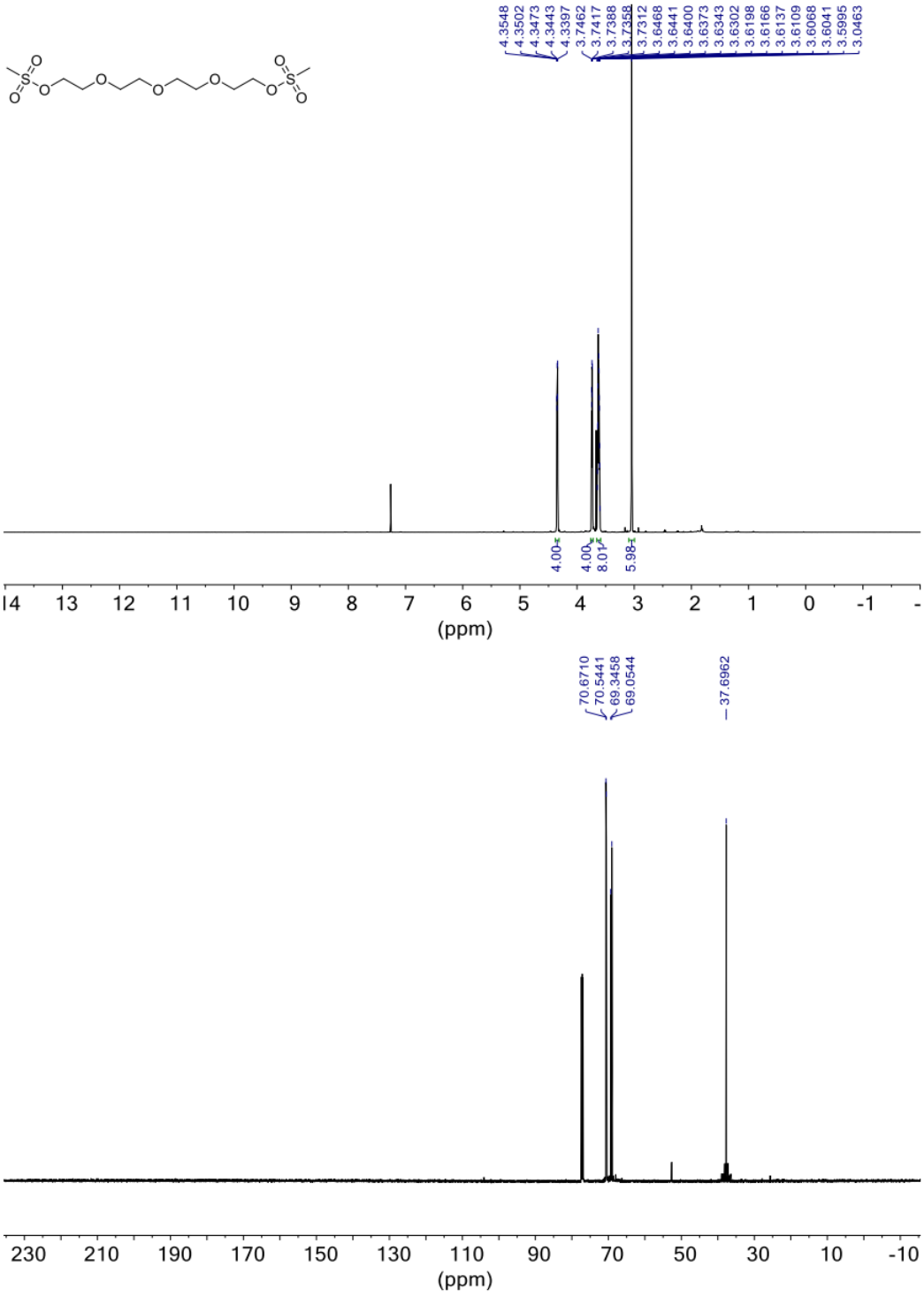

1-Azido-2-(2-(2-(2-azidoethoxy)ethoxy)ethoxy)ethane (S62)

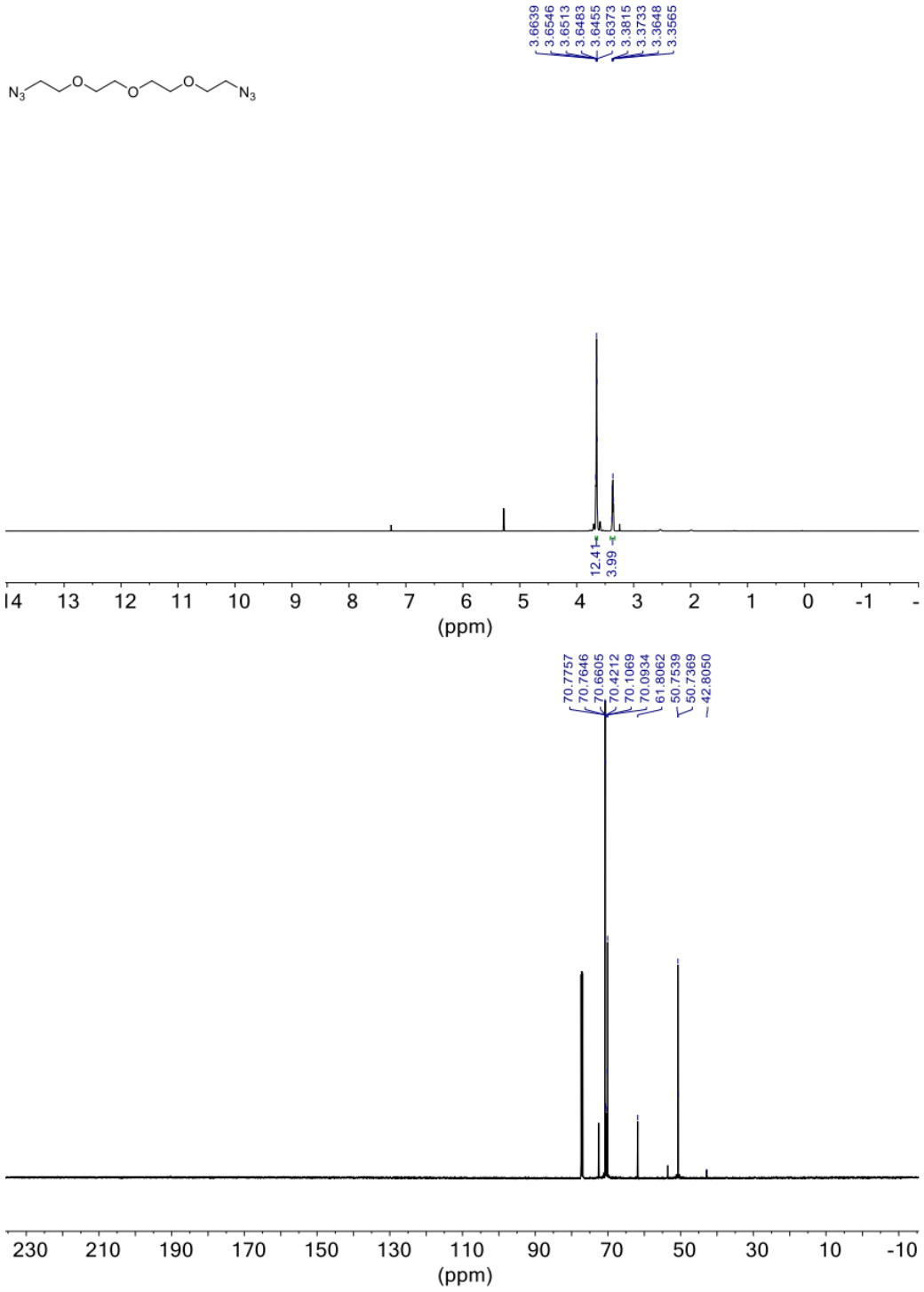

2-(2-(2-(2-Azidoethoxy)ethoxy)ethoxy)ethan-1-amine (S63)

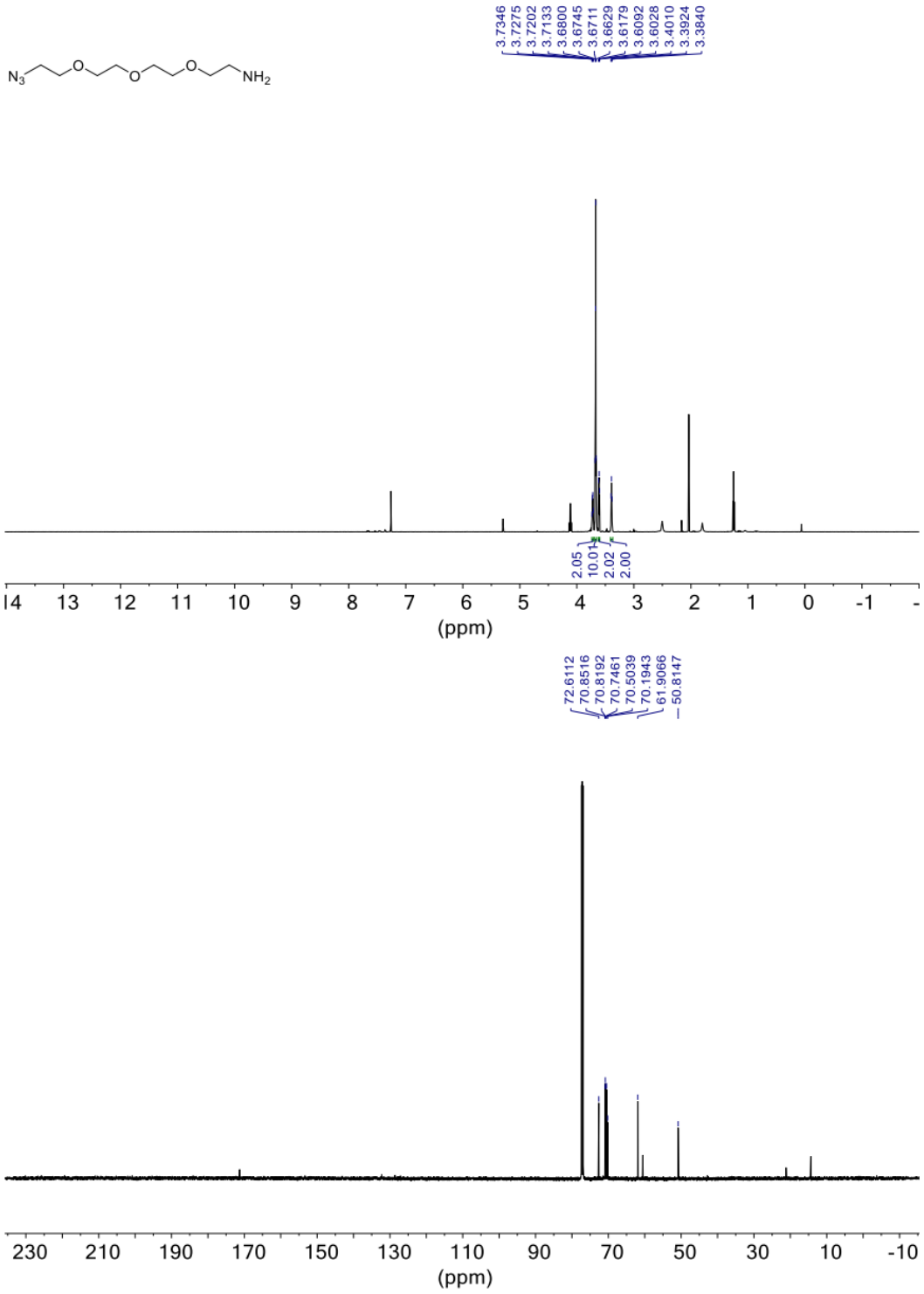

1,7-Dimethyl-3,5-styryl-8-(4-nitrophenyl)-BODIPY (S64)

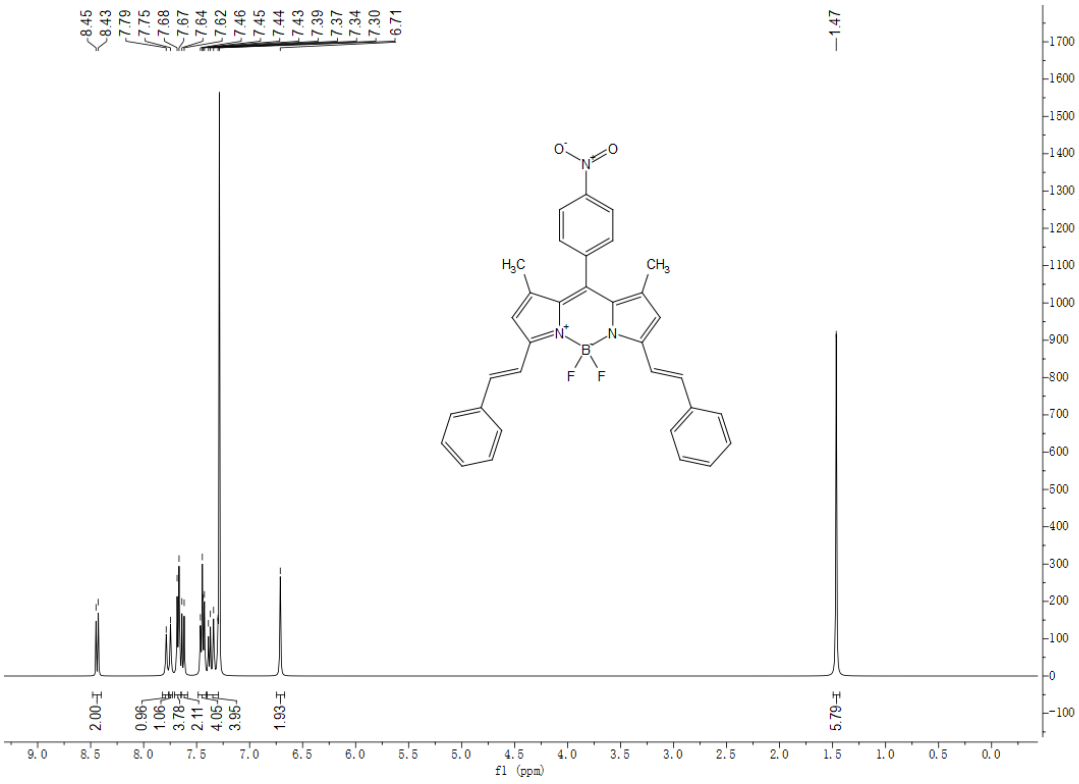

2-(2-(2-Methoxyethoxy)ethoxy)ethyl 4-methylbenzenesulfonate (S66)

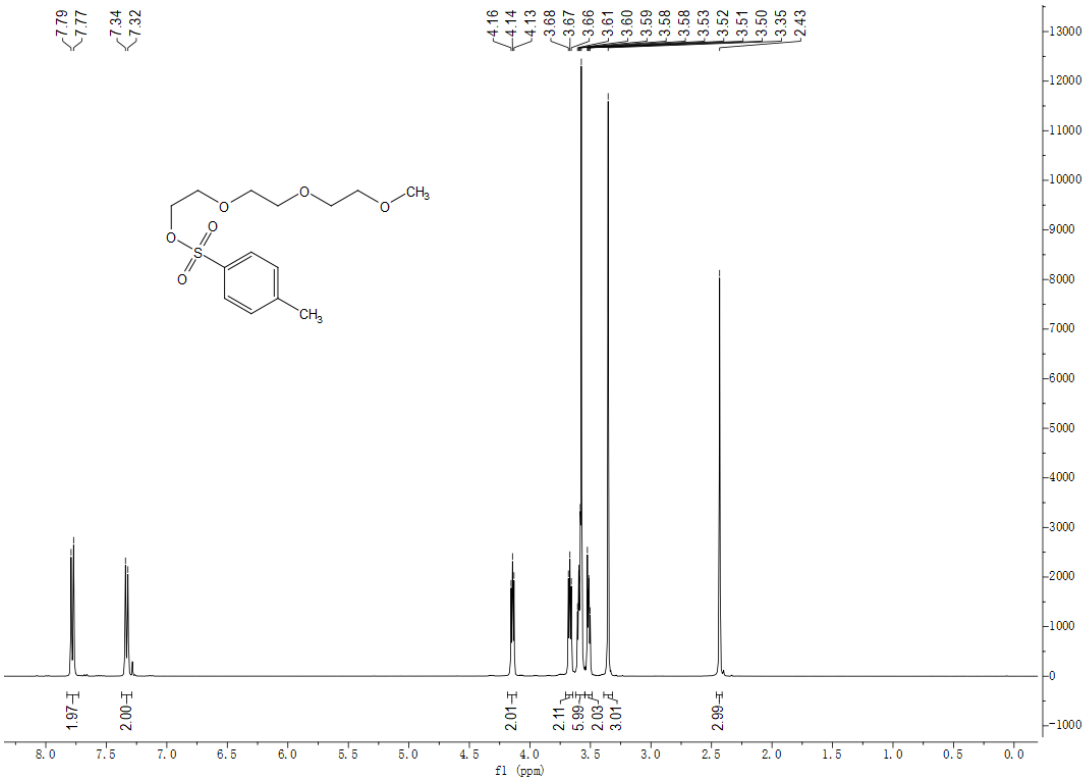

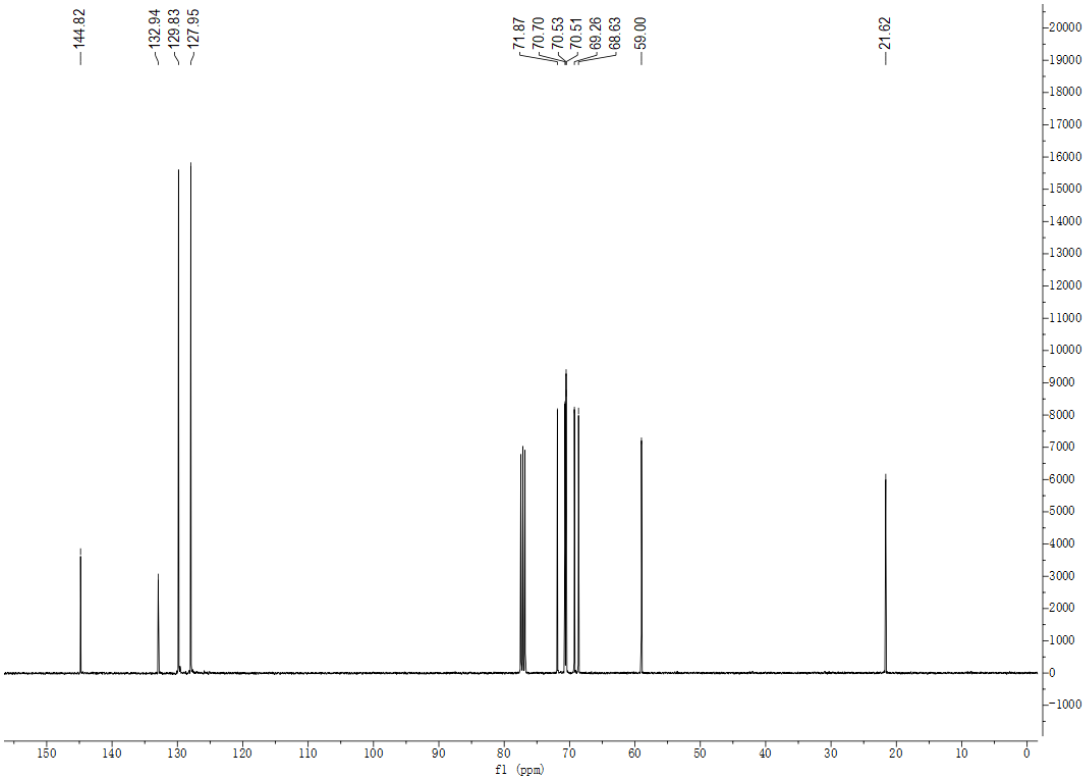

4-(2-(2-(2-Methoxyethoxy)ethoxy)ethoxy)benzaldehyde (S67)

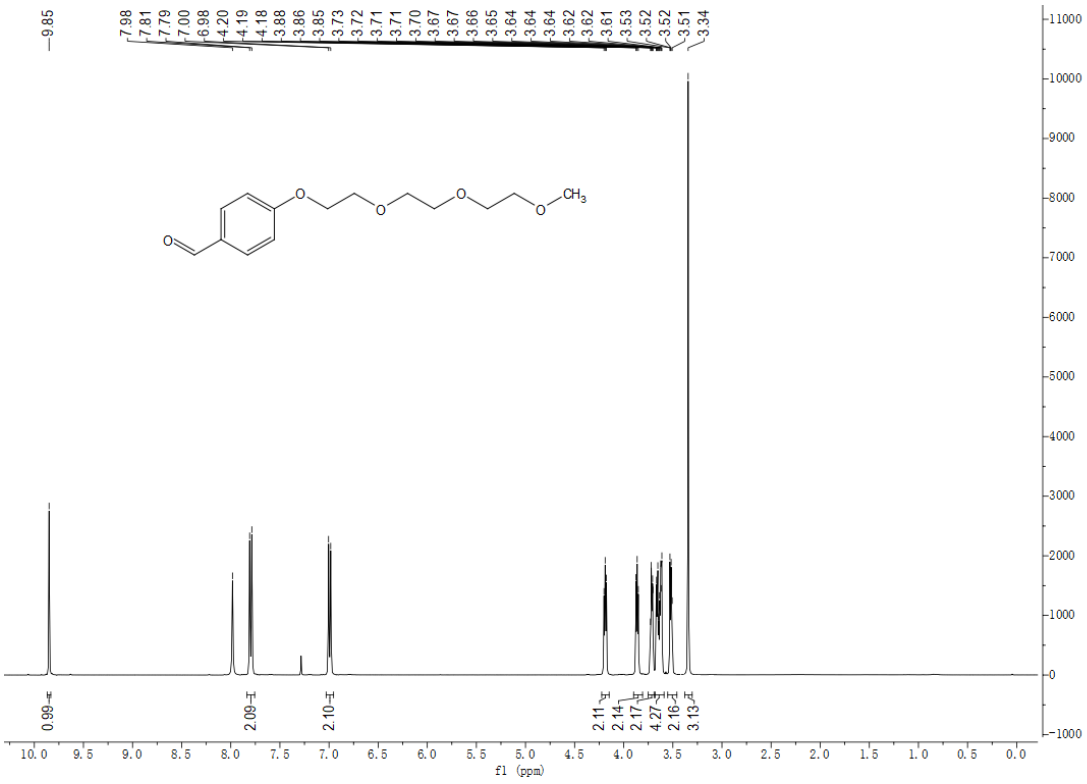

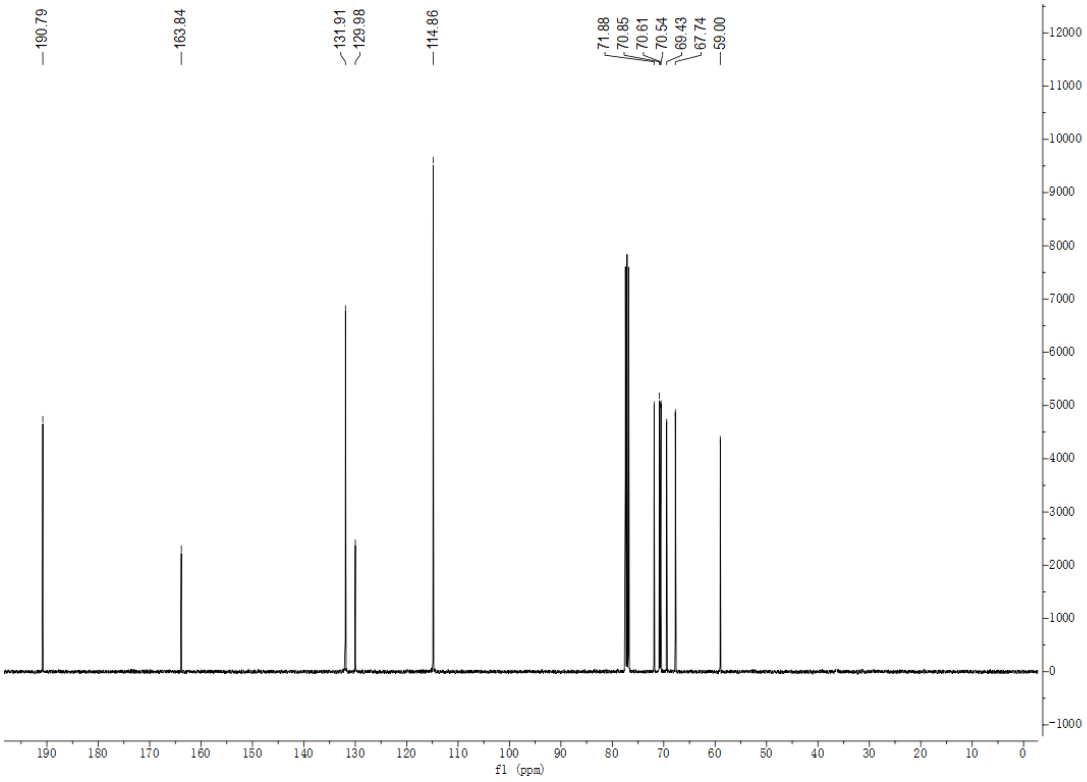

4-Morpholinobenzaldehyde (S68)

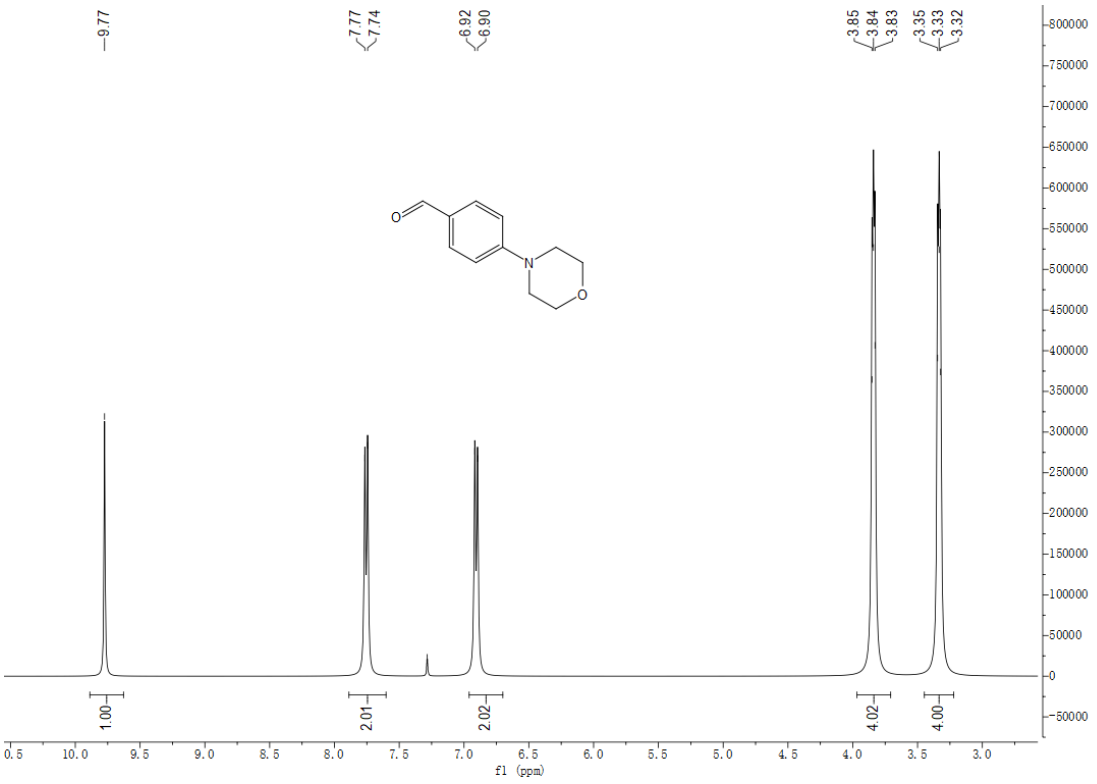

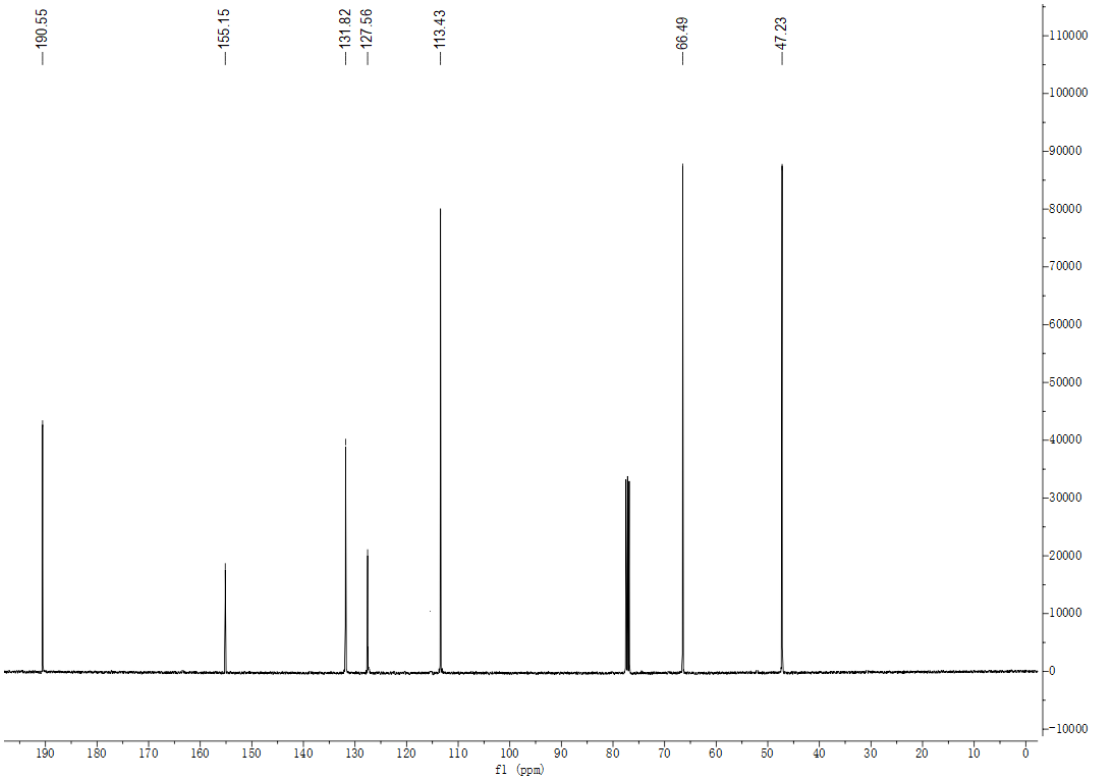

1-Methyl-1H-indole-5-carbaldehyde (S69)

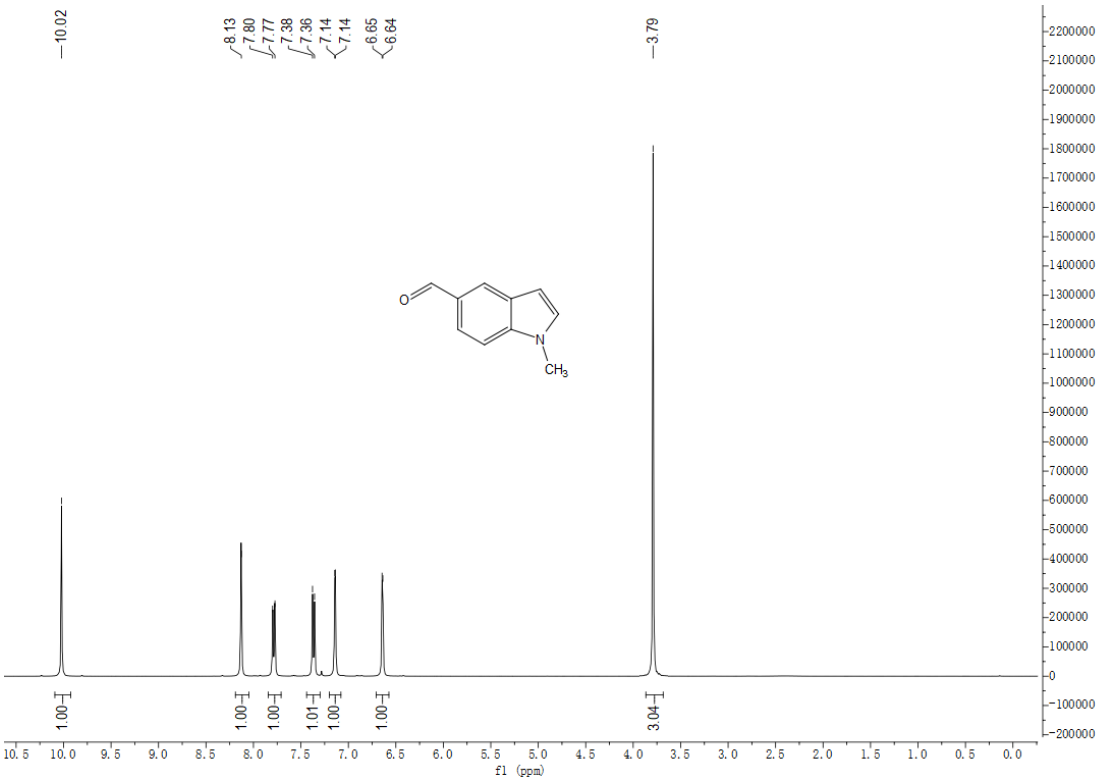

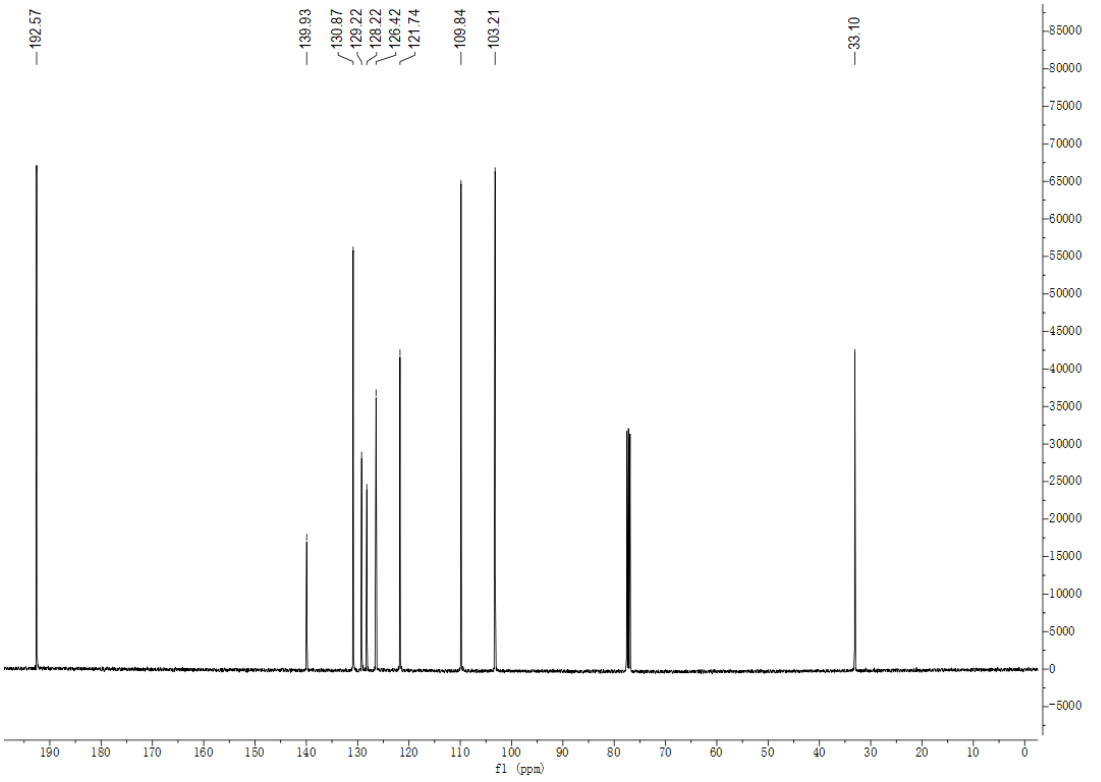

1,7-Dimethyl-3-phenyl-5-methoxystyryl-8-(4-nitrophenyl)-BODIPY (S70)

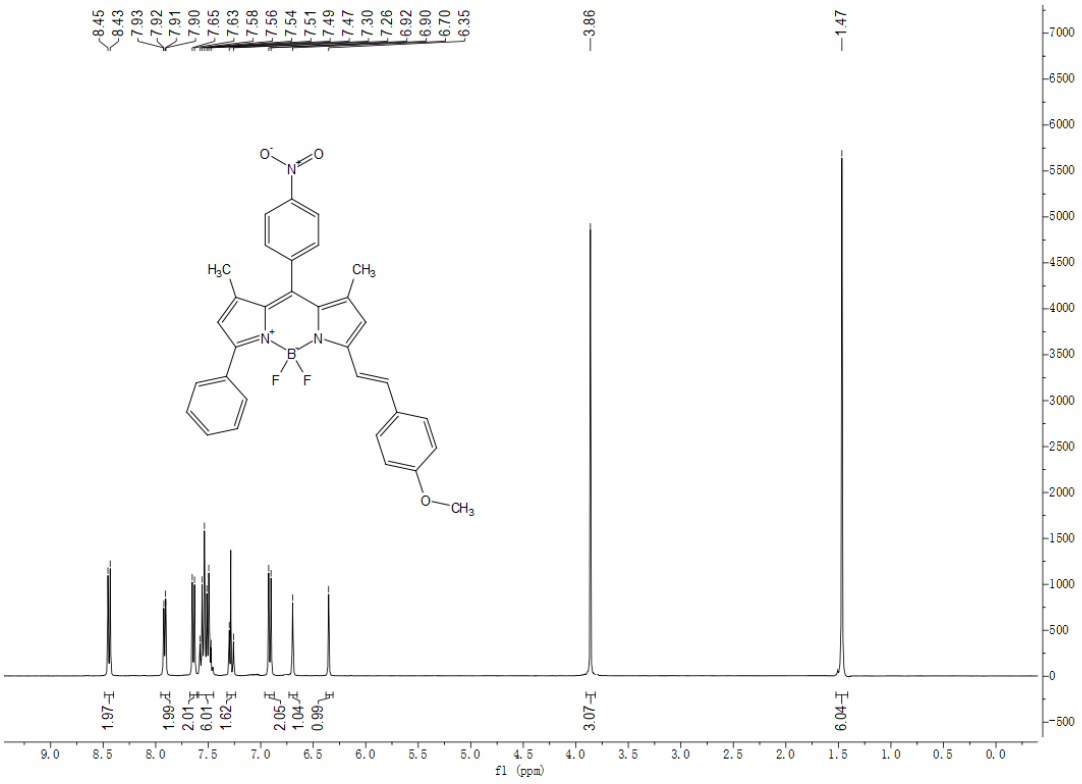

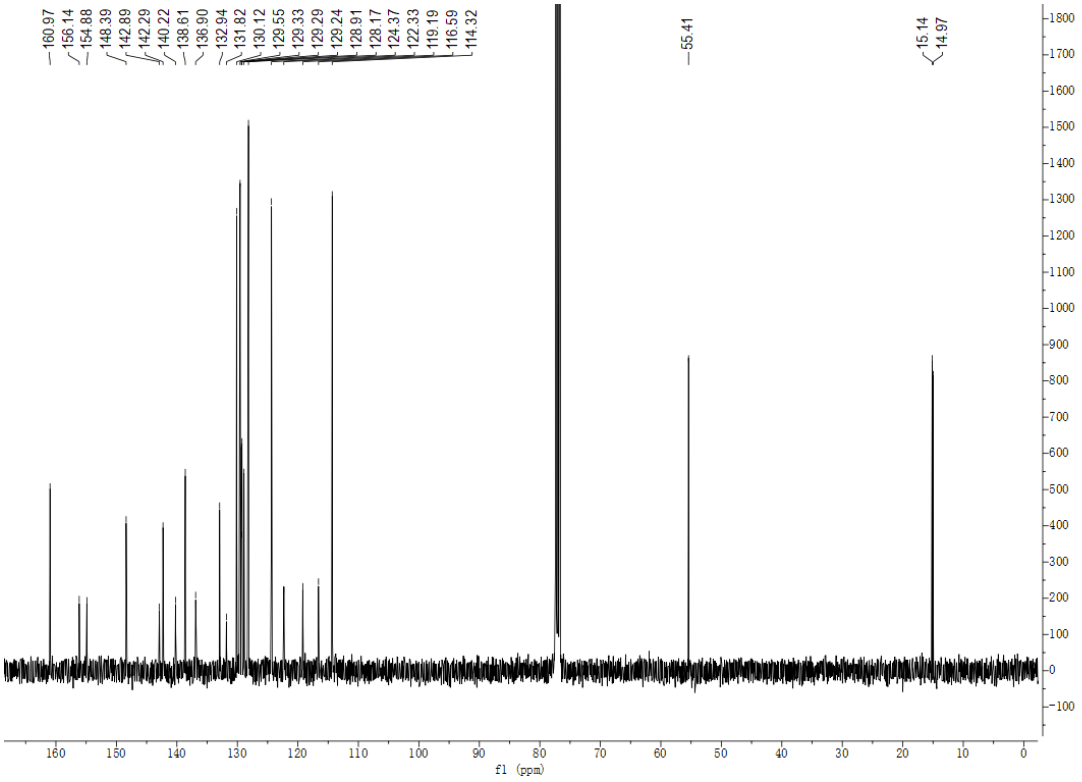

1,7-Dimethyl-3-phenyl-5-(2-(1-methyl-1H-indol-5-yl)vinyl)-8-(4-nitrophenyl)-BODIPY (S71)

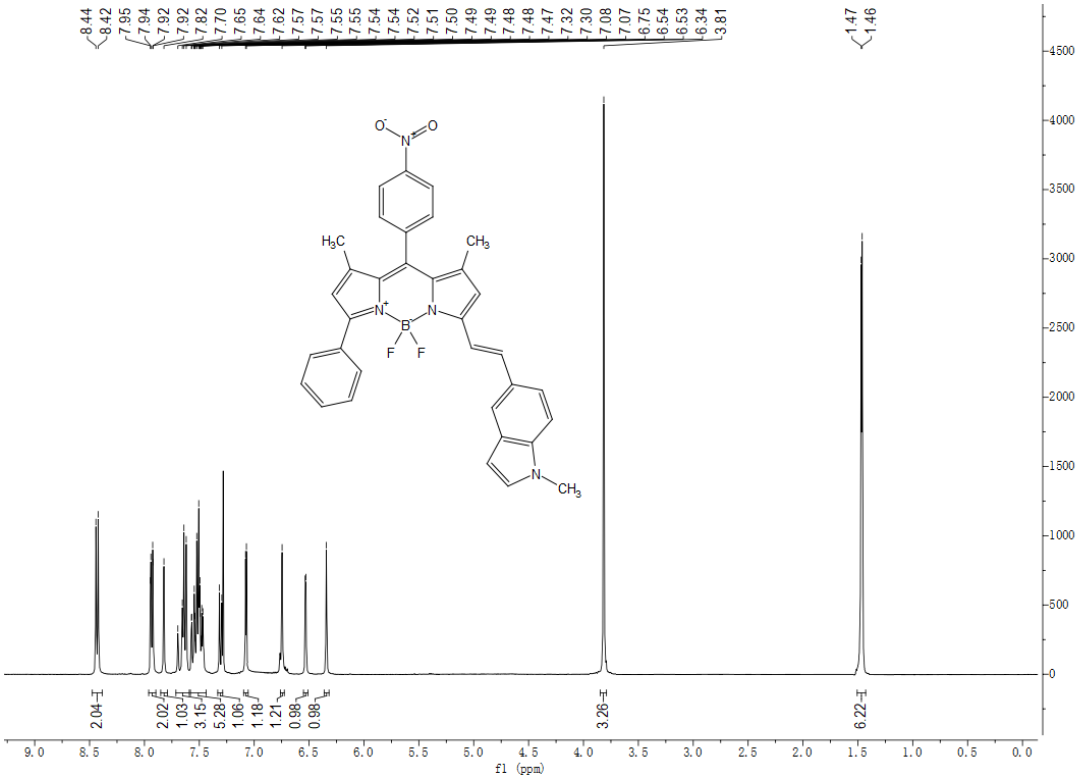

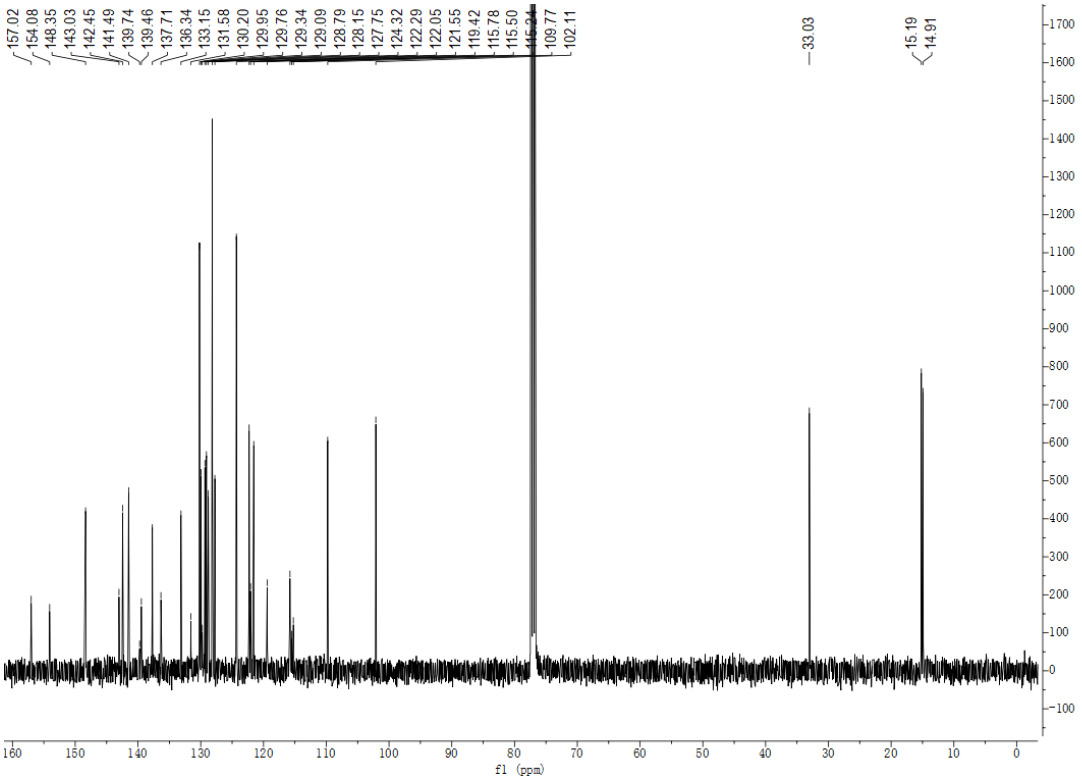

1,7-Dimethyl-3-phenyl-5-yl)vinyl)phenyl)morpholine-8-(4-nitrophenyl)-BODIPY (S72)

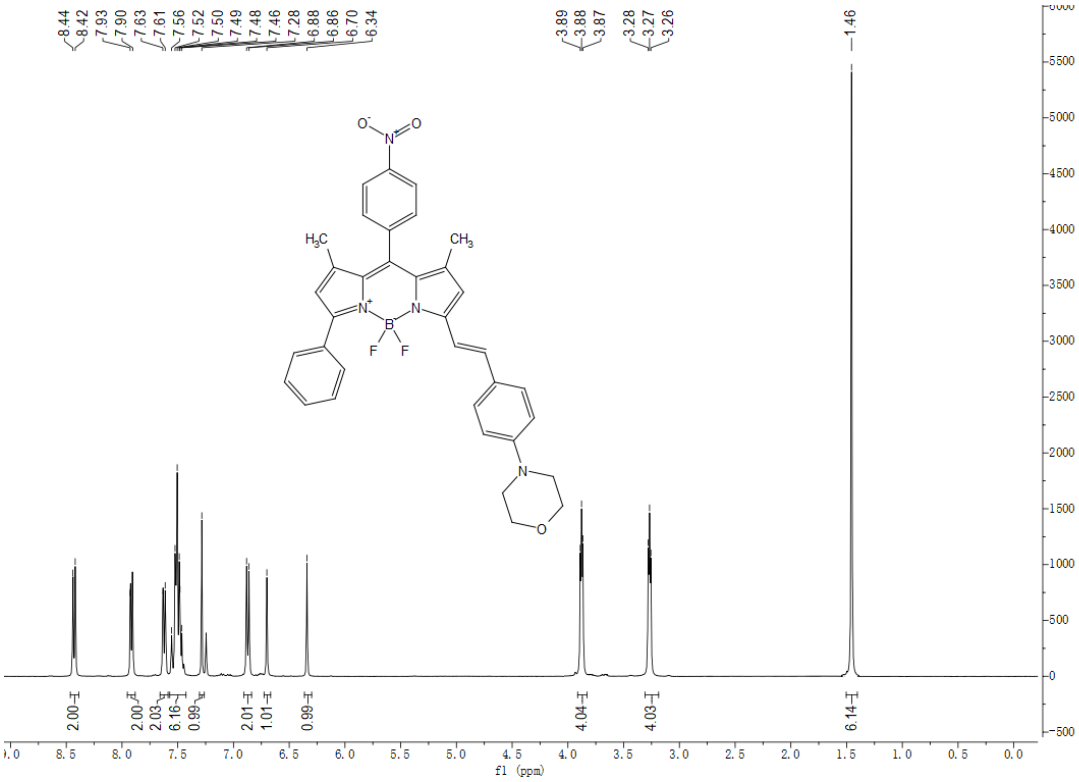

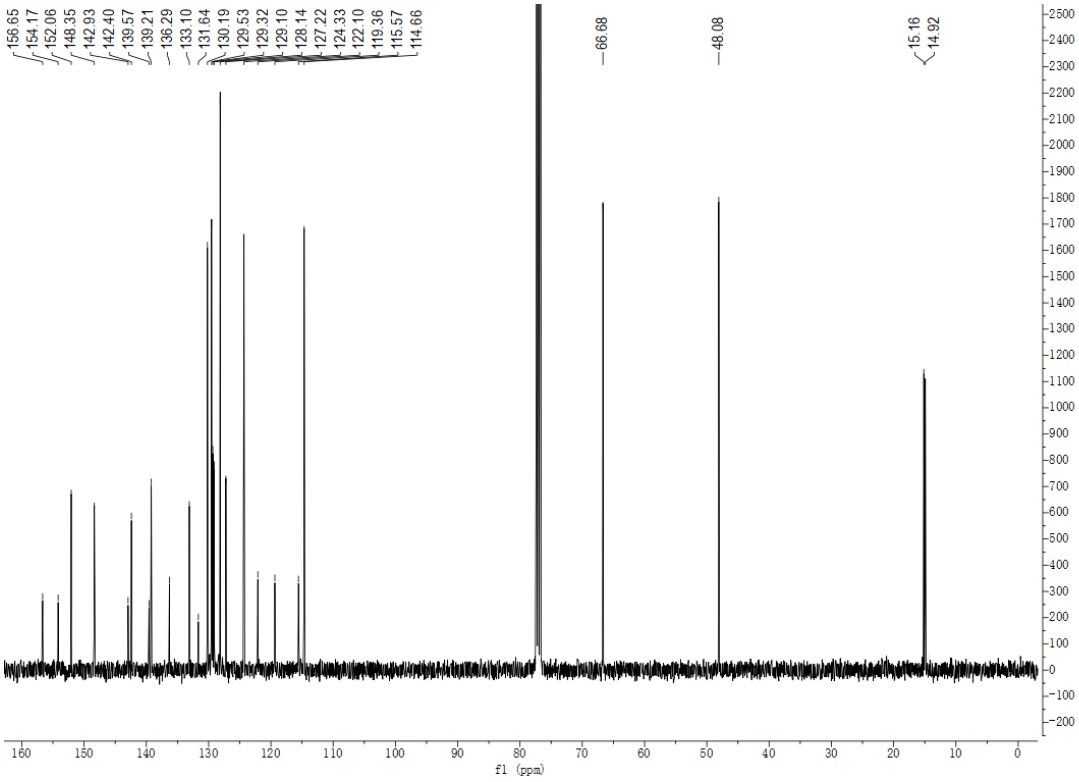

1-Methyl-3-methoxystyryl-8-(4-nitrophenyl)-BODIPY (S73)

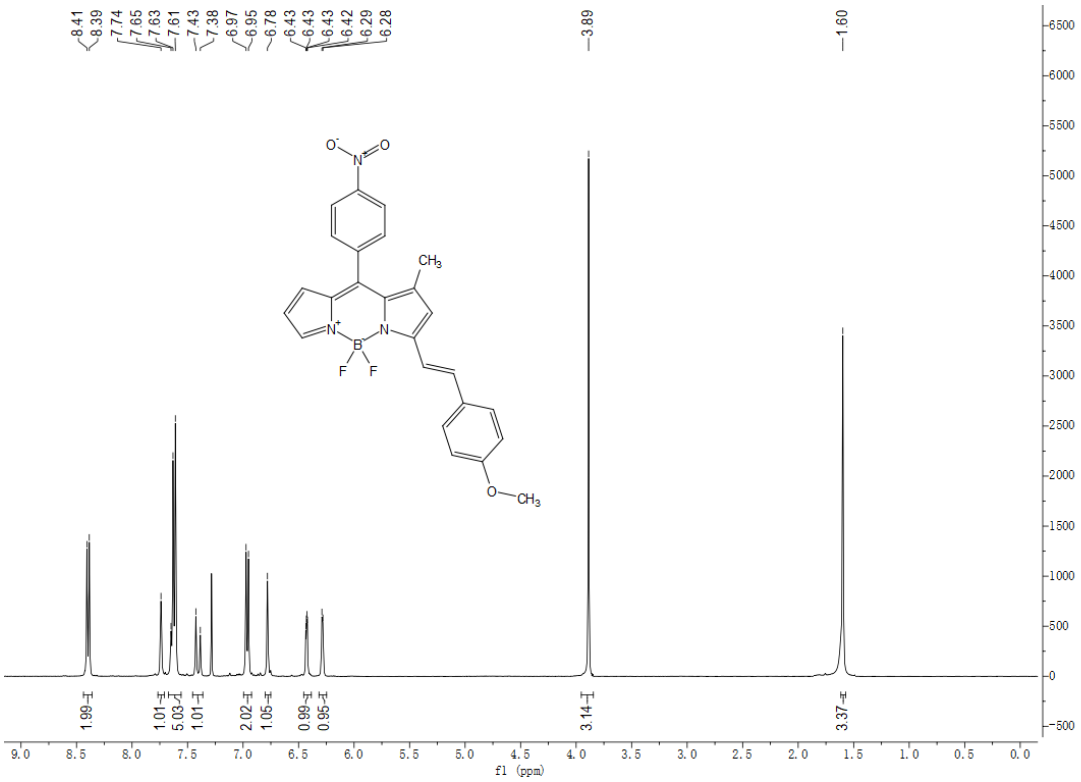

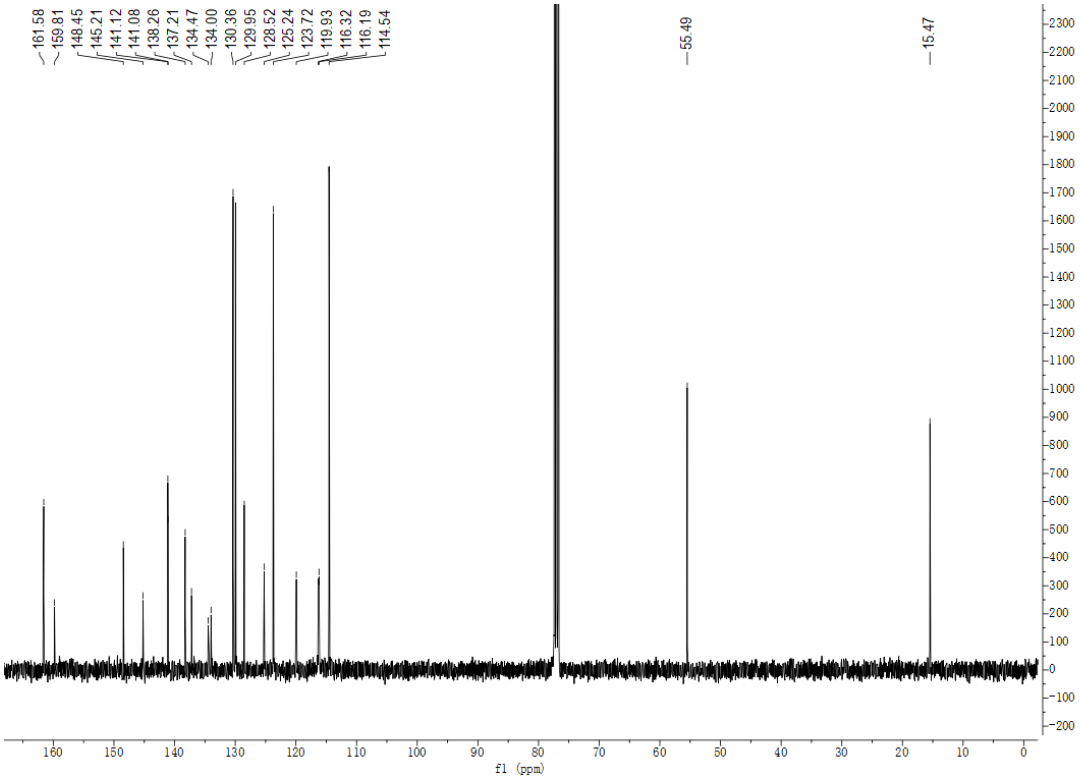

1-Methyl-3-(2-(1-methyl-1H-indol-5-yl)vinyl)-8-(4-nitrophenyl)-BODIPY (S74)

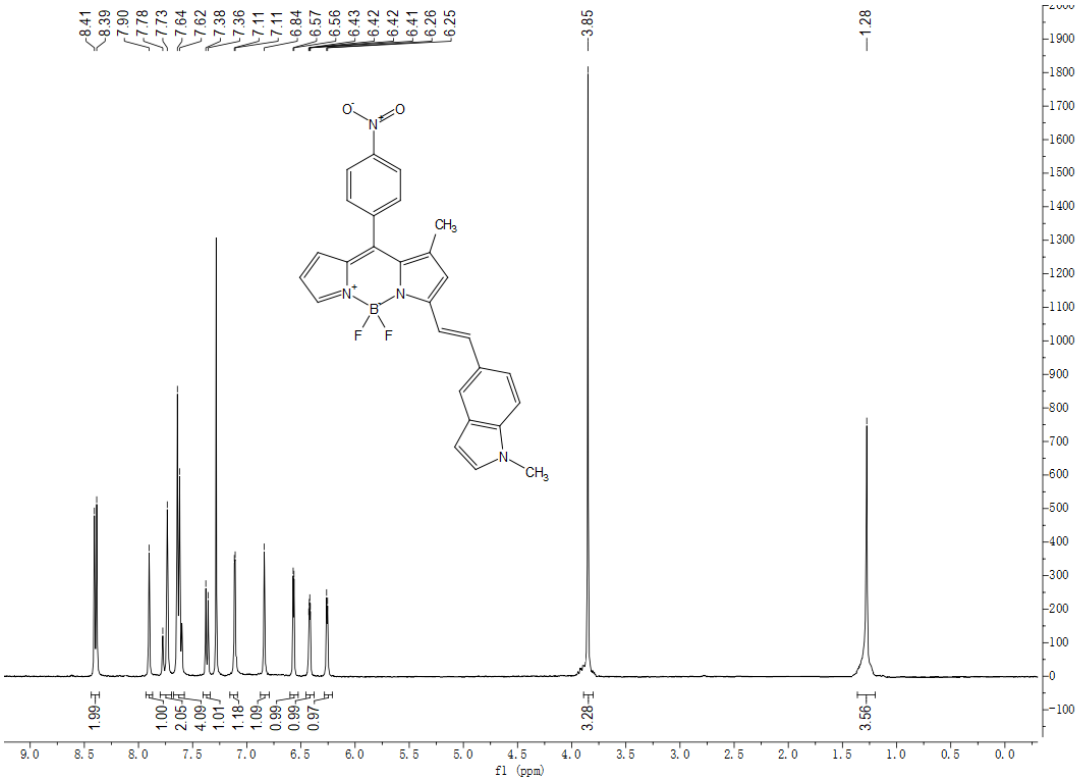

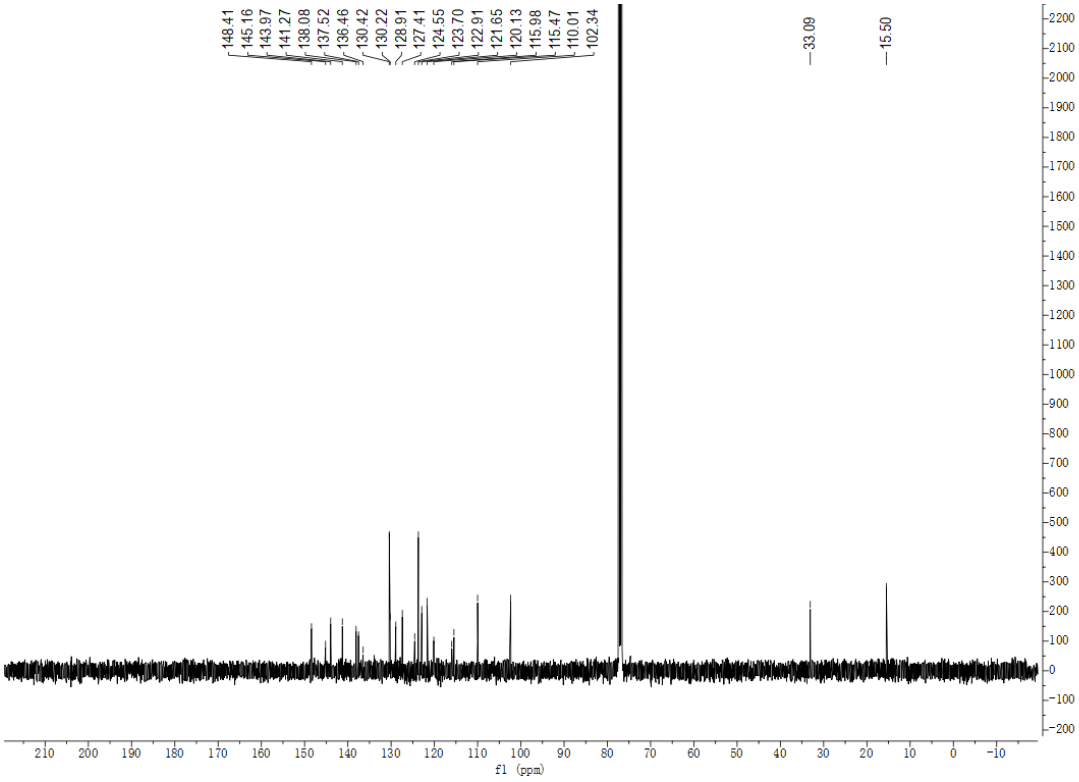

1,7-Dimethyl-3-phenyl-(4-(2-(2-(2-methoxyethoxy)ethoxy)ethoxy)styryl)-8-(4-nitrophenyl)-BODIPY (S75)

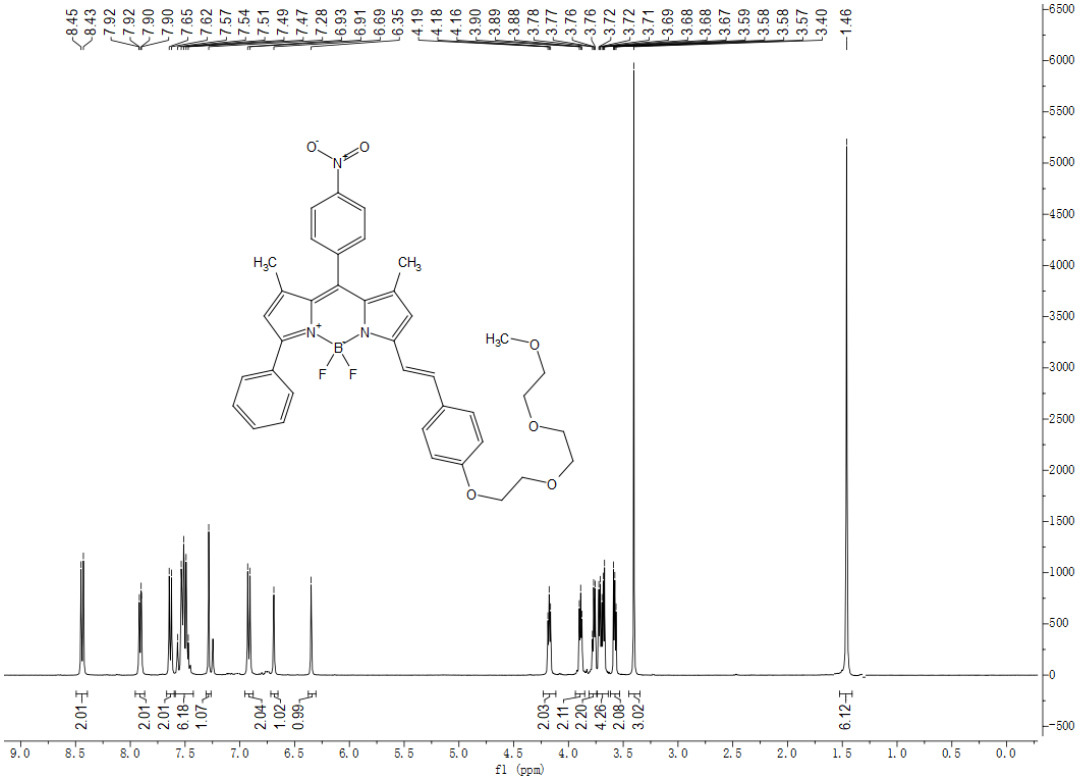

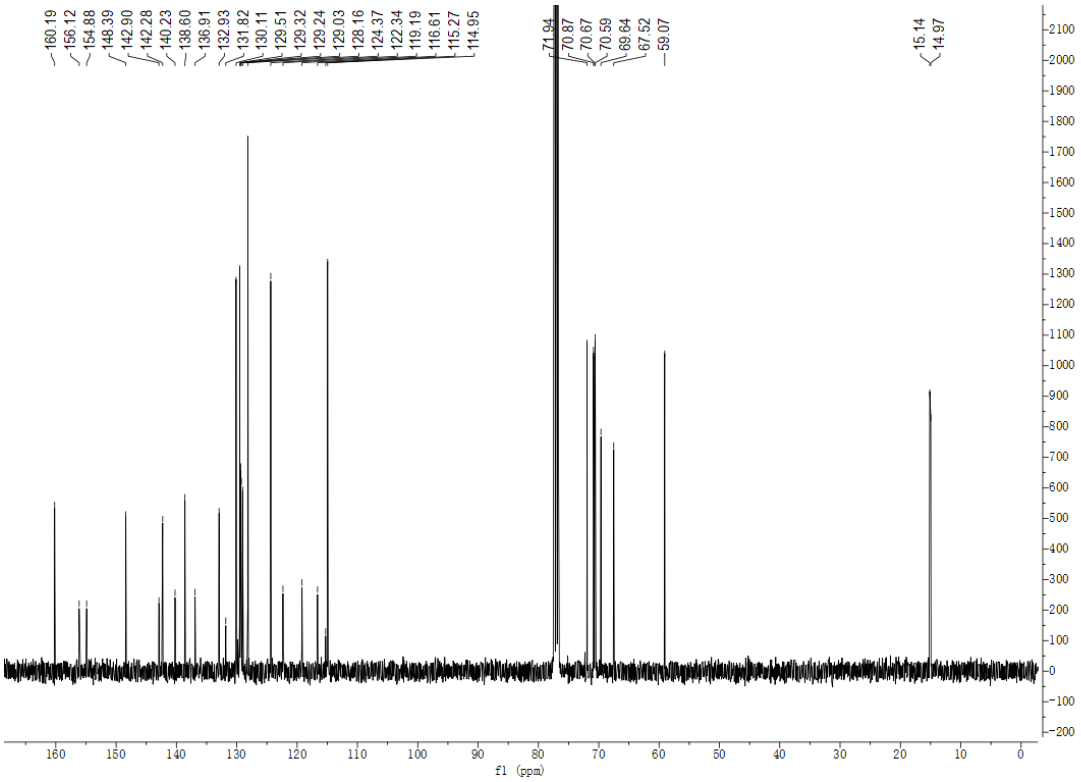

1,7-Dimethyl-3,5-bis(4-(2-(2-(2-methoxyethoxy)ethoxy)ethoxy)styryl)-8-(4-nitrophenyl)-BODIPY (S76)

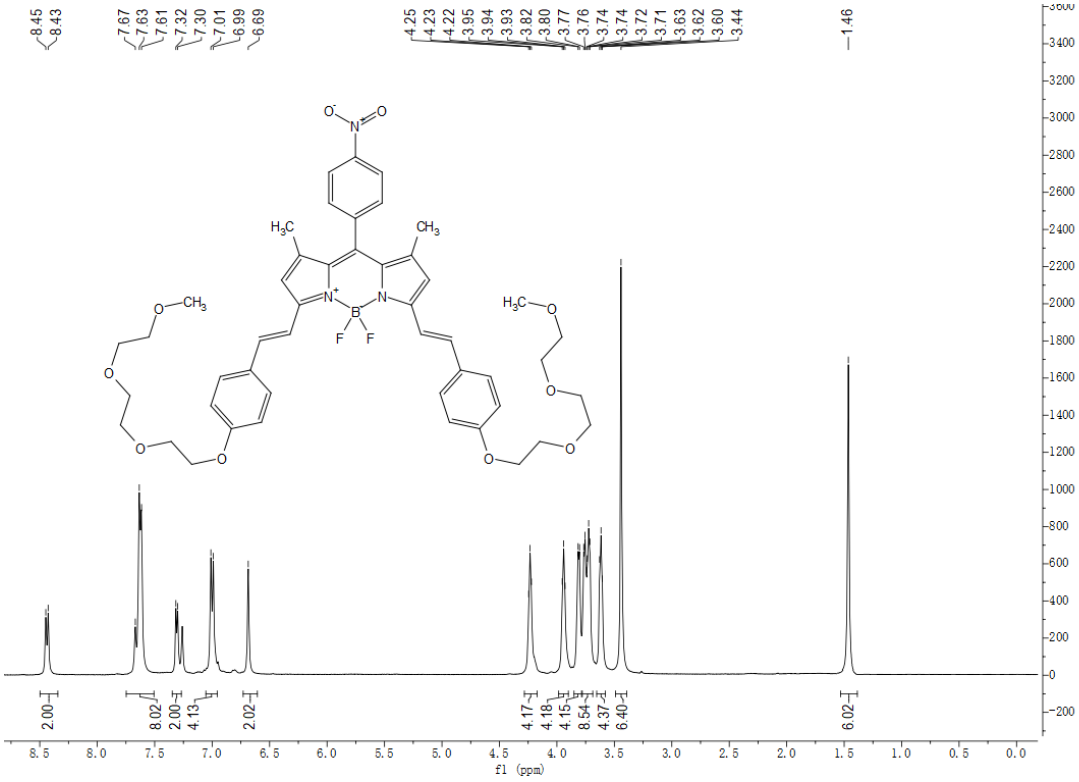

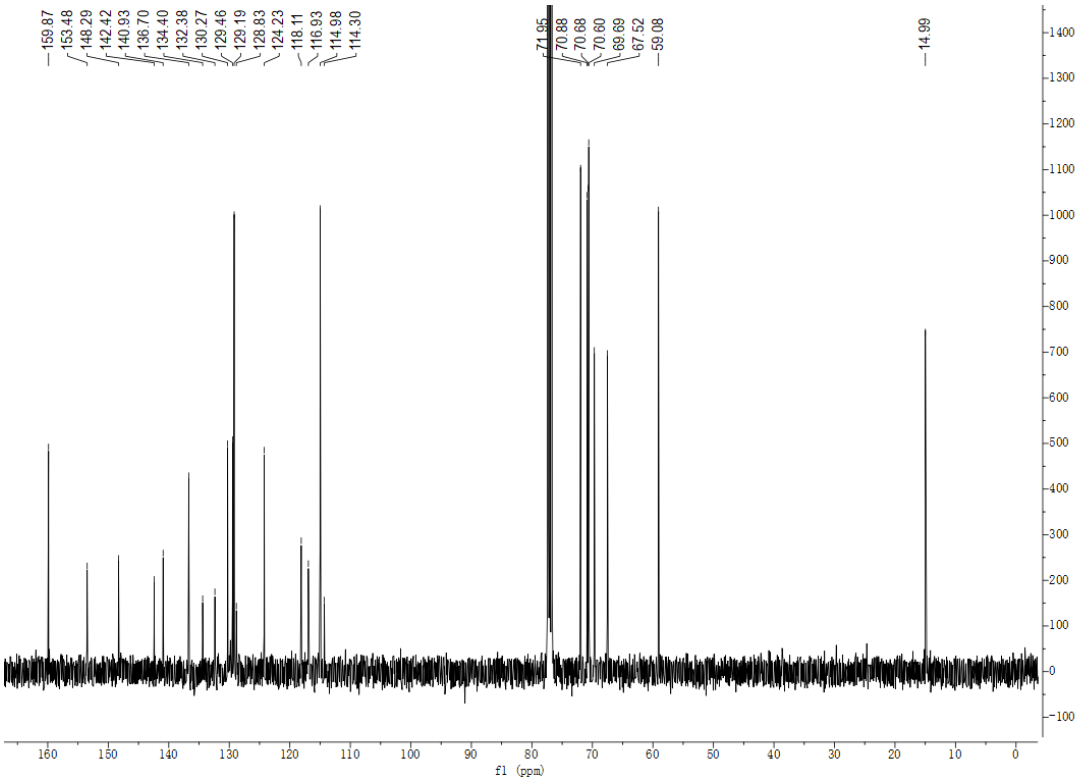

1,5,7-Trimethyl-3-(4-(2-(2-(2-methoxyethoxy)ethoxy)ethoxy)styryl)-8-(4-nitrophenyl)-BODIPY (S77)

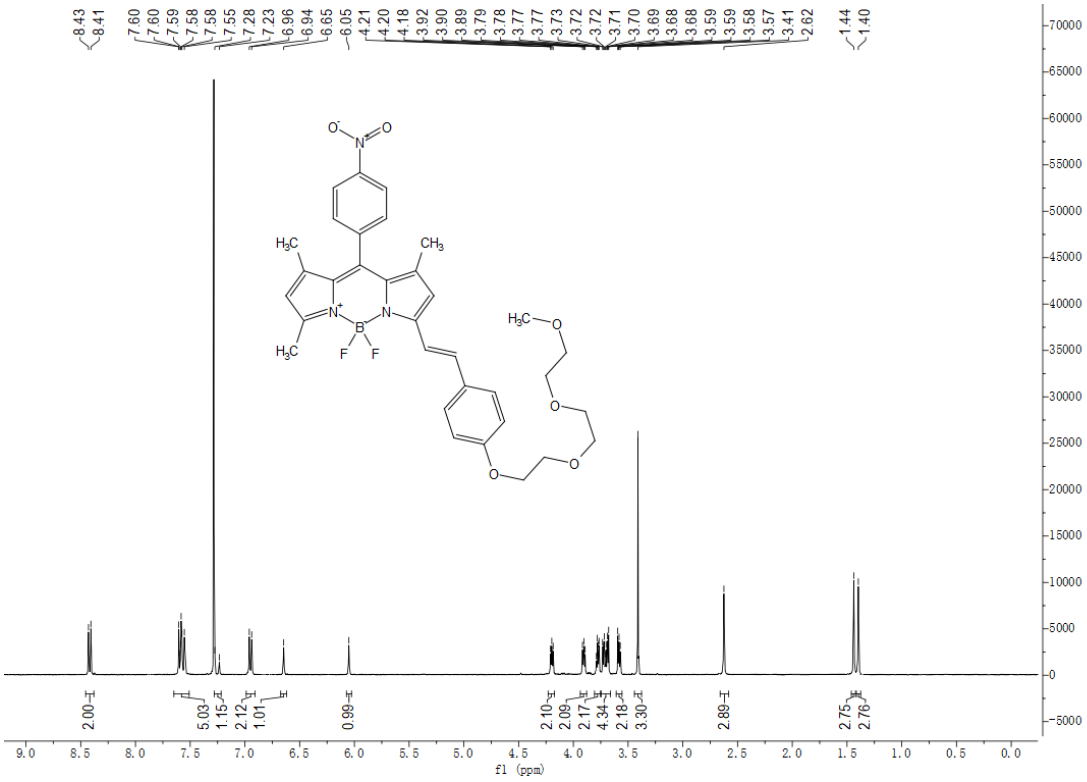

1,3,5,7-Tetramethyl-2,6-disulfonic acid-8-(4-nitrophenyl)-BODIPY (S79)

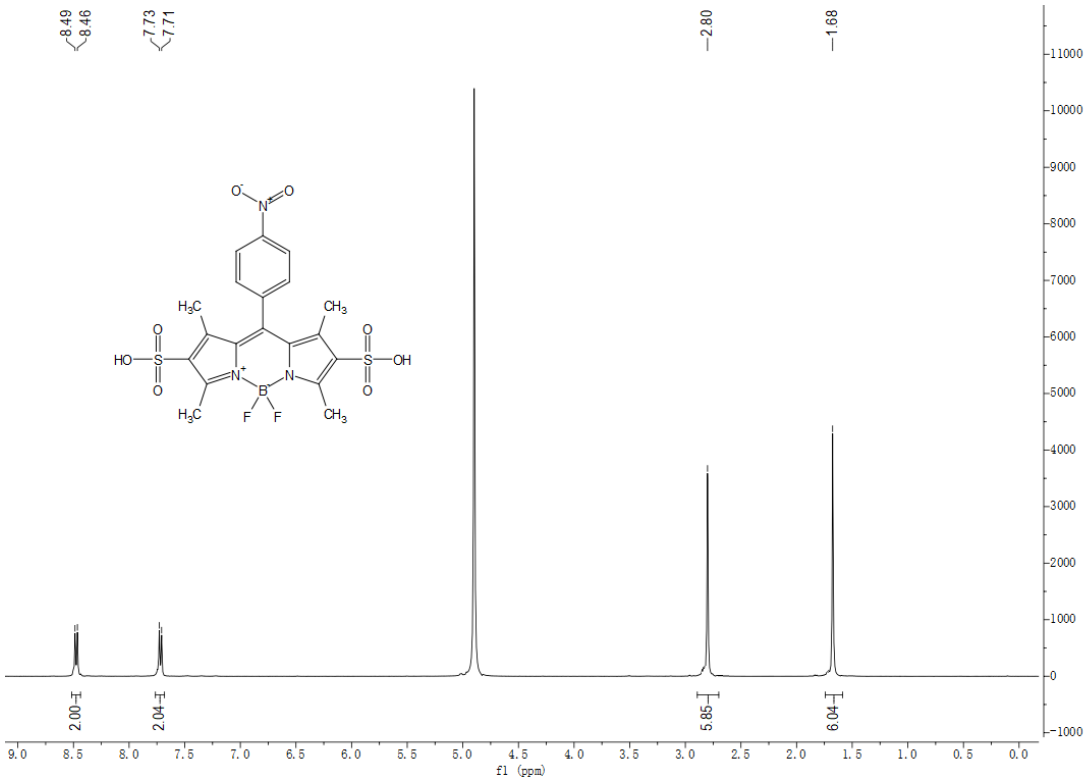

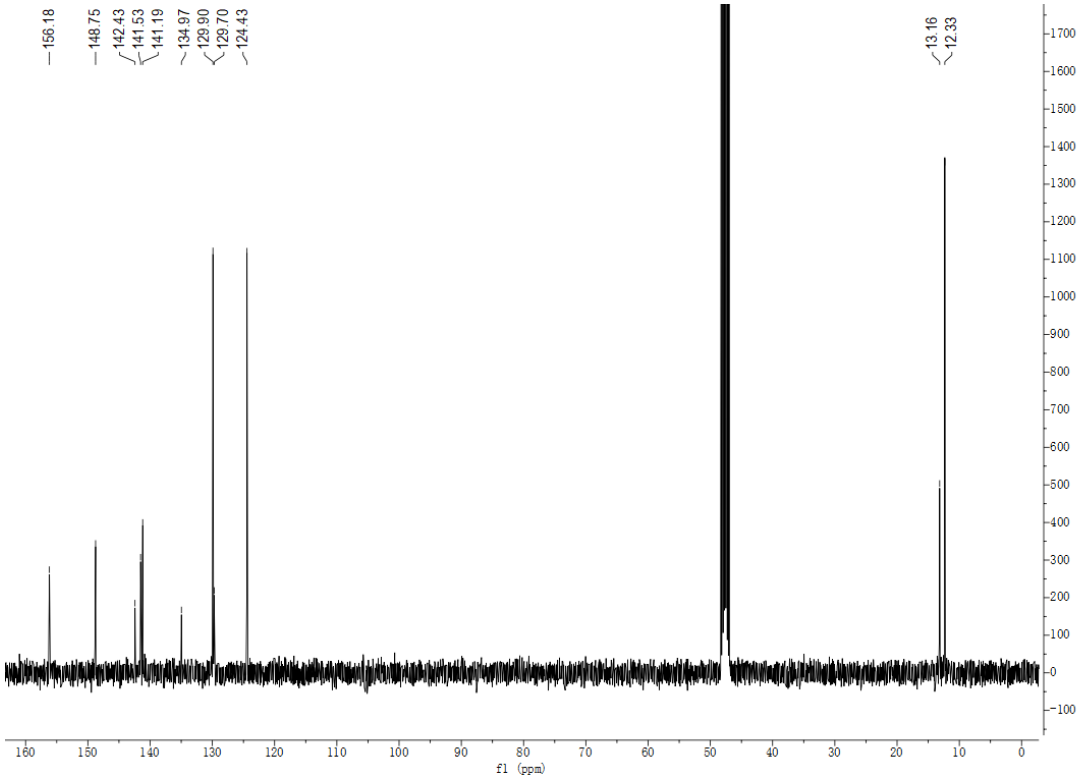

1,3,5,7-Tetramethyl-8-phenyl-BODIPY (S80)

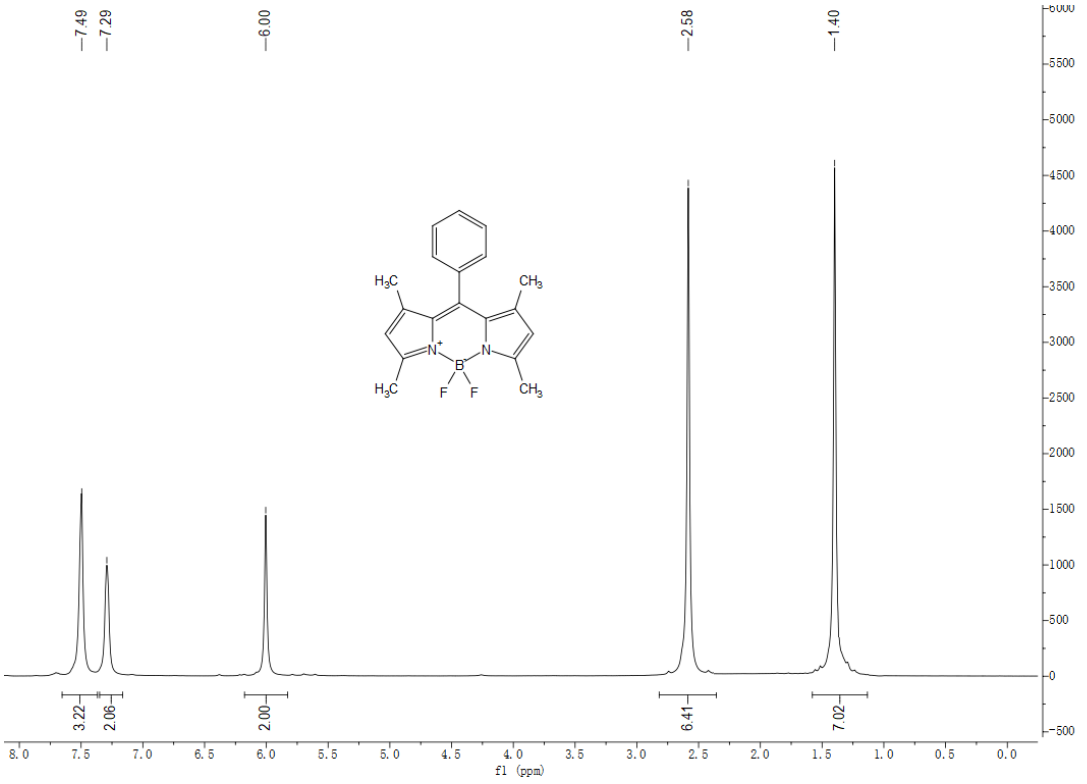

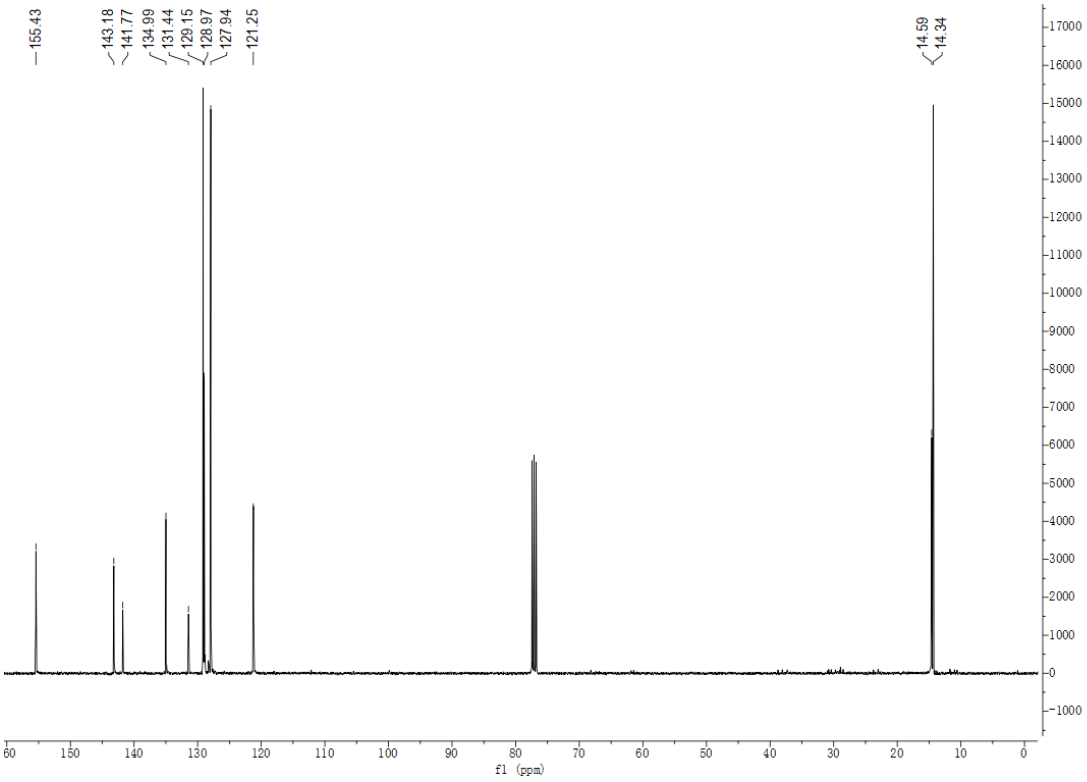

Ethyl 3-(5-benzoyl-2,4-dimethyl-1H-pyrrol-3-yl)propanoate (S81)

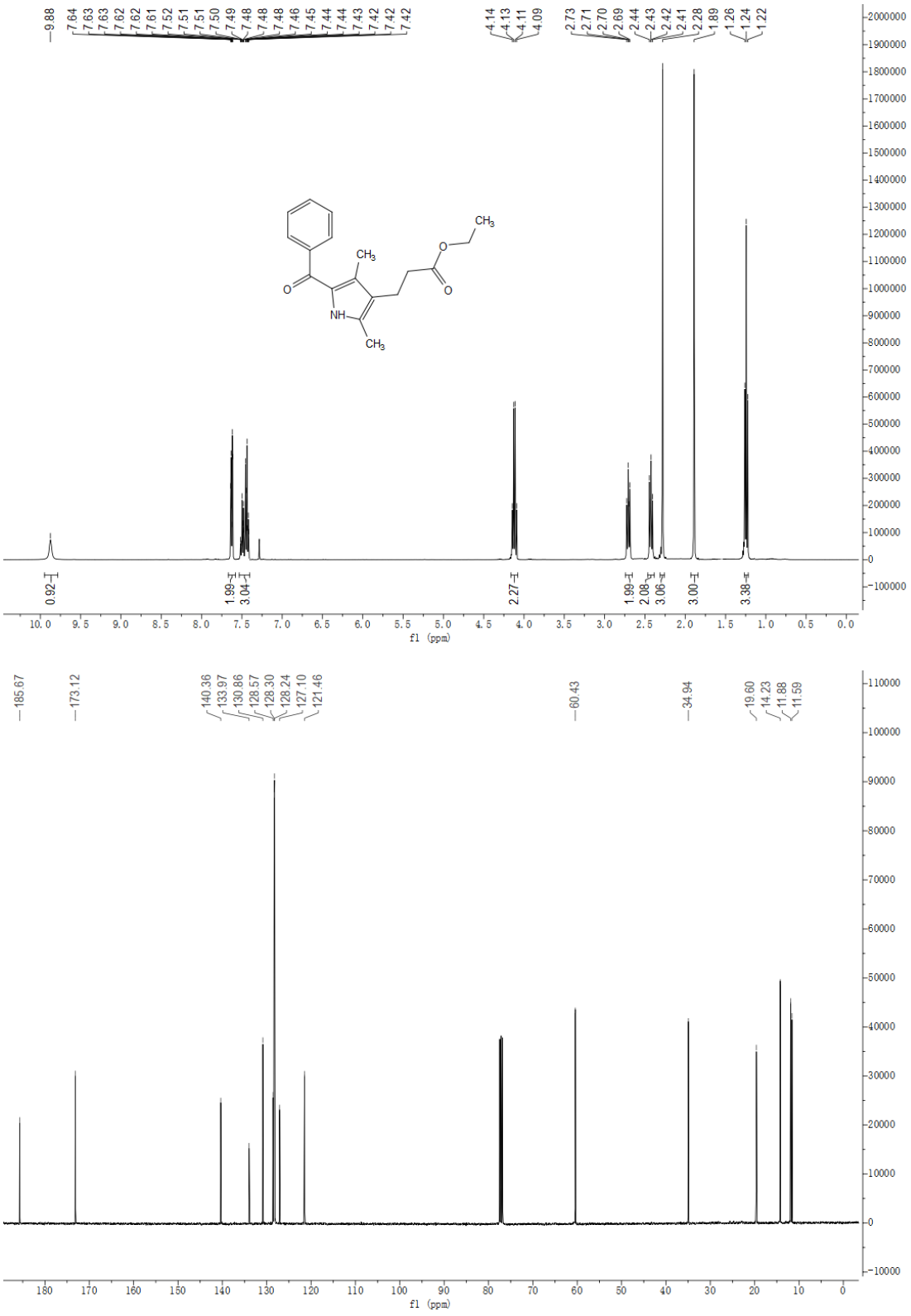

Methyl 3-(5-benzoyl-2,4-dimethyl-1H-pyrrol-3-yl)propanoate (S82)

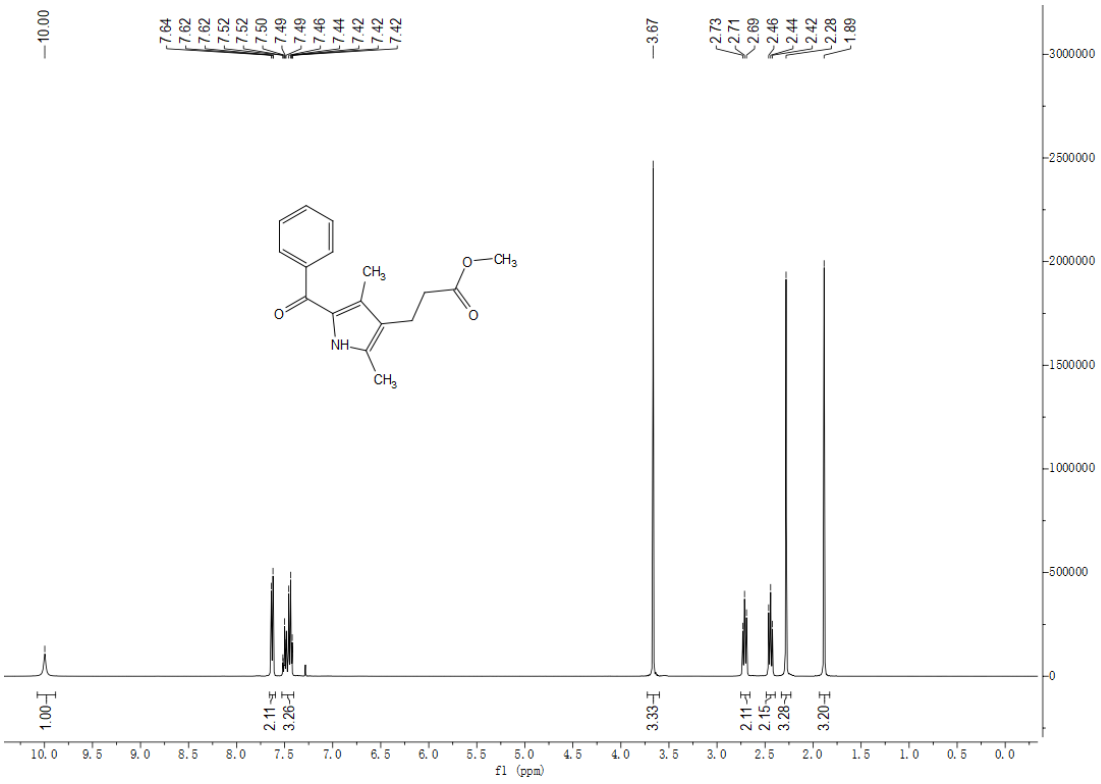

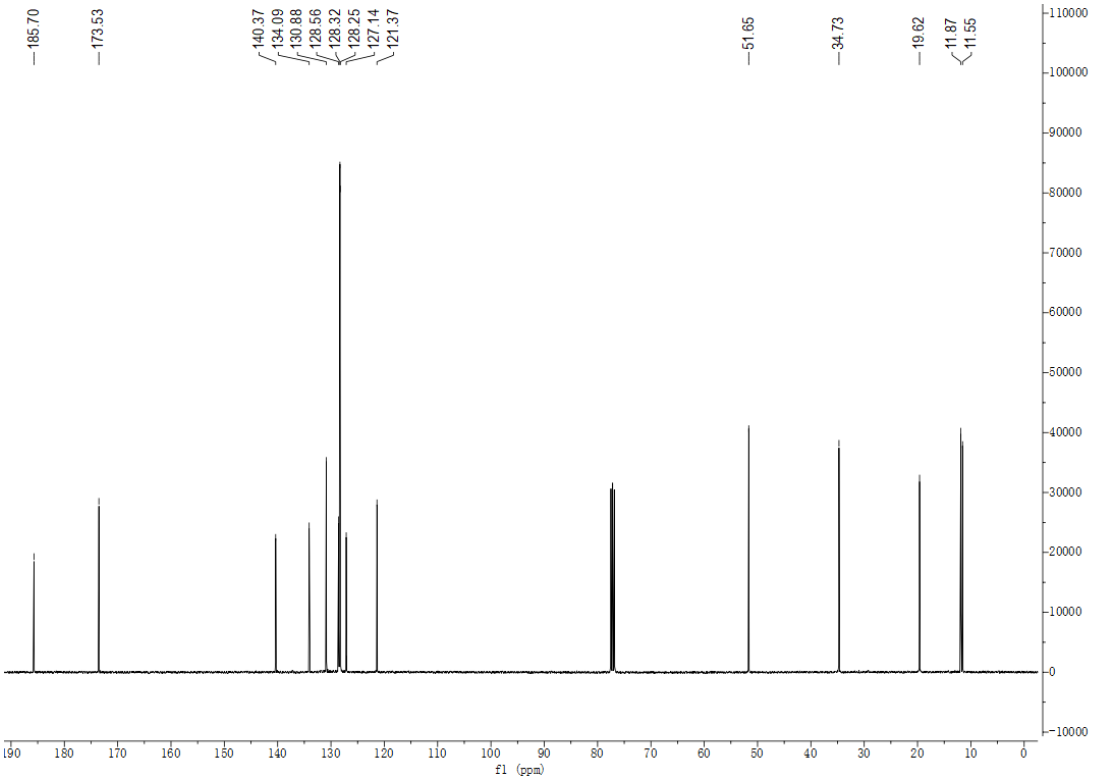

1,3,5,7-Tetramethyl-2-ethyl propanoate-8-(4-nitrophenyl)-BODIPY (S83)

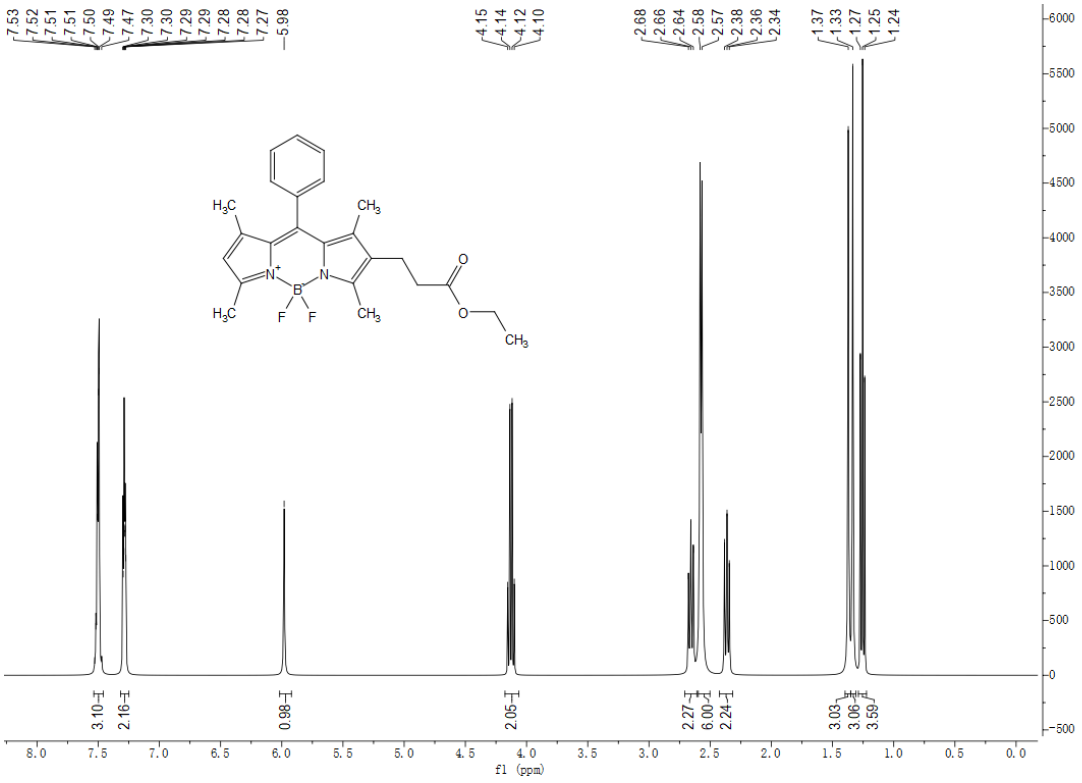

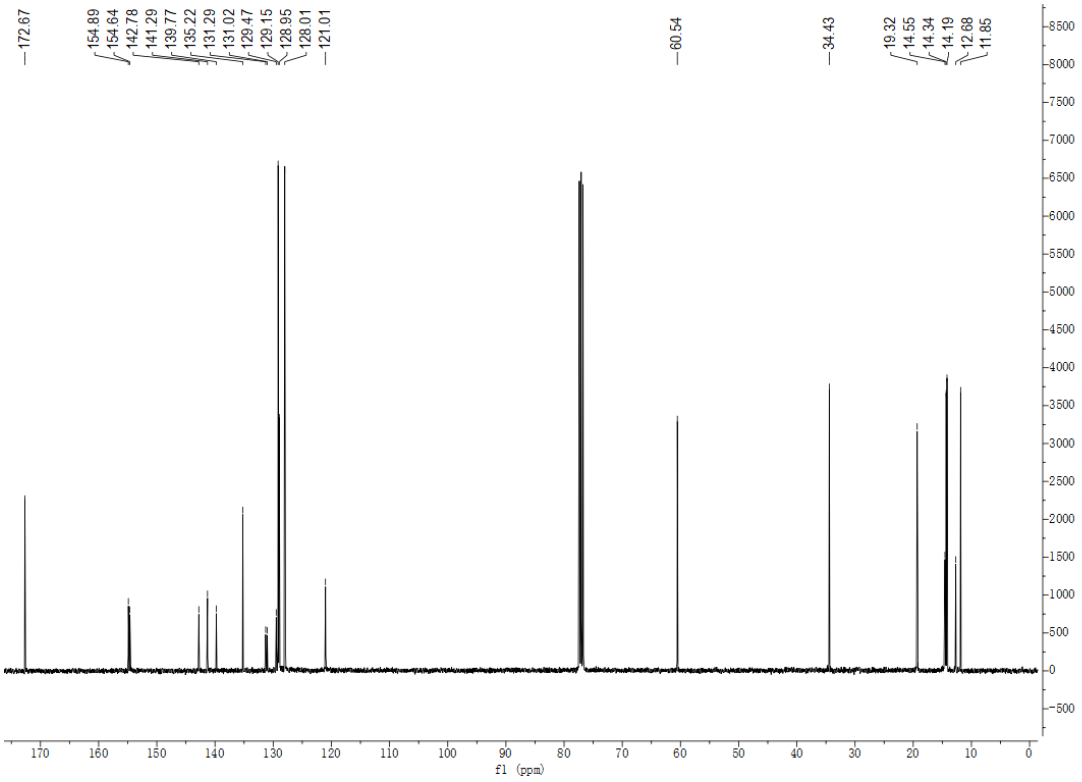

1,3,5,7-Tetramethyl-2-ethyl propanoate-8-(4-nitrophenyl)-BODIPY (S84)

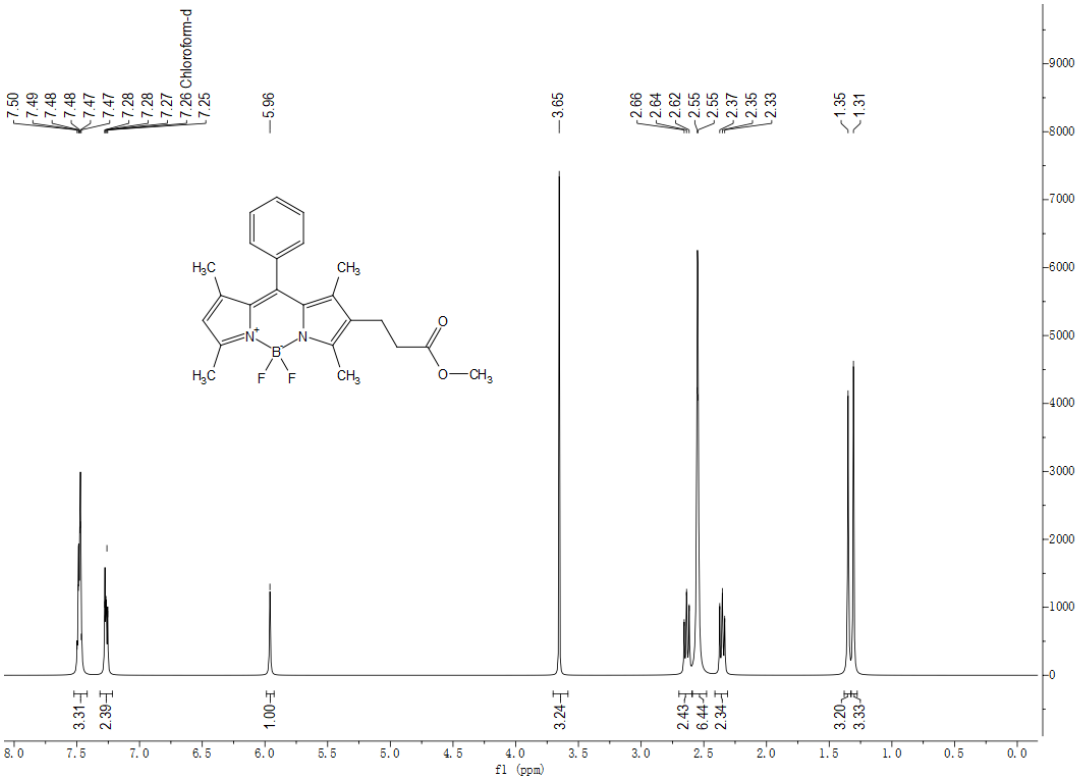

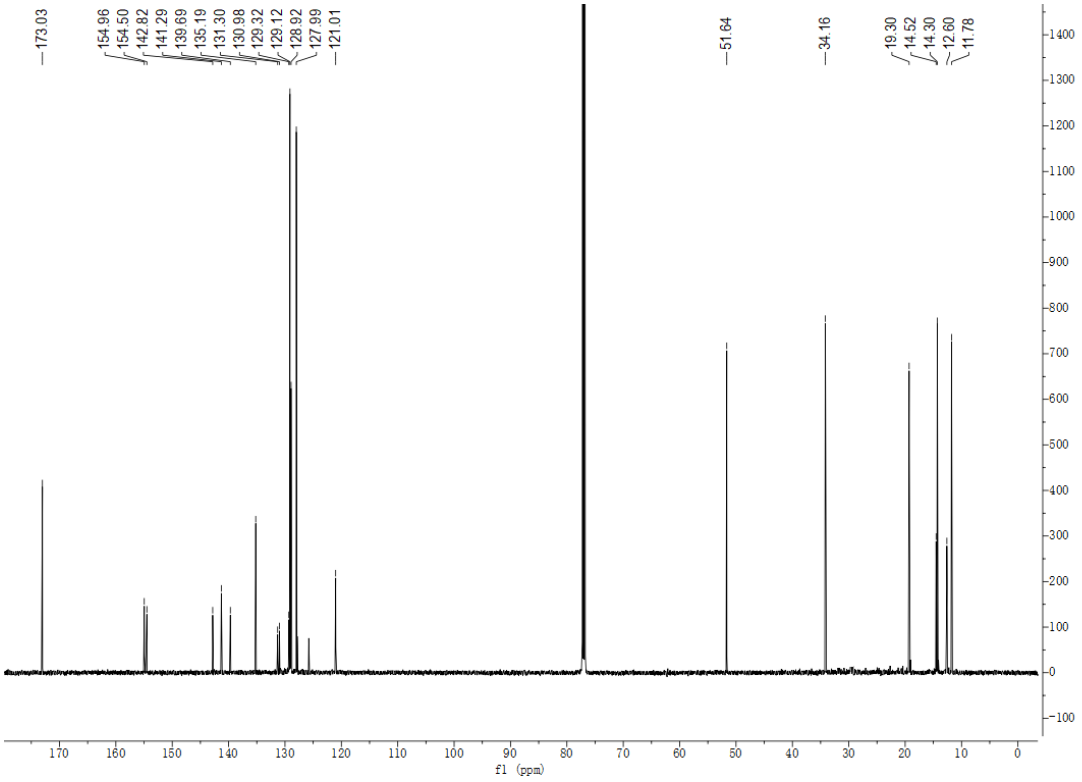

6-((7-Nitrobenzo[c][1,2,5]oxadiazol-4-yl)amino)hexan-1-ol (S85)

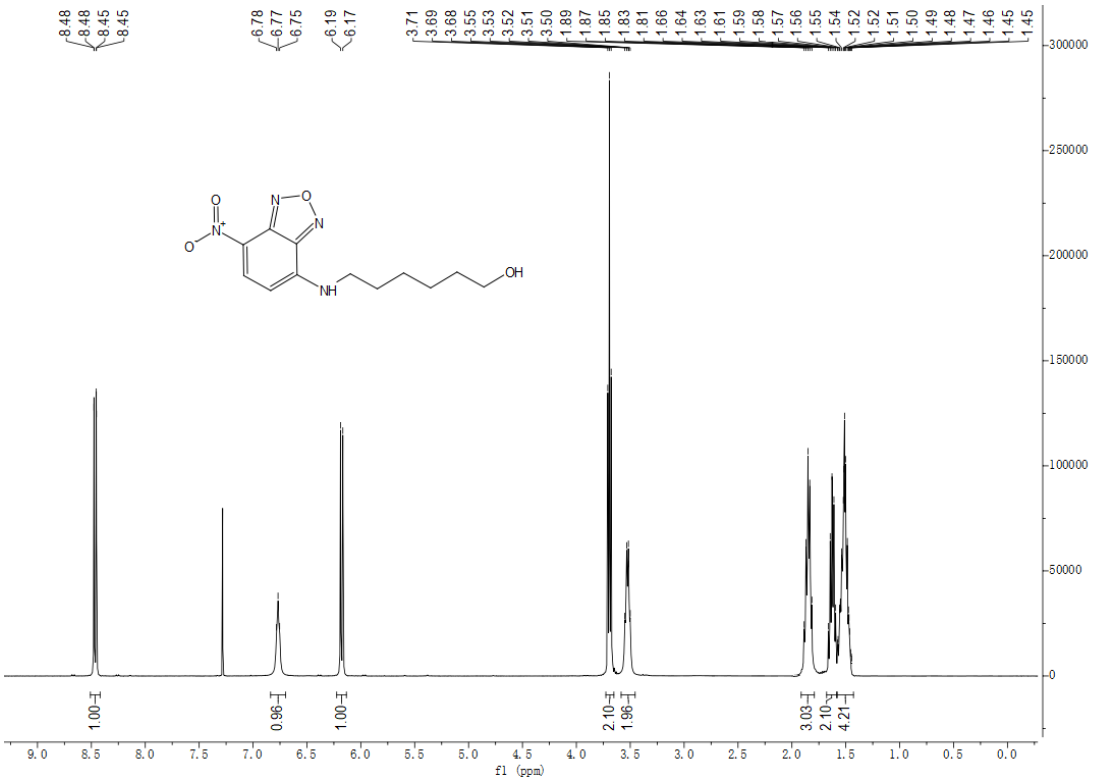

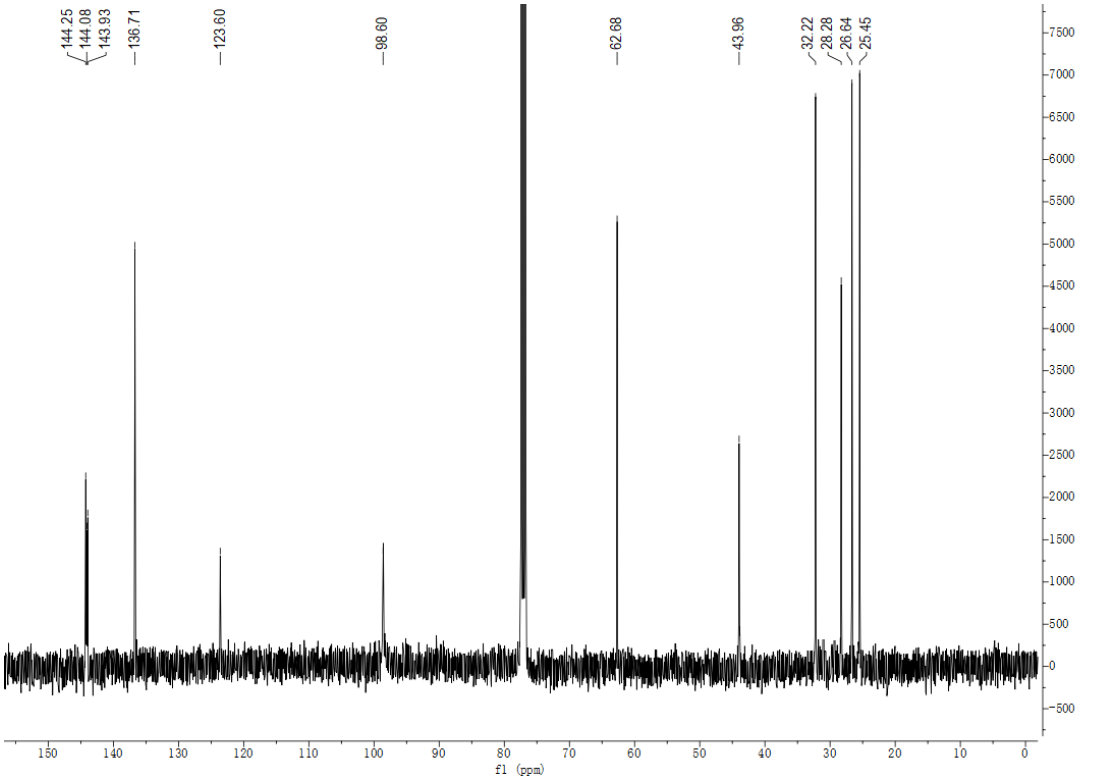

N-(6-iodohexyl)-7-nitrobenzo[c][1,2,5]oxadiazol-4-amine (S86)

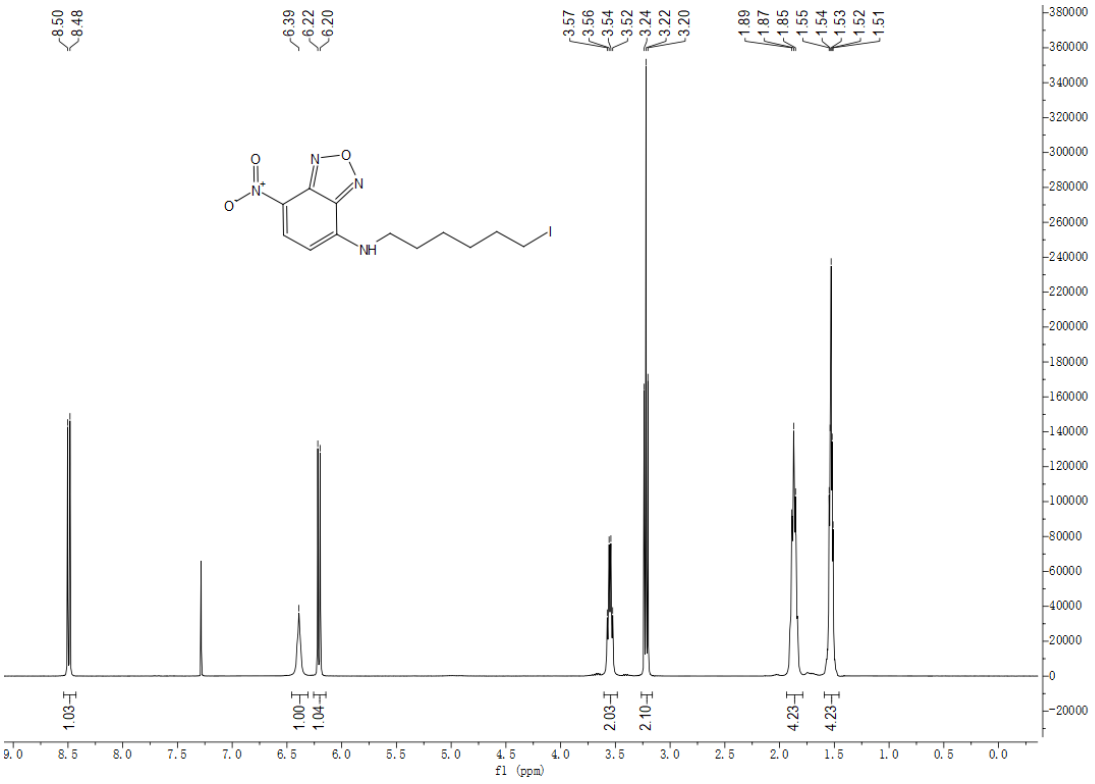

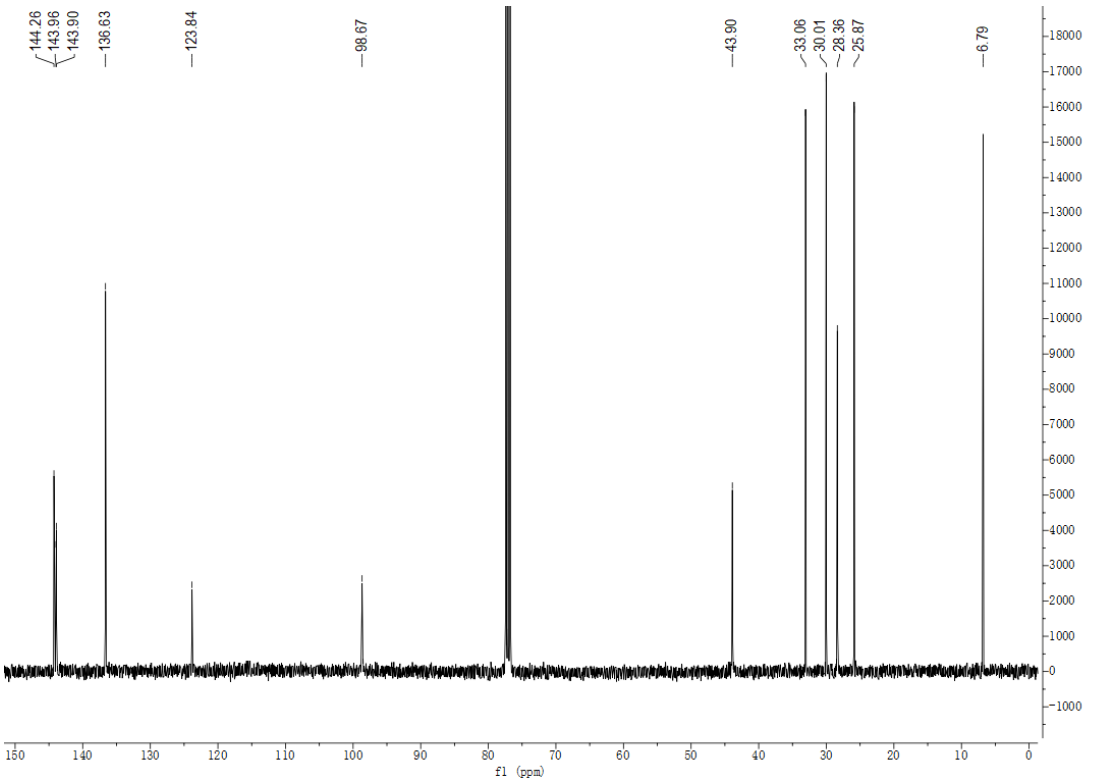

4-((6-((7-nitrobenzo[c][1,2,5]oxadiazol-4-yl)amino)hexyl)oxy)benzaldehyde (S87)

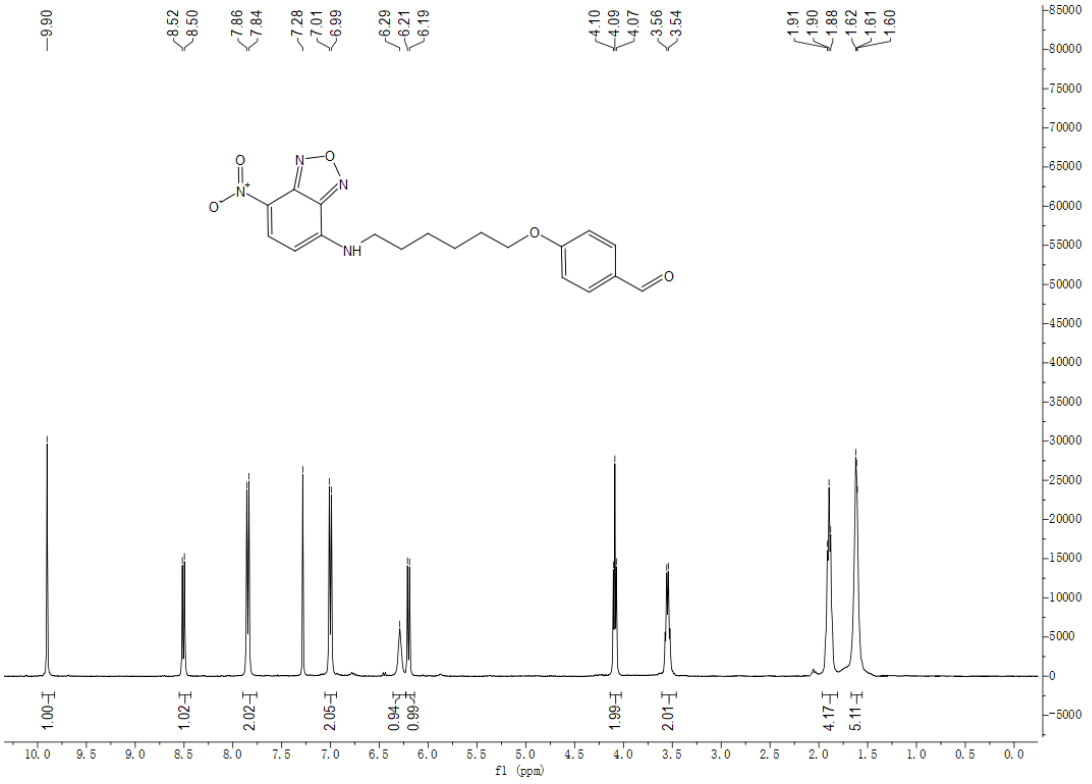

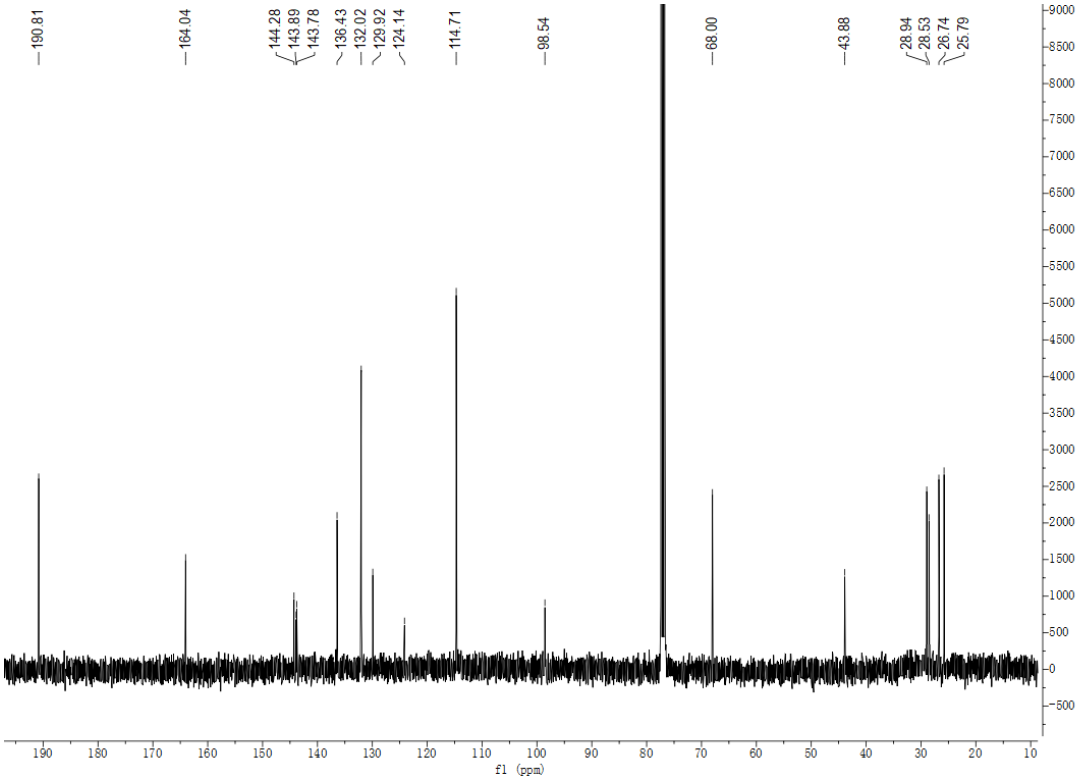

1-(6-((7-nitrobenzo[c][1,2,5]oxadiazol-4-yl)amino)hexyl)-1H-indole-5-carbaldehyde (S88)

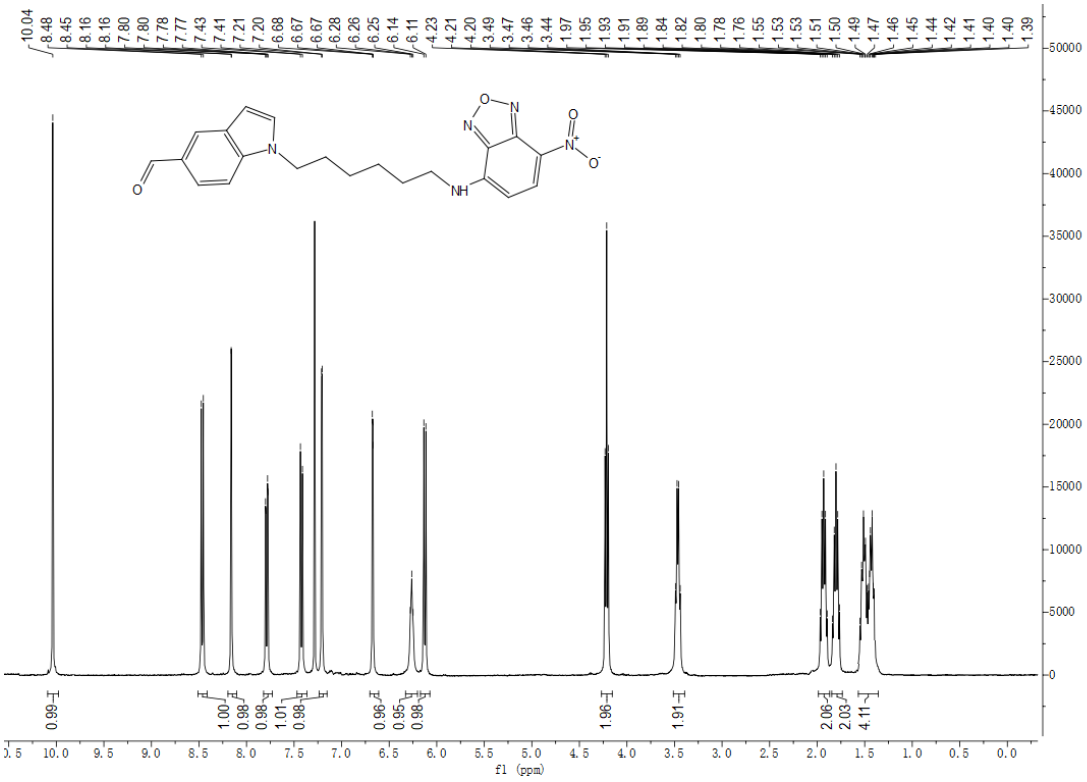

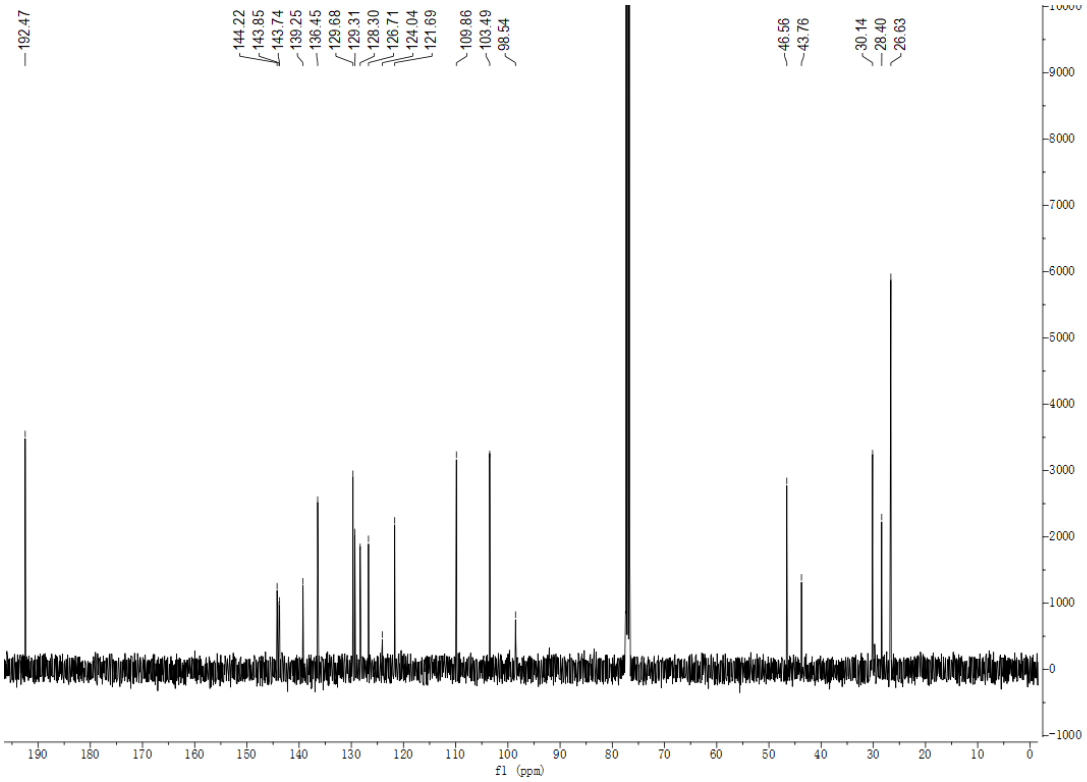

N-(6-(diethylamino)-9-(2-(((2,5-dioxopyrrolidin-1-yl)oxy)carbonyl)phenyl)-3H-xanthen-3-ylidene)-N-ethylethanaminium (Rhodamine B-NHS ester) (S89)

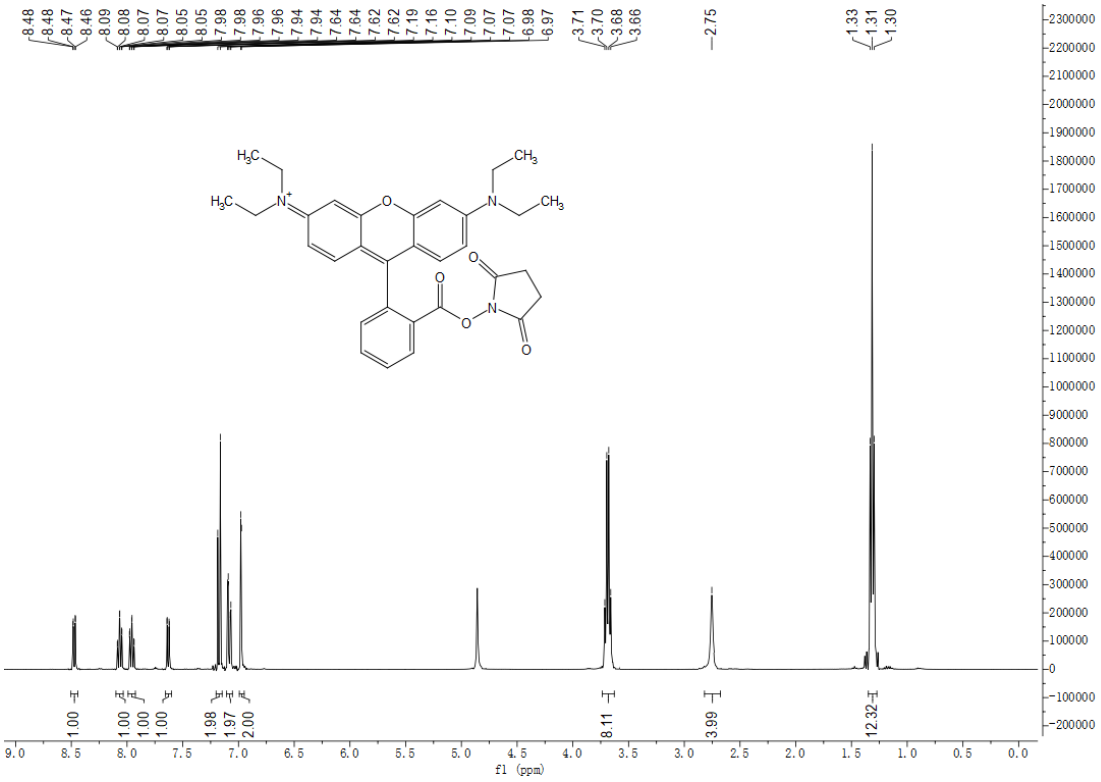

2-(6-Azidohexyl)-3',6'-bis(diethylamino)spiro[isoindoline-1,9'-xanthen]-3-one (S90)

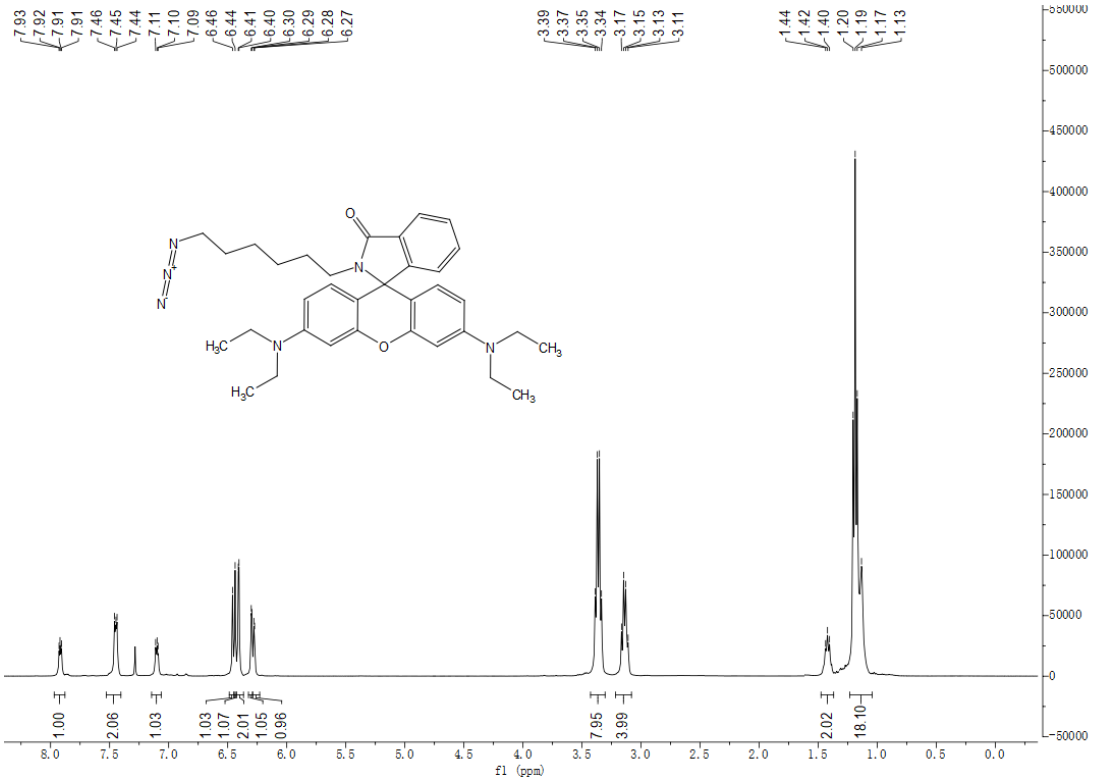

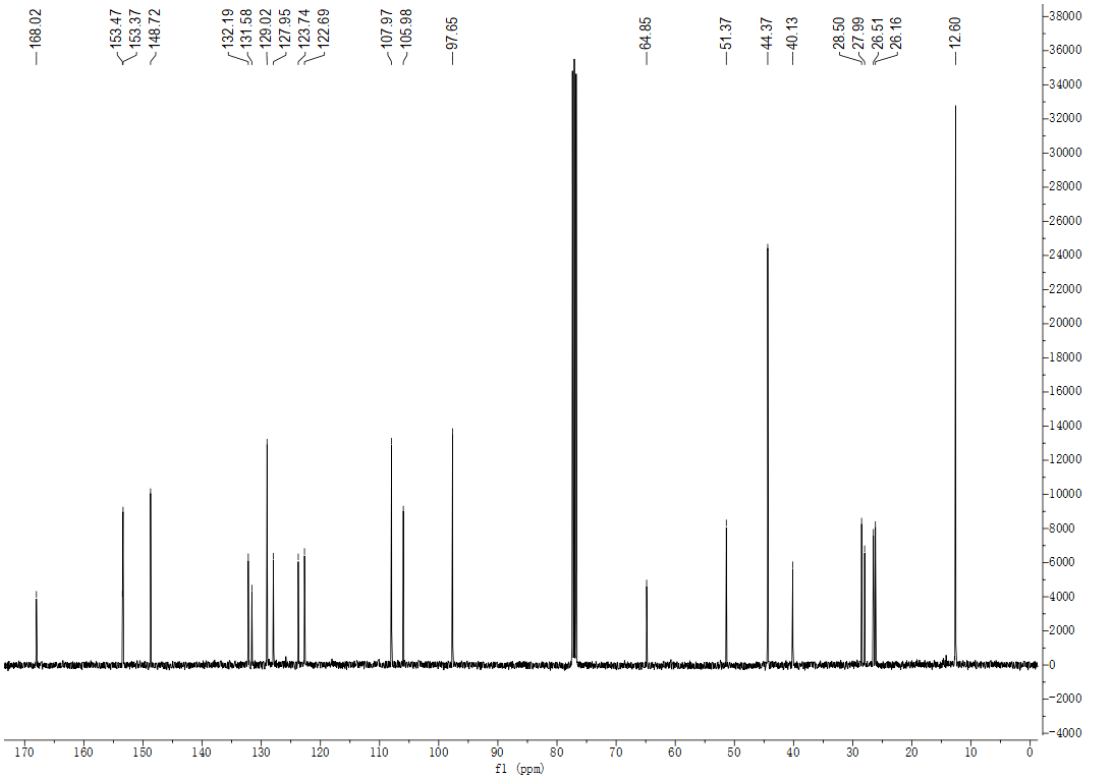

2-(2-(2-(2-(2-Azidoethoxy)ethoxy)ethoxy)ethyl)-3',6'-bis(diethylamino)spiro [isoindoline-1,9'-xanthen]-3-one (S91)

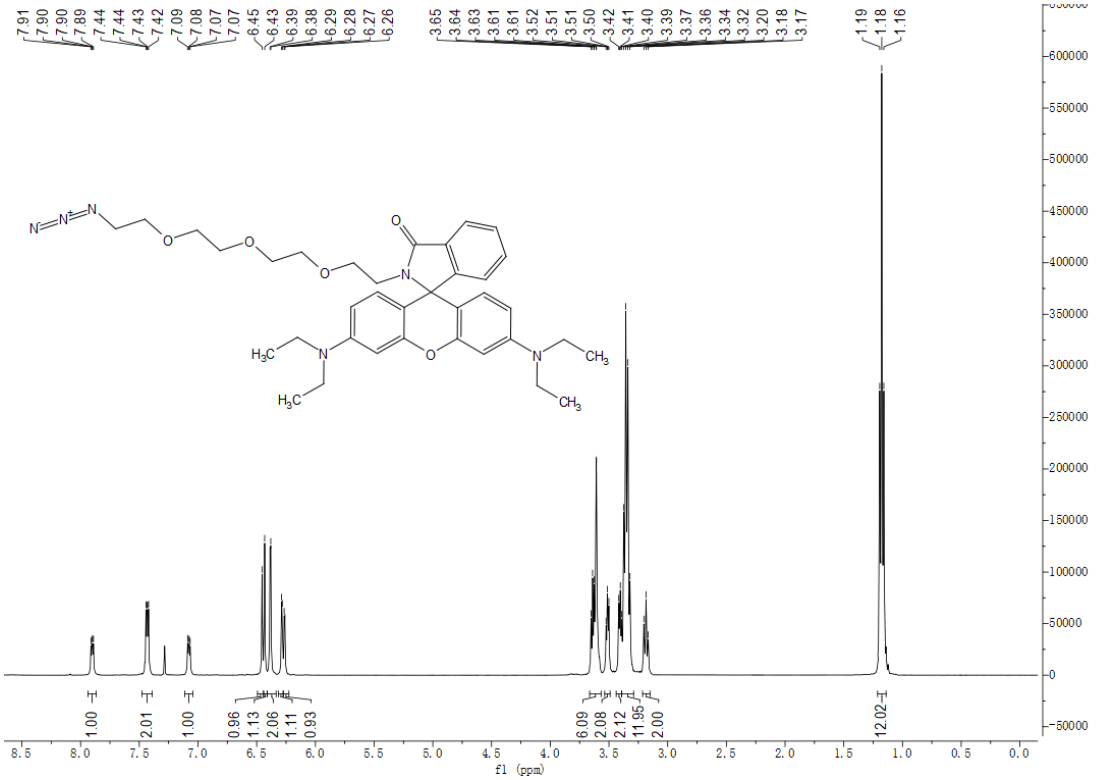

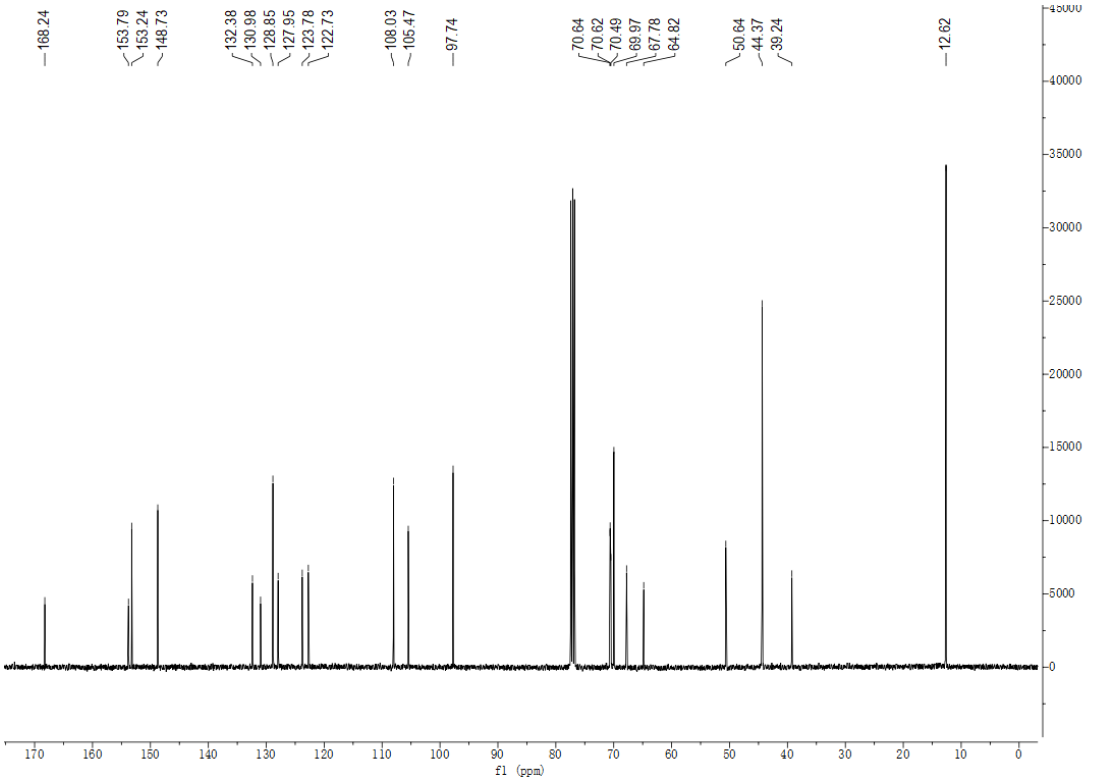

1-(5-Carboxypentyl)-2,3,3-trimethyl-3*H*-indolium bromide (S92)

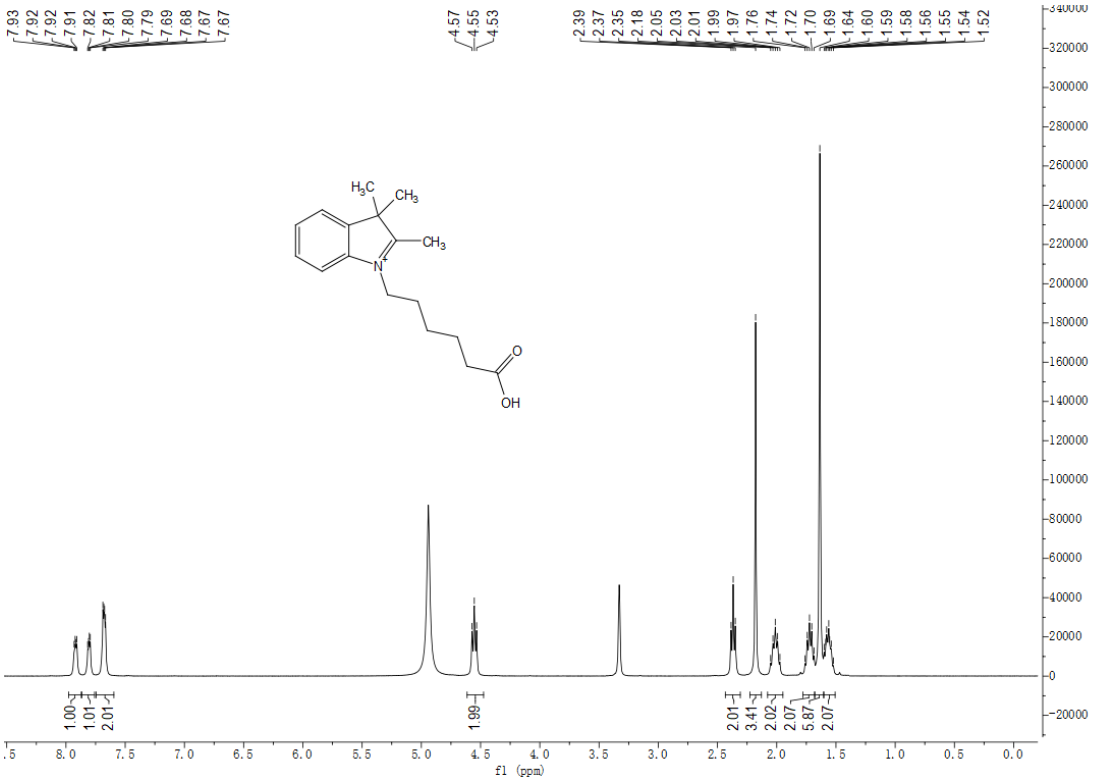

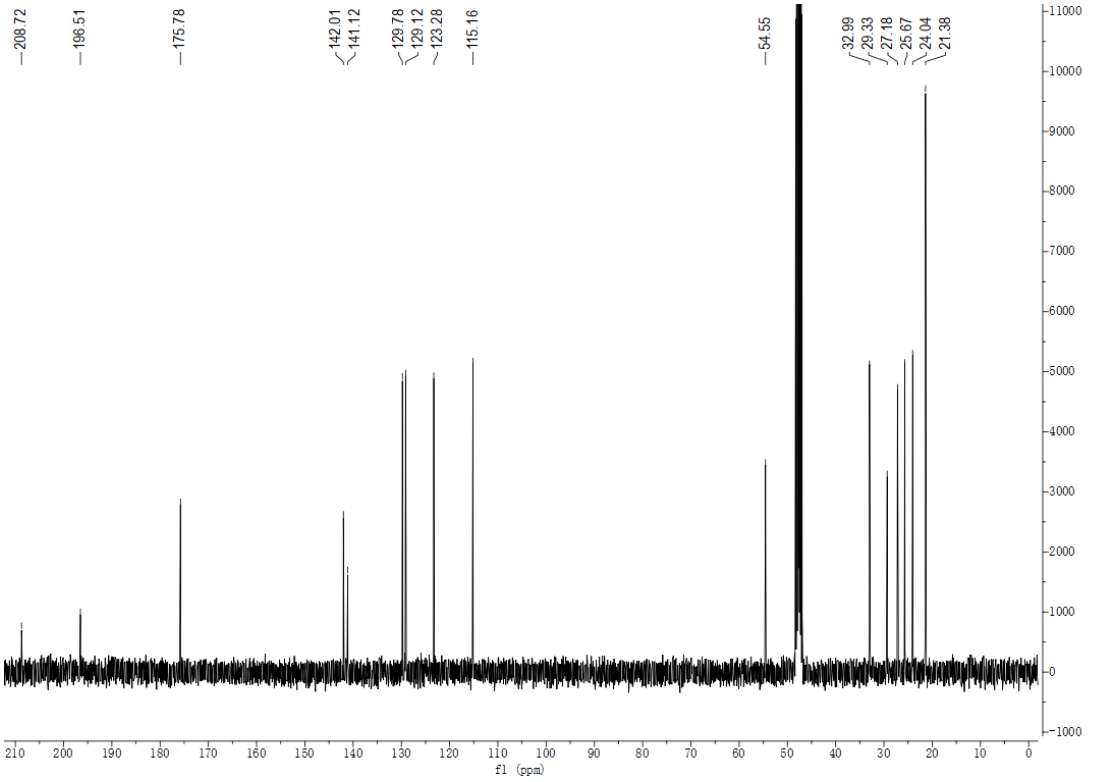

1,2,3,3-Tetramethyl-3*H*-indolium iodide (S93)

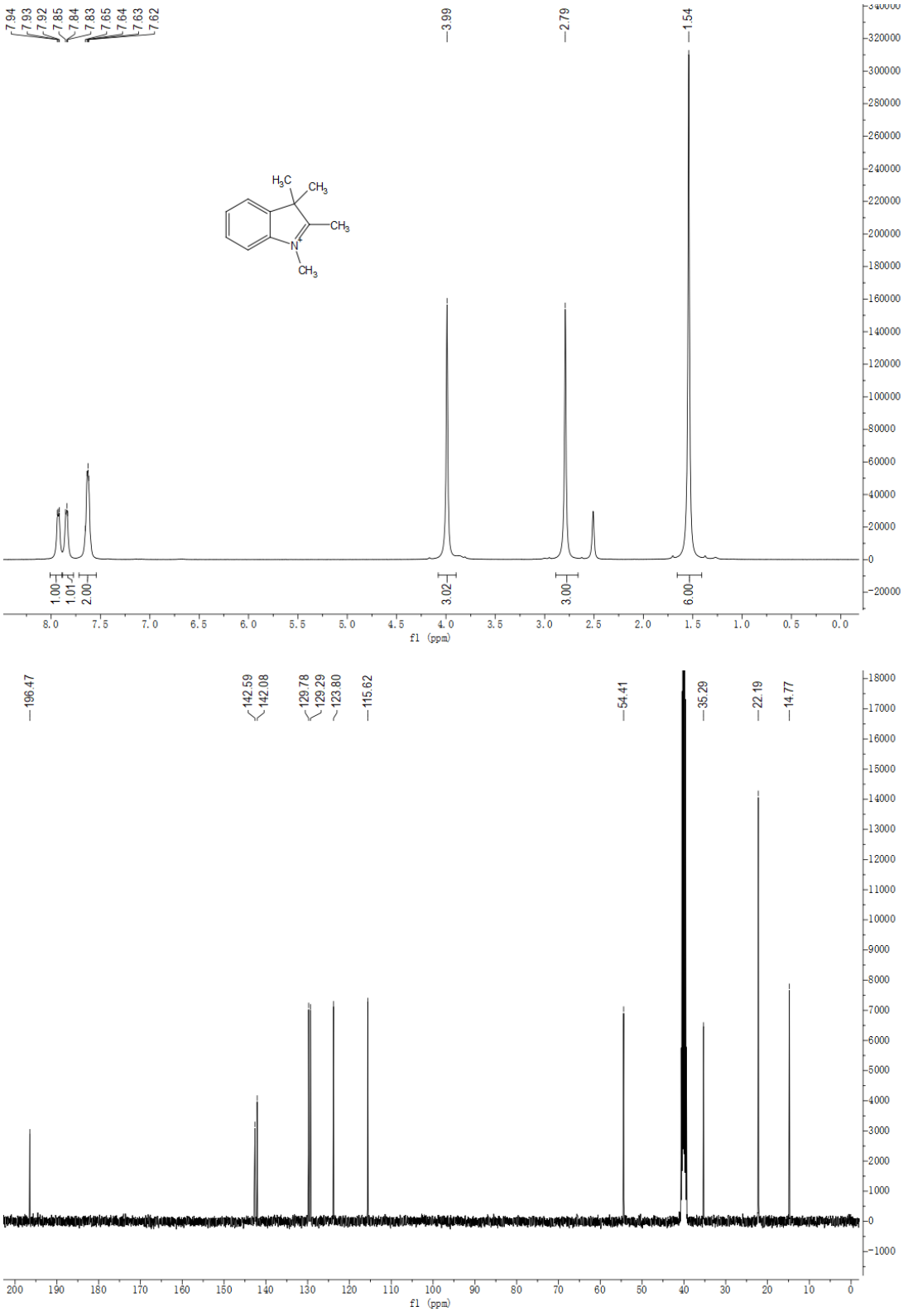

2-((1E,3E)-5-((E)-1-(5-carboxypentyl)-3,3-dimethylindolin-2-ylidene)penta-1,3-dien-1-yl)-1,3,3-trimethyl-3H-indol-1-ium chloride (S94)

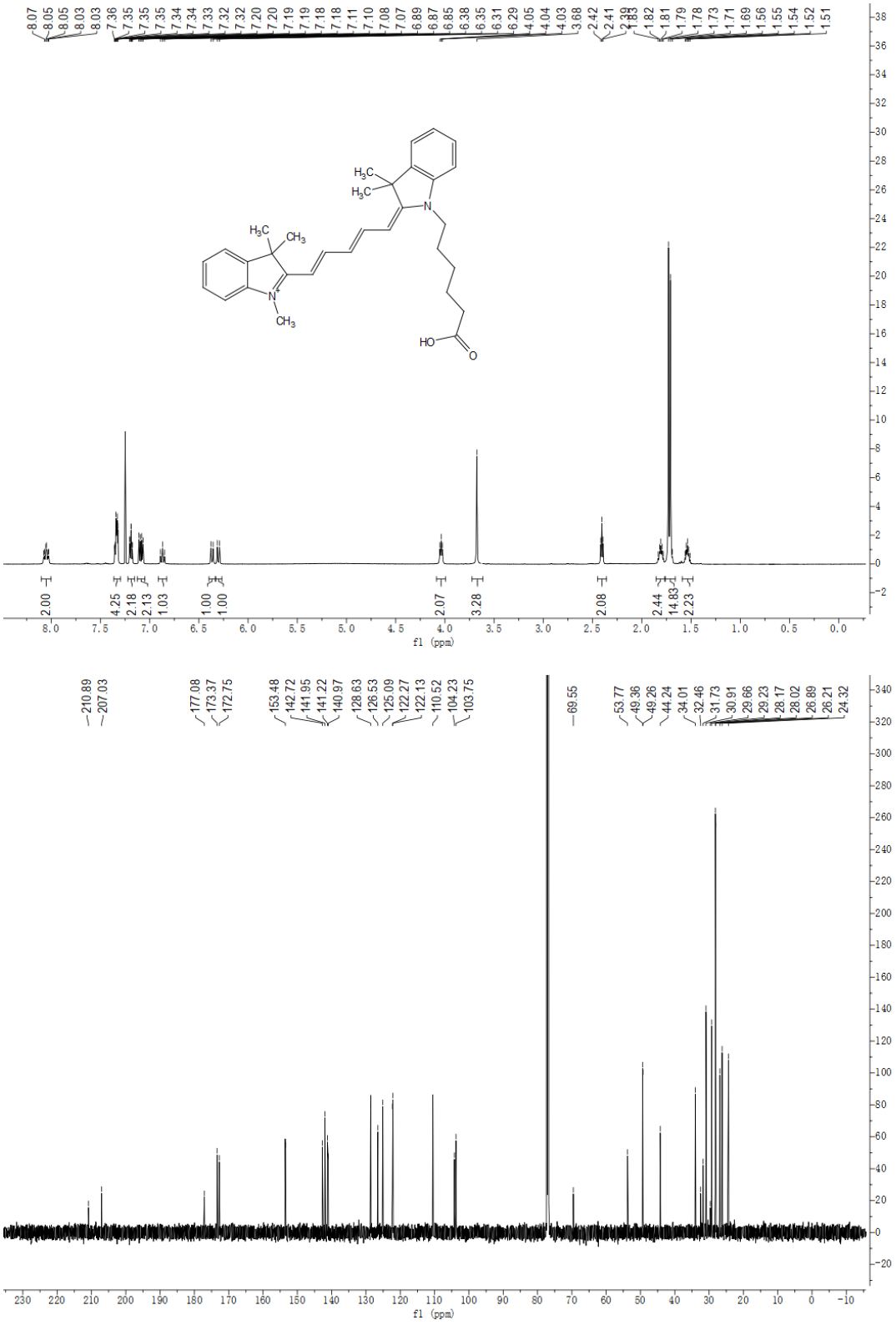

2-((1E,3E)-5-((E)-1-(6-((2,5-dioxopyrrolidin-1-yl)oxy)-6-oxohexyl)-3,3-dimethylindolin-2-ylidene)penta-1,3-dien-1-yl)-1,3,3-trimethyl-3H-indol-1-ium chloride (S95)

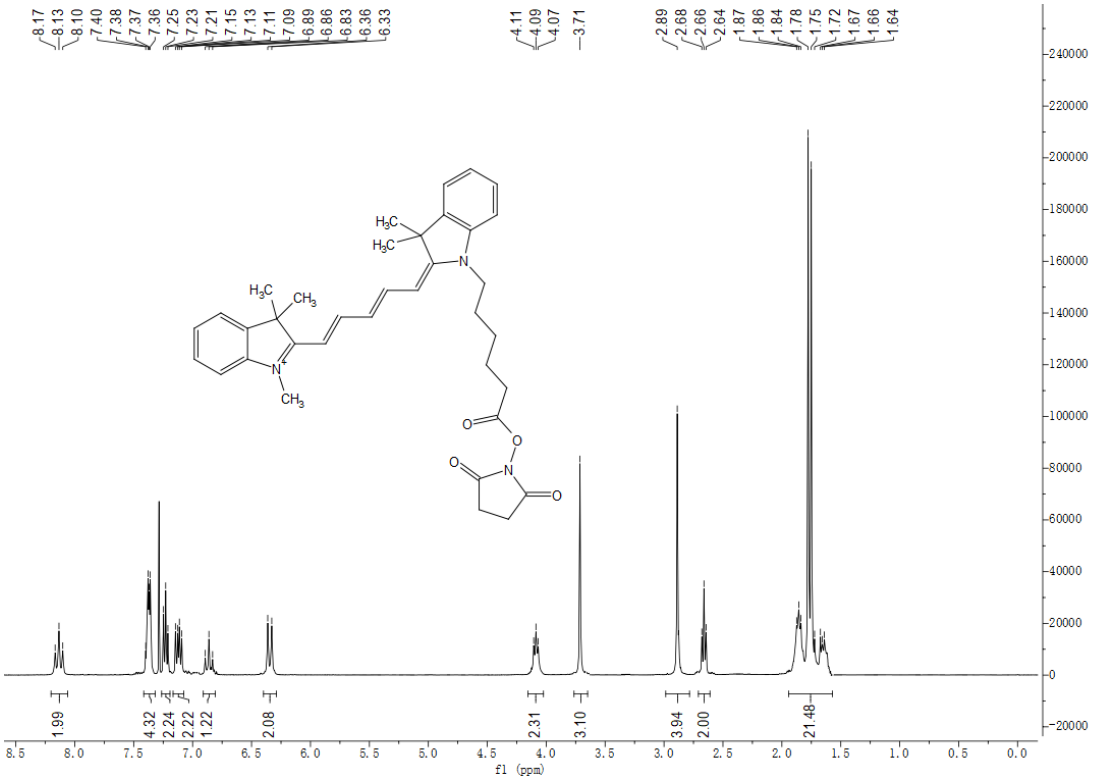

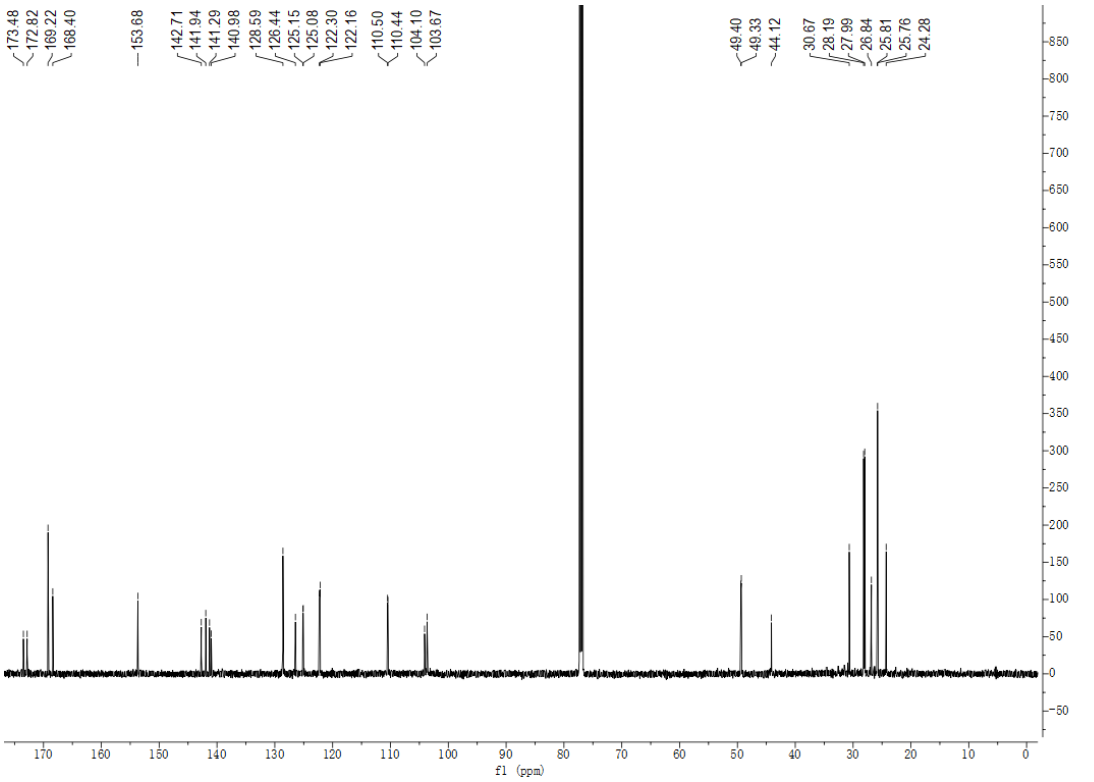

Nitro-BODIPY-NBD probe (S99)

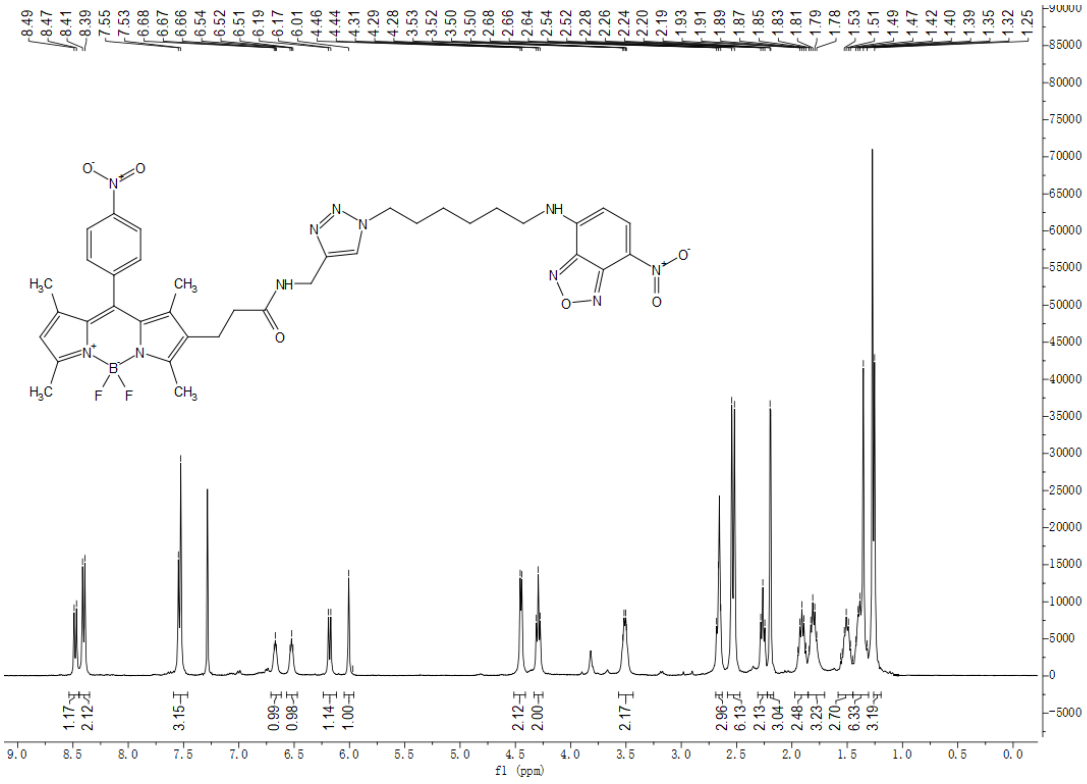

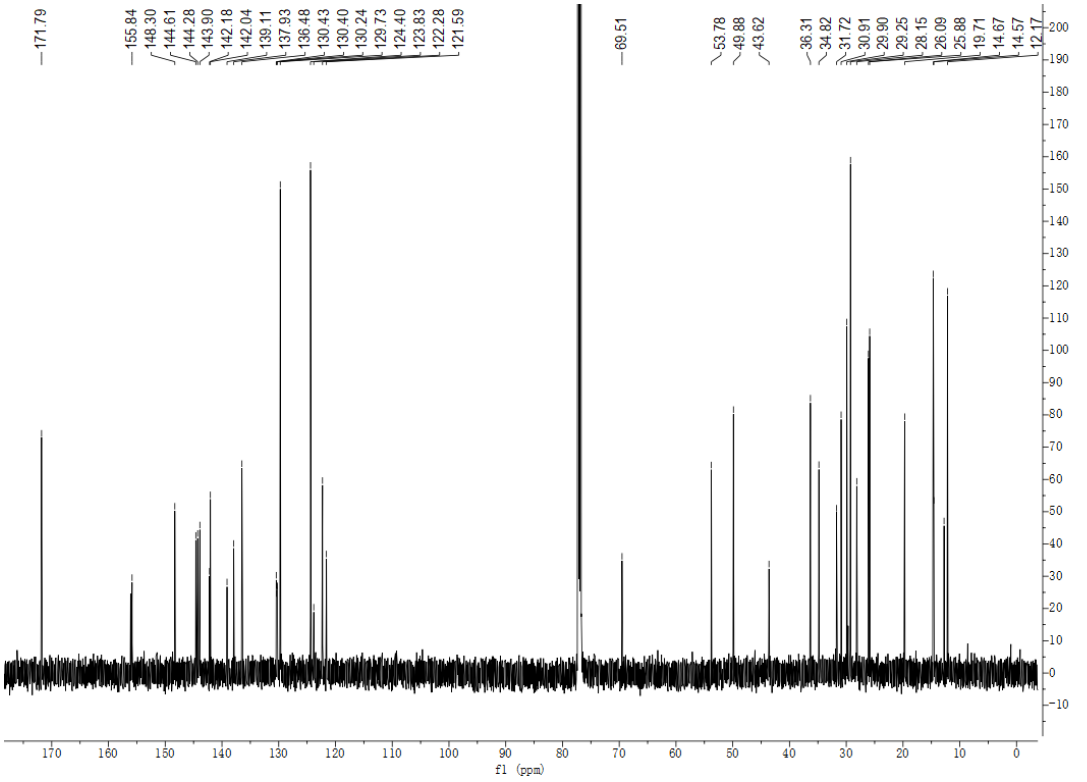

Nitro-BODIPY-dansyl probe (S100)

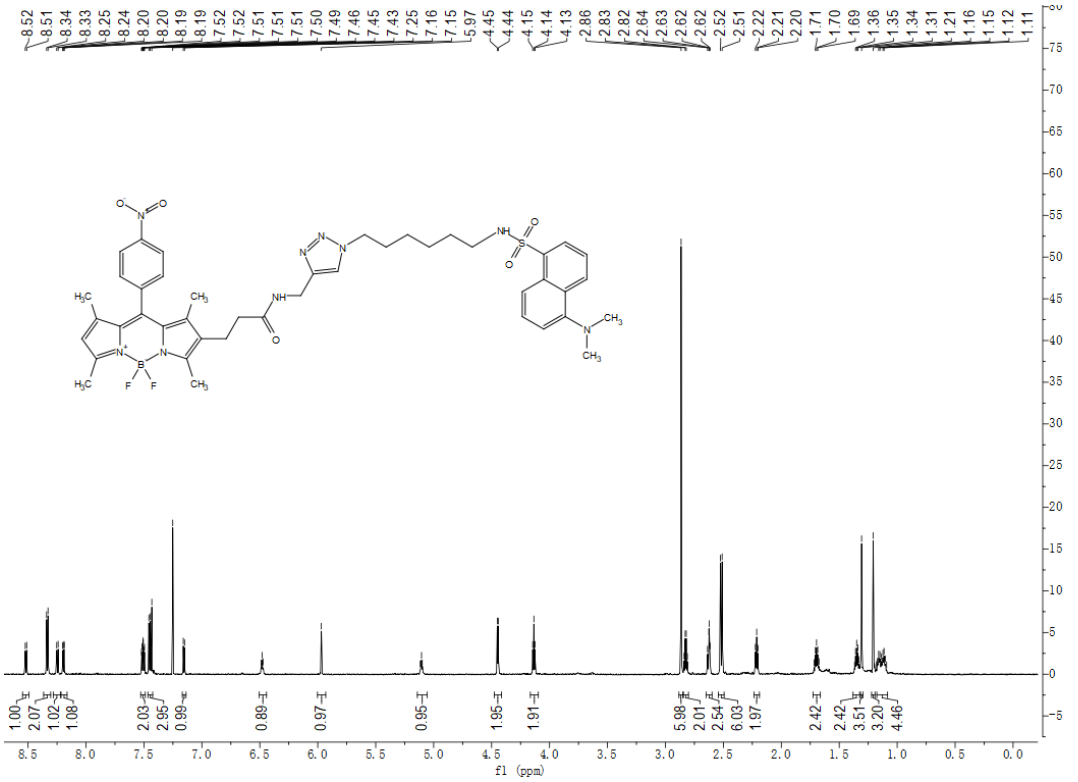

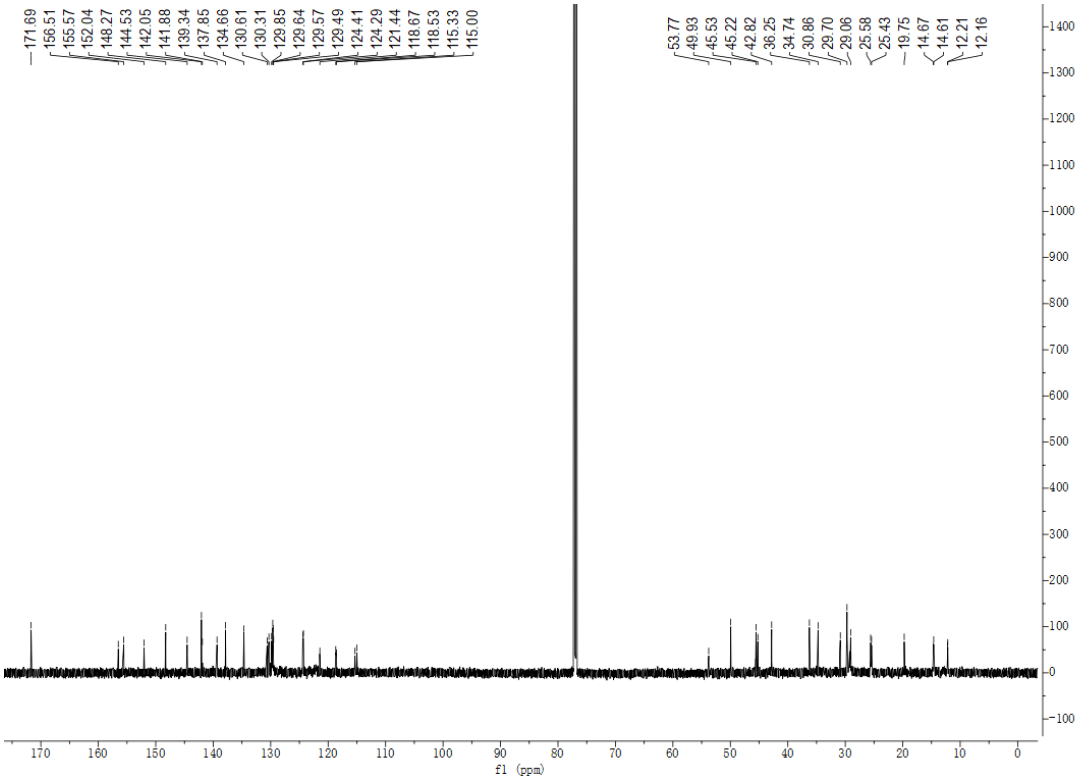

Nitro-BODIPY-Cy5 probe (S101)

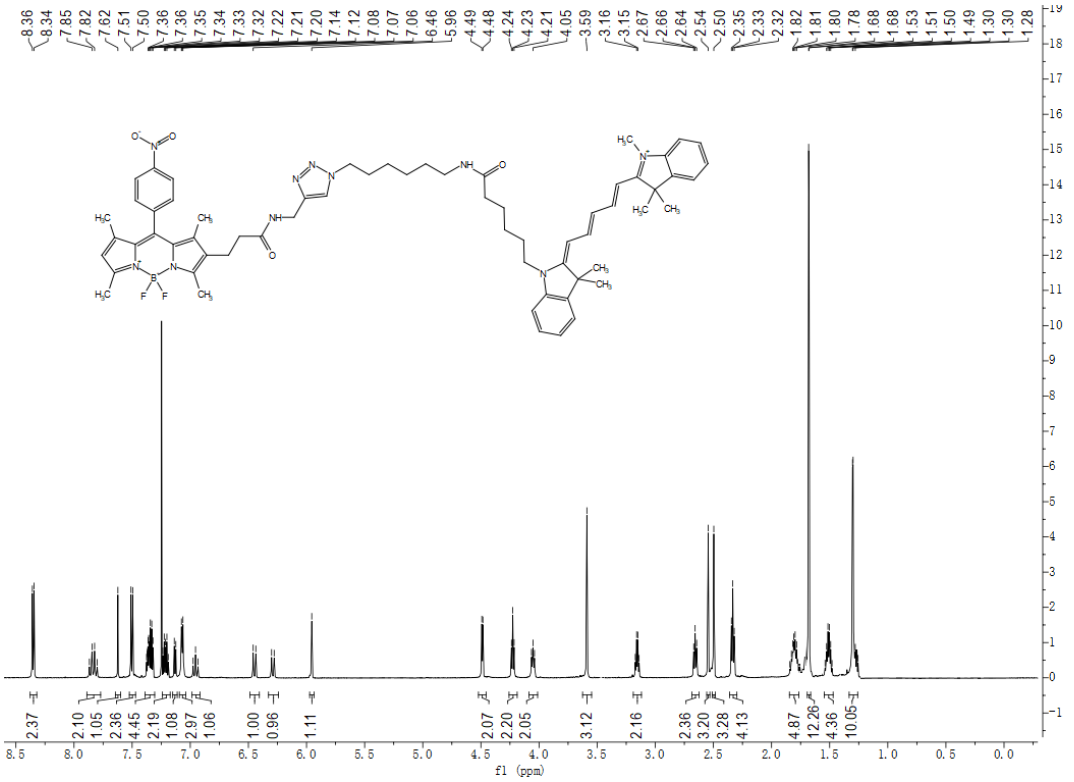

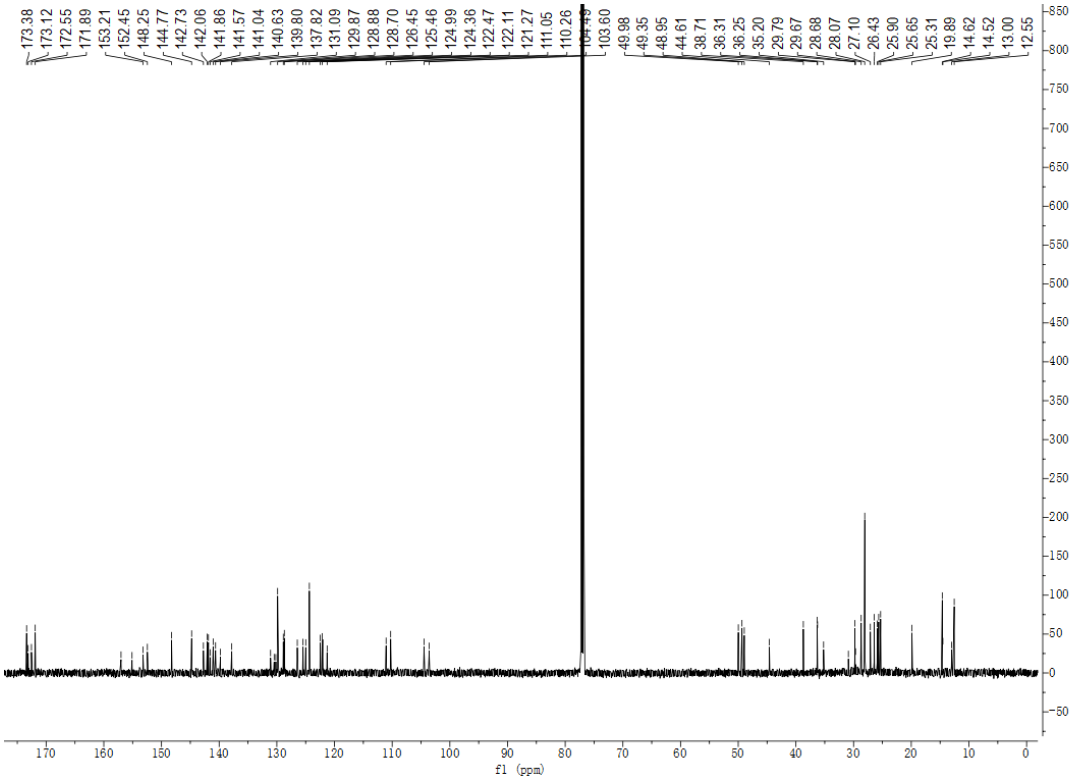

Nitro-BODIPY-C_6H_{12}-Rhodamine B probe (S102)

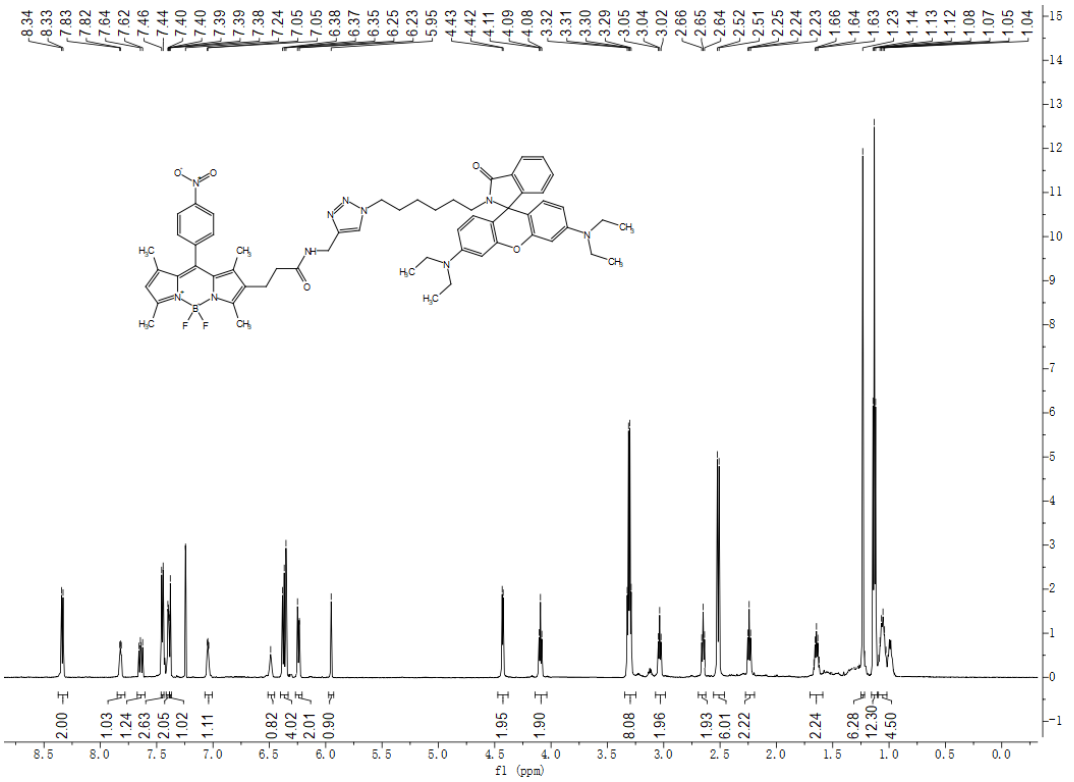

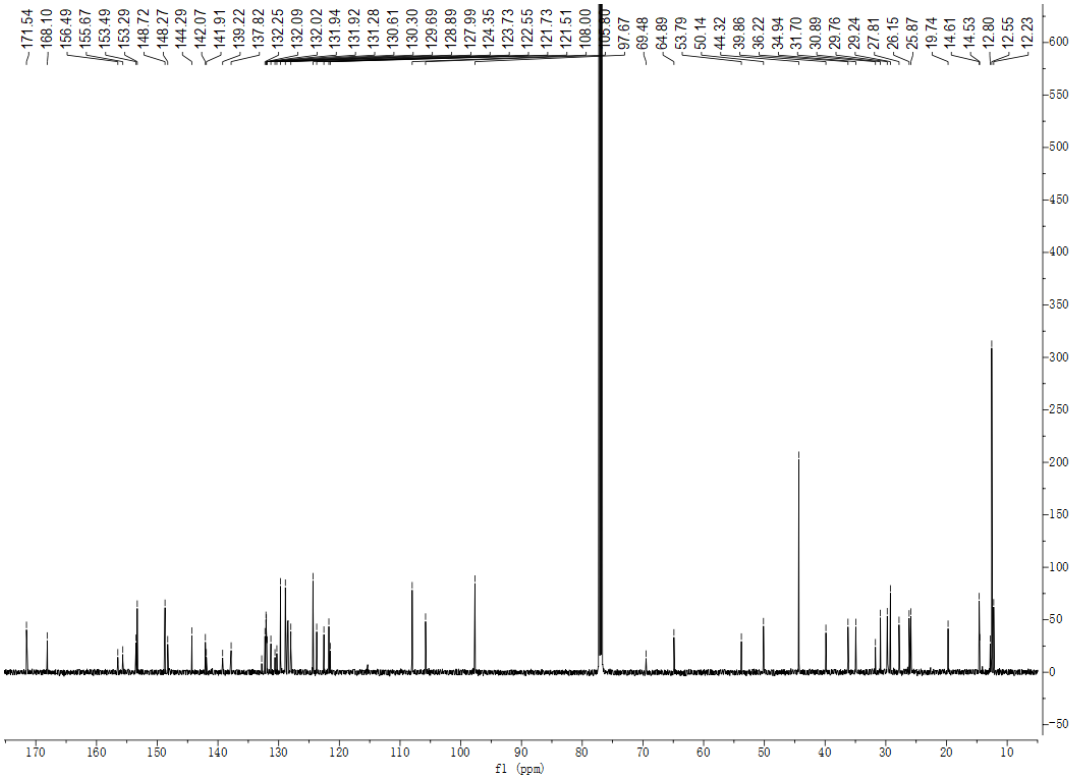

Nitro-BODIPY-PEG-Rhodamine B probe (S103)

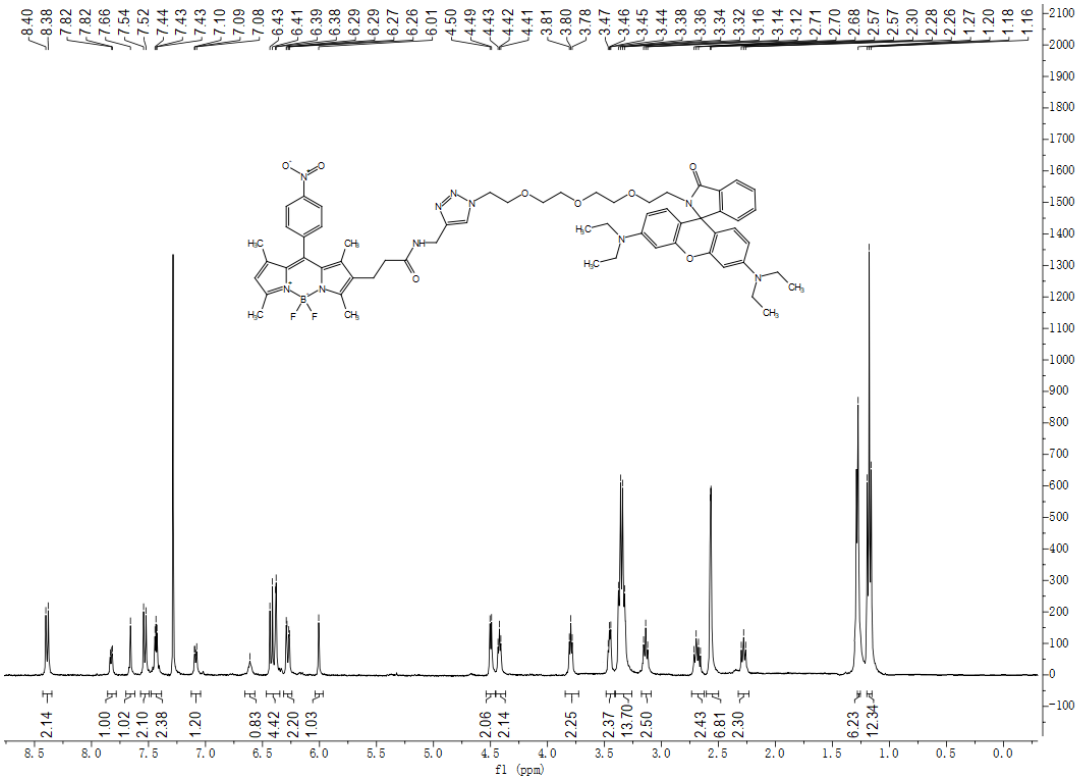

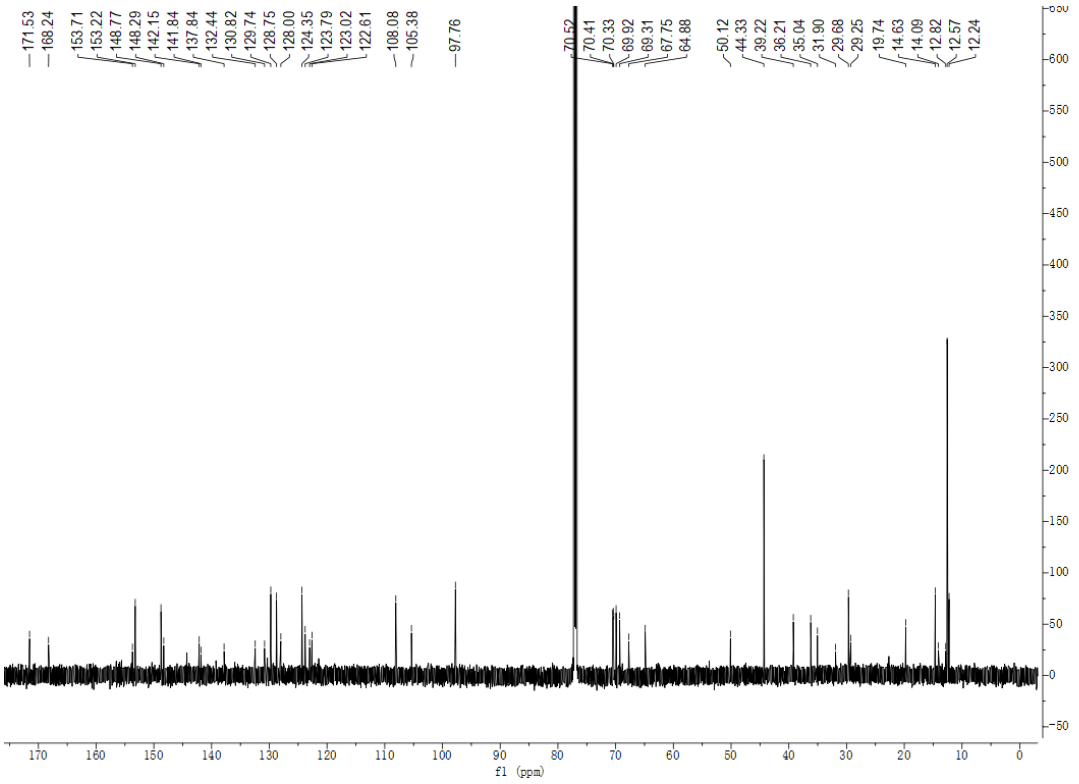

Nitro-BODIPY-NBD probe (S104)

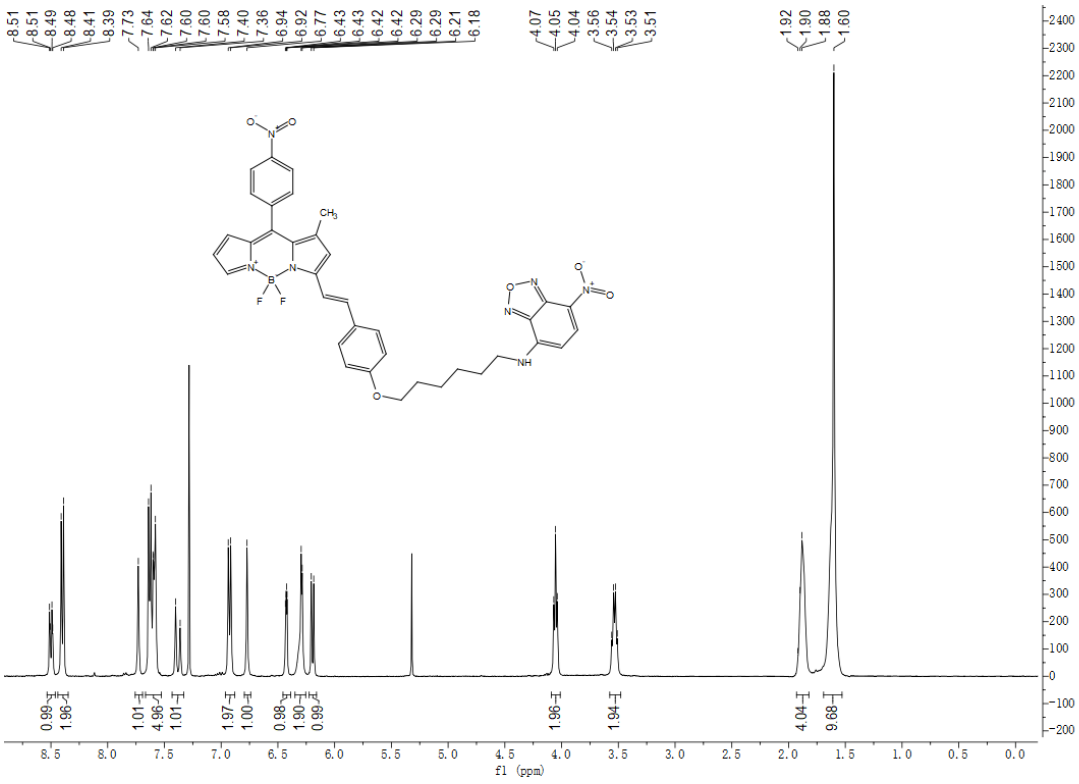

Nitro-BODIPY-NBD probe (S105)

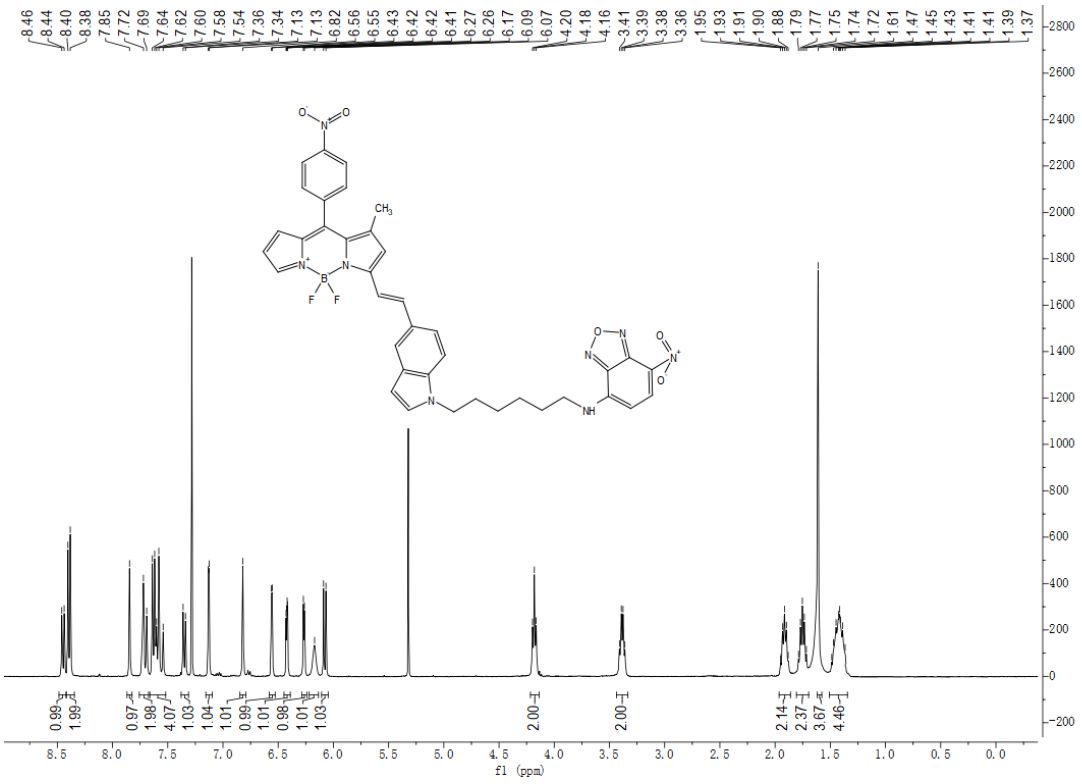

Nitro-BODIPY-NBD probe (S106)

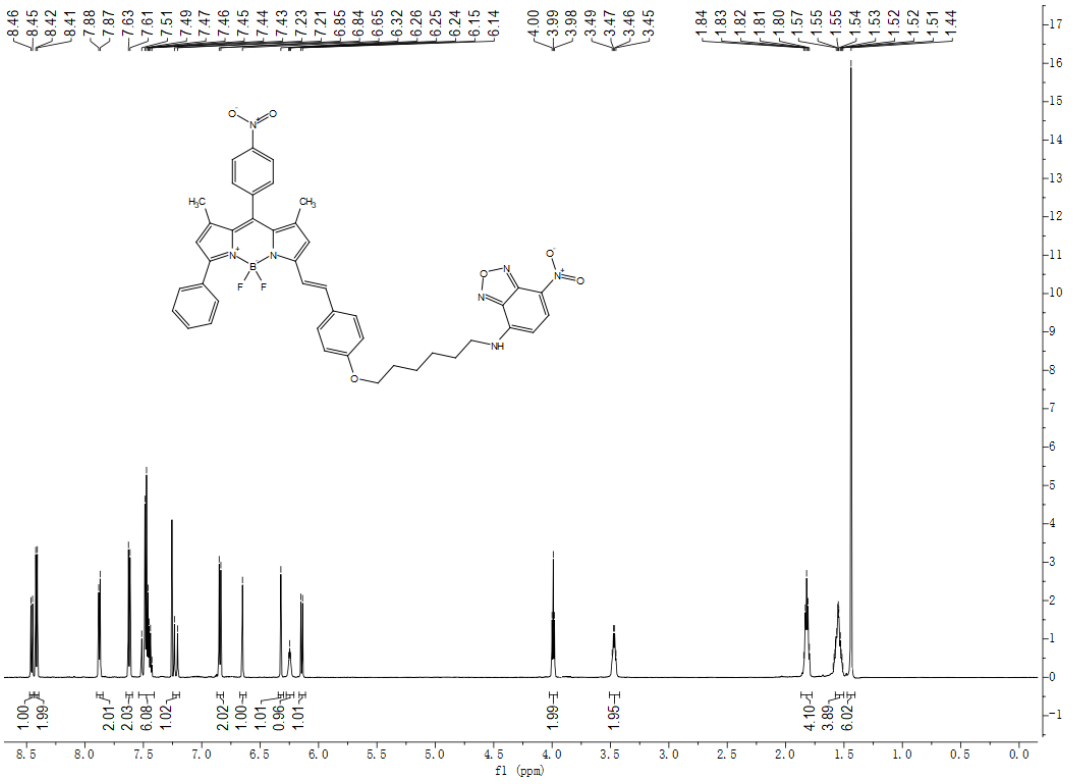

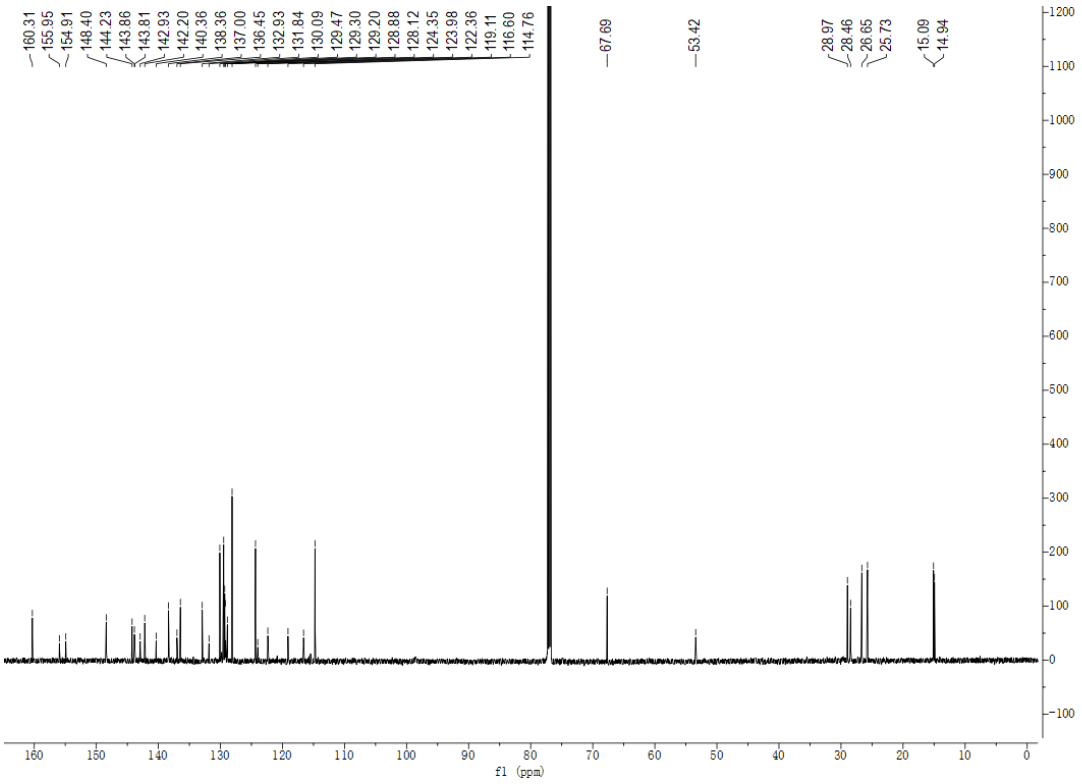

Nitro-BODIPY-NBD probe (S107)

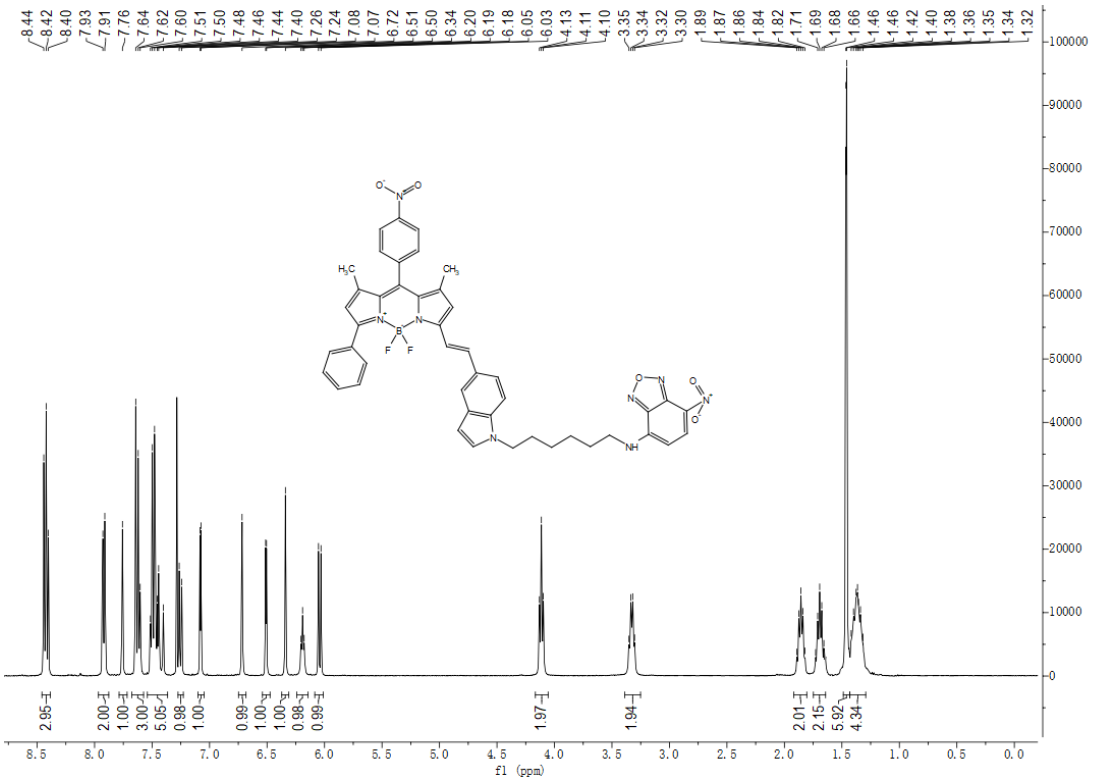

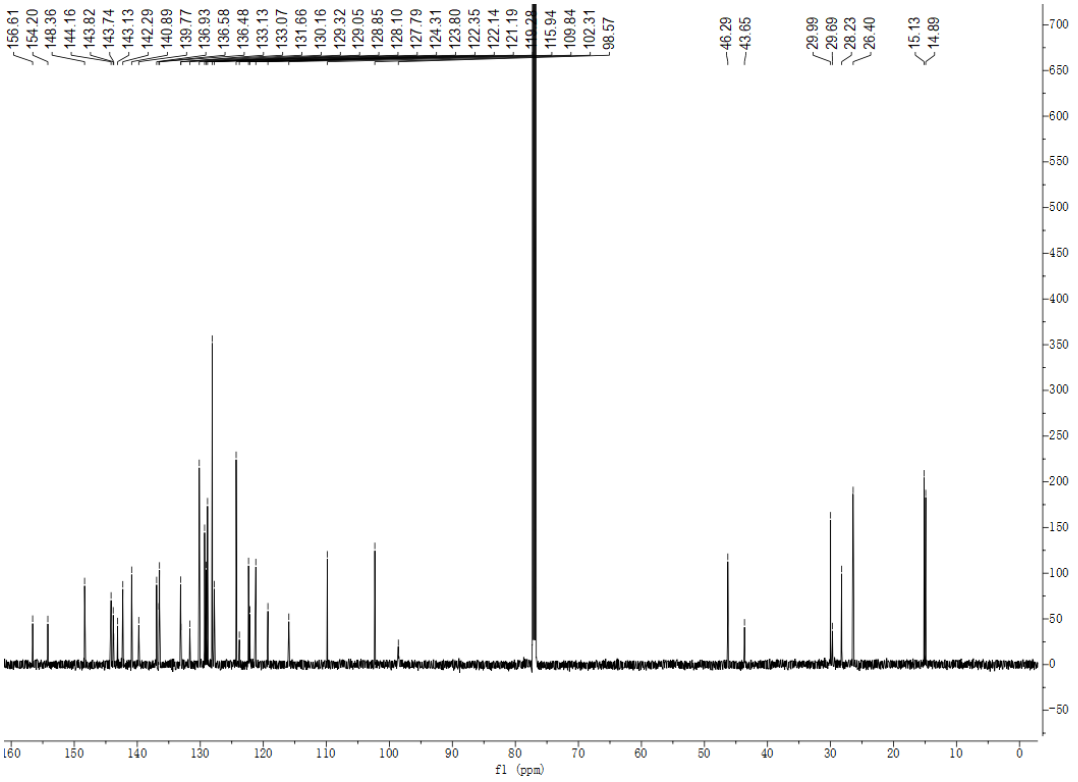

Methyl 4-(4-methoxybenzoyl)benzoate (S108)

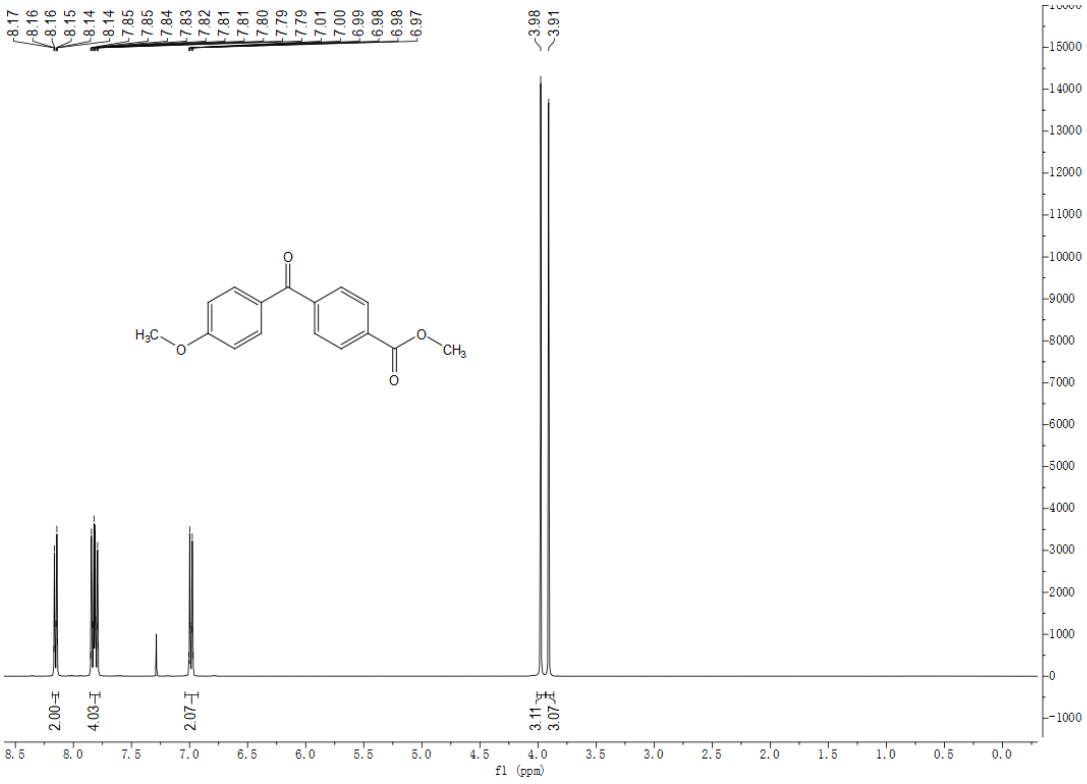

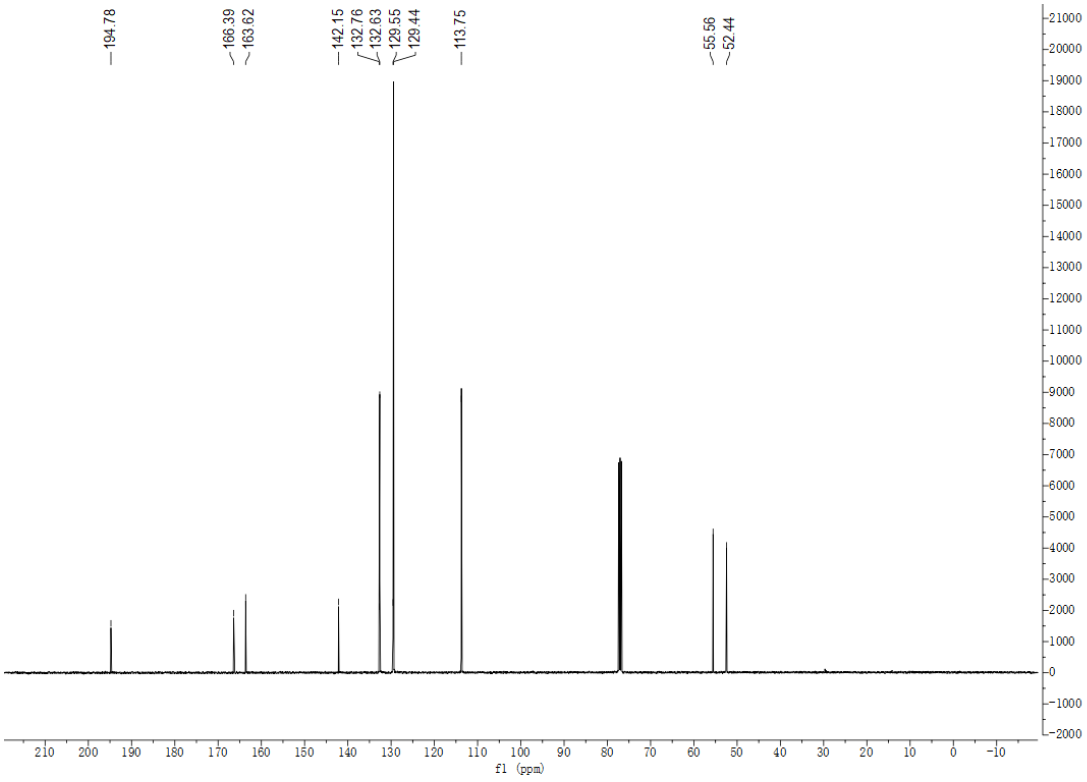

Methyl 4-(4-hydroxybenzoyl)benzoate (S109)

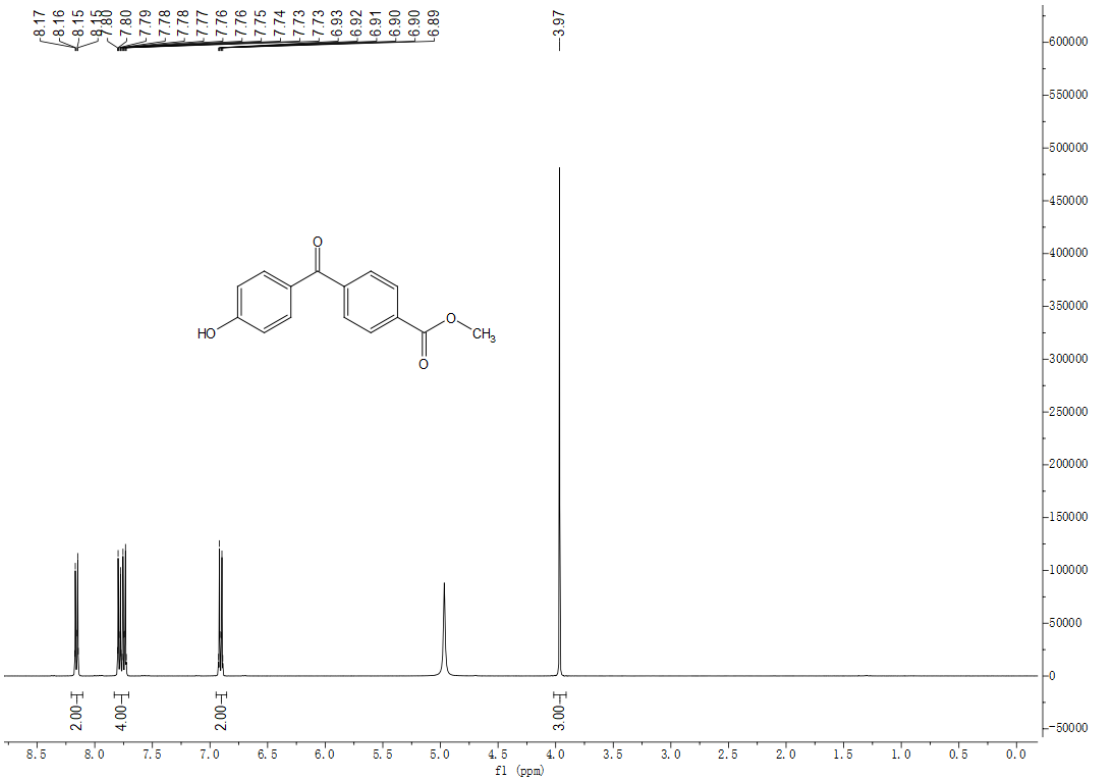

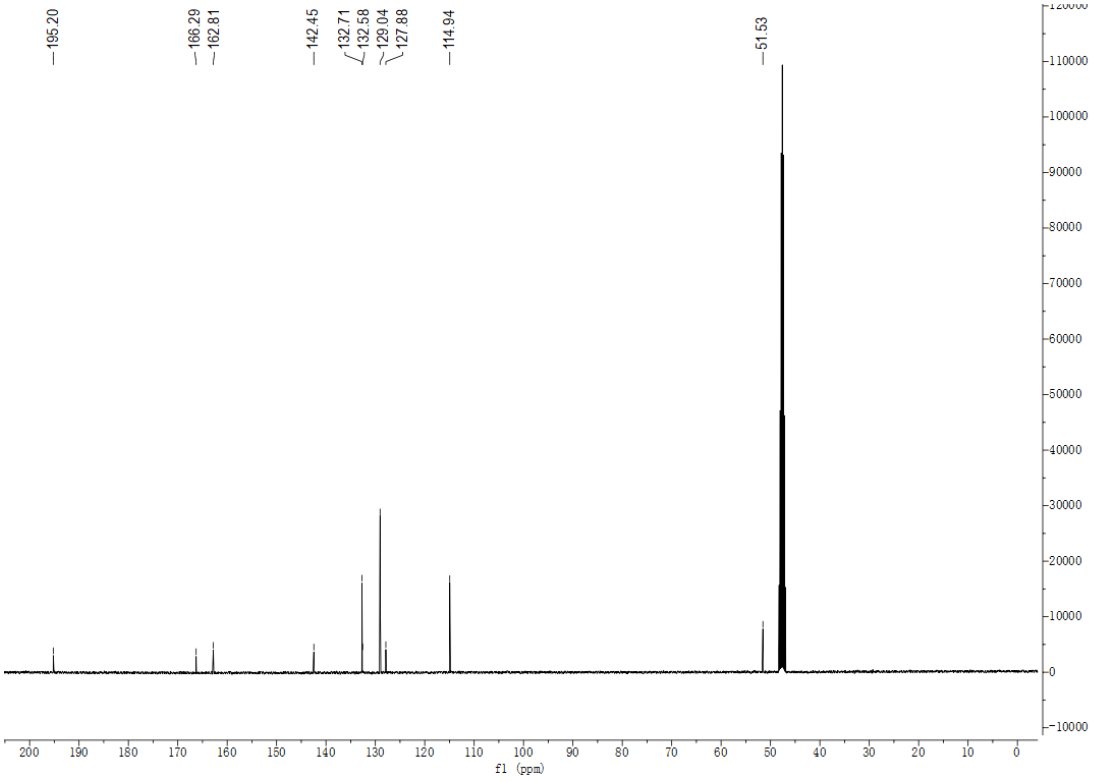

Methyl 4-(4-(hex-5-yn-1-yloxy)benzoyl)benzoate (S110)

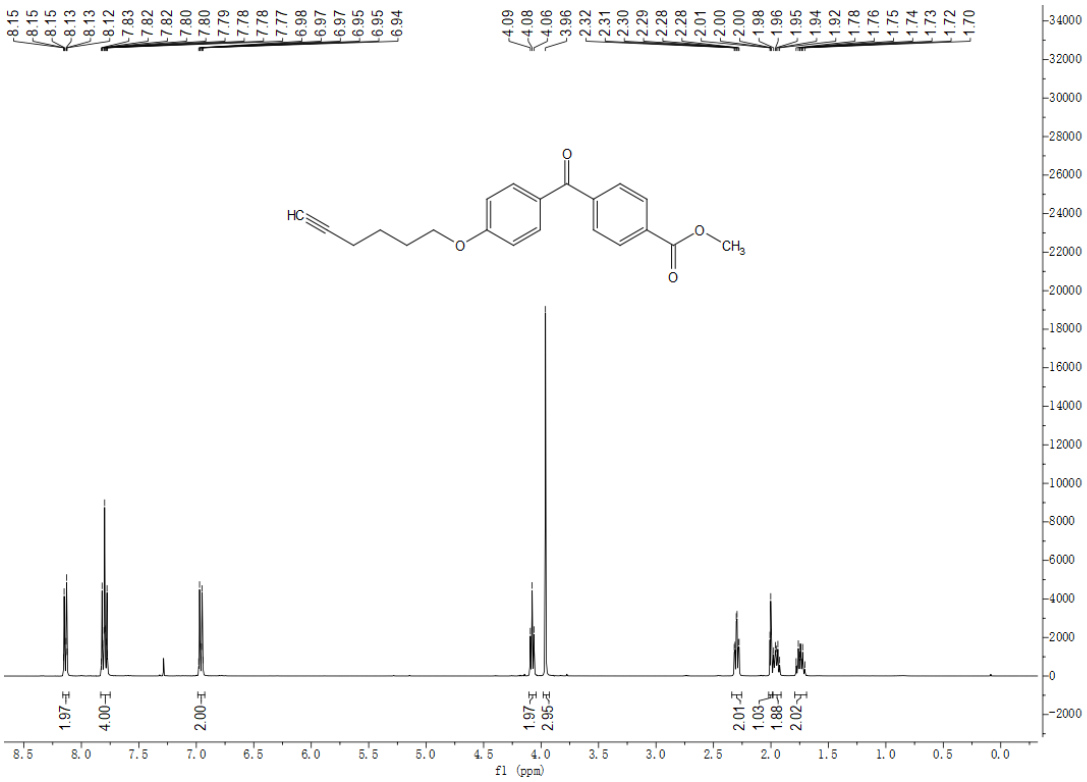

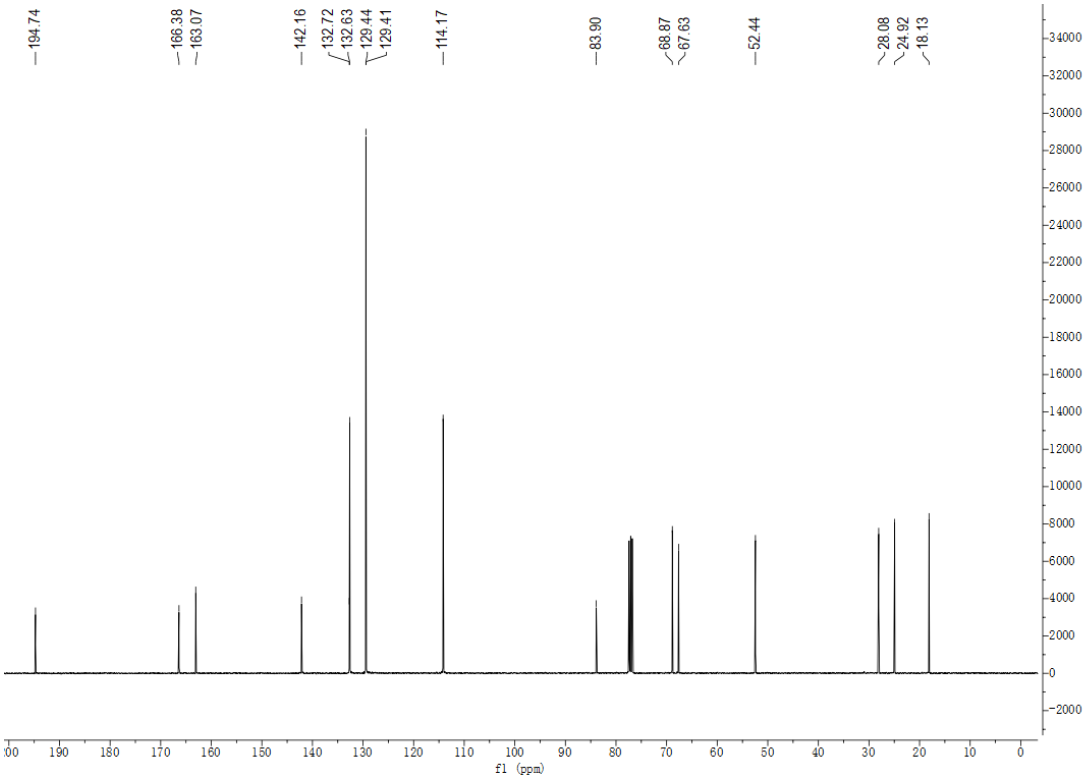

4-(4-(Hex-5-yn-1-yloxy)benzoyl)benzoic acid (S111)

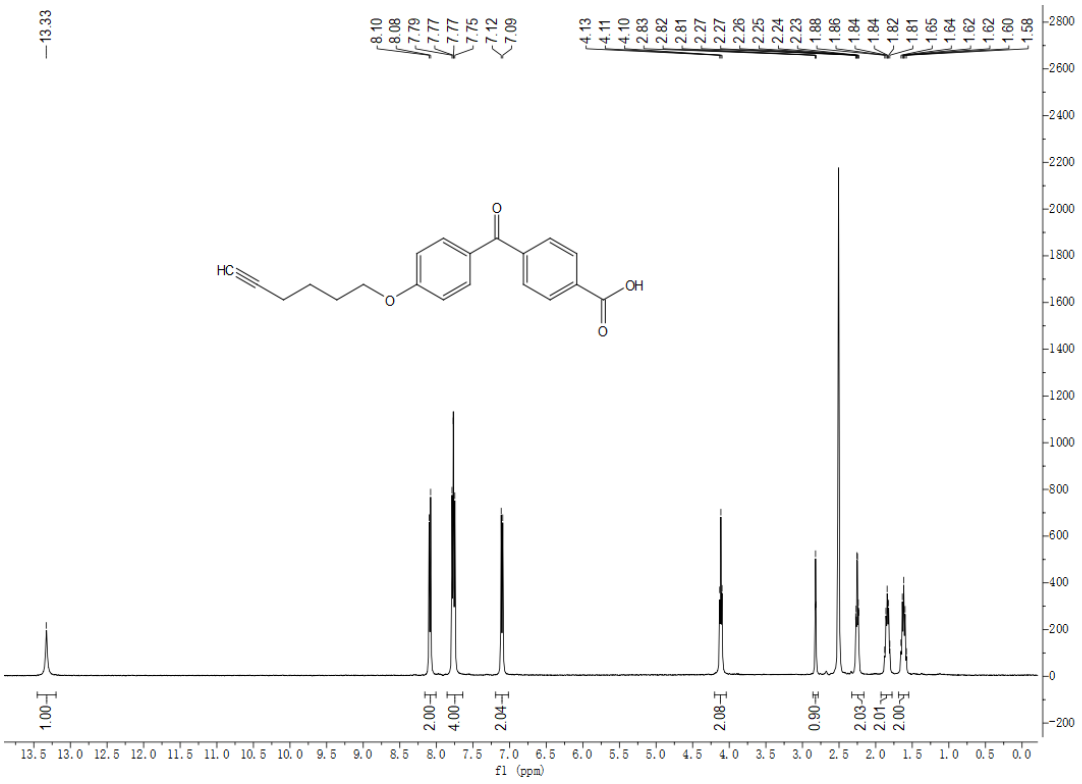

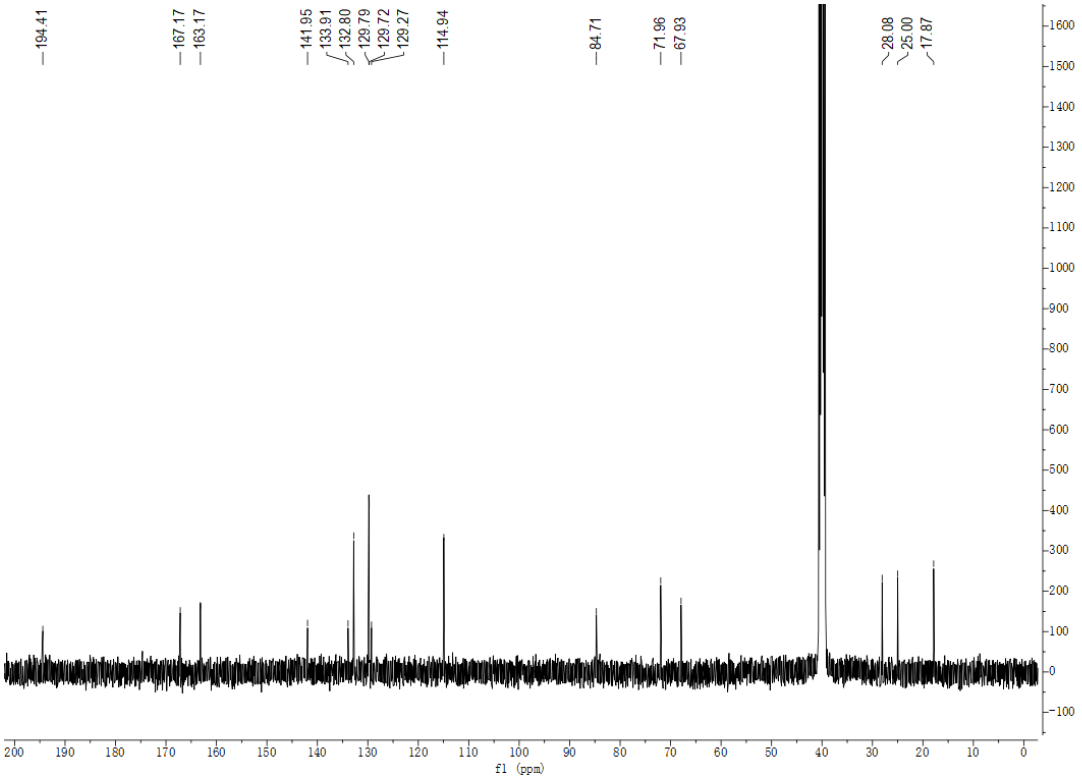

Tert-butyl (6-(4-(4-(hex-5-yn-1-yloxy)benzoyl)benzamido)hexyl)carbamate (S112)

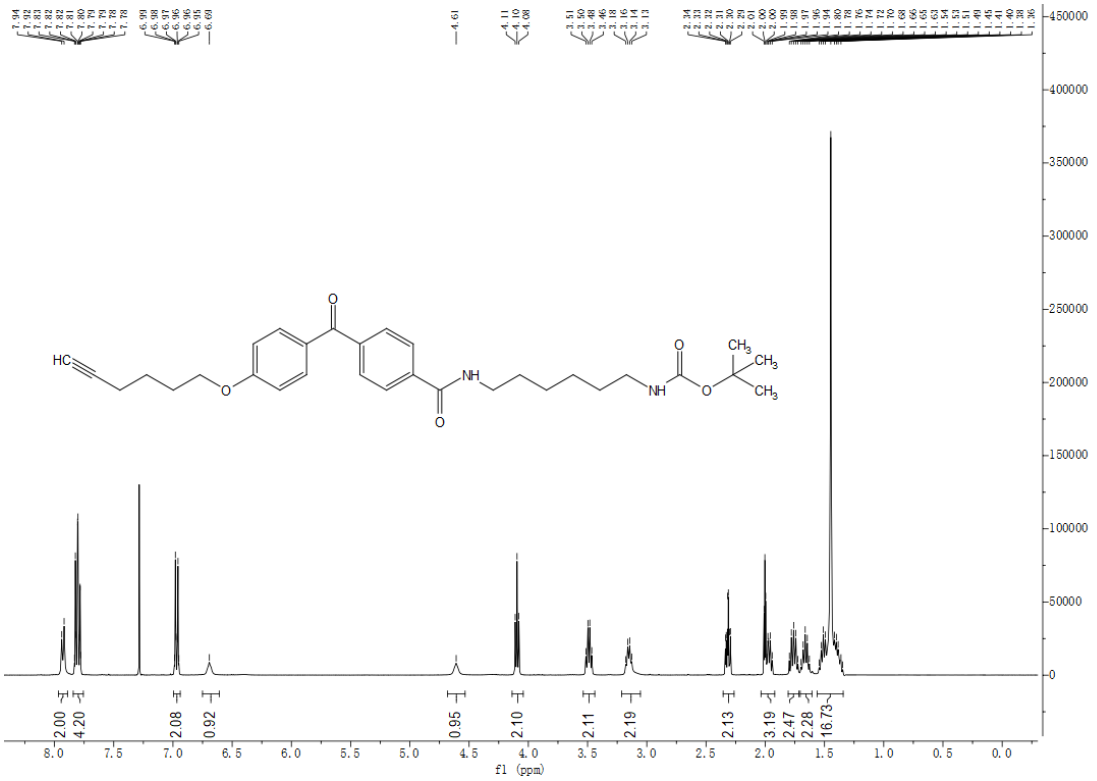

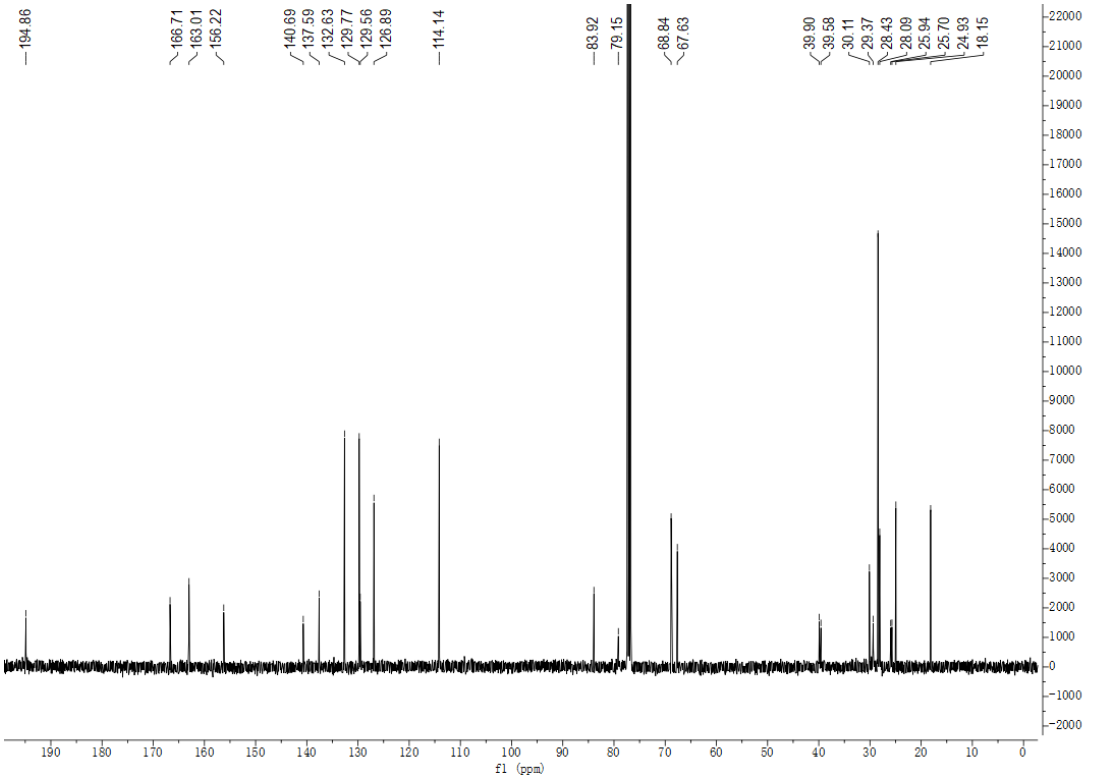

Photoaffinity labelling probe (S114)

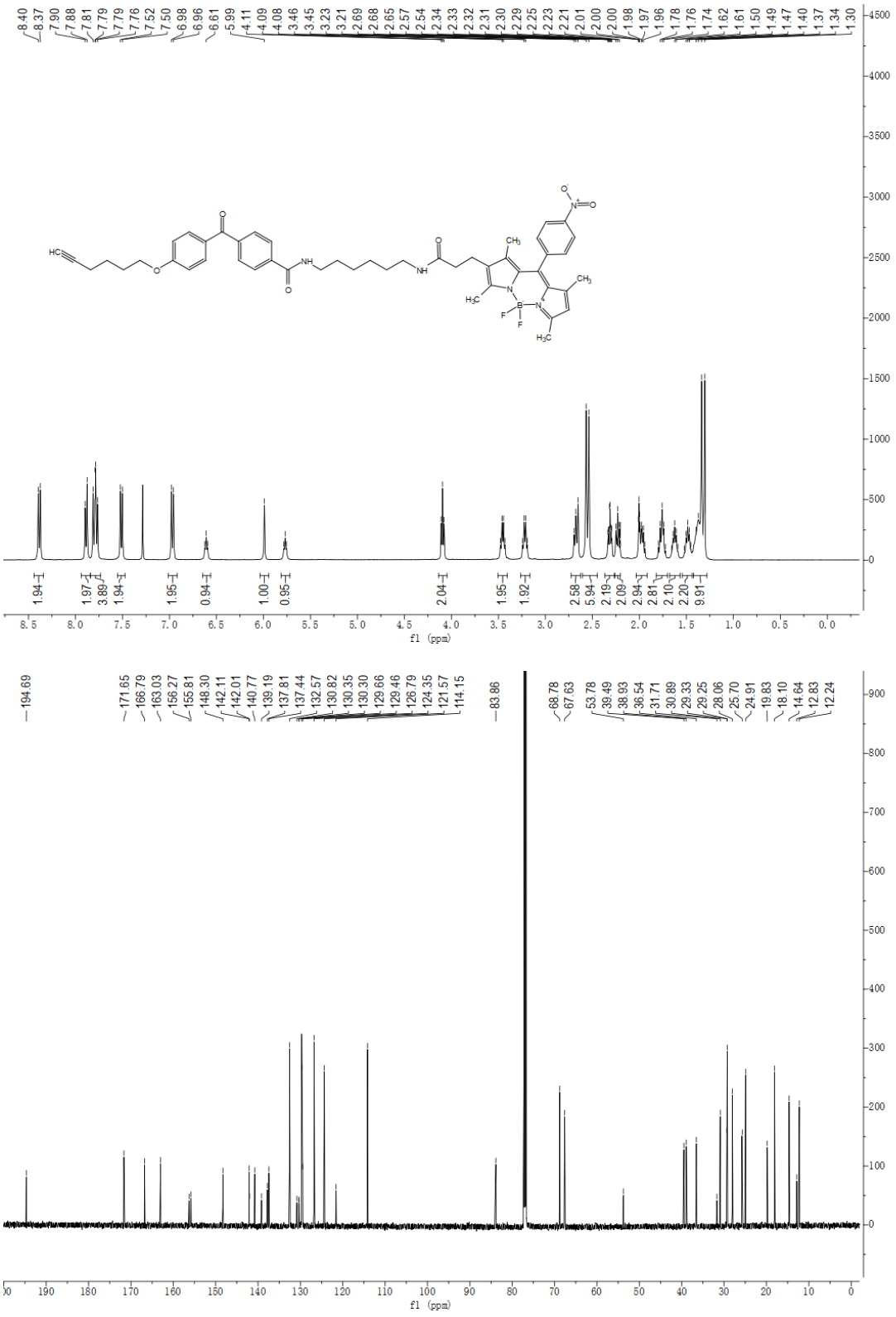

8 REFERENCES

1. Tram, K.; Yan, H.; Jenkins, H. A.; Vassiliev, S.; Bruce, D., The synthesis and crystal structure of unsubstituted 4,4-difluoro-4-bora-3a,4a-diaza-s-indacene (BODIPY). *Dyes Pigments* **2009,** *82* (3), 392-395.
2. Alfred, T.; Franz, H. K., Difluorboryl-Komplexe von Di- und Tripyrrylmethenen. *Liebigs Ann. Chem.* **1968,** *718*, 208-223.
3. Dixon, H. B. F.; Cornish,.B. A.; Liebecq, C.; Loening K. L.; Moss G. P.; Reedijk, J.; Velick, S. F.; Venetianer, P.; Vliegenthart, J. F. G., Nomenclature of tetrapyrroles. *Pure Appl. Chem.* **1987,** *59*, 779-832.
4. Aurore, L.; Kevin, B., BODIPY Dyes and Their Derivatives: Syntheses and Spectroscopic Properties. *Chem. Rev.* **2007,** *107*, 4891-4931.
5. Brandon, R. G.; Sarah, M. C.; Travis, L.; Cherif, F. M.; Shahin, S. H.; Alison, T., Synthesis and characterisation of the unsubstituted dipyrrin and 4,4-dichloro-4-bora-3a,4a-diaza-s-indacene: improved synthesis and functionalisation of the simplest BODIPY framework. *Chem. Commun.* **2013,** *49*, 816-818.
6. E. Vos de Wael; J. A. Pardoen; J. A. van Koeveringe; J. Lugtenburg, Pyrromethene-BF2 complexes (4,4′-difluoro-4-bora-3a,4a-diaza-s-indacenes). Synthesis and luminescence properties. *J. Recl. TraV. Chim. Pays-Bas* **1977,** *96*, 306-309.
7. Esnal, I.; Valois, E. I.; Gomez, D. C. F.; Urias, B. A.; Betancourt, M. M. L.; Lopez, A. I.; Banuelos, J.; Garcia, M. I.; Costela, A.; Pena, C. E., Blue-to-orange color-tunable laser emission from tailored boron-dipyrromethene dyes. *Chemphyschem* **2013,** *14* (18), 4134-4142.
8. Lucas, C. D. D. R.; Miguel, M. V.; Juliana, C. B. M.; Flavio, D. S. E., Synthesis, Photophysical Properties and Solvatochromism of Meso-Substituted Tetramethyl BODIPY Dyes. *J. Fluoresc.* **2014,** *24*, 257-266.
9. Thompson, A.; Lund, K. L. A. R., Synthesis of Symmetric meso-H-Dipyrrin Hydrobromides from 2-Formyl-pyrroles. *Syn. lett.* **2014,** *25* (08), 1142-1144.
10. Zhang X. F.; Zhang G. Q.; Zhu J.; Methylated Unsymmetric BODIPY Compounds: Synthesis, High Fluorescence Quantum Yield and Long Fluorescence Time. *J. Fluoresc.* **2019,** *29* (2), 407-416.
11. Watanabe, H.; Ono, M.; Matsumura, K.; Yoshimura, M.; Kimura, H.; Saji, H., Molecular Imaging of β-Amyloid Plaques with Near-Infrared Boron Dipyrromethane (BODIPY)-Based Fluorescent Probes. *Mol. Imaging* **2013,** *12* (5), 338-347.
12. Yutanova, S. L.; Berezin, M. B.; Semeikin, A. S.; Antina, E. V.; Guseva, G. B.; V'yugin, A. I., Thermal oxidative degradation of the functionally substituted 2,2′-dipyrrolylmethenes hydrobromides and difluoroborates. *Russ. J. Gen. Chem.* **2013,** *83* (3), 545-551.
13. Ulrich, G.; Ziessel, R.; Harriman, A., The chemistry of fluorescent bodipy dyes: versatility unsurpassed. *Angew. Chem. Int. Ed. Engl.* **2008,** *47* (7), 1184-201.
14. Schlachter, A.; Fleury, A.; Tanner, K.; Soldera, A.; Habermeyer, B.; Guilard, R.; Harvey, P. D., The TDDFT Excitation Energies of the BODIPYs: The DFT and TDDFT Challenge Continues. *Molecules* **2021,** *26* (6).
15. Khalid, N.; Sreejisha, T. N.; Pranjali, Y.; Asifkhan, S.; Prakash, P. N., Supramolecular Confinement within Chitosan Nanocomposites Enhances Singlet Oxygen Generation. *Chem. Plus. Chem.* **2018,** *83*, 418-422.
16. Gibbs, J. H.; Robins, L. T.; Zhou, Z.; Bobadova-Parvanova, P.; Cottam, M.; McCandless, G. T.; Fronczek, F. R.; Vicente, M. G., Spectroscopic, computational modeling and cytotoxicity of a series of meso-phenyl and meso-thienyl-BODIPYs. *Bioorg. Med. Chem.* **2013,** *21* (18), 5770-5781.

17. Reddy, G.; Duvva, N.; Seetharaman, S.; D'Souza, F.; Giribabu, L., Photoinduced energy transfer in carbazole-BODIPY dyads. *Phys. Chem. Chem. Phys.* **2018,** *20* (43), 27418-27428.
18. Richard, W. W.; Jonathan, S. L., Boron-dipyrromethene dyes for incorporation in synthetic multi-pigment light-harvesting arrays. *Pure & Appl. Chem.* **1996,** *68*, 1373-1380.
19. Wallace, D. M.; Leung, S. H.; Senge, M. O.; Smith, K. M., Rational tetraarylporphyrin syntheses: tetraarylporphyrins from the MacDonald route. *J. Org. Chem.* **1993,** *58* (25), 7245-7257.
20. Tahtaoui, C.; Thomas, C.; Rohmer, F.; Klotz, P.; Duportail, G.; Mely, Y.; Bonnet, D.; Hibert, M., Convenient method to access new 4,4-dialkoxy- and 4,4-diaryloxy-diaza-s-indacene dyes: Synthesis and spectroscopic evaluation. *J. Org. Chem.* **2007,** *72* (1), 269-272.
21. Guo, Z.; Wei, X.; Hua, Y.; Chao, J.; Liu, D., Synthesis of 2-benzoylpyrrole derivatives via C–H functionalization adjacent to nitrogen of pyrrole. *Tetrahedron Lett.* **2015,** *56* (25), 3919-3922.
22. Liu, X.; Nan, H.; Sun, W.; Zhang, Q.; Zhan, M.; Zou, L.; Xie, Z.; Li, X.; Lu, C.; Cheng, Y., Synthesis and characterisation of neutral mononuclear cuprous complexes based on dipyrrin derivatives and phosphine mixed-ligands. *Dalton Trans.* **2012,** *41* (34), 10199-10210.
23. K. Nicolaou; D. Claremon; D. Papahatjis, A Mild Method For The Synthesis of 2-Ketopyrroles from Carboxylic Acids. *Tetrahedron Lett.* **1981,** *22* (46), 4647-4650.
24. Gupta, M.; Mula, S.; Tyagi, M.; Ghanty, T. K.; Murudkar, S.; Ray, A. K.; Chattopadhyay, S., Rational design of boradiazaindacene (BODIPY)-based functional molecules. *Chem.* **2013,** *19* (52), 17766-17772.
25. Scheps, R.; Pavlopoulos, T. G., Photostability of some pyrromethene laser dyes. *Proceedings of SPIE* **1999,** *3613*, 112-118.
26. Prasannan, D.; Raghav, D.; Sujatha, S.; Hareendrakrishna kumar, H.; Rathinasamy, K.; Arunkumar, C., Synthesis, structure, photophysical, electrochemical properties and antibacterial activity of brominated BODIPYs. *RSC Advances* **2016,** *6* (84), 80808-80824.
27. Jiao, L.; Pang, W.; Zhou, J.; Wei, Y.; Mu, X.; Bai, G.; Hao, E., Regioselective stepwise bromination of boron dipyrromethene (BODIPY) dyes. *J. Org. Chem.* **2011,** *76* (24), 9988-9996.
28. Jia-Hai Ye; G. W.; Chengmei Huang; Zhengjuan Hu; Whenchao Zhang; Yan Zhang, An efficient and convenient bromination of BODIPY derivatives with copper (II) bromide. *Synthesis* **2012,** *1*, 104-110.
29. Mahmood, Z.; Xu, K.; Kucukoz, B.; Cui, X.; Zhao, J.; Wang, Z.; Karatay, A.; Yaglioglu, H. G.; Hayvali, M.; Elmali, A., DiiodoBodipy-perylenebisimide dyad/triad: preparation and study of the intramolecular and intermolecular electron/energy transfer. *J. Org. Chem.* **2015,** *80* (6), 3036-3049.
30. Fan Song; H. Z.; De‐Gao Wang; Tao Chen; Sheng Yang; Gui-Chao Kuang, Imine‐linked porous organic polymers showing mesoporous microspheres architectures with tunable surface roughness. *Polym. Chem.* **2018,** *56* (3), 319-327.
31. Chase, D. T.; Young, B. S.; Haley, M. M., Incorporating BODIPY fluorophores into tetrakis(arylethynyl)benzenes. *J. Org. Chem.* **2011,** *76* (10), 4043-4051.
32. Ye, J. H.; Hu, Z.; Wang, Y.; Zhang, W.; Zhang, Y., A new practical and highly efficient iodination of BODIPY derivatives with hypervalent iodine reagent. *Tetrahedron Lett.* **2012,** *53* (50), 6858-6860.
33. Wang, X. F.; Yu, S. S.; Wang, C.; Xue, D.; Xiao, J., BODIPY catalyzed amide synthesis promoted by BHT and air under visible light. *Org. Biomol. Chem.* **2016,** *14* (29), 7028-7037.
34. Baruah, M.; Qin, W.; Vallee, R. A.; Beljonne, D.; Rohand, T.; Dehaen, W.; Boens, N., A highly potassium-selective ratiometric fluorescent indicator based on BODIPY azacrown ether excitable with visible light. *Org. Lett.* **2005,** *7* (20), 4377-4380.

35. Leen, V.; Braeken, E.; Luckermans, K.; Jackers, C.; Van der Auweraer, M.; Boens, N.; Dehaen, W., A versatile, modular synthesis of monofunctionalized BODIPY dyes. *Chem. Commun. (Camb)* **2009,** (30), 4515-4517.
36. Zhou, X.; Yu, C.; Feng, Z.; Yu, Y.; Wang, J.; Hao, E.; Wei, Y.; Mu, X.; Jiao, L., Highly Regioselective alpha-Chlorination of the BODIPY Chromophore with Copper(II) Chloride. *Org. Lett.* **2015,** *17* (18), 4632-4635.
37. Kang, J.; Huo, F.; Yue, Y.; Wen, Y.; Chao, J.; Zhang, Y.; Yin, C., A solvent depend on ratiometric fluorescent probe for hypochlorous acid and its application in living cells. *Dyes Pigments* **2017,** *136*, 852-858.
38. More, A. B.; Chakraborty, G.; Mula, S.; Ray, A. K.; Sekar, N., Modulation of the Photophysical Properties of beta-substituted BODIPY Dyes. *J. Fluoresc.* **2018,** *28* (1), 381-392.
39. Li, L.; Han, J.; Nguyen, B.; Burgess, K., Syntheses and spectral properties of functionalized, water-soluble BODIPY derivatives. *J. Org. Chem.* **2008,** *73* (5), 1963-1970.
40. Kim, J.; Kim, Y., A water-soluble sulfonate-BODIPY based fluorescent probe for selective detection of HOCl/OCl(-) in aqueous media. *Analyst.* **2014,** *139* (12), 2986-2989.
41. Chan, J.; Dodani, S. C.; Chang, C. J., Reaction-based small-molecule fluorescent probes for chemoselective bioimaging. *Nat. Chem.* **2012,** *4* (12), 973-984.
42. Kolemen, S.; Akkaya, E. U., Reaction-based BODIPY probes for selective bio-imaging. *Coordin. Chem. Rev.* **2018,** *354*, 121-134.
43. Chen, X.; Zhou, Y.; Peng, X.; Yoon, J., Fluorescent and colorimetric probes for detection of thiols. *Chem. Soc. Rev.* **2010,** *39* (6), 2120-2135.
44. Jung, H. S.; Chen, X.; Kim, J. S.; Yoon, J., Recent progress in luminescent and colorimetric chemosensors for detection of thiols. *Chem. Soc. Rev.* **2013,** *42* (14), 6019-6031.
45. Isik, M.; Ozdemir, T.; Turan, I. S.; Kolemen, S.; Akkaya, E. U., Chromogenic and fluorogenic sensing of biological thiols in aqueous solutions using BODIPY-based reagents. *Org. Lett.* **2013,** *15* (1), 216-219.
46. Isik, M.; Guliyev, R.; Kolemen, S.; Altay, Y.; Senturk, B.; Tekinay, T.; Akkaya, E. U., Designing an intracellular fluorescent probe for glutathione: two modulation sites for selective signal transduction. *Org. Lett.* **2014,** *16* (12), 3260-3263.
47. Dickinson, B. C.; Chang, C. J., Chemistry and biology of reactive oxygen species in signaling or stress responses. *Nat. Chem. Biol.* **2011,** *7* (8), 504-511.
48. Liu, S. R.; Wu, S. P., Hypochlorous acid turn-on fluorescent probe based on oxidation of diphenyl selenide. *Org. Lett.* **2013,** *15* (4), 878-881.
49. Bove, P. F.; van der Vliet, A., Nitric oxide and reactive nitrogen species in airway epithelial signaling and inflammation. *Free Radic. Biol. Med.* **2006,** *41* (4), 515-527.
50. Gabe, Y.; Urano, Y.; Kikuchi, K.; Kojima, H.; Nagano, T., Highly sensitive fluorescence probes for nitric oxide based on boron dipyrromethene chromophore-rational design of potentially useful bioimaging fluorescence probe. *J. Am. Chem. Soc.* **2004,** *126* (10), 3357-3367.
51. Yao, H. W.; Zhu, X. Y.; Guo, X. F.; Wang, H., An Amphiphilic Fluorescent Probe Designed for Extracellular Visualization of Nitric Oxide Released from Living Cells. *Anal. Chem.* **2016,** *88* (18), 9014-9021.
52. Zhu, X. Y.; Yao, H. W.; Fu, Y. J.; Guo, X. F.; Wang, H., Effect of substituents on Stokes shift of BODIPY and its application in designing bioimaging probes. *Anal. Chim. Acta.* **2019,** *1048*, 194-203.
53. De Duve, C., Baudhuin, Peroxisomes (microbodies and related particles). *Physiol. Rev.* **1966,** *46*, 323-357.
54. H. Dariush F.; Helmut S., *Peroxisomes in Biology and Medicine*. Springer-Verlag, Berlin.: 1987.

55. Río, L. A. D., *Peroxisomes and their Key Role in Cellular Signaling and Metabolism*. Springer, Dordrecht, The Netherlands: 2013.
56. Lodhi, I. J.; Semenkovich, C. F., Peroxisomes: a nexus for lipid metabolism and cellular signaling. *Cell Metab.* **2014,** *19* (3), 380-392.
57. Schrader, M. G. S.; Fahimi, H.D., Islinger, M., Peroxisome interactions and cross-talk with other subcellular compartments in animal cells. In. *Subcell. Biochem.* **2013,** 69, 1-22.
58. Wanders, R. J.; Ferdinandusse, S.; Brites, P.; Kemp, S., Peroxisomes, lipid metabolism and lipotoxicity. *Biochim. Biophys. Acta.* **2010,** *1801* (3), 272-280.
59. Del Rio, L. A.; Lopez-Huertas, E., ROS Generation in Peroxisomes and its Role in Cell Signaling. *Plant. Cell Physiol.* **2016,** *57* (7), 1364-1376.
60. Hu, J.; Baker, A.; Bartel, B.; Linka, N.; Mullen, R. T.; Reumann, S.; Zolman, B. K., Plant peroxisomes: biogenesis and function. *Plant Cell* **2012,** *24* (6), 2279-2303.
61. I., B. A. a. G., *Plant Peroxisomes. Biochemistry, Cell Biology and Biotechnological Applications.* Kluwer, Dordrecht, The Netherlands.: 2002.
62. Eastmond, P. J., MONODEHYROASCORBATE REDUCTASE4 is required for seed storage oil hydrolysis and postgerminative growth in Arabidopsis. *Plant Cell* **2007,** *19* (4), 1376-1387.
63. Agrawal, G.; Subramani, S., De novo peroxisome biogenesis: Evolving concepts and conundrums. *Biochim. Biophys. Acta.* **2016,** *1863* (5), 892-901.
64. Reumann, S.; Quan, S.; Aung, K.; Yang, P.; Manandhar-Shrestha, K.; Holbrook, D.; Linka, N.; Switzenberg, R.; Wilkerson, C. G.; Weber, A. P.; Olsen, L. J.; Hu, J., In-depth proteome analysis of Arabidopsis leaf peroxisomes combined with in vivo subcellular targeting verification indicates novel metabolic and regulatory functions of peroxisomes. *Plant Physiol.* **2009,** *150* (1), 125-143.
65. Tobias B. D.; Eward H. W. P.; Ronald, J. A. W.; Karel W. A. W., Targeted fluorescent probes in peroxisome function. *J. Histochem. Cytochem.* **2001,** *33*, 65-69.
66. Gould, S. G.; Keller, G. A.; Subramani, S., Identification of a peroxisomal targeting signal at the carboxy terminus of firefly luciferase. *J. Cell. Biol.* **1987,** *105* (6 Pt 2), 2923-2931.
67. Gould, S. J.; Keller, G. A.; Hosken, N.; Wilkinson, J.; Subramani, S., A conserved tripeptide sorts proteins to peroxisomes. *J. Cell. Biol.* **1989,** *108* (5), 1657-1664.
68. Ewald, H. H., Ben, D., Henk F. T., Import of proteins into peroxisomes. *Biochim. Biophys. Acta.* **1999,** *1451*, 17-34.
69. Brocard, C.; Hartig, A., Peroxisome targeting signal 1: is it really a simple tripeptide. *Biochim. Biophys. Acta.* **2006,** *1763* (12), 1565-1573.
70. Yano, T.; Oku, M.; Akeyama, N.; Itoyama, A.; Yurimoto, H.; Kuge, S.; Fujiki, Y.; Sakai, Y., A novel fluorescent sensor protein for visualization of redox states in the cytoplasm and in peroxisomes. *Mol. Cell. Biol.* **2010,** *30* (15), 3758-3766.
71. E. Z. Monosov; T. J. Wenzel; G. H. Lüers; J. A. Heyman; S. Subramani, Labeling of Peroxisomes with Green Fluorescent Protein in Living P. pastoris Cells. *J. Hisrochem. Cyrochem.* **1996,** *44*, 581-589.
72. Landrum, M.; Smertenko, A.; Edwards, R.; Hussey, P. J.; Steel, P. G., BODIPY probes to study peroxisome dynamics in vivo. *Plant J.* **2010,** *62* (3), 529-538.
73. Zhou, Y.; Li, P.; Fan, N.; Wang, X.; Liu, X.; Wu, L.; Zhang, W.; Zhang, W.; Ma, C.; Tang, B., In situ visualization of peroxisomal peroxynitrite in the livers of mice with acute liver injury induced by carbon tetrachloride using a new two-photon fluorescent probe. *Chem. Commun.* **2019,** *55* (47), 6767-6770.
74. Jankowski, A.; Kim, J. H.; Collins, R. F.; Daneman, R.; Walton, P.; Grinstein, S., In situ measurements of the pH of mammalian peroxisomes using the fluorescent protein pHluorin. *J. Biol. Chem.* **2001,** *276* (52), 48748-48753.

75. Fahy, D.; Sanad, M. N.; Duscha, K.; Lyons, M.; Liu, F.; Bozhkov, P.; Kunz, H. H.; Hu, J.; Neuhaus, H. E.; Steel, P. G.; Smertenko, A., Impact of salt stress, cell death, and autophagy on peroxisomes: quantitative and morphological analyses using small fluorescent probe N-BODIPY. *Sci. Rep.* **2017,** *7*, 39069-39084.
76. Singh, A. T., E. R.; Westheimer, F. H., The Photolysis of Diazo-acetylchymotrypsin. *J. Biol. Chem.* **1962,** *237*, 3006-3008.
77. Sinz, A., Investigation of protein-ligand interactions by mass spectrometry. *Chem. Med. Chem.* **2007,** *2* (4), 425-431.
78. Zhao, B.; Burgess, K., Click-Addressable Cassette for Photoaffinity Labeling. *ACS Med. Chem. Lett.* **2018,** *9* (2), 155-158.
79. Lapinsky, D. J., Tandem photoaffinity labeling-bioorthogonal conjugation in medicinal chemistry. *Bioorg. Med. Chem.* **2012,** *20* (21), 6237-6247.
80. Park, J.; Koh, M.; Koo, J. Y.; Lee, S.; Park, S. B., Investigation of Specific Binding Proteins to Photoaffinity Linkers for Efficient Deconvolution of Target Protein. *ACS Chem. Biol.* **2016,** *11* (1), 44-52.
81. Lee, B. C.; Lee, K. C.; Lee, H.; Mach, R. H.; Katzenellenbogen, J. A., Strategies for the labeling of halogen-substituted peroxisome proliferator-activated receptor gamma ligands: potential positron emission tomography and single photon emission computed tomography imaging agents. *Bioconjug. Chem.* **2007,** *18* (2), 514-523.
82. Collins, E. S. A. I., Photoaffinity labeling in target- and binding-site identification. *Future. Med. Chem.* **2015,** *7*, 159-183.
83. Georg, C.; Terstappen, C. S.; Roberto R.; Giovanni, G., Target deconvolution strategies in drug discovery. *Nat. Rev. Drug. Discov.* **2007,** *6*, 891-903.
84. Yutaka S.; Yasumaru H., Photochemical Fishing Approaches for Identifying Target Proteins and Elucidating the Structure of a Ligand-binding Region Using Carbene-generating Photoreactive Probes. *Anal. Sci.* **2006,** *22*, 209-218.
85. Dubinsky, L.; Krom, B. P.; Meijler, M. M., Diazirine based photoaffinity labeling. *Bioorg. Med. Chem.* **2012,** *20* (2), 554-570.
86. Paul, P. G.; Laurette, M. P.; Gijs, A. V. D. M.; Rainer, B.; Herman, S. O., Photoaffinity Labeling in Activity-Based Protein Profiling. *Top. Curr. Chem.* **2012,** *324*, 85-114.
87. Ali, H.; Guerin, B.; Van L. J. E., gem-Dibromovinyl boron dipyrrins: synthesis, spectral properties and crystal structures. *Dalton Trans.* **2019,** *48* (30), 11492-11507.
88. Wei, Y.; Zhou, M.; Zhou, Q.; Zhou, X.; Liu, S.; Zhang, S.; Zhang, B., Triplet-triplet annihilation upconversion kinetics of C60-Bodipy dyads as organic triplet photosensitizers. *Phys. Chem. Chem. Phys.* **2017,** *19* (33), 22049-22060.
89. Jiangzhang, Z.; Jinnan C.; Zhao, W., China Patent, **2015,** CN104277061.
90. Kubheka, G.; Sanusi, K.; Mack, J.; Nyokong, T., Optical limiting properties of 3,5-dipyrenylvinyleneBODIPY dyes at 532nm. *Spectrochim. Acta. A Mol. Biomol. Spectrosc.* **2018,** *191*, 357-364.
91. Aydin, T. D.; Viswanathan, G.; Zehra, T. S.; Looi, C. Y.; Wong, W. F.; Min Y. T.; Zorlu, Y.; Gurek, A. G.; Lee, H. B.; Dumoulin, F., Antimicrobial activity of a quaternized BODIPY against Staphylococcus strains. *Org. Biomol. Chem.* **2016,** *14* (9), 2665-70.
92. Alnoman, R. B.; Stachelek, P.; Knight, J. G.; Harriman, A.; Waddell, P. G., Synthesis of 2-aminoBODIPYs by palladium catalysed amination. *Org. Biomol. Chem.* **2017,** *15* (36), 7643-7653.
93. Wang, E.; Qiao, H.; Zhou, Y.; Pang, L.; Yu, F.; Zhang, J.; Ma, T., A novel "turn-on" fluorogenic probe for sensing hypochlorous acid based on BODIPY. *RSC Advances* **2015,** *5* (89), 73040-73045.

94. Tsai, Y. H.; Essig, S.; James, J. R.; Lang, K.; Chin, J. W., Selective, rapid and optically switchable regulation of protein function in live mammalian cells. *Nat. Chem.* **2015,** *7* (7), 554-561.
95. Richard P. H.; Hee, C. K., Chemically Reactive Dpyrrometheneboron Difluoride Dyes. *United States Patent* **1988,**4774339.
96. Davison, E. C.; Fox, M. E.; Holmes, A. B.; Roughley, S. D.; Smith, C. J.; Williams, G. M.; Davies, J. E.; Raithby, P. R.; Adams, J. P.; Forbes, I. T.; Press, N. J.; Thompson, M. J., Nitrone dipolar cycloaddition routes to piperidines and indolizidines. Part 9.† Formal synthesis of (-)-pinidine and total synthesis of (-)-histrionicotoxin, (+)-histrionicotoxin and (-)-histrionicotoxin 235A. *J. Am. Chem. Soc., Perkin Transactions 1* **2002,** (12), 1494-1514.
97. Du, S.; Kimball, E. A.; Ragains, J. R., Visible-Light-Promoted Remote C-H Functionalization of o-Diazoniaphenyl Alkyl Sulfones. *Org. Lett.* **2017,** *19* (20), 5553-5556.
98. Han, Y.; Han, M.; Shin, D.; Song, C.; Hahn, H. G., Exploration of novel 3-substituted azetidine derivatives as triple reuptake inhibitors. *J. Med. Chem.* **2012,** *55* (18), 8188-92.
99. Shah, S.; Lee, C.; Choi, H.; Gautam, J.; Jang, H.; Kim, G. J.; Lee, Y. J.; Chaudhary, C. L.; Park, S. W.; Nam, T. G.; Kim, J. A.; Jeong, B. S., 5-Hydroxy-7-azaindolin-2-one, a novel hybrid of pyridinol and sunitinib: design, synthesis and cytotoxicity against cancer cells. *Org. Biomol. Chem.* **2016,** *14* (21), 4829-41.
100. Andrade, S. F.; Oliveira, B. G.; Pereira, L. C.; Ramos, J. P.; Joaquim, A. R.; Steppe, M.; Souza-Fagundes, E. M.; Alves, R. J., Design, synthesis and structure-activity relationship studies of a novel focused library of 2,3,4-substituted oxazolidines with antiproliferative activity against cancer cell lines. *Eur. J. Med. Chem.* **2017,** *138*, 13-25.
101. Zhang, L. Y.; Tu, F. Q.; Guo, X. F.; Wang, H.; Wang, P.; Zhang, H. S., A new BODIPY-based long-wavelength fluorescent probe for chromatographic analysis of low-molecular-weight thiols. *Anal. Bioanal. Chem.* **2014,** *406* (26), 6723-33.
102. Ling, H.; Xuerong, Y.; Wanhua W.; Jianzhang Z., Styryl Bodipy-C60 Dyads as Efficient Heavy-Atom-Free Organic Triplet Photosensitizers. *Org. Lett.* **2012,** 14 (10), 2594-2597.
103. Shi, Z.; Suri, M.; Glorius, F., Aerobic synthesis of pyrroles and dihydropyrroles from imines: palladium(II)-catalyzed intramolecular C-H dehydrogenative cyclization. *Angew. Chem. Int. Ed. Engl.* **2013,** *52* (18), 4892-6.
104. Wei, Y.; Deb, I.; Yoshikai, N., Palladium-catalyzed aerobic oxidative cyclization of N-aryl imines: indole synthesis from anilines and ketones. *J. Am. Chem. Soc.* **2012,** *134* (22), 9098-101.
105. Kang, N. Y.; Lee, S. C.; Park, S. J.; Ha, H. H.; Yun, S. W.; Kostromina, E.; Gustavsson, N.; Ali, Y.; Chandran, Y.; Chun, H. S.; Bae, M.; Ahn, J. H.; Han, W.; Radda, G. K.; Chang, Y. T., Visualization and isolation of Langerhans islets by a fluorescent probe PiY. *Angew. Chem. Int. Ed. Engl.* **2013,** *52* (33), 8557-60.
106. Kwon, H. Y.; Kim, J. Y.; Lee, J. Y.; Yam, J. K. H.; Hultqvist, L. D.; Xu, W.; Rybtke, M.; Tolker-Nielsen, T.; Kim, J. J.; Kang, N. Y.; Yang, L.; Park, S. J.; Givskov, M.; Chang, Y. T., CDy14: a novel biofilm probe targeting exopolysaccharide Psl. *Chem. Commun. (Camb)* **2018,** *54* (84), 11865-11868.
107. Romuald, C.; Busseron, E.; Coutrot, F., Very contracted to extended co-conformations with or without oscillations in two- and three-station [c2]daisy chains. *J. Org. Chem.* **2010,** *75* (19), 6516-31.
108. Masuya, T.; Murai, M.; Ifuku, K.; Morisaka, H.; Miyoshi, H., Site-specific chemical labeling of mitochondrial respiratory complex I through ligand-directed tosylate chemistry. *Biochemistry* **2014,** *53* (14), 2307-17.

109. Wang, L.; Fan, J.; Qiao, X.; Peng, X.; Dai, B.; Wang, B.; Sun, S.; Zhang, L.; Zhang, Y., Novel asymmetric Cy5 dyes: Synthesis, photostabilities and high sensitivity in protein fluorescence labeling. *J. Photochem. Photobiol. A* **2010,** *210* (2-3), 168-172.
110. Kvach, M. V.; Ustinov, A. V.; Stepanova, I. A.; Malakhov, A. D.; Skorobogatyi, M. V.; Shmanai, V. V.; Korshun, V. A., A Convenient Synthesis of Cyanine Dyes: Reagents for the Labeling of Biomolecules. *Eur. J. Org. Chem.* **2008,** *2008* (12), 2107-2117.
111. Khan, A. A.; Kamena, F.; Timmer, M. S.; Stocker, B. L., Development of a benzophenone and alkyne functionalised trehalose probe to study trehalose dimycolate binding proteins. *Org. Biomol. Chem.* **2013,** *11* (6), 881-5.
112. Dobretsov, G. E.; Syrejschikova, T. I.; Smolina, N. V., On mechanisms of fluorescence quenching by water. *Biophysics* **2014,** *59* (2), 183-188.
113. Li, H.; Guan, H.; Duan, X.; Hu, J.; Wang, G.; Wang, Q., An acid catalyzed reversible ring-opening/ring-closure reaction involving a cyano-rhodamine spirolactam. *Org. Biomol. Chem.* **2013,** *11* (11), 1805-9.
114. Nagata, T.; Okada, K.; Takebe, I.; Matsui, C., Delivery of tobacco mosaic-virus RNA into plant protoplasts mediated by reverse-phase evaporation vesicles (liposomes). *Mol. Genet. Genom.* **1981,** *184* (2), 161-165.